



**2020 International Conference on  
"Physics and Mechanics  
of New Materials  
and Their Applications"**

**PHENMA 2020**

**Kitakyushu, Japan, March 26–29, 2021**

 [phenma2020.sfedu.ru](http://phenma2020.sfedu.ru)



2020 International Conference on "Physics and Mechanics of New Materials and Their Applications" (PHENMA 2020)  
Kitakyushu, Japan, March 26 – 29, 2021

## Sponsored by



Kyushu Branch

The Society of Materials Science, Japan  
Kyushu Branch, Japan



公益 北九州観光コンベンション協会  
財団法人  
**Kitakyushu Convention & Visitors Association**

Kitakyushu Convention & Visitors Association, Japan



**KSCM** The Korean Society for Composite  
Materials, South Korea



Rostov Regional Administration, Russia



Ministry of Science and High Education  
of the Russian Federation, Russia



Russian Foundation for Basic Research, Russia



Ministry of Science and Technology  
of Taiwan, Taiwan

Kyushu Institute of Technology  
Southern Federal University  
National Kaohsiung University of Science and Technology  
Korea Maritime and Ocean University

**2020 International Conference  
on “Physics and Mechanics of New Materials  
and Their Applications” (PHENMA 2020)**

**Kitakyushu, Japan, March 26–29, 2021**

**<http://phenma2020.sfedu.ru/>**

**Abstracts & Schedule**

Rostov-on-Don – Taganrog  
Southern Federal University Press  
2021

UDK 53+531 - 027.22(063)

2020 International Conference on “Physics and Mechanics of New Materials and Their Applications” (PHENMA 2020) (Kitakyushu, Japan, March 26–29, 2021) : Abstracts and Schedule / I. A. Parinov, Y.-H. Kim, N.-A. Noda, S.-H. Chang (Eds.) ; Southern Federal University. – Rostov-on-Don ; Taganrog : Southern Federal University Press, 2021. – 356 p.

ISBN 978-5-9275-3768-6

The success of the Russian-Taiwanese Symposium “Physics and Mechanics of New Materials and Their Applications”, PMNM-2012 (Russia, 2012), 2013 International Symposium “Physics and Mechanics of New Materials and Underwater Applications”, PHENMA-2013 (Taiwan, 2013), 2014 International Symposium “Physics and Mechanics of New Materials and Underwater Applications”, PHENMA-2014 (Thailand, 2014), 2015 International Conference “Physics and Mechanics of New Materials and Their Applications”, PHENMA-2015 (Russia, 2015), 2016 International Conference “Physics and Mechanics of New Materials and Their Applications”, PHENMA-2016 (Indonesia, 2016), 2017 International Conference “Physics and Mechanics of New Materials and Their Applications”, PHENMA-2017 (India, 2017), 2018 International Conference “Physics and Mechanics of New Materials and Their Applications”, PHENMA-2018 (South Korea, 2018) and 2019 International Conference “Physics and Mechanics of New Materials and Their Applications”, PHENMA-2019 (Vietnam, 2019) predefined objectives and scientific directions of the new conference PHENMA-2020, conducted by the Kyushu Institute of Technology (Japan). Due to COVID-19 pandemic, this conference has been postponed from 2–5 October, 2020 to 26–29 March, 2021.

The following PHENMA abstracts cover five scientific directions: (i) processing techniques of new materials, (ii) physics of new materials, (iii) mechanics of new materials, (iv) applications of new materials, and (v) industry and management. These are present by scientists from 17 countries, demonstrating strong scientific collaboration, formed for last years.

Published in author’s edition.

UDK 53+531 - 027.22(063)

ISBN 978-5-9275-3768-6

© Southern Federal University, 2021



2020 International Conference on "Physics and Mechanics of New Materials and Their Applications" (PHENMA 2020)  
Kitakyushu, Japan, March 26 – 29, 2021

**Sponsored by**



Kyushu Branch

The Society of Materials Science, Japan  
Kyushu Branch, Japan



公益 北九州観光コンベンション協会  
財団法人  
Kitakyushu Convention & Visitors Association

Kitakyushu Convention & Visitors Association, Japan



**KSCM** The Korean Society for Composite  
Materials, South Korea



Rostov Regional Administration, Russia



Ministry of Science and High Education  
of the Russian Federation, Russia



Russian Foundation for Basic Research, Russia



Ministry of Science and Technology

Ministry of Science and Technology  
of Taiwan, Taiwan



National Foundation for Science & Technology Development, Vietnam



Vietnam Union of Science and Technology Associations (VUSTA), Vietnam



Vietnam Association of Science Editing (VASE), Vietnam



South Scientific Center of Russian Academy of Science, Russia



*New Century Education Foundation*

New Century Education Foundation, Taiwan



Ocean & Underwater Technology Association, Taiwan



Unity Opto Technology Co., Taiwan



Fair Well Fishery Co., Taiwan



Woen Jinn Harbor Engineering Co., Taiwan



Lorom Group, Taiwan



Longwell Co., Taiwan



Korea Maritime and Ocean University, South Korea



Hanoi University of Science and Technology, Vietnam



Vietnam Maritime University, Vietnam



Vinh Long University of Technology Education, Vietnam



Hanoi University of Industry, Vietnam



Vietnamese-German University, Vietnam



Ho Chi Minh City University of Agriculture and Forestry, Vietnam



Research Institute of Agriculture Machinery, Vietnam



Don State Technical University, Russia



University of 17 Agustus 1945 Surabaya, Indonesia



Perkumpulan Ahli dan Dosen Republik Indonesia



University of Maarif Hasyim Latif, Sidoarjo, Indonesia



PDPM Indian Institute of Information Technology, Design and Manufacturing, India



South Russian Regional Centre for Preparation and Implementation of International Projects, Ltd., Russia





## Organizing Committee

### Conference Chairs

- Y.-H. Kim (Korea Maritime and Ocean University, South Korea)
- N.-A. Noda (Kyushu Institute of Technology, Japan)
- I. A. Parinov (Southern Federal University, Russia)
- S.-H. Chang (National Kaohsiung University of Science and Technology,  
Taiwan, ROC)

### Advisory Chairs

- C.-K. Chou (New Century Education Foundation, Taiwan, ROC)
- T. Duc-Quy (Hanoi University of Industry, Vietnam)
- V. K. Gupta (PDPM-Indian Institute of Information Technology, Design and  
Manufacturing Jabalpur, India)
- L. Hai-An (Ministry of Education and Training, Vietnam)
- M. Hatta (University of 45 Surabaya, Indonesia)
- N. Hay (Nong Lam University, Ho Chi Minh City, Vietnam)
- I.-C. Huang (Fair Well Fishery Group, Taiwan, ROC)
- C. Hung- Phi (Vinh Long University of Technology Education, Vietnam)
- S. Jain (PDPM Indian Institute of Information Technology, Design and  
Manufacturing, Jabalpur, India)
- M. A. Jani (University of 17 Agustus 1945 Surabaya, Indonesia)
- V. I. Kolesnikov (Rostov State Transport University, Russia)
- K. Kolmetz (International Association of Certified Professional Engineers,  
USA)
- G. G. Matishov (South Scientific Center of Russian Academy of Sciences,  
Russia)
- B. Ch. Meskhi (Don State Technical University, Russia)
- M. Nugroho (University of 17 Agustus 1945 Surabaya, Indonesia)
- A. Ojha (PDPM Indian Institute of Information Technology, Design and  
Manufacturing, Jabalpur, India)
- D. Pham-Xuan (Vietnam Maritime University, Vietnam)
- P. Seshu (Indian Institute of Technology Dharwad, India)

I. K. Shevchenko (Southern Federal University, Russia)  
B. Tien-Long (Vietnam Association for Science Editing – VASE, Vietnam)  
D. Van-Phong (Hanoi University of Science and Technology, Vietnam)  
P. Van-Song (Vietnamese-German University, Vietnam)  
D. Vu-Minh (Vietnam Union of Science and Technology, Vietnam)  
D.-S. Wu (National Chung Hsing University, Taiwan, ROC)  
P. Xuan-Duong (Vietnam Maritime University, Vietnam)  
C.-Y. Yang (National Kaohsiung University of Science and Technology,  
Taiwan, ROC)

### **Conference Co-Chairs**

L. Anh-Tuan (Hanoi University of Science and Technology, VASE,  
Vietnam)  
L.-K. Chien (National Taiwan Ocean University, Taiwan, ROC)  
N. Duc - Chien (Hanoi University of Science and Technology, Vietnam)  
N. Duc-Toan (Hanoi University of Science and Technology, VASE,  
Vietnam)  
A. Fatoni, R (Perkumpulan Ahli dan Dosen Republik Indonesia)  
R. Hastijanti (University of 17 Agustus 1945 Surabaya, Indonesia)  
K. Hasyim (University of Darul Ulum, Jombang, Indonesia)  
H.-C. Huang (National Kaohsiung University of Science and Technology,  
Taiwan, ROC)  
V. V. Kalinchuk (South Scientific Center of Russian Academy of Sciences,  
Russia)  
P.K. Kankar (Indian Institute of Technology Indore, India)  
M. I. Karyakin (Southern Federal University, Russia)  
Y. H. Kim (Korea Maritime and Ocean University, South Korea)  
C.-T. Lin (National Kaohsiung University of Science and Technology,  
Taiwan, ROC)  
M. B. Manuilov (Southern Federal University, Russia)  
A. V. Metelitsa (Southern Federal University, Russia)  
V. I. Minkin (Southern Federal University, Russia)  
E.L. Mukhanov (Southern Federal University, Russia)  
Nurmawati (University of 45 Surabaya, Indonesia)  
N. Phu- Khanh (Hanoi University of Science and Technology, Vietnam)  
I. Prasetyawan (Lloyd Register Asia, Malaysia)  
N. Quoc-Hung (Vietnamese-German University, Vietnam)  
M. A. Rahim (University of 17 Agustus 1945 Surabaya, Indonesia)

Sajiyo (University of 17 Agustus 1945 Surabaya, Indonesia)  
T.-T. Shih (National Kaohsiung University of Science and Technology,  
Taiwan, ROC)  
A. N. Soloviev (Don State Technical University, Russia)  
H. Trung-Hai (Hanoi University of Science and Technology, Vietnam)  
P. Van- Hung (Hanoi University of Science and Technology, Vietnam)  
T. Van- Nghia (Ministry of Science and Technology, Vietnam)  
I. A. Verbenko (Southern Federal University, Russia)  
W. Widiasih (University of 17 Agustus 1945 Surabaya, Indonesia)  
J.-K. Wu (National Kaohsiung University of Science and Technology,  
Taiwan, ROC)  
M.-C. Wu (National Tsing Hua University, Taiwan, ROC)

### **Secretariats**

D. Anh-Tuan (Hung Yen University of Technology and Education, Vietnam)  
V. A. Chebanenko (South Scientific Center of Russian Academy of Sciences,  
Russia)  
A. V. Cherpakov (Southern Federal University, Russia)  
P. Duc-An (Hanoi University of Science and Technology, VASE, Vietnam)  
N.T. Hong-Minh (Hanoi University of Science and Technology, VASE,  
Vietnam)  
N. Huu- Quang (Hanoi University of Science and Technology, VASE,  
Vietnam)  
Yu. V. Klunnikova (Southern Federal University, Russia)  
S. J. Park (Korea Maritime and Ocean University, South Korea)  
E. P. Putri (University of 17 Agustus 1945 Surabaya, Indonesia)  
M. S. Shevtsova (RheinMain University of Applied Sciences, Germany)  
T. The-Van (Hung Yen University of Technology and Education, Vietnam)  
H.-W. Tin (National Kaohsiung University of Science and Technology,  
Taiwan, ROC)  
T. Van-The (Hung Yen University of Technology and Education, Vietnam)  
C. E. Vassilchenko (Southern Federal University, Russia)

### **Scientific Program Committee**

O. A. Ageev (Southern Federal University, Russia)  
B. Anh- Hoa (Hanoi University of Science and Technology, Vietnam)  
N. Anh-Tu (Hanoi University of Industry, Vietnam)

M.Z. Ansari (PDPM Indian Institute of Information Technology, Design and Manufacturing Jabalpur, India)

R. G. Atram (Institute of Science, Nagpur, India)

B. M. Bahirwar (Gurunanak College of Science, Ballarpur, India)

Y.-Y. Bu (National University of Tainan, Taiwan, ROC)

S. I. Builo (Southern Federal University, Russia)

J.-C. Chen (Vanung University, Taiwan, ROC)

R.-B. Chen (National Kaohsiung University of Science and Technology, Taiwan, ROC)

C.-L. Chiu (National Kaohsiung University of Science and Technology, Taiwan, ROC)

K.-K. Chong (National Kaohsiung University of Science and Technology, Taiwan, ROC)

L. Cong-Nho (Vietnam Maritime University, Vietnam)

D. Dinh-Phuong (Institute of Materials Sciences, Vietnam Academy of Science and Technology, Vietnam)

N. Dinh-Tung (Research Institute of Agricultural Machinery, RIAM, Vietnam)

Y.-C. Fang (National Kaohsiung University of Science and Technology, Taiwan, ROC)

J.-J. Ho (National Taiwan Ocean University, Taiwan, ROC)

T. Hoanh-Son (Hanoi University of Science and Technology, Vietnam)

H. Hong-Hai (Hanoi University of Science and Technology, Vietnam)

Y.-Z. Hsieh (National Taiwan Ocean University, Taiwan, ROC)

C.-L. Huang (National Kaohsiung University of Science and Technology, Taiwan, ROC)

J.-H. Go (Korea Maritime and Ocean University, South Korea)

B. S. Jagdale (Science and Commerce College, India)

F.-S. Juang (National Formosa University, Taiwan, ROC)

P. Koinkar (Tokushima University, Japan)

S. B. Kondawar (R.T.M. Nagpur University, Nagpur, India)

G. Kusnanto (University of 17 Agustus 1945 Surabaya, Indonesia)

Kuswanto (University of Darul Ulum, Jombang, Indonesia)

C.-Y. Lee (National Kaohsiung University of Science and Technology, Taiwan, ROC)

J. J.-Y. Lee (National Kaohsiung University of Science and Technology, Taiwan, ROC)

J.-W. Lee (Korea Institute of Industrial Technology, South Korea)

T.-F. Lee (National Kaohsiung University of Science and Technology,

Taiwan, ROC)

P.-H. Lei (National Formosa University, Taiwan, ROC)

C.-F. Lin (National Taiwan Ocean University, Taiwan, ROC)

C.-H. Lin (National Kaohsiung University of Science and Technology,  
Taiwan, ROC)

C.-Y. Liu (National Kaohsiung University of Science and Technology,  
Taiwan, ROC)

H. Long (Hanoi University of Science and Technology, VASE, Vietnam)

T. R. Mahale (Science and Commerce College, India)

I. P. Miroshnichenko (Don State Technical University, Russia)

M. A. More (S.P. Pune University, Pune, India)

S. Mukherjee (PDPM-Indian Institute of Information Technology, Design  
and Manufacturing Jabalpur, India)

R.-I. Murakami (National Taiwan University of Science and Technology,  
Taiwan, ROC)

M. Nafi (University of 17 Agustus 1945 Surabaya, Indonesia)

A. N. Nakagaito (Tokushima University, Japan)

D. V. Nandanwar (Shri M. M. College of Science, Nagpur, India)

A. V. Nasedkin (Southern Federal University, Russia)

N. Ngoc-Trung (Hanoi University of Science and Technology, Vietnam)

A. E. Panich (Southern Federal University, Russia)

C.-W. Park (Korea Maritime and Ocean University, South Korea)

S.-J. Park (Korea Maritime and Ocean University, South Korea)

S.D. Patel (PDPM-Indian Institute of Information Technology, Design and  
Manufacturing, India)

A. V. Patil (L.V.H. College, India)

J.-H. Pee (Ministry of Trade, Industry and Energy, South Korea)

N. Phong-Dien (Hanoi University of Science and Technology, Vietnam)

J. N. Ramteke (Shri M. M. College of Science, Nagpur, India)

L. A. Reznichenko (Southern Federal University, Russia)

F. Rodli (University of Maarif Hasyim Latif, Sidoarjo, Indonesia)

V. Sangawar (Institute of Science, India)

H. Seputro (University of 17 Agustus 1945 Surabaya, Indonesia)

T. Sheorey (PDPM-Indian Institute of Information Technology, Design and  
Manufacturing, India)

S. N. Shevtsov (South Scientific Center of Russian Academy of Sciences,  
Russia)

M.-C. Shihg (National University of Kaohsiung, Taiwan, ROC)

D.-H. Shin (Korean Air Tech Center, South Korea)

T.-J. Su (National Kaohsiung University of Science and Technology, Taiwan)  
 M. A. Sumbatyan (Southern Federal University, Russia)  
 J. C. Sun (Dalian Maritime University, China)  
 R. Sunder (BiSS (P) Ltd, India)  
 H. Tien-Dung (Hanoi University of Industry, Vietnam)  
 N. Tien-Han (Hanoi University of Industry, Vietnam)  
 V. Toan-Thang (Hanoi University of Science and Technology, Vietnam)  
 V. Yu. Topolov (Southern Federal University, Russia)  
 B. Trung-Thanh (Hung Yen University of Technology and Education,  
 Vietnam)  
 T. Trung Thanh (Vietnamese-German University, Vietnam)  
 D. Van-Chien (Vietnam Association for Science Editing, Vietnam)  
 D. Van- Hai (Hanoi University of Science and Technology, Vietnam)  
 P. Van-Hieu (Hanoi University of Science and Technology, VASE, Vietnam)  
 N. Van- Ngu (Hoa Binh University, Vietnam)  
 N. Van-Thien (Hanoi University of Industry, Vietnam)  
 A. O. Vatulyan (Southern Federal University, Russia)  
 T. Viet-Anh (Hanoi University of Science and Technology, Vietnam)  
 F.-T. Wang (Hwa Hsia University of Technology, Taiwan, ROC)  
 H.-Y. Wang (National Kaohsiung University of Science and Technology,  
 Taiwan, ROC)  
 J.-P. Wang (National Kaohsiung University of Science and Technology,  
 Taiwan, ROC)  
 C.-E. Weng (National Kaohsiung University of Science and Technology,  
 Taiwan, ROC)  
 C.-M. Wu (National Taiwan University of Science and Technology, Taiwan)  
 C.-C. Yang (National Kaohsiung University of Science and Technology,  
 Taiwan, ROC)  
 C.-D. Yang (National Kaohsiung University of Science and Technology,  
 Taiwan, ROC)  
 C.-F. Yang (National University of Kaohsiung, Taiwan, ROC)  
 S.-H. Yang (National Kaohsiung University of Science and Technology,  
 Taiwan, ROC)  
 M.-Y. Yeh (National Kaohsiung University of Science and Technology,  
 Taiwan, ROC)  
 C.-Y. Yen (National Kaohsiung University of Science and Technology,  
 Taiwan, ROC)  
 S.-W. Yoon (Research Institute of Medium & Small Shipbuilding, South  
 Korea)

S.-F. Zhao (National Kaohsiung University of Science and Technology,  
Taiwan, ROC)

**Local Organizing Committee**

Y.-H. Kim (Korea Maritime and Ocean University, South Korea)

N.-A. Noda (Kyushu Institute of Technology, Japan)

G. Hotta (National Institute of Technology, Ariake College, Japan)

Y. Nakamura (Kagoshima University, Japan)

K. Oda (Oita University, Japan)

H. Sakamoto (Doshisha University, Japan)

Y. Sano (Maruei Kako Corporation, Japan)

Y. Takase (Kyushu Institute of Technology, Japan)



Preface..... 30

**TABLE OF ABSTRACTS**

Adeel Ahmad Jamil, Chitsan Lin, Zulfiqar Ali. A Bag of Expressions-based Method for the Recognition of Vehicle Make and Model ..... 31

S. M. Afonin. Absolute Stability of Control System for Deformation of Electromagnetoelastic Actuator under Random Impacts in Nanoresearch..... 32

Alexandra Starnikova, Irina Gulyaeva, Khabibulla Abdullin, Victor Petrov. Study of Gas-sensitive Properties of Materials Based on ZnO Nanorods to Nitrogen Dioxide (IV)..... 33

Alexey M. Kolesnikov. Tubular Dielectric Elastomer Actuator Reinforced with two Families of Fibers ..... 34

T. M. Andreeva, Yu. E. Drobotov. On the Solution of Convolutional Equation in Spaces of Holomorphic Functions of Prescribed Growth..... 35

Andrey S. Vasiliev, Sergei S. Volkov, Sergei M. Aizikovich. Approximated Analytical solutions for Contact Problems for Piezoelectric Solids with Functionally Graded Coatings ..... 36

N.V. Andros, I.V. Morshneva. Occurrence of 3D Periodic Convective Flows in a Vertical Layer with Moving Boundaries..... 36

K.P. Andryushin, I.N. Andryushina, L.A. Reznichenko. The Effect of Biographical Defects on the Electrophysical Properties of *n*-component Ferroactive Solid Solutions of Composition PZT – PZN – PMN ..... 37

I.N. Andryushina, K.P. Andryushin, L.A. Reznichenko. The Structure, Microstructure and Piezoelectric Properties of Highly Sensitive Ferroelectric Ceramics ..... 38

I.N. Andryushina, E.V. Triger, N.A. Nikiforova, K.P. Andryushin, L.A. Reznichenko. Stability of the Polarized State in Ferroelectric Piezoelectric Ceramics of Various Ferrohardeness Degrees ..... 39

M. R. Aridi, N.A. Noda, Y. Sano, K. Takata, S. Zifeng. Effect of the Residual Stress to the Fatigue Failure of the Bimetallic Roll in 4-High Rolling Mill ..... 40

Arkadiy N. Soloviev, Alexander N. Epikhin, Denis V. Krasnov. Modeling the Interaction of Elastic Haptic Parts of Two Intraocular Lenses Located in the Capsular Bag of the Lens..... 41

A. N. Soloviev, D. K. Nadolin, Pavel A. Oganessian. Development of Standalone Computational Modules for ACELAN-COMPOS Package ..... 43

A.Soloviev, N. Glushko, A. Epikhin, M. Swain, O. N. Lesnyak, A. E. Ivanov. Finite Element Modeling of the Interaction of an Ocular Prosthesis with the Corneal Tissue of the Eye ..... 44

Arkadiy N. Soloviev, Pavel A. Oganessian, Evgenia Kirillova, V. A. Chebanenko. Modeling of Multisection Piezoelectric Energy Harvesting Devices Based on Applied Theory ..... 45

V.I. Avilov, N.A. Sharapov, N.V. Polupanov, V.A. Smirnov. Temperature Stability of Resistive Switching in Titanium Oxide Nanostructures ..... 46



R.A. Bardakova, A.A. Kotova, A.A. Matrosov. The Impact of Deterministic and Stochastic Loads on the Support of the Offshore Platform.....	47
E.M. Bayan, V.V. Petrov, V.Yu. Storozhenko, M.G. Volkova. Preparation and Characterization of Transparent Sn-ZnO Thin Films Obtained by Pyrolysis .....	48
O. A. Belyak. Wave Fields in an Orthotropic Strip Weakened by a Cylindrical Cavity of Small Characteristic Size .....	49
O.A. Belyak, T.V. Suvorova. On the Prediction of the Mechanical and Tribological Properties of Dispersively Filled Composites.....	50
T.I. Belyankova, E.I. Vorovich, V.V. Kalinchuk, O.M. Tukodova. Features of Rayleigh Waves Propagation in Structures with FGPM Coating Made of Various Materials.....	51
T.I. Belyankova, E.I. Vorovich, V.V. Kalinchuk, O.M. Tukodova. Specific Features of SH-Waves Propagation in Structures with Prestressed Inhomogeneous Coating Made of Piezoceramics Based on $\text{LiNbO}_3$ .....	52
Biao Wang, Nao-Aki Noda, Yoshikazu Sano, Xi Liu, Yuto Inui, Bei-fen Siew. Nut Height Effect on Anti-loosening Performance of Pitch Difference Bolt Nut Connections.....	53
O. V. Bocharova, I. E. Andjiovich, A. V. Sedov, V. V. Kalinchuk. An Effective Method for Recognizing Heterogeneities in Composite Materials.....	53
I.V. Bogachev. Modeling of Biological Tissues Taking into Account the Residual Stress .....	54
I.V. Bogachev. On the Identification of the Characteristics of Functional-Gradient Plates in the Framework of the Kirchhoff and Timoshenko Models .....	55
I.V. Bogachev, A.O. Vatulyan. On the Modeling of Delamination of an Inhomogeneous Polymer Coating of a Strip .....	56
A. S. Bogatin, E. N. Sidorenko, S. P. Shpanko, K. G. Abdulvakhidov. Relaxation Processes in the Organic Anti-Corrosion Films.....	57
N.A. Boldyrev, E.I. Sitalo. Maxwell-Wagner Relaxation in the Layered $(1-x)\text{NaNbO}_3-x\text{Ca}_2\text{Nb}_2\text{O}_7$ Ceramics .....	58
Boris V. Bondarev. New Quantum Spaser Theory.....	60
Boris V. Bondarev. Theory of Ball Lightning.....	61
N.V. Boyev. Asymptotics of Displacements in Back-reflected Ultrasonic Waves from a 3D Defect Located in an Elastic Material .....	62
V.A. Brazhnikov, D. D. Fugarov, O. A. Purchina, N.V. Rasteryaev. Power Processing Equipment of Oil Refineries.....	63
B. Witjaksana, S. Astutik, W. Oetomo, Romadhon. Failure Risk Analysis of Centralized Domestic Wastewater Management System in Buleleng District (With Failure Mode Effect Analysis Method) .....	64
I.Zh. Bunin, I.A. Khabarova. Effect of High-Voltage Nanosecond Pulses Treatment on the Surface Properties and Floatability of Pentlandite and Pyrrhotite.....	65
N.I. Buravchuk, O.V. Guryanova, E. P. Putri. Influence of Technogenic Raw Materials on the Physical and Mechanical Properties of Ceramic Products.....	66
N.I. Buravchuk, O.V. Guryanova. E. P. Putri. Technological Aspects of Obtaining Disperse-grained Composites Based on Solid Combustible Carbon-Containing Waste .....	69
Chang-Wook Park, Sung-Won Yoon. Mechanical Properties of Large-Scale Composite Structures according to Process Conditions.....	73
M.I. Chebakov, S.A. Danilchenko. Modeling the Contact Interaction of Spherical Hinge Joint in the Presence of Wear .....	73

M.I. Chebakov, A.A. Poddubny, E.M. Kolosova. Contact Problems on the Interaction of Indenter and Poroelastic Base .....	74
N. E. Chernenko, S.V. Balakirev, M. M. Eremenko, M. S. Solodovnik. Effect of the Arsenic Molecular Form on the Indium Nanodroplet Crystallization .....	75
A.V. Cherpakov, A.N. Soloviev, I.A. Parinov, V.A. Chebanenko, E. V. Rozhkov, S.-H. Chang, C.-C. Yang. Modeling a Rotary Drive of a Piezoelectric Generator.....	76
A.V. Cherpakov, A.N. Soloviev, I.A. Parinov, O.V. Shilyaeva, S.-H. Chang, C.-F. Lin. Application of Neural Network Technologies for Identifying Defect Sizes in a Half-plane.....	77
A.V. Cherpakov, A.N. Soloviev, I.A. Parinov, O.V. Shilyaeva, S.-H. Chang, C.-F. Lin. Using Neural Networks to Analyze the Shape of a Defect in a Layered Structure during Its Modeling .....	78
C. C. Yen, W.C. Lin, Z. H. Wang, G. F. Chen, D. Y. Chou, D. M. Lin, S. Y. Lin, M. H. Zhan, T. F. Lee. Correlation between Calcaneal Quantitative Ultrasound and Dual-energy X-ray Absorptiometry Bone Density.....	79
Chih Chin Yang, Hung Yeh Lin. Volt-ampere Type Relative Humidity Sensing Devices using Indium-Based Sensing Film on a Porous Silicon Substrate.....	80
C. C. Yang, Y. L. Hsiao, Z. H. Wu, Y. H. Hsu, I. A. Parinov, S. H. Chang. Respiration Sensing Devices Based on Indium Nitride p-n Heterostructure on Silicon Porous Substrate ...	81
C. C. Yang, Z. H. Wu, Y. L. Hsiao, Y. T. Li, S. H. Chang, I. A. Parinov. Capacitance Type p-InN/n-Si Heterostructure Sensing Devices on Silicon Unpolished Substrate.....	83
C. F. Lin, C. C. Chuang, S. H. Chang, I. A. Parinov, S. Shevtsov. Space Time Block Code Based FBMC Advanced Underwater Image Communication Technology.....	85
C. K. Yeh, C. Lin, H. C. Shen, Z. W. Kuo, W. Lukkhasorn. Using Activated Quantum Reagent to Transform the Quality of Poultry and Animal Manure and its Recycling .....	86
C. Lin, N. K. Cheruiyot, W. Lukkhasorn, L. T. Hieu. Using a Novel Graphene-Ceramic Composite Material in the Adsorption of Aromatic Volatile Organic Compounds .....	87
Daniil O. Nepryakhin, Michael Yu. Zhukov. Numerical Study of the Plane Free Liquid Surface Oscillations in an Elliptical Paraboloid .....	88
V.G. Dneprovski, I.A. Parinov. Surface Acoustic Wave Sensors of Breath.....	89
Dong-Ho Yang, Sung-Youl Bae. Design and Evaluation of Automated Preform Equipment for Ship Manufacturing.....	90
Dong-Hun Yang, Soo-Jeong Park, Yun-Hae Kim. A Study on Lightweight Design of Ultra High-Pressure Composite Pressure Vessel for Hydrogen Gas.....	90
Yu. E. Drobotov. Method for Computing the General Inverse of Rectangular Matrix and its Applications in Engineering Problems.....	91
Yu. E. Drobotov, A. V. Cherpakov. On Mathematical Processing of Test Results of Structural Vibrations with Inhomogeneity.....	92
Yu. E. Drobotov, B. G. Vakulov. The Riesz Potential Type Operator with Power-Logarithmic Kernel in Mathematical Modelling.....	92
Yu. E. Drobotov, G. A. Zhuravlev. Method of Local Approximations for Calculating Stress Concentration in Elastic Bodies with Projections of Complex Shapes.....	93
S. I. Dudkina, L. A. Shilkina, L. A. Reznichenko, I. A. Verbenko. Phase Patterns and Electrophysical Macro-responses in Solid Solutions of the Multicomponent Systems Based on Lead Zirconate Titanate.....	94
D.D. Dukhan, S.V. Balakirev, M.M. Eremenko, N.E. Chernenko, M.S. Solodovnik.	

Investigation of Influence of Nonstationary Supersaturated Environment on Characteristics of In/GaAs Nanostructures Formed by Droplet Epitaxy .....	95
Duy-Hieu Nguyen, Chitsan Lin. Investigating the Effectiveness of Shore-line Power Using AERMOD Model under the Aspect of Ship Emission .....	96
Edi Santoso, Ichlas Wahid, Maula Nafi. Effect of Voltage and Current to MIG Welding with 1 mm Filler Diameter to The Mechanical Properties of Welded Joints of Commercial Steel....	97
V.V. Efremov, M.N. Palatnikov, O.B. Shcherbina. High Dielectric Constant at Room Temperature in a Family of Solid Solutions $Li_xNa_{1-x}Ta_yNb_{1-y}O_3$ ( $y = 0.1 - 0.5$ ) Synthesized at High Pressure.....	98
I.O. Egorochkina, I.A. Serebryanaya, E.A. Shlyakhova. Monitoring the Condition of Structures of an Existing Building Near New Construction.....	99
I.O. Egorochkina, E.A. Shlyakhova, A.V. Cherpakov, I.A. Parinov, M.-Y. Yeh, C.-D Yang. Formation of the Structure of Heavy Concrete with Increased Crack Resistance.....	100
I.O. Egorochkina, E.A. Shlyakhova, A.V. Cherpakov, I.A. Parinov, S.-H. Chang. Impact of Standard Aggregates on the Effectiveness of Chemical Additives .....	101
I.O. Egorochkina, E.A. Shlyakhova, A.V. Cherpakov, I.A. Parinov, M.-Y. Yeh, C.-D Yang. Influence of Chemical, Mineralogical and Textural Features of Aggregates on the Processes of Structure Formation in Concrete .....	102
I.O. Egorochkina, E.A. Shlyakhova, A.V. Cherpakov, I.A. Parinov, Y.-M. Liu. Optimization of the Composition of the Repair Mixture Based on Non-shrinking and Expanding Cements.....	103
I.O. Egorochkina, E.A. Shlyakhova, A.V. Cherpakov, I.A. Parinov, C.-Y. Jenny Lee, C.-C. Yang. Statistical Methods for Predicting and Preventing the Appearance of a Defect in Efflorescence on the Surface of Brickwork.....	104
Endija Namsone, Denis Ermakov. Characterisation of Woven Composite Material Properties by Using an Inverse Technique Based on Vibration Tests .....	105
M. M. Eremenko, S. V. Balakirev, N.E. Chernenko, M. S. Solodovnik, O. A. Ageev. Study of the Growth of GaAs on Silicon with Amorphized Areas .....	106
Erni Puspanantasari Putri, Sukon Aduldaecha. A Case Study: Application of Business Process Re-engineering in Company .....	107
Erni Puspanantasari Putri, Sukon Aduldaecha. Case Study of the Keys to Success of Supply Chain Management in Company.....	108
Erni Puspanantasari Putri, Victoria Aurellia Sri Paramita Putri. A Case Study of Creative Industry Development Strategy in Sidoarjo Regency, East Java Province, Indonesia .....	109
Erni Puspanantasari Putri, Victoria Aurellia Sri Paramita Putri. Development Strategy of Creative Economy and Creative Industry in Surabaya, Indonesia.....	110
Erni Puspanantasari Putri, Victoria Aurellia Sri Paramita Putri. The Survival Strategy of Indonesia MSMEs Development in Facing the Economic Crisis due to the COVID-19 Outbreak .....	110
Evgeny Barkanov, Pavel Akishin, Andris Chate. Non-direct Optimisation of Coupled Thermo-chemical Problem in Pultrusion of Thin-walled Angle Profile.....	111
O.A. Ezhova, I.E. Lysenko, D.V. Naumenko. Research of the Developed Design of Micromechanical Linear Acceleration Sensor in Systems of Stabilization and Registration of the Objects Position.....	112

S.I. Fomenko, M.V. Golub, A.D. Khanazaryan, A.N. Shpak. Elastic Wave Propagation in Layered Periodic Dielectric Elastomers.....	113
D. D. Fugarov, O. A. Purchina, A.Bondar, D.A. Onyshko. Catalytic Alkylation of Isobutane with Olefins as Automation Object.....	114
D. D. Fugarov, O. A. Purchina, N.I. Kazimirov, D.A. Onyshko. Monitoring of Normal Operating Modes of Operative DC Systems.....	114
D. D. Fugarov, O. A. Purchina, D.E. Kondratyev, D.A. Onyshko. Mathematical Modeling of Long Pipeline.....	115
D. D. Fugarov, O. A. Purchina, V.V. Terehov, D.A. Onyshko. Centralized and Uninterrupted Power Supply for Oil and Gas Enterprises.....	116
D. D. Fugarov, O. A. Purchina, A.D. Trofimenko, D.A. Onyshko. Measurement of Large Amplitude Currents during Diagnostics of AC Circuit Switches.....	117
D. D. Fugarov, O. A. Purchina, D.V. Vovchenko, D.A. Onyshko. Building Base Blocks of Imitation Simulation.....	117
G.A. Geguzina. Solid Solutions of Binary Perovskites and Their Ferroelectric and Magnetic Phase Transitions Temperature Differences.....	118
E.V. Glazunova, I.A. Verbenko, A.A. Nikulina. The Effect of Strontium Pyroniobate on Phase Formation and Properties of the KNN System.....	120
E.V. Glushkov, N.V. Glushkova, O.A. Miakisheva, S.I. Fomenko, A.M. Tatarinov. Analysis of the Influence of Cortical Bone Thickness, Soft Tissue, and Porosity on Ultrasonic Guided Waves for Osteoporosis Diagnostics.....	121
Ie.Ie. Gorbenko, E.P. Troitskaya, E.A. Pilipenko, I.A. Verbenko, E.V. Glazunova. Influences of the Three-Body Interaction and the Deformation of Electron Shells of Atoms on Phonons Energy of Compressed Rare-Gas Crystals.....	122
A.V. Guryanov, M.V. Il'ina, O.I. Osotova, O.I. Il'in. Establishing Conditions for the Manifestation of the Piezoelectric Response of Carbon Nanotubes.....	123
Gyanendra Pratap Singh, Mukesh Kumar Roy. Influence of Thermal Calcination on Dielectric and Impedance Properties of ZnO Nanostructures.....	124
Hanie Teki Tjendani, Nick Yanie, Dwi Yuli Rakhmawati, Tisno Subroto. Evaluation of Factors Affecting Costs Using Multiple Linear Regression Method on the Implementation of Rehabilitation and Renovation of School Infrastructure Facilities in Pasuruan District .....	125
Hanie Teki Tjendani, Wateno Oetomo, Risma Marleno. A System Dynamics Approach to Risk Mitigation in Performance-based Contract Projects .....	126
Hsueh Chen Shen, Chitsan Lin, Chin Ko Yeh, Wisanukorn Lukkhasorn, Suei Chamg Wu. A Study on Nitrogen Oxides from Coal and Waste Tires in Different Proportion of Mixed Burning.....	126
I Made Kastiawan, I Nyoman Sutantra, Sutikno. Characteristics of Bottom Ash as Reinforcement of the Polypropylene Composite .....	127
Ichlas Wahid, Maula Nafi. Mechanical Properties and Microstructure Analysis of Heated Aluminum-2042 with Variation of Aging Temperature and Aging Time.....	128
A.A. Ipatov, S.Yu. Litvinchuk. Numerical Analysis of the Dynamic Behaviour of Poroviscoelastic Solids Using Boundary Element Approach.....	128
A. N. Isaeva, V. Yu. Topolov. Figures of Merit of Novel Piezo-active Lead-free Composites..	129
T. H. Jang, M. K. Bae, J. G. Choi, T.G. Kim. Multi-layer Thin	

Film Deposition for High-performance X-ray Field Emission Characteristics.....	131
Jeong-Hyo Hong, Tianyu yu, Soo-Jeong Park, Yun-Hae Kim. Experimental Study on Mechanical Properties of Sandwich Composites with Integrating Auxetic-core Structure Using FDM 3D Printer.....	132
Jeong Wan Kim, Mun Ki Bae, Tae Gyu Kim. MgF <sub>2</sub> Nanoparticle coating to Improve the Efficiency of Light Hazard in DSLR Cameras.....	132
Jin-Cheol Ha, Soo-Jeong Park, Yun-Hae Kim. Corrosion Mechanism and Degradation Behaviour of Basalt Fiber Reinforced Composites in Sulfuric Acid Solution.....	133
I.L. Jityaev, A.M. Svetlichnyi, A.S. Kolomiitsev, G.D. Gavrishchakin, A.I. Kovalets. Planar Multitip Field Emission Nanostructures.....	134
I.L. Jityaev, A.M. Svetlichnyi, A.S. Kolomiitsev, A.I. Kovalets, G.D. Gavrishchakin. Matrix Blade Field Emission Cathodes.....	135
S.V. Kara-Murza, K.M. Zhidel, N.V. Korchikova, Yu.V. Tekhtev, A.V. Pavlenko, A.G. Silcheva. Optical Properties of Sr <sub>0.61</sub> Ba <sub>0.39</sub> Nb <sub>2</sub> O <sub>6</sub> (SBN-61) Films Depending on Their Thickness.....	136
G.Ya. Karapetyan, V.E. Kaydashev, M.E. Kutepov, T.A. Minasyan, V.A. Kalinin, V.O. Kislitsyn, E.M. Kaidashev. Investigation of the Dependence of the Velocity of SAW Propagation under FeNi Films, Located on Lithium Niobate Substrates, on Magnetic Field.....	137
G.Ya. Karapetyan, M.E. Kutepov, V.A. Kalinin, V.O. Kislitsyn, E.M. Kaidashev. SAW Current Sensor with FeNi Film.....	138
R. Kawano, B. Wang, N.A. Noda, Y. Sano, X. Liu, Y. Inui, B. Siew. Effect of Pitch Difference and Root Radius on Anti-loosening Performance of Bolt Nut Connections.....	139
M.I. Kazmenko, D. D. Fugarov, O. A. Purchina, N.V. Rasteryaev. Synthetic Ethyl Alcohol Synthesis Technology.....	140
S. V. Khasbulatov, A. V. Nagaenko, L. A. Shilkina, E. V. Glazunova, S. I. Dudkina, I. A. Verbenko, L. A. Reznichenko, N.A. Boldyrev. Features of the BST/Ln-Ceramic Microstructure.....	141
S. V. Khasbulatov, L. A. Shilkina, S. I. Dudkina, I. A. Verbenko, L. A. Reznichenko, N.A. Boldyrev. On the Dependence of the Curie Temperature of Solid Solutions of the BST/REE System on the Chemical Composition and Position on the Phase Diagram.....	142
J.E. Kim, M. K. Song, M. S. Han, J.D. Kim. A Study on the Removal of Paint and Oxide Layer on the Steel Surface by Laser Beam Scanning Method.....	143
J.S. Kim, J.D. Kim. Comparison of Weldability of Laser and Laser-Arc Hybrid Welding for Ship Manufacturing using Environmentally Friendly Aluminum Alloys.....	144
I.A. Kirichenko, I.B. Starchenko. Prospects for the Use of Hydroacoustic Tools Based on Nonlinear Interaction of Acoustic Waves in Underwater Archaeology.....	144
Kirtan K. Sahu, Vijay K. Gupta. Buckling Load Analysis of Single Stage and Multistage Hydraulic Cylinder by Successive Approximation Method.....	145
V.S. Klimin, A.A. Rezvan, T.A. Zubova. Nanoscale Carbon Cells with Gas and Gas Mixture Detection.....	148
Yu.V. Klunnikova, M.V. Anikeev. Molecular Dynamic Simulations of Sapphire Deformation Behavior.....	149

Yu.V. Klunnikova, S.P. Malyukov, A.V. Filimonov. Influence of Sapphire Substrates Defective Layer on Microelectronic Devices .....	150
A.A. Kompaniets, D. D. Fugarov, O. A. Purchina, N.V. Rasteryaev. Operation Modes of Power Protection Facilities.....	151
A.S. Kornievsky, A.V. Nasedkin. Computer Investigation of Nanoporous Elastic Composites with Various Sizes and Structure of Pores.....	152
S.V. Korolenko, D. D. Fugarov, O. A. Purchina, N.V. Rasteryaev. Analysis of Elemental Sulphur Production Flow Charts .....	153
M. I. Kovalenko, S. I. Dudkina, L. A. Reznichenko. Crack Formation and Self-destruction Effects in Ceramics Based on the Alkali Metal Niobates .....	154
T.V. Krasnyakova, D.V. Nikitenko, I.A. Verbenko, S.A. Mitchenko. The Effect of the Preparation Conditions on the Catalytic Activity of $K_2PdCl_4$ in the Reaction of Methyl Alcohol with Acetylene .....	155
D.A. Kravchuk, I.B. Starchenko. Reconstruction of the Optical Acoustic Signal for Visualization of Biological Tissues.....	156
S.P. Kubrin, S.I. Raevskaya, J. Zhuang, Z. Tang, E.P. Shihova, S.A. Shlyahova, V.V. Titov, I.P. Raevski, M.A. Malitskaya. Studies of Magnetic and Local States of $Fe^{3+}$ Ions in $(1-x)Bi_{10.9}Dy_{0.1}FeO_3-xPbTiO_3$ Solid Solution.....	157
S. P. Kubrin, M. Yu. Silin, I. P. Raevski, D. A. Sarychev, V. V. Titov, V. A. Ershin, S. I. Raevskaya, M. A. Malitskaya. Mossbauer Studies of Compositional Ordering in Ternary Perovskite $Pb_2CoWO_6$ and $Pb_2CoWO_6-PbTiO_3$ Solid Solution.....	158
O.V. Kudryakov, V.N. Varavka, I.Yu. Zabayaka, A.V. Sidashov, E.S. Novikov. Synthesis, Electronic Structure, Microstructure and Properties of Vacuum Ion-Plasma Coatings Based on Carbon.....	159
L.G. Kurakin, A.V. Kurdoglyan. Semi-Invariant Form of Equilibrium Stability Criteria for Systems with Two Cosymmetries.....	160
L.G. Kurakin, I.A. Lysenko, S.A. Lysenko. On the Stability of a Regular Vortex Polygon in a Two-fluid Plasma.....	161
L.G. Kurakin, N. V. Shilova. Analysis of the Stability of a Regular System of Vortex Charges outside the Circular Region in the Case of an Arbitrary Circulation around the Boundary.....	162
M.E. Kutepov, T.A. Minasyan, G.Ya. Karapetyan, V.E. Kaydashev, I.V. Lisnevskaya, K.G. Abdulvakhidov, A.A. Kozmin, E.M. Kaidashev. Optimizing $VO_2$ Film Properties for Use in SAW Devices .....	163
Kyo-Moon Lee, Soo-Jeong Park, Seong-Jae Park, Yu Tianyu, Yun-Hae Kim. Quantifying of the Internal Defects Content in CF-PEKK through Water Absorption Behavior.....	164
Laksono Djoko Nugroho, Tiwi Sri Rejeki, Hudhiyantoro, Budi Santoso. Optimization and Management Strategy Resources for Water Fulfillment of Community water in Mojokerto District, East Java.....	164
Levan Ichkitidze, Alexander Markov, Mikhail Savelev, Alexander Gerasimenko, Pavel Vasilevsky, Eugenia Davydova, Elizaveta Smirnova, Dmitry Telyshev, Sergei Selishchev. Ordering of Carbon Nanotubes in Aqueous Dispersion of Nanomaterials under the Influence of Femtosecond Laser Radiation.....	165
Levan Ichkitidze, Mikhail Belodedov, Sergei Selishchev, Dmitry Telyshev.	

Influence of Fractality of Normal Clusters on the Resistivity of a Ceramic Superconductor.....	166
G.Yu. Levi, I.B. Mikhailova. The Effect of Heat-conducting Coating on the Propagation of the Waves Excited by Heat in the Thermoelastic Bodies .....	168
I. V. Lisnevskaya, I. A. Aleksandrova. Interfacial Reactions and Functional Properties of Magnetolectric Composites of Lead-free Piezoelectrics and Yttrium Iron Garnet.....	169
Luyen The-Thanh, Mac Thi-Bich, Banh Tien-Long, Nguyen Duc-Toan. A Comparison Study by Simulation/Experiment to Verify the Effect of Predicted Forming Limit Diagram Based on Graphical Method at Elevated Temperature for SPCC Sheet Material.....	170
A. V. Lyasnikova, I. P. Melnikova, A. L. Nikolaev. Improving the Functional Characteristics of Biocompatible Coatings of Bone Implants due to Modification of the Initial Powders .....	170
A. V. Lyasnikova, V.M. Taran, M.V. Dodonov. Probability-network Modeling of Nanocomposite Porous Coatings Structure.....	171
I.E. Lysenko, D.V. Naumenko, O.A. Ezhova. Pantograph Lever Structure MEMS Accelerometer with High Aspect Ratio Torsion Suspension.....	172
I.V. Malyshev, N.V. Parshina. The Method of Definition the Electrophysical Parameters of Spiral Inclusions in Chiral Metamaterials.....	173
I. S. Malysheva. Asymptotics of Eigenvalues of Large Symmetric Toeplitz Matrices with Smooth Simple-loop Symbols.....	174
I.P. Markov, L.A. Igumnov, E.V. Boev. Dynamic Boundary Element Analysis of Three-dimensional Multiply Connected Linear Piezoelectric Solids.....	174
I.P. Markov, A.N. Petrov, A.V. Boev. An Algorithm for Iterative Selection of Complex Frequencies Applied to a One-dimensional Dynamic Poroelastic Problem .....	175
Maula Nafi, Harjo Seputro. Microstructure and Tensile Stress Analysis on T6 Heat Treated Aluminum-Bottom Ash Coal Composite made by Squeeze Casting.....	176
Yu. F. Migal. DFT Study of Strengths of TiAlN Coating on Iron Surface.....	176
Min-Gyu Jeon, Jeong-Woong Hong, Deog-Hee Doh, Yoshihiro Deguchi. Temperature Measurement of Turbulent Flame Using CT-TDLAS (Computed Tomography-Tunable Diode Laser Absorption Spectroscopy).....	178
Min Yen Yeh, Sheng Min Huang, Shun-Hsyung Chang, Jenny Chih-Yu Lee, Chih-Feng Yen, Chyi-Da Yang. Preparation of Zinc Silicate Doped with Manganese Phosphor by Hydrothermal Method.....	179
I.P. Miroshnichenko, I.A. Parinov. On Extension of Functional Possibilities of the Optical Interference Meter of the Surface Displacements of Control Objects.....	180
I.P. Miroshnichenko, V.P. Sizov. On the Features of Spatial Temporal Distribution of Displacements and Stresses in Layered Constructional Materials at Diagnostics of Their State by Acoustic Active Non-destructive Testing Methods .....	181
E.A. Moguchikh, K.O. Paperzh, A.A. Alekseenko, A.A. Palchikov. The Influence of the Structure on the Characteristics of Pt/C and Pt/C-N Electrocatalysts .....	182
M.O. Moysa, A.V. Nagaenko, K.P. Andryushin, L.A. Reznichenko. Features of the Microstructure of Ferroactive Ceramics of the KNN-Cd <sub>0.5</sub> NbO <sub>3</sub> System .....	183
Muhyin, Dwi Yuli Rakhmawati, Fahreza Rukmana Witjaksono. Effect of Variation in the Composition of the Basic Ingredients and Briquette Pressure on Calorific Value and Temperature value of the Briquette Mixture of Rice Husk and Coconut Shell.....	184
A. N. Nakagaito, Y. Katsumoto, H. Takagi. Fabrication of Strong Macromolecules from Plant Fiber Bundles.....	185

A.V. Nasedkin, M.E. Nassar. Regarding Unexpected Properties of Porous Piezocomposites with Different Maximal Electrical and Mechanical Properties on the Pore Boundary.....	186
Natalia V. Petrovskaya. Convective Motions in a Rotating Spheroid at Vanishing Dissipation .....	187
A.V. Nazarenko, A.V. Pavlenko, Y.I. Yurasov. Studying of Dielectric Spectra of YMNO <sub>3</sub> -based Solid Solutions with the Use of Complex Conductivity.....	188
R.D. Nedin. On Modelling and Identification of Prestress State in Inhomogeneous Structures Including Coatings and Delamination Zones.....	190
I.V. Nemchenko, D. D. Fugarov, O. A. Purchina, D.A. Onyshko. Automated System for Monitoring Electrical Parameters of Process Equipment for Oil Refineries .....	191
S.A. Nesterov. On the Problem of Identifying Variable Thermomechanical Characteristics of a Cylinder .....	192
Nevelskaya A.K., Belenov S.V. Investigation of the Activity of PtCuAu/C Electrocatalysts in Alcohols Electrooxidation Reaction in Alkaline Media .....	193
Nguyen Phu Thuong Luu. A New Design of Protection Device to Improve Car-to-Truck Rear Under-ride .....	194
Nguyen Phu Thuong Luu. An Optimal Design Truck Cabin by Using Finite Element Model Simulation.....	194
Nguyen Van Dung, Vu Thi Lan Anh. Natural Radioactivity of <sup>226</sup> Ra, <sup>232</sup> Th and <sup>40</sup> K in Domestic Well Water and its Impact on the Health of People in Hanoi Area (Extension), Vietnam.....	195
Nguyen Van Tho, A.N. Soloviev, M.A. Tamarkin, I.A. Panfilov. Theoretical and Experimental Analysis of Metal Removal from Workpiece Surface during Centrifugal Rotation Processing .....	196
A L Nikolaev, M. A. Kazmina, N. V. Lyanguzov, K. G. Abdulvakhidov, E. M. Kaidashev, S.M. Aizikovich. Design of Construction Elements for Chemisensors Based on Zinc Oxide Nanorods.....	197
N. A. Noda, D. Chen, R. Takaki, Y. Sano, Y. Takase. Intensity of Singular Stress Field in Pull-out Test and Micro-bond Test.....	198
D.A. Onyshko, A.V. Gaydychik, D. D. Fugarov, O. A. Purchina. Technical Support of Low-power Multi-cell Wireless Networks.....	199
D.A. Onyshko, A.A. Ponomarev, D. D. Fugarov, O. A. Purchina. Automation of Monitoring of Technological Processes in the Oil and Gas Industry.....	200
D.A. Onyshko, D.A. Saveliev, D. D. Fugarov, O. A. Purchina. Infocommunication Technologies for Monitoring Systems of Technological Parameters of Remote Objects.....	202
D.A. Onyshko, P.Yu. Zhmaylov, D.D. Fugarov, O.A. Purchina. Modern Technologies for Building a Wireless Sensor Network.....	204
Pankaj Koinkar, Siddhant Dhongade, Akihiro Furube. Controlling the Optoelectrical Properties of Two-dimensional Nanostructures Prepared by Laser Ablation in Liquid.....	205
K.O. Paperzh, A.A. Alekseenko, A.Y. Nikulin. Highly Stable Pt/C Catalysts with Different Mass Fraction of Platinum .....	206
A.A. Pavelko, A.V. Pavlenko, A.A. Martynenko, L.A. Reznichenko. Effect of Lithium Carbonate Modification on the Ferroelectric Phase Transition Diffusion in Lead Ferroniobate Ceramics.....	207
A.V. Pavlenko. Preparation and Structure of Thin PbFe <sub>0.5</sub> Nb <sub>0.5</sub> O <sub>3</sub> Films.....	208



Pavlenko A.V., Ter-Oganessian N.V. Piezoelectric and Dielectric Properties of the $\text{NaNbO}_3(001)/\text{SrRuO}_3(001)/\text{MgO}(001)$ Heterostructure.....	209
A.S. Pavlets, A.A. Alekseenko, N.Yu. Tabachkova, V.E. Guterman. Influence of Acid Treatment on the Functional Characteristics of PtCu/C Electrocatalysts.....	210
D.V. Petrenko, D. D. Fugarov, O. A. Purchina, D.A. Onyshko. Analysis of Process Preparation of Process Polymer Mixtures.....	211
A.N. Petrov, A.A. Belov, M.V. Grigoryev. Numerical Study on Screening of Surface Waves Using a Rectangular Open Trench.....	212
V.V. Petrov, V.V. Polyakov, Yu.N. Varzarev, V.V. Bespoludin, E.M. Bayan. The Investigation of the Influence of Rapid Thermal Annealing Temperature on the Formation of Cobalt Oxide Films.....	213
T.A. Petrukhina, N.M. Polyakova. Turbulent Blood Flow in a Cylindrical Vessel with an Irregular Walls Profile.....	214
A.E. Pianov, D. D. Fugarov, O. A. Purchina, N.V. Rasteryaev. Waste Water Treatment in Reservoir Pressure Support Systems.....	215
A. S. Piskunov, Yu. E. Drobotov. Random Vortex Method for Modelling Flow of Viscous Incompressible Fluid in Bounded Regions.....	216
O. A. Purchina, D. D. Fugarov, S.R. Cherenok, D.A. Onyshko. Applying Artificial Intelligence Techniques to Redistribute Connections between Outputs.....	217
O. A. Purchina, D. D. Fugarov, A.V. Fedorov, D.A. Onyshko. Algorithm for Redistribution of Connections between Outputs.....	217
O. A. Purchina, D. D. Fugarov, S.O. Lagoyda, D.A. Onyshko. Search Procedure Based on Modelling Collective Alternative Adaptation.....	218
O. A. Purchina, A.Y. Poluyan, D. D. Fugarov, D.A. Onyshko. Application of Hybrid Immune Algorithms to Solve Fuzzy Optimization Problems .....	219
S.I. Raevskaya, N.M. Olekhnovich, A.V. Pushkarev, Y.V. Radyush, S.P. Kubrin, V.V. Titov, E.A. Artseva, I.P. Raevski, S.I. Shevtsova, C-C. Chou, M.A. Malitskaya. Chemical Ordering, Magnetic and Ferroelectric Phase Transitions in Multiferroic $\text{BiFeO}_3 - A\text{Fe}_{1/2}\text{Sb}_{1/2}\text{O}_3$ ( $A = \text{Pb, Sr}$ ) Solid Solution Ceramics Fabricated by a High-pressure Synthesis.....	220
Rahimah Abdul Rafar, Nao-Aki Noda, Xuchen Zheng, Hiroyuki Tsurumaru, Yudai Taruya, Yoshikazu Sano. Effect of Driving Torque on Interfacial Creep Generation for Shrink-fitted Bimetallic Work Roll Considering Elastic Deformation of Shaft .....	221
A.Sh. Rakhmatulin, V.D. Popov. Microaxelerometer Based on Self-organizing Semiconductor Heterostructures.....	222
E.V. Raksha, A.A. Davydova, Yu.V. Berestneva, O.N. Oskolkova, P.V. Sukhov, V.A. Glazunova, G.K. Volkova, V.V. Gnatovskaya, O.M. Padun, M.V. Savoskin, I.A. Verbenko, Yu.I. Yurasov. Nitrate Graphite Co-intercalated with Carboxylic Acids: Structural Reorganization and Carbon Nanoparticles Obtaining.....	223
E. A. Reshetnikova, I. V. Lisnevskaya, A. I. Terekhin. Problems of Hydrothermal Synthesis of Sodium Bismuth Titanate.....	224
A.N. Reshetnyak, O.S. Reshetnyak. Use of Mathematical Methods in Hydrochemical Researches of Natural Waters.....	225
R.A. Retno Hastijanti, M. Bayu Abisatya. Eco-friendly Electric Tourism	

Boat Design for Prone Rivers. Case Study: at Kalimas River, Surabaya, Indonesia .....	226
S.V. Revina, A.S. Ryabov. Turing Instability in the Gierer-Meinhardt System.....	227
A.A. Rezvan, V.S. Klimin, I.N. Kots, O.A. Ageev. The Use of Plasma Chemical Methods for Producing Carbon Nanostructures Based on SiC.....	228
A.A. Rezvan, V.S. Klimin, J.V. Morozova. Carbon Based Nanoelectronics Device Sensitive to Gas Parameters.....	229
Ri-ichi Murakami, Wahyu Solafide. Effects of Water pH and Immersion Time on Water Absorption Behavior and Mechanical Properties of Carbon Fiber Reinforced Bio Plastic Composites.....	230
Risma Marleno, Fajar Romadhon, Gede Sarya, Hari Susanto. Cost and Quality Analysis of Using Steel Fibers in a Strong Pavement Using Laboratory Experimental Method.....	230
N.N. Rudyk, O.I. Il'in, A.V. Guryanov, M.V. Il'ina, A.A. Fedotov. The Effect of Temperature during the Growth of CNTs on the Structure of Ni/TiN/Si .....	231
E.V. Sadyrin, M.V. Swain, A.L. Nikolaev, A.S. Vasiliev, D.V. Yogina, N.V. Lyanguzov, S.Yu. Maksyukov, S.M. Aizikovich. Molecular Composition of the White Spot Lesion Detected on the Human Molar.....	232
Sajiyo, Faiz Muhammad Azhari, Haris Muhammadun, Priyoto. Analysis of Resistance Factor and Application Strategy of Work Safety and Health Applications Construction Project Workers in Tulungagung Regency.....	233
F.D. Savriddinov, D. D. Fugarov, O. A. Purchina, D.A. Onyshko. Monomethylamine Isolation Process.....	234
I.V. Semenchatenko, A.A. Matrosov. Topological Optimization of the Support of the Control Panel of a Numerically Controlled Machine .....	235
Seong-Jae Park, Yu Tianyu, Kyo-Moon Lee, Soo-Jeong Park, Yun-Hae Kim. Effect of Heating Rate on Mechanical Properties of Polymer Matrix of Carbon/PEKK Composites in Thermoforming Process.....	236
I.A. Serebryanaya, A.A. Matrosov, D.A. Nizhnik, N.A. Poryadina. Mathematical Simulation Testing of Some Building Materials.....	236
Sergei M. Aizikovich, Andrey S. Vasiliev, Boris I. Mitrin, Evgeniy V. Sadyrin. Simplified Analytical Expressions for Indentation Stiffness of Coated Solids and its Application for Experimental Analysis .....	237
O.B. Shcherbina, G.B. Kunshina, V.V. Efremov. Structure, Mechanical and Electrophysical Characteristics of Li-ion Conducting Ceramics $\text{Li}_{1.3}\text{Al}_{0.3}\text{Ti}_{1.7}(\text{PO}_4)_3$ .....	238
O.B. Shcherbina, S.M. Masloboeva, M.N. Palatnikov. Mixed Yttrium Tantalum-Niobates .....	239
L.A. Shilkina, S.V. Khasbulatov, L.A. Reznichenko. Solubility Features of Rare Earth Elements in BST-ceramics. Part I: Large-sized Ln .....	240
L.A. Shilkina, S.V. Khasbulatov, L.A. Reznichenko. Solubility Features of Rare Earth Elements in BST-ceramics. Part II: Small-sized Ln .....	241
L.A. Shilkina, S.V. Khasbulatov, L.A. Reznichenko, S.I. Dudkina. Experimental Confirmation of Spinodal Decomposition in the $\text{Ba}_{1-x}\text{Sr}_x\text{TiO}_3$ .....	243
O.V. Shilyaeva, A.V. Cherpakov, R.I. Shakhanov, C.-Y. Jenny Lee, Y.-M. Liu. Analysis of Material Properties Using Machine Learning.....	244
E.A. Shlyakhova, I.A. Serebryanaya, I.O. Egorochkina, A.V. Cherpakov. Assessment of Crack Resistance of Bridge Reinforced Concrete Piles.....	245
V.A. Shuvaeva, I.P. Raevski, A.M. Glazer, S.I. Raevskaya, G.A. Simachkova,	

V.V. Titov, M.A. Malitskaya. Optical and EXAFS Studies of $\text{NaNbO}_3 - \text{NaTaO}_3$ Solid Solution Crystals.....	246
E.N. Sidorenko, S.P. Shpanko, M.A. Bunin. Influence of Organic Coatings Formation Conditions on Their Morphology and Protective Properties .....	247
E.N. Sidorenko, V.G. Smotrakov, M.A. Marakhovskiy. Microwave Energy Absorption and Radiation Spectra of Lead Ferrowolframate Ceramics .....	248
N.V. Sidorov, N.A. Teplyakova, M.V. Smirnov, M.N. Palatnikov, V.B. Pikylev. Photoluminescence of Nominally Pure Lithium Niobate Crystals Grown by Different Technologies .....	249
N.V. Sidorov, N.A. Teplyakova, R.A. Titov, M.N. Palatnikov, I.V. Biryukova. Structural Particularities of $\text{LiNbO}_3:\text{B}$ (0.55, 0.69, 0.83 mol. % $\text{B}_2\text{O}_3$ ) with R (Li/Nb) Close to Stoichiometric .....	250
E.I. Sitalo, N.A. Boldyrev. Piezoelectric Characteristics of Ternary Solid Solutions $(1 - x - y)\text{BiFeO}_3 - x\text{PbFe}_{0.5}\text{Nb}_{0.5}\text{O}_3 - y\text{PbTiO}_3$ .....	251
E.I. Sitalo, V.G. Smotrakov. Microstructure, Ferroelectric and Piezoelectric Properties of Textured Bismuth-containing Ceramics .....	252
A.N. Soloviev, Do Thanh Binh, V.A. Chebanenko, A.V. Derkun. Determination of the Physical Constants of a Piezomagnetolectric Layered Composite .....	253
A.N. Soloviev, Do Thanh Binh, V.A. Chebanenko, E.V. Kirillova. Applied Theory of Bending Vibrations of a Bimorph with Two Active Composite Piezomagnetolectric Layers... 254	
A.N. Soloviev, Do Thanh Binh, V.A. Chebanenko, P.A. Oganessian. Study of the Efficiency of Using Porous Piezoceramics in a Stack-type Piezoelectric Generator .....	255
A.N. Soloviev, A.A. Matrosov, I.A. Panfilov, O.N. Lesnyak, D.A. Nizhnik. The Simplest Mathematical Models of Wheat Ear Dynamics.....	256
A.N. Soloviev, A.V. Nasedkin, Do Thanh Binh, V.A. Chebanenko, P.A. Oganessian. The Use of Porous Piezoelectric Ceramics in a Piezoelectric Composite of 1-3 Connectivity .....	257
A.N. Soloviev, A.S. Vasiliev, I.A. Panfilov, A.S. Lednov, E.V. Sadyrin. Finite-element Modeling of Soft Biological Tissues Indentation.....	257
M.K. Song, J.E. Kim, J.H. Jung, D.S. Shin, J. Suh, S.J. Lee, J.D. Kim. Effect of Focal Position on Cut Surface Quality in Laser Cutting of 50 mm Thick Stainless Steel.....	258
Soo-Jeong Park, Yun-Hae Kim. Reinforcing Effects of CNT Nanofiller for Enhancing the Interfacial Bonding Strength of Filament Wound FRP Composites .....	259
S.A. Stel'makh, E.M. Shcherban', I.A. Parinov, A.V. Cherpakov, J.-P. Wang. Study of the Influence of the Configuration of a Rotary Mixer on the Quality Indicators of the Mixture .....	260
D.V. Stryukov, A.V. Pavlenko. Structure Features of $\text{BiFeO}_3$ Thin Film on Magnesium Oxide Substrate.....	261
Sung-Won Yoon, Chang-Wook Park. Lamination Design for Composite Material Application of Ship Radar Mast .....	262
Sung-Youl Bae, Yun-Hae Kim. A Study on Structural Design and Analysis of 18ft CFRP Leisure Boat.....	263
Supardi, Elisa Sulistyorini. The Treatment of Restaurant Wastewater Containing Oil and Grease By Using Immersed Membrane Bioreactor: Design Concept, Application and its Maintenance in Indonesia.....	263

T.V. Suvorova, O.A. Belyak. Determination of the Tribological Properties of the Oil Saturated Composite under Dynamic Effects Depending on the Viscosity of the Liquid Phase.....	264
Ta-Chi Jeang, Po Cheng Ke, Hung-Yu Wang, Tsair-Fwu Lee, Chien-Liang Chiu. A Novel Universal Voltage-mode Inverse Filter for Signal Processing.....	265
R. Takaki, N. A. Noda, B. Wang, S. Wang, Y. Sano, Y. Takase. Intensity of Singular Stress Field Analysis for Scarf Joint.....	265
M. V. Talanov. Dielectric Tunability of Multicomponent Relaxor Ceramics .....	266
M.V. Talanov, A.A. Bush, K.E. Kamentsev. Dielectric Properties of Bismuth-containing Pyrochlores: A Comparative Analysis .....	267
Te-Jen Su, Feng-Chun Lee, Shih-Ming Wang. A Neural Network Analysis to the Risk Factors of Type 2 Diabetes.....	268
Te-Jen Su, Tzung-Shiarn Pan, Tsung-Ying Li. Particle Swarm Optimization Implementation on the Fault Diagnosis of Gearbox.....	269
Tejkaran Narolia, Vijay K. Gupta, I.A. Parinov. A Scissor Jack Mechanism Shear Mode Piezoelectric Energy Harvester for Wind Mill.....	269
V.A. Temnenko, D. D. Fugarov ,O. A. Purchina, D.A. Onyshko. Viscous Oil Cooling Unit...	272
Teplyakova N.A., Sidorov N.V., Palatnikov M.N., Bobreva L.A. Determination of OH-group Concentration and Point Defects in LiNbO <sub>3</sub> :Zn Crystals .....	273
Tianyu yu, Zixuan Chen, Soo-Jeong Park, Yun-Hae Kim. Experimental and Computational Studies on Stiffness Properties of Nanoclay-Incorporated FRPs with Different Nano-Structures.....	274
S.V. Titov, L.A. Shilkina, V.V. Titov, A.V. Pavlenko, I.A. Verbenko, L.A. Reznichenko. Meso- and Microstructural Anomalies in Ceramics of Ferroactive Solid Solutions .....	275
R.V. Tominov, V.I. Avilov, A.A. Avakyan, V.A. Smirnov. Resistive Switching in Nanocrystalline ZnO Films for Next Generation Memory Development .....	276
V. Yu. Topolov, A. O. Denisova. Piezoelectric Sensitivity of Modern Lead-Free 1–3-Type Composites Based on Domain-Engineered Single Crystals: Longitudinal and Hydrostatic Responses.....	277
V. Yu. Topolov, A. N. Isaeva, C. R. Bowen. Piezoelectric Sensitivity and Anisotropy in 1–3-type Composites Based on Ferroelectric Lead-free Single Crystals.....	278
H. Totori, N. A. Noda, G. Gao, Y. Sano, A. Kai. Strength of Protective Sheet in Multi-Layered Pipe Plug Used for Repair and Maintenance of Underground Piping.....	280
K. M. Ugrovatov, D. D. Fugarov, O. A. Purchina, D.A. Onyshko. Operation Modes of the Automated Gas Monitoring System in the Pipeline .....	281
Uniek Praptiningrum, W, Joko Santoso. Is the Majority Gypsum for Ceiling Choosing on Housing and Buildings in Surabaya, Indonesia?.....	282
B. G. Vakulov, Yu. E. Drobotov. The Variable Order Riesz Potential on Quasimetric Sphere in the Variable Exponent Hölder Space.....	282
B. G. Vakulov, Yu. E. Drobotov, G. S. Kostetskaya. On Smoothness of the Solution of an Integral Equation with the Spatial Riesz Potential Type Operator.....	283
Z.E. Vakulov, D.A. Khakhulin, A.A. Geldash, V.S. Klimin, O.A. Ageev. Effect of Laser Pulses Energy on the Morphology and Electrical Properties of LiNbO <sub>3</sub> Thin Films Grown by Pulsed Laser Deposition .....	284
A. V. Vasilev, E. V. Shiryayeva. Numerical Study of Impurity Transport in Thin	

Horizontal Layer with a Free Boundary for the Stationary Turbulent Fluid Flow.....	286
P.V. Vasiliev, A.V. Senichev, A.I. Novikova. Development and Application of a Convolutional Neural Network Based on the Generated Data Set in Identification Problems .....	287
A.O. Vatulyan, S.A. Nesterov. Investigation of Stress Localization at the Interface of a Coating and a Substrate Based on the Gradient Model of Thermoelasticity .....	288
A.O. Vatulyan, L.I. Parinova. On Boundary Integral Equations in the Problem of Wave Propagation in Topographic Waveguides .....	289
D.V. Velibekov, A.A. Matrosov. Numerical Calculation of Stresses Arising in the Steering Axle of the Combine .....	290
N.N. Ventsov, L.A. Podkolzina. Application of Neural Networks to the Sensors Data Processing Problem.....	291
Victoria Aurellia Sri Paramita Putri, Erni Puspanantasari Putri. A Case Study of Renewable Energy Development in Indonesia.....	292
V. Yu. Vishnevetskiy, A.V. Golda, A.A. Sliva. Stabilographic Complex Based on Virtual Games Using AR Technology for Training and Rehabilitation of Athletes .....	293
V. Yu. Vishnevetskiy, D.A. Kolesnik, I.B. Starchenko. Evaluation of Information Characteristics of Underwater Communication Channel of Divers Using Parametric Arrays.....	294
I.N. Vislousova, V.V. Kotov, O.N. Lesnyak, A.A. Matrosov, A.N. Soloviev. Correlation Method for Estimating Dynamic Loading of Drives of Active Working Tools.....	294
Vladislav Gamaleev, Masaru Hori. Generation and Diagnostics of Glow Discharges for Biomedical, Agricultural and Gas Conversion Applications.....	295
A.A. Voitash, E.V. Raksha, A.A. Davydova, Yu.V. Berestneva, A.V. Muratov, A.B. Eresko, V.A. Glazunova, M.V. Savoskin, I.A. Verbenko, Yu.I. Yurasov. Thermally Expanded Graphite: Sorption Properties and Carbon Nanoparticles Obtaining... ..	297
D.A. Volkov, D. D. Fugarov, O. A. Purchina, D.A. Onyshko. Cracker Control System Upgrade.....	298
P.Yu. Voloshchenko, Yu.P. Voloshchenko. Researching the Phenomenon of Nonlinear Diffraction in Structure of Microwave Integrated Circuits .....	299
P.Yu. Voloshchenko, Yu.P. Voloshchenko. Topology Synthesis of Integrated Circuits of the Giga and Terahertz Range by the Method of Non-autonomous Blocks .....	300
Wateno Oetomo, Bambang Andrianto, Herry Widhiarto, Dwi Yuli Rakhmawati. Monitoring and Evaluation System of Contractor's Performance Achievement in Road Preservation in Long Segment Contract in East Java.....	301
Wu Kejun, Pankaj Koinkar, Akihiro Furube. Preparation of TiO <sub>2</sub> -WS <sub>2</sub> -Au Composite Using Hydrothermal Synthesis for Photocatalytic Activity under Visible Light .....	302
Yang-Wei Hsieh, Chao-Hong Liu, I-Hsing Tsai, Zih-Xiang Su, Yu-Hao Chiu, Pei-Ju Chao, Hung-Yu Wang, Yu-Jie Huang, Tsair-Fwu Lee. Improve the Efficiency of the Patients' Specific Quality Assurance Procedure in Fields' Optimization Techniques of the Pencil Beam Linear Scanning Proton Therapy .....	303
Young Woo Kwon, Mun Ki Bae, Ri-ichi Murakami, Tae Gyu Kim. A Study on the Micro / Nano Texture Design to Improve the Friction Properties of DLC Thin Films.....	304
Yu-Hao Chiu, Jung-Ting Hsieh, Jia-Yu Chen, Chao-Hong Liu, I-Hsing Tsai, Pei-Ju Chao, Hung-Yu Wang, Shyh-An Yeh, Tsair-Fwu Lee. Using	

Supervised Learning algorithms to Predict the Risk of Thyroid Damage for Head and Neck Cancer Patients after Radiation Therapy.....	305
Yudai Taruya, Rahimah Abdul Rafar, Nao-Aki Noda, Xuchen Zheng, Hiroyuki Tsurumaru, Yoshikazu Sano. Experimental Verification for Interfacial Creep Generation for Shrink-fitted Bimetallic Work Roll by Using Miniature Rolling Mill.....	306
A.S. Yudin. Oscillations of Non-axisymmetric Shells: Parameterization and Equations.....	307
A.S. Yudin. Vibrations of the Auxetic Shell in the Liquid.....	308
Y.I. Yurasov, A.V. Nazarenko, G.K. Timoshenko. The Dielectric Spectra Study of Polyaniline.....	309
Zainun Achmad, Dikrie Alief Zaini, M. Kevin Firnanda, Ismail. Study of Fatigue Life Experiments in Bottom Ash/Aluminum Composite Getting T6 Heat Treatment and Artificial Aging.....	311
Yu.N. Zakharov, L.A. Reznichenko, I.A. Parinov, E.I. Sitalo, V.A. Chebanenko, A.A. Pavelko, L.I. Kiseleva. Pyroelectric, Bolometric and Flexoelectric Effects Excited in the Volume of Unpolarized Ferroelectric Plates by Periodic Heating of Electrode Surfaces by Modulated Thermal Radiation.....	312
K.M. Zhidel, A.V. Pavlenko. Dielectric, Piezoelectric and Magnetodielectric Characteristics of Ceramic Multiferroic Solid Solution Composition $0.5\text{BiFeO}_3 - 0.5\text{PbFe}_{1/2}\text{Nb}_{1/2}\text{O}_3$ .....	313
G.A. Zhuravlev, A. V. Cherpakov, Yu. E. Drobotov. Investigation of the Parameters of the Convergence of Two Axes of Contacting Circular Parallel Steel Cylinders in Numerical Modeling.....	314
G. A. Zhuravlev, Yu. E. Drobotov. Evaluation Criteria for the Influence of the Material Properties of Elastic Cylinders on Their Contact Approach.....	315
G. A. Zhuravlev, Yu. E. Drobotov. Method for Calculating Stress Concentration in Elastoplastic Rod with Two Symmetric Hyperbolic Recesses.....	316
J.Y. Zubarev, L.A. Reznichenko. Thermostability Ceramics Based on Sodium, Calcium, Strontium Niobates, Depending on the of Synthesis and Sintering Conditions, and Mechanical Processing.....	317
S. V. Zubkov. Crystal Structure and Dielectric Properties of Layered Perovskite-like Solid Solutions $\text{Bi}_{3-x}\text{Gd}_x\text{TiTaO}_9$ ( $x = 0, 0.1, 0.2, 0.3$ ) with High Curie Temperature.....	318
S. V. Zubkov. Crystal Structure and Dielectric Properties of Layered Perovskite-like Solid Solutions $\text{Bi}_{3-x}\text{Nd}_x\text{TiNbO}_9$ ( $x = 0, 0.2, 0.4, 0.6, 0.8, 1.0$ ).....	318
S. V. Zubkov. Crystal Structure and Ferroelectrics Properties of Mixed-layer $\text{Bi}_7\text{Ti}_{4-x}\text{Sn}_x\text{NbO}_{21}$ ( $x = 0.1, 0.2, 0.3, 0.4, 0.5$ ) Ceramics.....	319
S. V. Zubkov. Crystal Structure and Ferroelectrics Properties of Mixed-layer $\text{Bi}_{7-x}\text{Y}_x\text{TiNbO}_{21}$ ( $x = 0, 0.2, 0.4, 0.6$ ) Ceramics.....	320
S. V. Zubkov. Crystal Structure and Ferroelectrics Properties of Mixed-layer $\text{Bi}_{7-2x}\text{Nd}_{2x}\text{Ti}_4\text{NbO}_{21}$ ( $x = 0.2, 0.4, 0.6, 0.8, 1$ ) Ceramics.....	321
H. Tottori, N.A. Noda, G.Gao, R. Takaki, Y. Sano, A. Kai. Development of Multi-layered Sewer Pipe Plug-ruptured Test and Stress Analysis of Pretective Sheet.....	322
H. Tottori, N.A. Noda, G. Gao, R. Takaki, Y. Sano, A Kai. Development of Multi-layered Sewer Piper Pulug -Tensile Strength of Protective Sheet.....	322
R. Saito, N. A. Noda, Y. Sano, A. Miyagi, T. Okamura. Fatigue Strength Improvement of Roller Chain by Press Pitting between Pin and Plate.....	323

K. Saito, N. A. Noda. How to Estimate Fatigue Strength of Wood Material.....	323
N. A. Noda, R. Takaki, B. Wang, S. Wang, Y. Sano, Y. Takase. Adhesive Strength Evaluation of Scarf Joint by using Intensity of Singular Stress Field (ISSF).....	324
R. Takaki, N. A. Noda, D. Ishida, Y. Sano, Y. Suzuki. Fractographic Identification of Fracture Origin in Scarf Joint in Comparison to Butt Joint .....	324
Y. Takase, N. A. Noda. Convenient and Accurate Formulas for Stress Intensity Factor Distribution of Semi-Elliptical Surfacecrack.....	324
R. A. Rafar, N. A. Noda, H. Tsurumaru, Y. Sano, Y. Takase. Effect of Shaft's Rigidity and Motor Torque on Interfacial Slip for Shrink-fitted Bimetallic WorkRoll.....	325
K. Oda, T. Irie, T. Masuno, N. Tutsumi. Stress Intensity Factors of Interfacial Crack Associated with Different Interface Edge Singularities.....	325
N. Tutsumi, K. Oda, K. Miyaji. Effect of Hydrogen on Fracture Mechanism in Tensile Test of Carbon Steels.....	326
T. Miyazaki, D. Takasuka, K. Naka. Proportional Method for Evaluating Intensity of Singular Stress Field for Butt Joint with Adhesivespew.....	326
C. F. Yang. Mechanism of Growth ZnO Nanowires and Applications. ....	327
A. B. Deore, M. A. More, B. B. MUSMADE, S. D. Nerkar, P. G. CHAVAN, P. M. KOINKAR. Photo-Enhanced Field Emission Behavior of CDSSE Microflowers.....	327
B. B MUSMADE, Y. P. PATIL, B. M. PATRE. Robust Sliding Mode Control of Uncertain Nonlinear Systems.....	328
S. PATIL, V. BARHATE, A. MAHAJAN, H. XU, M. RASADUJJAMAN, J. ZHANG. Investigation of Electrical Properties of Peald Deposited Ti/Al/Si MIM Capacitors.....	328
S. GUPTA, A. GAIKWAD, A. MAHAJAN, L. ONGXIAO, Z. WEI. Sol-Gel Deposited Xeroge, Aerogel and Porogen Based Porous Low-K Thin Films: A Comparative Investigation.....	329
K. N. Boldyrev. Photochromic Effects in P- and B-Doped Diamond .....	329
K. N. Boldyrev, V.E. Anikeeva, O.I. Semenova, M.N. Popova. Infrared Spectra of the CH <sub>3</sub> NH <sub>3</sub> PbI <sub>3</sub> and CH <sub>3</sub> NH <sub>3</sub> PbBr <sub>3</sub> Hybrid Perovskites: Signatures of Phase Transitions and of Organic Cation Dynamics.....	330
K. I. MURAI, T. NISHIURA, R. NAGATA, T. MORIGA. Fabrication and Evaluation of Ca-doped SrTiO <sub>3</sub> Thermoelectric Materials by Molten Saltmethod.....	331
M. OISHI, T. SAKURAGI, F. FUJISHIRO, T. INA, H. YAMAGISHI, I. WATANABE, T. OHTA. Local Electronic and Atomic Structures of The mixed B-site Ions in SrFe <sub>1-x</sub> Mn <sub>x</sub> O <sub>3-δ</sub> Studied with X-RAY Absorption Spectroscopy.....	332
S. DHONGADE, P. KOINKAR, A. FURUBE , S. SUGANO. Liquid Exfoliation of Graphene Oxide Nanoribbons using Chemical Assisted Laser Ablation .....	333
-----	
Author Index.....	334
Participating Countries and Organizations.....	340
Schedule.....	346
Offline Conference Venue .....	354



2020 International Conference on “Physics and Mechanics of New Materials and Their Applications” (PHENMA 2020)  
Kitakyushu, Japan, March 26 – 29, 2021

## PREFACE

The success of the Russian-Taiwanese Symposium “Physics and Mechanics of New Materials and Their Applications”, PMNM-2012 (Russia, 2012), 2013 International Symposium “Physics and Mechanics of New Materials and Underwater Applications”, PHENMA-2013 (Taiwan, 2013), 2014 International Symposium “Physics and Mechanics of New Materials and Underwater Applications”, PHENMA-2014 (Thailand, 2014), 2015 International Conference “Physics and Mechanics of New Materials and Their Applications”, PHENMA-2015 (Russia, 2015), 2016 International Conference “Physics and Mechanics of New Materials and Their Applications”, PHENMA-2016 (Indonesia, 2016), 2017 International Conference “Physics and Mechanics of New Materials and Their Applications”, PHENMA-2017 (India, 2017), 2018 International Conference “Physics and Mechanics of New Materials and Their Applications”, PHENMA-2018 (South Korea, 2018) and 2019 International Conference “Physics and Mechanics of New Materials and Their Applications”, PHENMA-2019 (Vietnam, 2019) predefined objectives and scientific directions of the new conference PHENMA-2020, conducted by the Kyushu Institute of Technology (Japan). Due to COVID-19 pandemic, this conference has been postponed from 2 -5 October, 2020 to 26 -29 March, 2021.

A significant interest to the PHENMA-2020 has led to the great sponsor support from The Society of Materials Science, Japan Kyushu Branch; Kitakyushu Convention & Visitors Association (Japan); The Korean Society for Composite Materials, (South Korea); Ministry of Science and High Education of the Russian Federation; Russian Foundation for Basic Research; Ministry of Science and Technology of Taiwan; National Foundation for Science & Technology Development (Vietnam); Vietnam Union of Science and Technology Associations (VUSTA); Vietnam Association of Science Editing (VASE); South Scientific Center of the Russian Academy of Science; New Century Education Foundation (Taiwan); Ocean & Underwater Technology Association (Taiwan); Unity Opto Technology Co. (Taiwan); Fair Well Fishery Co. (Taiwan); Woen Jinn Harbor Engineering Co. (Taiwan); Lorom Group (Taiwan); Longwell Co. (Taiwan); Korea Maritime and Ocean University; Hanoi University of Science and Technology (Vietnam); Vietnam Maritime University; Vinh Long University of Technology Education (Vietnam); Hanoi University of Industry; Vietnamese-German University (Vietnam); Ho Chi Minh City University of Agriculture and Forestry (Vietnam); Research Institute of Agriculture Machinery (Vietnam); Don State Technical University (Russia); University of 17 Agustus Surabaya (Indonesia); Perkumpulan Ahli dan Dosen Republik Indonesia; University of Maarif Hasyim Latif, Sidoarjo (Indonesia); PDPM Indian Institute of Information Technology, Design and Manufacturing (India); South Russian Regional Centre for Preparation and Implementation of International Projects, Ltd.

The following PHENMA abstracts cover five scientific directions: (i) processing techniques of new materials, (ii) physics of new materials, (iii) mechanics of new materials, (iv) applications of new materials, and (v) industry and management. These are present by scientists from 17 countries, demonstrating strong scientific collaboration, formed for last years.

Conference Chairs,

Prof. Yun-Hae Kim, Prof. Nao-Aki Noda, Prof. Ivan A. Parinov, Prof. Shun-Hsyung Chang



# ABSTRACTS

## A Bag of Expressions-based Method for the Recognition of Vehicle Make and Model

Adeel Ahmad Jamil<sup>1</sup>, Chitsan Lin<sup>2\*</sup>, Zulficar Ali<sup>3</sup>

<sup>1</sup>Ph.D. Program in Maritime Science and Technology, College of Maritime, National Kaohsiung University of Science and Technology, Kaohsiung 81157, Taiwan

<sup>1,2</sup>Department of Marine Environmental Engineering, National Kaohsiung University of Science and Technology, Kaohsiung 81157, Taiwan

<sup>3</sup>Department of Electrical Engineering, National Kaohsiung University of Science and Technology, Kaohsiung 807618, Taiwan

\*[ctlin@nkust.edu.tw](mailto:ctlin@nkust.edu.tw)

The recognition of vehicle make-model is a challenging task for various intelligent transportation and automated vehicular surveillance applications. This report presents a bag of expressions (BoE) method for the recognition of vehicle make and model. In addition to visual words, we included neighborhood information for feature extraction. The proposed method improves the existing strength of a bag of words approach, including view independence, scale invariance, and occlusion handling. First, we used the Invariant Feature Transform (SIFT) and Maximally Stable Extremal Regions (MSERs) detectors for vehicle detection, and histogram of oriented gradients (HOGs) based BoE descriptor for feature extraction. Then, we formed an optimized expressions dictionary on the base of visual words acquired through  $k$ -mean clustering. Occurrences of each expression in the image are counted to create the histogram of expressions. Finally, for classification, the BoE-based features representation are used to train multiclass linear support vector machines (SVMs). The approach was assessed by implementing cross-validation tests on easily accessible dataset NTOU-MMR. With multiclass SVM classification, the average accuracy and processing speed using SIFT were 96.4% and 13 fps, while using the MSER were 92.2% and 9 fps, respectively. Experimental results outperform recent approaches, making applicable to real-time vehicle make and model recognition systems.

# Absolute Stability of Control System for Deformation of Electromagnetoelastic Actuator under Random Impacts in Nanoresearch

S. M. Afonin

*National Research University of Electronic Technology  
(Moscow Institute of Electronic Technology MIET) Moscow, Russia*

[eduems@mail.ru](mailto:eduems@mail.ru)

The electromagnetoelastic actuator based on the piezoelectric, piezomagnetic, electrostriction, magnetostriction effects is used in nanoresearch, adaptive optics, nanobiology and biomechanics for the precision matching. The piezo-actuator is applied in nanotechnology, scanning microscopy, interferometry, automatic focus system, gene manipulator for the compensation of the temperature and gravitational deformations, the atmospheric turbulence [1–10]. We used the Yakubovich criterion absolute stability of the control system with the condition on the derivative for the hysteresis nonlinearity of the electromagnetoelastic actuator. The Yakubovich absolute stability criterion with the condition on the derivative is development of the Popov absolute stability criterion [11–14]. The stationary set of the control system for the electromagnetoelastic actuator with the hysteresis deformation is the segment of the straight line. This segment contains points of the intersection of the hysteresis partial loops and the straight line. We obtained the absolute stability condition on the derivative for the control systems with the piezo-actuator at the longitudinal, transverse and shift piezoeffect. We also obtained condition of the absolute stability on the derivative for the control system for the deformation of the electromagnetoelastic actuator under random impacts in nanoresearch. For the Lyapunov stable control system, the Yalubovich absolute stability criterion for the control system with the hysteresis nonlinearity provides the simplest and pictorial representation of the result of the investigation of the absolute stability and the possibility of the synthesis of the correcting device.

## References

- [1] Schultz, J., Ueda, J., Asada, H. *Cellular Actuators*. Butterworth-Heinemann Publisher, Oxford, 2017.
- [2] *Physical Acoustics: Principles and Methods. Vol.1. Part A. Methods and Devices*; W. Mason (Ed.), Academic Press, New York, 1964.
- [3] Afonin S.M. Chapter 9. In: *Piezoelectrics and Nanomaterials: Fundamentals, Developments and Applications*. I.A. Parinov (Ed.), Nova Science Publisher, New York, 225-242, 2015.
- [4] Afonin S.M. // *Journal of Computer and Systems Sciences International*. Pleiades Publishing, Springer, New York, **44**(2), 266–272, 2005.
- [5] Afonin S.M. // *Doklady Physics*. Pleiades Publishing, Springer, New York, **53**(3), 137–143, 2008.
- [6] Afonin S.M. // *Russian Engineering Research*. Allerton Press, Springer, New York, **35**(2), 89-93, 2015.
- [7] Afonin S.M. // *Actuators*. MDPI, Basel, **7**(1), 1-9, 2018.
- [8] Afonin S.M. // *Actuators*. MDPI, Basel, **8**(3), 1-14, 2019.
- [9] Afonin S.M. // *Mechanics of Solids*. Allerton Press, Springer, New York, **44**(6), 935-950, 2009.

- [10] Afonin S.M. // *Transactions on Networks and Communications*. Society for Science and Education, United Kingdom, 7(3), 11-21, 2019.
- [11] Yakubovich, V.A. // *European Journal of Control*, Elsevier, Amsterdam, 8(3), 200-208, 2002.
- [12] Afonin S.M. // *Doklady Mathematics*. Pleiades Publishing, Springer, New York, 74(3), 943–948, 2006.
- [13] Gelig A. Kh., Leonov G. A., Fradkov A. L. *Nonlinear System. Frequency and Matrix Inequalities*. Fizmatlit, Moscow, 2008 (In Russian).
- [14] Naumov B.N. *Theory of Nonlinear Automatic Systems. Frequency Methods*. Nauka, Moscow, 1972 (In Russian).

## **Study of Gas-sensitive Properties of Materials Based on ZnO Nanorods to Nitrogen Dioxide (IV)**

**Alexandra Starnikova<sup>1\*</sup>, Irina Gulyaeva<sup>1</sup>, Khabibulla Abdullin<sup>2</sup>, Victor Petrov<sup>1</sup>**

<sup>1</sup>*Southern Federal University, Research and Education Centre “Microsystem Technics and Multisensor Monitoring Systems”, Taganrog, 347922, Russia*

<sup>2</sup>*Al Farabi Kazakh National University, National Nanotechnology Laboratory of Open Type, Almaty, 050040, Kazakhstan*

[\\*a.starnikova@mail.ru](mailto:a.starnikova@mail.ru)

Arrays of ZnO nanorods were synthesized on glass substrates by the hydrothermal method. Formed ZnO nanorods with a predominantly vertical orientation have an average transverse size of about 30 – 40 nm and a length of 500 – 600 nm. On top of the obtained ZnO nanorods, one of the samples was sprayed with gold and tin in an amount at which a continuous layer would not form on top of the nanorods. Subsequently, the formed heterostructures were annealed at a temperature of 300 °C in air. For electrical contact, V-Ni metallization was also applied over the ZnO nanorods. The report investigates the gas-sensitive properties of the formed sensitive elements in relation to nitrogen dioxide (NO<sub>2</sub>). The gas-sensitive properties of the film samples were studied using a setup for studying the electrophysical properties of gas sensors [1]. The studies were carried out using the Mikrogaz-F installation. The measurements were carried out at an operating temperature of 150 °C. The NO<sub>2</sub> concentration equal to 50 ppm was formed by mixing with synthetic air, which was purged after the formation of the response. A mixture of air and NO<sub>2</sub> was introduced at a flow rate of 0.4 dm<sup>3</sup>/min. Figure 1 shows the responses of the samples to the effect of 50 ppm NO<sub>2</sub> at 150 °C. It is shown that a sensitive element based on ZnO nanorods with sputtered gold has 1.05 times higher sensitivity than similar structures with tin. The response and recovery times were approximately equal to 1120 s.

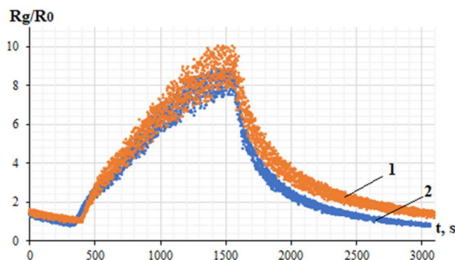


**Fig. 1.** Response of samples with arrays of ZnO nanorods to NO<sub>2</sub> with a concentration of 50 ppm with gold (1) and tin (2) sputtering at 150 °C

**Acknowledgement**

The work was carried out with the financial support of the RFBR grant No. 20-07-00653\_A.

**Reference**

[1] Petrov V.V., Starnikova A.P., Varzarev Y.N., Abdullin K.A., Makarenko D.P. // *IOP Conf. Ser. Mater. Sci. Eng.* **703**, 012038, 2019.

## **Tubular Dielectric Elastomer Actuator Reinforced with two Families of Fibers**

**Alexey M. Kolesnikov**

*Southern Federal University, Rostov-on-Don, Russia*

[Alexey.M.Kolesnikov@gmail.com](mailto:Alexey.M.Kolesnikov@gmail.com)

Dielectric elastomers are a class of electroactive polymers. Their property is the ability to undergo large elastic deformations under the influence of a static electric field. This ability has been known for a long time, the first studies of the electro-mechanical effect for rubber are presented in [1, 2]. Currently, dielectric elastomers are actively studied experimentally and theoretically. On their basis, various actuators, manipulators, soft robots are proposed. Dielectric elastomers are considered as one of the options for artificial muscles. Currently, the possibilities of using the unique properties of dielectric polymers are being investigated in various directions. Information about some of the capabilities of this material and designs based on it can be found in reviews [3 – 5]. In this report, we investigate a reinforced tube made of a dielectric elastomer. Reinforcement is carried out along two helical curves with different angles of inclination. The electric charge is set on the electroplated side surfaces. For the simplest electroelastic reinforced material, an analytical representation is obtained for external mechanical actions (longitudinal force, torque, pressure on the side surfaces) through the parameters of deformation and the magnitude of the electric charge. The aim of this work is to investigate the effect of reinforcement angles and stiffness of fibers on the behavior of a

tube under the action of a charge on the side surfaces. With asymmetric reinforcement, in addition to lengthening and changing the transverse dimension of the tube, twisting occurs.

### References

- [1] Röntgen W. C. // *Annalen der Physik*, **247**(13), 771 – 786, 1880.  
 [2] Quincke G. IV. // *The London, Edinburgh, and Dublin Philosophical Magazine and Journal of Science*, **10**(59), 30 – 39, 1880.  
 [3] Romasanta L. J., López-Manchado M. A., Verdejo R. // *Progress in Polymer Science*, **51**, 188 – 211, 2015.  
 [4] Gu G.-Y., Zhu J., Zhu L.-M., Zhu X. // *Bioinspiration & biomimetics*, **12**(1), 011003, 2017.  
 [5] Lu T., Ma C., Wang T. // *Extreme Mechanics Letters*, **38**, 100752, 2020.

## On the Solution of Convolutional Equation in Spaces of Holomorphic Functions of Prescribed Growth

T. M. Andreeva, Yu. E. Drobotov\*

*Southern Federal University, Rostov-on-Don, Russia*

\*[yu.e.drobotov@yandex.ru](mailto:yu.e.drobotov@yandex.ru)

Let  $G$  denotes a convex bounded region in the complex plane  $\mathbf{C}$ ,  $H(G)$  is the space of all functions which are holomorphic in  $G$ , and  $V = (v_n)_{n=1}^{\infty}$  represents the sequence of functions, continuous in  $G$  and increasing throughout  $n$ .  $V$  defines the space  $VH(G) := \bigcup_{n=1}^{\infty} H_{v_n}(G)$ ,

$$H_{v_n}(G) := \left\{ f \in H(G) : \|f\|_{v_n} := \sup_{z \in G} \frac{|f(z)|}{e^{v_n(z)}} < \infty \right\}, \quad n \in \mathbf{N}.$$

The presented abstract considers the solution of the convolutional equation:

$$\mu * f = g \tag{1}$$

where  $\mu: VH(G+K) \rightarrow VH(G)$  is an analytical functional with the support in  $K$ , while  $K$  is a convex compact in  $G$ . This solution is carried out in the form of the Neumann series, and is of interest within various applications in signal processing, vibration modelling and control, and other engineering disciplines. The general results of the study are based on the rigorous proof of the conditions for the convolutional operator being surjective between the considered spaces [1]. Under an additional specific condition that provides its injectivity, the convolutional operator is investigated for the inverse one, and the properties of (1) are described. Then, the method of successive approximations is used to formulate the solution of (1). All the arising conditions are illustrated in the engineering sense, and several specific issues are considered.

### Acknowledgement

Research was financially supported by Southern Federal University, grant No. VnGr-07/2020-04-IM (Ministry of Science and Higher Education of the Russian Federation).

### **Reference**

[1] Abanin A. V., Andreeva T. M. // *Vladikavkaz. Mat. Zh.* **20**(2), 3–15, 2018.

## **Approximated Analytical solutions for Contact Problems for Piezoelectric Solids with Functionally Graded Coatings**

**Andrey S. Vasiliev\***, **Sergei S. Volkov**, **Sergei M. Aizikovich**

*Research and Education Center "Materials", Don State Technical University,  
1, Gagarin Sq., Rostov-on-Don, 344000, Russia*

\*[andre.vasiliev@gmail.com](mailto:andre.vasiliev@gmail.com)

Contact problems for electroelastic piezoelectric transversely isotropic solids with functionally graded coatings are considered. The electromechanical properties of the coating are assumed to vary with depth, according to arbitrary continuously differentiable or piecewise constant functions. The problems are reduced to the solutions of the system of dual integral equations. Kernel transforms of the integral equations are obtained numerically. Asymptotic behavior of the kernel transforms is also studied. Specially designed approximations for the kernel transforms of the integral equations are used to obtain approximated analytical solutions of the contact problems. The solutions are asymptotically exact for large and small values of the characteristic geometrical parameters of the problem. Special attention is paid to the comparison of results with the classical solutions for homogeneous non-coated solids. Features of the deformation of coated solids are analyzed using analytical and numerical analysis of contact characteristic for thin coatings (both homogeneous and functionally graded). Numerical examples illustrating analytical results are also obtained.

### **Acknowledgement**

This work was supported by the Government of the Russian Federation (grant No. 14.Z50.31.0046).

## **Occurrence of 3D Periodic Convective Flows in a Vertical Layer with Moving Boundaries**

**N.V. Andros\***, **I.V. Morshneva\*\***

*I. I. Vorovich Institute of Mathematics, Mechanics and Computer Science,  
Southern Federal University, Rostov-on-Don, Russia*

\*[andross@mail.ru](mailto:andross@mail.ru); \*\*[ivmorshneva@sfedu.ru](mailto:ivmorshneva@sfedu.ru)

The problem of the occurrence of spatial secondary self-oscillating convection modes in an infinite vertical fluid layer with solid and isothermal boundaries moving vertically with the same value, but opposite in direction, velocities is considered. The behavior of such system is described by a system

of convection equations in Oberbeck-Boussinesq approximation. The equations of motion have a steady state solution (basic mode) with a cubic velocity profile and a linear temperature distribution. It is known that for some parameter values, this solution becomes unstable with oscillations. The occurrence of self-oscillations that appear with an oscillatory instability of the main mode with respect to spatial periodical perturbations is studied. The perturbation equations have a symmetry group  $O(2) \times O(2)$  and the theory of Andronov-Hopf bifurcation in systems with such symmetry is applicable [1]. Following the theory, as a governing parameter passes through its critical value the cycles can bifurcate from the main equilibrium solution. These cycles correspond to self-oscillations such as horizontal traveling waves, oblique traveling waves and various nonlinear superpositions of oblique traveling waves. For various critical values of the parameters corresponding to an oscillatory instability, the analysis of the branching type and stability of the occurring spatial self-oscillating modes in a vertical layer with moving boundaries is made. In order to do this, the analytical expressions for the coefficients of the branching equations system are derived. These coefficients are the functionals, expressed in terms of the eigenfunctions of the linear and conjugate stability problems, the solutions of a number of inhomogeneous boundary value problems with the right-hand sides depending on the same eigenfunctions are obtained. For the self-oscillatory modes, the first two members of the series are written by degrees of the supercritical parameter.

#### **Acknowledgement**

Research was financially supported by Southern Federal University, grant No. VnGr-07/2020-04-IM (Ministry of Science and Higher Education of the Russian Federation).

#### **Reference**

[1] Morshneva I. V. *The Andronov-Hopf Bifurcation in a Dynamical Systems with Symmetry and its applications in hydrodynamics*. Rostov-on-Don, Southern Federal University Press. 2010, 140 p. (In Russian)

## **The Effect of Biographical Defects on the Electrophysical Properties of $n$ -component Ferroactive Solid Solutions of Composition PZT – PZN – PMN**

**K.P. Andryushin\*, I.N. Andryushina, L.A. Reznichenko**

*Research Institute of Physics, Southern Federal University,  
344090 Rostov-on-Don, Stachki, Ave., 194, Russia*

\*[kpandryushin@gmail.com](mailto:kpandryushin@gmail.com)

Ferroactive materials based on the PZT system ( $\text{PbZr}_{1-x}\text{Ti}_x\text{O}_3$ ) with high values of piezoelectric responses are widely used in various types of modern instrument engineering being developed. Such devices almost always work in highly loaded cyclic modes (temperature, frequency/amplitude of an alternating electric field, etc.), which leads to the inevitable accumulation of various types of defects, and as a result, a change in performance. In view of the foregoing, studies are needed aimed at establishing correlations between the composition – structure – electric aging – phase hardening (PH) (irreversible accumulation of defects in the crystal structure, mainly edge dislocations, during cyclic thermally activated phase transitions (PT)). It is very narrow segment of work in this area.

Thus, the aim of the present work was to establish the effect of electric fatigue polarization properties, namely, the saturation polarization ( $P_s$ ), residual ( $P_r$ ) and coercive fields ( $E_c$ ), in multicomponent solid solutions (SSs) under conditions of a cyclically changing alternating electric field with a strength above  $E_c$  of each specific object, as well as the phenomenon of PH in multicomponent SS. The objects of the study were the SSs of the PZT – PZN – PMN system, modified by Ba and Sr, corresponding to the formula  $(\text{Pb}_{1-\alpha_1-\alpha_2}\text{Sr}_{\alpha_1}\text{Ba}_{\alpha_2})[\text{Ti}_x\text{Zr}_y((\text{Nb}_{2/3}\text{Zn}_{1/3})(\text{Nb}_{2/3}\text{Mg}_{1/3}))_{1-x-y}]\text{O}_3$  with  $\alpha_1 = 0.02 - 0.12$ ;  $\Delta\alpha_1 = 0.02$  [1]. The SSs with  $\alpha_1 = 0.02$ ,  $\alpha_1 = 0.1$  are most thoroughly studied. The FN study was carried out in the temperature range (373 – 723) K using a specially designed bench based on the LCR meter Agilent 4980A. Regularities of the manifestation of PH were studied in the process of observing the evolution of the Curie temperature ( $T_C$ ) and the dependences of the relative dielectric constant ( $\varepsilon/\varepsilon_0$ ) on temperature for multiple (up to  $n = 50$ ) consecutive phase transitions in the forward (heating) and reverse (cooling) modes. The  $P - E$  dielectric hysteresis loops were studied using the Sawyer – Tower circuit at  $f = 50$  Hz,  $T = (300 - 420)$  K, the number of cycles  $\sim 0 - 1.5 \times 10^6$ . The study of phase hardening showed that as the number of heating-cooling cycles increases, a shift of  $T_C$  occurs, a gradual decrease in  $\varepsilon/\varepsilon_0$ , and also an increase in its dispersion. From the  $P - E$  dielectric hysteresis loops, it was found that all the studied SSs are characterized by the preservation of the values of polarization characteristics, up to  $n \approx 5 \times 10^5$ , after which there is a significant decrease. The data obtained must be taken into account when developing components based on the system studied.

#### **Acknowledgement**

Research was financially supported by the Ministry of Science and Higher Education of the Russian Federation (State assignment in the field of scientific activity, Southern Federal University, 2020).

#### **References**

[1] K.P. Andryushin, L.A. Shilkina, I.N. Andryushina, et al. // *J. Ceramics International*, **45**, 14, 2019.

## **The Structure, Microstructure and Piezoelectric Properties of Highly Sensitive Ferroelectric Ceramics**

**I.N. Andryushina\*, K.P. Andryushin, L.A. Reznichenko**

*Research Institute of Physics, Southern Federal University,  
344090 Rostov-on-Don, Stachki, Ave., 194, Russia*

\*[futur6@mail.ru](mailto:futur6@mail.ru)

Using of ferro-piezoelectric ceramic materials (FPCM) opens up broad prospects in various fields of science and technology. The development of highly efficient piezoceramic elements requires the development of new high-tech techniques for their manufacture. This problem can be resolved in two areas: (i) the creation of a new generation of FPCM; (ii) improving the manufacturing technology of FPCM mastered by industry. The first area requires long-term painstaking research and comprehensive testing, the second uses innovative approaches and technologies, which should



be based on the most modern achievements of basic and applied sciences. In our work, a choice is made in favor of the second direction. In this regard, the aim of the work is to create highly sensitive FPCM for diagnostic devices based on PZT without the use of exotic methods (for example, the hot-pressing method), but with the preservation of the properties inherent to them. The solid solutions (SSs) based on the PZT system were used as objects of study:  $\text{PbTiO}_3 - \text{PbZrO}_3 - \text{PbNb}_{2/3}\text{Zn}_{1/3}\text{O}_3 - \text{PbNb}_{2/3}\text{Mg}_{1/3}\text{O}_3 + \text{MnO}_2$  (1),  $\text{PbTiO}_3 - \text{PbZrO}_3 - \text{PbW}_{1/2}\text{Cd}_{1/2}\text{O}_3$  (2),  $\text{PbTiO}_3 - \text{PbZrO}_3 - \text{PbW}_{1/2}\text{Cd}_{1/2}\text{O}_3 + \text{Ta}_2\text{O}_5$  (3), in which high frequency FPCM can be implemented. The samples were obtained by conventional ceramic technology, including two-stage solid-phase synthesis. X-ray diffraction analysis was performed by powder diffraction using diffractometers DRON-3 and ADP ( $\text{Fe}_{K\alpha}$  radiation, Mn filter;  $\text{Fe}_{K\beta}$  radiation; Bragg-Brentano focusing scheme). The microstructure of sintered ceramics was evaluated using a JSM-6390L scanning electron microscope. The electrophysical parameters of SSs at 300 K were measured using Agilent 4980A precision LCR-meter and the resonance-antiresonance method. X-ray phase analysis of the samples showed that all SSs have a perovskite structure. The crystal lattice symmetry of SSs (1) is rhombohedral (*Rh*), since its basis is the SS of the PZT system from the *Rh* region of the phase diagram. Compositions SSs (2) and (3) are a mixture of tetragonal (*T*) and *Rh* phases. The laws formation of dielectric (loss), piezoelectric (piezoelectric sensitivity) and ferroelastic (mechanical *Q*-factor) properties of media based on a PZT system are established. In all compositions studied, a weak dispersion  $\varepsilon/\varepsilon_0$  is observed before the phase transition (PT) to the paraelectric phase (PE) phase. At the time of PT in the PE phase, the dispersion  $\varepsilon/\varepsilon_0$  becomes strong and weakens in the PE region to some temperatures of  $\sim 700$  K, after which it becomes significant at low frequencies. The dispersion depth at the time of the phase transition is  $\Delta\varepsilon/\varepsilon \approx 79\%$  for (1),  $\Delta\varepsilon/\varepsilon \approx 54\%$  for (2),  $\Delta\varepsilon/\varepsilon \approx 41\%$  for (3).

#### **Acknowledgement**

Research was financially supported by the Ministry of Science and Higher Education of the Russian Federation (State assignment in the field of scientific activity, Southern Federal University, 2020).

## **Stability of the Polarized State in Ferroelectric Piezoelectric Ceramics of Various Ferrohardeness Degrees**

**I.N. Andryushina\*, E.V. Triger, N.A. Nikiforova, K.P. Andryushin, L.A. Reznichenko**

*Research Institute of Physics, Southern Federal University,  
344090 Rostov-on-Don, Stachki, Ave., 194, Russia*

\*[futur6@mail.ru](mailto:futur6@mail.ru)

Recently, much attention has been paid to the use of ferroelectric piezoelectric ceramics of various degrees of ferrohardeness in devices experiencing cyclic effects of temperature in heating-cooling modes (rocket and space technology, sonar, seismic devices, etc.). In this case, both ferro-hard (FH) materials that are resistant to electrical and mechanical influences (due to a "rigidly" fixed domain structure) and ferro-soft (FS) materials with movable domain walls are in demand. For such applications, it is necessary to maintain a stable polarized state in the materials. In this regard, it seems urgent to carry out works aimed at establishing the regularity of the formation of a stable

polarized state of ferroelectric ceramics of various degrees of ferrohardness. This became the main aim of this study. The objects of the study were ferroelectric piezoelectric materials based on the  $\text{Pb}(\text{Ti}_x\text{Zr}_{1-x})\text{O}_3$  system of three ferro-hardness groups: ferro-hard, medium ferro-hardness, and ferro-soft. A huge set of measurements was carried out, including studies of dielectric, piezoelectric, elastic properties and structural characteristics of materials in a wide thermal frequency range. It should be noted that studies of the piezoelectric properties were carried out by three methods: single heating and cooling to the Curie temperature ( $T_C$ ) and multiple heating according to different schemes. It is concluded that the dependence of the piezomodule measured in the quasi-static mode ( $d_{33}^{\text{qst}}$ ) ( $T$ ) has effect on the increase in dielectric constant ( $\epsilon$ ) with increasing temperature ( $T$ ) up to  $T_C$  and a decrease in the residual polarization ( $P_r$ ). It is pointed that a sharp drop in the piezomodule in ferro-soft ceramics is probably due to relaxation processes, due to the composition of the FS materials contains complex oxides of ferroelectric relaxors of various chemical compositions, for example  $\text{PbMg}_{1/3}\text{Nb}_{2/3}\text{O}_3$ . It was found that the growth  $d_{33}^{\text{qst}}$  in FS materials in the cooling mode and its unusual behavior in the last cycles indicate the generation of a large number of new domains (ferroelastic, wedge-shaped, “removing part of inhomogeneous mechanical stresses”) with movable domain walls, which contribute to the dielectric constant, pyro- and piezoelectric effect. Therefore, the temperature dependences of parameters in FS materials, including piezomodules, may be completely different from the dependences following from the theory of a single-domain ferroelectric.

**Acknowledgement**

Research was financially supported by the Ministry of Science and Higher Education of the Russian Federation (State assignment in the field of scientific activity, Southern Federal University, 2020).

**Effect of the Residual Stress to the Fatigue Failure of the Bimetallic Roll in 4-High Rolling Mill**

M. R. Aridi\*, N. A. Noda, Y. Sano, K. Takata, S. Zifeng

*Department of Mechanical Engineering, Kyushu Institute of Technology, Kitakyushu, Japan*

[\\*radz7cr@gmail.com](mailto:radz7cr@gmail.com)

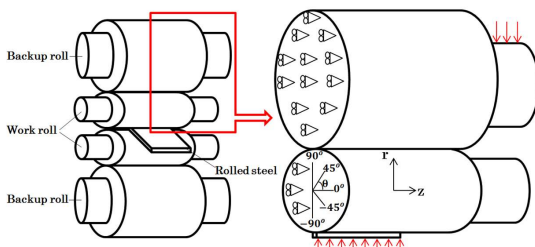


**Fig.1** Three-dimensional FEM model of 4-high rolling mill

In hot rolling mills, bimetallic work rolls are extensively used because of their excellent hardness and wear resistance of high-speed steel material (outer layer) and ductile casting iron (inner layer), see Fig. 1. Study of fatigue failure plays an important role in extending the life service of the rolls. In this report, the finite element method (FEM) simulation is performed to study the generated stress, when the rolling roll is used in the four-high rolling mill as shown in Fig.1. In order to study the effect of the residual stress, the heating treatment of the work roll is considered to the work roll. By using 3D model, we focus the fatigue failure at near the boundary layer where the work roll received load from the backup roll and the hot strip. We found that the residual stress gives significant effect to the fatigue failure of the work roll.

## **Modeling the Interaction of Elastic Haptic Parts of Two Intraocular Lenses Located in the Capsular Bag of the Lens**

**Arkadiy N. Soloviev<sup>1,2\*</sup>, Alexander N. Epikhin<sup>3\*\*</sup>, Denis V. Krasnov<sup>1\*\*\*</sup>**

*<sup>1</sup>Department of Theoretical and Applied Mechanics, Don State Technical University, Rostov-on-Don, Russia*

*<sup>2</sup>I. I. Vorovich Institute of Mathematics, Mechanics and Computer Sciences, Southern Federal University, Rostov-on-Don, Russia*

*<sup>3</sup>Rostov State Medical University, Rostov-on-Don, Russia*

\*[solovievarc@gmail.com](mailto:solovievarc@gmail.com); \*\*[epikhin-rus@yandex.ru](mailto:epikhin-rus@yandex.ru); \*\*\*[dinisiil@yandex.ru](mailto:dinisiil@yandex.ru)

The intraocular lenses (IOLs) implanted in the eye is used to treat diseases such as cataracts or myopia. One of the most common types of IOLs is a pseudophakic lens [1]. They are implanted during cataract surgery. A pseudophakic IOL provides the same function as a natural lens. The second type of IOLs is a phakic IOL. The IOL is placed on top of the existing natural lens and is used in refractive surgery as a treatment for myopia [2]. As a rule, IOL consist of a small plastic plate with side struts called haptics, which serve to hold the IOL in place in the eye's capsule bag. [3] IOLs were usually made from an inflexible material, although this was largely superseded by the use of flexible materials such as silicone and acrylic glass. Most IOLs, introduced to date, are fixed monofocal IOLs that provide a single focal length [4]. There are also types of IOLs, such as multifocal IOLs, which provide the patient with multi-focus vision, but this type of IOLs can create side effects in the form of reduced contrast vision in the dark, as well as glare [5]. Adaptive IOLs correct limited visual accommodation [6]. This report examines the problem of cataract healing while preserving the natural accommodation of the eye. The aim of this work is to model the system of IOLs, which has the possibility of accommodation, as well as the natural lens. The SpaceClaim CAD system was used for direct 3D modeling of an IOL with elastic haptic elements (Fig. 1) as well as the ANSYS Mechanical environment for creating a finite element mesh and a numerical model of deformations. Figure 2 shows the distribution of axial displacements that provide controlled accommodation under the action of radial pressure on the end elements of haptic connections. It is concluded that it is possible to create a working system of IOL with elements of accommodation, at the subsequent possibility of using them in cataract treatment operations. The purpose of further research is to select the optimal shape of haptic elements that provides their

stiffness properties in the radial and axial directions to achieve the necessary accommodation parameters.

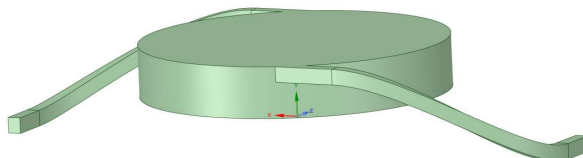


Fig. 1. CAD model of a single IOL

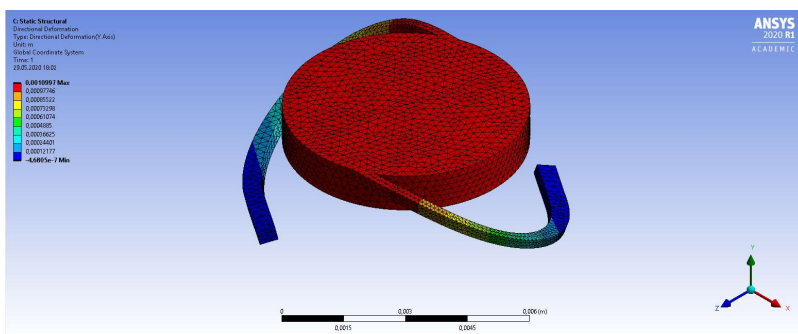


Fig. 2. Distribution of axial displacements

### Acknowledgement

This work was supported by the Government of the Russian Federation (grant No. 14.Z50.31.0046).

### References

- [1] Trivedi, R., Werner, L., Apple, D. et al. // *Eye*. **16**, 217-241, 2002.
- [2] Güell J.L., Morral M., Kook D., Kohnen T. // *Journal of Cataract and Refractive Surgery*. **36**(11), 1976 – 1993, 2010.
- [3] Sanders D., Vukich J.A. // *Cornea*. **25**(10), 1139 – 46, 2006.
- [4] de Silva S.R., Evans J.R., Kirthi V., Ziaei M., Leyland M. // *The Cochrane Database of Systematic Reviews*. **12**, CD003169, 2016.
- [5] Carson D., Hill W.E., Hong X., Karakelle M. // *Clinical Ophthalmology*. **8**, 2105 – 2113, 2014.
- [6] Ong H.S., Evans J.R., Allan B.D. // *The Cochrane Database of Systematic Reviews*. **5**, CD009667, 2014.

## Development of Standalone Computational Modules for ACELAN-COMPOS Package

Arkadiy N. Soloviev<sup>1,2\*</sup>, Dmitry K. Nadolin<sup>2\*\*</sup>, Pavel A. Oganessian<sup>2\*\*\*</sup>

<sup>1</sup>*Department of Theoretical and Applied Mechanics, Don State Technical University,  
Rostov-on-Don, Russia*

<sup>2</sup>*I. I. Vorovich Institute of Mathematics, Mechanics and Computer Sciences,  
Southern Federal University, Rostov-on-Don, Russia*

\*[solovievarc@gmail.com](mailto:solovievarc@gmail.com); \*\*[dknadolin@sfedu.ru](mailto:dknadolin@sfedu.ru); \*\*\*[oganesyan@hey.com](mailto:oganesyan@hey.com)

ACELAN-COMPOS is a package for composite materials property identification. The package is based on a modular architecture: a classic library responsible for performing calculations was used as a basis for developing web and desktop applications. While client-server architecture was a priority for ACELAN-COMPOS package and allowed one to perform all FEM-related computations on server side, the possibility to run specific modules with predefined scenarios for material properties identification was also valuable. The computational modules have built-in mesh generation algorithms for 3-3, 3-1 and 3-0 connectivity types, solvers for systems of linear equations with sparse symmetric matrices, mesh import program interfaces and a library of finite elements and post-processing tools. Such independent modules do not have ability to access material library and visualization tools of the package. The benefit of developing such modules lies not only in the possibility of using the computing resources of the client computer, but also in the ease of parallel execution of programs. Modules can be run independently, while their internal parallelization settings can be changed by the user. Thus, the simultaneous launch of a large number of independent processes, each of which uses a limited number of threads with a relatively small mesh size and does not take up a lot of RAM, is well suited for the needs of optimization methods, both deterministic and based, for example, on genetic algorithms. New version of ACELAN scripting language, based on Ruby programming language, was used as an input tool for standalone modules, which also allowed one to perform simultaneous tasks with various settings due to the possibility to modify scripts from external software. Both general FEM possibilities and simplified process of material identifications are available. Since homogenization method is used for material properties identification, set of boundary problems should be solved to obtain effective moduli, these sets are implemented as subroutines for scripting language. Further development of standalone modules will be related to data synchronization possibility between main client-server application and standalone modules. This will allow to perform distributed computations on server and client side simultaneously.

### ***Acknowledgement***

This work was supported by the Government of the Russian Federation, contract No. 075-15-2019-1928.

## Finite Element Modeling of the Interaction of an Ocular Prosthesis with the Corneal Tissue of the Eye

Arkadiy Soloviev<sup>1\*</sup>, Nadegda Glushko<sup>1\*\*</sup>, Alexander Epikhin<sup>2</sup>, Michael Swain<sup>3</sup>,  
O. N. Lesnyak<sup>1\*\*\*</sup>, A. E. Ivanov<sup>1\*\*\*\*</sup>

<sup>1</sup>*Department of Theoretical and Applied Mechanics, Don State Technical University,  
Rostov-on-Don, Russia*

<sup>2</sup>*Rostov State Medical University, Rostov-on-Don, Russia*

<sup>3</sup>*Sydney University, Sydney, Australia*

\*[solovievarc@gmail.com](mailto:solovievarc@gmail.com); \*\*[leksha\\_n@list.ru](mailto:leksha_n@list.ru); \*\*\*[lesniak.olga@yandex.ru](mailto:lesniak.olga@yandex.ru);  
\*\*\*\*[al.drobotow@yandex.ru](mailto:al.drobotow@yandex.ru)

In the development of ocular prostheses, a number of problems arise, one of which is the design of the connection between the hard optical part and the soft tissue of the cornea. Their Young's moduli can differ by three orders of magnitude. In this case, the problem arises of creating their connection, which will eliminate injury to soft biological tissues. A keratoprosthesis is considered, which has a support plate. For the first type, the stress-strain state is calculated. The purpose of this work is to study the stress-strain state of the keratoprosthesis and the cornea in the contact area. The mathematical models of the structure under consideration are a boundary value problem of the linear theory of elasticity. Spatial three-dimensional problems and problems in an axisymmetric formulation are solved by the finite element method. Finite element modeling of the structures under consideration was carried out in the CAE software ANSYS and ACELAN. CAD-models of keratoprostheses with the conditions of fixation and loading were built. The load on the keratoprosthesis under the action of internal ocular pressure was established. The stress-strain state of the elements of the keratoprosthesis and the cornea was calculated. Particular attention is paid to the vicinity of its contact with the keratoprosthesis. The results of calculating axial displacements and mechanical stresses in a keratoprosthesis of the first type show that the geometric parameters selected for it meet the kinematic and strength requirements. The models of the deformed state of soft biological tissues proposed in the work make it possible to assess their injury when using a keratoprosthesis of the type, and also to choose the most suitable conditions for its fixation.

### ***Acknowledgement***

This work was supported by the Government of the Russian Federation (Grant No. 14.Z50.31.0046)

## Modeling of Multisection Piezoelectric Energy Harvesting Devices Based on Applied Theory

Arkadiy N. Soloviev<sup>1,2\*</sup>, Pavel A. Oganessian<sup>2\*\*</sup>, Evgenia Kirillova<sup>3</sup>, V. A. Chebanenko<sup>4</sup>

<sup>1</sup>*Department of Theoretical and Applied Mechanics, Don State Technical University, Rostov-on-Don, Russia*

<sup>2</sup>*I. I. Vorovich Institute of Mathematics, Mechanics and Computer Sciences, Southern Federal University, Rostov-on-Don, Russia*

<sup>3</sup>*RheinMain University of Applied Sciences, Wiesbaden, Germany*

<sup>4</sup>*Southern Scientific Center of RAS, Rostov-on-Don, Russia*

\*[solovievarc@gmail.com](mailto:solovievarc@gmail.com); \*\*[oganesyan@hey.com](mailto:oganesyan@hey.com)

In the present study we build models of multisection energy harvesting devices based on applied theory of piezoelectric plate oscillations. In previous works we developed a method for solving problems with piecewise homogeneous transducers with two principal parts: part with transverse polarization and part with multidirectional longitudinal polarization. This theory was based on variational principle. Numerical results show growth of output potential of such devices compared to traditional uniformly polarized transducers. Sections with longitudinal polarization use  $d_{33}$  piezoelectric coefficient on working mode, which allows them to be more effective than parts with transversal polarization. However, the possibility to build needed field of preliminary polarization is limited by physical restrictions, so multisection devices can be used to combine multiple sections. In this study we are extending possibilities of suggested model by expanding it to multisection devices with any number of parts with different polarization. We obtained analytically the sets of equations and boundary conditions for different parts of transducers. The numerical solution is based on solving the resulting system of differential equations for a particular case. The final system of equations for various configurations of the converter is built automatically by forming boundary conditions that ensure the continuity of mechanical and electrical fields at the boundaries of individual parts of the converter. Numerical experiments are carried out using the MAPLE package, for which a parameterized script was implemented. The ability to automatically solve a series of problems for various geometric parameters, material properties, loading schemes and device configurations can significantly reduce the calculation time compared to traditional approaches based on the finite element method because changing geometry of the model usually leads to remeshing on FEM which is not required in suggested approach. Numerical results were obtained for different types of materials, including porous piezoceramics. Devices with passive metallic layer were also analyzed. Comparisons between FEM results and applied theory for multisection devices showed close results in limits of applicability of the theory.

### **Acknowledgement**

This work was supported by the Government of the Russian Federation, contract No. 075-15-2019-1928.

# Temperature Stability of Resistive Switching in Titanium Oxide Nanostructures

V.I. Avilov\*, N.A. Sharapov, N.V. Polupanov, V.A. Smirnov

*Southern Federal University, Institute of Nanotechnology, Electronics and Electronic Equipment Engineering, 2, Schevchenko Str., Taganrog, 347928, Russia*

\*[Avir89@yandex.ru](mailto:Avir89@yandex.ru)

Memristor structures are one of the promising elements of nanoelectronics that can find their application in a big-data processing system and neuromorphic devices. These elements have a high switching speed, low energy consumption, and are non-volatile. Analysis of the literature showed that the most preferred material for the manufacture of memristors is titanium oxide, structures based on it have a large resistance ratio in the HRS and LRS states, and a large storage time. Moreover, oxide nanostructures (ONSs) obtained by the method of local anodic oxidation (LAO) of titanium exhibit a memristor effect without an additional electroforming operation. This raises the urgent task of studying the influence of temperature stability on the patterns of resistive switching of such structures. To study the effect of temperature on the uniformity and stability of resistive switching in the memristor structure using the Ntegra probe nanolaboratory (NT-MDT, Russia), a 4.2 nm thick ONS of titanium was manufactured by the LAO method. Then, the current-voltage characteristics of the obtained structure were measured at a substrate temperature of 25 and 90 °C. An analysis of the results showed that titanium ONS at a substrate temperature of 25 and 90 °C, titanium oxide nanostructures exhibit a memristor effect (Fig. 1). Moreover, at a read voltage of 1 V, a current of  $3.52 \pm 1.08$  nA in the LRS state and  $0.71 \pm 0.32$  nA in the HRS state flows through the structure obtained at a temperature of 25 °C, while the ratio of the resistances in the HRS and LRS is 4.9. A current of  $0.63 \pm 0.48$  nA in the LRS state and  $0.09 \pm 0.02$  nA in the HRS state flows through the structure obtained at a temperature of 90 °C, while the ratio of resistances in the HRS and LRS state is 6.5.

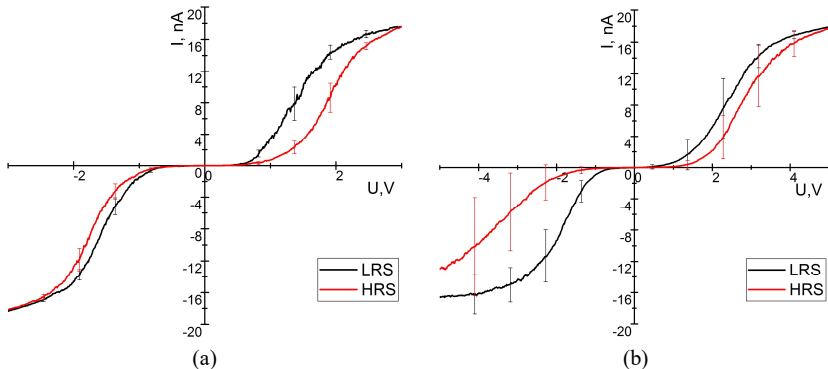


**Fig. 1.** Current-voltage characteristics of ONS of titanium measured at: (a) 25 °C and (b) 95 °C



It can be seen from the presented results that with an increase in the substrate temperature, the current through the structures decreases for the HRS and LRS states, however, the ratio of resistances does not change significantly. The results can be used in the development of technological processes for the formation of elements of nanoelectronics, as well as elements of resistive memory based on oxide nanoscale structures.

#### **Acknowledgement**

This work was supported by RFBR according to the research project No. 19-29-03041\_mk, and by grant of the President of the Russian Federation No. MK-767.2020.8.

## **The Impact of Deterministic and Stochastic Loads on the Support of the Offshore Platform**

**R.A. Bardakova, A.A. Kotova, A.A. Matrossov\***

*Don State Technical University, Gagarin Sq., 1, Rostov-on-Don, 344010, Russia*

[\\*amatrossov@donstu.ru](mailto:amatrossov@donstu.ru)

In the work, the problem of determining the distribution of stresses and strains in one of the supports of the oil platform is solved [1, 2]. A sea-based platform with fixed attachment to the seabed is considered. The functional purpose of the support is divided into drilling, marine riser, storage and auxiliary, which determines their internal structure and ultimately affects the stress-strain state. The problem is solved for the support, which acts as a reservoir for storing extracted oil. The support is a hollow cylinder of variable diameter, filled with a viscous fluid at three quarters of the height. The material of the cylinder walls is concrete. We believe that the base of the column is rigidly embedded in the bottom. The column is subjected to loads that can be divided into two types – deterministic and stochastic. Deterministic loads include: (i) the weight of various structures located on the platform; (ii) weight of the column itself; (iii) strength from the bulk effect of ice (relevant for structures located in the northern regions). Stochastic loads include: (i) the influence of underwater currents washing the column; (ii) exposure to surface waves in a storm; (iii) wind load on deck structures transmitted to the top of the column; (iv) seismic impact of the seabed on the base of the platform support. In a first approximation, we believe that these stochastic loads are determined by the deterministic component (constant value) and some random stochastic value. The problem is solved in the framework of the linear theory of elasticity. Numerical calculations for the support in question were performed in the ANSYS 19 R2 finite element analysis software package. A finite element mesh with SOLID 65 elements was used. According to the results of the calculation of finite element modeling, a picture of the stress distribution over the entire height of the support was obtained.

#### **References**

[1] Kislyakov E.A., Matrossov A.A. In: *Innovative Technologies in Science and Education "ITNO-2018": Materials of the VI Int. Sci. Practical Conf., September 5-9, 2018*. Rostov-on-Don, DSTU, 191-193, 2018 (In Russian).

[2] Kislyakov E.A., Matrosov A.A. In: *2018 International Conference on "Physics and Mechanics of New Materials and Their Applications" (PHENMA 2018), Busan, South Korea, August 9-11, 2018*, Busan, Korea Maritime and Ocean University Press, 196, 2018.

## **Preparation and Characterization of Transparent Sn-ZnO Thin Films Obtained by Pyrolysis**

**E.M. Bayan<sup>1\*</sup>, V.V. Petrov<sup>2</sup>, V.Yu. Storozhenko<sup>1</sup>, M.G. Volkova<sup>1</sup>**

<sup>1</sup>*Southern Federal University, Faculty of chemistry, Rostov-on-Don, Russia*

<sup>2</sup>*Southern Federal University, Institute of Nanotechnologies, Electronics, and Equipment Engineering, Taganrog, Russia*

\*[ekbayan@sfedu.ru](mailto:ekbayan@sfedu.ru)

Nanoscale zinc oxide films have transparency in the visible range and good optical properties, which give opportunities for their application in modern optical converters and solar cells. Promising results for obtaining films with different band gap can be achieved by synthesizing nanoscale ZnO films doped with tin (IV) oxide (ZTO) [1]. The aim of this work was to synthesize three-layer zinc oxide films doped with tin (IV) oxide by low-temperature pyrolysis.  $\text{SnCl}_4 \cdot 5\text{H}_2\text{O}$ ,  $\text{Zn}(\text{CH}_3\text{COO})_2 \cdot 2\text{H}_2\text{O}$  in different concentrations, dioxane and organic acid were used as precursors for the synthesis of ZTO films. The molar ratios of zinc and tin were Sn:Zn = 0:100, 0.5:99.5, 1:99 and 5:95. Salts solution in the organic solvent was applied to pre-prepared glass substrates, dried in the air and calcined at 550 °C for 2 hours. Obtained materials were studied by XRD (diffractometer Thermo ARL, Switzerland) in  $\text{Cu}_{\text{K}\alpha}$  radiation and scanning electron microscopy methods (SEM, electron microscopy EMXplus 10/12 Bruker, Germany). Optical properties were studied using optical absorption spectra obtained on the Varian Cary-100 spectrophotometer (Australia). The wurzite structure, which is typical for zinc oxide was confirmed by the XRD method. The average size of the coherent scattering regions calculated using the Scherrer equation was about 20 nm. According to SEM data, the thickness of three-layer films was 200-220 nm. When studying the optical properties, it was shown that in comparison with pure zinc oxide, there is a slight narrowing of the band gap at the ratio of tin and zinc ions concentration of 0.5:99.5. Thus, low-temperature pyrolysis method was used to synthesize film materials based on zinc oxide, which can be recommended for using in functional electronic elements and power engineering.

### **Acknowledgements**

*This work was financially supported by the RFBR, project 20-07-00653 A. The authors are grateful to the Molecular Spectroscopy Center of Southern Federal University for the registration of spectra.*

### **References**

[1] Petrov V.V., Varzarev Y.N., Bayan E.M., Storozhenko V.Yu., Rozhko A.A. // Proceedings of the 2019 IEEE International Conference on Electrical Engineering and Photonics, 8906834, P. 242, 2019.

## **Wave Fields in an Orthotropic Strip Weakened by a Cylindrical Cavity of Small Characteristic Size**

**O. A. Belyak**

*Rostov State Transport University, Rostov-on-Don, Russia*

[o\\_bels@mail.ru](mailto:o_bels@mail.ru)

The problems of oscillations of elastic semi-bounded bodies have long attracted the attention of many researchers, since the analysis of dynamic processes is very important, for example, in assessing the dynamic strength of elements of heavily loaded vehicles, machines and mechanisms, in geophysics and mining mechanics. Note that for isotropic homogeneous media, dynamic processes in such structures are well studied. In this paper, we consider the problem of vibrations of an orthotropic layer weakened by a cylindrical cavity of a small characteristic size. A steady-state oscillation regime with a frequency  $\omega$  of a layer of thickness  $h$  with a cylindrical cavity not extending to the boundary of the layer whose guide is a smooth closed curve  $l$  with a generator parallel to the  $y$ -axis is considered. The lower edge of the layer is rigidly pinched and coincides with the  $x$ -axis, the  $z$ -axis is directed perpendicular upward. The axes of elastic symmetry of the orthotropic material coincide with the axes of the coordinate system. Fluctuations in the layer are caused by an oscillating load applied to the upper part of the layer boundary. The study of the described problem was carried out on the base of information on the system of boundary integral equations with irregular kernels based on the ideas of potential theory [1]. It should be noted that the obtained boundary integral equations are formulated only along the boundary of the cavity  $l$ . The fields of displacements on the cavity were determined from the constructed systems of boundary integral equations based on the asymptotic approach under the assumption that the relative characteristic size of the cavity is small. Based on numerical experiments, the areas of correct operation of the asymptotic approach are determined in comparison with the boundary element method [2].

***Acknowledgement***

The author is grateful to Prof. Vatulyan A.O. for attention to the work.

***References***

[1] Vatulyan A.O., Belyak O.A. // *Journal of Applied Mechanics and Technical Physics*, **3**(50), 512–518, 2009.

[2] Vatulyan A.O., Belyak O.A. // *Acoustical Physics*, **3**(66), 235–241, 2020.

**On the Prediction of the Mechanical and Tribological Properties of  
Dispersively Filled Composites**

**O.A. Belyak\*, T.V. Suvorova**

*Rostov State Transport University, Rostov-on-Don, Russia*

\*[o\\_bels@mail.ru](mailto:obels@mail.ru)

Modification of polymers to obtain composite materials with new or improved physico-mechanical properties has attracted the constant interest of researchers, since the starting materials often do not have a set of properties and characteristics necessary for one or another of their practical applications. Among the most promising areas of creating composite materials with polymer matrices for the manufacture of a wide range of structural and tribotechnical parts is the functional modification of base matrices with components of various compositions and purposes. The introduction of various types and concentrations of nanomodified fillers and nanosized additives into the polymer matrix allows the directional formation of a composite with desired properties. An important problem in this case is directed modeling of the physico-mechanical properties of the composite. To this end, a study was made of the stress-strain state of a composite material under tribological contact, depending on the physico-mechanical characteristics of the matrix and additives, their shape, concentration, and distribution method in the matrix. The study was implemented in two stages. At the first stage, the effective elastic properties of the composite material were determined based on the differential scheme. In order to test the computational model, the obtained data were compared with the data of experiment, based on the nanoindentation method. At the second stage, the stress – strain state of the material during tribological contact was calculated based on the solution of the contact problem of sliding a rigid punch with a flat sole along a half-space with mechanical properties of an equivalent elastic medium corresponding to a composite material [1]. The calculations were performed for a composite material with a matrix of aromatic polyamide phenylone C-2 reinforced with short unidirectional arimide fibers or nanosized additives of aluminum-magnesium spinel [2].

#### ***Acknowledgement***

This study was supported by the Russian Science Foundation (project No. 20-08-00614).

#### ***References***

- [1] Belyak O.A., Suvorova T.V. // *Ecological Bulletin of Research Centers of the Black Sea Economic Cooperation*, **3**(16), 33-39, 2019.  
[2] Ivanochkin P.G., Suvorova T.V., Danilchenko S.A., Novikov E. S., Belyak O.A. // *Vestnik of Rostov State Transport University*, **4**(72), 18-25, 2018.

## **Features of Rayleigh Waves Propagation in Structures with FGPM Coating Made of Various Materials**

**T. I. Belyankova<sup>1\*</sup>, E. I. Vorovich<sup>2</sup>, V. V. Kalinchuk<sup>1</sup>, O. M. Tukodova<sup>2</sup>**

<sup>1</sup>*Southern Scientific Centre of the Russian Academy of Sciences (SSC RAS),  
Rostov-on-Don, Russia*

<sup>2</sup>*Don State Technical University (DSTU), Rostov-on-Don, Russia*

[\\*tbelen415@mail.ru](mailto:tbelen415@mail.ru)

In the framework of a model for piezoelectric structure with an inhomogeneous coating of two and three materials, the behavior of Rayleigh waves is studied. The structure is a homogeneous half-space made of PZT-5H ferroelectric ceramics with a functionally graded coating, whose properties vary continuously in a non-monotonic manner from the parameters of one material to another. As coating materials, combinations of high- and low-speed PZT-based ceramics with various localization regions in thickness are considered. The study of the features of the surface waves propagation is based on solving boundary value problems of the electro-elasticity theory for media with an inhomogeneous coating, constructing the Green functions of the medium, and analyzing its dispersion properties. The solution is constructed in Fourier images with subsequent inversion; a combination of the analytical representation for its homogeneous components with high-precision numerical recovery for heterogeneous ones is used. The problems of the surface waves propagation from a remote point source of harmonic oscillations in a piezoelectric structure with an electrically free and shorted surface are considered. The influence of the ratio of physical parameters for the coating materials, the localization region, and the size of the transition zone of one material into another on the propagation features of Rayleigh waves at various oscillation frequencies is studied. Within the framework of models, the patterns of the frequency distribution for the effective coefficient of electromechanical coupling are studied depending on the nature of coating heterogeneity and its location. The results obtained are useful for understanding the dynamic processes in prestressed piezoelectric structures, and for optimizing and designing new constructions and devices based on surface acoustic waves (SAWs) with high operational characteristics.

#### ***Acknowledgements***

The work was carried out as part of the implementation of the state assignment for the Southern Scientific Centre of the Russian Academy of Sciences (SSC RAS), project No. 01201354242, and with partial financial support from the Russian Foundation for Basic Research, grants Nos. 19-08-01051 and 19-01-00719.

## **Specific Features of SH-Waves Propagation in Structures with Prestressed Inhomogeneous Coating Made of Piezoceramics Based on LiNbO<sub>3</sub>**

**T.I. Belyankova<sup>1\*</sup>, E.I. Vorovich<sup>2</sup>, V.V. Kalinchuk<sup>1</sup>, O.M. Tukodova<sup>2</sup>**

<sup>1</sup>*Southern Scientific Centre of Russian Academy of Sciences, Rostov-on-Don, Russia*

<sup>2</sup>*Don State Technical University, Rostov-on-Don, Russia*

[\\*tbelen415@mail.ru](mailto:*tbelen415@mail.ru)

Within the framework of the linearized theory of electro-elasticity, a model is considered for a piezoelectric structure with a prestressed functionally graded coating made of piezoceramics of a trigonal system with a 3m symmetry class in the natural state. Ferroelectric LiNbO<sub>3</sub> is used as the base material of the structure. It is assumed that the stress-strain state of the coating material is homogeneous and is induced by the action of initial mechanical stresses and an electric field. The properties of the coating vary in a continuous non-monotonic manner over the thickness. The propagation features are studied for surface acoustic waves (SAWs) caused by the action of a distant source of harmonic oscillations in structures with an electrically free and short-circuited surface. The constitutive relations and equations of motion for the electro-elastic medium, linearized in the vicinity of a certain equilibrium state, are used, which allow us to consider the effect of initial deformation on both the elastic and the piezoelectric and dielectric properties of the coating material. The model takes into account both coherent and separate influences of mechanical and electrical effects. The analysis of structural features of the surface wave field was carried out based on solving the boundary value problems of the electro-elasticity theory for media with an inhomogeneous coating, using the numerical-analytical method for constructing the Green functions, and analyzing the dispersion properties of the medium. The influence of coating inhomogeneity and the magnitude and area of its localization on the frequency distribution of SAW velocities is investigated. Within the framework of the model, the separate and combined influence of the initial effects on the change in the physical properties of the structure, the transformation of the surface wave field, and the change in the SAW velocities are studied in a wide frequency range, depending on the parameters of the electric field, and the type and magnitude of mechanical stresses. The results obtained in this work are useful for understanding the dynamic processes in prestressed piezoelectric structures and optimizing and designing new constructions and devices on surface acoustic waves with high-performance characteristics.

#### ***Acknowledgements***

This work was carried out as part of the implementation of the State assignment for the Southern Scientific Centre of Russian Academy of Sciences (state registration number 01201354242) and with the partial financial support of the Russian Foundation for Basic Research (grants Nos. 19-01-00719-a, 19-08-01051-a).

## **Nut Height Effect on Anti-loosening Performance of Pitch Difference Bolt Nut Connections**

**Biao Wang\*, Nao-Aki Noda, Yoshikazu Sano, Xi Liu, Yuto Inui,  
Bei-fen Siew**

*Department of Mechanical Engineering, Kyushu Institute of Technology,  
1-1 Sensui-cho, Tobata-ku, Kitakyushu-shi 804-8550, Japan*

[\\*gongliwangbiao@163.com](mailto:gongliwangbiao@163.com)

Prevailing torque is quite a popular way to prevent the self-loosening of bolt nut connections. In previous studies, it has been proven that when introducing a suitable pitch difference between the nut and the bolt, a prevailing torque appears so that the anti-loosening performance of the bolts can be improved a lot. For bolts with standard height, to obtain big enough prevailing torque to acquire good anti-loosening performance, the suitable pitch difference is quite large. However, when the pitch difference is too large, the improvement of fatigue life of the bolt nut connections will decrease. Therefore, to obtain a better combination of anti-loosening performance and fatigue life, the anti-loosening performance of long nut with pitch differences are investigated in this study. It is found that by increase the nut height, the same prevailing torque as that of the nut with standard height can be obtained.

## **An Effective Method for Recognizing Heterogeneities in Composite Materials**

**O. V. Bocharova<sup>1\*</sup>, I. E. Andjikovich<sup>2</sup>, A. V. Sedov<sup>1</sup>, V. V. Kalinchuk<sup>1</sup>.**

<sup>1</sup>*Southern Scientific Center, Russian Academy of Sciences, Rostov-on-Don, 344006, Russia*

<sup>2</sup>*Southern Federal University, Rostov-on-Don, 344090, Russia*

[\\*olga\\_rostov1983@mail.ru](mailto:olga_rostov1983@mail.ru)

Currently, composite materials are increasingly used in various industries. Sandwich composites are a special class of composite materials. These construction materials are becoming more and more popular due to their unique ability to reduce the weight of the finished product without losing mechanical properties. Sandwich composites have such important characteristics as low weight, high rigidity, strength, thermal insulation, vibration resistance, corrosion resistance, good dielectric properties, which allow their successive use in various industries, including aircraft construction, shipbuilding, wind energy, aerospace, transport, etc. During operation under conditions of high loads and vibrations, significant stresses arise in structures, which can lead to the appearance of delaminations, hidden defects in them, which sharply reduce their strength characteristics that can cause their destruction. This circumstance necessitates the development of new methods for identifying defects and heterogeneities in composite materials.

In the present work, an effective approach has been proposed that allows recognizing the presence of heterogeneity and determining its type, based on monitoring changes in the parameters of surface wave fields. To increase the informativeness of the wave field, an original method has been developed that allows capturing minor differences in wave fields. This method is based on the use of optimal signal expansions on a basis that is adaptively tuned to the maximum possible sensitivity to defects characteristics. A series of experimental studies has been conducted to investigate the possibility of using this approach to identify heterogeneities in a sandwich composite. The possibility of recognizing the presence and type of heterogeneity (separation of fiberglass, rigid

inclusions) from the reflected and transmitted wave field has been investigated. The experimental results showed that using of the proposed approach provides a clear recognition of the type of heterogeneity in the diagnostic space of images. When recognizing the presence of heterogeneity and determining its type in a sandwich composite, the transmitted wave field is more informative, which must be taken into account by choosing the sensor location.

#### ***Acknowledgement***

This work was supported by the Russian Foundation for the Basic Research (18-08-01012, 19-01-00719, 19-48-230042).

## **Modeling of Biological Tissues Taking into Account the Residual Stress**

**I. V. Bogachev**

*Southern Federal University, Rostov-on-Don, Russian Federation*

[bogachev89@yandex.ru](mailto:bogachev89@yandex.ru)

At the present time, the relevant task of biomechanics is to create an adequate models of various biological tissues as inhomogeneous media of complex structure. Models of this kind should take into account both the essential inhomogeneity of tissues and organs, as well as the possible presence of fields of residual stresses (prestress) in them. Prestress can have a natural occurrence, for example, in bones, blood vessels, muscle tissue, and appear after scarring of the tissue due to damage or surgery. Moreover, in medicine, a special place is occupied by the tasks of monitoring the physiological state of tissues and organs, which allows predicting the onset and development of various diseases and pathologies at the early stages, as well as monitoring the stages of restoration of damaged tissues (bones, tendons, soft tissues), and assessing the level of prestresses. One of the most common diagnostic methods is the ultrasound diagnostic method, which belongs to the class of acoustic methods. Its advantages include simplicity of practical implementation, universality of application for the whole organism and, most importantly, non-destructive effect. Numerous experimental data show that the behavior of the skin corresponds to a substantially nonlinear viscoelastic material, it is a composite material consisting of discrete parts. In this case, it is necessary to take into account the presence of several layers in it (epidermis, dermis and subcutaneous fat), which have their own characteristics. Due to these features, conventional solid models cannot adequately describe the experimental results of studies in the skin. It is also worth noting the need to take into account the factor of prestress that occurs in the upper layers of the skin in the result of scarring during damage, for example, after plastic surgery. Their contribution to the deformation pattern is quite significant. In this work, we consider the problem of restoring the properties of a viscoelastic layer inhomogeneous in thickness (modeling the skin), which in turn consists of three layers modeling the subcutaneous fat, dermis, and epidermis. These three layers are considered prestressed. A model of a standard viscoelastic body is used to describe viscoelastic behavior. The statement of the problem is written out on the base of a general linearized statement of the problem of oscillations of a body with residual stress-strain state. Mechanical characteristics and residual stress were considered as functions of the transverse coordinate. The inverse problem, which consists in determining the complex modules of each of the layers and the complex function



of prestress from the data on the acoustic response (amplitude-frequency characteristics) at a certain point on the surface of the skin, is formulated. To construct a computational scheme using the Fourier transform along the longitudinal coordinate, the initial two-dimensional problem is written in transformants. To solve the inverse problem, a projection solution scheme is constructed based on the expansion of the functions of complex modules, residual stress, and transformants of the displacement functions in some systems of linearly independent functions and the subsequent solution of systems of linear and nonlinear equations with respect to the expansion coefficients. The results of computational experiments of the restoration of various functions, characterizing the complex modules and prestresses of each of the layers of the skin, are presented.

#### ***Acknowledgement***

The work was supported by the Russian Science Foundation (project code 18-71-10045).

## **On the Identification of the Characteristics of Functional-Gradient Plates in the Framework of the Kirchhoff and Timoshenko Models**

**I. V. Bogachev**

*Southern Federal University, Rostov-on-Don, Russian Federation*

[bogachev89@yandex.ru](mailto:bogachev89@yandex.ru)

In modern mechanics, new models of functionally gradient plates are often used in solving problems associated with technical objects: plates with spraying from various materials used in the manufacture of blades and cutting discs, membrane pressure sensors, pipe flanges, piston systems. In this regard, the problems of identifying their characteristics, including the components of the tensor of elastic characteristics and density, which are functions of spatial coordinates, are very relevant. Their solution requires the development of effective non-destructive diagnostic methods based on the acoustic approach, as one of the simplest in practical implementation and therefore has several advantages. This study is a development of previous studies on the modeling of inhomogeneous round plates in the framework of the Kirchhoff and Timoshenko models. Moreover, in these studies, the density was considered known and constant, which is not always satisfied for functionally gradient materials. However, when using the iterative approach from one experiment, it is not possible to restore two functions at once. In the problem of plate vibrations in the framework of the Timoshenko model, a different projection approach was developed to solve the inverse problem. It consists in the unknown functions of mechanical characteristics, in particular, cylindrical stiffness, as well as the deflection and angle of rotation of the normal, were represented as expansions in some systems of linearly independent functions, and then systems of linear and nonlinear equations with respect to the coefficients of these expansions are successively solved. Later it was found that due to the fact that when using the projection method, a solution is searched for in a given class of functions, due to which the initial ill-posed inverse problem is regularized, this technique can be used to identify two or more unknown functions at once. In this report, two new statements of inverse problems on the identification of the functions of cylindrical stiffness in the analysis of steady-state oscillations of a circular functionally gradient plate inhomogeneous in the radial coordinate in the framework of the Kirchhoff and Timoshenko models are formulated.

Oscillations are excited by a uniformly distributed load applied to the upper face of the plate. The plate is considered symmetrical in angular coordinate and rigidly fixed along the contour. As input information for the inverse problem, we used the acoustic response at some point of the plate in a given set of frequencies. To solve the direct problems of calculating oscillations, solution schemes based on the Galerkin method are constructed. In this case, the influence of both sought functions on the amplitude-frequency characteristics is analyzed. In both cases, a generalized projection technique for solving inverse problems was constructed, the results of which are illustrated by sets of computational experiments to identify various functions.

#### ***Acknowledgement***

Research was financially supported by Southern Federal University, grant No. VnGr-07/2020-04-IM (Ministry of Science and Higher Education of the Russian Federation).

## **On the Modeling of Delamination of an Inhomogeneous Polymer Coating of a Strip**

**I.V. Bogachev\*, A.O. Vatulyan**

*Southern Federal University, Rostov-on-Don, Russian Federation*

[\\*bogachev89@yandex.ru](mailto:bogachev89@yandex.ru)

Functionally gradient polymer coatings are one of the most actively developing types of protective coatings. Moreover, modeling the appearance of defects in them, in particular, the appearance of delamination in coatings, is an urgent modern task. For protective and insulating coatings, the occurrence of delamination is a critical factor, and in diagnostics it is important to localize delamination, determining its nature and location, as well as to identify the causes of its occurrence. Functional gradient polymer coatings, whose properties depend on coordinates and can vary over wide ranges, are one of the common coating classes. Also, rheological properties are characteristic of such coatings and creep and relaxation processes take place. For such coatings, it is important to develop new effective non-destructive methods for diagnosing delamination. For modelling the delamination of functional gradient polymer coatings, we consider in this study the problem of calculating the vibrations of an inhomogeneous elastic strip with a peeling viscoelastic coating. The viscoelastic properties of the coating are described on the basis of the concept of complex modules, the equations of oscillations are written using the correspondence principle, in which elastic modules are replaced by functions of complex modules, which depend not only on spatial coordinates, but also on the frequency of oscillations. The lower edge of the strip is rigidly pinched, a load is applied to the upper edge in a given area. Between the substrate and the coating there is a peeling region, the coordinates of which are known. In this study, the mechanical characteristics of the strip and coating were considered as functions of the transverse coordinate. At the first stage, to construct disclosure functions in the delamination region using the integral Fourier transform, the problem is reduced to solving individual boundary value problems for the substrate and coating in transformants. The solution to each of the problems is presented as a linear combination of solutions to auxiliary Cauchy problems for various types of boundary conditions. Then, to construct the disclosure functions from the conditions that the stresses in the delamination region are zero

(delamination is modeled as a mathematical section), based on the inverse of the Fourier transform, the corresponding operator relations are formulated in the form of integral equations of the first kind. The kernels of the constructed operator relations are singular and are integrals over an infinite interval; special approaches are used to calculate them. Based on a similar approach, a scheme for calculating the displacement function at the upper boundary of the coating is constructed. The results of computational experiments on the influence of various sets of initial parameters of the problem are presented: (i) ratios of the modules of each layer; (ii) coating thickness on the opening and (iii) displacement functions at the upper boundary of the layer.

#### **Acknowledgement**

This work was supported by the Russian Science Foundation (project code 18-11-00069).

## **Relaxation Processes in the Organic Anti-Corrosion Films**

**A. S. Bogatin, E. N. Sidorenko\*, S. P. Shpanko, K. G. Abdulvakhidov**

*Southern Federal University, Rostov-on-Don, 344006, Russia*

[\\*si-do-re@mail.ru](mailto:si-do-re@mail.ru)

Previously, we have studied the properties of protective films based on an organic compound of the imidazole class and its compositions with chloride and rodanide anions. It was found that the impedance of these films is an inductive type impedance, regardless of the nature of anions, their concentration ( $C$ ), and the time of experience ( $t$ ). The electrical conductivity of the films with an area of  $1 \text{ cm}^2$  is large and varies from  $0.1$  to  $2 \text{ S}$  when exposed to uniaxial pressure up to  $2.5 \times 10^5 \text{ Pa}$  [1, 2]. It is known that various groups of relaxers are present in organic materials. Therefore, these films with high through conductivity are of increased interest for the study of relaxation processes in them [3]. In the frequency range of  $10^2 - 10^6 \text{ Hz}$ , the electric capacity and the tangent of the dielectric loss angle  $\text{tg} \delta$  of freshly prepared films obtained by adsorption of a composite inhibitor with different concentrations of the rodanide anion ( $C_{\text{KNCS}} = 0.01 - 0.09 \text{ mol/l}$ ) and the time of formation ( $t = 1 - 5 \text{ days}$ ) of the adsorption film were measured. In the frequency dependence of the complex permittivity the real part  $\varepsilon'(v)$  of films with the maximum values of  $C_{\text{KNCS}}$  and  $t$ , a deep relaxation-type dielectric dispersion is observed, accompanied by a multiple decrease in  $\varepsilon'$  with increasing frequency  $v$  of the measuring field. These films are characterized by very high low-frequency capacitance values (hundreds of  $\text{mkF}$ ) or static dielectric permittivity  $\varepsilon_0$ . At the plot of the  $\text{tg} \delta(v)$  dependence in the frequency range of  $10^4 - 10^5 \text{ Hz}$ , a blurred minimum is observed, which is typical for materials with highly developed relaxation processes and large through electrical conductivity. The frequency dependence of the imaginary part of the complex permittivity  $\varepsilon''(v)$  has no extrema: the value of  $\varepsilon''$  smoothly decreases tenfold with increasing frequency. The frequency dependence of the imaginary part of the complex conductivity  $\sigma''(v)$  has a clear maximum at a frequency of  $10^3 \text{ Hz}$ . The high electrical conductivity of the films changes the standard appearance of the Cole-Cole diagram. In the low-frequency region of the diagram  $\varepsilon'' \neq 0$ , with decreasing  $\varepsilon'$  the value of  $\varepsilon''$  does not increase, but, on the contrary, first sharply and then more smoothly decreases. The dependence  $\varepsilon'' = f(\varepsilon')$  has not a maximum and only in the high frequency region it is a part of the deformed circle. The phase shift between the current and the

voltage applied to the film is  $\varphi > 0$ , which indicates that the current oscillations is lagging relative to the voltage oscillations. The frequency dependence  $\varphi(\nu)$  is a curve with a maximum ( $\varphi_{\max} = 85^\circ$ ) at a frequency of 20 kHz. Over time, the relaxation processes are weakened, and when the uniaxial pressure is applied to the film, on the contrary, they increase. Zero values of the total capacitance of parallel connected film samples with capacitors of different ratings were obtained at different frequencies. This result confirms the previously obtained inductive character of these films impedance. Thus, the investigated organic films can be considered as disordered systems with a large through inertial electrical conductivity, non-Debye spectrum of dielectric permittivity, high phase sensitivity, highly developed relaxation processes, and with a high coefficient of steel corrosion inhibition.

### **References**

- [1] Shpanko S.P., Sidorenko E.N., Kuznetsova L.E., Sosin E.A. In: *Advanced Materials - Proceedings of the International Conference on "Physics and Mechanics of New Materials and Their Applications"*, PHENMA 2018, Springer Proceedings in Physics, Ivan A. Parinov, Shun-Hsyung Chang, Yun-Hae Kim (Eds.). Springer Nature, Cham, Switzerland, **224**, 123-130, 2019.
- [2] Shpanko S.P., Sidorenko E.N., Kuznetsova L.E., Abdolvakhidov K.G., Obuhov D.S. In: *Proceedings of the 2018 International Conference on Physics and Mechanics of New Materials and Their Applications*, Ivan A. Parinov, Shun-Hsyung Chang, Yun-Hae Kim (Eds.). Nova Science Publishers, New York, 13-19, 2019.
- [3] Bogatin A.S., Turik A.V. // *Processes of Relaxation Polarization in Dielectrics with High through Electrical Conductivity*. Rostov-on-Don. SFedU. Phoenix, 2013, 255 p. (In Russian).

## **Maxwell-Wagner Relaxation in the Layered $(1 - x)\text{NaNbO}_3 - x\text{Ca}_2\text{Nb}_2\text{O}_7$ Ceramics**

**N.A. Boldyrev\*, E.I. Sitalo**

*Research Institute of Physics, Southern Federal University, 344090, Rostov-on-Don, Russia*

[\\*nboldyrev@sfedu.ru](mailto:*nboldyrev@sfedu.ru)

Ceramics of binary systems solid solutions  $(1 - x)\text{NaNbO}_3 - x\text{Ca}_2\text{Nb}_2\text{O}_7$  ( $0 \leq x \leq 1$ ,  $\Delta x = 0.1$ ) with non-isostructural extreme components were prepared by the solid-phase reactions technique with following sintering using conventional ceramic technology.

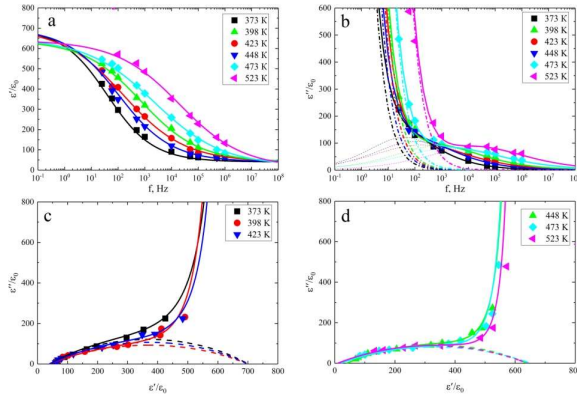


**Fig. 1.** Dependences of  $\varepsilon'/\varepsilon_0(f)$ ,  $\varepsilon''/\varepsilon_0(f)$  и  $\varepsilon''/\varepsilon_0(\varepsilon'/\varepsilon_0)$  in the  $0.7\text{NaNbO}_3 - 0.3\text{Ca}_2\text{Nb}_2\text{O}_7$  ceramics; the solid lines correspond to the calculation results for the case taking into account the contribution of the singular term; the dashed lines correspond to the calculation results without taking into account the contribution of the singular term

It was established that in a number of samples from layered zone, the Maxwell-Wagner polarization [1] and the corresponding relaxation are present. It manifested itself in the presence of frequency-dependent maxima in the dependences  $\varepsilon'/\varepsilon_0(T)$  and  $\text{tg}\delta(T)$ . It is shown that the anomalies, which are the consequence of the non-Debye dielectric relaxation, shift to the high temperature region with an increase in the frequency of the measuring electric field. The most probable cause of the revealed process can be described by Cole – Cole distribution function (Fig. 1) of Maxwell–Wagner relaxation with the wide spectrum of the distribution of relaxation times in the crystallite–interlayer heterogeneous system.

#### **Acknowledgements**

The work was supported by the Ministry of Science and Higher Education of the Russian Federation (State assignment in the field of scientific activity, Southern Federal University, 2020) with equipment of the CCU "EETPS", RIF SFedU.

#### **Reference**

[1] I.P. Raevski, S.A. Prosandeev, A.S. Bogatin, M.A. Malitskaya, L. Jastrabik // *J. Appl. Phys.*, **93**, 4130, 2003.

# New Quantum Spaser Theory

**Boris V. Bondarev**

*Moscow Aviation Institute, Moscow, Russia*

[bondarev.b@mail.ru](mailto:bondarev.b@mail.ru)

In nanophysics, structures of very small sizes were predicted theoretically and experimentally created – so-called spasers, which are analogous to lasers [1, 2]. Previously, the author of this report developed the laser theory based on the density matrix method [3, 4]. In this report, the new laser theory is applied to the description of the spaser operation. The kinetics of transitions between atomic energy levels is described by the equation:

$$dN_1/dt = - [ Q + B W(\omega) ] N_1 + [ A + B W(\omega) ] N_2, \quad (1)$$

where  $N_1 + N_2 = N$ ,  $N_1 = N_1(t)$  and  $N_2 = N_2(t)$  is the number of atoms in states 1 and 2 at time  $t$ ,  $N$  is the total number of active atoms,  $Q$  is the pumping intensity,  $A$  is the intensity of the spontaneous transition,  $B W(\omega)$  is the intensity of the transition under the action of radiation,  $W(\omega)$  is the spectral energy density of radiation. This formula is valid for spaser operation.

The operator  $\tilde{H}$  of the active atom in the coordinate representation may look as

$$H_{\alpha\beta} = \varepsilon_{\alpha}^{(0)} \delta_{\alpha\beta} + V_{\alpha\beta}, \quad (2)$$

where  $\alpha, \beta = 1, 2$ ;  $\varepsilon_1^{(0)}$  and  $\varepsilon_2^{(0)}$  are the energies at the first and second levels, and  $V_{\alpha\beta}$  are the matrix elements of the operator of the dipole interaction of a stationary atom and radiation. If the intensity of the electric field that acts on the atom is equal to  $\mathbf{E} = \mathbf{E}_0 \cos \omega t$ , where  $\mathbf{E}_0$  and  $\omega$  are the amplitude and frequency of the light incident on the atom, then the matrix elements will be equal:

$$V_{11} = V_{22} = 0, \quad V_{12} = V_{21}^* = -\mathbf{d} \cdot \mathbf{E}_0 \cos \omega t = -\hbar \Omega \cos \omega t, \quad (3)$$

where  $\mathbf{d}$  is the electric dipole moment of atom. The frequency  $\Omega = \mathbf{d} \cdot \mathbf{E}_0 / \hbar$ , is called the Rabi frequency. The eigenvalue of the atom energy can simply be found, if we know the Hamiltonian  $\tilde{H}_{\kappa\kappa'}$ , which is in diagonal form:

$$\tilde{H}_{\kappa\kappa'} = \varepsilon_{\kappa} \delta_{\kappa\kappa'}, \quad (4)$$

where  $\varepsilon_{\kappa}$  is the desired eigenvalue of the atom energy.

To go from the Hamiltonian  $H_{\alpha\beta}$  to the diagonal Hamiltonian  $\tilde{H}_{\kappa\kappa'}$ , one must find the unitary matrix  $U_{\alpha\kappa}$ . So, we know two Hamiltonians in  $\alpha$ - and  $\kappa$ -representations. Now, we can find the relations, connecting the density matrices  $\varrho_{\alpha\beta}$  and  $\tilde{\varrho}_{\kappa\kappa'}$  in these representations. To find the matrix  $\tilde{\varrho}_{\kappa\kappa'}$  write the equation:

$$i \hbar \partial \tilde{\varrho}_{\kappa\kappa'} / \partial t = \sum_{\eta} ( \tilde{H}_{\kappa\eta} \tilde{\varrho}_{\eta\kappa'} - \tilde{\varrho}_{\kappa\eta} \tilde{H}_{\eta\kappa'} ) + i \hbar \tilde{D}_{\kappa\kappa'}. \quad (5)$$

In the paper [5], it was proved that when the density matrix  $\tilde{\varrho}_{\kappa\kappa'}$  has a diagonal form, equation (5) transforms into the kinetic equation (1). In this way, we can find the dissipative matrix  $\tilde{D}_{\kappa\kappa'}$ , and then we find the density matrix in the  $\kappa$ -representation. Now we will find the spectral densities of radiation energies  $\Delta^+(x)$  and  $\Delta^-(x)$ , which fly along the length  $h$  of the resonator in opposite directions:

$$\mu c / N_A d\Delta^+ / dx = (A/2 + B \Delta^+) \varrho_{22} - B \Delta^+ \varrho_{11}, \quad (6)$$

$$-\mu c / N_A d\Delta^- / dx = (A/2 + B \Delta^-) \varrho_{22} - B \Delta^- \varrho_{11}, \quad (7)$$

where  $\mu$  is the constant of dimension,  $c$  is the speed of light,  $N_A$  is the number of active atoms on the path  $h$ ,  $\varrho_{11}$  and  $\varrho_{22}$  are the elements of the density matrix in the  $\alpha$ -representation. Solving these equations, we find the spectral density of the radiation emitted from the spaser:

$$\Delta_{\text{output}}^+(\omega) = F(\alpha, R, h) N_A \Omega^2 / \{ \mu \omega_0^2 [ (\omega - \omega_0)^2 + \Gamma^2 ] \}, \quad (8)$$

where  $F(\alpha, R, h)$  is the coefficient,  $R$  is the rate of reflection of light,  $\omega_0 = (\varepsilon_2^{(o)} - \varepsilon_1^{(o)})/\hbar$ ,  $\Gamma$  is the relaxation coefficient,  $\alpha = \mu N_A B (\varrho_{22} - \varrho_{11})/(2c)$ .

### References

- [1] Bergman D.J., Stockman M.I. // *Physical Review Letters*, **90**, 027402, 2003.  
 [2] Noginov M.A., Zhu G., Belgrave A.M., Bakker R., Shalaev V.M., Narimanov E.E., Stout S., Herz E., Suteewong T., Wiesner U. // *Nature*, **460**, 1110, 2009.  
 [3] Bondarev B.V. // *News Donetsk National University, Ser. A: Natural Sciences*, **4**, 54-68, 2017.  
 [4] Bondarev B.V. *My scientific articles. Book 3*. Moscow: Sputnik +, 2018.  
 [5] Bondarev B.V. // *Theor. Math. Phys.*, **100**, 33-43, 1994.

## Theory of Ball Lightning

**Boris V. Bondarev**

*Moscow Aviation Institute, Moscow, Russia*

[bondarev.b@mail.ru](mailto:bondarev.b@mail.ru)

Ball lightning is a glowing ball that moves randomly in the air. The temperature inside the balloon is assumed to be very high. Therefore, we will consider it such that all the atoms will be ionized, so that there are only electrons and nuclei of atoms in the ball, which we will consider all the same. Electrons are several thousand times lighter than nuclei. Therefore, we assume that the electrons are evenly distributed over the volume of the ball with the concentration  $w^{(e)} = 3 N Z / (4 \pi R^3)$ , where  $N$  is the number of nuclei,  $Z$  is the number of electrons in the atom, and  $R$  is the radius of the ball lightning. The potential energy of the nuclei in the electron field will be considered approximately equal to

$$U(r) = Z e^2 w^{(e)} r^2, \quad (1)$$

where  $e$  is the elementary electric charge,  $r$  is the distance from the center of the ball. Then the electrons will act on the nucleus with the force:

$$\mathbf{F} = - 2 Z e^2 w^{(e)} \mathbf{r}. \quad (2)$$

The most important equation that all quantum physics obeys is the equation for the statistical operator  $\hat{\rho}$ . This equation was phenomenologically written by Lindblad [1] as

$$i \hbar \partial \hat{\rho} / \partial t = [ \hat{H} \hat{\rho} ] + i \hbar \sum_{jk} C_{jk} \{ 2 \hat{a}_j \hat{\rho} \hat{a}_k^\dagger - \hat{a}_k^\dagger \hat{a}_j \hat{\rho} - \hat{\rho} \hat{a}_k^\dagger \hat{a}_j \}, \quad (3)$$

where  $\hat{H}$  is the Hamiltonian of the system,  $C_{jk}$  is some matrix, and  $\hat{a}_j$  is an arbitrary operator that still needs to be found.

In [2], two dissipative diffusion and attenuation operators were proposed:

$$\hat{\mathbf{a}}_1 = \hat{\mathbf{p}} + i \hbar \beta \hat{\mathbf{F}}/4, \quad \hat{\mathbf{a}}_2 = \hat{\mathbf{r}} + i \hbar \beta \hat{\mathbf{p}}/(4 M), \quad (4)$$

where  $\hat{r}$ ,  $\hat{p}$  and  $\hat{F}$  are the coordinate, momentum and force operators;  $M$  is the mass of the particle,  $\beta = 1/(k_B T)$  is the inverse temperature. Substituting these operators into the Linblad equation gives:

$$i \hbar \partial \hat{Q} / \partial t = [ \hat{H} \hat{Q} ] + i D / \hbar \{ [ \hat{p} [ \hat{p} \hat{Q} ] ] + i \hbar \beta / 2 [ \hat{p} [ \hat{F} \hat{Q} ]_+ ] \} + i \gamma / \hbar \{ [ \hat{r} [ \hat{r} \hat{Q} ] ] + i \hbar \beta / (2 M) [ \hat{r} [ \hat{p} \hat{Q} ]_+ ] \}, \quad (5)$$

where  $D$  and  $\gamma$  are the diffusion and attenuation coefficients. In this equation, the terms that contain  $\beta^2$  are discarded. Now substitute the formulas (1) and (2) in Equation (5). We will have an equation that describes the motion of nuclei in the ball lightning:

$$i \hbar \partial \hat{Q} / \partial t = [ \hat{p}^2 / (2 M) + Z e^2 w^{(e)} \hat{r}^2, \hat{Q} ] + i D / \hbar \{ [ \hat{p} [ \hat{p} \hat{Q} ] ] - 2 Z e^2 w^{(e)} i \hbar \beta / 2 [ \hat{p} [ \hat{r} \hat{Q} ]_+ ] \} + i \gamma / \hbar \{ [ \hat{r} [ \hat{r} \hat{Q} ] ] + i \hbar \beta / (2 M) [ \hat{r} [ \hat{p} \hat{Q} ]_+ ] \}. \quad (6)$$

In [3, 4], the following average values for atomic nuclei in the ball lightning were derived from Equation (6):

$$\partial \langle \mathbf{r} \rangle / \partial t = \langle \mathbf{p} \rangle / M, \quad \partial \langle \mathbf{p} \rangle / \partial t = - 2 Z e^2 w^{(e)} \langle \mathbf{r} \rangle - 2 \gamma \beta / M \langle \mathbf{p} \rangle; \quad (7)$$

$$\langle \hat{r}^2 \rangle = 2 N / F \{ [ (\gamma \beta)^2 + 2 \gamma \beta^2 D g + 2 g ] D + \gamma / M \}, \quad (8)$$

$$\langle \hat{p}^2 \rangle = 4 g N / F \{ 2 g D M + (D \beta^2 \gamma + 2 D^2 \beta^2 g M + 1) \gamma \}, \quad (9)$$

where  $g = 4 g \beta \{ D \gamma \beta (\gamma \beta / M + 2 D g \beta) + \gamma / M + 2 D g \}$ ,  $g = Z e^2 w^{(e)}$ . Consider two extreme cases, when either  $D = 0$  or  $\gamma = 0$ . In all these cases, we have:

$$\langle \hat{r}^2 \rangle = N / (2 Z e^2 w^{(e)} \beta), \quad \langle \hat{p}^2 \rangle = M N / \beta.$$

It is shown that the atomic nuclei will be distributed over the volume of the ball lightning approximately according to the formula:

$$w(\mathbf{r}) = N B(R, \alpha) \exp(-\alpha r^2). \quad (10)$$

where  $B = 2 \beta Z e^2 w^{(e)}$ .

### References

- [1] Lindblad G. // *Commun. Math. Phys.*, **48**, 119-130, 1976.
- [2] Bondarev B.V. // *Physica A*, **176**(2), 366-386, 1991.
- [3] Bondarev B.V. // *Scientific Discussion*, **1**(38), 37-44, 2019.
- [4] Bondarev B.V. // *Scientific Discussion*, **1**(39), 10-16, 2020.

## Asymptotics of Displacements in Back-reflected Ultrasonic Waves from a 3D Defect Located in an Elastic Material

N.V. Boyev

*I. I. Vorovich Mathematics, Mechanics and Computer Science Institute,  
Southern Federal University, Rostov-on-Don, Russia*

[nvboev@sfedu.ru](mailto:nvboev@sfedu.ru)

Within the framework of the geometric theory of diffraction (GTD), the leading term of the asymptotic behavior of the displacement amplitude is obtained in the case of backscattering of longitudinal and transverse waves in the far field approximation. The practical importance of this study is that obstacles in acoustic media and defects in elastic media are detected during ultrasonic



non-destructive testing (UNT) by high-frequency acoustic and elastic waves in the echo mode. This type of scan allows one to get in any direction the transit time of the reflected echo signal and its amplitude. Such data form the basis of the method of reconstruction of obstacles with a complex shape. Often, in UNT, to detect defects in structural elements, separately combined sensors are used that operate on longitudinal waves both in contact mode with the surface of the defect and in installations that implement the immersion monitoring method. Such sensors usually operate in echo mode. However, the existence of two types of waves in an elastic medium and their possible transformation on the boundary surface of an obstacle located in an elastic medium require substantiation of the models used in UNT. This is of particular relevance in the inverse problems of UNT. To excite acoustic waves in an elastic medium with possible defects, we will use a temporarily finite impulse. We suppose that the tonal filling of the pulse contains enough wavelengths (for example, 6 – 10 waves) of harmonic oscillations. This allows us to consider the problem in the approximation of a model of steady-state oscillations of an elastic medium. Moreover, we suppose that the defect is located at a sufficient distance from the oscillation source, which makes it possible to use the far field approximation at high vibration frequencies in the calculations of the waves incident and reflected from the defect surface. An ultrasonic longitudinal plane wave introduced into the elastic material interacts with the obstacle surface, is scattered on it, and the sensor detects the backward wave that came from the defect. If the scattering surface is smooth, then the first pulse received will be reflected from the vicinity of the surface point, the normal in which is parallel to the direction of propagation of the high frequency radiated longitudinal wave. By replacing plane wave introduced into the material with the superposition of point sources of spherical waves, each of which is caused by a concentrated force that varies in time according to a harmonic law, the original problem is reduced to studying the problem in a local setting. The study of the local problem is based on the physical theory of Kirchhoff diffraction. In the framework of the GTD for reflected longitudinal and transverse waves from obstacle surfaces in two-dimensional and spatial cases, it is shown that the main term of the reflected incoming wave will be determined by the longitudinal wave.

## **Power Processing Equipment of Oil Refineries**

**VA. Brazhnikov, D. D. Fugarov\*, O. A. Purchina, N.V. Rasteryaev**

*Don State Technical University, Rostov-on-Don, Russia*

\*[ddf\\_1@mail.ru](mailto:ddf_1@mail.ru)

One of the most important elements of the general modernization of oil and gas industry is the replacement of obsolete converters and motor drives for automation systems for in-field oil collection, treatment, transportation and refining [1]. Application of electric converters in industry, on transport and in life constantly extends [2]. Now already more than 60% of all electric energy developed in the world are consumed by electric motors [3]. Therefore, the efficiency of energy saving technologies is defined considerably by efficiency of converters of electric drives [4]. Development of high-performance, compact and economical power converters is the priority direction of the development of modern equipment. Growth of extent of integration in the

microprocessor equipment and transition from microprocessors to microcontrollers with a built-in set of specialized peripheral devices, made irreversible a trend of mass replacement of analog control systems of drives by the systems of direct digital control [5].

### **References**

- [1] Fugarov D.D. In: *2019 International Conference on "Physics and Mechanics of New Materials and Their Applications", PHENMA 2019*, Hanoi, Vietnam, November 7 – 10, 2019, Hanoi University of Science and Technology: Hanoi. 119-120, 2019.
- [2] Y.O. Chernyshev, O.A. Purchina, A.Y. Poluyan, D.D. Fugarov, A.V. Basova, O.V. Smirnova // *Journal of Theoretical and Applied Information Technology*. **80**(1), 13-20, 2015.
- [3] Poluyan A.Y., Fugarov D.D., Purchina O.A., Nesterchuk V.V., Smirnova O.V., Petrenkova S.B. // *Journal of Physics: Conference Series "International Conference Information Technologies in Business and Industry 2018 - Microprocessor Systems and Telecommunications"*. 022013, 2018.
- [4] Fugarov D.D., Gerasimenko Y.Y., Nesterchuk V.V., Gerasimenko A.N., Onyshko D.A. // *Journal of Physics: Conference Series*. 012055, 2018.
- [5] Solomentsev K.Y., Fugarov D.D., Purchina O.A., Poluyan A.Y., Nesterchuk V.V., Petrenkova S.B. // *Journal of Physics: Conference Series*. **1015**, 032179, 2018.

## **Failure Risk Analysis of Centralized Domestic Wastewater Management System in Buleleng District (With Failure Mode Effect Analysis Method)**

**Budi Witjaksana\*, Sri Astutik, Wateno Oetomo, Romadhon**

*Civil Engineering Department, University of 17 Agustus 1945 Surabaya Indonesia*

\*[budiwitjaksana@untag-sby.ac.id](mailto:budiwitjaksana@untag-sby.ac.id)

Domestic wastewater is waste that comes from the activities of everyday human life related to water usage. Disposal of domestic wastewater without a treatment process will result in pollution of the sources of raw water for drinking water, both surface water (river, lake, or territory) and groundwater. Wastewater management consists of treating on-site wastewater on an individual basis by providing wastewater treatment tanks or septic tanks and off-site sewage systems carried out collectively or communally through sewerage collection channels and then processed in Wastewater Treatment Plant (WWTP). Some obstacles in the centralized management of domestic wastewater systems, among others, are caused by the legislation that does not yet support, the lack of community participation, high cost in financial factors, and also weak technology aspects. The construction of the WWTP unit uses a large number of funds, so it is unfortunate if it cannot be utilized according to its function. To avoid all types of failures related to the non-operation of WWTP, failure analysis can be done. This analysis is expected to be an effort to support the functioning of the Central Domestic Wastewater Management System sustainably. The risk modeling that can be used is Fishbone Analysis and Failure Mode Effect Analysis (FMEA). Failure Mode Effect Analysis (FMEA) is a powerful method for identifying risks. FMEA is implemented to identify potential forms of failure, determine their impact on production, and define the operations to reduce failure. The results of failure risk analysis using Fishbone Analysis and FMEA obtained 19 risks and the highest priority failure risks for the sustainability of the Centralized

Domestic Waste Management System, namely: (i) maintenance of WWTP buildings, (ii) HR capacity, (iii) payment of contributions and subsidies for regional government funding. To minimize failures in the Central Domestic Wastewater Management System, it is necessary to (i) make the Standard Operating Procedure (SOP) for main building maintenance (IPAL), (ii) periodically clean and maintain the WWTP building, (iii) participate in the system management training Centralized Domestic Waste Water Management and (iv) evaluate financial aspects in the context of operational efficiency and maintenance of Centralized Domestic Waste Water Management Systems.

## **Effect of High-Voltage Nanosecond Pulses Treatment on the Surface Properties and Floatability of Pentlandite and Pyrrhotite**

**I. Zh. Bunin\*, I.A. Khabarova**

*Institute of Comprehensive Exploitation of Mineral Resources of the Russian Academy of Sciences (IPKON RAS), Moscow, Russia*

[\\*bunin\\_i@mail.ru](mailto:bunin_i@mail.ru)

In recent years, the various kinds of power influences on minerals, mineral suspensions and water, such as electrochemical, microwave treatment, electro-pulse, magnetic-pulse processing, the effect by accelerated electrons flow, high-power nanosecond electromagnetic pulses are used in order to improve the selective disintegration of mineral complexes and to increase contrast between technological properties of mineral raw material [1, 2]. The study of processing mechanisms by the concentrated energy flows and electromagnetic pulse fields of high intensity on mechanical, structural, chemical and technological properties of geomaterials with the aim of their application for the directed change of their chemical and phase surface composition is a major scientific and technological problem [2]. According to the modern experimental data [3, 4], the research into the application of microwave irradiation in the comminution and flotation of ores has made great progress. Microwave irradiation promotes the oxidation of sulfide minerals during exposure, and the extent of the oxidation is an important factor in the flotation of microwave-treated sulfides [2 – 4]. Microwave irradiation ( $t_{\text{treat}} = 5, 10$  and  $20$  s) led to the decrease in the floatability of chalcopyrite and pyrrhotite in the presence of xanthate, at the pH values equal to 4, 7 and 10, whereas no significant change was observed for pentlandite. The results presented by the works [4] indicate potential conditions to achieve selectivity between the microwave-pretreated chalcopyrite, pentlandite and pyrrhotite. In our study, we present the main experiment results on the *nonthermal* effect of high-power (high-voltage) nanosecond pulses (HPEMP) on the chemical surface composition and flotation properties of pyrrhotite and pentlandite. It should be noted that, for the mineral samples pulse processing, we used the special mode of the nanosecond repetitively pulsed discharges in air at atmospheric pressure, namely the spark regime. In the result of made microscopic and spectroscopic researches the relationship between the chemical composition of surface micro- and nanophases with the electrochemical, sorption and flotation properties of pyrrhotite and pentlandite under the influence of HPEMP has been established. Using scanning electron microscopy, X-ray microanalysis, chemical analysis of the liquid phase, the stage of

sequential oxidation of the surface of pyrrhotite together with the formation of oxides (hydroxides) and divalent and ferric sulfates under pulsed spark discharges in air were established. Whereas the formation of elemental sulfur on pentlandite was observed. This effect provides the contrast of electrochemical, sorption and flotation properties of pyrrhotite and pentlandite. HPEMP caused a different change in the electrode potential of minerals: an increase in the negative value of the electrode potential of pyrrhotite and an increase in the positive value of the pentlandite potential. The shift of the pentlandite electrode potential to the region of more positive values increased the anionic collector adsorption and the hydrophobization of the mineral surface. The transition of the pyrrhotite potential to the region of negative values prevented the xanthate adsorption and decreased the mineral floatability. For monomineral flotation of pyrrhotite and pentlandite, we established the optimal mode of preliminary electromagnetic pulsed processing of minerals ( $t_{\text{treat}} = 10$  s,  $N_{\text{imp}} = 10^3$ ), at which the contrast of their flotation properties increases in the mean on 20%.

#### **References**

- [1] Chanturiya V.A. // *Gornyi Zhurnal (Mining J.)*, **11** (2017).
- [2] Bunin I.Zh., Ryazantseva M.V., Samusev A.L., Khabarova I.A. // *Mining J.*, **11** (2017).
- [3] Batchelor A.R., Jones D.A., Plint S., Kingman S.W. // *Minerals Engineering*. **94** (2016).
- [4] Silva G.R., Waters K.E. // *Advanced Power Technology*, **29** (2018).

## **Influence of Technogenic Raw Materials on the Physical and Mechanical Properties of Ceramic Products**

**N.I. Buravchuk<sup>1\*</sup>, O.V. Guryanova<sup>1\*\*</sup>, E. P. Putri<sup>2</sup>**

<sup>1</sup>*I. I. Vorovich Mathematics, Mechanics and Computer Sciences Institute, Southern Federal University, Rostov-on-Don, Russia*

<sup>2</sup>*Department of Industrial Engineering, University of 17 Agustus 1945 (UNTAG) Surabaya, Indonesia*

\*[burav44@mail.ru](mailto:burav44@mail.ru), \*\*[guryanovaolga@mail.ru](mailto:guryanovaolga@mail.ru)

Ceramic goods are among the most ancient building materials. Due to the fire resistance and high durability of bricks and ceramic stones, the walls of buildings and structures made of them have advantages over walls made of wood, concrete, cinder blocks and other materials. The use of durable and expressive ceramic finishing materials improves the architectural appearance of buildings and reduces their operating costs. Recently, the rate of civil and industrial building, has noticeably increased and the need in bricks has increased. The goods with high consumer properties at a relatively low cost can win the competition for markets. It is possible to solve these two problems: to improve the quality and reduce the cost of production of building bricks. It is possible through the use of waste from the extraction and combustion of coal-mine rocks and ash-slag waste. Most of the waste of ash-slag and mine dumps by the amount of mineral raw materials contained in them, by the composition and properties of the stored rocks, are technogenic deposits, and the man-made masses (ash-slag and rocks) accumulated in the dumps are similar in properties to natural mineral raw materials used in the ceramic industry. The use of coal waste as a technological additive makes it possible to improve the technological properties of the charge based on local clay raw

materials, to correct the physical and mechanical properties of ceramic wall materials, to replace some of the clay raw materials, and to solve some environmental aspects of environmental protection. Deposits of clays suitable for the production of wall building ceramics are limited and are depleted every year. In most regions, low-quality loamy raw materials are used for brick production, from which it is difficult to obtain wall ceramic products with increased strength and frost resistance. Scientific research and the experience of enterprises show that it is possible to correct the physical and mechanical properties of ceramic goods by introducing coal waste and ash-slag mixtures similar in chemical composition to the clay raw materials into the raw charge [1 – 4]. The specific features of ash-slag waste and mine rocks are the proximity of the material composition to clay raw materials, dispersion, the presence of residual carbon and low-melting oxides, which can be used in the firing process. It creates the preconditions for the widespread use of these wastes in the manufacture of ceramic wall materials. Large-scale use of carbon waste is restrained mainly due to the low organization of supplies to consumers of this raw material that meets the requirements for granularity, humidity, lack of technical conditions for their use, taking into account the chemical composition, and heterogeneity. To use ash-slag waste and burnt rocks in the technology of ceramic bricks, technological samples of technogenic and clay raw materials were taken, a comprehensive assessment of the quality of technogenic raw materials was carried out. Studies were carried out on the effect of additives of burnt rocks, ash-slag waste on the technological and physical-mechanical properties of ceramic masses for wall, roofing materials, refractories, facade tiles and artistic ceramics. Physical, mechanical and technological tests were carried out at the enterprises of building ceramics in the Rostov region. Ash-slag mixture is a product of coal combustion in boiler furnaces at temperatures above 1000 °C, up to 1700 °C. The ash-slag mixture contains up to 30% fly ash with a specific surface area of 300 – 350 m<sup>2</sup>/kg. A glass phase is present in the ash-slag mixture. When coal is mined, associated rocks are stored on the surface in dumps. In the result of long-term self-burning of rocks in ovals at temperatures above 1000 °C, burnt rocks are formed. Burned rocks and ash-slag mixtures are inherently non-plastic materials. In the composition of the raw material charge for ceramic goods, ash-slag mixture and burnt rocks play the role of a lean additive, flux, microfiller, improve the granulometric composition of the charge, reduce the sensitivity of clay raw materials to drying, and increase the sintering capacity of the charge. The presence of spherical particles in the grain composition of the ash-slag mixture creates a plasticizing effect that improves the formation of goods. Burned rocks and ash-slag mixtures contain metakaolinite, reactive modifications of silica, alumina, iron oxides that have arisen in the process of firing in dumps or boiler furnaces. The presence of these active components contributes to the formation of strong contacts, the formation of a spatial structural framework of the composition during drying, which turns into a homogeneous structure of a ceramic shard during firing. Pilot tests of the existing developments were carried out at the factories of the construction industry of the Rostov region. Burnt rocks of the mine dump and ash-slag mixture are subjected to crushing, grinding and fractionation. The moisture content of lean additives is 2-3%. The content of burnt rocks in ceramic masses is from 15 to 35%, ash-slag mixture is from 15 to 40%. The molding moisture content of the charge decreases and for semi-dry pressing is 7 – 9%, for plastic, it is 18 – 22%. The firing temperature of goods is in the range of 970 – 1100 °C. Structural and mechanical properties of ceramic goods begin to form in the process of compaction of the raw mix and are fixed during drying and firing. The dispersed-reinforcing component is quartz grains that form the quartz strengthening skeleton of the composition. The source of quartz grains is burnt rocks and ash-slag mixture. Clay is a technological binder at the stage of formation of coagulation

structures during pressing and condensation-crystallization ceramic shards during firing. The introduction of complex additives to clay intensifies the sintering process of the charge due to the appearance of low-melting eutectics and an increase in the glassy phase. The selected composition of lean additives helps to reduce volumetric changes in the composition and the stability of the forming structure of the composition at all stages of the technological process. The greatest indicators of strength, frost resistance of a ceramic shard is associated with the presence of mullite, anorthite, wollastonite. These minerals are present in burnt rocks and ash-slag materials and are formed during the firing of the components of the ceramic mass. In addition, wollastonite, which is present in the non-plastic starting materials of the mixture and formed during firing, reduces volumetric changes, internal stresses and shrinkage of the ceramic shard. In the result of the joint manifestation of the properties of the charge components during molding, drying and firing, the structure of a ceramic shard of high strength and frost resistance is formed. Strength grade can reach "600" in frost resistance, namely not less than 300 cycles of alternate freezing and thawing. Ceramic products have a sintered ceramic shard of a homogeneous structure (Fig. 1). Quartz, anorthite, mullite, wollastonite were identified from the crystalline phases in the ceramic structure. The increased amount of glass phase and the absence of feldspars in the form of crystalline phases allows us to conclude that the formation of the ceramic shard is completed. There are no signs of deformations, cracks, or burn marks in the goods. The products have an even color with various shades, a clear shape, and an expressive architectural appeal (Fig. 2). With the appearance in the Rostov region on some waste heaps and ash dumps of crushing and sorting complexes for the processing and preparation of conditioned raw materials from burnt rocks and ash-slag mixture, the construction industry enterprises have a real opportunity to improve using technogenic waste in the production of building ceramics, refractories, tiles, facing tiles and decorative ceramics.

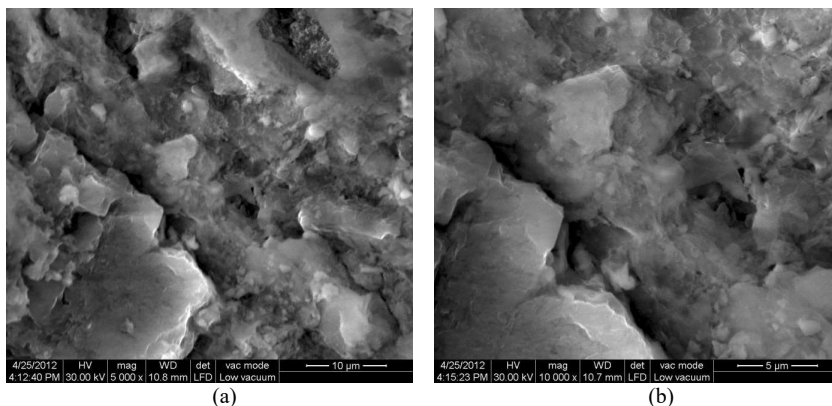


**Fig. 1.** Microstructure of a ceramic sample, containing burnt rocks:

(a) magnification - 5,000×; resolution - 10 µm; (b) magnification - 10,000×; resolution - 5 µm



**Fig. 2.** Samples of ceramic products made in the ceramic workshops of building materials factories

#### **Acknowledgement**

Research was financially supported by Southern Federal University, grant No. VnGr-07/2020-04-IM (Ministry of Science and Higher Education of the Russian Federation).

#### **References**

- [1] Abdrakhimova E.S. // *Coal*. 7, 67–69, 2019 (In Russian).
- [2] Fedorova N.V., Shaforost D.A. // *Teploenergetika*. 1, 53–58, 2015 (In Russian).
- [3] Abdrakhimov V.Z., Shevando V.V., Abdrakhimov A.V. et al. // *News of Universities. Building*. 7, 20 – 25, 2008 (In Russian).
- [4] Buravchuk N.I. *Resource Saving in Building Materials Technology*. Rostov-on-Don: Southern Federal University Press, 2009 (In Russian).

## **Technological Aspects of Obtaining Disperse-grained Composites Based on Solid Combustible Carbon-Containing Waste**

**N.I. Buravchuk<sup>1\*</sup>, O.V. Guryanova<sup>1\*\*</sup>, E. P. Putri<sup>2</sup>**

<sup>1</sup>*I. Vorovich Mathematics, Mechanics and Computer Sciences Institute, Southern Federal University, Rostov-on-Don, Russia*

<sup>2</sup>*Department of Industrial Engineering, University of 17 Agustus 1945 (UNTAG) Surabaya, Indonesia*

\*[burav44@mail.ru](mailto:burav44@mail.ru), \*\*[guryanovaolga@mail.ru](mailto:guryanovaolga@mail.ru)

The coal industry occupies one of the leading places in the mineral-industrial complex of Russia and is an intensive source of technogenic impact on the environment. Coal regions, due to their

specific socio-economic development, experience significant technogenic pressures, as a result of which intensive changes occur in all components of the environment. So, in the process of coal mining, during the enrichment, transportation, storage and transportation to the consumer, a large amount of coal waste (anthracite mine, coke and coal fines, coal sludges) is generated. Unused coal mining wastes are dumped. Significant areas of land suitable for agriculture are allocated for such dumps having the status of technogenic deposits [1, 2]. Dumps occupy about 20% of the area of all disturbed lands and, in addition, pollute the environment with greenhouse gases, toxic and harmful substances, soil and water with harmful ingredients. Long-term storage of significant volumes of fine-grained and finely dispersed fines in the open air leads to its ingress with flood and storm waters into the basins of nearby rivers. At the same time, the study of such qualitative characteristics of carbon-containing materials as: ash, sulfur content, calorific value, yield of volatile substances, made it possible to establish their prospects for use after proper processing as a full-fledged household fuel. Stocks of such waste having a certain energy potential are large. One of the major consumers of solid fuels is layered furnace devices for industrial energy and public utilities. For these purposes, ordinary, fine-grained or low-grade coals with a high yield of volatile substances are used that emit a lot of smoke, soot, and dust when burning. The use of such coals does not ensure the completeness of fuel combustion and, accordingly, the high thermal performance of power plants. The fuel, used in power plants, is subject to quality requirements in the direction of reducing environmental pollution by coal dust, harmful oxides of sulfur, nitrogen, etc. This is especially true for coal intended for burning in domestic stoves, small boiler houses and other small power plants, where there is no centralized system for collecting harmful emissions. It is almost impossible to control the quality of emissions of such power plants. Consumers in the household sector need fuel. Demand for high-quality coal will increase. Given the current tendency to reduce the production of high-quality coals for domestic needs, there is a need for additional types of solid fuel. Meanwhile, the reserves of coal fine-grained materials are huge. However, their use is difficult, and often almost impossible because of the complexity of transportation, dusting, incomplete combustion. Under these conditions, it is necessary to look for opportunities for the rational use of technological trifles and low-grade coals and other energy-bearing waste, to create technologies that replenish the reserves of conditioned fuel. It is possible to obtain a product with the necessary properties from substandard, but having a certain energy potential, raw materials by applying briquetting technology. If there is a raw material base for obtaining fuel briquettes, a technology is needed that ensures environmentally efficient production of products with specified quality indicators. The most justified technological direction, which can provide fuel with satisfactory consumer characteristics, is briquetting of substandard carbon-containing waste with binders. This is a universal way to obtain briquettes from virtually any material. Fine-grained coals were briquetted: anthracite cobs, coke, coal fines, coal sludges. The following materials were used as coal raw materials for research:

- (i) *anthracite fines (bayonet)* are the screenings of anthracite and waste from coal processing plants, fraction is 0-6 mm; carbon content in organic matter is 93.0–95.0% and density is 1.4–1.8 g/cm<sup>3</sup>;
  - (ii) *coal fines* are the screenings of coal and waste from coal processing plants; carbon content is 76–90% and density is 1.2–1.8 g/cm<sup>3</sup>;
  - (iii) *coal sludge* is waste from coal preparation plants, fine grades of anthracite, bituminous coal, particle size is 0–1 mm.
  - (iv) *coke breeze* is coke screenings, contain 82–88 % of carbon, density is 1.4–1.95 g/cm<sup>3</sup>.
- Technical characteristics of coal technogenic raw materials are given in Table 1.



**Table 1.** Technical properties of coal technogenic raw materials

Type of raw material	Quality indicators			
	Ash content, %	Humidity, %	Calorific ability, MJ/kg	Volatiles output, %
Culm	5.0–33.0	9.0–12.0	18.8–28.2	3.0–9.0
Coal fines	14.6–20.0	4.0–12.8	12.4–27.2	11.0–43.5
Coal sludge	26.0–45.0	8.0–28.0	14.9–18.5	5.0–9.0
Coke breeze	10.0–12.0	4.0–16.0	15.2–36.4	21.0–28.0

Molasses, a by-product of sugar beet production, belonging to the group of disaccharides, was used as the basis of the binder for briquetting carbonaceous raw materials. The chemical averaged composition of molasses ash is given in Table. 2.

**Table 2.** Chemical composition of molasses, weight. %

K <sub>2</sub> O	Na <sub>2</sub> O	CaO	MgO	Al <sub>2</sub> O <sub>3</sub>	SO <sub>3</sub>	Other oxides
76.4	11.2	3.5	0,5	3.7	0.2	4.5

Briquetting technology is developed in laboratory under semi-factory conditions [3–5]. Experimental batches of briquettes were manufactured at the IOTT production base in the city of Zhilevo, Moscow Region. Accredited laboratories carried out technical analysis and burning of fuel briquettes (see, Table 3 and Fig. 1).

**Table 3.** Results of experimental combustion of experimental batches of fuel briquettes

Type of fuel	Weight of the sample, kg	Ash content, $A^d$ , %	Mass fraction of moisture in the working fuel, $W_f$ , %	Weight of the unburnt residue from the furnace, %	Weight of the unburnt residue from the ashpit, %	Amount of fuel burnt, %	Epy amount (remainder) of unburned fuel, %
Briquettes	39.4	13.9	4.0	1.05	12.95	64.5	35.5
Coal grade AM	41.1	9.0	3.2	1.5	8.7	75.2	24.8

The nature of the combustion of molasses briquettes and high-quality coal is almost identical. The temperature resistance of briquettes is characterized as "very good", the briquettes do not crumble during combustion, retain their shape, withstand mechanical stress, korzhes do not form, combustion proceeds without smell, the ash residue does not sinter, and is dusty in structure. By technical characteristics, briquettes satisfy consumer requirements. Briquette quality indicators are: mechanical abrasion resistance (89 – 91%), dropping strength (90 – 100%), compression (12 – 16 MPa), ash content (6.5 – 19.7%), volatiles yield (3.3 – 9.0%), sulfur content (0.81 – 1.9%), water

absorption (1.1 – 3.8%), calorific value of working fuel (24.60 – 28.78 MJ/kg). The prepared briquettes can be used as fuel in fireplaces, stoves, boiler rooms or reprocessed in gas generators into heat, into generator gas and then into electricity. The demand for solid fuel is growing steadily, the fuel market is almost empty. The organization of production of conditioned briquetted fuel makes it possible to at least partially reduce the growing coal deficit and, above all, for furnace devices in the household sector and thermal units of industrial energy. Involvement of coal fines in the heat balance will make it possible to obtain additional fuel and at the same time reduce the level of environmental pollution.



**Fig. 1.** Samples of fuel briquettes made in laboratory and industrial conditions

#### ***Acknowledgement***

Research was financially supported by Southern Federal University, grant No. VnGr-07/2020-04-IM (Ministry of Science and Higher Education of the Russian Federation).

#### ***References***

- [1] Trubetskoy K.N., Umanets V.N. // *Mining Journal*. **1**, 12–16, 1992 (In Russian).
- [2] Trubetskoy K.N. Terpogosoov Z.A. Shitarev V.G. // *Mining Journal*. **3**, 44–66, 1994 (In Russian).
- [3] Buravchuk N.I., Guryanova O.V. // *Chemistry of Solid Fuels*. **4**, 49–53, 2014 (In Russian).
- [4] Buravchuk N.I., Guryanova O.V. *A method of Manufacturing a Fuel Briquette (Options)*. Russian Patent No. 2396306, 08.10.2010 (In Russian).
- [5] Buravchuk N.I., Guryanova O.V. Composition for Obtaining a Fuel Briquette. Russian Patent No. 2629365, 08.29.2017 (In Russian).

## **Mechanical Properties of Large-Scale Composite Structures According to Process Conditions**

**Chang-Wook Park, Sung-Won Yoon\***

*Research Institute of Medium & Shipbuilding, 38-6 Noksan Industrial Complex-232 Ro, Gangseo-Gu, Busan, Republic of Korea*

[\\*swyoon@rims.re.kr](mailto:swyoon@rims.re.kr)

The purpose of this study is to determine the correct estimation of the concept design and laminating pattern for composites. In this study, the effect of carbon tow prepreg on the composite structure has been investigated. Also, this work evaluated the structural safety according to the laminating pattern and process technique by computer simulation. The laminating pattern of three kinds was designed through the normal shape. Also, process technique of two kinds were carried out in dry and wet method to produce composites structure. The result of FEA showed that the structural safety of carbon tow prepreg is not significantly superior to that of the shaft with wet method material. However, considering the benefits of working environment and the reduction of the number of process, the possibility of replacing materials and process technique will be sufficient for composite structure.

## **Modeling the Contact Interaction of Spherical Hinge Joint in the Presence of Wear**

**M. I. Chebakov\*, S. A. Danilchenko**

*South Federal University, Rostov-on-Don, Russia*

[\\*michebakov@yandex.ru](mailto:michebakov@yandex.ru)

Hinge joints are used to couple machine elements and mechanisms that are movable relative to each other in sliding mode. Moreover, such compounds are used in biomechanics in the manufacture of prostheses. Ball joints and tips exist in various designs, with different sliding surfaces for a specific application. So, for example, self-lubricating joints are actively used. They consist of an inner ring with a convex spherical outer surface, which corresponds to an outer ring with a concave spherical inner surface. The sliding surfaces of these joints have special coatings made of modern materials. They have a low coefficient of friction and do not require periodic maintenance. These joints are used when a long period of operation of the hinge is required, or when operating conditions (for example, no lubrication system) make the use of steel/steel hinges undesirable. Self-lubricating hinges are fundamentally designed for use with increased loads and with a constant load direction. In the present work, the contact problem of the wear of the joint is considered. To solve the set problems, the finite element method and the ANSYS software package were used. As a model describing the wear process, the Archard model was used. The wear of the contacting surfaces was

calculated for various mechanical characteristics of the coatings, loading and rotation parameters. The effect of various combinations of coatings on the wear rate under the same operating conditions is investigated.

**Acknowledgment**

Research was financially supported by Southern Federal University, grant No. VnGr-07/2020-04-IM (Ministry of Science and Higher Education of the Russian Federation).

## **Contact Problems on the Interaction of Indenter and Poroelastic Base**

**M.I. Chebakov\*, A.A. Poddubny, E.M. Kolosova**

*I. I. Vorovich Institute of Mathematics, Mechanics and Computer Sciences  
Southern Federal University, Rostov-on-Don, Russia*

[\\*michebakov@yandex.ru](mailto:michebakov@yandex.ru)

The Cowin-Nunziato theory of elastic materials with voids is one of the common generalizations of the classical theory of elasticity. This theory concerns elastic materials with small pores (voids), distributed throughout the volume. In the report, the axisymmetric contact problems on the interaction of a hard stamp with the surface of a porous-elastic layered base are considered on the basis of equations of the theory of porous-elastic bodies of Cowin-Nunziato. It is assumed, that the stamp base has a flat or parabolic shape, there is no friction in the contact zone. The posed problems are reduced to an integral equation with a logarithmic kernel in relation to an unknown contact stress using the Hankel integral transform. The solution of the constructed integral equation is obtained by the asymptotic method and the direct collocation method. The scheme for obtaining a solution of the posed problem and its accuracy are tested on similar problems for an elastic half-space and an elastic layer, the exact solution of which is well-known. In the collocation method, it is enough to limit ourselves to 50 equations to obtain a solution with an error of 3%. The calculations of contact stresses, displacements of the free surface outside the punch and the size of the contact area for the case of a parabolic punch for some values of the problem parameters were carried out. The size of the contact area was found by the method of successive approximations. The relationship between the force, acting on the stamp, and its displacement was investigated. This relationship is one of the main characteristics in determining the mechanical parameters of the material by the indentation method. The results of the finding contact stresses and free surface displacements are presented in the form of graphs and tables for some values of the base porosity. It is shown that with an increase in porosity at a constant value of the displacement of the stamp the contact stresses and the value of the applied force decrease, and the surface outside the stamp has a large drawdown, while the contact area decreases. A comparative analysis of the studied values for various values of the porosity parameters was carried out

**Acknowledgment**

Research was financially supported by Southern Federal University, grant No. VnGr-07/2020-04-IM (Ministry of Science and Higher Education of the Russian Federation).

## Effect of the Arsenic Molecular Form on the Indium Nanodroplet Crystallization

N. E. Chernenko<sup>1,2\*</sup>, S.V. Balakirev<sup>2</sup>, M. M. Eremanko<sup>1</sup>, M. S. Solodovnik<sup>1,2</sup>

<sup>1</sup>*Southern Federal University, Research and Education Center "Nanotechnologies",  
Taganrog, Russia*

<sup>2</sup>*Southern Federal University, Department of Nanotechnologies and Microsystems,  
Taganrog, Russia*

[\\*nchernenko@sfnu.ru](mailto:*nchernenko@sfnu.ru)

Droplet epitaxy is currently one of the most interesting methods of molecular beam epitaxy due to its capabilities in the formation of semiconductor and hybrid nanostructures of various types and shapes in a wide range of conditions and material systems. At the same time, despite a number of advantages, the use of this technology is still very limited due to its complexity and a huge number of control parameters [1]. The goal of this work is to experimentally study the effect of the arsenic molecular form on the crystallization of indium nanodroplet structures and their transformation into InAs nanostructures during droplet epitaxy. For this purpose, we exposed GaAs samples with preformed arrays of In-nanodroplets under identical conditions in equivalent As-fluxes at two different cracking zone temperatures of the valve source, providing As-supply in the form of dimers ( $As_2$ ) or tetramers ( $As_4$ ). We present a comparative analysis of the obtained experimental data, which show that the use of tetramers makes it possible to obtain ensembles of crystalline InAs nanostructures that correlate in their morphological parameters (size, density, shape of elementary structures) with arrays of indium metal nanodroplets. This is true over the entire range of considered temperatures (100 – 300°C) and equivalent thicknesses of indium deposition (1.5 – 3.0 monolayers). The use of a flux of arsenic dimers leads to the formation of structures with a diameter of 20 – 50 nm in the entire range of considered conditions. At the same time, the correlation between the parameters of the ensemble of metal nanodroplets and the final crystal structures is practically not traced either in density or in size. Thus, we obtained that the arsenic molecular form is critically important in the droplet epitaxy of  $A_3B_5$  nanostructures.

### **Acknowledgement.**

The study was carried out with the financial support of the Russian Science Foundation (project No. 19-79-10099) and grant from the President of the Russian Federation (project MK-477.2019.8). The results were obtained using the equipment of the Research and Education Centre "Nanotechnologies" of Southern Federal University.

### **Reference**

[1] Balakirev S.V. et. al. // *Nanotechnology*, **31**, 485604, 2020.

## Modeling a Rotary Drive of a Piezoelectric Generator

A.V. Cherpakov<sup>1,2\*</sup>, A.N. Soloviev<sup>1,2</sup>, I.A. Parinov<sup>1</sup>, V.A. Chebanenko<sup>1</sup>,  
E. V. Rozhkov<sup>1</sup>, S.-H. Chang<sup>3</sup>, C.-C. Yang<sup>3</sup>

<sup>1</sup>*Southern Federal University, Rostov-on-Don, Russia*

<sup>2</sup>*Don State Technical University, Rostov-on-Don, Russia*

<sup>3</sup>*Department of Microelectronics Engineering, National Kaohsiung University of Science and Technology, Kaohsiung, Taiwan (R.O.C.)*

\*[alex837@yandex.ru](mailto:alex837@yandex.ru)

The problem of full-scale modeling of a rotary drive of a piezoelectric power generator (PEG) is considered. A feature of the PEG is that it uses two types of piezoelectric elements: piezoelectric elements in the form of a bimorph under bending load and piezoelectric cylindrical elements for pressure loading. The mechanical drive wheel with a diameter of 67 cm acts as an excitation element, bending the generator substrate with a magnet (see Fig. 1).

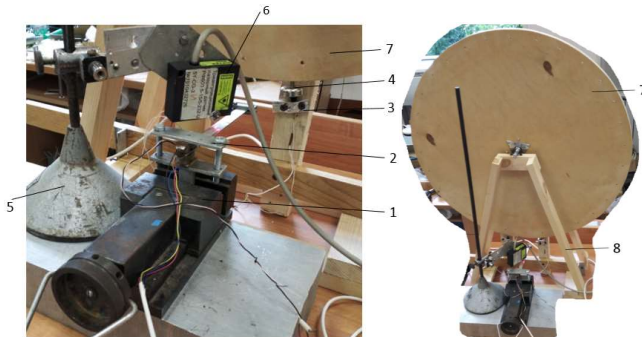


**Fig. 1.** Vibration set-up for PEG excitation. 1 – retainer; 2 – PEG; 3 – induction sensor; 4 – magnet; 5 – fastening elements of the RF603 laser sensor (6); 6 – laser triangulation displacement meter RF603; 7 – rotating drive; 8 – drive base elements (7)

The set-up consists of a drive wheel with a C25 type magnet attached to it; the diameter of the magnet is 25 mm. The drive is mounted on a base rod structure on a bearing support. The PEG is secured in a retainer. The laser displacement meter records the oscillations of the PEG cantilever in the vicinity of the extreme point of the bimorph fixing. The drive wheel is made of 12 mm plywood. Inductance sensors located on both sides of the end of the PEG allow recording the transit time of the magnet. The operation of the set-up was carried out as follows. During the rotation of the drive wheel (7), the oscillations and output characteristics of the PEG were investigated (1). There was a fixed magnet (4) on the drive wheel. When the wheels rotated, the magnet excited an electric

potential when passing by two induction sensors (3, 4) located before and after the PEG proof mass. Thus, the excitation time of the first and second induction sensors was recorded and the average rotation speed was calculated. When the magnet passed over the PEG proof mass (1), the metal mass was attracted to the magnet (5). After passing through the magnet (5), and thus removing the load in the form of attraction, PEG (1) continued to oscillate with a certain damping. The output excitation voltage of the induction sensors and the PEG output voltages taken from the bimorph and piezoelectric elements at the base of the PEG were recorded (1). The loading time was calculated from the possible parameters of rotation of the drive wheel and ranged from 2.98 to 4.92 rad/s. The maximum power taken from the piezoelectric plates at an active load of 1 M $\Omega$  at an output voltage of  $U_1 = 3.095$  V was 4.55  $\mu$ W for a bimorph based on PEG. The peak power value for the top piezocylinders is reached at a load of 1 M $\Omega$  with an output voltage of 0.47 V and is equal to 0.109  $\mu$ W. For the lower piezocylinders, the peak value is equal to 0.01  $\mu$ W at a load of 1 M $\Omega$  and an output voltage of 0.04 V. This loading did not take place at resonant modes of PEG oscillations. In the future, it makes sense to investigate the resonance modes of excitation by a rotating PEG drive.

#### **Acknowledgement**

The study was performed under partial support of the Russian Foundation for Basic Research (No. 19-08-00365).

#### **References**

- [1] T.V. Polyakova, A.V. Cherpakov, I.A. Parinov, M.N. Grigoryan // *IOP Conference Series: Material Science Engineering*, **913**, 022014 (10 p.), 2020.
- [2] A.N. Soloviev, I.A. Parinov, A.V. Cherpakov, V.A. Chebanenko. In: *Abstract Collection of The Second International Conference on Material, Machines and Methods for Sustainable*

## **Application of Neural Network Technologies for Identifying Defect Sizes in a Half-plane**

**A.V. Cherpakov<sup>1,2\*</sup>, A.N. Soloviev<sup>1,2</sup>, I.A. Parinov<sup>1</sup>, O.V. Shilyaeva<sup>2</sup>, S.-H. Chang<sup>3</sup>,  
C.-F. Lin<sup>4</sup>**

<sup>1</sup>*Southern Federal University, Rostov-on-Don, Russia*

<sup>2</sup>*Don State Technical University, Rostov-on-Don, Russia*

<sup>3</sup>*Department of Microelectronics Engineering, National Kaohsiung University of Science and Technology, Kaohsiung, Taiwan (R.O.C.)*

<sup>4</sup>*Department of Electrical Engineering, National Taiwan Ocean University, Taiwan (R.O.C.)*

\*[alex837@yandex.ru](mailto:alex837@yandex.ru)

The work is devoted to solving one of the most important and practically significant problems in the field of solid mechanics, namely the restoration of data on the parameters of structures by performing numerical experiment calculations of building structures with defects using CAE modeling packages [1, 2]. Data analysis was carried out by the authors using artificial neural networks. In the development of various devices and structures in world practice in recent years,

methods of mathematical modeling and finite element technologies, presented in the form of software packages, have been increasingly used. The use of such packages makes it easy to optimize structural models, reduce calculation time, and quickly change and analyze design parameters. The relevance of the chosen research topic is due to the creation of optimal algorithms for researching the state of structures, a quick assessment of the state and reliability of materials. Using the methods of finite-element analysis and the ANSYS software package, in this work, the modeling of a layered structure with a defect is implemented. The problem of reconstructing the radius of a defect based on the application of simulation modeling of oscillations in the ANSYS finite element complex and artificial neural network (ANN) in the MATLAB complex is considered. The results of unsteady oscillations of a half-plane with a circular internal defect are obtained and presented. The transverse displacements are calculated at the control points of the structure during the propagation of a wave from a pulsed loading. As a result, an approach was developed to restore the radius of a defect in a structure based on a combination of the finite element method and ANN.

#### **Acknowledgement**

Research was financially supported by Southern Federal University, grant No. VnGr-07/2020-04-IM (Ministry of Science and Higher Education of the Russian Federation).

#### **References**

- [1] Solov'ev A.N., Cherpakov A.V., Vasil'ev P.V., Parinov I.A., Kirillova E.V. // *Advanced Engineering Research*. **20**(3), 205-215, 2020.
- [2] A. V. Cherpakov, P. V. Vasiliev, A. N. Soloviev, I. A. Parinov, B. V. Sobol. In: *Advanced Materials - Proceedings of the International Conference on "Physics and Mechanics of New Materials and Their Applications"*, PHENMA 2019, Springer Proceedings in Materials, Ivan A. Parinov, Shun-Hsyung Chang, Banh Tien Long (Eds.). Springer Nature, Cham, Switzerland, **6**, 439-447, 2020.

## **Using Neural Networks to Analyze the Shape of a Defect in a Layered Structure during Its Modeling**

**A.V. Cherpakov<sup>1,2\*</sup>, A.N. Soloviev<sup>1,2</sup>, I.A. Parinov<sup>1</sup>, O.V. Shilyaeva<sup>2</sup>, S.-H. Chang<sup>3</sup>, C.-F. Lin<sup>4</sup>**

<sup>1</sup>*Southern Federal University, Rostov-on-Don, Russia*

<sup>2</sup>*Don State Technical University, Rostov-on-Don, Russia*

<sup>3</sup>*Department of Microelectronics Engineering, National Kaohsiung University of Science and Technology, Kaohsiung, Taiwan (R.O.C.);* <sup>4</sup>*Department of Electrical Engineering, National Taiwan Ocean University, Taiwan (R.O.C.)*

[\\*alex837@yandex.ru](mailto:alex837@yandex.ru)

The methods for solving the problems of restoring the parameters of a layered structure have been present in [1, 2]. They use analytical and numerical solutions based on the formulation of inverse problems. To solve the problem of restoring properties, an information about the wave parameters of a certain area of the structure is required. The time parameter of the vibrational response of the structure should cover the areas requiring restoration of the parameters. The application of artificial



neural networks (ANNs) is considered as an analysis tool. In many works, some solutions to the problems of reconstruction of the damaged state of structural elements are considered. Modeling of a layered structure (with a width of 10 m and a depth of 7 m) with a defect was carried out in the FE complex ANSYS. The defect is located at a depth of 1.5 m from the surface and at a distance of from the point of loading in the form of a shock pulse. The displacement field of a flat structure is calculated in the result of a short-term impulse action. The shape of the defect area is considered as the variable parameter under study. The shape of the defect area can be in the form of the following configurations: (i) a circle of radius  $R$ , (ii) an ellipse-like structure  $R_1$ - $R_2$ , (iii) a rectangular structure  $h$ - $l$ , (iv) a triangular structure  $h$ - $l_1$ - $l_2$ . Thus, 4 clusters of defective areas are modeled. The magnitude of the variation of the corresponding dimensional parameters lies in the range  $R_i = 0 - 0.5$  m. To identify the layer thickness, we used a fully connected multilayer ANN model in the Matlab software. The neural network model, containing 10 hidden layers, consisted of 43 input neurons and 1 output neuron. The calculation results showed that at the use of ANN, it is possible to reconstruct the configuration of the defect region with a sufficiently high degree of correlation (0.99).

#### **Acknowledgement**

Research was financially supported by Southern Federal University, grant No. VnGr-07/2020-04-IM (Ministry of Science and Higher Education of the Russian Federation).

#### **References**

- [1] Solov'ev A.N., Cherpakov A.V., Vasil'ev P.V., Parinov I.A., Kirillova E.V. // *Advanced Engineering Research*. **20**(3), 205-215, 2020.
- [2] Alexander A. Lyapin, Ivan A. Parinov, Nina I. Buravchuk, Alexander V. Cherpakov, Ol'ga V. Shilyaeva, Ol'ga V. Guryanova. *Improving Road Pavement Characteristics - Applications of Industrial Waste and Finite Element Modelling*. Series: Innovation and Discovery in Russian Science and Engineering. Springer Cham, Switzerland, 2020, 238 p.

## **Correlation between Calcaneal Quantitative Ultrasound and Dual-energy X-ray Absorptiometry Bone Density**

**Chia-Chi Yen<sup>1,2,3</sup>, Wei-Chun Lin<sup>1\*</sup>, Zi-Hao Wang<sup>1</sup>, Guan-Fan Chen<sup>1</sup>, Da-Ying Chou<sup>1</sup>, Dian-Min Lin<sup>1</sup>, Shu-Yuan Lin<sup>1</sup>, Min-He Zhan<sup>1</sup>, Tsair-Fwu Lee<sup>4,5\*\*</sup>**

<sup>1</sup>*Department of Orthopedic, Kaohsiung Municipal Min-Sheng Hospital, Kaohsiung, Taiwan*

<sup>2</sup>*Department of Nutrition, Institute of Biomedical Nutrition, Hung-Kuang University, Taichung, Taiwan*

<sup>3</sup>*Department of Business Management, National Sun Yat-Sen University, Kaohsiung, Taiwan*

<sup>4</sup>*Medical Physics and Informatics Laboratory of Electronics Engineering, National Kaohsiung University of Applied Sciences, Kaohsiung, 80778, Taiwan*

<sup>5</sup>*PhD program in Biomedical Engineering, Kaohsiung Medical University, Kaohsiung, 80708, Taiwan*

\*[patdrwc@gmail.com](mailto:patdrwc@gmail.com); \*\*[tflee@nkust.edu.tw](mailto:tflee@nkust.edu.tw); [tflee@kuas.edu.tw](mailto:tflee@kuas.edu.tw)

Calcaneal quantitative ultrasonography (QUS) is useful prescreening tool for osteoporosis but there still exists discrepancy between the QUS and dual-energy X-ray absorptiometry (DXA). In this

study, the correlation between QUS and DXA in Taiwanese population is evaluated. Totally 772 patients were enrolled, demographic data was recorded with QUS and DXA T-score over hip and spine. Correlation coefficient of QUS with DXA-hip is 0.171 ( $p < 0.001$ ). Correlation coefficient of QUS with DXA-spine is 0.135 ( $p < 0.001$ ). In females, the correlation between QUS and DXA-spine is 0.237 ( $p < 0.001$ ). For males, the correlation coefficient is 0.255 ( $p < 0.001$ ). Logistic regression model using DXA-spine as dependent variable was established, and classification table has 66.2% accuracy. ROC analysis with Youden's index revealed the optimal cut-off point of QUS for predicting osteoporosis is 2.72. This study reveals a meaningful correlation between QUS and DXA in Taiwanese population. The potential for pre-screening osteoporosis with calcaneus QUS is warranted.

## **Volt-ampere Type Relative Humidity Sensing Devices using Indium-Based Sensing Film on a Porous Silicon Substrate**

**Chih Chin Yang\*, Hung Yeh Lin**

*Department of Microelectronics Engineering, National Kaohsiung University of Science and Technology, Kaohsiung city 81157, Taiwan, Republic of China*

\*[chchyang@nkust.edu.tw](mailto:chchyang@nkust.edu.tw)

The volt-ampere type respirator using a relative humidity (RH) sensing device with  $p$ - $n$  heterostructure has been proposed to apply the sensor in respiration voltammetry (RV) measurement. The RV measurement was used in the concentration detection of breath sampling under oxidation-reduction (redox) reaction. In this research, the RH sensing device was fabricated on  $n$ -type silicon ( $n$ -Si) porous substrate with a native silicon dioxide (native-SiO<sub>2</sub>) layer, so called native-SiO<sub>2</sub>/ $n$ -Si porous substrate. The RH sensing device was constructed with a  $p$ - $n$  heterostructure. An  $n$ -type indium oxide ( $n$ -In<sub>2</sub>O<sub>3</sub>) sensing film was deposited by sputtering an indium metal target with 99.99% purity and 4-in diameter under optimized growth conditions at room temperatures. A  $p$ - $n$  heterostructure by deposited the  $n$ -type indium oxide ( $n$ -In<sub>2</sub>O<sub>3</sub>) sensing film on  $p$ -type silicon ( $p$ -Si) buffer layer was fabricated as shown in Fig. 1. The  $p$ -type silicon ( $p$ -Si) buffer layer on the  $n$ -type silicon ( $n$ -Si) porous substrate was also deposited at room temperature. Subsequently, the top electrical contact was made on the surface of the  $n$ -type indium oxide ( $n$ -In<sub>2</sub>O<sub>3</sub>) sensing film by depositing an aluminum metal circular dot and interdigit pattern using sputtering method respectively as the electrodes of aluminum drain-source (Al-DS) electrode and aluminum gate (AG) electrode. The electrical properties of  $n$ -type indium oxide ( $n$ -In<sub>2</sub>O<sub>3</sub>) sensing film and  $p$ -type silicon ( $p$ -Si) buffer layer were simultaneously evidenced by Hall measurement, which design constructed the volt-ampere type RH sensing device with a  $p$ - $n$  heterostructure. However, to obtain well-defined sensing performance, the current-voltage ( $I$ - $V$ ) curve of RH sensing device with a  $p$ - $n$  heterostructure was measured using D-S terminals structure. The current-voltage ( $I$ - $V$ ) curves of volt-ampere type RH sensing device with a  $p$ - $n$  heterostructure in D-S terminals structure related in various RH values were obtained which revealed the low output current value with mA-scale when the RH value was high at the same negative-bias-voltages (from -5 V to 0 V). However, when the bias voltages were operated at positive values (from 0 V to 5 V),

the output current value of volt-ampere type RH sensing device was as high as  $\mu\text{A}$ -scale at high RH value. The different volt-ampere phenomena at different bias directions could be applied in different measured environments.

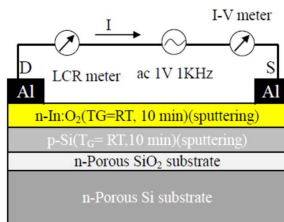


**Fig.1.** Scheme and measurement of  $n\text{-In}_2\text{O}_3/p\text{-Si}$  RH sensing device on native- $\text{SiO}_2/n\text{-Si}$  porous substrate

### Acknowledgments

The authors would like to thank the Ministry of Science and Technology, Taiwan, for the financial support under contract number of MOST 109-2813-C-992-019-E and the National Kaohsiung University of Science and Technology, Taiwan, for the financial support under contract number of NKUST 109A13.

## Respiration Sensing Devices Based on Indium Nitride $p\text{-}n$ Heterostructure on Silicon Porous Substrate

Chih Chin Yang<sup>1</sup>, Yu Liang Hsiao<sup>\*1</sup>, Zong Hsien Wu<sup>1</sup>, Yu Hsuan Hsu<sup>1</sup>,  
Ivan A. Parinov<sup>2</sup>, Shun Hsyung Chang<sup>1</sup>

<sup>1</sup>Department of Microelectronics Engineering, National Kaohsiung University of Science and Technology, Kaohsiung City, 81157, Taiwan, Republic of China

<sup>2</sup>I. I. Vorovich Mathematics, Mechanics and Computer Science Institute, Southern Federal University, Rostov-on-Don, 344006, Russia

\*[C107187111@nkust.edu.tw](mailto:C107187111@nkust.edu.tw)

The voltam-type respirator using a relative humidity (RH) sensing device with  $p\text{-}n$  heterostructure on  $n$ -type silicon ( $n\text{-Si}$ ) porous substrate was proposed in this research. The  $p\text{-}n$  heterostructure of semiconductor sensing device was constructed using layer by layer sputtering deposition method on an  $n$ -type silicon substrate with native silicon dioxide (native- $\text{SiO}_2$ ) layer on substrate surface. The  $p\text{-}n$  heterostructure includes  $p$ -type indium nitride ( $p\text{-InN}$ ) sensing film and  $n$ -type silicon ( $n\text{-Si}$ ) buffer layer, in which the  $n\text{-Si}$  buffer layer was deposited on native- $\text{SiO}_2/n\text{-Si}$  porous substrate.

Moreover, the aluminum drain-source (Al-DS) electrode and Al gate back (Al-GB) electrode were respectively settled on the surfaces of  $p$ -InN sensing film and  $n$ -Si buffer layer, as shown in Fig.1.

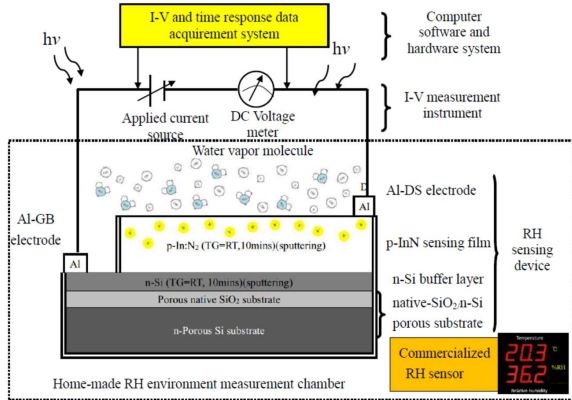


**Fig.1.** Scheme and measurement of  $p$ -InN/ $n$ -Si RH sensing device on native-SiO<sub>2</sub>/ $n$ -Si porous substrate

In this study, the Al-DS and Al-GB electrodes,  $p$ -InN sensing film, and  $n$ -Si buffer layer were layered on a substrate using DC sputtering system and the semiconductor sensing device was fabricated using lift-off technique by a metal mask. Afterward, the electrical properties of  $p$ -InN sensing film and  $n$ -Si buffer layer including carrier concentration, carrier mobility, carrier type, and resistivity values at room temperature was examined using Hall measurement instrument. However, the RH sensing characteristic of RH sensing device including responsivity and current-voltage ( $I$ - $V$ ) curves at various RH values was measured using a home-made RH environment measurement system by integrating a current-voltage meter and a computer system. Then, the sensitivity of the RH sensing device was evaluated using calculated resistance values from  $I$ - $V$  curves at various RH values [1, 2]. Finally, the respiration response was also detected using the home-made RH environment measurement system including a current-voltage meter and a data acquisition system.

#### Acknowledgments

The authors would like to thank the Ministry of Science and Technology, Taiwan, for the financial support under Contract No. MOST 105-2923-E-992-302-MY3.

#### References

- [1] Maryam Gholizadeh Arashti, Mohammad Ali Sadeghzadeh // *Vacuum*, **93**, 1-6, 2013.
- [2] Timothy David Veal, Christopher F. McConville, William J. Schaff, *Indium Nitride and Related Alloys*, CRC Press, 2017.

# Capacitance Type $p$ -InN/ $n$ -Si Heterostructure Sensing Devices on Silicon Unpolished Substrate

Chih Chin Yang<sup>1</sup>, Zong Hsien Wu<sup>\*1</sup>, Yu Liang Hsiao<sup>1</sup>, Yi Tseng Li<sup>1</sup>,  
Shun Hsyung Chang<sup>1</sup>, Ivan A. Parinov<sup>2</sup>

<sup>1</sup>*Department of Microelectronics Engineering, National Kaohsiung University of Science and Technology, Kaohsiung City 81157, Taiwan, Republic of China*

<sup>2</sup>*Vorovich Mathematics, Mechanics and Computer Science Institute, Southern Federal University, Rostov-on-Don, 344006, Russia*

[\\*C107187156@nkust.edu.tw](mailto:*C107187156@nkust.edu.tw)

The capacitance type  $p$ -InN/ $n$ -Si heterostructure ( $p$ -InN/ $n$ -Si HS) relative humidity (RH) sensing device with drain (D) and source (S) upper contact electrodes was proposed in this research. The  $p$ -InN/ $n$ -Si HS RH sensor was fabricated on (100)  $n$ -silicon unpolished substrate with native silicon dioxide (native-SiO<sub>2</sub>) using DC sputtering system and lift-off technique to deposit  $p$ -InN/ $n$ -Si HS layer and construct D-S electrodes, respectively. Firstly, the first layer of  $p$ -InN/ $n$ -Si HS RH sensor is defined as a buffer layer which a  $n$ -type silicon layer was deposited on the unpolished native-SiO<sub>2</sub> using DC sputtering system kept with the growth pressure of 10<sup>-4</sup> torr, DC power of 100 W, applied voltage of 800 V, and applied current of 2 A at the growth temperature (so called substrate temperature) of room temperature for 10 minutes. Moreover, the flow rate of argon gas into the growth chamber was maintained at 10 sccm using the mass flow controllers to sputtering the silicon target. Afterward, the second layer of  $p$ -InN/ $n$ -Si HS RH sensor was deposited on the  $n$ -type silicon buffer layer as a sensing layer defined by a  $p$ -type InN sensing film to detect the moisture in environment measurement chamber. The sputtering conditions of  $p$ -type InN sensing film in DC sputtering system were the same as those of  $n$ -type silicon buffer layer including the growth pressure, DC power, applied voltage, applied current, growth temperature, and growth time. However, while fabricating the  $p$ -type InN sensing film, the flow rates of argon gas and nitrogen gas continuously flowed into the growth chamber were identically maintained at 10 sccm to sputter the indium target and to adsorb the sputtered indium ions from indium target in sputtering chamber. The growth of the  $p$ -type InN sensing film onto  $n$ -type silicon buffer layer constructs a  $p$ -InN/ $n$ -Si HS which can be applied in RH sensor for the enhancement of the sensitivity and responsivity. Finally, two aluminum contact electrodes including D-electrode and S-electrode were deposited onto  $p$ -type InN sensing film using a specific metal mask to fabricate a capacitance type RH sensor, as shown in Fig.1. In this capacitance type RH sensor, the  $p$ -type InN sensing film was simultaneously served as a sensing layer of the RH sensor, a channel of the FET structure, and a dielectric material of the capacitor. In summary, the capacitor structure of the capacitance type  $p$ -InN/ $n$ -Si heterostructure ( $p$ -InN/ $n$ -Si HS) relative humidity (RH) sensing device was constructed including a drain (D) and source (S) upper contact electrodes, and a  $p$ -type InN sensing dielectric material which the permittivity could be significantly altered as the water molecules were adsorbed onto the surface of the  $p$ -type InN sensing film, as shown in Fig. 2. Therefore, not only the  $p$ -InN/ $n$ -Si HS is a critical device of RH sensor which can be applied in environment monitoring, but also the  $p$ -InN/ $n$ -Si HS can be used as a key element of the respirometer which can be applied in breath detection of human body [1, 2].

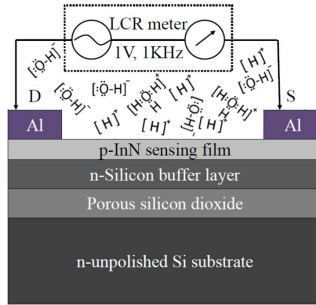


**Fig. 1.** D-S electrode measurement of capacitance type *p*-InN/*n*-Si HS RH sensor on *n*-type silicon unpolished substrate with porous native silicon dioxide

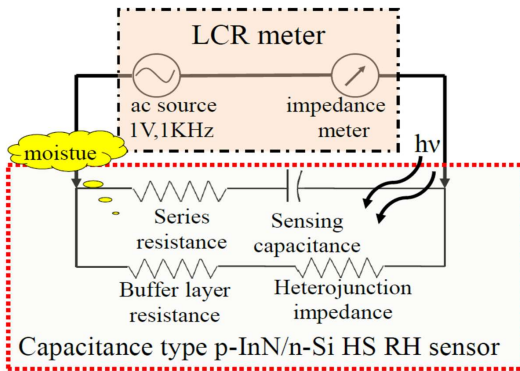


**Fig. 2.** Equivalent circuit scheme of capacitance type *p*-InN/*n*-Si HS RH sensor

**Acknowledgment**

The authors would like to thank the Ministry of Science and Technology, Taiwan, for the financial support under Contract No. MOST 105-2923-E-992 -302 -MY3.

**References**

- [1] Maryam Gholizadeh Arashti, Mohammad Ali Sadeghzadeh // *Vacuum*, **93**, 1-6, 2013.
- [2] Timothy David Veal, Christopher F. McConville, William J. Schaff, *Indium Nitride and Related Alloys*, CRC Press, 2017.

# Space Time Block Code Based FBMC Advanced Underwater Image Communication Technology

Chin-Feng Lin<sup>1\*</sup>, Chih-Chin Chuang<sup>1</sup>, Shun-Hsyung Chang<sup>2</sup>, Ivan A. Parinov<sup>3</sup>,  
Sergey Shevtsov<sup>4</sup>

<sup>1</sup>Deaprtment of Electrical Engineering, National Taiwan Ocean University, Taiwan, ROC

<sup>2</sup>Deaprtment of Microelectronic Engineering, National Kaohsiung University of Science and Technology, Taiwan, Kaohsiung, ROC

<sup>3</sup>I. I. Vorovich Mathematics, Mechanics, and Computer Science Institute, Southern Federal University, Rostov-on-Don, Russia

<sup>4</sup>Head of Aircraft Systems and Technologies Laboratory, South Center of the Russian Academy of Science, Rostov-on-Don, Russia

\*[lcf1024@mail.ntou.edu.tw](mailto:lcf1024@mail.ntou.edu.tw)

In the report, a  $2 \times 4$  space time block code (STBC) based filter bank multicarrier (FBMC)- low density parity check (LDPC) code underwater image communication technology (UICT) is proposed. The adaptive binary phase shift keying (BPSK) modulation and four offset quadrature amplitude modulation (4-OQAM), are integrated into the proposed UICT. The performances of bit error rates (BERs) and peak signal-to-noise ratios (PSNRs) of the proposed UICT with perfect channel estimation (PCE)(0%) are investigated. From these simulation results, we evaluate the performances of the proposed advanced UICT with a PCE.

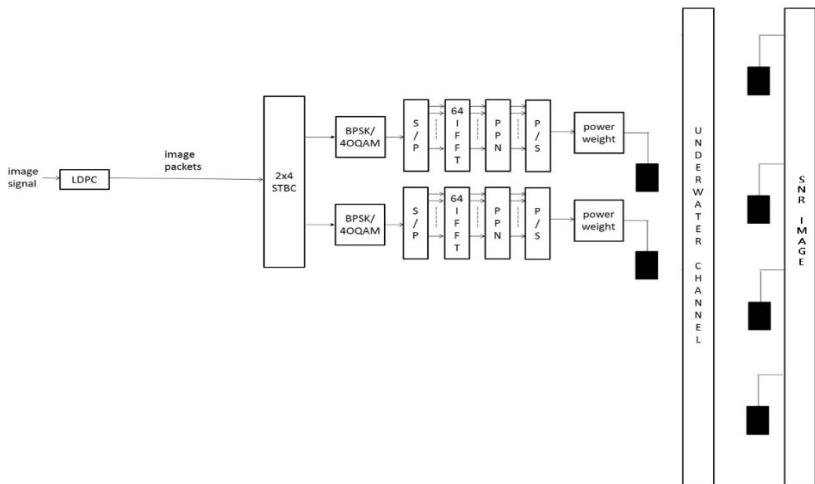
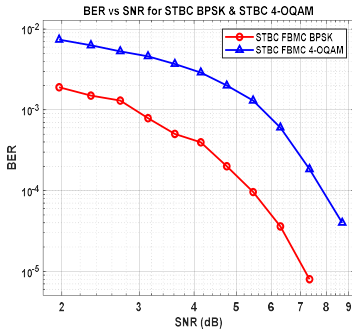
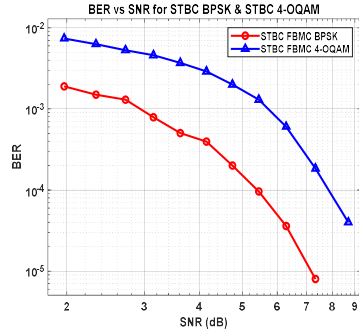


Fig. 1. Proposed STBC based FBMC-LDPC advanced UICT



**Fig. 2.** BER performance of the STBC FBMC-LDPC UICT with a PCE



**Fig. 3.** PSNR performance of the STBC FBMC LDPC UICT with a PCE

### Acknowledgement

The authors acknowledge the support of the grant from The Ministry of Science and Technology of Taiwan, under contract No. MOST 108-2221-E-992 -026.

## Using Activated Quantum Reagent to Transform the Quality of Poultry and Animal Manure and its Recycling

Chin Ko Yeh<sup>1</sup>, Chitsan Lin<sup>1,2\*</sup>, Hsueh Chen Shen<sup>1</sup>, Zau Wen Kuo<sup>3</sup>,  
Wisanutkorn Lukkhasorn<sup>2</sup>

<sup>1</sup>Ph.D. Program in Maritime Science and Technology, College of Maritime, National Kaohsiung University of Science and Technology, Kaohsiung 81157, Taiwan (R.O.C.).

<sup>2</sup>Department of Marine Environmental Engineering, National Kaohsiung University of Science and Technology, Kaohsiung 81157, Taiwan (R.O.C.).

<sup>3</sup>Tygood Cosmos Vital Force Technology Corporation, Taiwan (R.O.C.).

\*[ctlin@nkust.edu.tw](mailto:ctlin@nkust.edu.tw)

According to the current livestock breeding scale in Taiwan, there are 5,514,211 pigs, 105,059 cattle, and 100,480,021 chickens. If the average daily excretion of adult livestock and poultry is 2 kg for big pigs, 0.15 kg for adult chickens, and 20 kg for cattle, and then 60% of adult livestock and poultry weights are used to estimate the average weight of livestock and poultry, the annual excretion of livestock. The solid matter amounts to approximately 16,920,963 metric tons, which is the primary source of livestock waste. This project will conduct a 7-day kitchen waste composting experiment in a greenhouse space. Under the same operating parameters, compare a group of control reactors without a quantum active agent and another group of experimental reactors with a quantum active agent to compare the biochemical effects of composting and the differences in monitoring data of



two groups for research and discussion. The results of the experiment showed that the index gas data ( $\text{NH}_3$ ,  $\text{H}_2\text{S}$ ) of the experimental pile was not detected, which was significantly better than the control pile, and it could reduce the fat content in the food waste compost by 50% on the fourth day of the experiment. Through the method of paving and drying, when the moisture content is lower than 35%, the parameters of the experimental pile tend to be stable, which is easy to control the experiment and achieves the removal of the peculiar smell caused by the fermentation during the composting process, and the time required to accelerate the composting process reduce the fat content in the compost pile and improve the quality of the fertilizer. The traditional mechanical transformation processing methods most focus on the chemical aspect. They use quantum active substances to automatically transform poultry and animal manure, mainly through quantum physical modifications. Suppose it can be successful, in the expected to significantly enhance the various efficiencies of traditional chemical treatment, which subsequent experiments need to confirm.

## **Using a Novel Graphene-Ceramic Composite Material in the Adsorption of Aromatic Volatile Organic Compounds**

**Chitsan Lin\*, Nicholas Kiprotich Cheruiyot, Wisanukorn Lukkhasorn, Le Thi Hieu**

*Department of Marine Environmental Engineering, National Kaohsiung University of Science and Technology, Kaohsiung 81157, Taiwan*

\*[ctlin@nkust.edu.tw](mailto:ctlin@nkust.edu.tw)

Benzene and toluene are ones of the most common volatile organic compounds (VOCs) in industrial processes. Carbon-based adsorbents, including activated carbon and graphene, have been widely used to remove these aromatic compounds in both air and water. This study evaluates the adsorption capacity of a 10 pixels per inch (PPI) novel graphene-ceramic composite material at inlet concentrations of 100 ppm and 25 °C. The graphene-ceramic material weighed was 17 – 21 g and had a length of 5 cm, and a diameter of 4 cm. The flow rate was set equal to 0.8 – 1.0 L·min<sup>-1</sup>. The average adsorption capacity of the adsorbent was 21.4 ± 1.06 mg·g<sup>-1</sup> and 16.8 ± 1.47 mg·g<sup>-1</sup> for benzene and toluene, respectively. The adsorbent achieved removal efficiencies of 99% and 96% of benzene and toluene, respectively. These preliminary results show that the graphene-ceramic material can successfully adsorb these compounds at 25 °C. Further work would test the adsorption capacity at different concentrations and temperatures, as well as compare its performance with other commonly used adsorbents.

## Numerical Study of the Plane Free Liquid Surface Oscillations in an Elliptical Paraboloid

Daniil O. Nepryakhin\*, Michael Yu. Zhukov\*\*

*Southern Federal University, Rostov-on-Don, Russia*

\*[nepryahin@sfedu.ru](mailto:nepryahin@sfedu.ru), \*\*[myuzhukov@mail.ru](mailto:myuzhukov@mail.ru)

The problem on the oscillations of the plane liquid unperturbed surface which fill an elliptical paraboloid or paraboloid is numerically investigated on the basis of classical shallow water equations. In the latter case, due to the axial symmetry, the problem is reduced to a spatially one-dimensional one. Well known, that shallow water equations are hyperbolic and allow shock waves and rarefaction waves as solutions. To solve similar equations, we need to use Riemann solvers and other special methods. In this report, the finite element method and the finite volume method are used for numerical solution of the problem. Effective numerical algorithms have been developed to successfully prevent the effects of mesh viscosity. In the case of the finite volume method, the classical version of the method and the method using HLL approximation are used for approximation. In addition, the method for implementing the finite volume method using the FreeFem++ finite element package is specified. The computational experiments showed that the use of the finite volume method is more preferable than the use of the finite element method. The choice of the problem of vibrations of a flat surface in a paraboloid is due to the fact that under certain special initial conditions the problem has an exact analytical solution. This, in turn, allows us to evaluate the effectiveness of methods, approximations, the accuracy of the solution, etc. The numerical experiment allowed us to choose the optimal scheme of calculations. The results of calculations for oscillation frequencies of the order  $O(1)$  show that almost all the solution algorithms used give a good agreement with the analytical solution everywhere except for a narrow area near the walls of the paraboloid (on the order of several grid steps). This effect is explained by the degradation of the approximation in the vicinity of the boundary. It is interesting to note that the amount of deviation from the exact solution does not tend to increase over time. A theoretical estimate of the error is given, which is in good agreement with the experiment. The presented algorithms can be used to solve similar problems.

### ***Acknowledgement***

Research was financially supported by Southern Federal University, grant No. VnGr-07/2020-04-IM (Ministry of Science and Higher Education of the Russian Federation).

## Surface Acoustic Wave Sensors of Breath

V.G. Dneprovski\*, I.A. Parinov

*I. I. Vorovich Mathematics, Mechanics and Computer Science Institute, Southern Federal University,  
Rostov-on-Don, Russia*

\*[valdnepr@ya.ru](mailto:valdnepr@ya.ru)

A breathing is one of the basic vital functions of a person; knowledge of its parameters and quality is necessary in medicine. Respiratory monitoring methods are important for monitoring the quality of sleep or sudden infant death syndrome (SIDS). The respiratory control in the intensive care units of hospitals, especially in patients affected by coronavirus, is particularly important. It is known, that detecting of the gas composition exhaled by a patient can be used to diagnose certain diseases. Therefore, one of the most important applications of respiratory sensors is their use for the diagnosis of diseases. No doubt, the use of the surface acoustic waves (SAWs) sensors [1, 2] are very promising here. This is due to the possibility of their remote work in the passive wireless no-touch mode, their small size and the fact that they should not burden of the patients. In the present report, a comparative analysis of the methods for monitoring human respiration using SAWs sensors developed by various researchers has been carried out. Air exhaled by humans contains more than 3,000 volatile organic compounds (VOCs) such as carbon dioxide, acetone, methanol, ethanol, butane, etc. Exhaled gas analysis is the non-invasive technique whose goal is to detect its composition. The paper [3] discusses the technique for detecting several gases, for example, acetone. To achieve the goal, the SAWs sensor was developed using the COMSOL Multiphysics 5.0® software. Adsorption rate and conductivity were monitored by a gas sensor based on electric potential. The biosensor is manufactured in such a way that the detection and analysis of VOCs exhaled by humans becomes possible. Various sensors have already been developed that were used to detect respiratory diseases (for example, asthma, lung cancer, tuberculosis, sleep apnea, etc.) by analyzing VOCs during expiration [4]. In view of the listed advantages of SAW sensors, they should be widely used in respiratory monitoring and disease diagnosis.

### **Acknowledgements**

This work was financially supported by the Internal Grant of Southern Federal University VnGr-07/2020-06-MM and the Grant No. 19-08-00365 & No.18-29-02076 of the Russian Foundation for Basic Research.

### **Reference**

- [1] Dneprovski V.G., Karapetyan G.Y., Parinov I.A. *Surface Acoustic Wave Devices*. Nova Science Publishers, New York, 2016.
- [2] Bagdasaryan A.S., Dneprovski V.G., Karapetyan G.Y., Nefedova N.A., Sinitsyna T. // *Electronics: Science, Technology, Business*. 1(83), 46-51, 2008 (in Russian).
- [3] Nagamalli A., Alli D. *The Proceedings of the 2019 COMSOL Conference in Bangalore*. [http://cn.comsol.com/paper/download/682731/Bangalore\\_2019\\_Poster\\_Nagamalli.pdf](http://cn.comsol.com/paper/download/682731/Bangalore_2019_Poster_Nagamalli.pdf)
- [4] Hashoul D., Haick H. // *European Respiratory Review*. 152(28), 190011, 2019.

## **Design and Evaluation of Automated Preform Equipment for Ship Manufacturing**

**Dong-Ho Yang<sup>1\*</sup>, Sung-Youl Bae<sup>2</sup>**

*<sup>1</sup>Center of Ceramic Fiber Commercialization, Korea Institute of Ceramic Engineering and Technology, Busan, Korea*

*<sup>2</sup>R&D Center, Control Factory, Busan, Korea*

[\\*dongho.yang@controlfactory.co.kr](mailto:dongho.yang@controlfactory.co.kr)

In this study, the results of design and evaluation of automated preform equipment in the manufacturing process of composite ships are presented. The existing composite ship was expensive and had low mechanical properties because hand lay-up process is applied on the ship manufacturing. In this study, the equipment for automated preform and resin spraying in the manufacturing process of composite ships was designed. Moreover, the performances of developed equipment were evaluated by performance tests. Through the performance evaluation, it was confirmed that the developed preform manufacturing equipment had a productivity of 5 kg/min and had product reproducibility of 1.0 mm or less.

## **A Study on Lightweight Design of Ultra High-Pressure Composite Pressure Vessel for Hydrogen Gas**

**Dong-Hun Yang<sup>1</sup>, Soo-Jeong Park<sup>2</sup>, Yun-Hae Kim<sup>1,2†</sup>**

*<sup>1</sup>Department of Marine Equipment Engineering, Graduate School, Korea Maritime and Ocean University, 727 Taejong-ro, Busan, 49112, Republic of Korea*

*<sup>2</sup>Department of Ocean Advanced Materials Convergence Engineering, Korea Maritime and Ocean University, 727 Taejong-ro, Yeongdo-gu, Busan, 49112, Republic of Korea*

[†yunheak@kmou.ac.kr](mailto:yunheak@kmou.ac.kr)

Carbon fiber reinforced composite (CFRP) materials are widely used as fuel tanks for storing hydrogen gas. Manufactured by the filament winding method, CFRP works reliably at high pressures of 70 MPa and provides a product life of up to 20 years through stringent international safety certifications such as GTR No.13. A lightweight fuel tank for hydrogen gas storage provides higher energy efficiency and extends the total mileage of hydrogen fuel cell vehicles. The hydrogen gas storage efficiency is expressed in wt.%, which is the value dividing the weight of storable hydrogen gas by the total weight of container. The currently commercialized fuel tank for hydrogen fuel cell vehicles' hydrogen gas storage efficiency is 5.2 wt.%. The fuel tank's hydrogen gas storage efficiency for the next-generation hydrogen fuel cell vehicle is 6-7 wt.%. Therefore, high toughness and low viscosity epoxy resin were used as a lightweight design method using the same carbon fiber

in this study. It was found that performance improvement in the same winding pattern is an essential factor in achieving the lightweight design goal.

## Method for Computing the General Inverse of Rectangular Matrix and its Applications in Engineering Problems

Yu. E. Drobotov

*Southern Federal University, Rostov-on-Don, Russia*

[yu.e.drobotov@yandex.ru](mailto:yu.e.drobotov@yandex.ru)

The presented abstract considers a method for computing a rectangular complex matrix inversion and demonstrates its applications to balancing of flexible rotors by means of influence coefficients, and several other problems of mechanical engineering and signal processing. The method is based on the theory of weighted pseudoinverse [1] and assumes constructing iterative reflections between vector spaces with inner products of special type. Let  $R_m$  and  $R_n$  denote the complex vector spaces with the following inner products and norms:

$$(u, v)_B = (u, Bv^*)_m, \quad (u, v)_C = (u, Cv^*)_n,$$

$$\|u\|_B = (u, u)_B^{1/2}, \quad \|u\|_C = (u, u)_C^{1/2},$$

where  $B$  and  $C$  are Hermitian positive definite matrices of orders  $m$  and  $n$ , respectively,

$$(u, v)_k = \sum_{i=1}^k u_i v_i, \quad k = m, n,$$

and  $v^*$  denotes conjugation of vector  $v$ . Then the  $m \times n$  complex matrix  $A$  has the unique pseudoinverse  $n \times m$  matrix  $A^\dagger$ , defined by the following properties:  $AA^\dagger A = A$ ;  $A^\dagger A A = A^\dagger$ ;  $(B A A^\dagger)^* = B A A$ ;  $(C A^\dagger A)^\dagger = C A$ , which implies the pseudosolution of  $Ax = b$  with

$$\|Ax - b\|_B = \min_{x \in R_n}, \quad \|x\|_C = \min_{x \in R_n}.$$

The presented method appeals to the conditioning theory and backward error analysis [2] to investigate weights for the pseudoinverse at each step of the workflow in order to reach demanded accuracy of the solution. To compute the pseudoinverse matrix, an approach based on [3] is used, and the role of the weights is discussed.

### **Acknowledgement**

Research was financially supported by Southern Federal University, grant No. VnGr-07/2020-04-IM (Ministry of Science and Higher Education of the Russian Federation).

### **References**

- [1] Molchanov I. N., Galba E. F. // *Ukr. Math. J.*, **35**, 46–50, 1983.
- [2] Rice J. H. *Matrix Computations and Mathematical Software*. McGraw-Hill Book Company, 1981.
- [3] Pennisi L. L. // *Mathematics Magazine*, **60**(1), 31–33, 1987.

## On Mathematical Processing of Test Results of Structural Vibrations with Inhomogeneity

Yu. E. Drobotov<sup>1\*</sup>, A. V. Cherpakov<sup>1,2\*\*</sup>

<sup>1</sup>*Southern Federal University, Rostov-on-Don, Russia*

<sup>2</sup>*Don State Technical University, Rostov-on-Don, Russia*

\*[yu.e.drobotov@yandex.ru](mailto:yu.e.drobotov@yandex.ru), \*\*[alex837@yandex.ru](mailto:alex837@yandex.ru)

The abstract states the problem on vibration control for systems with inhomogeneity and proposes an approach for mathematical modelling of such vibration processes basing on their test results. Specifically, the output values of vibration acceleration are represented as the response function  $f_i^*(t)$ ,  $t \in [0, T_H]$ , where the time interval  $T_H$  is sufficiently large for the system state numbered  $i$  under diagnostics. Every  $f_i^*(t)$  can be considered in a discretized form, i.e.

$$f_i^* = [f_{i,1}^*, \dots, f_{i,n}^*]^T \in \mathbb{R}^n,$$

where  $\mathbb{R}^n$  denotes the space of all real vectors with a specific metrics, by default with the Euclidean one. The discretization step  $\Delta t$  is chosen with regard to the discretization theorem, however the presented paper considers the problem on varying  $\Delta t$  in dependence on the informativity of sub-intervals. Wavelet analysis is used to reveal such sub-intervals, and the following study is carried out to express the considered signal in the form of a series on an orthonormal system of functions with the local effects being taken into account.

### **Acknowledgement**

Research was financially supported by Southern Federal University, grant No. VnGr-07/2020-04-IM (Ministry of Science and Higher Education of the Russian Federation).

## The Riesz Potential Type Operator with Power-Logarithmic Kernel in Mathematical Modelling

Yu. E. Drobotov\*, B. G. Vakulov

*Southern Federal University, Rostov-on-Don, Russia*

\*[yu.e.drobotov@yandex.ru](mailto:yu.e.drobotov@yandex.ru)

Let  $\mathbb{R}^n$  is the space of all vectors  $x = (x_1, x_2, \dots, x_n)$  with real coordinates, supplied with the Euclidean metric  $|x - \sigma| = \sqrt{(x_1 - \sigma_1)^2 + \dots + (x_n - \sigma_n)^2}$ , and  $x \cdot \sigma = x_1 \sigma_1 + \dots + x_n \sigma_n$  is an inner product in it. A multidimensional spherical convolution operator in its general definition is

$$(Kf)(x) = \int_{S^{n-1}} k(x \cdot \sigma) f(\sigma) d\sigma, \quad x \in S^{n-1},$$

where  $S^{n-1} := \{x \in \mathbb{R}^n : |x|=1\}$  is an unit sphere in  $\mathbb{R}^n$  and the kernel  $k(x \cdot \sigma)$  defines the specific operator researched. Such operators can be studied with applying the Fourier–Laplace multiplier theory [1, p. 10], which provides a way, in which the image  $Kf$  of the operator can be expanded into a Fourier series, if there is a Fourier decomposition of the preimage  $f$ . The presented research considers a special kind of the spherical convolution operators, namely the Riesz potential type operators with a power-logarithmic kernel:

$$(K^{\alpha,\nu} f)(x) = \int_{S^{n-1}} \frac{f(\sigma)}{|x-\sigma|^{m-1-\alpha}} \ln^{\nu} \frac{r}{|x-\sigma|} d\sigma, \quad \nu \in \mathbb{R}, \quad x \in S^{n-1},$$

and it is to outline the basic reflection properties of  $K^{\alpha,\nu} f$  [2], as well as to express its Fourier–Laplace multiplier explicitly and to invert the operator for specific values of the parameters. These theoretical results are applied to analysis of integral equations with the potential type operators on functions from the generalized Hölder spaces, which provide convenient terminology for formalizing the smoothness concept. The integral equations of such kind are of interest within mathematical modelling in both theoretical and applied disciplines, as they are used for analysis of fractal sets and considering objects with significantly specific properties, such as porous medium, polymers, colloid aggregates, aerogels, etc. [3, p. 20].

#### **Acknowledgement**

Research was financially supported by Southern Federal University, grant No. VnGr-07/2020-04-IM (Ministry of Science and Higher Education of the Russian Federation).

#### **References**

- [1] Samko S. G. *Hypersingular Integrals and Their Applications*. Taylor & Francis, 2002.
- [2] Vakulov B. G., Karapetjanc N. K., Shankishvili L. D. // *Izv. Vuzov. Matem.*, 2, 3–14, 2003.
- [3] Tarasov V. E. *Fractional Dynamics: Applications of Fractional Calculus to Dynamics of Particles, Fields and Media*. Berlin, Germany: Springer, 2010.

## **Method of Local Approximations for Calculating Stress Concentration in Elastic Bodies with Projections of Complex Shapes**

**Yu. E. Drobotov\*, G. A. Zhuravlev\*\***

*Southern Federal University, Rostov-on-Don, Russia*

\*[yu.e.drobotov@yandex.ru](mailto:yu.e.drobotov@yandex.ru), \*\*[zhur.okp@yandex.ru](mailto:zhur.okp@yandex.ru)

The problem considered is the calculation of stress concentration in the elastic bodies with projections of complex shapes. The significantly small geometric concentrators were estimated on the stress-strain state with applying the analytical solutions of plane and spatial problems in [1, 2]. In the presented abstract, the distribution of stresses in the elastic bodies with complex shape in the neighborhood of the concentrator is investigated with the method of local approximations, based on the composition of two analytical solutions: (i) the stress-strain state of a rod with two symmetric

hyperbolic recesses under pure bending, and (ii) the deflections in a cantilever plate. In the plane problem, the stress function is expressed as [3]

$$\begin{cases} F = \Phi_0 + x\Phi_1, & \Phi_i = \Phi_i(x, y), \\ \Delta\Phi_i = 0, & i = 0, 1. \end{cases}$$

The following isometric curved coordinate system is considered here:

$$\begin{cases} x(u, v) = \sinh(u)\varphi(v), \\ y(u, v) = -\cosh(u)\varphi'(v), \end{cases} \quad \varphi(v) = A \cos(v) + B \sin(v),$$

and the particular values  $A=1$  and  $B=0$  provide the one used by H. Neuber [3], while using the arbitrary values of the coefficients correspond to the problem on stresses in a rod with the dangerous section of arbitrary width. As the main result, the presented abstract proposes applying the method of local approximations to investigate the problem of reducing stress concentration in elastic bodies with projections of complex shapes, which is simultaneously accompanied by miniaturization of radius of curvature and other geometric parameters of a concentrator.

#### **Acknowledgement**

Research was financially supported by Southern Federal University, grant No. VnGr-07/2020-04-IM (Ministry of Science and Higher Education of the Russian Federation).

#### **References**

- [1] Zhuravlev G. A., Drobotov Yu. E. // *Applied Mechanics and Materials*, **404**, 350–356, 2013.
- [2] Zhuravlev G. A., Drobotov Yu. E. In *2015 International Conference on "Physics and Mechanics of New Materials and Their Applications" (PHENMA 2015) Abstracts & Schedule*. Southern Federal University Press, 275–276, 2015.
- [3] Neuber, H. *Kerbspannungslehre. Theorie der Spannungskonzentration Genaue Berechnung der Festigkeit*. Springer-Verlag Berlin Heidelberg, 2001.

## **Phase Patterns and Electrophysical Macro-responses in Solid Solutions of the Multicomponent Systems Based on Lead Zirconate Titanate**

**S. I. Dudkina\*, L. A. Shilkina, L. A. Reznichenko, I. A. Verbenko**

*Research Institute of Physics, Southern Federal University, Rostov-on-Don, Russia*

\*[s.i.dudkina@yandex.ru](mailto:s.i.dudkina@yandex.ru)

The basis of many known ferroelectric materials with high piezoelectric activity are the compounds related to complex oxides with a perovskite-type structure (OSP) and used in practice in the form of their solid solutions (SSs). The most important place among them is occupied by SSs of the lead-containing OSPs, first of all, the representatives of the binary system  $\text{PbZrO}_3 - \text{PbTiO}_3$  (PZT) and multicomponent media based on it. The latter are of considerable interest due to the fact that with increasing complexity of the composition, i.e., with an increase in the number of components in the system, the dimension of morphotropic region (MR) increases (the  $k$ -component system has  $(k - 1)$ -dimensional MR), that allows one to change the concentration of components over a wide range and provides great opportunities for creating materials with various properties (MR is the region of



the structural phase transition in the vicinity of which the electrophysical parameters are extreme). In this work, SSs of a four-component system based on PZT, including the ferro-soft complex oxide  $\text{PbW}_{1/2}\text{Ni}_{1/2}\text{O}_3$ , were fabricated and studied. The compositions were selected in the MR of the system approximated by the plane, built on the basis of data on the MR of its simpler systems. The nature of the change in the unit cell parameters depending on the composition indicates the formation of SS in the studied region. It was shown that with an increase in the  $\text{PbTiO}_3$  content in the compositions, selected in the vicinity of the MR, a transition from rhombohedral (pseudocubic) to tetragonal symmetry is observed. In all cases, when approaching the MR, the value of the homogeneous parameter of the deformation, which characterizes the spontaneous deformation of the perovskite cell, decreases especially sharply when passing from the tetragonal to the heterophase region and less clearly during a similar transition from the rhombohedral region to the MO. In all cases, the extreme behavior of the dielectric and piezoelectric parameters, mechanical  $Q$ -factor, and sound velocity were revealed, the values of which sharply increase or decrease in the small (3 – 5 mol. %) concentration range. It was established that in the 4-component system more effective compositions were obtained, the main parameters of which ( $\epsilon_{33}^T/\epsilon_0$ ,  $K_p$ ) exceed the values of the parameters of its component systems. These compositions can be effectively used in low-frequency devices (microphones, hydrophones, pickups, robotics devices, optical system deflectors, etc.).

#### **Acknowledgement**

Research was financially supported by the Ministry of Science and Higher Education of the Russian Federation (State assignment in the field of scientific activity, Southern Federal University, 2020).

## **Investigation of Influence of Nonstationary Supersaturated Environment on Characteristics of In/GaAs Nanostructures Formed by Droplet Epitaxy**

**D.D. Dukhan\*, S.V. Balakirev, M.M. Eremenko, N.E. Chernenko, M.S. Solodovnik**

*Institute of Nanotechnologies, Electronics and Equipment Engineering,  
Southern Federal University, Taganrog, 347928, Russia*

\*[duhan@sfedu.ru](mailto:duhan@sfedu.ru)

In this work, we present results of modeling the processes of In/GaAs droplet epitaxy in conditions of nonstationary supersaturation of the medium, that shows us a possibility to achieve mutually independent control of size and surface density of nanostructures. Performed theoretical studies have revealed that during the exposure processes without deposition, the material is redistributed on the surface. Due to the fact that probability of decay of a stable supercritical island is extremely small, atoms migrate mainly from wetting layer to regions of drops. In the result of material redistribution during the interruption of deposition, average droplet size increases, while the thickness of the wetting layer decreases. This process has a more pronounced effect when exposure time is increased from 1 to 3 seconds. In addition, the difference in droplet size increases with increase in deposition temperature. At a temperature of 150 °C, the average diameter of droplets, deposited in a continuous mode with double interruption for a 3 second period, increases from 18 to 22 nm (by 18%), while at a temperature of 300 °C, a change occurs from 107 to 144 nm (26%).

It was also found that unsteady supersaturation of the medium affects intensity of islands nucleation, which is caused by an increased intensity of adatoms surface diffusion, which by itself, is caused by a decrease in the deposition rate. As a result, the final surface density of droplets at a temperature of 300 °C decreases from  $1.8 \times 10^8$  to  $5.2 \times 10^7$  cm<sup>-2</sup> with a double interruption of growth for 3 seconds compared to continuous deposition. Wherein decrease in double interruption intervals to just 1 second has not brought any significant change in the surface density of nanostructures. Taking into account the effect of deposition interruption on the average size of droplets and the critical thickness of their formation, the change in the surface density upon changing the conditions of unsteady supersaturation of the medium, makes it possible to conclude that there is an additional control parameter affecting growth of In/GaAs nanostructures during the process of droplet epitaxy. The revealed regularities make it possible to improve the technology of fabrication of heterostructures with quantum dots for promising opto- and nanoelectronic devices.

#### ***Acknowledgements***

This study was performed with financial support from Russian Science Foundation (grant No. 19-79-10099) and grant of the President of the Russian Federation (project MK-477.2019.8).

## **Investigating the Effectiveness of Shore-line Power Using AERMOD Model under the Aspect of Ship Emission**

**Duy-Hieu Nguyen<sup>1,2</sup>, Chitsan Lin<sup>1,2\*</sup>**

*<sup>1</sup>Ph.D. Program in Maritime Science and Technology, College of Maritime, National Kaohsiung University of Science and Technology, Kaohsiung 81157, Taiwan (R.O.C.)*

*<sup>2</sup>Department of Marine Environmental Engineering, National Kaohsiung University of Science and Technology, Kaohsiung 81157, Taiwan (R.O.C.)*

*\*[ctlin@nkust.edu.tw](mailto:ctlin@nkust.edu.tw)*

Green ports (eco-ports) have become international trends. In recent years, many projects have aimed to improve the port's environment. Among them, Kaohsiung Port has successively installed shore power systems since 2012 to reduce air pollution caused by maritime transportation. However, this system has not been in full operation because of high operating costs. Moreover, there is a lack of international standards on ship power voltage and grid frequency. When including the environmental impact, shore power can still compete with fossil fuel. Therefore, this research studies the feasibility of a green port with respect to ship emissions. The AERMOD atmospheric diffusion model simulates the air quality impact of ship emission in the Kaohsiung harbor area. There are 27 piers simulated with four major emission factors: PM10, PM2.5, SO<sub>2</sub>, and NO<sub>2</sub>. Scenarios are simulated under the long-term goal of expanding Kaohsiung harbor to include more piers. The results show that PM pollution in the ambient air was below the Taiwan standard. Since the ship's energy comes from combustion of fuel, the hourly NO<sub>2</sub> and SO<sub>2</sub> concentrations were significantly high at 1303 µg·m<sup>-3</sup> and 326 µg·m<sup>-3</sup>, respectively. The project results can be used to evaluate the effectiveness of using shore power to reduce air pollution in the port area. Study results

can also be referenced to assess other effects of air pollution on nearby areas such as NO<sub>x</sub> cycle or secondary pollution.

## **Effect of Voltage and Current to MIG Welding with 1 mm Filler Diameter to the Mechanical Properties of Welded Joints of Commercial Steel**

**Edi Santoso\*, Ichlas Wahid, Maula Nafi**

*Department of Mechanical Engineering, University of 17 Agustus 1945 Surabaya, Indonesia*

[\\*edisantoso@untag-sby.ac.id](mailto:edisantoso@untag-sby.ac.id)

The welding process is undergone heating, which causes changes in physical properties affecting the mechanical properties of the raw material. The changes in these properties will result in changes in the strength of the welds, which cause cracks and fractures in the joints, thus affecting the safety of the machine construction. To determine changes in physical and mechanical properties in commercial steels, tensile strength and hardness testing of commercial steels were performed and welding results with different voltage and current strength obtained. Welding was done by MIG welding on 3 mm thick steel plates with filler ER-50-6 of 1 mm diameter with CO<sub>2</sub> gas flow rate of 7 L/min. Voltage variations used in this study were 24 volts, 25 volts and 26 volts, and the variation of current strength used in this study were 100 A, 110 A and 120 A. Then hardness testing and tensile testing were performed. From the tensile test data, we obtained that the highest hardness value of 64.5 HRC was found at 25 V and 120 A and the lowest hardness value of 51.5 HRC was found at 19 V and 100 A. For each voltage variation, the current 120 A gave the highest hardness value and at each increase in current, the hardness value increased. From the tensile test data, we obtained that the higher the MIG welding voltage and current used gave the higher the tensile stress value. MIG welding with variations in the current strength of 100 A, 110 A, 120 A and the voltage of 19 V, 22 V, 25 V produces unequal tensile strength values. The highest tensile strength value of 50.2 kgf/mm<sup>2</sup> was produced in the welding by using 120 A current and 25 V voltage, while the lowest tensile strength value of 22.8 kgf/mm<sup>2</sup> was in the welding by using 100 A current and 19 V voltage.

## High Dielectric Constant at Room Temperature in a Family of Solid Solutions $\text{Li}_x\text{Na}_{1-x}\text{Ta}_y\text{Nb}_{1-y}\text{O}_3$ ( $y = 0.1 - 0.5$ ) Synthesized at High Pressure

V.V. Efremov\*, M.N. Palatnikov, O.B. Shcherbina

*I.V. Tananaev Institute of Chemistry – Subdivision of the Federal Research Centre «Kola Science Centre of the Russian Academy of Sciences», Apatity, Russia*

[\\*v.efremov@ksc.ru](mailto:v.efremov@ksc.ru)

Ferroelectric solid solutions (SSs)  $\text{Li}_x\text{Na}_{1-x}\text{Ta}_y\text{Nb}_{1-y}\text{O}_3$  are based on sodium niobate. They have perovskite structure type which allows different structure distortions. This fact determines a great amount of concentration phase transitions and existence of morphotropic areas. Several competing instabilities make  $\text{Li}_x\text{Na}_{1-x}\text{Ta}_y\text{Nb}_{1-y}\text{O}_3$  sensitive towards outer forces and leads to co-existence of several phases in a wide range of temperatures. Such a sensitivity to outer actions is perspective for application because varying obtaining conditions and composition can change its physical properties. SSs  $\text{Li}_x\text{Na}_{1-x}\text{Ta}_y\text{Nb}_{1-y}\text{O}_3$  ( $y = 0.1 - 0.5$ ) were synthesized under pressure  $P = 6$  GPa,  $T = 1800$  K for 3 min on press plant DO138A. Due to XRD analysis (Fig. 1) synthesized samples correspond to  $\text{NaNbO}_3$ . Sodium niobate has a crystal structure of perovskite which is characterized by ordered distortions, collective shifts of anions and cations of a certain type. It is a common knowledge that this compound is ferroelectric active and has six phase transitions in dependence on temperature, i.e. it can have seven main phases. But it is a known fact that even nominally pure  $\text{NaNbO}_3$  has a substantial admixture of a ferroelectric phase Q(P21ma). An increase in Li concentration leads to stabilization of Q-phase in pure sodium niobate; the Q-phase co-exists with P-phase. At large amounts of Li, samples become uniform ferroelectrics with a structure characteristic of Q-phase. Thus, lithium and tantalum concentration in the system, as well as synthesis temperature influence phase composition connected with polymorphism in high pressure ceramics. Temperature dependences of dielectric conductivity contain anomalies in the shape of maxima in the area of room temperatures. These anomalies were detected to be caused by a structure phase transition  $N \leftrightarrow Q$  in studied samples. Values of  $\varepsilon'$  at room temperature at a frequency 100 KHz have already high values. A dispersy of dielectric constant was studied. Fig. 2 demonstrates the result. The dispersy deepness is huge, as Fig. 2 reveals. In the area of low frequencies  $\varepsilon'$  is  $\sim 10^6 - 10^8$  in dependence on tantalum concentration. For ceramics with  $y = 0.4$ ,  $\varepsilon' \sim 10^4$  and values do not show strong dependence on the measurement of field frequency. The obtained great dielectric constant dispersy is usually caused by migration polarization due to Maxwell-Wagner, if there is simultaneously an ion conductivity in heterogeneity systems. Charge carriers gain on the component boundaries and contribute to polarization, i.e. lead to an increase in dielectric constant of a material. In ceramic samples such contribution is proportional to the volume of electrode-composite boundaries and dielectric spontaneous polarization. This effect can be used for creation of condensers.

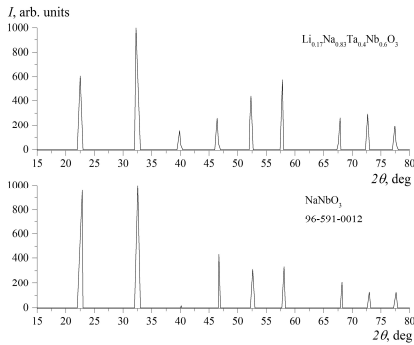


**Fig. 1.** XRD patterns of  $\text{Li}_{0.17}\text{Na}_{0.83}\text{Ta}_{0.4}\text{Nb}_{0.6}\text{O}_3$  and  $\text{NaNbO}_3$  compositions

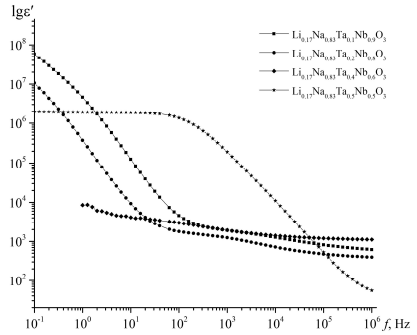


**Fig. 2.** Frequency dependence of real part of dielectric constant  $\text{Li}_{0.17}\text{Na}_{0.83}\text{Ta}_y\text{Nb}_{1-y}\text{O}_3$  ( $y = 0.1 - 0.5$ ) at room temperature

## Monitoring the Condition of Structures of an Existing Building Near New Construction

I. O. Egorochkina, I. A. Serebryanaya\*, E. A. Shlyakhova

*Don State Technical University, 1, Gagarin Sq., Rostov-on-Don, 344010, Russia*

\*[silveririna@mail.ru](mailto:silveririna@mail.ru)

In the process of building a new construction in dense urban area, there is high risk of destruction and damage for structures of adjacent buildings [1]. One of the common problems is the development of cracks in the supporting structures of buildings that appear in the result of the damaging effects of shock and vibration when installing pile foundations of new buildings. Monitoring allows one to record the amplitude-time characteristics of fluctuations during the operation of the hydraulic hammer and equipment for driving piles and to compare them with the maximum permissible. Installation of beacons at the locations of existing defects (cracks) in the bearing walls of the monitoring object allows one to monitor the development of deformations during the driving of test piles of new construction. To register the amplitude-time characteristics of the vibrational velocities, the Vibran-2.2 analyzer was used, the use of which is effective for the purpose of technical diagnostics of building structures [2, 3]. The digitized results of measurements of the amplitude-frequency characteristics (AFCs) were processed using the specialized ANSYS software package. The developed program for signal processing is based on the transformation of the data array and the construction of the dependence of the frequency response on the intensity and duration of the vibration (shock) effect. Frequency response reflect the integral values of the amplitudes for each of the frequencies in a given range of the original signals. According to the

results of processing, the values of the maximum amplitude of vibrations when driving piles were obtained. The results were compared with the standard values of the maximum allowable amplitudes of acceleration of foundation vibrations according to Russian standard "Design and installation of pile foundations and sheet piling in the conditions of reconstruction of industrial enterprises and urban development". The parameters of the safe driving mode of piles without starting a diesel hammer engine with leader drilling were established.

#### **References**

- [1] Livadnaya D.B., Serebryanaya I.A. // *Engineering Journal of Don*, **6**, 2019, [jvdon.ru/ru/magazine/archive/N6y2019/6010](http://jvdon.ru/ru/magazine/archive/N6y2019/6010).
- [2] Egorochkina I.O., Serebryanaya I.A., Shlyakhova E.A., Matrosov A.A., Maltseva I.V., Lukhneva Yu.N. // *Engineering Journal of Don*, **2**, 2020, [jvdon.ru/ru/magazine/archive/N2y2020/6330](http://jvdon.ru/ru/magazine/archive/N2y2020/6330).
- [3] Cherpakov A., Egorochkina I., Shlyakhova E., Kharitonov A., Zarovny A., Dobrohodskaya S. // *MATEC Web of Conferences*, **106**, 04009, 2017 [doi.org/10.1051/mateconf/201710604009](https://doi.org/10.1051/mateconf/201710604009).

## **Formation of the Structure of Heavy Concrete with Increased Crack Resistance**

**I.O. Egorochkina<sup>1\*</sup>, E.A. Shlyakhova<sup>1</sup>, A.V. Cherpakov<sup>1,2</sup>, I.A. Parinov<sup>2</sup>, M.-Y. Yeh<sup>3</sup>, C.-D Yang<sup>3</sup>**

<sup>1</sup>*Don State Technical University, Rostov-on-Don, Russia*

<sup>2</sup>*Southern Federal University, Rostov-on-Don, Russia*

<sup>3</sup>*Department of Microelectronics Engineering, National Kaohsiung University of Science and Technology, Kaohsiung, Taiwan (R.O.C.)*

[\\*arin77@bk.ru](mailto:*arin77@bk.ru)

Concrete products and reinforced concrete structures are considered one of the main and high-quality materials for the construction of building complexes. Every year the scale of construction is increasing, and the issues of choosing materials for the objects under construction are becoming more and more responsible. Ensuring the performance of building structures is considered a key issue in modern technology for the production of concrete and reinforced concrete. Crack resistance is one of these characteristics. The issue of crack resistance of concrete and reinforced concrete structures has been relevant for a long time and remains so to this day. There are many different factors that have a dominant influence on fracture toughness. The literature has repeatedly described possible ways to increase crack resistance, such as the use of special additives, replacement of part of the sand in concrete, reduction or replacement of a part of cement, the formation of the most suitable concrete structure for a particular case. One of the indirect methods for assessing the crack resistance of piles can be testing concrete for tensile strength during splitting (Russian GOST 10180-2012), with the help of which the effectiveness of the developed compositions of increased crack resistance was evaluated. The studies were carried out on concretes of various compositions, while the composition and type of fine aggregate of all size ranges were varied (from the nanoscale to the macrolevel). The compositions used a fine aggregate in the form of quartz sand with a size

modulus of  $M_s = 1.5$ ; screening out of stone crushing of sandstone with a size modulus of  $M_s = 3.3$ ; microsilica and nanosilica. The performed studies have shown the effectiveness of using a combined fine aggregate in order to increase the crack resistance of concrete.

#### **Acknowledgement**

Research was financially supported by Southern Federal University, grant No. VnGr-07/2020-04-IM (Ministry of Science and Higher Education of the Russian Federation).

#### **Reference**

[1] Cherpakov A., Egorochkina I., Shlyakhova E., et al. // *MATEC Web of Conferences*, **106**, 04009, 2017.

## **Impact of Substandard Aggregates on the Effectiveness of Chemical Additives**

**I.O. Egorochkina<sup>1\*</sup>, E.A. Shlyakhova<sup>1</sup>, A.V. Cherpakov<sup>1,2</sup>, I.A. Parinov<sup>2</sup>, S.-H. Chang<sup>3</sup>**

<sup>1</sup>*Don State Technical University, Rostov-on-Don, Russia*

<sup>2</sup>*Southern Federal University, Rostov-on-Don, Russia*

<sup>3</sup>*Department of Microelectronics Engineering, National Kaohsiung University of Science and Technology, Kaohsiung, Taiwan (R.O.C.)*

[\\*arin77@bk.ru](mailto:arin77@bk.ru)

In the construction industry, the issue of the quality of precast concrete and reinforced concrete products is very acute. It is known that the main indicators of the quality of concrete directly depend on the characteristics of the raw materials, including the content of pollutants (CPTs) in the aggregates used. Aggregates with the required characteristics for the production of concrete mixes are available in most regions of the Russia in limited quantities. As practice shows, at present, many enterprises of the Rostov Region have significant difficulties with conditioned fine aggregates. The sands used have a low value of the modulus of size ( $M_s$ ) from 1.2 to 1.5 and a high value of the content of silty-clay particles – above 5%. It is noted that the effectiveness of the use of chemical additives to regulate the rheological characteristics of concrete mixtures in the production of concrete can change significantly with a change in the characteristics of aggregates. Currently, there is a tendency to use plasticizing additives based on polycarboxylate (PCX) ethers. The effectiveness of polycarboxylates depends on the charge density of the main chain, as well as on the chemical structure, length and number of side branches. In Russia, the share of PCX accounts for an insignificant part of the total volume of plasticizing additives, which is associated not so much with their high cost as with strict restrictions on the content of CPTs in aggregates. Often, when using fine sands, which include most of the sands used in the Rostov Region, with an increased content of CPTs, it is required to increase the consumption of expensive PCX. In addition, the effectiveness of their action in concrete mixes decreases. Our studies to assess the effectiveness of PCX in concrete mixtures using fine sands from deposits of the Rostov Region with a modulus of size from 1.2 to 1.8 and a content of CPTs from 2.0 to 6.8% made it possible to establish the possibility of their application.

#### **Acknowledgement**

Research was financially supported by Southern Federal University, grant No. VnGr-07/2020-04-IM (Ministry of Science and Higher Education of the Russian Federation).

## References

- [1] Egorochkina I.O., Shlyahova E.A., Cherpakov A.V., Soloviev A.N. // *Engineering Journal of Don*, 4, 2015 (In Russian).
- [2] Egorochkina I.O., Shlyahova E.A., Cherpakov A.V., Manvelyan L.A., Kucherenko D.Yu. // *Engineering Journal of Don*, 4, 2016 (In Russian).
- [3] Shlyakhova E. A., Holostova A. I. In: Proc. Int. Sci.-Pract. Conf. CONSTRUCTION - 2015: CONTEMPORARY PROBLEMS OF CONSTRUCTION, Rostov-on-Don, 565-567, 2015 (In Russian).

## Influence of Chemical, Mineralogical and Textural Features of Aggregates on the Processes of Structure Formation in Concrete

I.O. Egorochkina<sup>1\*</sup>, E.A. Shlyakhova<sup>1</sup>, A.V. Cherpakov<sup>1,2</sup>, I.A. Parinov<sup>2</sup>,  
M.-Y. Yeh<sup>3</sup>, C.-D Yang<sup>3</sup>

<sup>1</sup>Don State Technical University, Rostov-on-Don, Russia

<sup>2</sup>Southern Federal University, Rostov-on-Don, Russia

<sup>3</sup>Department of Microelectronics Engineering, National Kaohsiung University of Science and Technology, Kaohsiung, Taiwan (R.O.C.)

\*[arin77@bk.ru](mailto:arin77@bk.ru)

High performance indicators of concretes are achieved by using high-quality raw materials and technological methods aimed at forming a defect-free structure, providing a high degree of adhesion of components [1 – 3]. A whole complex of processes and phenomena is involved in the formation of the structure of concrete, the degree of study of which is not the same and requires detailed research. The work of domestic and foreign researchers is devoted to the question of the role of the adhesion of cement stone with aggregates in creating concrete strength. It is emphasized that ensuring high adhesion strength is achieved both by optimizing the shape and relief of aggregates, and by intensifying physicochemical processes in the contact zone. To assess the effect of the mineralogical, chemical and textural features of various aggregates on the structure formation in the contact zone, we carried out X-ray phase and differential thermal analyzes of the aggregate surfaces directly in contact with the cement stone. The decoding of the X-ray diffraction patterns showed that complex physical and chemical processes are taking place in the contact zone. The phase analysis showed that the contact zone is formed by substances whose composition and structure are intermediate in comparison with the composition and structure characteristic of cement stone and aggregate. Compounds characteristic of Portland cement stone in the process of cement hydration on the surface of the aggregate are recrystallized into complex compounds of the types:  $2CaOSiO_{2n}H_2O$ ,  $2CaOAl_2O_{3n}H_2O$ ,  $3CaOAl_2O_3(Ca, Mg)CO_{3n}H_2O$ . So, the most probable is the arrangement of substances to the following order: carbonate –  $2CaOAl_2O_3SiO_{2n}H_2O$  – cement stone, which represents a gradual transition from aggregate to cement stone. Compounds with a stable crystal lattice were found in the contact zone:  $4CaOAl_2O_3Fe_2O_{3n}H_2O$ ,  $2CaOAl_2O_3SiO_{2n}H_2O$ ,  $3MgO_2SiO_{2n}H_2O$ ,  $2CaOSiO_{2n}H_2O$ . Chemisorption processes at the interface largely determine the adhesion of the cement stone to the aggregate grains, which increases with the increase in the



chemical activity of the aggregate to the cement stone. The data obtained confirmed the assumption that the presence of hydrated formations of cement stone on the surface of fillers, similar in structure and chemical composition to crystallizing new formations, promotes the formation of strong isomorphic and epitaxial intergrowths between calcite of carbonate fillers and calcium oxide hydrate due to the closeness of the lattice parameters of these crystals. The result of the formation of the "fibrous" structure of the cement stone and the low-defect contact zone is a more preferable structure of the capillary-porous structure, which largely has a positive effect on the performance properties of concrete.

#### **Acknowledgement**

Research was financially supported by Southern Federal University, grant No. VnGr-07/2020-04-IM (Ministry of Science and Higher Education of the Russian Federation).

#### **Reference**

- [1] Egorochkina I. O. // News of South-Ural State University. Building and Architecture Series, **3**, 49-53, 2014.
- [2] Shlyakhova, E. A., Akopyan, A. F., Akopyan, A. V. // *Engineering Journal of Don*, 2012, **4**(Pt. 2).
- [3] Shlyakhova E.A., Egorochkina I.O., Cherpakov A.V. In: *Proceedings of the 2018 International Conference on Physics and Mechanics of New Materials and Their Applications*, Ivan A. Parinov, Shun-Hsyung Chang, Yun-Hae Kim (Eds.). Nova Science Publishers, New York, 227-232, 2019.

## **Optimization of the Composition of the Repair Mixture Based on Non-shrinking and Expanding Cements**

**I.O. Egorochkina<sup>1\*</sup>, E.A. Shlyakhova<sup>1</sup>, A.V. Cherpakov<sup>1,2</sup>, I.A. Parinov<sup>2</sup>, Y.-M. Liu<sup>3</sup>**

<sup>1</sup>*Don State Technical University, Rostov-on-Don, Russia*

<sup>2</sup>*Southern Federal University, Rostov-on-Don, Russia*

<sup>3</sup>*Department of Electric Communication Engineering, National Kaohsiung University of Science and Technology, Kaohsiung, Taiwan (R.O.C.)*

\*[arin77@bk.ru](mailto:arin77@bk.ru)

Power transmission lines (PTLs) are strategic facilities, the reliability of which depends on the country's life support. Most of the currently operated transmission lines were put into operation in the twentieth century, and by now the problem of assessing their technical condition, repairing, if necessary, and maintaining it in a working condition has ripened. Many works have been devoted to the issues of technical diagnostics and repair of structures of power transmission lines. Defects that appear during the operation of reinforced concrete elements of power lines have different localization and degree of manifestation, but the destruction of the surface layer of concrete with exposure of reinforcement is characteristic, more often at the base of the power line rack. The purpose of this research work is to select the optimal composition of the repair mixture based on non-shrinking and expanding cements, which ensure reliable adhesion of the repair compounds to the concrete of the structure, which will ensure the bearing and operational characteristics in the restored reinforced concrete elements of the power transmission line at the design level. The studies

were carried out using a complex of physicochemical, acoustic and dynamic research methods, in particular the methods of ultrasonic flaw detection and vibration diagnostics. In the result of mathematical planning and optimization, repair compositions were selected containing a four-component expanding complex additive of the sulfoaluminate type, the positive effect of which lies in the directional modeling of the fine-porous structure of the cement stone with the intensification of the process of pore clogging by crystallizing complex salts such as hydrosulfoaluminates and calcium hydrochloroaluminates. As a result, a fine-pored cement stone structure is formed with evenly distributed, partially sealed pores. Due to, the strength indicators, crack resistance, water resistance and frost resistance of the resulting repair composition are significantly increased.

#### ***Acknowledgement***

Research was financially supported by Southern Federal University, grant No. VnGr-07/2020-04-IM (Ministry of Science and Higher Education of the Russian Federation).

#### ***References***

- [1] Cherpakov A., Egorochkina I., Shlyakhova E., et al. // *MATEC Web of Conferences*, **106**, 04009, 2017.
- [2] Shlyakhova E.A., Egorochkina I.O., Serebryanaya I.A., Matrosov A.A. // *Materials Science Forum*, **931**, 618-623, 2018.

## **Statistical Methods for Predicting and Preventing the Appearance of a Defect in Efflorescence on the Surface of Brickwork**

**I.O. Egorochkina<sup>1\*</sup>, E.A. Shlyakhova<sup>1</sup>, A.V. Cherpakov<sup>1,2</sup>, I.A. Parinov<sup>2</sup>,  
C.-Y. Jenny Lee<sup>3</sup>, C.-C. Yang<sup>3</sup>**

<sup>1</sup>*Don State Technical University, Rostov-on-Don, Russia*

<sup>2</sup>*Southern Federal University, Rostov-on-Don, Russia*

<sup>3</sup>*Department of Microelectronics Engineering, National Kaohsiung University of Science and Technology, Kaohsiung, Taiwan (R.O.C.)*

\*[arin77@bk.ru](mailto:arin77@bk.ru)

Brick buildings are characterized by high strength, heat engineering and aesthetic properties. The appearance of such a defect as efflorescence on the masonry surface, in addition to reducing aesthetics over time, leads to a decrease in the strength and durability of brick structures. Efflorescence can be located locally or diffusely over the entire surface of the wall and have different intensities. Measures to prevent efflorescence are mainly reduced to hydrophobization of the surface. For the purposes of predicting and preventing the appearance of a defect in efflorescence, the reasons for the appearance of efflorescence were established, the factors influencing this process were studied, and a system for preventing and eliminating the defect was developed [1, 2]. The use of statistical methods of quality management made it possible to establish the factors causing the appearance of salts on the wall surface. For diagnostic purposes, a modern instrumental base was used, the methodology and technology of using which is highlighted in the works. The chemical and mineralogical composition of the cement binder, the main component of

the solution, plays a significant role in the processes of efflorescence. For masonry work, the following binders are mainly used: Portland cement without additives, Portland cement with additives, slag Portland cement, pozzolanic Portland cement. The conducted spectral, X-ray phase, differential thermal analyzes, the results presented here, made it possible to establish a variation in clinker content in the range from 98.5 to 20%, and the amounts of additives from 0 to 80%. If we assume that all binders are made on the basis of one clinker of normal composition and initially do not take into account the role of additives, then based on the regulated binder compositions, the amount of calcium hydroxide and, accordingly, the intensity of efflorescence in the cement stone will change in the following order: PC – PC – D – SHPC – PPTs. To prevent the appearance of efflorescence, it is necessary to use cements with a limited alite content and with a low water-cement ratio, as well as introduce mineral adsorbents or chemical surface-active additives. It is recommended to use active silica additives as mineral additives that reduce the diffusion process of  $\text{Ca}(\text{OH})_2$  and bind it into insoluble low-basic hydrosilicates. In the result of the research, an analysis of the causes of efflorescence, the type of violation of the requirements that led to the appearance of this defect and the development of preventive recommendations were proposed. Compliance with the recommendations for the prevention of efflorescence allows one to ensure the durability, safety, aesthetics and commercial attractiveness of brick buildings and structures.

#### ***Acknowledgement***

Research was financially supported by Southern Federal University, grant No. VnGr-07/2020-04-IM (Ministry of Science and Higher Education of the Russian Federation).

#### ***References***

- [1] Egorochkina I.O., Serebryanaya I.A., Shlyakhova E.A., Matrosov A.A., Pronina K.A. // *Engineering Journal of Don*, 4, 2019.
- [2] Shlyakhova E.A., Akopyan A.F., Akopyan A. V. // *Engineering Journal of Don*, 4(Pt 2), 2012.

## **Characterisation of Woven Composite Material Properties by Using an Inverse Technique Based on Vibration Tests**

**Endija Namsone<sup>1\*</sup>, Denis Ermakov<sup>2</sup>**

*<sup>1</sup>Institute of Materials and Structures, Riga Technical University  
Kalku Str. 1, LV-1658, Riga, Latvia*

*<sup>2</sup>Department of Mechanics of Composite Materials and Structures, Perm National Research Polytechnic University, Komsomolski Ave. 29, 614990 Perm, Russia*

\*[barkanov@latnet.lv](mailto:barkanov@latnet.lv)

Nowadays, use of woven composite materials has increased and, due to their high stiffness and low weight properties, these materials are utilized widely in different engineering applications like aircraft, automobile, ship, railway constructions, etc. Unfortunately, not always all necessary material data are available from manufactures for the design and optimisation purposes of advanced lightweight structures. For this reason, a mixed numerical-experimental technique based on vibration tests is modified and applied in the present study to determine the elastic material properties of woven composites. The non-destructive technique consists of physical experiments,

numerical modelling and material identification procedure, where an identification of material properties is performed minimising the error functional between the experimental and numerical parameters of structural responses. The computational effort has been substantially reduced by using non-direct optimisation methodology developed on the planning of experiments and response surface technique. For the characterisation of woven composite material properties, two carbon fibre panels made of four anisotropic layers with different reinforcement schemes  $[0^\circ/90^\circ/0^\circ/90^\circ]$  and  $[-45^\circ/45^\circ/-45^\circ/45^\circ]$  have been prepared. The selected thicknesses and reinforcement schemes of specimens have been chosen in relation to the design requirements for a manufacture of power shells widely used in aircraft structures. Samples have been made of CM-PregF-T27 200/1250 CP0041 45 prepreg carbon fibre material by manual layout technology, vacuuming under the polyethylene film and curing in an autoclave at high temperature and pressure. The plans of experiments with regular distribution of the points of experiments in the domain of factors for both samples have been formulated for 3 design parameters and 20 experiments. Then in each experimental point the finite element vibration analysis based on the first-order shear deformation theory have been carried out in ANSYS for the samples with completely free boundary conditions. Physical experiments have been executed by using non-contact excitation with loudspeaker and optical sensing with POLYTEC scanning laser vibrometer PSV-400-B. During vibration testing, 11 first frequencies have been measured for specimen 1 and 12 first frequencies – for specimen 2. Different order polynomial functions have been estimated in their applicability to approximate accurately the numerical results. The identified elastic material properties have been successfully validated by comparison of numerical and experimental resonant frequencies.

## **Study of the Growth of GaAs on Silicon with Amorphized Areas**

**M. M. Eremenko\*, S. V. Balakirev, N.E. Chernenko, M. S. Solodovnik, O. A. Ageev**

*Southern Federal University, REC “Nanotechnologies”, Taganrog, Russia*

[\\*eryomenko@sfnedu.ru](mailto:*eryomenko@sfnedu.ru)

The integration of highly efficient light emitting sources based on III/V structures with silicon technology remains a difficult task today [1], but it could allow the creation of photonic integrated circuits compatible with well-established silicon complementary metal oxide semiconductor (CMOS) technology. This is expected to combine the advantages of GaAs technology (high-performance laser sources) and Si technology (high-speed information processing). The use of various surface patterning methods allows not only to localize the structure on a certain area of the substrate, but also to reduce the density of dislocations in the growing layers by orders of magnitude while reducing the thickness of the grown nanostructures. In this work, the focused ion beam (FIB) method was used to localize and improve the nucleation of the grown GaAs on Si structures. For growth processes, on-axis Si (001) substrates with preliminary FIB processing were used. Surface modification was carried out by implanting Ga atoms in predetermined areas of the Si substrate. To identify optimal regimes of the FIB procedure, the dose and current of implantation were varied. After removing the oxide, the substrate was cooled to 600 °C and 200 nm of GaAs buffer was deposited at a rate of 0.1 ML/s. The epitaxial materials were fabricated using a SemiTEq STE 35

molecular beam epitaxy system with solid-state sources. At the lowest dose of Ga implantation equal to  $1 \text{ pC}/\mu\text{m}^2$ , the deposition of GaAs on modified areas occurs as separate crystallites with an irregular shape. An increase in the implantation dose leads to GaAs coalescence and further filling of the areas. However, it is worth noting that at the highest dose of implantation, the morphology of the grown nanostructures is deteriorated. We suggest that this is due to significant damage to the crystal structure of the modified regions during FIB processing. An analysis of the surface roughness showed that with an increase in the dose of implanted Ga from  $1$  to  $7 \text{ pC}/\mu\text{m}^2$ , the roughness of the grown nanostructure decreases. For nanostructures grown in areas with an implantation current of  $1 \text{ pA}$ , a lower surface roughness is observed compared to  $10 \text{ pA}$ . However, in both cases, with an increase in the implantation dose from  $7$  to  $21 \text{ pC}/\mu\text{m}^2$ , the roughness increases, which confirms the processes of surface and quality deterioration of the grown nanostructures.

### ***Acknowledgements***

This work was supported by the Russian Science Foundation (grant No. 20-69-46076). The results were obtained using the equipment of the Research and Education Center "Nanotechnologies" of Southern Federal University.

### ***Reference***

[1] Tang M., Park J.-S., Wang Z., Chen S., Jurczak P., Seeds A., Liu H. // *Prog. Quant. Electron*, **66**, 1-18, 2019.

## **A Case Study: Application of Business Process Re-engineering in Company**

**Erni Puspanantasari Putri<sup>1</sup>, Sukon Aduldaecha<sup>2</sup>**

<sup>1</sup>*Department of Industrial Engineering, University of 17 Agustus 1945 (UNTAG) Surabaya, Indonesia*

<sup>2</sup>*Faculty of Business Administration and Accountancy, Khon Kaen University (KKU), Thailand*

\*[erniputri@untag-sby.ac.id](mailto:erniputri@untag-sby.ac.id)

Organizations are consistently searching for approaches to reduce expenses and increment yields. With the quick movement of innovation, the appropriation of new innovation inside organizations is a consistent need. Thus, these progressions could state the requirement for business process improvement. There is a more extensive and increasingly unique way to deal with upgrading current business forms, in particular business process reengineering (BPR). Normally, in the present day and age, this will incorporate innovation. However, there is a whole other world to it than just utilizing innovation for change. BPR assists organizations with lessening costs and boost yields. The company process has to be invariably analyzed to comply with the requirement and expectancy of the expanding people. Hence, it can scheme the work-streams and evaluates the company processes. In applying the BPR method, the company can attain the following benefits: meet customer satisfaction overall, gain the expense benefit, increase the competency benefit, establish customer value, and existence the obvious company vision. In this report, the case studies of the BPR method application in the company are discussed as follows: (i) restructuring strategy at

Garuda Indonesia Aircraft; (ii) work reengineering in Ford Motor Company; (iii) redesign of recruitment procedure in Google Company; (iv) reengineering of item advancement in Hallmark Cards Inc. and (v) reengineering guideline in Taco Bell Company.

## **Case Study of the Keys to Success of Supply Chain Management in Company**

**Erni Puspanantasari Putri<sup>1\*</sup>, Sukon Aduldaecha<sup>2</sup>**

*<sup>1</sup>Department of Industrial Engineering, University of 17 Agustus 1945 (UNTAG) Surabaya, Indonesia*

*<sup>2</sup>Faculty of Business Administration and Accountancy, Khon Kaen University (KKU), Thailand*

*[\\*erniputri@untag-sby.ac.id](mailto:erniputri@untag-sby.ac.id)*

Supply chain management (SCM) creates benefits advantages as well as novel efficiency, great benefits, fewer costs, and intensifies cooperation. SCM sustains enterprises to better organize demand, lead the proper inventory quantity, handle disruptions, preserve minimum costs, and meet customer satisfaction effectively. These SCM advantages are attained by selecting an effective strategy and the right technology to organize the plurality growth of supply chains. SCM takes possession of important effects on both company and consumer. The main company processes will be integrated by SCM to the final consumers via original providers, manufacturers, marketing, and third-side logistics association according to the supply chain. These integrations are as follows: (i) crucial success aspects in an enthusiastic trade atmosphere; (ii) requirement for improving grade in the structure; (iii) effective supply chain achievement through distributing and applying sources, capitals, facilities, processes, information, science, systems among different degrees; and (iv) improving the service time, efficiency and expenses of the applying systems, process quality, inventory values, and the information transference. Integration guides to preferable teamwork for equalized production organizing, cooperation product establishment, cooperation requirement, and logistics designing. In this report, it will be discussed the case study of keys to the SCM success in companies as follows: (i) success keys of McDonald's SCM; (ii) Starbucks SCM modification; (iii) Nestlé's SCM strengths and (iv) strategy works of Amazon's SCM.

## **A Case Study of Creative Industry Development Strategy in Sidoarjo Regency, East Java Province, Indonesia**

**Erni Puspanantasari Putri<sup>1\*</sup>, Victoria Aurellia Sri Paramita Putri<sup>2</sup>**

<sup>1</sup>*Department of Industrial Engineering, University of 17 Agustus 1945 (UNTAG) Surabaya, Indonesia*

<sup>2</sup>*Department of Industrial Engineering, University of Pembangunan Nasional Veteran (UPN Veteran) East Java, Surabaya, Indonesia*

\*[erniputri@untag-sby.ac.id](mailto:erniputri@untag-sby.ac.id)

Creative industries have an important role in the economy of a country. At this time, creative industry players are faced with the era of the ASEAN Economic Community (AEC). The implementation of the Southeast Asian free market is a challenge as well as an opportunity for industry creative of Small and Medium Enterprises (SMEs). Therefore, industry creative products must have standards to be able to compete. The era of the industrial revolution 4.0 has begun. Synergy with the development of information technology is the key for creative industry players to be able to compete in the global market. Creative industries have a characteristic of their superiority in the creative side of a product's design. Sidoarjo Regency is located in East Java Province, Indonesia. This regency has a border with Surabaya City, Madura Strait, and several regencies, namely: Gresik Regency, Pasuruan Regency, and Mojokerto Regency. Sidoarjo Regency is one of the main buffer cities of Surabaya City and is also a member of the Gerbangkertosusila Region. The Gerbangkertosusila Region consists of Gresik Regency, Bangkalan Regency, Mojokerto Regency, Surabaya City, Sidoarjo Regency, and Lamongan Regency. This region is the second-largest metropolitan area in Indonesia. Surabaya City is the center of the Gerbangkertosusila Region. Sidoarjo Regency is also called the City of Indonesian SMEs. Some of the reasons are as follows: (i) it has the largest number of small and medium enterprises (SMEs) in Indonesia; (ii) it has many people's economic activities with small and medium scale business sectors; (iii) it has around 82 creative industry centers of SMEs; and (iv) it has creative business villages, such as batik villages, snack villages, cracker villages, sandals, and shoe villages, etc. The Sidoarjo Regency Government encourages the creative industries to continuously improve their innovations. By increasing these innovations, the creative industry will be able to compete in the global market. The efforts, made by the Sidoarjo Regency Government to develop the creative industries, provide guidance and assistance to improve SMEs businesses. Several creative industry development programs in the Sidoarjo Regency consist of (i) Tanggulangin SMEs Revitalization Center Program; (ii) Sidoarjo Youth Center Program; (iii) Agro Tourism Village Development Program; (iv) Independent and Prosperous Industrial Village Program; (v) Minapolitan Area Development; and (vi) Digital SMEs Village Program.

## **Development Strategy of Creative Economy and Creative Industry in Surabaya, Indonesia**

**Erni Puspanantasari Putri<sup>1\*</sup>, Victoria Aurellia Sri Paramita Putri<sup>2</sup>**

<sup>1</sup>*Department of Industrial Engineering, University of 17 Agustus 1945 (UNTAG) Surabaya, Indonesia*

<sup>2</sup>*Department of Industrial Engineering, University of Pembangunan Nasional Veteran (UPN Veteran) East Java, Surabaya, Indonesia*

[\\*erniputri@untag-sby.ac.id](mailto:erniputri@untag-sby.ac.id)

The creative economy is a concept that intensifies information and creativity based on ideas and knowledge from human resources as the main production factor. This concept will be supported by the existence of a creative industry. To achieve successful business development, companies need a strategy to manage the effort. Therefore, the company will be able to produce maximum profit. Surabaya is the second-largest city in Indonesia after Jakarta as the capital city. With a population of around 3 million people, Surabaya has become: (i) metropolis city with some diversity; (ii) the center for business, commerce, industry, and education; (iii) a major port and commercial trading center in Eastern Indonesia and (iv) one of the largest cities in Southeast Asia. Creative industries have an important role to encourage economic growth in the region and nationally. Surabaya has the potential to become a center for creative industries in the future. The creative economy industry development program is considered successful in improving the economy of Surabaya City. Several programs to develop the economy and creative industries that have been launched in Surabaya City are as follows: (i) Economic Heroes and Young Fighters Program, (ii) Millennial Economic Festival, and (iii) Surabaya Start-up Program.

## **The Survival Strategy of Indonesia MSMEs Development in Facing the Economic Crisis due to the COVID-19 Outbreak**

**Erni Puspanantasari Putri<sup>1\*</sup>, Victoria Aurellia Sri Paramita Putri<sup>2</sup>**

<sup>1</sup>*Department of Industrial Engineering, University of 17 Agustus 1945 (UNTAG) Surabaya, Indonesia*

<sup>2</sup>*Department of Industrial Engineering, University of Pembangunan Nasional Veteran (UPN Veteran) East Java, Surabaya, Indonesia*

[\\*erniputri@untag-sby.ac.id](mailto:erniputri@untag-sby.ac.id)

Micro, Small, and Medium Enterprises (MSMEs) are the driving wheels of the Indonesian economy. MSMEs have contributed greatly to the development and economic growth of this country. Based on data released by the Ministry of Cooperatives and Small and Medium Enterprises of the Republic of Indonesia concerning Data Development of Micro, Small, Medium Enterprises (MSMEs) and



Large Enterprises (LEs) in 2016-2017, MSMEs are amounted to 62,922,617 business units and LEs are only amounted 5,460 business units. Therefore, the number of MSMEs in Indonesia reaches 99.9 % of the total business units. Indonesia has experienced in two period of economic crisis, namely: a monetary crisis (1998) and a global financial crisis (2008). MSMEs remain strong in sustaining the national economy and are still able to absorb labor during the two economic crisis periods. However, this is not the case with the effects of the economic and financial crisis during the global spread of the corona virus (COVID-2019). MSMEs have become the most vulnerable sector in the economic crisis. The resilience of micro, small and medium enterprises (MSMEs) in Indonesia is again being tested in the face of the economic crisis as the impact of the spread of COVID-19. In addition to requiring government support, MSMEs need to make breakthroughs and strategies in order to remain able to survive amid the economic downturn. Therefore, MSMEs as a pile of the Indonesia economy can keep on to cultivate rectify. It is because MSMEs are able to preserve the survival of their business to grow and contend in the deal with strict worldwide competition.

## **Non-direct Optimisation of Coupled Thermo-chemical Problem in Pultrusion of Thin-walled Angle Profile**

**Evgeny Barkanov\*, Pavel Akishin, Andris Chate**

*Institute of Materials and Structures, Riga Technical University  
Kalku Str. 1, LV-1658, Riga, Latvia*

[\\*barkanov@latnet.lv](mailto:*barkanov@latnet.lv)

Pultrusion is a technological process, where fibres impregnated with resin move through the heated die and solidify into composite profile with a constant cross-section as in the metallic die. In many modern pultrusion processes the temperature measurements in different die points are executed by thermocouples to control the work of electrical heaters. To improve an effectiveness of conventional pultrusion processes, preserving the quality of pultruded profiles, new optimisation methodology is developed and applied for a production of thin-walled angle profiles in the present study. Due to the large dimension of numerical problem solved and multiple iterations applied for the solution of governing equations, an optimisation methodology is developed, employing the method of experimental design and response surface technique. In each point of the plan of experiments the coupled thermo-chemical problem is solved iteratively by the mixed time integration scheme and nodal control volumes method. It is necessary to note that ANSYS in this case is used only for the solution of transient thermal problem. This approach has been successfully validated by an experimental trial, when new cure sensors have been used for the measurement of electrical resistivity and temperature on the profile surface. Different order polynomial functions are evaluated for a development of suitable approximation of simulation results by using a conventional un-weighted least square estimation. To demonstrate an application of the developed non-direct optimisation methodology, the real industrial process, producing thin-walled angle profiles made of glass fibres TEX4800 with the fibre mass fraction of 56% and epoxy resin RESOLTECH 1401+1407+AC140, has been chosen. In the present study the objective function is formulated as

the minimum energy applied per one meter of pultruded profile. The design variables describe important parameters of the technological process (pull speed, control temperature on electrical heaters, position of electrical heaters) and ambient room temperature. Constrains are introduced into optimisation procedure with the aim to provide a qualitative profile production, when the resin is fully cured and no overheated during the pultrusion process. Since the curing is allowed after the die exit, an additional constraint requiring the minimal degree of cure in the profile cross-section at the die exit is introduced additionally. With this constraint it is guaranteed that resin, leaving the die, is in a solid state and does not flow. The developed optimisation approach has allowed one to estimate effectiveness and productivity of the industrial pultrusion process with the temperature control executed by the heaters switch-on and switch-off strategy. By this way more realistic process optimisation has been achieved and more accurate values of electrical energy spent for a die heating have been obtained.

## **Research of the Developed Design of Micromechanical Linear Acceleration Sensor in Systems of Stabilization and Registration of the Objects Position**

**O. A. Ezhova\*, I. E. Lysenko, D. V. Naumenko**

*Southern Federal University, Taganrog, Russia*

\*[ezhova.08.05@gmail.com](mailto:ezhova.08.05@gmail.com)

Micromechanical sensors of angular velocities and linear accelerations are used widely in modern technical means for various purposes: from specialized products of aerospace and defense systems to household appliances such as cell phones and gaming platform of new generation. For example, the MEMS sensors in navigation systems with GLONASS or GPS receiver allow us to maintain accuracy and continuity of navigation upon loss of signal reception from the satellite. The report presents the developed design of a MEMS linear acceleration sensor with three sensitivity axes. The modal and static analysis is performed, design parameters are found that ensure equality of natural frequencies along the sensitivity axes, and experimental samples are created and studied. Based on the studies of the developed single-mass design, projects of linear acceleration sensors were created, which are developed designs with different parameters of elements. By creating projects, the same natural frequencies were obtained for the three axes of sensitivity of the linear acceleration sensor, which ensures the same response of the sensor to external influences on the sensitivity axes and the same limit conditions for each axis, under which the sensor operation mode is violated. During the research, static and modal analysis of the developed projects was carried out. The error in the simulation of vibrations of the structure in order to determine the eigenfrequencies in comparison with the results of numerical methods is less than 15%. Software tools have been developed to investigate the movement of the sensing element under the influence of external accelerations, to calculate the stiffness of the developed design. Parametrizable geometric and finite element models of the proposed sensor are developed, which allow us to carry out numerical modeling in the ANSYS software package. An experimental sample of a single-mass sensor was studied. During the studies, it was found that the parameters of the experimental samples of the micromechanical accelerometer meet the following requirements: (i) the number of axes of

sensitivity is 3, (ii) the range of measured accelerations is  $\pm 10$  g, (iii) sensitivity is not less than 0.5 FF/g, (iv) the level of cross-talk suppression is not less than 50 dB.

#### **Acknowledgements**

The results were received with use of the equipment of student's design office "Elements and Instruments of Inertial Navigation Systems of Robotic Technology" of the Institute of Nanotechnologies, Electronics and Instrument Making of the Southern Federal University (Taganrog). Work was performed with financial support of task No. FENW-2020-0022 for performing scientific research at the expense of the Federal budget, in terms of scientific activities on the topic "Development and research of methods and tools for monitoring, diagnosing and predicting the state of engineering objects based on artificial intelligence".

## **Elastic Wave Propagation in Layered Periodic Dielectric Elastomers**

**S.I. Fomenko\*, M.V. Golub, A.D. Khanazaryan, A.N. Shpak**

*Institute for Mathematics, Mechanics and Informatics, Kuban State University,  
Krasnodar, Russia*

[\\*sfom@yandex.ru](mailto:*sfom@yandex.ru)

Nowadays composite materials and smart structures are used extensively in aerospace, mechanical and civil engineering, and many high-performance products due to their enhanced properties. Moreover, a novel class of composites providing unique properties and called metamaterials is now being intensively introduced into practice. Metamaterials are composites periodically designed to have special properties arising from the consolidation of several material components. Wave propagation in acoustic/elastic metamaterials or phononic crystals is intensively studied to manipulate mechanical waves. Thus, acoustic metamaterials can provide required acoustic properties, e.g. wider band-gap, specific resonances or negative refractive index. Accordingly, the dynamic behaviour of complex structures made of acoustic metamaterials should be efficiently simulated and understood. In this report, the results of studies of wave motion in layered phononic crystals composed of elastic and dielectric elastomers are presented. At first, infinite periodic structures and structures composed of a finite number of unit-cells surrounded by two elastic half-spaces are considered. A semi-analytical method is developed to simulate and analyse the wave-fields in a layered phononic crystal of finite thickness in the case of oblique incidence when the wave-fields are calculated in terms of transfer matrix eigenvalues of a unit-cell that provides numerical stability. Dispersion equation for periodic layered composite made of elastomers is also formulated and solved via the spectral element method employing Lagrange interpolation polynomials at Gauss – Lobatto – Legendre points and periodic boundary conditions. The influence of material and geometrical properties of layers on wave transmission through various kinds of layered phononic crystals made of dielectric elastomers are investigated.

#### **Acknowledgement**

The authors are grateful to the support of the Russian Foundation for Basic Research and the Krasnodar Regional Administration (Project 19-41-230012).

## Catalytic Alkylation of Isobutane with Olefins as Automation Object

D. D. Fugarov<sup>1\*</sup>, O. A. Purchina<sup>1</sup>, A. Bondar<sup>1</sup>, D. A. Onyshko<sup>2</sup>

<sup>1</sup>Don State Technical University, Rostov-on-Don, Russia

<sup>2</sup>M.I. Platov South-Russian State Polytechnic University (NPI), Novocherkassk, Russia

\*[ddf\\_1@mail.ru](mailto:ddf_1@mail.ru)

The alkylation process is a chemical reaction of isobutane with light olefins using strong sulfuric acid as catalyst [1]. During the alkylation process it is possible to use gases which release during catalytic cracking and coking processes [2]. The system of automation of isobutane alkylation process with olefins should provide the following functions [2]: (i) to perform alarm signalization; (ii) to provide automatic monitoring of the air situation at the production facility in order to determine the concentration of powerful and toxic substances; (iii) to perform continuous monitoring and control of ventilation system; (iv) to monitor processing parameters; (v) to calculate the optimal process mode; (vi) to generate and implement the necessary control actions on the control object; (vii) to calculate and record current technical and economic indicators [3].

### References

[1] Poluyan A.Y., Fugarov D.D., Purchina O.A., Nesterchuk V.V., Smirnova O.V., Petrenkova S.B. // *Journal of Physics: Conference Series*, **1015**, 022013, 2018.

[2] Fugarov D.D., Gerasimenko Y.Y., Nesterchuk V.V., Gerasimenko A.N., Onyshko D.A. // *Journal of Physics: Conference Series*, **1015**, 012055, 2018.

[3] Solomentsev K.Y., Fugarov D.D., Purchina O.A., Poluyan A.Y., Nesterchuk V.V., Petrenkova S.B. // *Journal of Physics: Conference Series*, **1015**, 032179, 2018.

## Monitoring of Normal Operating Modes of Operative DC Systems

D. D. Fugarov<sup>1\*</sup>, O. A. Purchina<sup>1</sup>, N. I. Kazimirov<sup>1</sup>, D. A. Onyshko<sup>2</sup>

<sup>1</sup>Don State Technical University, Rostov-on-Don, Russia

<sup>2</sup>M.I. Platov South-Russian State Polytechnic University (NPI), Novocherkassk, Russia

\*[ddf\\_1@mail.ru](mailto:ddf_1@mail.ru)

Protection of operative DC systems is most often carried out with the help of internal protections of automatic switches (AS), which most often do not meet modern requirements for emergency protection [1]. AS are often insensitive to short circuits in distribution networks and cannot provide redundancy of protection failures that depart from connection buses [2]. These protections have considerable time delays that reduce the efficiency of relay protections [3]. This determines the need to improve the monitoring of the operation of the on-line DC systems [1]. General protection tasks are timely determination of emergency modes at powered and powering connections: short

circuit at the facilities of powered and powering connections; reverse current at powering connections; overload current at powered and powering connections [4].

### References

- [1] Fugarov D.D., Gerasimenko Y.Y., Nesterchuk V.V., Gerasimenko A.N., Onyshko D.A. // *Journal of Physics: Conference Series*, **1015**, 012055, 2018.  
 [2] Solomentsev K.Y., Fugarov D.D., Purchina O.A., Poluyan A.Y., Nesterchuk V.V., Petrenkova S.B. // *Journal of Physics: Conference Series*, **1015**, 032179, 2018.  
 [3] Chernyshev Y.O., Purchina O.A., Poluyan A.Y., Fugarov D.D., Basova A.V., Smirnova O.V. // *Journal of Theoretical and Applied Information Technology*, **80**(1), 13-20, 2015.  
 [4] Poluyan A.Y., Fugarov D.D., Purchina O.A., Nesterchuk V.V., Smirnova O.V., Petrenkova S.B. // *Journal of Physics: Conference Series*, **1015**, 022013, 2018.

## Mathematical Modeling of Long Pipeline

D. D. Fugarov<sup>1\*</sup>, O. A. Purchina<sup>1</sup>, D.E. Kondratyev<sup>1</sup>, D.A. Onyshko<sup>2</sup>

<sup>1</sup>Don State Technical University, Rostov-on-Don, Russia

<sup>2</sup>M.I. Platov South-Russian State Polytechnic University (NPI), Novocherkassk, Russia

\*[ddf\\_1@mail.ru](mailto:ddf_1@mail.ru)

Main pipelines are an important component of the oil and gas complex of the Russian Federation [1]. The relevance of work is caused by the fact that mathematical modeling of the modes of operation of oil pipelines was included into practice of the companies which are engaged in transportation of oil, oil products and gas and became necessary component of operational management of the enterprises [2]. Dynamic model of long oil pipeline [3] is considered in this work. The model, obtained by the authors, describes the movement of raw materials in a linear oil pipeline [4]:

$$\begin{cases} -\frac{\partial P}{\partial t} = C^2 \cdot \frac{\partial(\rho v)}{\partial x_1} \\ -\frac{\partial P}{\partial x_1} = 2 \cdot a \cdot (\rho v) \end{cases}$$

where  $\rho$  is the density of the substance,  $x = (x_1, x_2, x_3)$  is the point coordinates,  $a$  is the diameter of the pipe,  $v$  is the flow rate,  $P$  is the pressure,  $C$  is the speed of sound in the liquid. The obtained mathematical model can be used in technical calculations of pipeline transport, as well as in increasing the complexity of automatic control algorithms [2].

### References

- [1] Chernyshev Y.O., Purchina O.A., Poluyan A.Y., Fugarov D.D., Basova A.V., Smirnova O.V. // *Journal of Theoretical and Applied Information Technology*, **80**(1), 13-20, 2015.

[2] Fugarov D.D., Gerasimenko Y.Y., Nesterchuk V.V., Gerasimenko A.N., Onyshko D.A. // *Journal of Physics: Conference Series*, **1015**, 012055, 2018.

[3] Solomentsev K.Y., Fugarov D.D., Purchina O.A., Poluyan A.Y., Nesterchuk V.V., Petrenkova S.B. // *Journal of Physics: Conference Series*, **1015**, 032179, 2018.

[4] Poluyan A.Y., Fugarov D.D., Purchina O.A., Nesterchuk V.V., Smirnova O.V., Petrenkova S.B. // *Journal of Physics: Conference Series*, **1015**, 022013, 2018.

## Centralized and Uninterrupted Power Supply for Oil and Gas Enterprises

D. D. Fugarov<sup>1\*</sup>, O. A. Purchina<sup>1</sup>, V.V. Terehov<sup>1</sup>, D.A. Onyshko<sup>2</sup>

<sup>1</sup>Don State Technical University, Rostov-on-Don, Russia

<sup>2</sup>M.I. Platov South-Russian State Polytechnic University (NPI), Novocherkassk, Russia

\*[ddf\\_1@mail.ru](mailto:ddf_1@mail.ru)

Very often at the enterprises of the oil and gas complex, at the stage of their creation, the climatic factor is not taken into account and these enterprises work at capacities that are much higher than the normative ones [1]. Due to these circumstances, all elements of power systems and other electrical components of the enterprise wear out much faster and require more frequent inspection and measures connected with repair of equipment [2]. The main causes of emergency incidents at the oil and gas complex facilities can be divided into several groups [3]: (i) late implementation of organizational measures in terms of accident prevention and emergency situations; (ii) low level of the preparation of the specialists of oil and gas complex enterprises; (iii) poor technical conditions and wear of main and auxiliary equipment. These problems are common for a whole industry, but they are very acute at the facilities of the oil and gas enterprises, where *a priori* should be not situations that can create a man-made disaster [2, 4].

### References

[1] Poluyan A.Y., Fugarov D.D., Purchina O.A., Nesterchuk V.V., Smirnova O.V., Petrenkova S.B. // *Journal of Physics: Conference Series*, **1015**, 022013, 2018.

[2] Fugarov D.D., Gerasimenko Y.Y., Nesterchuk V.V., Gerasimenko A.N., Onyshko D.A. // *Journal of Physics: Conference Series*, **1015**, 012055, 2018.

[3] Chernyshev Y.O., Purchina O.A., Poluyan A.Y., Fugarov D.D., Basova A.V., Smirnova O.V. // *Journal of Theoretical and Applied Information Technology*, **80**(1), 13-20, 2015.

[4] Solomentsev K.Y., Fugarov D.D., Purchina O.A., Poluyan A.Y., Nesterchuk V.V., Petrenkova S.B. // *Journal of Physics: Conference Series*, **1015**, 032179, 2018.

## Measurement of Large Amplitude Currents during Diagnostics of AC Circuit Switches

D. D. Fugarov<sup>1\*</sup>, O. A. Purchina<sup>1</sup>, A.D. Trofimenko<sup>1</sup>, D.A. Onyshko<sup>2</sup>

<sup>1</sup>Don State Technical University, Rostov-on-Don, Russia

<sup>2</sup>M.I. Platov South-Russian State Polytechnic University (NPI), Novocherkassk, Russia

\*[ddf\\_1@mail.ru](mailto:ddf_1@mail.ru)

Annual failures of various circuit switches (CS) of 0.4 kV connections are recorded in the power networks of enterprises, which appear at the most unfavorable moment in the emergency mode of the network [1]. The main problem of the existing CS diagnostics devices is the error of measuring the effective value of the test current. It is due to the absence of universal mathematical methods, which allow us to calculate the effective values of the test currents according to the data obtained from induction sensors at the non-sinusoidal form of the test current [2]. Comparative analysis showed that the use of current transformers does not provide a specific range of linearity for the whole scale of setting values of load currents at acceptable weight and size characteristics [3]. The solution is to use current sensors with a magnet dielectric core made of carbonyl iron powders of grades P10, P20, P100 or IR. [4]. The results of the calculations showed that measurement errors within the range of current setting at optimal selection of design parameters of the sensor do not exceed 5% [2].

### References

- [1] Solomentsev K.Y., Fugarov D.D., Purchina O.A., Poluyan A.Y., Nesterchuk V.V., Petrenkova S.B. // *Journal of Physics: Conference Series*, **1015**, 032179, 2018.
- [2] Fugarov D.D., Gerasimenko Y.Y., Nesterchuk V.V., Gerasimenko A.N., Onyshko D.A. // *Journal of Physics: Conference Series*, **1015**, 012055, 2018.
- [3] Poluyan A.Y., Fugarov D.D., Purchina O.A., Nesterchuk V.V., Smirnova O.V., Petrenkova S.B. // *Journal of Physics: Conference Series*, **1015**, 022013, 2018.
- [4] Chernyshev Y.O., Purchina O.A., Poluyan A.Y., Fugarov D.D., Basova A.V., Smirnova O.V. // *Journal of Theoretical and Applied Information Technology*, **80**(1), 13-20, 2015.

## Building Base Blocks of Imitation Simulation

D. D. Fugarov<sup>1\*</sup>, O. A. Purchina<sup>1</sup>, D. V. Vovchenko<sup>1</sup>, D. A. Onyshko<sup>2</sup>

<sup>1</sup>Don State Technical University, Rostov-on-Don, Russia

<sup>2</sup>M.I. Platov South-Russian State Polytechnic University (NPI), Novocherkassk, Russia

\*[ddf\\_1@mail.ru](mailto:ddf_1@mail.ru)

Properties of APCS are often investigated by simulation of its subsystems and information parts [1]. Currently, the information part of the system is modeled by the SCADA system, but it cannot

perform the modeling of objects [2]. For this kind of tasks, it is advisable to use simulation models that were created in external specialized software [3]. The authors carried out studies, which allowed us to develop the theoretically justified and practically confirmed methodology of automatizing the process of the construction of dynamic models for spatially distributed objects, which significantly increased productivity and reliability of imitation experiments [2]. We ground theoretically a frame model of knowledge representation, allowing us to use the knowledge base on models of distributed objects in CAD, as well as to provide functionally complete and consistent possibilities of operation with numerical models in their imitation simulation [4].

#### References

- [1] Solomentsev K.Y., Fugarov D.D., Purchina O.A., Poluyan A.Y., Nesterchuk V.V., Petrenkova S.B. // *Journal of Physics: Conference Series*, **1015**, 032179, 2018.
- [2] Fugarov D.D., Gerasimenko Y.Y., Nesterchuk V.V., Gerasimenko A.N., Onyshko D.A. // *Journal of Physics: Conference Series*, **1015**, 012055, 2018.
- [3] Poluyan A.Y., Fugarov D.D., Purchina O.A., Nesterchuk V.V., Smirnova O.V., Petrenkova S.B. // *Journal of Physics: Conference Series*, **1015**, 022013, 2018.
- [4] Chernyshev Y.O., Purchina O.A., Poluyan A.Y., Fugarov D.D., Basova A.V., Smirnova O.V. // *Journal of Theoretical and Applied Information Technology*, **80**(1), 13-20, 2015. and *Applied Information Technology*. 2015. T. 80. № 1. C. 13-20.

## Solid Solutions of Binary Perovskites and Their Ferroelectric and Magnetic Phase Transitions Temperature Differences

G.A. Geguzina

*Southern Federal University, Science Research Institute of Physics,  
Rostov-on-Don, 344090, Russia*

[geguzina@sfedu.ru](mailto:geguzina@sfedu.ru)

Some of the known binary  $A^{\text{III}}B^{\text{III}}\text{O}_3$  perovskites and hexagonal manganites  $A^{\text{III}}\text{Mn}^{\text{III}}\text{O}_3$  with ferro- (FE) or antiferroelectric (AFE) and different magnetic phase transitions: ferro- (FM), antiferro- (AFM) are considered. They have FE or AFE properties below their phase transition (PT) temperatures,  $T_C$ , together with magnetic properties below their magnetic phase transition temperatures,  $T_N$ . Not only these temperature values, but their difference  $T_C - T_N$  plays a significant role to construct multiferroics using them. For a multiferroics functioning this difference should be minimized and the temperatures themselves should be raised to at least room temperature. This task is difficult if at all solvable. Some correlations between their ferro- (Fig. 1) or antiferroelectric ( $T_C$ ) and magnetic ( $T_N$ ) phase transition temperatures, on the one hand, and their interatomic bond  $A$ -O strains, on the other hand, have been constructed. The influence of their interatomic bond  $A$ -O strains on the temperatures  $T_C$  and  $T_N$ , as well as of their difference  $T_C - T_N$  was revealed, i.e. there are the correlations between their values and strain values, which can help with the search for new systems of solid solutions between different ferroelectrics-magnetics. Important laws that call special attention of researchers were and remain laws of relationships "chemical (elemental)



composition – crystalline structure – phase transitions – physical properties". The energy characteristics and features of near and far interatomic interactions in the compound structure also play a significant role. The most acceptable and accessible characteristics of such interactions in the structure of complex oxides may be the lengths of interatomic bonds that can be determined theoretically with the help of the quasi-elastic model of the perovskite structure. The main feature of the quasi-elastic model of the perovskite structure is the assumption that the interatomic bonds  $A$ -O lengths ( $L_{AO}$ ) in real oxides with perovskite structure can significantly differ (by our estimates, up to ~25 %) from the corresponding unstrained (free) interatomic bond lengths ( $L_{AO}^0$ ). When atoms  $A$  and  $B$  enter a complex compound lattice, they inevitably strain. The  $A$ -O interatomic bond strains are defined as its relative deformation:  $\delta_{AO} = (L_{AO} - L_{AO}^0) / L_{AO}^0$  and  $L_{AO}^0$  values are tabulated. Thus, to circumvent such fundamental difficulties of individual ferroelectric-magnetics, ferroelectric solid solutions between ferroelectrics and magnetics are created with the hope to get closer to each other and to increase the temperatures of their different phase transitions. Nevertheless, to do this it was necessary to systematize the PTs temperatures of potential components of possible solid solutions between magnetics and find out what structural parameters they can depend on. Then it was necessary to determine where these temperatures come closest to each other on the correlations constructed here (see Fig. 1) between the arguments of their structure, namely the  $A$ -O interatomic bond strains  $\delta_{AO}$ , on the one hand, and the temperatures of their different PTs and their differences, on the other hand.

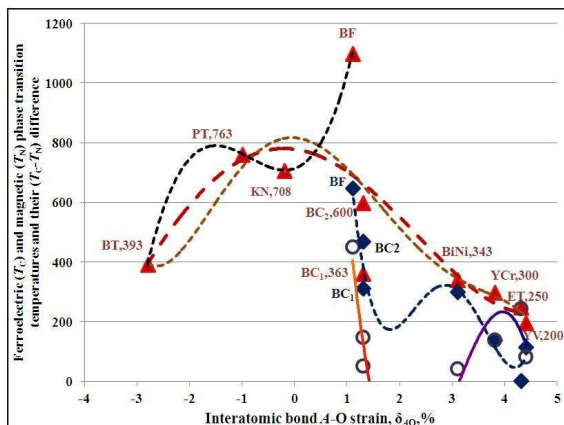


Fig. 1.

We previously established that the  $T_C$  of ferro- and/or antiferroelectric PTs depend on their  $A$ -O interatomic bond strains  $\delta_{AO}$ . Nevertheless, it is not yet clear whether the temperatures of magnetic PTs are depended on the interatomic bond elastic characteristics and if so, how? It was established here that the differences between temperatures of ferroelectric and magnetic phase transitions  $T_C$  –

$T_N$  (lower empty circles) depend on  $\delta_{AO}$  values to some extent. Thus, it is possible to find out such solid solution systems that are characterized negative or positive  $\delta_{AO}$  values, but enough high temperatures  $T_C$  and  $T_N$  and to bring together their  $T_C$  and  $T_N$  for them. Systems, that could be recommended in this sense are the following: BiFeO<sub>3</sub> – BiNiO<sub>3</sub>, BiFeO<sub>3</sub> – BiCoO<sub>3</sub>, BiFeO<sub>3</sub> – YVO<sub>3</sub> (see Fig. 1) or systems with hexagonal manganites, as the solid solutions with the most low  $T_C - T_N$  differences, and some systems, for example, BiFeO<sub>3</sub> – KNbO<sub>3</sub> or BiFeO<sub>3</sub> – BaTiO<sub>3</sub> that have already been investigated. If to take into attention the antiferroelectric components not shown here in Fig. 1, then such systems could be the following systems: BiMnO<sub>3</sub> – BiGaO<sub>3</sub>, or BiMnO<sub>3</sub> – BiCoO<sub>3</sub>, or BiMnO<sub>3</sub> – BiNiO<sub>3</sub> or others.

## The Effect of Strontium Pyroniobate on Phase Formation and Properties of the KNN System

E.V. Glazunova\*, I.A. Verbenko, A.A. Nikulina

*Research Institute of Physics, Southern Federal University,  
344090, Rostov-on-Don, Russia*

\*[kate93g@mail.ru](mailto:kate93g@mail.ru)

Presently, the much attention is given to the development of lead-free piezoelectric materials. The base for their production can be, for example, the solid solutions of potassium sodium niobate (K, Na)NbO<sub>3</sub> (KNN), which have been investigating very intensively in recent decades, due to the proximity of their piezoelectric properties to used in industry PbZr<sub>1-x</sub>Ti<sub>x</sub>O<sub>3</sub> (PZT) materials. However, producing quality and high-density KNN ceramics is difficult because of a number of issues, such as hydrolysis of the reagents during synthesis, a limited range of optimal temperatures of synthesis and sintering, violation of the stoichiometric composition due to the high volatility of alkaline components at relatively low temperatures that result to low experimental density and high conductivity of ceramics. These difficulties can be eliminated by doping various modifiers into the system. Because the strontium pyroniobate Sr<sub>2</sub>Nb<sub>2</sub>O<sub>7</sub> has high values of the phase transition temperature  $T_C \approx 1615$  K, and solid solutions of the KNN have relatively high values of piezoelectric activity, they in combination with each other can provide the necessary conjunction of properties to developing a new generation of high-temperature devices. Thus, is current to establishing the laws of phase formation and the formation of the dielectric properties of solid solutions of the system KNN doped Sr<sub>2</sub>Nb<sub>2</sub>O<sub>7</sub>. The objects of investigating were solid solutions of multicomponent system  $(1-x)\text{K}_{0.5}\text{Na}_{0.5}\text{NbO}_3 - x\text{Sr}_2\text{Nb}_2\text{O}_7$ ,  $0.0 \leq x \leq 0.1$ ,  $\Delta y = 0.025$ , produced by two-stage solid-phase synthesis followed by sintering with using traditional ceramic technology. The X-ray phase analysis was performed by powder X-ray diffraction on a DRON-3 diffractometer. The microstructure of the fragment of samples was investigated by using a scanning electron microscope JSM-6390L. The dielectric spectra were measured in the range temperature  $T = (300 - 900)$  K, using a specially designed setup, including the LCR-meter Agilent 4980A, at frequencies of 1 kHz – 1 MHz. X-ray phase analysis of the solid solutions system  $(1-x)\text{K}_{0.5}\text{Na}_{0.5}\text{NbO}_3 - x\text{Sr}_2\text{Nb}_2\text{O}_7$ ,  $0.0 \leq x \leq 0.1$ ,  $\Delta y = 0.025$ , demonstrated that all samples had a perovskite-type structure. At increasing

concentration of  $\text{Sr}_2\text{Nb}_2\text{O}_7$  in the range  $0.0 \leq x \leq 0.1$  in the system, a number of phase transitions occurs:  $\text{R(M)} \rightarrow \text{R(M)+Psc} \rightarrow \text{Psc+T}$ . The doped of the system by strontium pyroniobate also leads to reducing grain size and loosening the microstructure that affects on the density of objects. The dielectric spectra of the investigated objects are characterized by a strong frequency dispersion of the dielectric permeability and increasing the temperatures of its maxima, when the frequency increases, that is typical for ferroelectric-relaxers. The doping by more than 5 mol%  $\text{Sr}_2\text{Nb}_2\text{O}_7$  results with sharply increasing electrical conductivity of the material, what can be caused by an increase in the number of free charge carriers at the domain boundaries due to the additive of bivalent strontium into the system. The charged grain boundaries interact with an alternating electric field, what leads to the appearance polarization of Maxwell-Wagner's type. An additional contribution to the mechanism of polarization can be provided by the appearance of interfacial boundaries ceramic-air during porosity formation. Future work on the study of the piezoelectric characteristics of the investigating samples is planned.

#### **Acknowledgement**

Research was financially supported by the Ministry of Science and Higher Education of the Russian Federation (State assignment in the field of scientific activity, Southern Federal University, 2020) topic No. 0110/20-3-07 IP.

## **Analysis of the Influence of Cortical Bone Thickness, Soft Tissue, and Porosity on Ultrasonic Guided Waves for Osteoporosis Diagnostics**

**E.V. Glushkov<sup>1\*</sup>, N.V. Glushkova<sup>1</sup>, O.A. Miakisheva<sup>1</sup>, S.I. Fomenko<sup>1</sup>, A.M. Tatarinov<sup>2</sup>**

*<sup>1</sup>Institute for Mathematics, Mechanics and Informatics, Kuban State University,  
Krasnodar, 350040 Russia*

*<sup>2</sup>Riga Technical University, Riga, LV-1048, Latvia*

[\\*evg@math.kubsu.ru](mailto:evg@math.kubsu.ru)

In recent years, in the field of diagnosis and prevention of osteoporosis, there has been an increase in interest in determining the condition of compact bone tissue, namely the main supporting element of the skeleton, which quality determines the risk of atraumatic bone fractures in osteoporosis. Quantitative Ultrasound (QUS) is a promising tool for diagnosing the risk of osteoporotic fractures since the ultrasound propagation parameters reflect the material properties of the compact bone tissue. Ultrasonometers have such advantages over X-ray densitometry as the absence of ionizing radiation, compactness, and lower cost, which makes them a well-suitable tool for screening and monitoring the bone condition. Understanding the dependence of the traveling wave propagation on a number of factors related to the state of the bone, such as the thickness of cortical layer, porosity, radial gradient, and degree of mineralization, as well as possible artifacts such as surrounding soft tissues can reveal hidden signs of osteoporosis improving its diagnostics. The present work is focused on the simulation of dispersion and amplitude-frequency characteristics of ultrasonic guided waves (GWs) piezoelectrically generated in samples mimicking real bones (phantoms) in order to identify signs predicting osteoporosis. Here we use analytically-based computer models that we have been also developing for the ultrasonic inspection of composite materials and assessing

the deterioration of their properties in the framework of Structural Health Monitoring (SHM) technologies. The models are based on the explicit GWs representation in terms of the inverse Fourier transform path integrals of the waveguide's Green matrix, followed by the GWs extraction using the residue technique. The experimental and numerical results obtained for the phantoms under consideration are analyzed and discussed.

#### **Acknowledgement**

The work is supported by the Russian Science Foundation (project No. 17-11-01191).

## **Influences of the Three-Body Interaction and the Deformation of Electron Shells of Atoms on Phonons Energy of Compressed Rare-Gas Crystals**

**Ie.Ie. Gorbenko<sup>1\*</sup>, E.P. Troitskaya<sup>2</sup>, E.A. Pilipenko<sup>2</sup>, I.A. Verbenko<sup>3</sup>, E.V. Glazunova<sup>3</sup>**

<sup>1</sup>*Lugansk National Agrarian University, Lugansk, Ukraine*

<sup>2</sup>*Donetsk A.A. Galkin Physics and Technology Institute, Donetsk, Ukraine*

<sup>3</sup>*Research Institute of Physics, Southern Federal University, Rostov-on-Don, Russia*

\*[e\\_g81@mail.ru](mailto:e_g81@mail.ru)

The most convenient objects for the study of a number of fundamental problems of solid-state physics are rare-gas crystals (Ne, Ar, Kr, and Xe), since they comprise a relatively simple system: they consist of atoms with closed electron shells and contain one atom in the unit cell. In this work, the dynamic matrix is constructed based on the nonempirical version of the quantum-mechanical model of deformed and polarized atoms (Tolpygo model) with allowance for both types of the three-body interactions (due to overlap of electron shells and their deformation). *Ab initio* calculations phonon frequencies are performed at two and ten mean-value points of the Chadi-Kohen method and the influence of all three-body forces on them for compressed crystals of the Ne – Xe series. As previously, the contribution from three-body forces due to the electron shell overlap was small against the background of the pair interaction even at high pressure and most pronounced for Xe, while the effects of electron shell deformations within the pair and three-body approximations differ for different mean-value points. Contribution from the electron shell deformation (for example, for Ne) is varied from 0% to 0.39% at compression  $u = p = 0$  and from 0.35% to 55.9% at  $u = 0.76$ . The average contribution value increases with an increase in pressure from 0.15% to 17.2%. The calculation of  $\hbar\omega_i(X)$  performed by us for Ar with a pure pair potential, with neglect of the deformation of the electron shells gives a discrepancy with the experiment of 2.6% for  $\hbar\omega_L(X)$  and 8% for  $\hbar\omega_T(X)$ . The discrepancy with the experiment of our calculations  $\hbar\omega_i(X)$  of in the model with neglect of the deformation of the electron shells but with allowance for the three-body interaction due to the overlap of the electron shells is 3.7% for  $\hbar\omega_L(X)$  and 6.4% for  $\hbar\omega_T(X)$ . The allowance for the three-body interaction and the deformation of the electron shells in the pair and three-body approximations reduces this discrepancy for  $\hbar\omega_L(X)$  to 1.5% and for  $\hbar\omega_T(X)$  to 5.9%, which is close to the experimental error of 5%. The absence of a qualitative experiment makes it very problematic to test the theory by adequate description of phonon frequencies at the boundary

of the Brillouin zone, although the short-wave phonons region is most sensitive to details of the theory even at zero pressure.

#### ***Acknowledgement***

Research was financially supported by the Ministry of Science and Higher Education of the Russian Federation (State assignment in the field of scientific activity, Southern Federal University, 2020).

## **Establishing Conditions for the Manifestation of the Piezoelectric Response of Carbon Nanotubes**

**A. V. Guryanov, M. V. Il'ina\*, O. I. Osotova, O. I. Il'in**

*Southern Federal University, Institute of Nanotechnologies, Electronics and Electronic Equipment Engineering, Taganrog, 347922, Russia*

\*[mailina@sfedu.ru](mailto:mailina@sfedu.ru)

Recent studies have shown that carbon nanotubes (CNTs) can demonstrate abnormal piezoelectric properties when they form a deformation which dislocate the atomic lattice symmetry [1 – 3]. Such a deformation can be formed during the CNTs growth process or under the influence of an external local pressure, for example, using a probe of an atomic force microscope (AFM) [1 – 3]. Thus, it can be assumed that the value of the piezoelectric response will depend on the CNTs growth parameters and on the magnitude of the CNTs deformation resulting from external influence. The aim of this work is to identify the conditions for the appearance of the piezoelectric response of carbon nanotubes. To determine the conditions for the CNTs piezoelectric response appearance, the influence of the diameter, height, and growth temperature of CNTs was studied. Arrays of aligned carbon nanotubes grown by plasma enhanced chemical vapor deposition (PECVD) were used as the samples. Experimental studies were carried out by AFM force spectroscopy with the detection of piezoelectric current using a built-in microscope oscilloscope. An analysis of the dependence of the piezoelectric current on the diameter of the CNTs showed that with an increase in the diameter of the nanotubes from 35 to 65 nm, a decrease in the current from 22.6 to 17.3 nA is observed. This can be due to an increase in the bending stiffness of CNTs with an increase in diameter and, as a result, to a decrease in the magnitude of deformation of CNTs at a given load. An analysis of the dependence of the piezoelectric current on the height of nanotubes showed that with an increase in the height from 6 to 12  $\mu\text{m}$ , the current decreases from 19 to 5 nA. Studies of the carbon nanotubes growth temperature influence on their piezoelectric response have shown that the magnitude of the piezoelectric response nonlinearly decreased from 22.5 to 15 nA with increasing growth temperature from 615 to 690  $^{\circ}\text{C}$ . This may be due to a gradual increase in the disorientation of nanotubes and a decrease in structural defects with increasing growth temperature. Thus, in this work, the conditions for the appearance of the carbon nanotubes piezoelectric response were shown. It is shown that the value of the CNTs piezoelectric response depends both on the magnitude of the deformation determined by the geometrical parameters of the CNTs and the magnitude of the external pressure, as well as on the structural characteristics of CNTs determined by growth temperature. However, further research is required to establish the effect of growth parameters on

structural perfection of the CNTs. The results can be used to develop promising elements of nanoelectronics based on aligned CNTs.

#### **Acknowledgements**

The results were obtained using the equipment of the REC and CCU "Nanotechnology" of the Southern Federal University. This work was financially supported by the RFBR (project No. 20-37-70034).

#### **References**

- [1] Il'ina M.V., Il'in O.I., Blinov Yu.F., Smirnov V.A., Ageev O.A. // *Technical Physics*, **63**(11), 1672 – 1677, 2018.
- [2] Il'ina M.V., Il'in O.I., Blinov Yu.F., Smirnov V.A., Kolomiitsev A.S., Fedotov A.A., Konoplev B.G., Ageev O.A. // *Carbon*, **123**, 514 – 524, 2017.
- [3] Il'ina M.V., Il'in O.I., Blinov Y.F., Konshin A.A., Konoplev B.G., Ageev O.A. // *Materials* **11**, 638, 2018.

## **Influence of Thermal Calcination on Dielectric and Impedance Properties of ZnO Nanostructures**

**Gyanendra Pratap Singh\*, Mukesh Kumar Roy**

*Natural Science Discipline, PDPM, Indian Institute of Information Technology, Design and Manufacturing Jabalpur, Madhya Pradesh 482005, India*

\*[1616602@iiitdmj.ac.in](mailto:1616602@iiitdmj.ac.in)

The dielectric materials have immense potential for use in modern microelectronics as well as for high-energy density storage applications for the miniaturization of electronic devices. Many groups are doing research to explore new dielectric materials for application purpose. So, in this work, we have detailed study for the effect of thermal calcination on dielectric properties of ZnO nanostructures. We have synthesized ZnO nanostructures using sol-gel auto combustion method. Sol-gel auto combustion method is adopted because this method is fast, less equipment used, environment friendliness, cost effective and able to produce large amount of sample. We have prepared three samples named as Z1, Z2, and Z3 using different calcination temperature 400 °C, 500 °C, and 600 °C, respectively. The structural and dielectric observations have been investigated for each sample. The XRD (X-ray diffraction) outcomes reveal that each sample has high crystallinity with wurtzite hexagonal structure without any impurity. The average crystallite size for each sample is calculated using Scherrer's formula. Average crystallite size is found equal to 17 – 19 nm for as prepared samples. It has been observed a small change in lattice parameters of the samples with thermal calcination. The dielectric properties are measured in the frequency range from 20 Hz to 1 MHz. The plots for dielectric constant and dielectric loss show that both parameters are decreasing for all samples as frequency is increasing. At higher frequencies, dielectric constant and dielectric loss become almost constant. The sample calcinated at lower temperature exhibits highest dielectric constant and lowest dielectric loss value at 1 kHz. The plot of AC conductivity show that conductivity is in increasing trend with frequency. The complex impedance study for all samples is also investigated to identify whether the long-range or short-range movement of charge

carriers is dominant in the relaxation process. The Nyquist or Cole-Cole plots for as prepared samples show formation of semicircle arc, which indicate the presence of grain effect and single relaxation process in prepared samples. The diameter of semicircle arc decreases with the rise of thermal calcination, which indicate that Z3 sample has lowest bulk resistance. It can be concluded that ZnO sample at low thermal calcination is an appropriate dielectric material for electronic devices in high frequency applications.

## **Evaluation of Factors Affecting Costs Using Multiple Linear Regression Method on the Implementation of Rehabilitation and Renovation of School Infrastructure Facilities in Pasuruan District**

**Hanie Teki Tjendani<sup>1\*</sup>, Nick Yanie<sup>1</sup>, Dwi Yuli Rakhmawati<sup>2</sup>, Tisno Subroto<sup>1</sup>**

*<sup>1</sup>Department of Civil Engineering, University of 17 Agustus 1945 Surabaya Indonesia*

*<sup>2</sup>Department of Industrial Engineering, University of 17 Agustus 1945 Surabaya Indonesia*

[\\*hanie\\_tekitjendani@yahoo.com](mailto:hanie_tekitjendani@yahoo.com)

Efforts to improve human resources can be done in several ways, one of them is through improving the quality of education. However, when viewed from the quality of educational infrastructure in Indonesia, there is still some educational infrastructure that is not yet feasible, so that it can result in inhibition of teaching and learning activities. Supervision of School Infrastructure and Facilities Improvement for the Pasuruan District was conducted in 10 (ten) scattered public elementary schools. The purpose of this study is to analyze the use of the number of workers, get the factors that affect the cost of implementing rehabilitation and renovation of school infrastructure facilities in Pasuruan Regency, get a regression model of the costs of implementing rehabilitation and renovation of school infrastructure facilities in Pasuruan District. The data analysis technique used is multiple linear regression analysis. The results of this study are work progress reports showing the use of the number of workers in accordance with the planned, evidenced an increase in the acceleration of work in the period from 6th to 15th week. Factors affecting the cost of implementing rehabilitation and renovation of school infrastructure in the Pasuruan District are the number of workers. Regression model of the cost of implementing rehabilitation and renovation of school infrastructure facilities in Pasuruan District is  $Y = -87,452,639,807 + 50,520,875 X_2$ . The regression equation shows that the cost of implementing rehabilitation and renovation ( $Y$ ) is reduced by Rp. 87,452,639,807 if not accompanied by the number of workers ( $X_2$ ). The cost of implementing the rehabilitation and renovation of school infrastructure will increase in value by Rp. 50,520,875 if the number of workers ( $X_2$ ) increases by 1 person.

## **A System Dynamics Approach to Risk Mitigation in Performance-based Contract Projects**

**Hanie Teki Tjendani\*·Wateno Oetomo , Risma Marleno**

*Magister Teknik Sipil Universitas 17 Agustus 1945 Surabaya, Indonesia*

[\\*hanie\\_tekitjendani@yahoo.com](mailto:*hanie_tekitjendani@yahoo.com)

The Indonesian government is applying performance-based contracting in few pilot projects as a solution to handle premature deterioration on the national road problems. Nowadays, the delivery of national road projects mostly applies the conventional system design-bid-build (DBB), namely the planning, implementation, monitoring, and maintenance of roads are handled by different stakeholders. The way of contracting out road preservation is based on unit price contracts. Conversely, Performance-Based Contracts assign minimum conditions of road and traffic facility that have met by the contractor, such as the management of asset data, mobilize and servicing to emergencies, and reaction to public requests, complaints, and response. Thus, the Indonesian government has adopted performance-based contracting, a new delivery system that has been successfully implemented in both developing and developed countries. The use of performance-based contracting commenced in 2011 as a pilot project in the construction of five national roads along west Java, central Java and east Java. In this report, a strategy for the successful implementation of performance-based contracting in Indonesia using a dynamic system is discussed. A dynamic system was selected because it does not require many samples. The results of this study are expected to provide guidance in taking actions to reduce the risks that may occur in the implementation of performance-based contracting in the future.

## **A Study on Nitrogen Oxides from Coal and Waste Tires in Different Proportion of Mixed Burning**

**Hsueh Chen Shen<sup>1</sup>, Chitsan Lin<sup>2\*</sup>, Chin Ko Yeh<sup>1</sup>, Wisanukorn Lukkhasorn<sup>2</sup>,  
Suei Chang Wu<sup>2</sup>**

*<sup>1</sup>Ph.D. Program in Maritime Science and Technology, College of Maritime, National Kaohsiung University of Science and Technology, Kaohsiung, 81157, Taiwan (R.O.C.)*

*<sup>2</sup>Department of Marine Environmental Engineering, National Kaohsiung University of Science and Technology, Kaohsiung, 81157, Taiwan (R.O.C.)*

[\\*ctlin@nkust.edu.tw](mailto:*ctlin@nkust.edu.tw)

With the rapid development of industry and lack of energy, various alternative fuels appear. Scrap tires are a kind of auxiliary fuel with high calorific value in waste recycling. They are commonly used in power generation or the cement industry, but they are derived from combustion. A large number of nitrogen oxides will produce acid when exposed to moisture and then form acid rain and



haze, which causes environmental air pollution and damages humans and animals' health. This study takes a power plant in southern Taiwan as an example. It uses a circulating fluidized bed boiler with an evaporation capacity of 200 tons per hour (t/h). The combustion temperature is set at 870 °C to 950 °C to record the two-month combustion power generation process. Under different co-firing ratios of coal and waste tires, monitor the concentration of nitrogen oxides (NO<sub>x</sub>) in the exhaust smoke to find the best fuel co-firing ratio with the lowest NO<sub>x</sub> emission concentration. The preliminary results show that the co-firing ratio of waste tires used in power plants is 0 ~ 52%. When coal is used as fuel (the co-firing ratio is 0%), the maximum NO<sub>x</sub> emission concentration is 131 ± 16 ppm; when the co-firing ratio is 50%, the emission concentration of ~ 52% of NO<sub>x</sub> is 93 ± 3 ppm. Pearson, correlation coefficient analysis, showed that the proportion of waste tires in co-firing and NO<sub>x</sub> emission concentration is negatively correlated ( $r = -0.797$ ,  $p = 0.000$ ), which means that the proportion of co-firing is high, the NO<sub>x</sub> emission concentration is lower. In the future, we will continue to discuss the influence of particle size, air-fuel ratio, stirring, residence time, and even different furnace temperatures on the production of NO<sub>x</sub> based on this optimal co-firing ratio. In addition to improving the efficiency of energy reuse, the results of this study are also expected to reduce the impact of resource waste reuse on the environment, especially for acid rain, fine suspended particulates, and ozone air quality.

## Characteristics of Bottom Ash as Reinforcement of the Polypropylene Composite

I Made Kastawan\*, I Nyoman Sutantra\*\*, Sutikno\*\*\*

*Departement of Mechanical Engineering, Faculty of Industrial Technology, Institut Teknologi Sepuluh Nopember Surabaya, Indonesia*

\*[madekastiawan@untag-sby.ac.id](mailto:madekastiawan@untag-sby.ac.id), \*\*[tantra@me.its.ac.id](mailto:tantra@me.its.ac.id), \*\*\*[sutikno@me.its.ac.id](mailto:sutikno@me.its.ac.id)

Bottom ash particles as reinforcement of polypropylene matrix composites were considered. Due to the surfaces of the bottom ash particles are angular, irregular and porous, it is an advantage for a reinforcement that relies on the interface bond as a mechanical bond. Bottom ash particles were processed by a simple treatment and without the addition of chemical elements as a coupling agent, that allows one to increase the strength of the composite significantly. The composition was washed twice, with freshwater and hot water (80 °C) for 3 hours, and dried in the open space with following heating at 120 °C for 3 hours. This treatment had a pretty good impact on bottom ash particles as composite reinforcement. Observations on variations in the size of bottom ash particles have found several physical characteristics of bottom ash particles that affect the strength of the composite. These characteristics were the presence of layers and surface cracks, the level of surface cleanliness, the level of dryness of particles in the result of the treatment, which had an impact on the quality of composites. Composites produce the best value of mechanical properties with particle sizes of 250 – 300 mesh. The tensile strength value was 49.39 MPa, and the bending stress was 97.45 MPa. These values are above the strength of pure polypropylene. These results indicate that the bottom ash particles are reinforcements.

# Mechanical Properties and Microstructure Analysis of Heated Aluminum-2042 with Variation of Aging Temperature and Aging Time

Ichlas Wahid\*, Maula Nafi

Department of Mechanical Engineering, University of 17 Agustus 1945 Surabaya

[\\*ichlaswahid@untag-sby.ac.id](mailto:ichlaswahid@untag-sby.ac.id)

This study determines the effect of variations in the aging temperatures of 130 °C, 160 °C, and 190 °C with aging times of 40 minutes, 80 minutes, and 120 minutes. After the heat treatment process, mechanical properties testing includes hardness test, tensile test, and microstructure study. Material used in the study is Aluminum 2042. The results of the research show that the highest hardness test result corresponds to the case without heat treatment and is equal to 82.4 HRB. The lowest hardness test result is obtained in aluminum 2024 after heat treatment with an aging temperature of 190 °C and an aging time of 120 minutes and is equal to 67.8 HRB. The highest tensile value of 59.68 kgf/mm<sup>2</sup> belongs to aluminum 2024 without heat treatment and the lowest tensile value is obtained for aluminum 2024 after heat treatment with an aging temperature of 190 °C and an aging time of 120 minutes and is equal to 40.56 kgf/mm<sup>2</sup>. The largest average grain size of microstructure is found for 2024 aluminum after heat treatment with an aging temperature of 190 °C and an aging time of 120 minutes; it is equal to 60.47 μm and the smallest average grain size is obtained in aluminum 2024 without heat treatment; it is equal to 42.2 μm. The results of the study showed that aluminum 2024 by being treated with variations in temperature and aging time can reduce mechanical properties and can change the grain size of microstructure.

## Numerical Analysis of the Dynamic Behaviour of Poroviscoelastic Solids Using Boundary Element Approach

A. A. Ipatov<sup>1,2\*</sup>, S. Yu. Litvinchuk<sup>1,2</sup>

<sup>1</sup>Research Institute for Mechanics, National Research Lobachevsky State University of Nizhny Novgorod, 23 Gagarin Avenue, building 6, Nizhny Novgorod 603950, Russia

<sup>2</sup>Research and Education Mathematical Center "Mathematics for Future Technologies", Nizhny Novgorod 603950, Russia

[\\*ipatov@mech.unn.ru](mailto:ipatov@mech.unn.ru)

Study of wave propagation in saturated porous media is an important issue of engineering sciences. The poroelasticity theory was developed and nowadays is an important to engineering applications. However, in addition to the macroscopic effects, there exist many other time-dependent physical mechanisms. For example, the rock mass itself without fluid can exhibit creep behavior. These phenomena can be modeled as apparent viscoelastic mechanisms at the macroscopic level. In the present paper, wave propagation poroviscoelastic solids is studied. Moreover, the research is

dedicated to modeling of a slow compressional wave in poroviscoelastic media by means of boundary-element method. Poroviscoelastic formulation is based on Biot's model of fully saturated poroelastic media with a correspondence principal usage. Standard linear solid model is employed in order to describe viscoelastic behavior of the skeleton in porous medium. Fundamental and singular solutions play a key role in BEM, the expressions of which in the case of poroelasticity are known only in the Laplace domain. The boundary-value problem of the three-dimensional dynamic poroviscoelasticity is written in terms of Laplace transforms. Direct approach of the boundary integral equation method is employed. The boundary-element approach is based on the mixed boundary-element discretization of surface with generalized quadrangular elements. Subsequent application of collocation method leads to the system of linear equations, and then to the solution in Laplace domain. Numerical inversion of Laplace transform is used to obtain time-domain solution. It is known that in porous medium due to the presence of a fluid phase, two kinds of compressional waves exist. The first one is similar to an elastic wave, and called a fast wave, with a small amount of attenuation. The second wave is with a much slower propagation speed and highly dissipative, and is called a slow wave. A problem of a Heaviside-type load acting on a poroviscoelastic column is considered in order to demonstrate slow wave phenomena. An influence of permeability of porous material on dynamic responses is studied. The problem of a vertical Heaviside-type force acting on a halfspace is considered in the case of surface waves investigation, such as Rayleigh. An influence of viscoelastic parameter on dynamic responses of displacements and pore pressure is demonstrated.

#### ***Acknowledgement***

The work was carried out with the financial support of the Ministry of education (task 0729-2020-0054).

## **Figures of Merit of Novel Piezo-active Lead-free Composites**

**A. N. Isaeva, V. Yu. Topolov\***

*Department of Physics, Southern Federal University, 344090 Rostov-on-Don, Russia*

[\\*yutopolov@sfedu.ru](mailto:yutopolov@sfedu.ru)

In recent years, piezoelectric energy harvesting has received increasing attention with the development of low-powered electronics, wireless sensor technologies and piezotechnical applications. Among piezoelectric materials to be of great interest are composites based on ferroelectric lead-free single crystals (SCs) [1, 2], and on the connectivity patterns these composites are mainly of the 1–3- and 2–2-types. To the best of our knowledge, despite the known piezoelectric performance of a series of the lead-free composites [2, 3], their figures of merit (FOMs) were not yet studied in detail. Moreover, a study is topical because the new (modified) FOMs [4] were put forward very recently for a more careful characterization of piezoelectrics at the energy conversion and harvesting under mechanical loading. In the present study, we analyze an influence of the electromechanical properties of the ferroelectric single-crystal component on the following FOMs of the lead-free composites:

- (i) electric-field FOM  $F_E = (k_{33}^*)^4/(Z^*)^2$ , where  $k_{33}^*$  is the longitudinal electromechanical coupling factor.  $Z^*$  is the acoustic impedance,
- (ii) electric-charge FOM  $F_Q = (d_{33}^*)^2$ , where  $d_{33}^*$  is the longitudinal piezoelectric coefficient,
- (iii) voltage FOM  $(Q_{33}^*)^2 = d_{33}^*g_{33}^*$ , where  $g_{33}^*$  is the longitudinal piezoelectric coefficient,
- (iv) hydrostatic FOM  $(Q_h^*)^2 = d_h^*g_h^*$ , where  $d_h^*$  and  $g_h^*$  are hydrostatic piezoelectric coefficients,
- (v) modified FOM at the applied mechanical stress  $F_{ij}^{\sigma\sigma} = \lambda_{max}(d_{ij}^*)^2/[(k_{ij}^*)^2\varepsilon_{ii}^{\sigma\sigma}]$ , where  $\lambda_{max} = [(k_{ij}^*)^{-1} - ((k_{ij}^*)^{-2} - 1)^{1/2}]^2$  is the maximum transmission coefficient,  $k_{ij}^*$  is the electromechanical coupling factor,  $\varepsilon_{ii}^{\sigma\sigma}$  is the dielectric permittivity at stress  $\sigma = \text{const}$ ,
- (vi) modified FOM at the applied mechanical strain  $F_{ij}^{\varepsilon\varepsilon} = \lambda_{max}(d_{ij}^*)^2/[(k_{ij}^*)^2\varepsilon_{ii}^{\sigma\sigma}s_{jj}^{E*}s_{jj}^{D*}]$ , where  $s_{jj}^{E*}$  and  $s_{jj}^{D*}$  are elastic compliances at the electric field  $E = \text{const}$  and electric displacement  $D = \text{const}$ , respectively.

In addition to  $(Q_{33}^*)^2$  and  $(Q_h^*)^2$  from (ii) and (iii), the similar FOMs  $(Q_{31}^*)^2 = d_{31}^*g_{31}^*$  and  $(Q_{32}^*)^2 = d_{32}^*g_{32}^*$  are introduced for the transverse piezoelectric effect. The FOMs (i) – (vi) are analyzed for some composites based on ferroelectric alkali niobate – alkali tantalate SCs poled along [001] of the perovskite unit cell. The main connectivity formulae of the composites to be of interest are 1–3–0 SC / porous polymer (including a case of two porosity levels in the polymer matrix), 1–0–3 ferroelectric SC-1 / piezoelectric SC-2 / polymer, and 2–0–2 ferroelectric SC-1 / piezoelectric SC-2 / polymer. Hereby large FOM values [e.g.  $(Q_{33}^*)^2 \sim 10^{-10} \text{ Pa}^{-1}$  and  $(Q_h^*)^2 \geq 50 \times 10^{-12} \text{ Pa}^{-1}$ ] are achieved in some volume-fraction and porosity ranges, and a large anisotropy [e.g.  $(Q_{33}^*)^2/(Q_{31}^*)^2 \sim 10^2$ ] is observed due to a composite microgeometry. New diagrams that link the FOMs and volume fractions of components (or porosity in the polymer medium) are put forward and interpreted in terms of the piezoelectric performance of the composite. The studied FOMs are compared to the similar parameters of the conventional composites based on PZT-type ceramics, and advantages of the novel lead-free composites are shown.

#### Acknowledgement

Research was financially supported by Southern Federal University, grant No. VnGr-07/2020-04-IM (Ministry of Science and Higher Education of the Russian Federation).

#### References

- [1] D. Zhou, K. H. Lam, Y. Chen et al. // *Sens. a. Actuat. A* **182**, 95, 2012.
- [2] V. Yu. Topolov, C. R. Bowen, A. A. Panich, A. N. Isaeva // *Mater. Chem. Phys.* **201**, 224, 2017.
- [3] V. Yu. Topolov, C. R. Bowen, A. N. Isaeva // *IEEE Trans. Ultrason., Ferroelec., a. Freq. Cont.* **65**, 1278, 2018.
- [4] J. I. Roscow, H. Pearce, H. Khanbareh et al. // *Eur. Phys. J. Special Topics* **228**, 1537, 2019.

# Multi-layer Thin Film Deposition for High-performance X-ray Field Emission Characteristics

T. H. Jang<sup>1</sup>, M. K. Bae<sup>1</sup>, J. G. Choi<sup>2</sup>, T.G Kim<sup>3\*</sup>

<sup>1</sup>*Department of Nano Fusion Technology, Pusan National University, Busan, Korea*

<sup>2</sup>*Electro-Medical Device Research Center, Korea Electrotechnology Research Institute, Ansan, Korea*

<sup>3</sup>*Department of Nanomechatronics Engineering, Pusan National University, Busan, Korea*

[\\*tekim@pusan.ac.kr](mailto:*tekim@pusan.ac.kr)

In order to develop high speed operation FDXS (full digital X-ray source), which has advantages such as light weight and high-speed operation, the size of X-ray tube should be small and simplified. The issue of heat emission is one of the problems that needs to be solved in the manufacture of FDXS, as the size of the X-ray tube is small and generates a lot of heat. Currently, DLC (diamond-like carbon) has excellent characteristics of low friction coefficient and sliding ability, good wear resistance, high hardness, and is applied to wide variety of areas such as various semiconductor displays, bio medical field, machinery and materials [1, 2]. By applying the advantage of the excellent heat emission of DLC, it acts as the back plate of the W layer where field emissions occur directly, and DLC is expected to be able to perform its role as a heat release device. In this study, the substrate used for thin film deposition was 100  $\mu\text{m}$  thick Sapphire. The highly conductive W thin film deposition method used DC power, which is characterized by low temperature process ability, and a PVD (physical vapor deposition) method with high safety and high-quality thin film advantage. Next, we used RF-CVD (radio frequency chemical vapor deposition) method, which enables DLC thin film deposition at low temperature and enables excellent throughput. Based on the substrate, deposition was carried out in the form of a multilayer structure consists of W and DLC thin films. The thickness and shape of each layer was analyzed by SEM (scanning electron microscope) and then we discussed the field emission.

## References

- [1] Li F., Zhang S., Kong J., Zhang Y., Zhang W. // *Thin Solid Films*, **519**(15), 4910-4916, 2011.
- [2] Alawajji R. A., Kannarpady G. K., Nima Z. A., Kelly N., Watanabe F., Biris A. S. // *Applied Surface Science*, **437**, 429-440, 2018.

## **Experimental Study on Mechanical Properties of Sandwich Composites with Integrating Auxetic-core Structure Using FDM 3D Printer**

**Jeong-Hyo Hong<sup>1</sup>, Tianyu yu<sup>1</sup>, Soo-Jeong Park<sup>2</sup>, Yun-Hae Kim<sup>1,2\*</sup>**

<sup>1</sup>*Department of Marine Equipment Engineering, Graduate School, Korea Maritime and Ocean University, 727 Taejong-ro, Busan, 49112, Republic of Korea*

<sup>2</sup>*Department of Ocean Advanced Materials Convergence Engineering, Korea Maritime and Ocean University, 727 Taejong-ro, Yeongdo-gu, Busan, 49112, Republic of Korea*

[†yunheak@kmou.ac.kr](mailto:yunheak@kmou.ac.kr)

Sandwich composites are being used in various industries for light-weight and high mechanical properties. In particular, the hexagonal honeycomb core is mainly used in the aerospace industry. However, comparing with a conventional hexagonal honeycomb core, auxetic core-structure possesses many superior properties such as shear resistance, fracture resistance, and energy absorption. In this respect, this study proposes integrating auxetic core-structure to improve the mechanical properties of sandwich composites further to prevent various damage. The integration of auxetic core-structure was manufactured of carbon fiber using a 3D printer of the Fused Deposition Modeling (FDM) type. Then, sandwich panels were fabricated using an integrated auxetic core and hexagonal core structure, and mechanical properties were compared.

### ***Acknowledgment***

This work was supported by the Technology Innovation Program (No. 20005403), funded by the Ministry of Trade, Industry & Energy (MOTIE, Korea).

## **MgF<sub>2</sub> Nanoparticle coating to Improve the Efficiency of Light Hazard in DSLR Cameras**

**Jeong Wan Kim<sup>1</sup>, Mun Ki Bae<sup>1</sup>, Tae Gyu Kim<sup>2\*</sup>**

<sup>1</sup>*Department of Nano Fusion Technology, Pusan National University, Busan, Korea*

<sup>2</sup>*Department of Nanomechatronics Engineering, Pusan National University, Busan, Korea*

[\\*tekim@pusan.ac.kr](mailto:*tekim@pusan.ac.kr)

The transmission properties of the antireflection (AR) coating depend on the wavelength of the light used, the refractive index of the substrate, the refractive index of the thin film, the coating thickness and the incident angle of the light. In this study, MgF<sub>2</sub> nanoparticles were coated on a DSLR lens by spin coating. The nanoparticle coating serves to reduce the harmfulness of the imaging surface by reducing the light reflectance of the aspherical lens and increasing the absorption rate. The size of the prepared MgF<sub>2</sub> nanoparticles was analyzed by FESEM, and the particles were very fine at 10 μm or less. The crystal growth and crystallization of MgF<sub>2</sub> nanoparticles had a great influence over the autoclave heat treatment conditions and time, and ion crystals such as fluoride crystallized well

even at relatively low temperatures. When the sol solution was not heat treated, the refractive index of the film was measured as equal to 1.40, and during autoclave heat treatment, an antireflection film having a low refractive index was formed. The crystal grains formed at this time were produced as a porous film having a certain ratio of nano porous between particles. In the case of coating MgF<sub>2</sub> with a porous film having nano porous, a disadvantage in that the mechanical strength of the film was lowered was generated, and the adhesion was improved by using a SiO<sub>2</sub> binder while maintaining a low refractive index. At this time, the adhesion strength according to the presence or absence of SiO<sub>2</sub> binding was measured by a nano-scratch tester. Therefore, in this study, the MgF<sub>2</sub>-based antireflection coating layer having a refractive index of 1.26 was first deposited, and secondly, SiO<sub>2</sub> binder was used as a binder between pores to enhance mechanical properties. In the result of applying this coating film to a DSLR aspheric lens, it was confirmed that the coating hazard of the imaging surface was improved by about 30%.

## **Corrosion Mechanism and Degradation Behaviour of Basalt Fiber Reinforced Composites in Sulfuric Acid Solution**

**Jin-Cheol Ha<sup>1\*</sup>, Soo-Jeong Park<sup>2</sup>, Yun-Hae Kim<sup>2\*\*</sup>**

*<sup>1</sup>College of Engineering, Dali University, No. 2 Hongsheng Road, Dali, Yunan, P.R. China*

*<sup>2</sup>Department of Ocean Advanced Materials Convergence Engineering, Korea Maritime and Ocean University, 727 Taejong-ro, Yeongdo-gu, Busan, Republic of Korea*

*\*[chnhjc@naver.com](mailto:chnhjc@naver.com); \*\*[yunheak@kmou.ac.kr](mailto:yunheak@kmou.ac.kr)*

Basalt fiber reinforced composites were treated with a sulfuric acid solution for different periods and concentrations. The strength, oxidation-reduction potential, Young's modulus of the composites were examined, and fracture energy was calculated after the treatment. The fracture surfaces were characterized using scanning electron microscopy and energy dispersive X-ray. In general, the tensile strengths and Young's modulus of the sulfuric acid solution treated samples showed a decreasing trend with treating times and concentrations. However, after 500 hours of treatment time, the tensile strengths and Young's modulus showed an increasing trend. Based on the experimental results, possible corrosion mechanisms were explored, indicating that the weight of the Fe, Si, Ca element content in the basalt fiber could improve resistance to environmental degradation of the basalt fiber reinforced composites in a sulfuric acid solution.

## Planar Multitip Field Emission Nanostructures

I.L. Jityaev\*, A.M. Svetlichnyi, A.S. Kolomiitsev, G.D. Gavrishchakin, A.I. Kovalets

*Southern Federal University, Institute of Nanotechnologies, Electronics, and Electronic Equipment Engineering, Taganrog, 347922 Russia*

[\\*izhityaev@sfnu.ru](mailto:izhityaev@sfnu.ru)

Improving the performance of the element base has several difficulties. This is due to technological and physical limitations in the manufacture of the element base. The use of field emission nanostructures implies an increase in the operating speed of electronic devices. Carbon nanomaterials are used to increase the stability and durability of field emission structures. In this work, the material of the field emission cathode is based on graphene films obtained on the surface of silicon carbide. Increasing the power of nanoscale field emission elements is possible by using blade cathodes or arrays of pointed nanostructures [1]. At the same time, it is necessary to take into account the destabilizing factors that may arise during the emission process. It is possible to minimize the destruction processes of a nanoscale field emission cathode of a matrix shape at the design stage. It is important to consider the processes of local amplification of the electric field and strive for its homogeneity near the emitting surface. The aim of this report is to study a nanoscale field emission cell containing a multitip cathode based on graphene films on silicon carbide. The paper simulates the distribution of the electric field strength in the interelectrode space of a planar nanoscale field emission cell. The influence of the distance between the planar tips in the array and the interelectrode distance on the uniformity of the electric field strength at the emitting surface is studied. The interelectrode distance was studied in the range from 50 to 100 nm, and the distance between the tips in the array varied from 100 to 200 nm. We obtained pictures of the electric field strength distribution. Theoretical dependences of the electric field strength at different field emission cell parameters were obtained. The simulation results confirmed the presence of a local increase in the electric field strength at the edge tips of the array. The theoretical dependences made it possible to determine the minimum parameters of the distance between the tips in the array and the interelectrode distance with uniformity of the electric field strength at the emitting surface of each tip. It was found that the minimum distance between the tips in the array changes from 130 to 160 nm in the considered range of interelectrode distance.

### **Acknowledgement**

This work was funded by the Grant of the President of the Russian Federation for state support of young Russian scientists - candidates of sciences (Project No. MK-1811.2019.8).

### **References**

[1] Jityaev I.L., Svetlichnyi A.M. // *Journal of Vacuum Science and Technology B: Nanotechnology and Microelectronics*, **37**, 012201, 2019.



## Matrix Blade Field Emission Cathodes

I.L. Jityaev\*, A.M. Svetlichnyi, A.S. Kolomiitsev, A.I. Kovalets, G.D. Gavrishchakin

*Southern Federal University, Institute of Nanotechnologies, Electronics, and Electronic Equipment Engineering, Taganrog, 347922, Russia*

[\\*izhityaev@sfnu.ru](mailto:izhityaev@sfnu.ru)

Nanoscale field emission cathodes are promising for nanoelectronics application. Reducing the size of the field emission cell to nanometers helps to reduce the threshold voltage. It is important to take into account the effect of the geometrical dimensions of the nanoscale field emission cell and emitter materials on the field emission characteristics. The use of nanocarbon materials is expedient because they are characterized by high electrical and thermal conductivity, as well as high resistance to ion bombardment. In this report, we consider the design of a field emission cathode consisting of an array of blade cathodes. An increase in the emission surface due to the use of multiemitter field emission blade cathodes promotes an increase in the emission current. However, the negative impact of the destruction processes of the blade edge imposes some restrictions on the operating time of the emitter, as well as on the stability of its characteristics. This is due to the local concentration of the electric field and cathode temperature [1]. The study evaluates the influence of the cathode density in the array and the interelectrode distance on the uniformity of the electric field strength at the emitting surface. The blades are made of silicon carbide with a multilayer graphene film on the surface. Multilayer graphene film is formed by thermal decomposition of silicon carbide in vacuum. By etching the field emission cathodes with nanometer accuracy is ensured by using the method of focused ion beams [2]. An increase in the distance between the blade emitters in the matrix of more than 100 nm at the interelectrode distance of 100 nm makes it possible to achieve the same value of the electric field strength at the emitting surface. The electric field strength at the outer corners of the blades in the matrix exceeds the value in the flat section by more than 3 times. The dependence of the electric field strength at the blade angles on the distance between the electrodes is nonlinear.

### **Acknowledgement**

This work was funded by the Grant of the President of the Russian Federation for state support of young Russian scientists - candidates of sciences (Project No. MK-1811.2019.8).

### **References**

- [1] Jityaev I.L., Svetlichnyi A.M. // *Journal of Vacuum Science and Technology B: Nanotechnology and Microelectronics*, **37**, 012201, 2019.
- [2] Kolomiitsev A.S., Jityaev I.L., Svetlichnyi A.M., Fedotov A.A., Ageev O.A. // *Diamond and Related Materials* **108**, 107969, 2020.

## Optical Properties of Sr<sub>0.61</sub>Ba<sub>0.39</sub>Nb<sub>2</sub>O<sub>6</sub> (SBN-61) Films Depending on Their Thickness

S.V. Kara-Murza<sup>1\*</sup>, K.M. Zhidel<sup>2</sup>, N.V. Korchikova<sup>1</sup>, Yu.V. Tekhtev<sup>1</sup>, A.V. Pavlenko<sup>3</sup>  
A.G. Silcheva<sup>1</sup>

<sup>1</sup>Lugansk Taras Shevchenko State University, Lugansk, Ukraine

<sup>2</sup>Research Institute of Physics, Southern Federal University, Rostov-on-Don, Russia

<sup>3</sup>[Federal Research Center The Southern Scientific Centre of the Russian Academy of Sciences, Rostov-on-Don, Russia](#)

[\\*skaramurza@gmail.com](mailto:skaramurza@gmail.com)

The properties of the films of Sr<sub>0.61</sub>Ba<sub>0.39</sub>Nb<sub>2</sub>O<sub>6</sub> (SBN-61) composition were studied by spectrophotometry and ellipsometry methods. The films were deposited by HF cathode atomization in oxygen atmosphere on single-crystal substrates of MgO with orientation (001). The time of deposition was 5 min, 10 min, and 115 min. The transmission spectra were measured in the wavelength range of 300–800 nm using a Shimadzu UV-50 spectrophotometer. In order to determine the thickness of the films and to perform a detailed study of their surface, ellipsometric measurements were performed using a multi-angle reflective ellipsometer at a wavelength of 632.8 nm helium-neon laser. To determine the optical parameters of the films, we used a two-layer model of the surface, including a base transparent layer with a thickness  $d_0$  with a refractive index  $n$  and a disturbed layer with effective parameters  $d_{ef}$  and  $n_{ef}$ . The effective refractive index of the surface of the damaged layer was recalculated into the coefficient of volumetric filling with the material of the damaged layer. Spectral measurements of optical transmittance made it possible to find the dispersion of the refractive index of an ordinary ray  $n_o$ , which for all studied films is consistent with the data presented in the literature for crystals. Ellipsometry data show that the measurement results are independent of the plane of incidence of the probe beam. These results are confirmed by X-ray diffraction analysis, according to which all films are heteroepitaxially grown, and the natural growth direction of [001] coincides with the direction of the  $c$ -axis of the SBN-61 structure. In addition, it was found that the parameter  $c$  of the films is somewhat larger compared to a single crystal, and it increases with decreasing film thickness. It should be noted that the accuracy of ellipsometric measurements does not make it possible to reliably determine the influence of the parameter  $c$  and, therefore, the contribution of anisotropy to the results. Nevertheless, the results of ellipsometric measurements of films of various thicknesses are of interest from the viewpoint of the formation of a surface disturbed layer. Table 1 shows the results obtained by ellipsometry for all three SBN-61 films.

**Table 1**

Sputtering time, $t$ , min	Film thickness, $d_0$ , nm	Refractive index, $n$	Disturbed layer		Volumetric factor of filling out
			$d_{ef}$ , nm	$n_{ef}$	
5	29	2.3	5	1.65	0.6
10	47	2.3	5	1.65	0.6
115	623	2.31	8	1.47	0.45

A decrease in the refractive index of the thin films is associated possibly with an increase in the anisotropy parameter  $c$  and its influence on an increase in the unit cell volume; it leads to a decrease in the refractive index  $n$ . Of particular interest in the results obtained is the large thickness of the disturbed layer in the thickest film, which is due, in our opinion, to the peculiarity of their growth (Volmer-Weber mechanism).

**Acknowledgement**

Research was financially supported by the Ministry of Science and Higher Education of the Russian Federation (State assignment in the field of scientific activity, Southern Federal University, 2020).

**Investigation of the Dependence of the Velocity of SAW Propagation under FeNi Films, Located on Lithium Niobate Substrates, on Magnetic Field**

G.Ya. Karapetyan<sup>1\*</sup>, V.E. Kaydashev<sup>2</sup>, M.E. Kutepov<sup>1</sup>, T.A. Minasyan<sup>1</sup>, V.A. Kalinin<sup>3</sup>, V.O. Kislitsyn<sup>3</sup>, E.M. Kaidashev<sup>1</sup>

<sup>1</sup>Laboratory of Nanomaterials, Southern Federal University, 200/1, Stachki, 344090 Rostov-on-Don, Russi.

<sup>2</sup>Moscow Institute of Physics and Technology, 9, Institutskiy per., Dolgoprudny, 141701, Russia

<sup>3</sup>LLC STC "RUS", 199178, Saint-Petersburg, Maly Ave., V. I. 54, Built 5, Russia

\*[jorichkaka@vandex.ru](mailto:yorichkaka@vandex.ru)

The propagation of surface acoustic waves (SAWs) under the thin-film piezo-magnetic structure of FeNi/ZnO/LiNbO<sub>3</sub> was studied. FeNi magnetostrictive films were obtained by pulsed laser deposition with a ZnO sublayer on the surface of lithium niobate. The deposition was carried out from a target of the FeNi alloy with a percentage of iron and Nickel of 2:1, the thickness of The FeNi film was equal to 500 nm, and the ZnO sublayer was 250 nm. The length of the film was 4 mm. A special setup was also developed to measure the effect of magnetic on the SAW propagation velocity (Fig. 1).

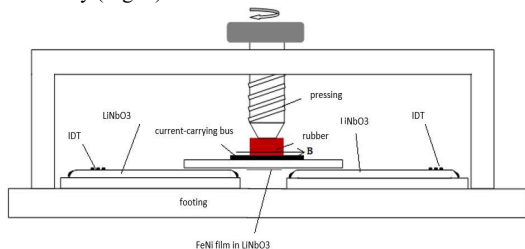


**Fig. 1**

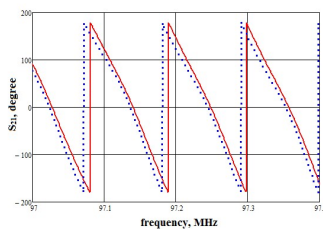


**Fig. 2**

This setup allowed measuring the SAW velocity in  $YX/128^\circ$  lithium niobate substrates, which were coated with a FeNi film. This substrate was pressed against two substrates located on the both side

of this substrate. This allowed SAW propagation from one substrate to another due to the SAW is accompanied by an electric field in the piezoelectric, which excites the SAW in the substrate to which it pressed. Excitation and reception of SAWs in the substrates to which the substrate with the film is pressed were carried out using interdigital transducers (IDT). The magnetic field was excited using a copper bus with a width of 1 cm and a thickness of 0.3 mm, through which a current was passed in the range of 1 – 10 A, which allowed one to obtain a magnetic field induction of up to 0.02 T. The phase of the transmission coefficient (parameter  $S_{21}$ ) was measured using the Obzor-304 device. Fig. 2 shows the phase shift at the current in the bus with 1 A in respect to the case when there is no current in the bus (no magnetic field). This method of investigation differs from the method of investigation proposed in [1], where it is necessary to excite the SAW directly using IDT. In [2], we proposed the concept of monitoring multiple SAW reflections by Fourier transform of the frequency response ( $S_{21}$ ) to increase the sensitivity of UV sensors. The proposed approach can be used to increase the sensitivity of SAW of magnetic field sensors based on the thin-film piezo-magnetic structure FeNi/ZnO/LiNbO<sub>3</sub>.

### Reference

- [1] Jie Tong, Yang Wang, Shiyue Wang, Wen Wang, Yana Ji, Xinlu Liu, // *Appl. Sci.*, **7**, 755, 2017  
 [2] G. Y. Karapetyan, V. E. Kaydashev, T. A. Minasyan, D. A. Zhilin, K. G. Abdulvakhidov, E. M. Kaidashev // *Smart Materials and Structures*, **26**, 035029, 2017.

## SAW Current Sensor with FeNi Film

G.Ya. Karapetyan<sup>1\*</sup>, M.E. Kutepov<sup>1</sup>, V.A. Kalinin<sup>2</sup>, V.O. Kislyitsyn<sup>2</sup>, E.M. Kaidashev<sup>1</sup>

<sup>1</sup>Laboratory of Nanomaterials, Southern Federal University,  
 200/1, Stachki, Rostov-on-Don, 344090, Russia

<sup>2</sup>LLC STC “RUS”, Maly av., V. I. 54, built 5, Saint-Petersburg, 199178, Russia

\*[jorichkaka@yandex.ru](mailto:jorichkaka@yandex.ru)

In a current-conducting bus with a width  $b = 8$  cm and a thickness  $a = 5$  mm, the magnetic field strength is  $H = 10/0.08 = 125$  A/m = 1.56 Oe at a current of 10 A, and  $H = 15.6$  Oe at a current of 100 A. As shown in [1] for a magnetic field sensor based on FeNi films, the change in the SAW velocity  $\Delta V/V = 0.007\%$  (1/15000), when the magnetic field strength is changed by 10 Oe. This is quite enough to noticeably change the ripples on the frequency dependence of parameter  $S_{11}$  in the sensor design shown in Fig. 1.

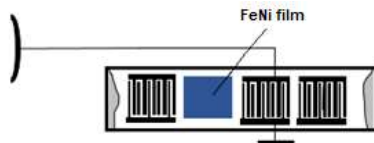
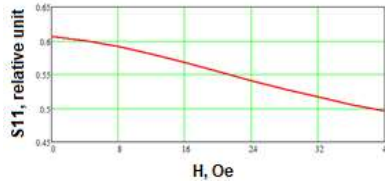


Fig. 1. Design of the current sensor and its location on the conducting bus



**Fig. 2.** Calculated dependence of parameter  $S_{11}$  on the magnetic field at 433.49 MHz; the length of the magnetosensitive film is equal to 1000 SAW lengths at the central frequency

The sensor is a SAW delay line, which has three interdigital transducers (IDTs), and between the middle and end IDT, FeNi film is located, which leads to a dependence of the SAW velocity on the magnetic field magnitude, and, consequently, of the current in the bus. When a reading signal is applied to the middle IDT, the SAWs excited by it are reflected from the end IDTs. Since, the end IDTs are located at different distances from the central IDT, it leads to the ripples of the frequency dependence of  $S_{11}$  parameter, which will depend on current changes because the SAW phase will depend on the SAW speed, which changes under the influence of a magnetic field. That is, for a fixed frequency, the amplitude changes on the frequency dependence of the  $S_{11}$  parameter. Fig. 2 shows the calculation of the change in the amplitude of parameter  $S_{11}$  at a frequency of 433.29 MHz when the magnetic field strength changes from 0 to 40 Oe, which corresponds to a change in the magnetic field induction from 0 to 0.004 T. From Fig. 2, it can be seen that the amplitude of the parameter  $S_{11}$  will change noticeably even for fields of 1 – 2 Oe, which correspond to the magnetic field strength on the bus equal to 10 – 20 A. Then this means that such a magnetic field sensor can be installed on the bus without any magnetic cores, which will greatly simplify and reduce the cost of the magnetic field sensor.

### Reference

[1] Jie Tong, Yang Wang, Shiyue Wang, Wen Wang, Yana Jia, Xinlu Liu // *Appl. Sci.* 7, 755, 2017.

## Effect of Pitch Difference and Root Radius on Anti-loosening Performance of Bolt Nut Connections

R. Kawano\*, B. Wang, N.A. Noda, Y. Sano, X. Liu, Y. Inui, B. Siew

*Department of Mechanical Engineering, Kyushu Institute of Technology, Kitakyushu, Japan*

\*[kawano.ryo621@mail.kyutech.jp](mailto:kawano.ryo621@mail.kyutech.jp)

Bolt nut connections are widely used in the industry. To ensure the safety of structures, both good anti-loosening performance and high fatigue are needed. In previous studies, it has been proven that by enlarging the root radii of bolt nut connections or introducing a pitch difference between the bolt and the nut, the fatigue life can be improved significantly. Based on this, in this study, the anti-loosening performance of the root enlarged bolt nut connections are studied. The prevailing torque

and the loosening process of M16 bolt nut connections are simulated by FEM analysis. It is found that even though the anti-loosening performance of the bolt nut connections decreases, introducing suitable pitch differences improves the anti-loosening performance compared to a common bolt nut connection.

## Synthetic Ethyl Alcohol Synthesis Technology

M.I. Kazmenko, D. D. Fugarov\*, O. A. Purchina, N.V. Rasteryaev

*Don State Technical University, Rostov-on-Don, Russia*

\*[ddf\\_1@mail.ru](mailto:ddf_1@mail.ru)

Synthetic ethyl alcohol is an alcohol from refining gases [1]. Oil is the third, most important raw material for alcohol production. When oil is heated (this is carried out at large oil refineries), a number of fractions are successively separated from it, namely gasoline, kerosene, naphtha, etc. [2]. These fractions are a mixture of light hydrocarbons. In the residue, heavy fuel oil is obtained. In order to increase the production of gasoline, which was urgently demanded by the rapidly developing automotive industry and aviation based on the use of internal combustion engines, oil is began to undergo special processing [3]. This processing associated with the use of high temperatures and pressures is called pyrolysis or cracking, depending on the conditions of the process [4]. Nowadays, when oil cracking and pyrolysis have been greatly developed in many countries, Butlerov's reaction has been carried out on an industrial scale. Hundreds of thousands of tons of alcohol are obtained from ethylene from refining gases. This is alcohol from oil. To obtain it, the cost of food raw materials is not required and therefore the production of such alcohol has unlimited development prospects [5].

### References

- [1] Fugarov D.D., Gerasimenko Y.Y., Nesterchuk V.V., Gerasimenko A.N., Onyshko D.A. // *Journal of Physics: Conference Series*. 012055, 2018.
- [2] Poluyan A.Y., Fugarov D.D., Purchina O.A., Nesterchuk V.V., Smirnova O.V., Petrenkova S.B. // *Journal of Physics: Conference Series "International Conference Information Technologies in Business and Industry 2018 - Microprocessor Systems and Telecommunications"*. 022013, 2018.
- [3] Fugarov D.D. In: *2019 International Conference on "Physics and Mechanics of New Materials and Their Applications", PHENMA 2019*, Hanoi, Vietnam, November 7 – 10, 2019, Hanoi University of Science and Technology: Hanoi. 119-120, 2019.
- [4] Y.O. Chernyshev, O.A. Purchina, A.Y. Poluyan, D.D. Fugarov, A.V. Basova, O.V. Smirnova // *Journal of Theoretical and Applied Information Technology*. **80**(1), 13-20, 2015.
- [5] Solomentsev K.Y., Fugarov D.D., Purchina O.A., Poluyan A.Y., Nesterchuk V.V., Petrenkova S.B. // *Journal of Physics: Conference Series*. **1015**, 032179, 2018.

## Features of the BST/Ln-Ceramic Microstructure

S. V. Khasbulatov<sup>1,2\*</sup>, A. V. Nagaenko<sup>1</sup>, L. A. Shilkina<sup>1</sup>, E. V. Glazunova<sup>1</sup>,  
S. I. Dudkina<sup>1</sup>, I. A. Verbenko<sup>1</sup>, L. A. Reznichenko<sup>1</sup>, N.A. Boldyrev<sup>1</sup>

<sup>1</sup>Research Institute of Physics, Southern Federal University, Rostov-on-Don, Russia

<sup>2</sup>Chechen State University, Grozny, Russia

\*[said\\_vahaevich@mail.ru](mailto:said_vahaevich@mail.ru)

Microstructures of (Ba, Sr)TiO<sub>3</sub> system ceramics with Ln modifier were studied. It is shown that regardless of the type of input modifiers, the grain landscape of solid solutions with different amounts of SrTiO<sub>3</sub> decreases to the size of crystallites not exceeding (2–3) microns, and compacted. In the initial system the average grain size at  $x = 0.20$  is equal to 6  $\mu\text{m}$ ; at  $x = 0.50$ , it is 4  $\mu\text{m}$ ; at  $x = 0.80$  it is 18  $\mu\text{m}$ . And the use of mechanoactivating procedures leads to an even greater reduction in the size  $\bar{d}$  and density of ceramics, and an increase in the concentration of modifiers in each group (within the considered limits of dopant variation) against the background of such a fine-grained structure has little effect on the dynamics of  $\bar{d}$  changes. Observed phenomena can be explained by the introduction of the large size of the rare-earth elements (REEs). It often leads to the transformation of ceramics symmetry with  $x = 0.20$  from tetragonal to cubic, the phase change of solid solutions with  $x = 0.50$  – shear on the phase diagram in the initial stage of spinodal decomposition or in the metastable region, the defective development of the situation in ceramics with  $x = 0.80$ . All these factors contribute to reducing spontaneous cell deformation, easing internal stresses in ceramics and, as a result, facilitating diffusion processes and mass transfer during recrystallization. It often leads to the increase of  $\bar{d}$ . However, this does not happen: in contrast to the traditional inverse dependence  $\bar{d}(\delta)$ , we observe a symbiotic behavior of these characteristics. The reason, probably, is that with very small distortions of the structure or in their practical absence (cubic phases), conditions are created for the simultaneous appearance of several recrystallized centers – the embryos of a new grain structure with a naturally reduced mass capacity, which in the future at the stage of grain growth "forced" to provide a smallness of their size. In the case of modification of ceramics with small-sized REEs, they replace the basic elements in very small quantities (limited solubility) with the loss of ballast phases, which act as catalysts for recrystallization processes that provoke multicenter grain structure at the primary stage of its formation and, as described above, contribute to its grinding.

### **Acknowledgement**

The research was carried out with the financial support of the Ministry of Science and Higher Education of the Russian Federation (State task in the field of scientific activity, Southern Federal University, 2020).

## On the Dependence of the Curie Temperature of Solid Solutions of the BST/REE System on the Chemical Composition and Position on the Phase Diagram

S. V. Khasbulatov<sup>1,2\*</sup>, L. A. Shilkina<sup>1</sup>, S. I. Dudkina<sup>1</sup>,  
I. A. Verbenko<sup>1</sup>, L. A. Reznichenko<sup>1</sup>, N.A. Boldyrev<sup>1</sup>

<sup>1</sup>Research Institute of Physics, Southern Federal University, Rostov-on-Don, Russia

<sup>2</sup>Chechen State University, Grozny, Russia

\*[said\\_vahaevich@mail.ru](mailto:said_vahaevich@mail.ru)

Dielectric spectra of solid solutions  $(1-x)\text{BaTiO}_3 - x\text{SrTiO}_3$  ( $x = 0.20; 0.50; 0.80$ ), modified by rare earth elements (REEs), in the frequency range  $(20 - 10^6)$  Hz (BST/REE) were studied. It is found that regardless of type of introduced into the system modifier the Curie temperature ( $T_C$ ) of ceramics with  $x = 0.20$  shifts towards to the low temperature region by  $\sim 80 - 100$  deg., in ceramics with  $x = 0.50$  it practically does not change its position ( $\Delta T = 0$ ), and in solid solutions with  $x = 0.80$ ,  $T_C$  shifts towards higher temperatures by  $\sim 170$  deg. It can be explained by the greater mobility of ceramic structures with  $x = 0.20$  and  $x = 0.80$  compared to ceramics with  $x = 0.50$  due to their proximity to morphotropic regions and spinodals of the BST system. Moreover, in the first case, with small amounts of Sr and modifiers in the structure, it is likely that a crystal-chemical disorder is formed, which contributes to a decrease in its stability and, as a result, a decrease in  $T_C$ . In ceramics with  $x = 0.80$ , it would seem that the situation is similar due to the small content of Ba and modifiers. However, in this case, the  $T_C$  increases, which may be the result of a very small (1.0 mol. %) amount (4 times less than in the first case) of the introduced dopants, which, probably, in addition to  $A$ -positions, mainly occupy vacant places in the perovskite structure (always available in this family), making it more resistant to various external influences, including chemical (isomorphic substitutions). The fact that the  $T_C$  position in ceramics is unchanged with  $x = 0.50$  may indicate its high stability, most likely due to equal amounts of structure-forming components-titanates, barium and strontium, and, as a result, the parity role of each of these compounds in the formation of chemical bonds. Moreover, these samples are located almost in the center of a single-phase (pseudocubic) region, equidistant from the morphotropic regions formed in the system. Thus, the position of the samples on the phase diagram of the BST system and the number of modifiers entered have a decisive influence on the shift of the Curie temperature in the modified ceramics of the BST system.

### **Acknowledgement**

The research was carried out with the financial support of the Ministry of Science and Higher Education of the Russian Federation (State task in the field of scientific activity, Southern Federal University, 2020).



## A Study on the Removal of Paint and Oxide Layer on the Steel Surface by Laser Beam Scanning Method

J.E. Kim<sup>a</sup>, M. K. Song<sup>b</sup>, M. S. Han<sup>c</sup>, J.D. Kim<sup>d\*</sup>

<sup>a</sup>*Ocean Science and Technology School, Korea Maritime and Ocean University,  
Busan, Republic of Korea*

<sup>b</sup>*Laser Advanced Machining Support Center, Korea Maritime and Ocean University,  
Busan, Republic of Korea*

<sup>c</sup>*Daewoo Shipbuilding & Marine Engineering Co., Ltd., Busan, Republic of Korea*

<sup>d</sup>*Division of Marine Engineering, Korea Maritime and Ocean University,  
Busan, Republic of Korea*

\*[jdkim@kmou.ac.kr](mailto:jdkim@kmou.ac.kr)

This study is aimed to develop eco-friendly pretreatment technology and surface cleaning technology for designing the smart yard, and conducted a study to replace the existing technology based on manual work, which has problems in terms of worker safety and environment, with laser cleaning technology [1 – 3]. The cleaning characteristics of the antifouling paint and oxide layer on the steel surface were analyzed according to the laser beam scanning method, which is the main process parameter. In the result of the experiment, the line beam pattern of the stage movement method showed a difference in the amount of heat input for the cleaning area. On the other hand, it was confirmed that the square area beam pattern of the galvano scanner movement method has uniform cleaning characteristics throughout. This study should be helpful to develop the eco-friendly surface cleaning technology for designing the smart yard by showing that laser cleaning technology can precisely remove not only the paint but also the oxide layer on the steel surface.

### References

- [1] Ji-Eon Kim, Myoung-Soo Han, Jong-Do Kim // *Modern Physics Letters B*, **34**, 2040042, 2020.
- [2] Guangxing Zhang, Xueming Hua, Ye Huang, Yuelong Zhang, Fang Li, Chen Shen, Jian Cheng // *Applied Surface Science*, **506**, 144666, 2020.
- [3] Guodong Zhu, Shouren Wang, Wei Cheng, Yuan Ren, Daosheng Wen // *Optics and Laser Technology*, **132**, 106475, 2020.

## Comparison of Weldability of Laser and Laser-Arc Hybrid Welding for Ship Manufacturing Using Environmentally Friendly Aluminum Alloys

J.S. Kim<sup>a</sup>, J.D. Kim<sup>b\*</sup>

<sup>a</sup>*Korea Marine Equipment Research Institute, Busan, Republic of Korea*

<sup>b</sup>*Division of Marine Engineering, Korea Maritime and Ocean University,  
Busan, Republic of Korea*

\*[jdkim@kmou.ac.kr](mailto:jdkim@kmou.ac.kr)

Since aluminum alloy is recyclable, it is considered as an environmentally friendly material for cruise, fishing boats, yachts, etc. The aluminum alloy 5083 of the 5000 series is an Al-Mg alloy that maintains mechanical strength through the solid solution strengthening effect of the Mg alloy. Thus, it has the highest strength among the non-thermal treatment alloys. Therefore, aluminum alloy 5083 with high strength is applicable to almost all parts of an aluminum ship, such as side of the ship, external board of ship bottom, rip plate, separating panel, rib, engine pedestal, operational room funnel, deck, and bulwark. However, when laser welding 5000 series aluminum alloys, the Mg is selectively evaporated by welding heat due to low melting and vaporization points, resulting in a reduction in strength of welds. Therefore, laser welding application is difficult to because laser welding of 5000 series aluminum alloy results in such a reduction in strength [1, 2]. In this study, laser and laser-arc hybrid welding were performed on 8 mm-thick aluminum alloy 5083 sheets and their weldabilities were compared and the effects of alloying elements on weldability were examined.

### References

[1] M. Mazar // *Optik*, **127**, 6782-6804, 2016.

[2] Dongsheng Wu // *International Journal of Heat Transfer*, **113**, 730-740, 2017.

## Prospects for the Use of Hydroacoustic Tools Based on Nonlinear Interaction of Acoustic Waves in Underwater Archaeology

I.A. Kirichenko<sup>1\*</sup>, I.B. Starchenko<sup>2</sup>

<sup>1</sup>*Southern Federal University, Taganrog, 347922, Russia*

<sup>2</sup>*Parametrika LCC, Taganrog, 347902, Russia*

\*[ikirichenko@sfnedu.ru](mailto:ikirichenko@sfnedu.ru)

The shallow water environment is one of the most dynamic elements, including coastal zones subject to rapid sedimentary flows and a significant focus for human activity throughout history. Coastal zones are characterized by shallow water, strong waves, strong currents and a large tidal range, as well as the presence of shallow gas, which can severely restrict the penetration of sound. As a result, such areas are rarely explored, which is unfortunate, since it is known that the land-sea

transition areas are rich in archaeological features. Obtaining information about the bottom structure requires the use of tools that are used to emit an acoustic signal with a specific physical parameter, such as output power, signal frequency, and signal duration. Typical frequencies of such acoustic systems are in the range from 10 to 200 kHz. Currently, a new class of underwater acoustics equipment is being developed, namely active location hydroacoustic devices with parametric arrays and transducers. The narrow beam pattern of the parametric array allows one to significantly increase the accuracy and angular resolution at short and medium distances of modern sonar devices, such as profilers. The absence of side lobes combined with a narrow directivity minimizes (often almost completely eliminates it) reverberation interference from the sea surface and bottom, which makes it possible to create precision sonar devices based on parametric arrays for marine archaeological work. In order to consider the parametric method of acoustic radiation formation, it is necessary to briefly consider the physical foundations of nonlinear acoustics, since many physical phenomena in the process of acoustic wave propagation cannot be described linearly. Such phenomena include cavitation, radiation force, and a number of others. Based on the results of a methodology for the evaluation of energy parameters of acoustic wave propagation, the technical characteristics of profiler can be assessed, such as operating frequency range, the energy potential in the given hydrological conditions, the parameters of the transmitted signal, including the signal duration and sounding period, noise conditions, the acoustic properties of bottom sediments, which will significantly expand the use of hydroacoustic tools in the interests of underwater archaeology.

***Acknowledgement***

The reported study was funded by RFBR and ASA according to the research project No. 19-52-40005.

## **Buckling Load Analysis of Single Stage and Multistage Hydraulic Cylinder by Successive Approximation Method**

**Kirtan K. Sahu\*, Vijay K. Gupta**

*PDPM IITDM Jabalpur, India*

\*[1913615@iiitdmj.ac.in](mailto:1913615@iiitdmj.ac.in)

Stability plays an important role in the structural analysis of the column. The hydraulic cylinder behaves as a structural member or column, which is subjected to axial loading. One of the major failure modes in the hydraulic cylinder is a buckling failure, which occurs due to instability. As the load increases, the instability also increases. For higher slenderness ratio, instability is more as compare to the lower slenderness ratio. Various theories like Euler, Rankine and Johnson theories have been developed for the uniform column, which has the constant flexural rigidity throughout the length. The flexural rigidity of the hydraulic cylinder changes constantly for the length of the cylinder and the rod. These theories are not suitable to solve the variable flexural rigidity columns. In this work, a successive approximation method and energy method have been developed for the single stage and a multistage hydraulic cylinder to determine the critical buckling load. The result of the buckling load by successive approximation method is compared with the result of the finite element method. The conjugate beam is used to derive the displacement and slope of the real beam.

It is an imaginary beam, which has the same dimension as the dimension of the real beam. The load at the conjugate beam is the moment divided by flexural rigidity (i.e.  $M/EI$ ) of the real beam. The shear force of the conjugate beam is the slope of the real beam, and the bending moment of the conjugate beam is the deflection of the real beam. The pin-pin end hydraulic cylinder is assumed as a conjugate beam to determine the buckling load. The change in the flexural rigidity of the hydraulic cylinder complicates it. The successive approximation method is used to derive the buckling load of a uniform column with the help of a conjugate beam. This method is an iterative method, which is used to determine the buckling load in the case, when the exact solution is unknown or complicated. The successive approximation method gives the accurate result as well as it also gives the lower and upper bound of the buckling load.

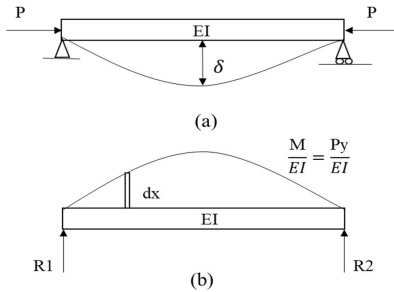


**Fig. 1.** (a) Real uniform beam with deflection curve; (b) conjugate uniform beam with variable load

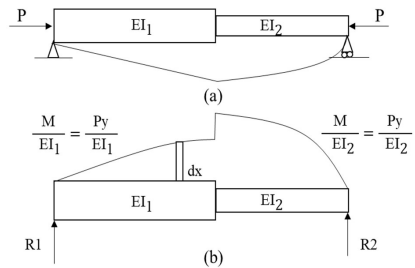


**Fig. 2.** (a) Real beam of hydraulic cylinder with deflection curve; (b) conjugate beam of hydraulic cylinder with variable load

A parabolic deflection curve is assumed for the uniform buckled beam. With the help of this assumed deflection curve the bending moment is calculated in the term of axial load. The new calculated deflection equation can be obtained by the conjugate beam method, and it is equated with the original assumed deflection curve at any section along the length of the beam, which gives the equation of the critical load. To obtain the accurate value of the critical load, the procedure is repeated. Using the average value of the deflection can reduce the value of the error. The lower and upper bound of the critical load is obtained by the ratio of two consecutive deflections. The assumed deflection curve for the uniform conjugate beam:

$$y_1 = \frac{4L\delta_1}{L^2}(L-x)^2 \quad (1)$$

Reaction forces due to a fictitious load ( $\frac{M}{EI} = \frac{Py_1}{EI}$ ):

$$R_1 = \frac{Pl\delta_1}{EI} \text{ and } R_2 = \frac{Pl\delta_1}{EI} \quad (2)$$

The fictitious bending moment in the conjugate beam:

$$y_2 = R_1x - \int_0^L \frac{Py_1}{EI}(x_1-x) \quad (3)$$

$$y_2 = \frac{Pl\delta_1 x}{3EI} \left( 1 - \frac{2x^2}{L^2} + \frac{x^3}{L^3} \right) \quad (4)$$

The critical load will be calculated by equating the deflection  $y_1$  and  $y_2$  at  $x = L/2$  along the length of the beam:

$$(y_1)_{x=L/2} = \delta_1 \text{ and } (y_2)_{x=L/2} = \delta \quad (5)$$

The calculated buckling load:

$$P_{Cr} = \frac{48EI}{5L^2} = \frac{9.6EI}{L^2} \quad (6)$$

Euler buckling load:

$$P_{Cr} = \frac{\pi^2 EI}{L^2} = \frac{9.869EI}{L^2} \quad (7)$$

Lower bound and upper bound of the critical load can be calculated by putting  $x = 0$  and  $x = L/2$  in the ratio of deflection curve:

$$\left( \frac{y_1}{y_2} \right) = \frac{12EI}{P} \frac{(L-x)}{L^3 - 2x^2L + x^3} \quad (8)$$

$$\left( \frac{y_1}{y_2} \right)_{min} = \frac{9.6EI}{L^2} \text{ and } \left( \frac{y_1}{y_2} \right)_{max} = \frac{12EI}{L^2} \quad (9)$$

$$\frac{9.6EI}{L^2} < P_{Cr} < \frac{12EI}{L^2} \quad (10)$$

The critical buckling load in successive approximation method is 2.7 % smaller than the Euler buckling load. The error can be reduced by equating the average value of  $y_1$ -deflection to the average value of  $y_2$ -deflection.

### References

- [1] S. Timoshenko, J.M. Gere. *Theory of Elastic Stability*. Pdf, 1963.
- [2] Gamez-Montero P. J., Salazar E., Castilla R., Freire J., Khamashta M., Codina E. // *Int. J. Mech. Sci.*, **51**(2), 105–113, 2009.
- [3] Pinarbasi S. // *J. Mech. Mater. Struct.*, **7**(5), 2012.
- [4] Pinarbasi S., Okay F., Akpinar E., Erdogan H. // *Math. Probl. Eng.*, 858906, 2013.
- [5] Zdravković N., Gašić M., Savković M., // *FME Trans.*, **41**(3), 222–229, 2013.
- [6] Ramasamy V., Junaid Basha A. M., “// *Def. Sci. J.*, **68**(2), 167–174, 2018.
- [7] Jatin P., Aniket N., Kankar P. K., Gupta V. K., Jain P. K., Ravindra T., Vinayak N., Ismail M., *Estimation of Load Carrying Capacity for Pin-Mounted Hydraulic Cylinders*, Springer, Singapore, 2019.
- [8] Prakash, J., Gupta, S. K., Kankar, P. K. // *Proc. Inst. Mech. Eng. Part C, J. Mech. Eng. Sci.*, **234**(19), 3919–3934, 2020.

## Nanoscale Carbon Cells with Gas and Gas Mixture Detection

V.S. Klimin, A.A. Rezvan\*, T.A. Zubova

*Institute of Nanotechnologies, Electronics, and Electronic Equipment Engineering,  
Southern Federal University, Taganrog, Russia*

\*[arezvan@sfedu.ru](mailto:arezvan@sfedu.ru)

The development of science and technology in the field of carbon nanostructures formation has reached great heights. There are a huge number of different techniques for obtaining these materials, ranging from mechanical exfoliation to laser stimulated deposition [1 – 3]. However, the most favorable from the viewpoint of the quality of obtained structure is still plasma chemical vapor deposition (PECVD), due to which it is possible to vary parameters of both – deposition process and structure's topology without presence of defect formation in the formed micro- and nanoelectronics element. The main idea of this report is formation of a gas sensor based on carbon nanostructures using plasma chemical deposition from gas phase. To perform, we chose Si (100) plates, surface of which was subjected to standard chemical treatment processes. Next, Ni was used to form contact layers, which were simultaneously applied to several Si wafers, by magnetron sputtering. Thereby, an upper and lower electrode were obtained for our gas detection device. A carbon nanostructure was formed on one of the plates by plasma chemical vapor deposition. Acetylene was used as carbon containing gas, and Ar was used to transport it to the substrate surface. As a result, it was determined that the fabricated model of a gas sensor based on a sensitive element consisting of a carbon nanosystem is sensitive to acceptor NO<sub>2</sub> gas molecules and NH<sub>3</sub>, CO gas donor molecules, H<sub>2</sub>O pairs with varying degrees of concentration-dependent sensitivity. According to the experimental estimates for CH<sub>4</sub>, CO<sub>2</sub>, CO, at a working temperature of 300 K and a concentration of 0.01 mol/liter, the sensitivity was 63, 135, 5468, respectively, the response time was 0.1 sec; recovery time 1.0 sec.

### **Acknowledgements**

This work was supported by Grant of the President of the Russian Federation No. MK-3512.2019.8. The results were obtained using the equipment of the Research and Education Center and Center for Collective Use "Nanotechnologies" of Southern Federal University.

### **Reference**

- [1] Klimin V.S., Rezvan A.A., Ageev O.A. // *Journal of Physics: Conference Series*, **1124**(2), 022035, 2018.
- [2] Klimin V.S., Rezvan A.A., Ageev O.A. // *Journal of Physics: Conference Series*, **1124**(7), 071020, 2018.
- [3] Nagase M., Nakamatsu K., Matsui S., Namatsu H. // *Journal of Applied Phys.* **44**(7), 5409, 2005.

## Molecular Dynamic Simulations of Sapphire Deformation Behavior

Yu. V. Klunnikova\*, M. V. Anikeev

*Southern Federal University, Taganrog, Russia*

[\\*jklunnikova@rambler.ru](mailto:*jklunnikova@rambler.ru)

Sapphire has a number of desirable chemical, electrical, mechanical, optical surface, thermal, and durability properties that make it an attractive material for a wide range of applications. Many experiments have been carried out before to evaluate its properties and determine some atomic reaction during the loading. Computational approaches are extensively used to explore various properties and behavior of sapphire. The molecular dynamics (MDs) simulation is a powerful method to study the material in atomic scale. In MDs simulation, Newton's equations of motion are numerically integrated for a discrete number of atoms whose interactions are governed by interatomic potentials. We used the molecular dynamics simulation with empirical potentials to study of sapphire deformation behavior. We considered the effect of parameters like sample size and strain rate on the sapphire tensile deformation. The MDs calculations are carried out by the Large-scale Atomic/Molecular Massively Parallel Simulator (LAMMPS) package. For the LAMMPS simulations we used the  $\text{Al}_2\text{O}_3$  interaction potential developed by Streitz and Mintmire. Sapphire was obtained from the melt by heating while high temperature liquid was 3000 K, then this melt was cooled to ambient temperature in 40000 time steps ( $\Delta t = 2$  fs). The atomic radial distribution function (RDF)  $G(r)$  showed peaks corresponding to the inter-atomic distances existing in the material. So, at a radial distance up to 1.6 Å the probability of finding two atoms is zero. The maximum probability is in between 1.6 Å to 2 Å, and then it shows some down and up behavior. Since crystal is a close packed structure, maximum probability is exceeding 3 for the radial distance from 1.6 Å to 2 Å. We analyzed the uniaxial tensile deformation of the obtained specimen along  $y$ -direction. Simulations have also been conducted to study the initiation of fracture during tensile deformation at different strain rates. We analyzed the sample fracture by formation of voids whose openings tend to occur under tensile loading conditions. We found the structure transition and significantly oxygen chains displacements under tensile effect in sapphire. The obtained results correspond to the experimental ones and allow us to develop the recommendations for determining the sapphire properties and increasing its quality for further application.

## Influence of Sapphire Substrates Defective Layer on Microelectronic Devices

Yu. V. Klunnikova<sup>1\*</sup>, S. P. Malyukov<sup>1</sup>, A. V. Filimonov<sup>2,3</sup>

<sup>1</sup>*Southern Federal University, Taganrog, Russia*

<sup>2</sup>*St. Petersburg Academic University RAS, St. Petersburg, Russia*

<sup>3</sup>*Peter the Great St. Petersburg Polytechnic University, St. Petersburg, Russia*

[\\*klunnikova@rambler.ru](mailto:*klunnikova@rambler.ru)

Sapphire crystals are one of the promising materials for microelectronic devices. The quality of the substrates surface layer significantly affects the structural perfection of the films obtained on their surface. The presence of thermoelastic stresses and defects, such as voids, dislocations, or microcracks in substrate, leads to the formation of defects in films. Dislocations and structure defects appear from the substrate and inherit its negative properties and worsen operational properties of microelectronic devices. Therefore, for meeting requirements of modern microelectronics, it is necessary to find methods for obtaining the optimal surface structure at the internal phase boundary in the “growing layer – substrate” system. We are studying the effect of sapphire substrate defects on the quality of the resulting films on its surface. As the substrate, we use sapphire with a thickness of 0.43 mm, a diameter of 50 mm, C-orientation and sapphire with the area of  $1 \times 1$  cm<sup>2</sup>, and a thickness of 3 – 5 mm. We obtain thin films (Si, Cu, Cr, Fe<sub>2</sub>O<sub>3</sub>, and TiO<sub>2</sub>) with a thickness up to 1 μm by various methods (laser annealing, magnetron sputtering, plasma-chemical vapor deposition) on their surfaces. The obtained samples are studied using methods of stylus profilometry, atomic force microscopy, scanning electron microscopy, powder X-ray diffractometry and Mössbauer spectroscopy. The mechanisms of surface defects occurrence in sapphire substrates and their influence on the quality of the resulting films are investigated. Experimental studies for estimation of the effect of substrate defects (volume defects such as voids and thermoelastic stresses) on the quality of the initial films are consistent with theoretical ones. Experimental studies for measuring mechanical stresses in thin films were carried out on a Tencor FLX-232 equipment. The thermoelastic stresses in the films on a sapphire substrate are estimated from the processing conditions, film thickness, and film and substrate properties. The results allow us to develop the recommendations for determining the properties of the surface layers of sapphire and improving the quality of the films obtained on its surface, which can be used to create better micro- and nanoelectronics devices, in particular, in specialized integrated circuits, solar energy and gas sensors.

### **Acknowledgement**

This work was supported by the Ministry of Science and Higher Education of the Russian Federation and the German Academic Exchange Service (DAAD) within the framework of the joint program “Mikhail Lomonosov”.



## Operation Modes of Power Protection Facilities

A.A. Kompaniets, D. D. Fugarov\*, O. A. Purchina, N.V. Rasteryaev

*Don State Technical University, Rostov-on-Don, Russia*

\*[ddf\\_1@mail.ru](mailto:ddf_1@mail.ru)

We consider the main operation modes of protection units, namely storage batteries (SBs). SB operates in three modes: mainly charge and recharge [1]. In the basic operation mode, the SB provides load current for motors not exceeding 2500 A at supply voltage 230 V [2]. The battery operation duration is 15-20 minutes [3]. SB charging mode is possible after completion of main operation mode, at that charging the unit is switched on, and six electric motors and recharging unit are disconnected from power supply buses [4]. SB is charged from charging unit with rectified current of 600 A up to voltage 230 B. The charging unit is powered by a three-phase AC industrial network. In the recharging mode of the accumulator battery, the recharging unit (RU) recharges the SB with a current of up to 70 A. This is necessary to maintain the SB in a charged state. Thus, SB and RU are combined into a single system capable of providing a constant voltage value on the power supply bus. The recharging unit is powered by three-phase alternating voltage of the industrial network [5].

### References

- [1] Fugarov D.D. In: *2019 International Conference on "Physics and Mechanics of New Materials and Their Applications", PHENMA 2019*, Hanoi, Vietnam, November 7 – 10, 2019, Hanoi University of Science and Technology: Hanoi. 119-120, 2019.
- [2] Y.O. Chernyshev, O.A. Purchina, A.Y. Poluyan, D.D. Fugarov, A.V. Basova, O.V. Smirnova // *Journal of Theoretical and Applied Information Technology*. **80**(1), 13-20, 2015.
- [3] Poluyan A.Y., Fugarov D.D., Purchina O.A., Nesterchuk V.V., Smirnova O.V., Petrenkova S.B. // *Journal of Physics: Conference Series "International Conference Information Technologies in Business and Industry 2018 - Microprocessor Systems and Telecommunications"*. 022013, 2018.
- [4] Fugarov D.D., Gerasimenko Y.Y., Nesterchuk V.V., Gerasimenko A.N., Onyshko D.A. // *Journal of Physics: Conference Series*. 012055, 2018.
- [5] Solomentsev K.Y., Fugarov D.D., Purchina O.A., Poluyan A.Y., Nesterchuk V.V., Petrenkova S.B. // *Journal of Physics: Conference Series*. **1015**, 032179, 2018. Series 2018. C. 012055.

## Computer Investigation of Nanoporous Elastic Composites with Various Sizes and Structure of Pores

A.S. Kornievsky\*, A.V. Nasedkin\*\*

*Institute of Mathematics, Mechanics and Computer Sciences, Southern Federal University,  
344090 Rostov-on-Don, Russia*

\*[alexandr5koren@gmail.com](mailto:alexandr5koren@gmail.com); \*\*[nasedkin@math.sfedu.ru](mailto:nasedkin@math.sfedu.ru)

It is known from experiments that the values of the corresponding effective moduli of nanoscale and macroscale porous bodies are different. There are a lot of approaches to describe this effect. Currently one of the most popular is the Gurtin-Murdoch model. The report involves mathematical methods development and finite element technologies. This also includes the design of APDL ANSYS programs for solving homogenization problems with surface effects, modeling representative volumes and determination of effective properties for porous anisotropic elastic materials. In this work, the porous beryllium was considered as an example. Beryllium is an anisotropic material of the hexagonal crystal family. To determine the effective properties of such composites, we solved six boundary-value problems with special boundary conditions in displacement. Further, in the ANSYS post processor block, the averaged stresses were calculated, both for volume elements and for surface ones. Finally, the effective moduli of the porous composite with surface effects were calculated using the corresponding formulas of the effective modulus method with respect to the found average stresses. In order to take into account the size effect, the Gurtin-Murdoch model was used. Namely, at the boundaries between the two phases, special elastic membranes were placed. These membranes are determined by surface stresses. All the problems for a representative volume were solved numerically using the finite element method in the ANSYS software package. The work describes an algorithm for the automatic determination of interphase boundaries and the positions of membrane elements on them. The algorithm remains operational at various sizes of representative volumes, built in the form of a cubic grid of hexahedral finite elements. At the same time, we compared several types of representative volumes. To generate representative volumes with different types of phase connectivity, the ACELAN-COMPOS package was used. In the result of our computational experiments, we discovered some trends. These results are similar to those of other authors, both theoretical and experimental. For example, a nanoscale body with low porosity rate can have greater stiffness than a corresponding body of macroscale dimensions. Moreover, the effective elastic stiffness of ordinary size bodies decreases with increasing porosity while these characteristics of the nanosized composite can both decrease and increase. The computational results of the composites with various mesh generation were compared. It was noted that due to surface effects, the geometric features of nanosized bodies can have much greater influence than ones of ordinary sized bodies. It is also numerically confirmed that in the case of a fixed percentage of porosity, as the pore size decreases, the stiffness of the material increases.

### ***Acknowledgement***

This research was funded by the RFBR, project number 20-31-90057.

## Analysis of Elemental Sulphur Production Flow Charts

S.V. Korolenko, D. D. Fugarov\*, O. A. Purchina, N.V. Rasteryaev

*Don State Technical University, Rostov-on-Don, Russia*

[\\*ddf\\_1@mail.ru](mailto:ddf_1@mail.ru)

Gases generated during purification of hydrocarbon gases from acidic components are hydrogen sulfide gas, which is processed into elemental sulfur [1]. The Klaus process or its various modifications [2] is used for this operation. To date, sulfur-containing compounds in exhaust gases should not exceed 0.5 mg/m. Therefore, before discharging process of gases into the atmosphere, it is necessary to clean them, this is an integral part of the Klaus process [3]. The analysis made it possible to draw a number of conclusions [4]: (i) the process of obtaining SO<sub>2</sub> from sulfur has the best economic indicators; (ii) a process with pre-heating of the process gas is most preferred in the case of high oxygen costs; (iii) the oxygen process is economically more profitable at lower oxygen prices; (iv) the final cost of sulphur is affected positively by low concentrations of H<sub>2</sub>S in the processed gas; (v) the most expensive is a scheme including a stage of sulphur combustion, the use of this scheme is advisable in the case of complete absence of hydrocarbons in the feedstock (the hydrocarbons cause deposits of resin on the catalyst, which negatively affects the quality of the final product [5]).

### References

- [1] Fugarov D.D., Gerasimenko Y.Y., Nesterchuk V.V., Gerasimenko A.N., Onyshko D.A. // *Journal of Physics: Conference Series*. 012055, 2018.
- [2] Y.O. Chernyshev, O.A. Purchina, A.Y. Poluyan, D.D. Fugarov, A.V. Basova, O.V. Smirnova // *Journal of Theoretical and Applied Information Technology*. **80**(1), 13-20, 2015.
- [3] Fugarov D.D. In: *2019 International Conference on "Physics and Mechanics of New Materials and Their Applications"*, PHENMA 2019, Hanoi, Vietnam, November 7 – 10, 2019, Hanoi University of Science and Technology: Hanoi. 119-120, 2019.
- [4] Poluyan A.Y., Fugarov D.D., Purchina O.A., Nesterchuk V.V., Smirnova O.V., Petrenkova S.B. // *Journal of Physics: Conference Series "International Conference Information Technologies in Business and Industry 2018 - Microprocessor Systems and Telecommunications"*. 022013, 2018.
- [5] Solomentsev K.Y., Fugarov D.D., Purchina O.A., Poluyan A.Y., Nesterchuk V.V., Petrenkova S.B. // *Journal of Physics: Conference Series*. **1015**, 032179, 2018.

## Crack Formation and Self-destruction Effects in Ceramics Based on the Alkali Metal Niobates

M. I. Kovalenko, S. I. Dudkina\*, L. A. Reznichenko

*Research Institute of Physics, Southern Federal University, Rostov-on-Don, Russia*

[\\*s.i.dudkina@yandex.ru](mailto:s.i.dudkina@yandex.ru)

The adoption in 2002 and 2011 of legislative directives by the European Parliament on the inadmissibility in the electrotechnical fields of the use of Pb-containing ceramics, in which toxic lead is present as the main component, prompted the scientific community to develop alternative lead-free materials that can replace Pb-containing in piezotechnical applications. The most promising were ferroceramics (FCs) based on alkali metal niobates (NAMs). However, their well-known tendency to self-destruction prevents the wide practical use of such compositions. The main causes of crack formation and the effect of self-destruction in ceramics based on NAMs and ways to minimize them are considered. The obtained experimental data and their analysis make it possible to determine the following causes of destruction phenomena in the FCs:

- (i) secondary discontinuous recrystallization of type I, which causes the growth of individual crystallites to a critical size ( $\sim 14 \mu\text{m}$ ), above which the integrity of the samples is violated;
- (ii) secondary discontinuous recrystallization of type II, associated with the presence in the niobate ferroceramics of a fluorine-containing liquid phase (LP), which is a matrix for excessively fast growth of single crystals to gigantic sizes both in the edge regions ("cortical effect") and in the center of the sample; using various experimental methods (determination of strength, fracture toughness, etc.), it was found that the maximum permissible concentration F, which does not lead to destruction phenomena in the FCs based on NAMs, is less 0.2 mass. %; an increase in the F-content leads to a deterioration in the mechanical properties, suppression of the piezoelectric state (a decrease in  $K_p$ ,  $|d_{31}|$ ,  $g_{31}$ ,  $V_R$ ,  $Q_m$ ), as well as to an undesirable increase in the  $\varepsilon_{33}^T/\varepsilon_0$  by 50% for the FC;
- (iii) heterogeneity of the studied solid solutions, due to the simultaneous existence of crystalline and liquid phases in the process of sintering, each of a different composition;
- (iv) rheological characteristics (high caking and low flowability) of the initial powders, leading to an inhomogeneous density, and subsequently low sintering activity, which causes the formation of centers with a more (less) dense structure and heterogeneous microstructure, which are sources of internal stresses;
- (v) the existence of critical values of the specific surface area of  $\text{Nb}_2\text{O}_5$  particles of various qualifications, above which the strength of the FCs based on NAMs decreases sharply (for  $\text{Nb}_2\text{O}_5$  qualifications NbO-Pt – 550–650  $\text{m}^2/\text{kg}$ ; osch – 950–1000  $\text{m}^2/\text{kg}$ ; osch type – 2500–3500  $\text{m}^2/\text{kg}$ ). One of the ways to minimize the described effects is considered the iso- and heterovalent modifications of ceramics based on NAMs.

### **Acknowledgement**

Research was financially supported by the Ministry of Science and Higher Education of the Russian Federation (State assignment in the field of scientific activity, Southern Federal University, 2020)".

## The Effect of the Preparation Conditions on the Catalytic Activity of $K_2PdCl_4$ in the Reaction of Methyl Alcohol with Acetylene

T.V. Krasnyakova<sup>1,2\*</sup>, D.V. Nikitenko<sup>1</sup>, I.A. Verbenko<sup>3</sup>, S.A. Mitchenko<sup>1</sup>

<sup>1</sup>*Institute of Physical Organic and Coal Chemistry, Donetsk, Ukraine*

<sup>2</sup>*Lugansk Taras Shevchenko State University, Lugansk, Ukraine*

<sup>3</sup>*Research Institute of Physics, Southern Federal University, Rostov-on-Don, Russia*

[\\*ktv\\_list.ru](mailto:*ktv_list.ru)

The formation of new materials is one of the central problems of modern engineering and technology development. Engineering, materials science, medicine and other industries require the production of materials with special electrical, magnetic, temperature-dependent, chemical, etc. properties. One of the methods for obtaining of such materials is mechanochemical activation, which is a combination of uniaxial loading and shear deformation of a substance in various dispersion media. Methods of mechanochemical activation make it possible to obtain nano- and submicrocrystalline materials with special physicochemical characteristics, which differ significantly from the properties of the initial polycrystalline sample. Specific properties are often determined by the nanocrystalline structure, a high degree of defectiveness, and the presence of amorphous, quasicrystalline, and metastable phases. The creating localized on the surface defects of a crystal structure (active centers of heterogeneous catalysts) by mechanochemical grinding opens up wide possibilities for using this method in heterogeneous catalysis. For  $K_2PdCl_4$  salt, we showed:

- (i) salt without mechanical pre-treatment is inactive for the reaction of methyl alcohol with acetylene;
- (ii) the active sites of the catalyst are formed upon mechanically activation of the salt in an acetylene atmosphere;
- (iii) an increase in the time of mechanochemical pre-activation is accompanied by a rise of its catalytic activity.

The report will consider the effect of mechanochemical pre-activation on the catalytic properties of the  $K_2PdCl_4$  salt in the reaction of addition of methyl alcohol to the triple bond of acetylene.

### **Acknowledgement**

Research was financially supported by the Ministry of Science and Higher Education of the Russian Federation (State assignment in the field of scientific activity, Southern Federal University, 2020).

# Reconstruction of the Optical Acoustic Signal for Visualization of Biological Tissues

D.A. Kravchuk<sup>1\*</sup>, I.B. Starchenko<sup>2\*\*</sup>

<sup>1</sup>*Southern Federal University, Taganrog, 347922, Russia*

<sup>2</sup>*OOO "Parametrica", Taganrog, 347922, Russia*

\*\*[kravchukda@sfedu.ru](mailto:kravchukda@sfedu.ru); \*\*[ibstarchenko@gmail.com](mailto:ibstarchenko@gmail.com)

One of the most important applications of optoacoustics is the visualization of oxygenation, hemoglobin concentration, and monitoring. Currently, the most commonly used methods for determining optical properties require invasive procedures and *in vitro* autonomous work methods based on attenuation using spectrophotometry, reflection coefficient, fluorescence spectroscopy, Raman spectroscopy, and optoacoustics [1]. *In vivo* studies using a combination of optoacoustics and carbon nanoparticles were performed [2–5] and demonstrated an increase in image contrast [6]. Most of the results presented to date are qualitative, and there are no quantitative *in vivo* studies. The purpose of the work is a quantitative study of the characteristics of an optoacoustic signal in model liquid biological media. The reverse filtering method, based on the configuration of scanning with rotation, is applied. It is a classical algorithm for reconstructing a cross-sectional image. Optoacoustic signals with pressure  $P_r(t)$  were obtained by deconvolution of the recorded acoustic signal  $P_{a0}(t)$ , emanating from a point absorption source, with a fast inverse Fourier transform. The report presents the results of processing an acoustic signal obtained in the result of thermoelastic expansion under the influence of an ND: YAG laser with a duration of 84 ns on an aqueous solution using a modified back projection algorithm based on a combined wavelet for high-frequency optoacoustic tomography. The results show that the above wavelet-based back projection algorithm effectively improves the resolution and contrast of reconstruction images under conditions of strong background noise. It is shown that the method can be used in optoacoustic signal reconstruction to obtain images of biological tissues.

## References

- [1] Kolkman R.G.M. et. al. // *Phys. Med. Biol.* **49**(20), 4745–4756, 2004.
- [2] Orda-Zhigulina D.V., Starchenko I.B. // *Engineering Journal of Don.* **22**(4–1), 28, 2012 (In Russian)
- [3] Kravchuk D.A., Starchenko I.B. // *Appl. Phys. Federal Informational-Analytical Center of the Defense Industry*, **2018**(4), 89–93, 2018 (In Russian).
- [4] Kravchuk D.A., Starchenko I.B. // *J. Phys. Conf. Ser.* **1353**, 12088, 2019..
- [5] Kravchuk D.A., Voronina K.A. // *Journal of Biomedical Photonics & Engineering.* **6**(1), 010307, 2020.
- [6] Li C. et. al. // *Phys. Med. Biol.* **49**, 1329, 2004.

## Studies of Magnetic and Local States of Fe<sup>3+</sup> Ions in (1 - x)Bi<sub>0.9</sub>Dy<sub>0.1</sub>FeO<sub>3</sub> - xPbTiO<sub>3</sub> Solid Solution

S.P. Kubrin<sup>1</sup>, S.I. Raevskaya<sup>1</sup>, J. Zhuang<sup>2</sup>, Z. Tang<sup>2</sup>, E.P. Shihova<sup>1</sup>, S.A. Shlyahova<sup>1</sup>,  
V.V. Titov<sup>1</sup>, I.P. Raevski<sup>1\*</sup>, M.A. Malitskaya<sup>1</sup>

<sup>1</sup>Research Institute of Physics and Faculty of Physics, Southern Federal University,  
Rostov-on-Don, 344090, Russia

<sup>2</sup>Electronic Materials Research Laboratory, Key Laboratory of the Ministry of Education,  
International Center for Dielectric Research, School of Electronic and Information Engineering,  
Xi'anJiaotong University, Xi'an, Shaanxi, 710049, China

\*[igorraevsky@gmail.com](mailto:igorraevsky@gmail.com)

Recently a possibility of multiferroic morphotropic phase boundary separating two chemical regions with distinct crystal structures and ferro orderings were reported for several BiFeO<sub>3</sub>-based single phase multiferroics [1, 2]. The scope of the present work was to study magnetic and local states of Fe<sup>3+</sup> ions in one of such materials, namely in (1 - x)Bi<sub>0.9</sub>Dy<sub>0.1</sub>FeO<sub>3</sub> - xPbTiO<sub>3</sub> solid solution using Mössbauer spectroscopy. Ceramic samples of compositions with  $x = 0, 0.2, 0.25, 0.31, 0.34, 0.4, 0.5$  were prepared using solid phase reactions route as described in [1]. According to X-ray phase analysis, the samples obtained were single-phase and possessed a perovskite structure. At room temperature, Mössbauer spectra of the samples with  $x = 0.2 - 0.34$  appear to be superpositions of three Zeeman sextets. Each sextet corresponds to the local state of Fe<sup>3+</sup> ions in the vicinity of which there is a different number of Ti<sup>4+</sup> ions. The sextet with the highest value of the hyperfine magnetic field (HMF) is due to Fe<sup>3+</sup> ions in the vicinity of which Ti<sup>4+</sup> ions are absent. The HMF values of other sextets are smaller, the more Ti<sup>4+</sup> ions are present in the Fe<sup>3+</sup> environment corresponding to these sextets. The presence of several local states of Fe<sup>3+</sup> ions indicate the existence of compositional inhomogeneities in the B-sublattice of the samples under study. That is, for the studied samples, clustering of cations of the B-sublattice is observed. Room temperature Mössbauer spectra of samples with  $x = 0.4$  and  $0.5$  consist of two paramagnetic doublets. The presence of two doublet components indicates that there are regions with different concentration of Fe<sup>3+</sup> ions. To estimate the temperatures of the magnetic phase transitions  $T_N$ , a temperature scanning technique was applied. We performed the measurement of Mössbauer spectrum doublet intensity  $I_m$  under gradual stepwise cooling. An abrupt drop in the  $I_m$  temperature dependence corresponds to  $T_N$ . Values of  $T_N$  were found to decrease as  $x$  grows due to the dilution of the magnetic Fe-sublattice. However, in the  $x = 0.3 - 0.4$  compositional range roughly corresponding to the boundaries of the multimorphotropic region separating the ferromagnetic compositions with monoclinic symmetry and antiferromagnetic compositions with tetragonal symmetry [2] a slope of the  $T_N(x)$  dependence was substantially (by more than two times) larger than that for the lower and higher values of  $x$ .

### Acknowledgment

This work was supported in part by RFBR project 19-52-53030 GFEN\_a.

### References

[1] J. Zhuang, L. Chen, W. Ren, Z.-G. Ye // *Ceramics International*. **39**, S207 – S211, 2013.

[2] J. Zhuang, J. Lu, N. Zhang, J. Zhang, A. A. Bokov, S. Yang, W. Ren, Z.-G. Ye. // *J. Appl. Phys.* **125**(4), 044102, 2019.

## Mossbauer Studies of Compositional Ordering in Ternary Perovskite $\text{Pb}_2\text{CoWO}_6$ and $\text{Pb}_2\text{CoWO}_6 - \text{PbTiO}_3$ Solid Solution

S. P. Kubrin<sup>1</sup>, M. Yu. Silin<sup>2</sup>, I. P. Raevski<sup>1\*</sup>, D. A. Sarychev<sup>1</sup>, V. V. Titov<sup>1</sup>, V. A. Ershin<sup>1</sup>,  
S. I. Raevskaya<sup>1</sup>, M. A. Malitskaya<sup>1</sup>

<sup>1</sup>Research Institute of Physics and Faculty of Physics, Rostov State University, Stachki Ave. 194,  
Rostov-on-Don, 344090, Russia

<sup>2</sup>RITVERC JSC, Kurchatov Str., 10, St. Petersburg, 194223, Russia

\*[igorraevsky@gmail.com](mailto:igorraevsky@gmail.com)

Ternary ferroelectric and antiferroelectric perovskite-family oxides  $\text{Pb}_2(B'B'')\text{O}_6$  have been studied intensively in recent years. Of special interest, is the great impact of the degree  $S$  of ordering of  $B'$  and  $B''$ -ions over equivalent crystallographic positions on the temperatures of ferroelectric and magnetic phase transitions [1 – 4]. Such ordering is usually called compositional or chemical to differentiate it from the dipole (ferroelectric and antiferroelectric) or spin (ferromagnetic and antiferromagnetic) order. Mossbauer spectroscopy was successfully used to study the compositional ordering in Fe-containing perovskites. The Mossbauer spectra of disordered  $\text{Pb}_2\text{FeNbO}_6$  and  $\text{Pb}_2\text{FeTaO}_6$  in a paramagnetic phase are doublets [4]. In contrast to this, Mossbauer spectra of highly ordered  $\text{Pb}_2\text{FeSbO}_6$  and  $\text{Sr}_2\text{FeMoO}_6$  are singlets [5 – 7]. The cause of quadrupole splitting for the cubic phase appears to be the incompletely ordered distribution of  $B'$  and  $B''$ -ions over octahedral lattice sites. In this case, the symmetry of the environment of Mossbauer cation is not cubic. The goal of the present work was to study Mossbauer spectra of  $\text{Pb}_2\text{CoWO}_6$  and  $\text{Pb}_2\text{CoWO}_6 - \text{PbTiO}_3$  solid solution at room temperature in the emission mode. Mossbauer spectrum of  $\text{Pb}_2\text{CoWO}_6$  sample is a singlet being a fingerprint of a very high degree of ordering. Mossbauer spectrum of  $\text{Pb}_2\text{CoWO}_6 - \text{PbTiO}_3$  solid solution composition containing 20 mol.% of  $\text{PbTiO}_3$  is a superposition of singlet and doublet. The relative content of these components is 44 and 56% respectively. The data of Mossbauer studies corroborate well the results of the X-ray diffraction studies. The singlet likely corresponds to compositionally ordered regions (fairly large in size), whereas the doublet is associated with regions, where the long-range order in the arrangement of ions is disturbed.

### Acknowledgement

The work was partially supported by Russian Foundation for Basic Research (grant No. 20-03-00920\_a).

### References

- [1] C.G.F. Stenger, F.L. Scholten, A.J. Burggraaf // *Solid State Commun.* **32**, 989, 1979.
- [2] I.P. Raevski, V.Y. Shonov, M.A. Malitskaya et al // *Ferroelectrics*, **235**, 205, 1999.
- [3] I.P. Raevski, A.V. Pushkarev, S.I. Raevskaya, et al // *Ferroelectrics*, **501**, 154, 2016.
- [4] A.A. Gusev, S.I. Raevskaya, V.V. Titov, et al // *Ferroelectrics*, **496**, 231, 2016.
- [5] V. V. Laguta, V. A. Stephanovich, M. Savinov, et al // *New J. Phys.*, **16**, 11304, 2014.
- [6] B. Argymbek, T. Kmjec, V. Chlan, et al // *J. Magn. Magn. Mater.*, **477**, 334, 2019.



## Synthesis, Electronic Structure, Microstructure and Properties of Vacuum Ion-Plasma Coatings Based on Carbon

O.V. Kudryakov<sup>1\*</sup>, V.N. Varavka<sup>1\*\*</sup>, I.Yu. Zabiya<sup>1</sup>, A.V. Sidashov<sup>2</sup>, E.S. Novikov<sup>2</sup>

<sup>1</sup>*Don State Technical University, Rostov-on-Don, Russia*

<sup>2</sup>*Rostov State Transport University, Rostov-on-Don, Russia*

\*[kudryakov@mail.ru](mailto:kudryakov@mail.ru), \*\*[varavkavn@gmail.com](mailto:varavkavn@gmail.com)

The prospects for the development of ion-plasma methods today consist in the development of new materials and the production of multifunctional coatings. In this regard, one of the most attractive objects of research in the field of materials science and nanotechnology is carbon materials, in particular, diamond-like coatings (DLCs). Interest in DLCs is associated with the possibility of relatively simple technological regulation of the ratio of electronic carbon configurations in the coating:  $sp^2$ -bonds (characteristic of graphite) and  $sp^3$ -bonds (characteristic of diamond). Due to this variability, the properties of DLCs can also be changed within wide limits. In the present report, the carbon coatings obtained by vacuum ion-plasma technology using a gas mixture of acetylene and methylsiloxane at a temperature of 180 °C are studied. The coatings were applied to the substrate from steels with various types of thermal and chemical-thermal treatment. Some of the samples, before applying DLCs, were doped with Nb and Hf in the vacuum chamber of the ion-plasma device to increase the adhesion of the coating. The problem of adhesion of DLCs on various substrates is considered in our other publications. The total thickness of the coatings ranged from 0.5 to 1.6  $\mu\text{m}$ . The electron microscopic study of the coatings revealed that in the cross-section they consist of two layers: the layer on the surface of the sample is much more saturated with silicon (from methylsiloxane), and the outer coating layer is almost completely carbon. The transition zone between the layers is smooth, blurry and does not have the nature of the interphase boundary. A finer study of the composition of DLCs was carried out by X-ray photoelectron spectroscopy (XPES) by layer-by-layer ion profiling of the coating surface to its entire depth. Using the "SPECES" (surface analysis system, Germany), survey spectra were recorded from each profiled (vaporized) layer. To determine the  $sp^3/sp^2$  ratio, C (KLL) Auger spectra were used. An XPES study showed a graded distribution of the  $sp^3/sp^2$  ratio over the coating depth: from 2/1 on the surface to 1/9 at the substrate. The study of the physical and mechanical properties by means of the indentation method showed that the indentation hardness  $H$  of the studied DLCs is very sensitive to the magnitude of the applied load. At the same time, the Young's modulus  $E$  demonstrates a small dependence on the applied load. Apparently, this should be evaluated as the influence of the "size factor" on the mechanical properties. So, at a load of 100 mN, the spread of hardness was 9 – 21 GPa, and at 10 mN, it was 12 – 30 GPa. According to the  $H/E$  and  $H^3/E^2$  indicators, which determine the elastic and plastic deformation resistance, respectively, the studied carbon coatings are not inferior to ion-plasma wear-resistant nitride coatings. As for the tribological properties tested on a TRB friction machine equipped with "pin plate" unit in accordance with the methods of DIN 50324 and ASTM G99, the

studied carbon coatings did not show particular advantages in wear resistance over coatings of nitride systems and even over steels after chemical-thermal treatment (with the exception of the indicator – coefficient of friction  $\mu$ ). The study of the degradation of DLCs during tribological tests showed that their wear is carried out by the abrasion mechanism. Moreover, DLCs demonstrate lubricating properties and the ability to relax stresses in the surface contact layers during the unloading period. As the main applied result of the work, we conclude that the usage of carbon coatings (DLCs) with an optimum thickness of 1.2 – 1.4  $\mu\text{m}$  provides a significant decrease in the friction coefficient  $\mu$  in tribological tests. The maximum effect of reducing  $\mu$  (on average, 2.0 – 2.5 times) was obtained on the nitride samples from steel 38Cr<sub>2</sub>MoAl, additionally modified before coating by ion implantation of Nb and Hf.

#### **Acknowledgement**

This research was financially supported by RFBR grant No. 18-08-00546 and by the Ministry of Science and Higher Education of Russia (project identifier RFMEFI60718X0203).

## **Semi-Invariant Form of Equilibrium Stability Criteria for Systems with Two Cosymmetries**

**L.G. Kurakin<sup>1,2,3\*</sup>, A.V. Kurdoglyan<sup>3\*\*</sup>**

<sup>1</sup>*Water Problems Institute of the Russian Academy of Sciences, Moscow, Russia*

<sup>2</sup>*Southern Mathematical Institute of the Vladikavkaz Scientific Center of the Russian Academy of Sciences, Vladikavkaz, Russia*

<sup>3</sup>*I. I. Vorovich Institute of Mathematics, Mechanics and Computer Sciences,  
Southern Federal University, Rostov-on-Don, Russia*

\*[lgkurakin@sfedu.ru](mailto:lgkurakin@sfedu.ru), \*\*[aik\\_kurdoglyan@mail.ru](mailto:aik_kurdoglyan@mail.ru)

Critical cases of equilibria stability are considered for differential equations with two cosymmetries. Stability spectrum of such equilibrium consists of two spectral sets. The first is the non-trivial neutral spectrum that is on the imaginary axis. The second is a stable part of the spectrum that lies in the left half-plane. According to the general theory, research of the critical cases comes down to study of nonlinear model systems. To calculate the coefficients for such systems is a separate problem. Stability criteria for the model systems are described in the previous work of the authors. The purpose of given report is to express the coefficients of Taylor's series for model systems from such coefficients for the original equation. A usual algorithm constructing a model system consists of two coherent conversions of the original equation. The first is to form the reduction on the neutral surface for this equation. As a result, its dimension is decreased to the neutral subspace's dimension. Then the constriction is transformed to normal form to some finite order. The higher order terms are ignored. In this work the coefficients of the model systems are computed with the help of algorithm of V. I. Yudovich. It makes possible to unite both conversions into one. The obtained formulae for coefficients of model systems are independent of the original equation's dimension. Thus it is applicable to systems of finite or infinite dimension and usable to realize using packages of analytical calculations.

### **Acknowledgement**

The results of this research were published in the work [1], which was financially supported by the Southern Federal University, grant No. VnGr-07/2020-04-IM (Ministry of Education and Science of the Russian Federation).

### **Reference**

[1] Kurakin L. G., Kurdoglyan A. V. // Bulletin of Higher Educational Institutions. North Caucasus Region. Natural Sciences, 1, 11–16, 2020.

## **On the Stability of a Regular Vortex Polygon in a Two-fluid Plasma**

**L.G. Kurakin<sup>1,2,3\*</sup>, I.A. Lysenko<sup>3\*\*</sup>, S.A. Lysenko<sup>3\*\*\*</sup>**

<sup>1</sup>*Water Problems Institute of the Russian Academy of Sciences, Moscow, Russia*

<sup>2</sup>*Southern Mathematical Institute of the Vladikavkaz Scientific Center of the Russian Academy of Sciences, Vladikavkaz, Russia*

<sup>3</sup>*I. I. Vorovich Institute of Mathematics, Mechanics and Computer Sciences, Southern Federal University, Rostov-on-Don, Russia*

\*[kurakin@math.rsu](mailto:kurakin@math.rsu), \*\*[irina107ls@mail.ru](mailto:irina107ls@mail.ru), \*\*\*[sergey23ls@mail.ru](mailto:sergey23ls@mail.ru)

The motion of the system of  $N$  point vortices with identical intensity  $\Gamma$  in the Alfvén model of a two-fluid plasma is considered. The stability of the stationary rotation of  $N$  identical vortices disposed uniformly on a circle with radius  $R$  is studied for  $N = 2, \dots, 5$ . This problem has three parameters: the discrete parameter  $N$  and two continuous parameters  $R$  and  $c$ , where  $c > 0$  is the value characterizing the plasma. Two different definitions of the stability are used, namely the orbital stability and the stability of a three-dimensional invariant set founded by the orbits of a continuous family of stationary rotations. Instability is interpreted as instability of equilibrium of the reduced system. An analytical analysis of eigenvalues of the linearization matrix and the quadratic part of the Hamiltonian is given. As a result, the parameter space  $(N, R, c)$  of this problem for two stability definitions considered is divided into three parts: the domain  $\mathcal{A}$  of stability in an exact nonlinear problem setting, the linear stability domain  $\mathcal{B}$ , where the nonlinear analysis is needed, and the domain of exponential instability  $\mathcal{C}$ . The results of theoretical analysis for orbital stability [1] are checked by numerical calculations of the vortex trajectories. The application of the stability theory of invariant sets for the systems with a few integrals for  $N = 2, 3, 4$  allows one to obtain new statements about the stability in the domains, where nonlinear analysis is needed in investigating the orbital stability.

### **Acknowledgement**

The results of this research were published in the work [2], which was financially supported by the Southern Federal University, grant No. VnGr-07/2020-04-IM (Ministry of Science and Higher Education of the Russian Federation).

### **References**

[1] Lysenko I.A. // *University News. North-Caucasian Region. Natural Sciences Series*, 1, 17–23, 2019 (In Russian).

[2] Kurakin L.G., Lysenko I.A. // *Russian Journal of Nonlinear Dynamics*, **16**(1), 3–11, 2020.

# Analysis of the Stability of a Regular System of Vortex Charges outside the Circular Region in the Case of an Arbitrary Circulation around the Boundary

L.G. Kurakin<sup>1,2,3\*</sup>, N. V. Shilova<sup>3\*\*</sup>

<sup>1</sup>*Water Problems Institute of the Russian Academy of Sciences, Moscow, Russia*

<sup>2</sup>*Southern Mathematical Institute of the Vladikavkaz Scientific Center of the Russian Academy of Sciences, Vladikavkaz, Russia*

<sup>3</sup>*I. I. Vorovich Institute of Mathematics, Mechanics and Computer Sciences, Southern Federal University, Rostov-on-Don, Russia*

\*[lgkurakin@sfedu.ru](mailto:lgkurakin@sfedu.ru); \*\*[natalya.shilova7@mail.ru](mailto:natalya.shilova7@mail.ru)

The model of the motion of a system of point vortex charges (point vortices) outside a circular domain with a non-zero circulation around the boundary is considered. The interaction potential between the charges is inversely proportional to the distance between them. The stability of stationary rotation of a system of  $N$  identical vortices located at the vertices of a regular  $N$ -gon is studied. This work is a natural continuation of the paper [1], which considers the case of zero circulation. The stability theory of stationary motions for dynamical systems with symmetry, developed by V. I. Yudovich, is applied. The motion equations are a Hamiltonian system, so the paper uses methods for analyzing the stability of equilibria of Hamiltonian systems. Cases  $N = 2, \dots, 8$  are considered sequentially. The linearization matrix is analyzed and exponential instability conditions are obtained. Conditions are found under which the quadratic part of the Hamiltonian is positive-definite. In this case, the stationary rotation of the vortex  $N$ -gon is stable in a nonlinear setting. Conditions are obtained when all eigenvalues of the linearization matrix lie on the imaginary axis, and the quadratic part of the Hamiltonian is not positive-definite. It is well known that the stability problem requires the nonlinear analysis in this case.

## **Acknowledgement**

The results of this research were financially supported by the Southern Federal University, grant No. VnGr-07/2020-04-IM (Ministry of Science and Higher Education of the Russian Federation).

## **Reference**

[1] L.G. Kurakin, A.P. Melekhov<sup>1</sup>, I.V. Ostrovskaya // *University News. North-Caucasian Region. Natural Sciences Series*, **4-1**(196-1), 24 – 30, 2017.

## Optimizing VO<sub>2</sub> Film Properties for Use in SAW Devices

M.E. Kutepov<sup>1\*</sup>, T.A. Minasyan<sup>1</sup>, G.Ya. Karapetyan<sup>1</sup>, V.E. Kaydashev<sup>2</sup>,  
I.V. Lisnevskaya<sup>3</sup>, K.G. Abdulvakhidov<sup>4</sup>, A.A. Kozmin<sup>1</sup>, E.M. Kaidashev<sup>1</sup>

<sup>1</sup>Laboratory of Nanomaterials, Southern Federal University,  
200/1, Stachki, Rostov-on-Don, 344090, Russia

<sup>2</sup>Moscow Institute of Physics and Technology,  
9, Institutskiy per., Dolgoprudny, 141701, Russia

<sup>3</sup>Department of Chemistry, Southern Federal University,  
7, Zorge Str., Rostov-on-Don, 344090, Russia

<sup>4</sup>Smart Materials Research Institute, Southern Federal University,  
178/24, Sladkova, Rostov-on-Don, 344090, Russia

\*[kutepov.max@yandex.ru](mailto:kutepov.max@yandex.ru)

Vanadium dioxide (VO<sub>2</sub>) exhibits a metal-insulator transition (MIT) at a temperature of about 69 °C [1, 2]. At this transition, the resistivity of VO<sub>2</sub> changes up to 4 orders of magnitude [3]. The aim of the study was to optimize the conditions for producing thin VO<sub>2</sub> films for their use in SAW devices. We used the laser pulsed deposition (PLD) method to produce VO<sub>2</sub> films. We used metallic vanadium target. The dependence of the oxygen pressure during PLD on the resistive metal-insulator transition on substrates of *c*- and *R*-sapphire was studied. The resulting films had sharp metal-insulator temperature transitions in all used Al<sub>2</sub>O<sub>3</sub> cuts. The most high-quality films showed resistance change by 4 orders of magnitude. At the lower point of the hysteresis, the resistance of these samples was in the range of 50 – 100 Ω. The synthesized VO<sub>2</sub> films had a sharp temperature transition and a relatively small width of thermal hysteresis. The use of thin VO<sub>2</sub> films with low resistance after the transition to the metallic state allowed us to change the reflection coefficient of a SAW in a delay line by more than 3 times. We also used VO<sub>2</sub> film as a bridge of an acoustic coupler. The SAW transmission coefficient through the coupler into another channel changed by 2 times.

### References

- [1] F.J. Morin // *Phys. Rev. Lett.* **3**, 34–36, 1959.
- [2] D.P. Partlow, S.R. Gurkovich, K.C. Radford, L.J. Denes // *J. Appl. Phys.* **70**, 443–452, 1991.
- [3] H. Jerominek, F. Picard, D. Vincent // *Opt. Eng.* **32**, 2092–2099, 1993.

## **Quantifying of the internal defects content in CF-PEKK through water absorption behavior**

**Kyo-Moon Lee<sup>1</sup>, Soo-Jeong Park<sup>2</sup>, Seong-Jae Park<sup>1</sup>, Yu Tianyu<sup>1</sup>, Yun-Hae Kim<sup>1,2†</sup>**

<sup>1</sup>*Department of Marine Equipment Engineering, Graduate School, Korea Maritime and Ocean University, 727 Taejong-ro, Yeongdo-gu, Busan, 49112, Republic of Korea*

<sup>2</sup>*Department of Ocean Advanced Materials Convergence Engineering, Korea Maritime and Ocean University, 727 Taejong-ro, Yeongdo-gu, Busan, 49112, Republic of Korea*

†[yunheak@kmou.ac.kr](mailto:yunheak@kmou.ac.kr)

Along with the development of high-performance thermoplastic resin, various researches were being conducted on hot-press forming and oven consolidation, which are a part of the Out-of-Autoclave (OoA) process for thermoplastic composite structures. Thermoplastic composite is manufactured by using prepregs. In this manufacture, splicing, tow gap, overlap can be caused in internal laminate, and repeated of defects cause void, delamination. This defect in laminate can be inspected using C-scan (NDI), but it just show the presence, distance of defects. NDI is difficult to quantifying of internal defects content. Polyetherketoneketone(PEKK) has the charaterisitic of wate absorption resistance and degradation resistance in high temperature water. However, in water absorption condition, the void in laminate is filled with water and increases saturation absorption. In this study, the objectives is to quantifying of internal defect volume in carbon fiber reinforced PEKK composites (CF-PEKK) using water absorption behavior.

### ***Acknowledgment***

This work was supported by the Technology Innovation Program (No. 20007444), funded by the Ministry of Trade, Industry & Energy (MOTIE, Korea).

## **Optimization and Management Strategy Resources for Water Fulfillment of Community Water in Mojokerto District, East Java**

**Laksono Djoko Nugroho\*, Tiwi Sri Rejeki, Hudhiyantoro, Budi Santoso**

*Department of Civil Engineering, University of 17 Agustus 1945 Surabaya, Indonesia*

\*[laksononugroho7366@gmail.com](mailto:laksononugroho7366@gmail.com)

Current domestic and non-domestic drinking water needs are sourced from surface and groundwater. The increasing population and the need for residential land and other activities (industry and tourism) require an increase in the supply of water resources. The purpose of this study is to analyze the condition of existing water resources, to analyze the condition of the comparison of the amount of water needed with the availability of known water resources by calculating the water balance up to 2032 and to evaluate and formulate a strategy for optimizing the management of water resources in

Mojokerto Regency. From the calculation using the water balance method that has been done in Scenario I (the availability of existing water is considered constant), the water needs in Mojokerto Regency by optimizing the Brantas River. In Scenario II (we consider water sources, springs, and reservoirs) and taking into account the effects of environmental degradation. The conclusion of this research in the scenario I is that the carrying capacity of water resources in Mojokerto Regency is currently still sufficient until 2036 with a water demand of 41,892,326 m<sup>3</sup>/year compared to water availability of 6,949,846,656 m<sup>3</sup>/year. However, this condition will be different if not balanced with concrete steps to preserve the existing environment and efforts to optimize the potential of the Brantas River. While Scenario II in Mojokerto Regency will start experiencing water shortages in 2019, from the water demand of 41,892,326 m<sup>3</sup>/year compared to the availability of water of 38,493,377 m<sup>3</sup>/year. To meet the subsequent water needs, environmentally friendly policies are needed based on the concept of social learning with strategies that pay attention to demand and supply issues.

## **Ordering of Carbon Nanotubes in Aqueous Dispersion of Nanomaterials under the Influence of Femtosecond Laser Radiation**

**Levan Ichkitidze<sup>1,2\*</sup>, Alexander Markov<sup>2</sup>, Mikhail Savelev<sup>1,2</sup>,  
Alexander Gerasimenko<sup>1,2</sup>, Pavel Vasilevsky<sup>1</sup>, Eugenia Davydova<sup>1</sup>,  
Elizaveta Smirnova<sup>1</sup>, Dmitry Telyshev<sup>1,2</sup>, Sergei Selishchev<sup>1</sup>**

*<sup>1</sup>Institute of Biomedical Systems of National Research University of Electronic  
Technology "MIET", Moscow, 124498, Russia*

*<sup>2</sup>Institute for Bionic Technologies and Engineering of I.M. Sechenov First Moscow  
State Medical University, Moscow, 119991, Russia*

\*[ichkitidze@bms.zone](mailto:ichkitidze@bms.zone)

A composite nanomaterial with carbon nanotubes actively absorbs radiation from a femtosecond laser (FSL), which leads to a change in the characteristics of the material. In this work, we investigate the effect of PSL radiation on aqueous dispersions of a biological composite nanomaterial in the composition of bovine serum albumin (BSA) and single-wall carbon nanotubes (SWCNTs) at different concentrations of the components. The investigated biological nanomaterial (bionanomaterial) included: BSA from AMFESCO (USA) and SWCNT of "Carbon Chg Ltd" from Chernogolovka (Russia). SWCNTs were carboxylated in the form of an aqueous paste (2.5 wt% SWCNTs) and had a diameter of ~ 1.5 nm, a length of  $\geq 1 \mu\text{m}$ . For individual SWCNTs, a specific surface area of ~ 1300 m<sup>2</sup>/g was achieved, however, they strongly aggregated and their specific surface area decreased to 200 – 400 m<sup>2</sup>/g. After aggregation, the nanotube diameter was  $\geq 3 - 4 \text{ nm}$ , the length was  $\gg 1 \mu\text{m}$ . Layers of composite bionanomaterial BSA/SWCNT were prepared according to the route map: (i) instrumental dispersion of an aqueous dispersion of SWCNT and dispersion in the composition of BSA and SWCNT; (ii) application of a dispersion of SWCNT, BSA/SWCNT on substrates; (iii) irradiation of FSL layers in a liquid state; (iv) drying samples; (v) microscopic examinations and electrical measurements. Covering glass plates with a size of 24 ×

24 × 0.15 mm served as substrates. The dispersions contained: BSA/SWCNT – 10 wt.% BSA and (0.001 – 0.1) wt.% SWCNT, the rest was distilled water; SWCNT – (0.001 – 0.1) wt.%, the rest was distilled water. On the back side of the substrate, a marker was applied in the form of two parallel lines with a distance of ~ 1 mm between them. A laser beam with a spot diameter of ~ 1 mm was focused at this point. After the application of the aqueous dispersion onto the substrates using PSL radiation, the liquid evaporated, resulting in the formation of a continuous layer 0.1 – 10 μm thick. The radiation was generated by a Chameleon-ultra FSL (lasing wavelength 810 nm, power ~ 500 mW/mm<sup>2</sup>, pulse duration 140 fs, pulse intensity ~ 5 kW/mm<sup>2</sup>). The resulting layers were examined on a ZEISS LSM 880 confocal scanning microscope; their electrical resistance was measured with an Agilent 34401A device. It was found that in aqueous dispersions of a biological composite nanomaterial (BSA/SWCNT), PSL radiation orders nanotubes, their sheeds and aggregates – they are arranged in the form of a linear chain. In this arrangement, the nanotubes remain in the dried layers. Moreover, this ordering is observed at low concentrations of ≤ 0.01 wt. % SWCNTs and an intensity of ~ 5 kW/mm<sup>2</sup> in a laser pulse. This value is many times less than the threshold ≥ 1 MW/mm<sup>2</sup>, at which ablation occurs, SWCNT ordering, and an increase in resistance by several orders of magnitude in materials in the solid state [1]. In our case, the ablation of nanotubes does not occur. Nanotubes are ordered in an aqueous dispersion at low values of the intensity of PSL radiation, and the resistance of the films decreases several times. The observed effect is assumed to be due to the action of PSL radiation on catalytic ferromagnetic nanoparticles located at the ends of the SWCNT ends. The proposed approach to ordering nanotubes will be in demand in the development of various types of sensors, for example, strain sensors, with the possibility of using them in medical applications.

#### **Acknowledgements**

The authors are grateful to N. S. Struchkov and O. A. Burdukova for their help in the experiment. This work was financed by the Ministry of Science and Higher Education of the Russian Federation within the framework of state support for the creation and development of World-Class Research Centers "Digital biodesign and personalized healthcare" No. 075-15-2020-926.

#### **Reference**

[1] Spellauge M., Loghin F-C., Sotrop J., et al // *Carbon, N.-Y.* **138**, 234 – 242, 2018.

## **Influence of Fractality of Normal Clusters on the Resistivity of a Ceramic Superconductor**

**Levan Ichkitidze<sup>1,2\*</sup>, Mikhail Belodedov<sup>3</sup>, Sergei Selishchev<sup>1</sup>, Dmitry Telyshev<sup>1,2</sup>**

<sup>1</sup>*Institute of Biomedical Systems of National Research University of Electronic Technology  
"MIET", Moscow, 124498, Russia*

<sup>2</sup>*Institute for Bionic Technologies and Engineering of I.M. Sechenov First Moscow State Medical  
University, Moscow, 119991, Russia*

<sup>3</sup>*Bauman Moscow State Technical University, 105005, Russia*

\*[ichkitidze@bms.zone](mailto:ichkitidze@bms.zone)

As usual, HTSC ceramic materials have a granular structure, and numerous inhomogeneities can exist in them, in particular, at the grain boundaries in the form of Josephson junctions and within



the grains themselves in the form of various inclusions of non-superconducting or low-temperature superconducting phases. The pores in the space between the granules can join, i.e. they can become open pores and form channels, so-called normal clusters. Some of them are considered to be infinite normal clusters (INCs), when such a cluster extends from one edge (surface) of the sample to its opposite edge (surface). INCs can coexist together with infinite superconducting clusters (ISCs), which can form interconnected HTSC granules. ISCs form a percolation cluster of current flow lines from one surface of the sample to another. In a ceramic HTSC, numerous INCs can have a fractal distribution, which in a certain way can affect the resistive properties of the material. In this work, the fractal dimension of INC from open pores is determined and its effect on the resistive properties of samples of ceramic HTSC material of composition Bi-2223 is studied. Samples of two forms were investigated, namely a massive sample and a sample in the form of a thick film. Bulky samples were cut from compressed Bi-2223 pellets, while thick-film samples were formed by applying a Bi-2223 ceramic powder onto MgO substrates. Samples of both shapes were heat treated at 900 °C and had the following dimensions. Massive: length (distance between potential contacts)  $l \approx 6.0$  mm, width  $w \approx 1.5$  mm, thickness  $t \approx 0.5$  mm; thick film:  $l \approx 6.0$  mm,  $w \approx 1.5$  mm and  $t \approx 0.5$  mm, respectively. The processing of electron microscopic images of the samples was carried out for structures of granules and open pores forming INC. The fractal dimension of INC was determined for all samples. It was found that the fractal dimension of INC is higher in thick-film than in bulk samples. It was found that the higher the value of the INC fractal dimension, the wider the range of sample resistivity. The obtained relationship between the fractal dimension and the resistivity of the sample is qualitatively well described by the model proposed by Yu. I. Kuzmin [1]. The high value of the fractal dimension also correlates well with the high value of the volt-tesla magnetosensitivity of the image. For a layer of ceramic HTSC material of the Bi-2223 system, the magnetosensitivity per unit length of the layer was of the order of  $\sim 1$  V/T in the region of  $\leq 0.5$  mT, which is a high indicator. The prospects for using an increased fractal dimension in samples of a HTSC ceramic material and the possibility of creating on this basis magnetoresistive sensors of an ultra-weak magnetic field with a resolution of  $\leq 10$  pT are considered.

#### ***Acknowledgement***

This work was financed by the Ministry of Science and Higher Education of the Russian Federation within the framework of state support for the creation and development of World-Class Research Centers "Digital biodesign and personalized healthcare" No. 075-15-2020-926.

#### ***Reference***

[1] Yu. I. Kuzmin // *Technical Physics Letters*, **30**(6), 457 – 460, 2004.

# The Effect of Heat-conducting Coating on the Propagation of the Waves Excited by Heat in the Thermoelastic Bodies

G. Yu. Levi\*, I. B. Mikhailova

*Southern Scientific Center of the Russian Academy of Sciences, Rostov-on-Don, Russia*

\*[galias@yandex.ru](mailto:galias@yandex.ru)

The dynamic coupled contact problems on the harmonic vibration excitation on the thermoelastic body surface are studied. The body is the thermoelastic layer coupled with the thermoelastic half-space and homogeneous thermoelastic half-space. Oscillations are caused by an oscillating temperature  $\tau_0 e^{-i\omega t}$  distributed in a certain area on the body surface. The surfaces of the half-spaces are supposed to be free of mechanical stresses, outside the load area and thermally insulated. The half-space parameters are denoted as  $n=0$ , and  $n=1$  relates to layer parameters. In a structurally heterogeneous half-space at the interface, we assumed the conditions of thermal insulation and rigid adhesion. The contact problem is described as

(i) the linearized equations of motion of a thermoelastic medium:

$$\nabla \cdot \Theta^{(n)} = \rho^{(n)} \frac{\partial^2 \mathbf{u}^{(n)}}{\partial t^2}, \theta_j^{(n)} = c_{ijkl}^{(n)} u_{k,l}^{(n)} - \beta_{ij}^{(n)} u_4^{(n)}, \quad (1)$$

(ii) linearized heat equation:

$$K_{ik}^{(n)} u_{4,ik}^{(n)} = c_\varepsilon^{(n)} \rho^{(n)} \frac{\partial u_4^{(n)}}{\partial t} + \theta_0^{(n)} \beta_{ik}^{(n)} \frac{\partial u_{k,i}^{(n)}}{\partial t}, \quad n=0,1, i,j,k,l=1 \div 3, \quad (2)$$

and corresponding boundary conditions.

Oscillations are assumed to be steady, occurring according to the harmonic law, so all functions are represented as  $f = f_0 e^{-i\omega t}$ . Further exponents can be omitted. Boundary-value problems with mixed boundary conditions on the surface by using operational calculus methods are reduced to an integral equation of the first kind with respect to the unknown function of the heat flux distribution in the contact zone. By using the boundary element method, its solution is constructed. A solution to the contact problem is obtained, namely the distributions of displacements and temperatures in a layered body. The effect of the substrate material on the distribution of the displacement vector components excited in a thermoelastic body by the surface temperature is studied. The possibility of localizing near the soft coat deformations arising under the temperature action on the surface of a thermoelastic body was revealed.

## **Acknowledgements**

The work was performed as part of the implementation of the state assignment of the Southern Scientific Center of the Russian Academy of Sciences, project No. 01201354242 and with partial financial support from the Russian Foundation for Basic Research, grants Nos. 19-08-01051, 19-01-00719.

## Interfacial Reactions and Functional Properties of Magnetolectric Composites of Lead-free Piezoelectrics and Yttrium Iron Garnet

I. V. Lisnevskaya\*, I. A. Aleksandrova

*Faculty of Chemistry, Southern Federal University,  
7, Zorge Str., Rostov-on-Don, 344090, Russia*

\*[liv@sfedu.ru](mailto:liv@sfedu.ru)

A wide range of magnetolectric composites has been prepared:  $(100 - x)$  wt.% FE +  $x$  wt.% YIG ( $x = 30 - 70$  in steps of 10 wt.%), where YIG is yttrium iron garnet and FE is a lead-free ferroelectric material reported in the literature, namely, lithium sodium potassium niobate ( $[\text{Li}_{0.06}(\text{Na}_{0.52}\text{K}_{0.48})]_{1.04}\text{NbO}_3$ , KLNN), modified sodium bismuth titanate ([96 mol.%  $\text{Bi}_{0.5}(\text{Na}_{0.84}\text{K}_{0.16})_{0.5}\text{TiO}_3 + 4$  mol.%  $\text{SrTiO}_3 + 0.2$  wt.%  $\text{La}_2\text{O}_3$ ], BNT), or barium calcium zirconate titanate ( $\text{Ba}_{0.85}\text{Ca}_{0.15}\text{Ti}_{0.9}\text{Zr}_{0.1}\text{O}_3$ , BCZT). The interfacial reactions and dielectric, piezoelectric, magnetic and magnetolectric behaviors of the composites have been studied. The high-temperature calcination was found to yield the fergusonite-type impurity phase  $\text{YNbO}_4$  in KLNN-containing composites and the pyrochlore-like phase  $\text{Y}_2\text{Ti}_2\text{O}_7$  in BNT-containing ones. The BCZT-containing samples remain only phase-pure materials after heat treatment. As a result, among the materials studied, the samples of  $(100 - x)$  wt.% BCZT +  $x$  wt.% YIG show the best magnetolectric coupling coefficient  $\Delta E/\Delta H$  that reaches  $\sim 5$  mV/(cm-Oe) with  $x = 40$ . Despite showing significant piezoelectric response, the KLNN-containing ceramics exhibit  $\Delta E/\Delta H$  of 1.2 mV/(cm-Oe) or less. The composites containing BNT show weak piezoelectric and almost zero ME response ( $\Delta E/\Delta H$  does not exceed 0.2 mV/(cm-Oe)) due to the decomposition of ferroelectric phase caused by high-temperature interfacial reactions. The BCZT-containing composites appeared to be magnetically softer than KLNN-containing materials and magnetically harder than BNT-containing ones.

### Reference

[1] Lisnevskaya I. V., Aleksandrova I. A. // *Applied Physics A*, **126**(6), 406, 2020.

## **A Comparison Study by Simulation/Experiment to Verify the Effect of Predicted Forming Limit Diagram Based on Graphical Method at Elevated Temperature for SPCC Sheet Material**

**Luyen The-Thanh<sup>1</sup>, Mac Thi-Bich<sup>1</sup>, Banh Tien-Long<sup>1,2</sup> Nguyen Duc-Toan<sup>2\*</sup>**

*<sup>1</sup>Faculty of Mechanical Engineering, Hung yen University of Technology and Education, Hung yen, 100000, Vietnam*

*<sup>2</sup>School of Mechanical Engineering, Hanoi University of Science and Technology, 1A-Dai Co Viet Street, Hai Ba Trung District, Hanoi City, 100000, Vietnam*

*\*[toan.nguyenduc@hust.edu.vn](mailto:toan.nguyenduc@hust.edu.vn)*

Sheet Metal forming processing based on the deformation of materials has taken an important position with an increasing proportion in mechanical manufacturing and metallurgy. In this study, in order to predict more accuracy forming limit curve (FLC) at elevated temperature, the uniaxial tensile test of SPCC sheet material at 150 °C was first performed to obtain the stress-strain curve at 150 °C. The graphical method based on the Modified Maximum Force Criterion (MMFC) was then applied to estimate the FLCs according to various hardening laws of Swift, Voce, and Kim-Tuan at 150 °C elevated temperature. After that, the obtained FLCs data were used for numerical simulation using the finite element method (FEM) to predict the fracture heights of the SPCC sheet material cup by deep-drawing process and compare with corresponding experimental results. Comparison results between simulation and experiments show that Swift's hardening model shows good predictions for fracture height compared to experimental data at elevated temperature of 150 °C, followed by Kim-Tuan's and Voce's hardening model, respectively. So that Swift's hardening model should be suggested to estimate forming limit curve (FLC) at elevated temperature for SPCC sheet material.

## **Improving the Functional Characteristics of Biocompatible Coatings of Bone Implants due to Modification of the Initial Powders**

**A. V. Lyasnikova<sup>1\*</sup>, I. P. Melnikova<sup>2</sup>, A. L. Nikolaev<sup>1</sup>**

*<sup>1</sup>Don State Technical University, Rostov-on-Don, Russia*

*<sup>2</sup>Gagarin State Technical University, Saratov, Russia*

*\*[lyasnikovaav@mail.ru](mailto:lyasnikovaav@mail.ru)*

It is well known that by controlling the size and shape of the powders used in plasma spraying, it is possible to impart completely new functional characteristics to the sprayed materials, which are sharply different from those of bulk materials. Thus, the purpose of our study was to modernize the structure and properties of biocompatible coatings by modifying the particles of the original powder by fixing small particles on large granules. Using this method, it was possible to achieve an increase

in the uniformity, strength, open porosity of the coating, and an increase in the contact area of the surfaces of the bone tissue and the implant. It was also possible to achieve an increase in the bioactivity of the implant surface. The choice of the particle size for plasma spraying is explained by the need to obtain a porous structure of the coating with a pore size of 100-200  $\mu\text{m}$  and a maximum adhesion of 25-30 MPa. It is known that the pore size in a porous framework is related to the size of its constituent particles. In the technology developed and used by us for plasma spraying of ceramic coatings on intraosseous titanium implants with a porous titanium sublayer, a powder with a particle size of 40 to 100  $\mu\text{m}$  is used. Thus, we have proposed a method for nanostructuring biocompatible coatings of intraosseous implants while maintaining the required porosity and surface morphology. The proposed method consists in creating combined particles of the original powder for spraying by fixing small particles with a size of less than 40 microns on large particles with a size of 40-100 microns. In the process of plasma spraying in a high-temperature jet, heat removal from a small particle to a large one will keep some of the small fixed particles from melting. The combined particle will disintegrate upon impact on the substrate. This process will be accompanied by the separation of a small particle from a large one. In this case, it can be assumed that a small particle, having the kinetic energy of a large particle, will break into nanometer-sized particles. In this work, we investigated the effect of changes in the particle size distribution of powders of biocompatible materials (hydroxyapatite and aluminum oxide) on the properties of pressed and plasma-sprayed samples made from them. The possibility of hardening plasma-sprayed coatings based on hydroxyapatite (Young's modulus  $E = 50$  GPa) with  $\text{Al}_2\text{O}_3$  particles (Young's modulus  $E = 380$  GPa) was also investigated.

#### **Acknowledgment**

A. L. Nikolaev acknowledge support from the Russian Foundation for Basic Research within grant No. 20-07-00637 A.

## **Probability-network Modeling of Nanocomposite Porous Coatings Structure**

**A. V. Lyasnikova<sup>1\*</sup>, V.M. Taran<sup>2</sup>, M.V. Dodonov<sup>1</sup>**

<sup>1</sup>*Don State Technical University, Rostov-on-Don, Russia*

<sup>2</sup>*Gagarin State Technical University, Saratov, Russia*

[\\*lyasnikovaav@mail.ru](mailto:lyasnikovaav@mail.ru)

Porous coatings are used in various fields of technology and medicine as carriers of liquid substances. The main structural formation of porous coatings is a framework of powder particles, which forms pores (voids) due to loose packing of powder particles. The traditional methods for obtaining porous coatings are plasma spraying and powder metallurgy. These technological methods were developed to obtain heat- and corrosion-resistant coatings with the lowest possible porosity, since the porosity significantly worsened the functionality of the coating. Liquid substances can be introduced into porous coatings, for example, lubricants, electrolytes in electrochemical electrodes, drugs, etc. It is obvious that the amount of liquid substance in the pores and the intensity of its entry into the working contact zone should be controlled processes. In this regard, the problem of forming coatings with a predicted geometry of porous formations is of great

practical interest. To solve this problem, a model was considered that describes the porosity of nanocomposite coatings. The model is built using the method of probability-network modeling and is based on the concept of tortuosity of pore channels. In most experiments, when comparing statistical and experimental data, an insignificant difference was found.

## **Pantograph Lever Structure MEMS Accelerometer with High Aspect Ratio Torsion Suspension**

**I.E. Lysenko, D.V. Naumenko\*, O.A. Ezhova**

*Southern Federal University, Taganrog, Russia*

[\\*danil.naumenko@gmail.com](mailto:danil.naumenko@gmail.com)

The development of MEMS accelerometers is an important technical task to solve the problem of measuring linear acceleration, controlling speed, vibration and the position of an object in space. Such tasks arise in many areas, for example military consumer electronics, transportation, robotics, military equipment. Design of new MEMS inertial sensors is always associated with the development of manufacturing technologies. So, increase in the thickness of the instrument layer of inertial sensors manufactured on SOI structures using the technology of deep reactive-ion etching (DRIE) allows one to create designs with an instrument thickness of more than 100  $\mu\text{m}$  and an aspect ratio of up to 1:50. Such designs can increase the inertial mass without increasing the area of the sensitive element, so that we can reduce noise, increase sensitivity and reduce the cost of the MEMS sensors. Torsion suspensions are widely used in MEMS out-of-plane devices as like micromirrors, accelerometers, energy harvesters, switches. Thus, the report describes the problem of using high-aspect torsion suspension for acceleration measurement. A mathematical model based on the Lagrange equation of the 2nd kind is developed, which allows calculating the linear movement of the inertial mass and elastic suspensions of the structure. Software tools have been developed to investigate the movement of the sensing element under the influence of external accelerations, to calculate the stiffness of the developed design. Parametrizable geometric and finite element models of the proposed sensor are developed, which allow us to carry out numerical modeling in the ANSYS software package. The amplitude of displacements was obtained as a result of static finite element analysis and is proportional to the magnitude of the effective acceleration. At 1g-acceleration, we obtained 4.5 nm along z-axis, and 2.2 nm along x- and y-axis. At 10g-acceleration, we obtained 46 nm along z-axis, and 23 nm along x- and y-axis. The design of an integrated micromechanical accelerometer is proposed. This mechanism can be customized to different sensitivity, deviation and range. Customization is achieved by changing the length of the levers thereby changing the torque and deflection, as well as the rigidity of the flexible beams to adjust the range of measurement of acceleration. This makes it possible to manufacture sensors with high sensitivity or high acceleration on a single silicon crystal.

### ***Acknowledgement***

This work was supported by RFBR research project No. 19-37-90136 “Development of the fundamental foundations for the construction of high-aspect torsion suspensions for inertial MEMS sensors”.

# The Method of Definition the Electrophysical Parameters of Spiral Inclusions in Chiral Metamaterials

I.V. Malyshev\*, N.V. Parshina

*Southern Federal University, Taganrog, Russia*

[\\*im1960@mail.ru](mailto:*im1960@mail.ru)

It is known that metal spiral structures [1], modern strip multilayer metal-semiconductor hybrid InGaAs/GaAs/Ti/Al [2] or other spiral inclusions that are part of the dielectric resin hard alloy are used to produce artificial chiral metamaterials. (The concentration of such elements usually reaches about 500 units/mm<sup>2</sup> [2]). In this case, the electric and magnetic field densities included in the Maxwell equations ( $\vec{D}$  и  $\vec{B}$ ) will have chiral-dependent corrections for the isotropic Pasteur medium [1]:  $\vec{D} = \epsilon \vec{E} - jk\sqrt{\mu_0 \epsilon_0} \vec{H}$ ,  $\vec{B} = \mu \vec{H} + jk\sqrt{\mu_0 \epsilon_0} \vec{E}$ , where  $\vec{E}$  and  $\vec{H}$  are the intensities of electric and magnetic fields;  $\epsilon$ ,  $\epsilon_0$ ,  $\mu$ ,  $\mu_0$  are the dielectric and magnetic permeabilities of the medium and vacuum, respectively;  $k$  is the dimensionless chirality coefficient (it is often assumed that  $k \leq n \sqrt{\frac{\mu \epsilon}{\mu_0 \epsilon_0}}$ ,  $n$  is the reflection coefficient of the dielectric medium). The main parameters of the spiral are the area of its diameter  $S$  and length  $l$ , which is usually assumed to be equal to half the wavelength of the basic frequency  $l = \lambda / 2$ . It was established [1], that the polarization moments  $p_e$  and  $p_m$  of these spirals will be determined along unit vectors  $u$ , and, as planar parameters of the space of the medium, are find as  $p_e = \alpha_{ee} uuE + \alpha_{em} uuH$ ,  $p_m = \alpha_{mm} uuH + \alpha_{me} uuE$ . The polarizability  $\alpha_{ij}$  of the spiral determines the medium chiral properties and is expressed in terms of distributed parameters: inductance  $L$  of the spiral loops, capacitance  $C$  of the wire (or strip) and intrinsic resistance of the spiral radiator  $R$  [1]. For a considered case, it is known:  $\alpha_{ee} = \frac{cl^2}{1-\omega^2 LC + j\omega RC}$ ,  $\alpha_{mm} = \frac{\mu^2 \omega^2 CS^2}{1-\omega^2 LC + j\omega RC}$ ,  $\alpha_{em} = -\alpha_{me} = \frac{j\omega \mu CS l}{1-\omega^2 LC + j\omega RC}$ , where  $\mu$  is the dielectric constant of the own medium in which the spirals are located. In this report, we will determine  $R$ ,  $L$ ,  $C$  being the parameters for a spiral with dimensions  $l$  and  $S$  included in relations for the polarizability parameters of a spiral  $\alpha_{ij}$ , will ultimately take this into account in the electrodynamic properties of metamaterials. By using the substitution  $x + jy = (1 - \omega^2 LC) + j\omega RC$ , we rewrite these relations in the form:  $\frac{x + jy}{c} = \frac{l^2}{\alpha_{ee}}$ ,  $\frac{x + jy}{c} = \frac{S^2 \mu^2 \omega^2}{\alpha_{mm}}$ ,  $\frac{x + jy}{c} = j \frac{\mu \omega l S}{\alpha_{em}}$ , from which it follows:  $\frac{l^2}{\alpha_{ee}} = \frac{S^2 \mu^2 \omega^2}{\alpha_{mm}}$ . After corresponding permutations, we obtain:  $\frac{l}{S} = \mu \omega \sqrt{\alpha_{ee} / \alpha_{mm}}$ . Carrying out the separation of relations into the real and imaginary parts and the transformations leading them to 0, we finally have:  $R = \frac{\mu l S}{1 - \alpha_{em}}$ ,  $l = \omega \sqrt{\alpha_{ee}}$ ,  $S = \sqrt{\alpha_{mm} / \mu}$ ;  $L = (\frac{1}{1 + \omega^2} [\frac{\alpha_{mm} \mu^2 \omega^2 S^2}{\alpha_{em} - \alpha_{mm} \omega^2} + \frac{\alpha_{mm} \mu^2 \omega^2 S^2 - \alpha_{ee} l^2}{\alpha_{mm} - \alpha_{ee}}])$ ;  $C = \frac{\alpha_{mm} - \alpha_{ee}}{L(\alpha_{mm} \omega^2 - \alpha_{ee} \omega^2) + (\alpha_{mm} \mu^2 \omega^2 S^2 - \alpha_{ee} l^2)}$ . These relations determine the main electrophysical parameters of left- and right-twisted species of spirals, which are included as chiral-depending elements in the metamaterial composition.

## References

- [1] A. Sihvola, I. Lindell, M. Osanen, F. Hujanen. // *Electronic Letters*. 6(2), 378-383, 1990.  
[2] E.V. Naumova, V.Ya. Prince, S.V. Golod et al. // *Avtometriya*. 45(4), 12-22, 2009.

## Asymptotics of Eigenvalues of Large Symmetric Toeplitz Matrices with Smooth Simple-loop Symbols

I. S. Malysheva

*I. I. Vorovich Institute of Mathematics, Mechanics and Computer Sciences, Southern Federal University, Rostov-on-Don, Russia*

[malir2004@list.ru](mailto:malir2004@list.ru)

This report is devoted to the asymptotic behavior of all eigenvalues of symmetric (in general non-Hermitian) Toeplitz matrices with moderately smooth symbols which trace out a simple loop on the complex plane line as the dimension of the matrices increases to infinity. The main result describes the asymptotic structure of all eigenvalues. The constructed expansion is uniform with respect to the number of eigenvalues.

### Acknowledgement

The results of this research were financially supported by the Southern Federal University, grant No. VnGr-07/2020-04-IM (Ministry of Science and Higher Education of the Russian Federation).

## Dynamic Boundary Element Analysis of Three-dimensional Multiply Connected Linear Piezoelectric Solids

I.P. Markov<sup>\*1</sup>, L.A. Igumnov<sup>1,2</sup>, E.V. Boev<sup>1</sup>

<sup>1</sup>*Research Institute for Mechanics, National Research Lobachevsky State University of Nizhny Novgorod, Nizhny Novgorod, Russia*

<sup>2</sup>*Research and Education Mathematical Center "Mathematics for Future Technologies", Nizhny Novgorod, Russia*

\*[markov@mech.unn.ru](mailto:markov@mech.unn.ru)

Piezoelectric materials with coupled electroelastic fields are extensively used in many practical fields. Numerical modeling of transient dynamic responses of piezoelectric solids is an essential part of their effective technical utilization. In this report, a direct boundary element formulation in Laplace domain is used to model the dynamic behavior of the three-dimensional linear piezoelectric multiply connected solids. Contracted notation is used to combine electric and mechanical variables and quantities into generalized vectors and tensors. Boundary integral equations (BIEs) for generalized displacements are employed. These BIEs are regularized with the



singular piezoelectric fundamental solutions and thus do not contain strongly singular integrals. Dynamic piezoelectric displacement fundamental solutions and their derivatives are represented as integrals over a half of a unit sphere. Spatial discretization of the BIEs is performed using a mixed boundary elements and nodal collocation procedure. In order to obtain time-domain solutions, the classic Durbin's method is employed for numerical inversion of Laplace transform. For a numerical example, a prismatic multiply connected piezoelectric solid subjected to a mixed electroelastic loading is considered. Results of boundary element analysis are compared with finite element solutions.

### **Acknowledgement**

The work was carried out with the financial support of the Ministry of Science and Higher Education of the Russian Federation (task 0729-2020-0054).

## **An Algorithm for Iterative Selection of Complex Frequencies Applied to a One-dimensional Dynamic Poroelastic Problem**

**I.P. Markov\*, A.N. Petrov, A.V. Boev**

*Research Institute for Mechanics, National Research Lobachevsky State University of Nizhny Novgorod*

\*[markov@mech.unn.ru](mailto:markov@mech.unn.ru)

Studying the dynamic processes in poroelastic media and structural elements is particularly interesting and attracts special attention. Even analytical or semi-analytical poroelastic solutions often time exits only in frequency or Laplace domains. Studying effects of wave propagation in the time domain in such cases is in general only possible with subsequent application of one or another method for numerical inverse of Laplace or Fourier transform.

The Laplace transform of a function  $f(t): \mathbb{R} \rightarrow \mathbb{R}$ ,  $f(t) = 0$  for  $t < 0$ , is defined as

$$F(s) = L\{f(t)\} = \int_0^{+\infty} e^{-st} f(t) dt, \quad s = \alpha + i\omega.$$

We consider a proper rational approximation for  $F(s)$ :

$$F(s) \approx \frac{b_{N-1}s^M + b_{N-2}s^{M-1} + \dots + b_1s + b_0}{a_Ns^N + a_{N-1}s^{N-1} + \dots + a_1s + a_0} = \frac{P(s)}{Q(s)}, \quad M < N.$$

Then by utilizing the vector fitting by pole relocation method [1], we calculate a partial fraction decomposition of  $F(s)$  as

$$F(s) \approx \frac{P(s)}{Q(s)} = \sum_{k=1}^N \frac{r_k}{s - p_k}.$$

We propose an algorithm for obtaining partial fraction decompositions of  $F(s)$  with increasing order of approximation  $N$  by iterative adaptive selection of additional complex frequencies  $s$ . The algorithm is tested on a model problem of wave propagation in one-dimensional poroelastic column.

### ***Acknowledgement***

The reported study was funded by RFBR, project No. 20-08-00451.

### ***Reference***

[1] Gustavsen B., Semlyen A. // *IEEE Transactions on Power Delivery*, **14**(3), 1052-1059, 1999.

## **Microstructure and Tensile Stress Analysis on T6 Heat Treated Aluminum-Bottom Ash Coal Composite Made by Squeeze Casting**

**Maula Nafi\*, Harjo Seputro**

*Department of Mechanical Engineering, University of 17 Agustus 1945 Surabaya*

\*[maula.nafi@untag-sby.ac.id](mailto:maula.nafi@untag-sby.ac.id)

Squeeze casting is a casting method by forging molten metal in a mold with high pressure. This study analyzes the effect of variations in pouring time and duration of pressing on squeeze casting to the tensile stress and microstructure of aluminum-bottom ash coal composite. The pouring time used in this study is equal to 5 seconds, 10 seconds and 15 seconds. The duration of suppression is equal to 60 seconds, 90 seconds, and 120 seconds with a 100 kgf suppressor load. The percentage weight of the composite is 15 kgf with 96.5% aluminum alloy, 2.5% bottom ash coal, and 1% magnesium. This study obtained the highest tensile test results on specimens with a variation of 15 seconds pouring time and 120 seconds duration of suppression after the T6 heat treatment process. With the results of 167.2 N/mm<sup>2</sup>, the shape of the microstructure is rather small and dense which was analyzed by Scanning Electron Microscope. This means that the pouring time and the duration of the pressure on the squeeze casting of aluminum-bottom ash coal composite can improve its mechanical properties.

## **DFT Study of Strengths of TiAlN Coating on Iron Surface**

**Yu. F. Migal**

*Southern Scientific Center of the Russian Academy of Sciences, Rostov-on-Don, Russia*

[ymigal@mail.ru](mailto:ymigal@mail.ru)

In many areas of technology, there is currently a growing interest in various ways to increase the strength of the working surfaces of parts and assemblies. One of these ways is to provide hard coatings on work surfaces that increase their strength. Numerous papers (see, for example, [1, 2]) are devoted to the study of coatings of TiAlN compounds on iron. In this report, we consider a simple numerical model consisting of six atomic layers that simulates the TiAlN coating on iron. We use this model and the DFT-based ADF package [3] to consider the following issues:

(i) what is the mutual arrangement of Ti, Al, N atoms on the iron surface to provide the greatest strength of the surface layer under mechanical load?

(ii) how does a dense TiAlN coating affect the strength of the iron layer weakened by defects?

When constructing the model, it turns out to be important that N atoms have significantly smaller sizes than Ti and Al atoms. Due to this fact, by using these elements, we can create a system with a denser packaging than in iron itself. Along with the geometric factor, the strength of chemical binding of atoms of these elements is also important. Taking these two factors into account we can develop coatings that are more durable than traditional steels. The ADF package allows us to search quickly for optimal coating options. Fig. 1 shows the structure of the model TiAlN coating on a Fe surface, weakened by atomic defects. The presence of defects is simulated by the appearance of impurities (in this case, silicon atoms) in the metal. The destruction of this surface under a mechanical load perpendicular to the surface is shown in Fig. 1 on the right side. Calculations have shown that the tensile strength of such a system is slightly less than the strength of a defect-free system, but significantly higher than the strength of a defective system without a coating.

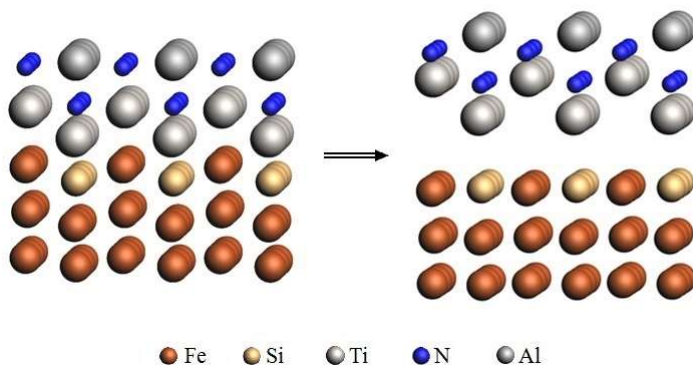


Fig. 1. TiAlN coating on the iron surface and destruction of the system under vertical load

### References

- [1] *Surface and Coating Technology* (Special Issue), **257**, 1 – 362, 2014.
- [2] R. E. Contreras, R. M. Gomez, et al. // *Surface and Coating Technology*, **378**, 12494, 2019.
- [3] G. te Velde, F.M. Bickelhaupt, et al. // *J. Comp. Chem.*, **22**(9), 931 – 967, 2001.

# Temperature Measurement of Turbulent Flame Using CT-TDLAS (Computed Tomography-Tunable Diode Laser Absorption Spectroscopy)

Min-Gyu Jeon<sup>1\*</sup>, Jeong-Woong Hong<sup>2</sup>, Deog-Hee Doh<sup>1</sup>, Yoshihiro Deguchi<sup>3</sup>

<sup>1</sup>*Division of Mechanical Engineering, Korea Maritime and Ocean University,  
Busan 49112, Republic of Korea*

<sup>2</sup>*Division of Refrigeration & Air-conditioning Engineering, Korea Maritime and Ocean  
University, Busan 49112, Republic of Korea*

<sup>3</sup>*Graduate School of Advanced Technology and Science, Tokushima University,  
Tokushima 770-8501, Japan*

\*[jeon85@kmou.ac.kr](mailto:jeon85@kmou.ac.kr)

In order to satisfy the requirements of high-quality and high-performance optimal material manufacturing process, it is essential to control the gas system of the manufacturing process. It is necessary to improve the quality of the product by adjusting various gases in the manufacturing process. The TDLAS (Tunable laser absorption spectroscopy) technique can be measured by the temperature and concentration of target gas simultaneously. Among the more advanced technologies, CT-TDLAS (Computed tomography-tunable diode laser absorption spectroscopy) is the most crucial technique for measuring temperature and concentration distributions across two-dimensional planes. This study suggests a two-dimensional useful measurement of irregular flow or exhaust gases. Furthermore, CT-TDLAS has been adopted to measure temperature distribution at a cross-section of the Propane-Air premixed flame. The equivalence ratio of fuel can control this system. The burner system consists of two sections (main flame, sub flame) for a turbulent flame. In the CT-TDLAS technique, it is essential to set the wavelength for target gases. Therefore, we compared two laser system types using a mixed laser (1388 nm, 1343 nm) and 1395 nm laser. The temperatures, obtained by using the CT-TDLAS technique, were relatively evaluated with those obtained by thermocouples.

## ***Acknowledgments***

This research was supported by Basic Science Research Program through the National Research Foundation of Korea (NRF) funded by the Ministry of Education (No.2020R111A1A01052771).

## Preparation of Zinc Silicate Doped with Manganese Phosphor by Hydrothermal Method

Min Yen Yeh\*, Sheng Min Huang, Shun-Hsyung Chang  
Jenny Chih-Yu Lee, Chih-Feng Yen, Chyi-Da Yang

*Department of Microelectronics Engineering, National Kaohsiung University of Science and Technology, No.142, Haijhuang Rd., Nanzih Dist., Kaohsiung, 81157, Taiwan*

\*[minyen@nkust.edu.tw](mailto:minyen@nkust.edu.tw)

Zinc silicate doped with manganese ( $\text{Zn}_2\text{SiO}_4:\text{Mn}^{2+}$ ) was synthesized by hydrothermal method. Zinc nitrate  $\text{Zn}(\text{NO}_3)_2$  and sodium metasilicate ( $\text{Na}_2\text{SiO}_3$ ) were used as raw materials. Manganese nitrate  $\text{Mn}(\text{NO}_3)_2$  was used as active dopant. NaOH was used to adjust PH value of solution. The effects of  $\text{Mn}(\text{NO}_3)_2$  doping ratio and NaOH concentration on the synthesis powder were characterized. The structure and fluorescent properties of the samples were analyzed by XRD, SEM and PL. From XRD analysis, the hydrothermally synthesized powder (with particle size of 20 – 30 nm) for 12 hours and 24 hours reveal good  $\text{Zn}_2\text{SiO}_4$  crystalline structure with or without the addition of NaOH. From SEM, it can be observed that the  $\text{Zn}_2\text{SiO}_4$  powder gradually agglomerates into rods as the NaOH concentration increases. The obtained  $\text{Zn}_2\text{SiO}_4:\text{Mn}$  phosphor shows green light fluorescent luminescence at the wavelength of about 545 nm under 270 nm UV-LED excitation. The best fluorescent  $\text{Zn}_2\text{SiO}_4:\text{Mn}$  was obtained using 0.14 mmol  $\text{Mn}(\text{NO}_3)_2$  and 3M NaOH for 12hr synthesis. Figure 1 shows the XRD patterns of phosphor powders prepared by hydrothermal synthesis for 12 hours reacted with different volume of NaOH. It can be observed that all of the samples reveal  $\text{Zn}_2\text{SiO}_4$  Willemite structure (JCPDS: 37-1485) with the identified diffraction peaks of (300), (220), (113), (410), (223), (333), (006), (713), (633) and (416), where the (113) is preferential diffraction peak of the Willemite zinc silicate. Fluorescence properties of the  $\text{Zn}_2\text{SiO}_4:\text{Mn}^{2+}$  powders prepared by different doping levels of manganese nitrate as sodium hydroxide kept at 1M were analyzed using UV excitation of 274 nm. The samples reveal a significant fluorescence at 547.8 nm. The fluorescent emission was caused by the transition of excited state  $^4\text{T}_1$  to ground state  $^6\text{A}_1$  of  $\text{Mn}^{2+}$ . It can be observed that the sample doped with 0.14 mmol manganese nitrate has a better fluorescence effect. With more doping amount of manganese nitrate, its fluorescence intensity decreases and the phenomenon means that over doping will result in concentration quenching for fluorescence.

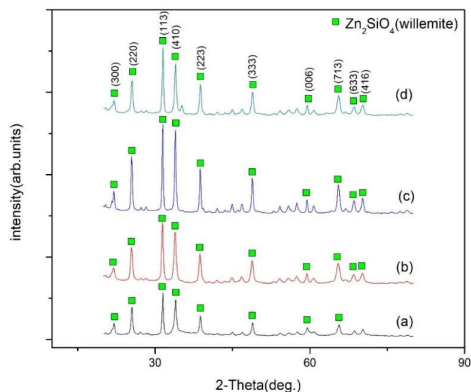


**Fig. 1.** XRD patterns of zinc silicate doped with manganese prepared by hydrothermal synthesis at NaOH concentration of (a) 0M; (b) 1M; (c) 2M; (d) 3M

## On Extension of Functional Possibilities of the Optical Interference Meter of the Surface Displacements of Control Objects

I.P. Miroshnichenko<sup>1\*</sup>, I.A. Parinov<sup>2</sup>

<sup>1</sup>*Don State Technical University, Rostov-on-Don, Russia,*

<sup>2</sup>*Southern Federal University, Rostov-on-Don, Russia*

\*[ipmir@rambler.ru](mailto:ipmir@rambler.ru)

The optical interference means for contactless measurements of the displacements of the control objects surfaces are well-known [1, 2]. They are developed on the base of a new measurement method, namely the method of highlighting the surface of the control object by laser radiation (or the method of "luminous point") [3]. The marked displacement meters allow contactless measurements of the linear and angular components of the surface displacement of the control object, and also provide the ability to change the range of measured displacements during the measurement process without making changes to the optical scheme. The results of calculation-theoretical and experimental studies of functional characteristics of the pointed meters, and the results of their trial operation allow us to note that there are limitations to their use due to the impossibility of simultaneous measurements by one device the linear and all angular displacement components of the control object (spatial displacement). Technical proposals have been developed to expand the functionality of known displacement meters by measuring the spatial displacements of the surfaces of control objects. The described results are aimed at creating new contactless optical interference means for measuring spatial displacements of the surfaces of control objects.

### **Acknowledgements**

The study was performed under partial support of the Russian Ministry of Education and Science and Russian Foundation for Basic Research (No. 19-08-00365).

### **References**

- [1] I.P. Miroshnichenko, I.A. Parinov, E.V. Rozhkov. *Optical Interferential Device for Measurements of Movements of Surfaces of Controlled Objects*. Russian Patent No. 2512697, 10.04.2014 (In Russian)
- [2] I.P. Miroshnichenko, I.A. Parinov, E.V. Rozhkov. *Optical Device for Measuring Displacements of Control Objects Surfaces*. Russian Patent No. 2343402, 10.01.2009 (In Russian)
- [3] I.P. Miroshnichenko, A.G. Serkin, V.P. Sizov // *Journal of Optical Technology*. **75(7)**, 437, 2008.

## **On the Features of Spatial Temporal Distribution of Displacements and Stresses in Layered Constructional Materials at Diagnostics of Their State by Acoustic Active Non-destructive Testing Methods**

**I.P. Miroshnichenko<sup>1\*</sup>, V.P. Sizov<sup>2</sup>**

<sup>1</sup>*Don State Technical University, Rostov-on-Don, Russia,*

<sup>2</sup>*Southern Federal University, Rostov-on-Don, Russia*

\*[ipmir@rambler.ru](mailto:ipmir@rambler.ru)

Analysis of the results of diagnostics of the state of layered structural materials of power elements of constructions by acoustic active methods of non-destructive testing showed that this raises the problem of recognition of the obtained measurement results and difficulties in determining their correspondence to typical internal defects. The noted problem also exists by performing diagnostics of the state of layered power elements of constructions made of composite materials. Computational and theoretical studies of the features of the spatial and temporal distribution of displacements and stresses in layered constructional materials of typical power elements of constructions were carried out by modeling the process of diagnosing their state by acoustic active methods of non-destructive testing. At the same time, mathematical models, methods and original software were used to determine the stress-strain state in isotropic and transverse isotropic layered plates and layered cylindrical shells, constructed on the base of the generalized scalarization method of dynamic elastic fields in transverse isotropic media [1]. Methods for *a priori* and *a posteriori* analysis were proposed to improve the quality of diagnostic results. The described results are most appropriate to use by analyzing the results of diagnostics of the state of layered structural materials of power structural elements of machines for various purposes in mechanical engineering, shipbuilding, and aircraft construction.

### **Acknowledgements**

The study was performed under partial support of the Russian Ministry of Education and Science and Russian Foundation for Basic Research (No. 19-08-00365).

### **Reference**

[1] V.P. Sizov, I.P. Miroshnichenko, *Elastic Waves in Layered Anisotropic Structures*. LAP LAMBERT Academic Publishing, Saarbrucken, Germany, 2012.

## The Influence of the Structure on the Characteristics of Pt/C and Pt/C-N Electrocatalysts

E.A. Moguchikh\*, K.O. Paperzh, A.A. Alekseenko, A.A. Palchikov

*Southern Federal University, Rostov-on-Don, Russia*

\*[liza.moguchix@mail.ru](mailto:liza.moguchix@mail.ru)

Nanoparticles of metals deposited on various types of carbon, such as activated carbon, carbon nanotubes, and graphene, are often used as electrocatalysts for low-temperature fuel cells (LTFC). Doping a carbon support with heteroatoms is an effective approach for increasing the catalytic characteristics of materials. Obtaining platinum-containing electrocatalysts based on a modified carbon carrier is an urgent task in the field of alternative energy [1]. In this study, several samples were obtained on various carbon supports: Pt/C<sub>1</sub> (M1), Pt/C<sub>2</sub> (M2), Pt/C<sub>2</sub>-N (M3), Pt/C<sub>3</sub>-N (M4). The synthesis was carried out in a liquid medium, formaldehyde was used as a reducing agent at elevated temperature. All catalysts have a mass fraction of platinum of about 20%. We would like to note that with the same initial metal loading, the mass fraction of platinum in catalysts with doped dopant is higher. This suggests that the introduction of nitrogen into the carbon structure positively affects the adhesion of the metal on the surface of the carrier. All catalysts have a platinum nanoparticle (NP) size of less than 1 nm. The introduction of nitrogen into the structure of the M2 carrier leads to a narrowing of the bilayer region, which indicates a decrease in capacitive characteristics.

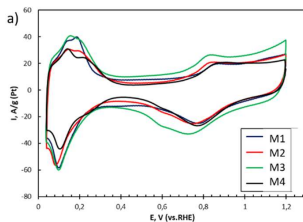


**Fig. 1.** Cyclic voltammograms (a) Pt/C samples; potential sweep speed is 20 mV/s; 2 cycle. 0.1 M HClO<sub>4</sub>, sat. Ar

The presence of N in the carrier structure favorably affects the deposition of metal nanoparticles on the surface. All catalysts show high ESA values, while in not all cases doping leads to an increase in activity in MOR. When nitrogen is introduced into the structure of the carbon carrier M2, the charge distribution between the C-N-Pt atoms occurs, facilitating the adsorption of O<sub>2</sub> on the metal surface.



## Reference

[1] Li Y., Feng Y., Li L., Wu K., Bo X., Jia J., Zhu L. // *Journal of Alloys and Compounds*. **823**, 153892, 2020.

## Features of the Microstructure of Ferroactive Ceramics of the KNN-Cd<sub>0.5</sub>NbO<sub>3</sub> System

M.O. Moysa<sup>1\*</sup>, A.V. Nagaenko<sup>2</sup>, K.P. Andryushin<sup>1</sup>, L.A. Reznichenko<sup>1</sup>

<sup>1</sup>Research Institute of Physics, Southern Federal University, Rostov-on-Don, Russia

<sup>2</sup>Institute of High Technology and Piezo Technic, Southern Federal University, Rostov-on-Don, Russia

\*[maksim.moysa@mail.ru](mailto:maksim.moysa@mail.ru)

The need to exclude toxic lead from the composition of electrotechnical ceramics, as stipulated in the European Parliament Directives 2002 and 2011, motivates researchers to search for alternative functional materials. This was done by us in [1], where solid solutions (SSs) of the  $(1 - x - y)\text{NaNbO}_3 - x\text{KNbO}_3 - y\text{Cd}_{0.5}\text{Nb}_2\text{O}_6$  system were chosen as the object. The optimal conditions for the preparation of ceramics were determined; built phase diagrams (PDs) of the system near  $\text{NaNbO}_3$ . The basic electrophysical characteristics were measured. Based on this, it was concluded that the SSs data are promising for practical applications. In this report, we have examined in detail the features of the microstructure of the SSs of one of the sections of the system ( $y = 0.10$ ), which largely determine the specifics of their macroresponses.

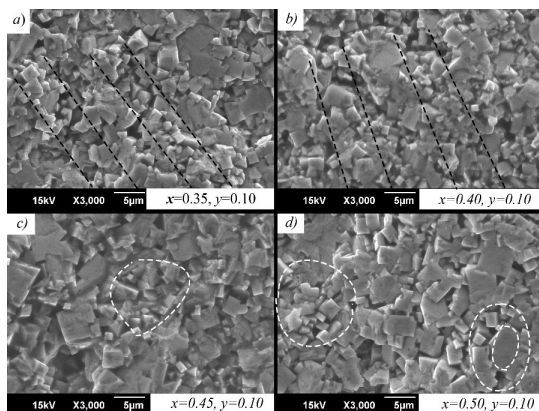


**Fig 1.** Fragments of the ceramic microstructure of the SS system  $(1 - x - y)\text{NaNbO}_3 - x\text{KNbO}_3 - y\text{Cd}_{0.5}\text{Nb}_2\text{O}_6$  ( $x = 0.35 - 0.50$ ,  $y = 0.10$ )

It could be seen in Fig. 1 that the bimodality of the structure with plate-shaped (larger) grains and crystallites similar in shape to a cube, which, generally speaking, is specific for non-bound ceramics sintered with the participation of the liquid phase, is common for all fragments of the grain landscape. In this case, at  $x = 0.35 - 0.40$ , small and large grains are arranged in layers (indicated by a red dotted line), then ( $x = 0.45 - 0.50$ ) this periodicity is violated, giving way mainly to coarse-grained fractions, and small grains are consolidated in certain areas (highlighted by dashed lines) or are framed by larger grains, forming figures of the “flower” type ( $x = 0.50$ ). Such a peculiarity of the grain structure of ceramics will undoubtedly affect their macroproperties (dielectric and piezoelectric), which we will report on later.

#### **Acknowledgement**

Research was financially supported by the Ministry of Science and Higher Education of the Russian Federation (State assignment in the field of scientific activity, Southern Federal University, 2020).

#### **Reference**

[1] Andryushin K.P. et al. *Sodium Solutions of Sodium-Potassium-Cadmium. Preparation, Structure, Electrophysical and Thermofrequency Properties*. LAP LAMBERT Academic Publishing, 2012.

## **Effect of Variation in the Composition of the Basic Ingredients and Briquette Pressure on Calorific Value and Temperature Value of the Briquette Mixture of Rice Husk and Coconut Shell**

**Muhyin<sup>1</sup>, Dwi Yuli Rakhmawati<sup>2\*</sup>, Fahreza Rukmana Witjaksono<sup>1</sup>**

<sup>1</sup>*Department of Mechanical Engineering, University of 17 Agustus 1945 Surabaya, Indonesia*

<sup>2</sup>*Department of Industrial Engineering, University of 17 Agustus 1945 Surabaya, Indonesia*

\*[dwi\\_yuli@untag-sby.ac.id](mailto:dwi_yuli@untag-sby.ac.id)

Due to the disbalance between energy needs and availability, it must be balanced continuing to create alternative energy. So, the sources of alternative energy, for example, biomass briquettes arose. In general, biomass briquettes are obtained from agricultural, plantation, and other wastes. The adhesive used in the composition of the briquette is tapioca flour because tapioca flour is a food ingredient that can be renewed. In this study, we used the basic ingredients of a matrix and filler and considered briquettes from agricultural and plantation waste, namely rice husks and coconut shells. The basic ingredients of briquettes go through a separate carbonation process. After the material becomes charcoal, it is sieved using mesh 60. Mixing briquette composition consists of several kinds of compositions with the same type of adhesive. The process of printing briquettes in this variation varies to determine the best pressure for the briquettes. For molds with measurements of  $2.5 \times 2.5 \text{ cm}^2$  in a rectangular shape, the briquette is sintered to reduce water pressure at a temperature of  $110 \text{ }^\circ\text{C}$  for 30 minutes. Based on the results of the analysis, we found that the briquettes with a composition of 55% rice husk, 35% coconut shell, and 10% tapioca flour demonstrated under pressure of  $300 \text{ kg/cm}^2$ , a calorific value of  $5432.730 \text{ cal/g}$  and a maximum

temperature value of 429 °C. So, by comparing with the standard briquettes, the heating value and temperature value are good.

## **Fabrication of Strong Macrofibers from Plant Fiber Bundles**

**A. N. Nakagaito<sup>1\*</sup>, Y. Katsumoto<sup>2</sup>, H. Takagi<sup>1</sup>**

*<sup>1</sup>Graduate School of Technology, Industrial and Social Sciences, Tokushima University,  
Tokushima 770-8506, Japan*

*<sup>2</sup>Graduate School of Advanced Technology and Science, Tokushima University,  
Tokushima 770-8506, Japan*

*\*[nakagaito@tokushima-u.ac.jp](mailto:nakagaito@tokushima-u.ac.jp)*

The manufacture of continuous fibers aiming a variety of uses such as in textiles, composite reinforcements, and filters is nowadays in great demand. In addition to high mechanical properties, these fibers must attend environmental requirements both in manufacture and at end-of-life disposal. In this sense, fiber bundles from many plants have been converted into yarns and used as reinforcements in composites. However, the mechanical properties are much lower than those of synthetic fibers and are dependent on variations in climate and nutrition that fiber-producing crops are subjected. The latest trend in bio-based materials for composite manufacture has been the exploration of cellulose nanofibers extracted from plant fibers. Even though having mechanical properties approaching those of the strongest synthetic fibers, controlling the proper alignment of nanofibers has been one of the major challenges. Many successful approaches are being proposed such as fiber spinning and hydrodynamic alignment, but they are still complex and costly. To address these issues, we propose a method to make long cellulosic fibers by maintaining the original plant cell wall structure and crosslinking the constituent cellulose nanofibers by hydrogen bonds. By chemically extracting non-cellulosic substances from plant fiber bundles and keeping the fibers arrangement intact, the drying from wet state produces interfibrillar hydrogen bonds that mechanically fix and stabilize the neighboring fibers and nanofibers. Manila hemp fiber bundles had lignin removed by the Wise method and hemicelluloses by alkali treatment, and subsequently rinsed with water. Wet fiber bundles were twisted and dried under tension to form long fiber bundles comprised of virtually pure cellulose. Most of the cellulose nanofibers were aligned along the length of the fibers due to the previous natural arrangement in the cell wall of the plant fibers. The gain in strength relative to the original Manila hemp fiber bundle was not so significant but the process might be able to keep the mechanical properties consistent regardless of the property variations coming from the starting fibers.

# Regarding Unexpected Properties of Porous Piezocomposites with Different Maximal Electrical and Mechanical Properties on the Pore Boundary

A.V. Nasedkin <sup>1\*</sup>, M.E. Nassar <sup>1,2\*\*</sup>

<sup>1</sup>*Southern Federal University, Rostov-on-Don, Russia*

<sup>2</sup>*Faculty of Electronic Engineering, Menoufia University, Menouf, Egypt*

\*[nasedkin@math.sfedu.ru](mailto:nasedkin@math.sfedu.ru), \*\*[mohammed.alsayed75@el-eng.menofia.edu.eg](mailto:mohammed.alsayed75@el-eng.menofia.edu.eg)

Smart structures are characterized by integrating active materials into passive structures using a control system. The piezoelectric transducers are integrated into smart structures as sensors or actuators. The material properties of piezoelectric materials can be tailored for specific applications by introducing porosity into them. For example, porous piezoceramics are preferred in hydrophone sensing applications. However, introducing porosity into the piezoceramics decreases its mechanical strength. To increase the stiffness of porous piezocomposites, A. N. Rybyanets, et al. in the Southern Federal University developed a novel approach for fabricating the piezocomposites by transporting micro or nanoparticles of specific metals or metal oxides into ceramic matrices. In this way, they created a metal layer on the pore surface. In this work, we modeled the porous piezocomposites assuming different extremal electrical conductivity and mechanical strength properties of that layer. We considered a simple representative volume composing of a cube of the piezoceramic material with a compound spherical pore at its center. The compound pore consists of a spherical vacuum pore and a spherical layer on its boundary. The spherical layer simulates the properties of the metal layer produced on the pore surface. We created the finite element model using SOLID227 ANSYS elements for all phases of the composite. The material properties of the spherical layer distinguish between the different systems under study. In the first system, the pore is coated by a conductive metal layer with negligible thickness. The material properties of the layer coating the pore is represented as a piezoelectric material with negligible piezoelectric and elastic moduli, and very high dielectric permittivity moduli. The high dielectric permittivity simulates the material conductivity; while the negligible elastic moduli indicate that the spherical layer's thickness is thin. For the second system, a mechanically rigid insulating layer covers the pore. The properties of the material filling this layer was represented as a piezoelectric material with negligible piezoelectric and dielectric moduli, and very high elastic moduli. The third system considers a pore surface with extremal electrical conductivity and mechanical rigidity. The piezoelectric phase acquires the material properties of the piezoceramics PZT-4. The vacuum is represented by a piezoelectric material with negligible elastic, piezoelectric, and dielectric permittivity moduli. We developed specific algorithms in ANSYS APDL to solve the homogenization problems using the finite element method. The theory of effective moduli was implemented in these algorithms under special essential boundary conditions to obtain the effective moduli of the piezocomposites under study. The findings of this work confirm that the effective moduli of these systems greatly depend on the material properties of the spherical layer on the pore surface. The conductive layer in the first and the third system enhances the electric field near the interface between the piezoelectric and the conductor phases. Also, the integral value of the electric induction inside the metal volume is very high. This greatly affects the effective piezoelectric and dielectric permittivity moduli of these

systems. The rigid layer for the second and third systems largely influences its moduli. The results of this study indicate that these new piezocomposites could have multiple practical applications.

**Acknowledgement**

This research was done in the framework of the RFBR project 20-31-90102.

## Convective Motions in a Rotating Spheroid at Vanishing Dissipation

Natalia V. Petrovskaya

*Southern Federal University, 8a, Milchakov Str., Rostov-on-Don, 344090, Russia*

[nvp108@gmail.com](mailto:nvp108@gmail.com)

The six-dimensional model of viscous fluid thermal convection in a uniformly rotating ellipsoidal cavity [1] is studied. It is known that in the case of an inviscid, non-heat-conducting fluid the problem under consideration has *exact* solutions with spatially linear velocity and temperature fields. In solutions of this kind the dimensionless vorticity  $\boldsymbol{\omega}$  and temperature gradient  $\mathbf{q}$  depend only on time and satisfy the following *ordinary* differential equations at  $\varepsilon = 0$ :

$$\begin{aligned} \dot{\mathbf{M}} &= [\boldsymbol{\omega}, \mathbf{M} + 2\mathbf{M}_0] + [\mathbf{k}, \mathbf{q}] - \varepsilon \sigma \mathbf{M} \\ \dot{\mathbf{q}} &= [\boldsymbol{\omega}, \mathbf{q}] + \varepsilon (\mathbf{Q} - \mathbf{q}), \quad \mathbf{M} = \mathbf{I} \boldsymbol{\omega}. \end{aligned} \tag{1}$$

Here  $\mathbf{I} = \text{diag}(I_1, I_2, I_3)$ ,  $I_k = \sum_{i=1}^3 a_i^2 - a_k^2$ ,  $a_k$  being the ellipsoid semiaxes;  $\mathbf{M}_0 = \mathbf{I} \boldsymbol{\Omega}_0$ , where  $\boldsymbol{\Omega}_0$  is the angular velocity of ellipsoid rotation; unit vector  $\mathbf{k}$  determines the gravity direction;  $\mathbf{Q}$  is a constant temperature gradient on the ellipsoid surface,  $\sigma$  and  $\varepsilon$  are parameters proportional to the Prandtl number and the fluid thermal conductivity, respectively. We assume that the ellipsoid is rotationally symmetric:  $a_1 = a_2$ . The gravity, angular velocity  $\boldsymbol{\Omega}_0$  and temperature gradient  $\mathbf{Q}$  are directed along the axis of symmetry:  $\mathbf{k} = -\mathbf{e}_3$ ,  $\boldsymbol{\Omega}_0 = (0, 0, \omega_0)$ ,  $\mathbf{Q} = \mathbf{k}$  (under heating is considered). At  $\varepsilon = 0$  (the ideal convection case), the system (1) is close to the well-known Euler-Poisson equations describing the motion of a rigid body with a fixed point, the two systems coincide, when  $\omega_0 = 0$ . Like the Euler-Poisson equations, the ideal convection model has an integral invariant (the phase volume) and three independent first integrals, which are the counterparts of the total energy, potential vorticity and entropy. In the rotationally symmetric case under consideration the quantity  $\omega_3$  represents an additional fourth integral, so that the system (1) can be integrated precisely in the same manner as the Euler-Poisson equations in the integrable Lagrange case [2]. Non-degenerate joint levels of the integrals are two-dimensional toruses. This allows us to use the averaging method for asymptotic analysis of steady state convective motions in the limiting case  $\varepsilon \rightarrow 0$  when  $\sigma$  and  $\omega_0$  are constant. The results are as follows. For  $\varepsilon$  small enough in some region of  $\sigma$  the asymptotically stable two-dimensional torus exists in the phase space of system (1). Then the steady state convective motions are periodic or quasiperiodic with two independent frequencies. Let  $\sigma$  be fixed. At  $\omega_0 = 0$  there is an oscillatory-type periodic

motion with zero mean angular velocity. The axis of rotation is constant for it (orthogonal to gravity) while the intensity and direction of rotation change periodically [3]. This is an analog of the pendulum oscillations of a rigid body with a fixed point. When  $0 < \omega_0 < \hat{\omega}$ ,  $\hat{\omega} = \mathbf{O}(1)$  (slow rotations), the motion is a superposition of such pendulum oscillations and the uniform rotation of the angular velocity vector in the horizontal plane. With increasing  $\omega_0$  the oscillation amplitude tends to zero and the motion becomes close to stationary rotation of the fluid around the vertical axis. The rearrangements of the phase flow on a 2D-torus (attractor) with a continuous growth of rotation number do not change the basic characteristics of motion. On the contrary in the previously considered case of fast rotations of the ellipsoid [4], the resonance ‘tongues’ corresponding to resonances 1:4, 1:3 and 1:2 are very extensive, so that we can observe the hysteresis phenomenon for periodic motions of this type.

#### **Acknowledgement**

Research was financially supported by Southern Federal University, grant No. VnGr-07/2020-04-IM (Ministry of Science and Higher Education of the Russian Federation).

#### **References**

- [1] Gledzer E. B., Dolzhanskii F. V., Obukhov E. M. *Hydrodynamic Type Systems and Their Application*. Moscow: Nauka, 1981 (In Russian)
- [2] Golubev V. V. *Lectures on the Integration of Equations of a Heavy Rigid Body Motion near a Fixed Point*. Moscow: GITTL, 1953 (in Russian)
- [3] Petrovskaya N. V. // *University News, North-Caucasus Region, Natural Sciences Series*. **3**, 20–26, 2019 (in Russian)
- [4] Petrovskaya N. V. // *Fluid Dynamics*. **30**(5), 673-675, 1995

## **Studying of Dielectric Spectra of YMNO<sub>3</sub>-based Solid Solutions with the Use of Complex Conductivity**

**A.V. Nazarenko<sup>1\*</sup>, A.V. Pavlenko<sup>1,2</sup>, Y.I. Yurasov<sup>1,2</sup>**

<sup>1</sup>*Southern Scientific Center, Russian Academy of Sciences, 344006, Rostov-on-Don, Russia*

<sup>2</sup>*Research Institute of Physics, Southern Federal University, 344090, Rostov-on-Don, Russia*

\*[avnazarenko1@gmail.com](mailto:avnazarenko1@gmail.com)

Scientists around the world have been studying the dielectric properties of functional materials for many years. Numerous objects with unique properties and combination of ferroelectric, piezoelectric and optical properties were created during this time. Moreover, there are many theories and models to describe physical processes occurring in these objects. Among the existing theories, the most general is the Havriliak-Negami model [1]:

$$\varepsilon^* = \varepsilon_\infty + \frac{\varepsilon_s - \varepsilon_\infty}{(1 + (i\omega\tau)^{1-\alpha})^\beta} \quad (1)$$

However, the physical properties of complex objects often have a pronounced relaxer character in the temperature-frequency dependences, which is associated with the presence of inhomogeneities, conductivity, and other nonlinear effects. This greatly complicates the description of the properties

of known models, including (1), so there is a need to refine theories in the study of such materials. The objects of studying are solid solutions of  $YCu_xMn_{1-x}O_3$  with  $x = 0.05; 0.10; 0.15$ , which were obtained using common ceramic technology. Investigations of their crystal structure and grain microstructure were carried out. The temperature-frequency dependences of the relative permittivity and dielectric loss tangent (in frequency range  $f = 10^2 - 10^5$  Hz) and electrical resistivity  $\rho$  at  $T = 300 - 700$  K were studied. As it is known, Mn-based oxides usually have high electrical conductivity. The introduction of Cu-ions in  $YMnO_3$  can provoke a change in the Mn-valency, which also increases the conductivity. So, it was expected that in  $YCu_xMn_{1-x}O_3$  solid solutions the study of dielectric properties would be difficult due to strong relaxation. Therefore, the aim of this work was to study the possibility of applying a new approach based on the Havriliak-Negami model (1) recorded for complex electrical conductivity [2, 3]:

$$\gamma^* = \gamma_\infty + \frac{\gamma_{st} - \gamma_\infty}{(1 + (i\omega\tau)^{1-\alpha})^\beta} + \varepsilon''_\infty \omega \varepsilon_0 + i \varepsilon'_\infty \omega \varepsilon_0 \quad (2)$$

where  $\alpha = \frac{kT}{E_a} \ln(Q_\infty)$ ;  $\beta = 1 - \alpha$ ;  $Q_\infty = \frac{\varepsilon'_\infty}{\varepsilon''_\infty}$  [3].

As expected, it was not possible to study the dependences of the dielectric constant using model (1) over the entire range of temperatures and frequencies. However, at high frequencies of the external field, it was fixed the anomalies in the  $\varepsilon'/\varepsilon_0(T)$  curves [4]. This anomaly was also confirmed by analyzing the  $\ln\rho(1/T)$  dependences. It was found that, unlike the classical models, the model (2) fully describes the dielectric spectra over the entire range of measuring frequencies in the temperature region with strong through conductivity. Thus, this model can be further used to describe the dielectric spectra of any nonlinear dielectrics, including those with high electrical conductivities.

#### **Acknowledgements**

The work is performed as part of the projects of the SSC RAS State Order (01201354240 and 01201354247) and the Ministry of Science and Higher Education of the Russian Federation (State assignment in the field of scientific activity, Southern Federal University, 2020) with the use of equipment of the Centers for Collective Use Nos. 1483136 and 501994.

#### **References**

- [1] Havriliak S., Negami S. // *Journal of Polymer Science Part C*. **14**(1), 99 – 117, 1966.
- [2] Yurasov Yu.I., Nazarenko A.V. // *Science of the South of Russia*. **15**(1), 31 – 41, 2019.
- [3] Yurasov Yu.I., Nazarenko A.V. // *Journal of Advanced Dielectrics*. **10**(1 & 2), 2060006, 2020.
- [4] Nazarenko A.V. et al. // *Science of the South of Russia*. **15**(4), 12 – 17, 2019.

# On Modelling and Identification of Prestress State in Inhomogeneous Structures Including Coatings and Delamination Zones

R. D. Nedin<sup>1,2</sup>

<sup>1</sup>*I.I. Vorovich Institute of Mathematics, Mechanics and Computer Sciences, Southern Federal University, Rostov-on-Don, Russia*

<sup>2</sup>*Southern Mathematical Institute of Vladikavkaz Scientific Center of RAS, Vladikavkaz, Russia*

[rdn90@bk.ru](mailto:rdn90@bk.ru)

Nowadays, modern materials with a complex inhomogeneous structure are currently widely used in military and civil engineering. Due to the features of the manufacturing process, most finished products made of such materials are in conditions of inhomogeneous residual stress-strain state. Deformation models of 1D and 2D inhomogeneous structures like rods, cylinders, plates and strips, which are common structural elements, are relevant in solving problems arising in modern construction, in the creation of a wide-range military and civilian technical systems. In production, prestresses (or residual stresses) are often implemented intentionally in such structures to improve their mechanical and operational properties. In this paper, we describe a model of a prestressed body, which does not explicitly take into account the initial deformation [1]. On its basis, a number of particular problems on steady state vibrations of 1D and 2D inhomogeneous structures made of a non-uniform functionally graded material in conditions of an initial stress-strain state is considered. Particularly, a problem on in-plane vibrations of a strip with a delaminating prestressed coating is studied. Variational formulations for all the considered problems are formulated. Numerical solutions of the direct problems were constructed using the finite element method based on the weak formulations provided, and the effects of prestress levels in the objects under study on the amplitude-frequency characteristics and resonant frequencies were investigated [2]. The change of dynamic characteristics depending on the type of complex prestressed state is studied. For a class of simple structures (e.g., rods, cylinders, strips), the numerical results obtained for the resonances and eigenfrequencies for different levels of initial stress state were compared to the published experimental results. The formulations obtained are convenient for solving a large class of inverse coefficient problems in which it is required to determine a level or non-uniform distributions of prestress fields with the known data on the displacement field. A number of inverse problems on the restoration of prestresses in plates are considered; their statements differ in the type of additional information known about the measured displacement field in the acoustic sounding mode. Several approaches to the reconstruction of a 1D and 2D residual stress states in rods, plates and 2D-regions are proposed based on iterative regularization, projection methods and other techniques. Computational experiments on the reconstruction of various types of prestressed state were carried out, effective modes of acoustic sounding of the plate were identified, and the most efficient and informative frequency ranges for fine reconstruction were determined.

## **Acknowledgement**

The study was supported by the Russian Science Foundation (grant No. 18-11-00069).

## **References**

[1] R.D. Nedin, V.V. Dudarev, A.O. Vatulyan // *Engineering Structures*, **151**, 391-405, 2017.



[2] R.D. Nedin, A.O. Vatulyan, I.V. Bogachev // *Mathematical Methods in the Applied Sciences*, 41(4), 1600–1618, 2018.

## **Automated System for Monitoring Electrical Parameters of Process Equipment for Oil Refineries**

**I.V. Nemchenko<sup>1</sup>, D. D. Fugarov<sup>1\*</sup>, O. A. Purchina<sup>1</sup>, D.A. Onyshko<sup>2</sup>**

<sup>1</sup>*Don State Technical University, Rostov-on-Don, Russia*

<sup>2</sup>*South-Russian State Polytechnic University (NPI) named after M.I.Platov, Novocherkassk, Russia*

[\\*ddf\\_1@mail.ru](mailto:ddf_1@mail.ru)

The modern rational power supply system of an industrial enterprise should be economical, reliable, safe, convenient to operate, and should also ensure the proper quality of energy and provide for the flexibility of the system, ensuring the possibility of expansion during the development of the enterprise without significant complicating and increasing the cost of the initial version [1]. Decisions requiring minimum consumption of non-ferrous metals and electricity should be made as far as possible [2]. Modern refineries consist of separate complex process units, the number of which is accepted in accordance with the annual capacity [3]. Depending on the selected product range, the process flow of the refinery [4] is changed. At oil refineries there are various electric receivers of process equipment of a general plant nature, from which the most powerful are cooling water units with pumping stations with a capacity of several thousand kilowatts and a raw material base with numerous pumps. The peculiarity of oil refineries is many different motors, asynchronous and synchronous, used for drives of powerful pumping stations and compressor units of various purposes. The development and research of an automated system for monitoring the electrical parameters of the refinery's process equipment is an urgent scientific and technical task.

### **References**

- [1] Poluyan A.Y., Fugarov D.D., Purchina O.A., Nesterchuk V.V., Smirnova O.V., Petrenkova S.B. // *Journal of Physics: Conference Series "International Conference Information Technologies in Business and Industry 2018 - Microprocessor Systems and Telecommunications"*. 022013, 2018.
- [2] Fugarov D.D., Gerasimenko Y.Y., Nesterchuk V.V., Gerasimenko A.N., Onyshko D.A. // *Journal of Physics: Conference Series*. 012055, 2018.
- [3] Y.O. Chernyshev, O.A. Purchina, A.Y. Poluyan, D.D. Fugarov, A.V. Basova, O.V. Smirnova // *Journal of Theoretical and Applied Information Technology*. **80**(1), 13-20, 2015.
- [4] Solomentsev K.Y., Fugarov D.D., Purchina O.A., Poluyan A.Y., Nesterchuk V.V., Petrenkova S.B. // *Journal of Physics: Conference Series*. **1015**, 032179, 2018.

## On the Problem of Identifying Variable Thermomechanical Characteristics of a Cylinder

S.A. Nesterov

*Southern Mathematical Institute - Branch of the VSC RAS, Vladikavkaz, Russia*

[1079@list.ru](mailto:1079@list.ru)

Currently, research in the field of functionally graded materials is attracting more and more attention of scientists. Knowledge of the real characteristics of the material allows us to evaluate its functional properties and the possibility of use. Direct measurements of thermomechanical characteristics in the case of inhomogeneous bodies are impossible. Therefore, non-destructive quality control of heterogeneous materials requires solving inverse coefficient problems. The direct problem of axisymmetric vibrations of an inhomogeneous hollow thermoelastic cylinder is considered. The edges of the cylinder are thermally insulated and are in conditions of sliding embedment. On the inner surface of the cylinder, zero stresses and zero temperature are maintained, and on the outer surface, a combined load is applied. Thermomechanical properties are considered variable along the radial coordinate. The direct problem of determining the stress-strain state of a cylinder is solved on the basis of the method of separation of variables. A set of canonical linear systems of first-order differential equations is obtained, the solution of each of which is obtained numerically using the shooting method. For this, solutions of auxiliary Cauchy problems are constructed. The influence of the laws of changes in the heterogeneity of thermomechanical characteristics on the boundary physical fields is analyzed. The inverse problem is posed for finding the thermomechanical characteristics of a cylinder with finite length according to additional information given on the outer surface of the cylinder. The dimensionless thermomechanical characteristics of the cylinder were restored in two stages. At the first stage, the initial approximation in the class of positive bounded functions was determined. At the second stage, based on the solution of the corresponding Fredholm integral equations of the first kind, corrections of the reconstructed functions were found, and an iterative process of their refinement was constructed. The numerical solution of the Fredholm equation of the first kind is an ill-posed problem, for the solution of which the regularization method of A.N. Tikhonov is used. Based on the computational experiments, it was found that monotonic characteristics were restored with good accuracy.

### ***Acknowledgement***

This work was supported by the Southern Mathematical Institute, a Branch of the VSC RAS, Vladikavkaz, Russia.

# Investigation of the Activity of PtCuAu/C Electro catalysts in Alcohols Electrooxidation Reaction in Alkaline Media

A.K. Nevelskaya\*, S.V. Belenov

Southern Federal University, Chemistry Department, 7, Zorge Str., Rostov-on-Don, Russia

\*[alya.nevelskaya@mail.ru](mailto:alya.nevelskaya@mail.ru)

For many years, methanol and ethanol have been used as fuels for alkaline direct alcohol fuel cells (ADAFCS). According to literature, the electrocatalytic activity for organic molecule oxidation of small molar mass in alkaline media is higher than that in acidic media [1]. Various catalysts are used for the efficient operation of FCs, and platinum-based catalysts are considered to be suitable catalysts for alcohol FCs. However, the presence of a noble metal increases catalyst production cost. To reduce its cost and to increase its specific characteristics, several concepts have been developed, one of which is alloying of Pt with various metals to obtain bi- and trimetallic nanoparticles. The synthesis of PtCuAu/C catalysts with different structures was carried out by the methods of simultaneous reduction of metal precursors and the galvanic substitution method developed previously [2]. Investigating the materials by the cyclic voltammetry (CV) method, it was found that the PtCuAu/C catalyst activity in the ethanol oxidation reaction is higher than that for the commercial Pt/C catalyst (Fig. 1b). According to the CV data, an increase in electricity amount in the ethanol oxidation reaction and earlier ethanol oxidation potentials were recorded for the synthesized materials in comparison with the commercial catalyst Pt/C. However, it was found that in the methanol electrooxidation reaction, PtCuAu/C catalyst (Fig. 1a) obtained in one synthesis step is more active compared to other materials studied. The chronoamperometry results show that for the synthesized PtCuAu/C catalysts, a higher initial specific current of ethanol oxidation is observed in comparison with the Pt/C catalyst. The result obtained correlates well with data on the materials activity obtained by the CV method.

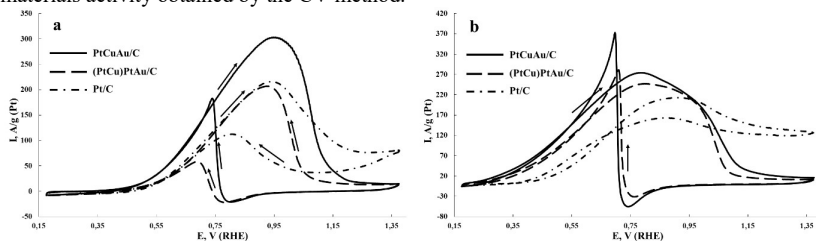


**Fig. 1.** Cyclic voltammograms of PtCuAu/C catalysts: (a) in 0.1M KOH + 0.5M CH<sub>3</sub>OH, (b) in 0.1M KOH + 0.5M C<sub>2</sub>H<sub>5</sub>OH

## Acknowledgement

This research was supported by BA30110/20-1-04KhF.

## References

[1] Santasalo-Aarnio A., Kwon Y., Ahlberg E. et al. // *Electrochemistry Communications*. **13**(5), 466, 2011.

[2] Alekseenko A.A., Guterman V.E., Belenov S.V. et al. // *Int. J. of Hydrogen Energy*. **43**(7), 3676, 2018.

## **A New Design of Protection Device to Improve Car-to-Truck Rear Under-ride**

**Nguyen Phu Thuong Luu**

*Department of Automotive Engineering, Ho Chi Minh City University of Technology (HUTECH),  
Ho Chi Minh City, Vietnam*

[npt.luu@hutech.edu.vn](mailto:npt.luu@hutech.edu.vn)

This paper studied on a new design of rear barrier for trucks to improve the car-to-truck rear underride crash accidents. Rear under-run crashes involving heavy vehicles with rear extension represents the extreme examples of incompatibility between heavy trucks and passenger cars. This type of crash often causes severe or fatal injuries to car occupants. The safety of the vehicle occupant space in car-to-truck rear-end collisions is directly related to the crashworthiness of the car body structure. This paper mainly studied the effect of the new rear truck barrier design on car structural impact in a rear-end accident. To provide a reference on the promotion of car crashworthiness and improvement of truck's underride guard, this paper analyzed the load path and deformation process of rear-end collisions by simulation method and mainly focused on the changes of car acceleration, intrusion volume. The simulation results show good agreement with the crash test indicating that such models could be used at a relatively low cost to design barrier truck structures and investigate injury prevention.

## **An Optimal Design Truck Cabin by Using Finite Element Model Simulation**

**Nguyen Phu Thuong Luu**

*Department of Automotive Engineering, Ho Chi Minh City University of Technology (HUTECH),  
Vietnam*

[npt.luu@hutech.edu.vn](mailto:npt.luu@hutech.edu.vn)

This paper studied an optimal design of truck cabin structure for improving the occupant safety by using finite element modeling. Occupant survive space of truck cab is required for all the commercial vehicles. According to ECE R29 real test conditions, the simulation methods of the front pillar impact test and the side 20° pendulum impact of the roof strength test for a truck model are proposed. Based on the current market truck dimensions, a reliable finite element model of a truck is built by using its CAD model. That is used for the modeling of the chosen cabin modules followed by using Hypermesh finite element meshing and then analysis is done using LS-DYNA

by setting the boundary conditions, material properties etc. Crash analysis of truck cab structure implemented using finite element analysis in order to prophesy the design parameters for curtailing injure to the passengers of the vehicle. To enhance the impact of the cabin truck, specific structural improvements are designed such as filling foam in the A-pillars and the side panels, adding a roof crossbeam, and reinforcing the rear wall of cab. The simulation results of the improved cab structure show that the cab stiffness is improved, the energy absorption is consistent and there is no intrusion into the survival space.

## **Natural Radioactivity of $^{226}\text{Ra}$ , $^{232}\text{Th}$ and $^{40}\text{K}$ in Domestic Well Water and its Impact on the Health of People in Hanoi Area (Extension), Vietnam**

**Nguyen Van Dung\*, Vu Thi Lan Anh**

*Faculty of Environmental, Hanoi University of Mining and Geology, Hanoi, Vietnam*

\*[dungnhumg@gmail.com](mailto:dungnhumg@gmail.com)

People are always exposed to background ionizing radiation. The interaction between ionizing radiation and the biological system can lead to changes in cells or tissues that cause serious diseases such as cancer, blood, etc. In this work, we determine activity of natural radioactive nuclei  $^{226}\text{Ra}$ ,  $^{232}\text{Th}$  and  $^{40}\text{K}$  in well water in households in Hanoi area (dragon extensions), Vietnam. Water samples were collected from households by winter and summer. The activity of natural radionuclides  $^{226}\text{Ra}$ ,  $^{232}\text{Th}$  and  $^{40}\text{K}$  were determined by low background gamma spectroscopy with ultra-pure Germanium semiconductor probe, the samples were analyzed at Institute for Nuclear Science and Technology, Vietnam Atomic Energy Institute. We obtained the following results: the average activity of the radionuclides  $^{226}\text{Ra}$ ,  $^{232}\text{Th}$  and  $^{40}\text{K}$  in domestic well water was, respectively,  $0.48 \pm 0.21 \text{ BqL}^{-1}$ ,  $1.43 \pm 0.46 \text{ BqL}^{-1}$  and  $8.35 \pm 5.45 \text{ BqL}^{-1}$  for winter. For summer, the average activity of radionuclides  $^{226}\text{Ra}$ ,  $^{232}\text{Th}$  and  $^{40}\text{K}$  in domestic well water was, respectively,  $0.58 \pm 0.16 \text{ BqL}^{-1}$ ,  $0.98 \pm 0.38 \text{ BqL}^{-1}$  and  $6.75 \pm 3.13 \text{ BqL}^{-1}$ . The contribution of radionuclides in water samples to the annual effective dose for adults is valued at  $0.011 - 0.278 \text{ mSv/year}$ , in average as  $0.176 \text{ mSv/year}$ . The study of results showed that the activity of natural radionuclides of  $^{226}\text{Ra}$ ,  $^{232}\text{Th}$  and  $^{40}\text{K}$  in domestic well water in Hanoi area (extension), Vietnam is lower than the level recommended by the report World Health Organization (WHO, 2011). Moreover, the average annual dose caused by natural radionuclides in the sample of domestic well water in the surveyed area is lower than the global average value ( $0.29 \text{ mSv/year}$ ), which is recommended by United Nations Science Commission on the Impact of Atomic Radiation (UNSCEAR 2000).

# Theoretical and Experimental Analysis of Metal Removal from Workpiece Surface during Centrifugal Rotation Processing

Nguyen Van Tho<sup>1,2,3\*\*</sup>, A.N. Soloviev<sup>2\*</sup>, M.A. Tamarkin<sup>3\*\*\*</sup>, I.A. Panfilov<sup>2\*\*\*\*</sup>

<sup>1</sup>Faculty of Mechanical Engineering, Haiphong University, Haiphong City, Vietnam

<sup>2</sup>Department of Theoretical and Applied Mechanics, Don State Technical University, Rostov-on-Don, Russia

<sup>3</sup>Department of Mechanical Engineering, Don State Technical University, Rostov-on-Don, Russia

\*[solovievarc@gmail.com](mailto:solovievarc@gmail.com); \*\*[thonv@dhhp.edu.vn](mailto:thonv@dhhp.edu.vn); \*\*\*[tehn\\_rostov@mail.ru](mailto:tehn_rostov@mail.ru);

\*\*\*\*[panfilov\\_i@prof-cad.ru](mailto:panfilov_i@prof-cad.ru)

In Centrifugal-rotary processing (Fig. 1), the surface of the workpiece is completed and a stable roughness is achieved. To improve machining efficiency, it is necessary to solve the optimization problem of the technological parameters of the centrifugal rotation: quality of abrasive particles, their shape and volume, rotation speed, processing time.

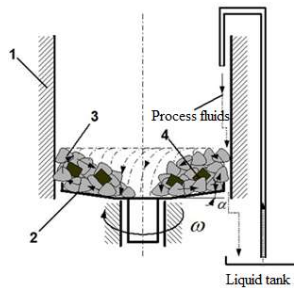


**Fig. 1.** Centrifugal-rotary processing: 1 – fixed cylindrical ring; 2 – rotor; 3 – abrasive particles; 4 – workpieces

Considering the process that a particle pressed the surface of the workpiece by the inertial pressure of the abrasive layer, the dependence of the contact interaction force on time is described by a theoretical curve, for example, the Gaussian distribution curve and characterized by the maximum value and interaction time. In this case, the particle moves along the workpiece surface at a constant speed depending on the angular speed of the centrifugal rotating chamber. The mathematical model of this interaction is the contact problem of the theory of elasticity for an elastoplastic body. The metal removal is calculated using the Archard model that we have studied. In this work, the finite element model of the interaction of a particle with the surface of the workpiece is solved in the ANSYS finite element package. A series of numerical experiments were carried out while altering technological parameter values of the particle and centrifugal rotating chamber. Based on the calculation data, a regression model of the metal removal process with a single interaction is

constructed. The scheme of metal removal from workpiece surface can be constructed on the basis of a probabilistic approach taking into account the random nature of the interaction. A lot of experiments have been performed in which various shapes of abrasive particles of different shapes are used. The dependences of the value of metal removed from workpiece surface on the angular velocity of the centrifugal rotating chamber are constructed. Through this research, the essential and important data-sheets will provide for the experiment works and real manufacturing. Hence, time and finance save a lot in achieving the desired surface quality.

## **Design of Construction Elements for Chemisensors Based on Zinc Oxide Nanorods**

**A L Nikolaev<sup>1\*</sup>, M. A. Kazmina<sup>1</sup>, N. V. Lyanguzov<sup>2</sup>, K. G. Abdulvakhidov<sup>2</sup>,  
E. M. Kaidashev<sup>2</sup>, S.M. Aizikovich<sup>1</sup>**

*<sup>1</sup>Don State Technical University, Rostov-on-Don, Russia*

*<sup>2</sup>Southern Federal University, Rostov-on-Don, Russia*

*\*[andreynicolaev@eurosites.ru](mailto:andreynicolaev@eurosites.ru)*

Zinc oxide is a very promising semiconductor material with a direct wide band gap  $\sim 3.37$  eV at room temperature. Various zinc oxide nanostructures, such as nanorods, nanobelts, thin films, stimulate a large research interest due to their exceptional properties and great potential for nanoelectronic applications. For example, the highly oriented arrays of zinc oxide nanorods are of great interest for modern sensorics and photodetection. This is possible due to the high sensitivity caused by surface defects a colossal effective surface area and consequently a high adsorption activity [1]. In addition to applications in nanoelectronics, bulk resonators based on zinc oxide nanorods can be used as mass sensors [3], UV detectors [4], infrared detectors [5], photodetectors [6], etc. The degree of sensitivity to a certain type of radiation, or a change of bulk resonator condition is expressed by the shift characteristic (resonant) frequency. The resonance frequency of the bulk resonator can be varied within wide limits, because it is directly dependent on the material and geometry as well as on the mass and dimensions of contacts [2]. Thus, bulk resonators based on ZnO are a flexible tool of modern sensor technology. The ability to change the geometry and characteristics of resonator sensors, creates the potential for broad range of detection effects.

As an active element of such devices is used nanobelts, thin films and ZnO nanorods with 753 MHz, 1.6 GHz and 3.9 GHz resonant frequencies, respectively [7]. As the top contact, Au, Pt, Al films and Au coated zinc oxide nanorods are used [8]. Also exist other designs of resonator sensors, such as microbalance resonators proven as high-sensitive devices. Thus, obviously that the development of high-sensitive devices requires high oriented ZnO nanorod arrays, grown on metal surfaces. This is essential for surface and microbalance resistors. Moreover, the resulting structures must have a high concentration of surface defects [9]. Moreover, a non-destructive method is needed, that allows one to apply the top electrode to the nanorod arrays for precise controlling the top contact options. In this work, we present three methods (hydrothermal, electrochemical and carbothermal CVD technique) to obtain a high oriented nanorod arrays on Au surface and a new

method of obtaining top Au contact. This is an important step on the way to create the high-sensitive gas sensors based on zinc oxide.

#### **Acknowledgments**

A. L. Nikolaev and S. M. Aizikovich acknowledged support from the Government of Russia within grant no. 14.Z50.31.0046. A. S. Kamencev acknowledged support from the Russian Foundation for Basic Research within grant no. 20-07-00637 A.

#### **References**

- [1] Prabhakar Rai, et al. // *Sens. Actuators B: Chem.* **165**, 140, 2012.
- [2] Zhi Yan, et al. // *Applied Surface Science.* **253**, 9372–9380, 2007.
- [3] Xiaolei Bian, et al. // *Scientific Reports.* **5**, 9123, 2015.
- [4] Ziyu Wang, et al. // *Thin Solid Films.* **519**, 6144–6147, 2011.
- [5] S. Kiruthika, et al. // *RSC Advances.* **6**(50), 44668-44672, 2016.
- [6] Z. Yan, Xiao-jie Zhou // *Materials Science. Proc. 2010 Symposium on Piezoelectricity, Acoustic Waves and Device Applications*, 2010.
- [7] Brent A. Buchine, et al. // *Nano Lett.*, **6**(6), 2006.
- [8] Dechao Yang, et al. // *Phys. Status Solidi A*, **212**, 1–4, 2015.
- [9] Nikolaev A. L., et al. In: *Advanced Materials - Proceedings of the International Conference on "Physics and Mechanics of New Materials and Their Applications", PHENMA 2018*, Springer Proceedings in Physics, Ivan A. Parinov, Shun-Hsyung Chang, Yun-Hae Kim (Eds.). Springer Nature, Cham, Switzerland, **224**, 103-113, 2019.

## **Intensity of Singular Stress Field in Pull-out Test and Micro-bond Test**

**N. A. Noda\*, D. Chen, R. Takaki, Y. Sano, Y. Takase**

*Department of Mechanical Engineering, Kyushu Institute of Technology, Kitakyushu, Japan*

\*[noda.naoaki844@mail.kyutech.jp](mailto:noda.naoaki844@mail.kyutech.jp)

Wide application of fiber composite technology in various fields is based on taking advantage of the high strength and high stiffness of fibers. Many different alternative test set-ups and experimental techniques have been developed in recent years to gain more insight into the basic mechanisms, dominating the properties of the fiber/matrix interface. Among these experimental tests, pull-out test and micro-bond test are most widely used. A lot of analytical studies have been done to clarify pull-out phenomena in pull-out test and micro-bond test as shown in Fig. 1, but no studies are available for the intensity of singular stress field (ISSF) at the singular points that cause crack initiation. In this study, this intensity will be analyzed to evaluate the fiber/matrix interface, properly. Previously, the finite element method and proportional method were used to evaluate the ISSF of butt joint and lap joint. These methods are used to study the ISSF in pull-out test and micro-bond test. Fig. 2 shows the ISSF ratio of pull-out test and micro-bond test by varying fiber bond length  $l_b$ . It is found that in micro-bond test, no matter how the fiber bond length  $l_b$  changes, the fiber entry point is more dangerous in micro-bond test. Instead, in fiber pull-out test, the fiber end point can be more dangerous, if the embedded length is shorter. The ISSF at the entry point in micro-bond test is about 1.5 times of the ISSF of pull-out test at the entry point under the same



geometries  $D$  and  $l_b$ . By using this knowledge, the ISSFs of pull-out test can be predicted from micro-bond test.

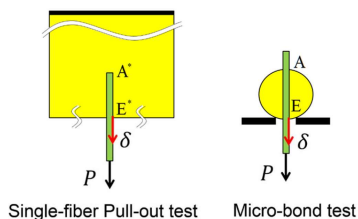


Fig. 1. Pull-out test and micro-bond test

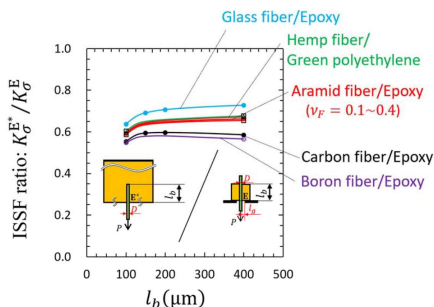


Fig. 2. ISSF ratio of pull-out test and micro-bond test

## Technical Support of Low-power Multi-cell Wireless Networks

D.A. Onyshko<sup>1</sup>, A.V. Gayduchik<sup>1</sup>, D. D. Fugarov<sup>2</sup>, O. A. Purchina<sup>2</sup>

<sup>1</sup>M.I. Platov South-Russian State Polytechnic University (NPI), Novocherkassk, Russia

<sup>2</sup>Don State Technical University, Rostov-on-Don, Russia

\*[ddf\\_1@mail.ru](mailto:ddf_1@mail.ru)

Recently, for the organization of distributed information collection systems, the use of Meshlogic built-in modules, which are designed to build low-power multi-cell wireless networks, has become widespread [1 – 3]. Compared with other standard technologies, such as Zigbee, the Russian development has several significant advantages. These include self-organization, auto-search for packet transmission routes, as well as energy efficiency. Meshlogic plug-ins are represented by the ML-Module-Z, MLM-CC1120-868 and MLM-LSR-P100 boards. The main differences between the modules are the frequency range, transmitter power and power consumption. The MLM-CC1120-868 module is designed for the frequency range 868.7-869.2 MHz, and the ML-Module-Z and MLM-LSR-P100 modules for the 2400-2483.5 MHz. These modules fully provide the necessary functions for working with the radio channel and network interaction, they are optimized for solving information exchange tasks, realizing a wireless sensor data acquisition network. The host device in the circuit is a microcontroller that uses a serial UART interface to communicate with the module (TXD and RXD signals). To control the module, the signals /CS, /RDY, /IRQ and /RST are used, as well as a set of API commands described in the technical documentation for the module. For a more efficient use of the energy reserve, the modules use the energy control of an autonomous power supply by measuring the analogue PM signal. The external DS2411 chip implements the 48-bit serial number of the module. For these purposes, we can also use the MAX31826 temperature sensor chip, which also has a unique identification code, which is

transformed into a network address in the module. In this case, in addition to the serial number and network address of the module, it is possible to read the temperature using the module. Meshlogic built-in modules have the necessary functionality and are able to effectively solve many control tasks, for example: the energy consumption, the environment, the technological parameters of industrial equipment, etc.

### **References**

- [1] Sedov A.V., Onyshko D.A., Lipkin M.S. // *Basic Investigations*, **12**(6), 1134-1138, 2015 (In Russian).
- [2] Onyshko D.A., Fugarov D.D., Nesterchuk V.V., Skakunova T.P. // *Prospective of Science*, **8**(107), 35-38, 2018 (In Russian).
- [3] Onyshko D.A., Fugarov D.D., Skakunova T.P., Gerasimenko A.N. // *Science and Business: Ways of Development*, **10**(88), 37-40, 2018 (In Russian).

## **Automation of Monitoring of Technological Processes in the Oil and Gas Industry**

**D.A. Onyshko<sup>1</sup>, A.A. Ponomarev<sup>1</sup>, D. D. Fugarov<sup>2\*</sup>, O. A. Purchina<sup>2</sup>**

<sup>1</sup>*M.I. Platov South-Russian State Polytechnic University (NPI), Novocherkassk, Russia*

<sup>2</sup>*Don State Technical University, Rostov-on-Don, Russia*

[\\*ddf\\_1@mail.ru](mailto:ddf_1@mail.ru)

Recently, large oil companies have introduced new technologies that are aimed at improving the efficiency and safety of the process by reducing overall costs. These technologies allow us to effectively manage more complex equipment together with fulfilment of all necessary regulatory requirements [1 – 3]. Many elements of such an equipment, as well as technological processes require constant monitoring of parameters by the serving staff. However, such monitoring is usually very inert and inaccurate due to the degree of influence of the human factor. The most effective is the use of continuous and automated monitoring of equipment elements, which ensures a reduction in the number of errors, and also allows for the implementation, under certain conditions, of a continuous flow of information about the current state of an object. Moreover, modern technologies make it possible to ensure a high transmission rate of such information, thereby increasing its efficiency. To automate the monitoring of technological processes on the components of the oil and gas complex infrastructure, wireless sensor network technologies are increasingly used. A wireless network sensor is a miniature computing and communication device, which consists of processor, memory, digital-to-analog and analog-to-digital converter, radio frequency transceiver, power supply and sensor. The type of sensor depends on the monitored parameters at the facility and its connection can be realized via digital or analog interfaces. The network sensor is used only for collecting, preprocessing and transmitting primary data.

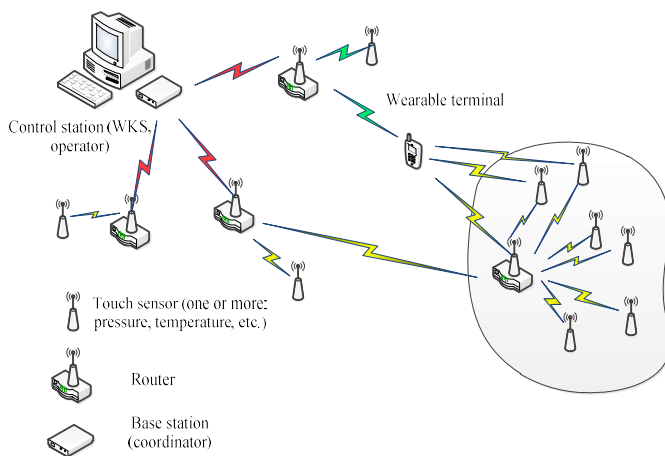


**Fig. 1.** General monitoring scheme

The main processing of information of the sensor network is performed on a node or gateway, implemented as a computer. The network sensors exchange data with each other using built-in transceivers of a certain radio range. Thus, data is transmitted from one sensor to another according to a predetermined topology, and, ultimately, sensors are close to the node, transmit the final data array to it. Moreover, if some of the sensors fail, then the network continues after its reconfiguration (Fig. 1). Wireless sensor systems are built taking into account the requirements of international standards governing the protocols of physical channel, as well as network levels of information transmission lines. At remote technological facilities, monitoring sensors with interfaces are installed, which are the “lower level” of the wireless monitoring system (Fig. 2). The key element of the top level is the AWP and the server.

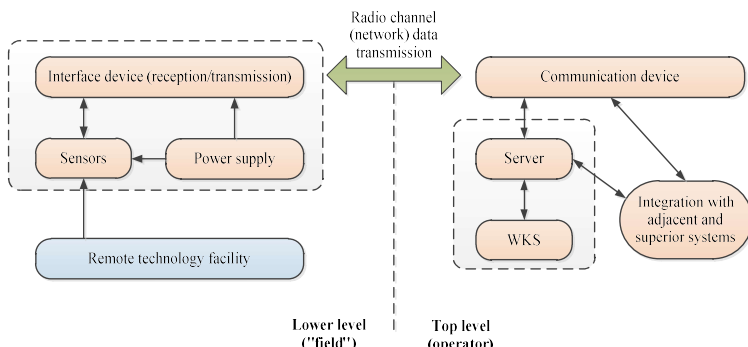


**Fig. 2.** General monitoring scheme

The confidentiality of information on the network is achieved by using appropriate authentication algorithms and message encryption. The main disadvantage of radio systems based on a sensor network compared to wired systems is their increased vulnerability to various attacks aimed at disrupting the operation of the radio line. This violation of work can manifest itself in a breakdown of synchronization, or the imposition of false modes and algorithms for its operation. Moreover, the purpose of the attacks may be a violation of the distribution of information flows, disruption of the implementation of services, etc. An analysis of such radio systems indicates the high vulnerability of the radio links of the information communication system for monitoring the parameters of remote objects of the oil and gas complex from attacks on the synchronization system by using deterministic synchronization signals in it. By providing the specific probabilistic - temporal characteristics of information transmission under attacks on the synchronization system requires the use of additional measures aimed at significantly reducing the likelihood of simulating false clocks.

#### **References**

- [1] Fugarov D.D., Solomentsev K. Yu., Onyshko D.A., Purchina O.A. // *Science and Business: Ways of Development*, **3**(81), 20-23, 2018 (In Russian).
- [2] Onyshko D.A., Fugarov D.D., Nesterchuk V.V., Skakunova T.P. // *Prospective of Science*, **8**(107), 35-38, 2018 (In Russian).
- [3] Onyshko D.A., Fugarov D.D., Skakunova T.P., Gerasimenko A.N. // *Science and Business: Ways of Development*, **10**(88), 37-40, 2018 (In Russian).

### **Infocommunication Technologies for Monitoring Systems of Technological Parameters of Remote Objects**

**D. A. Onyshko<sup>1</sup>, D. A. Saveliev<sup>1</sup>, D. D. Fugarov<sup>2\*</sup>, O. A. Purchina<sup>2</sup>**

<sup>1</sup>*M. I. Platov South-Russian State Polytechnic University (NPI), Novocherkassk, Russia*

<sup>2</sup>*Don State Technical University, Rostov-on-Don, Russia*

\*[ddf\\_1@mail.ru](mailto:ddf_1@mail.ru)

The objective of the study is to ensure the timely collection of reliable information about the technical condition of remote objects. The research hypothesis is based on the fact that ensuring trouble-free operation of remote objects requires constant monitoring of the technological parameters of the facility automation system. In the course of the study, methods of analysis of telecommunication and computing systems were used [1 – 3]. The results achieved allow us to provide the specified requirements for reliability and timeliness in the development of modern telecommunication devices for monitoring systems of parameters of remote objects. The advantage of a wireless network is the simplicity and speed of its deployment, as well as the possibility of spatial movement of the control system within a stable network connection. A network is a system with one host (Host) and several slave devices (Fig. 1), each of which includes a transceiver. It is necessary to use a computer as the Host device, since its software allows one to best manage information flows, process and present data in a convenient form for human perception (tables, graphs, histograms, mnemonic diagrams). Moreover, the computer software can be mobile upgraded, if necessary, change the functioning algorithm of the information processing system and introduce new devices into the system.

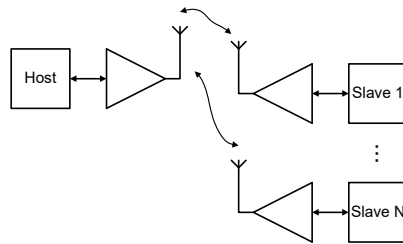


**Fig. 1.** Wireless network diagram

The programmatic description of the network uses the two-level MBus model, which allows one to control the process of exchanging information over the radio telemetric network. To implement the task of exchanging information in the system, information packages are used, which include: the packet header, the command code, the Slave address code of the device, the size of the information packet, the transmitted information and the information packet checksum. Each transmitted byte of the information packet consists of 14 bits (start bit, 8 data bits, 4 bits of the Hamming code and parity bit). The implementation of the protocol at the level of data representation – Data Link (second level) is performed by a microcontroller, which performs the function of determining the time of information bits, receiving information and processing it. Encoding and decoding of packets is provided by the Hamming algorithm. The transceiver performs the functions of the physical layer (level 1 – according to the MBus specification) of the network protocol software model. The use of a frequency synthesizer in a transceiver is due to the need to obtain a stable frequency grid in a given frequency range, a mobile transition with a busy or high level of noise frequency to one of the spare frequencies and the possibility of entering into a tuner-free communication. Together, the frequency synthesizer and the voltage-controlled generator form a loop of phase-locked loop, which is an automatic control system (for deviation). Cryptographic methods are used to protect the transmitted information at the level of data representation. In order to increase the reliability of information transmission, the system provides for multiple transmission of messages. With multiple transmission, you can vary the number and repetition period of messages, achieving the required noise immunity. Transmission parameters can be determined in advance if time distribution functions are known for each of them. If the conditions of the signal passage become worse, the system operation algorithm provides a transition to a higher-level code (from the point of view of noise immunity), for example, a cyclic code or the Bowes – Chowdhury – Hockingham code, which are easily implemented by the microcontroller software. Moreover, the analysis of the state of the communication channel is carried out indirectly, according to the time required to receive information from one source, taking into account the number of possible repetitions. If the situation has not improved with the transition to a new code, according to the algorithm of functioning the system, a transition to the spare frequency occurs. In order to ensure the efficient use of the radio path as a communication channel, a frequency selective feature of encoding information bits is implemented when transmitting data, which also increases the reliability of information transfer. The report studies functioning the telecommunication module for battery monitoring systems. The

structure of the module is justified, in which the specified requirements for the reliability and timeliness of monitoring the parameters of the batteries of remote objects are provided.

### **References**

- [1] Fugarov D.D., Solomentsev K. Yu., Onyshko D.A., Purchina O.A. // *Science and Business: Ways of Development*, **3**(81), 20-23, 2018 (In Russian).
- [2] Onyshko D.A., Fugarov D.D., Nesterchuk V.V., Skakunova T.P. // *Prospective of Science*, **8**(107), 35-38, 2018 (In Russian).
- [3] Onyshko D.A., Fugarov D.D., Skakunova T.P., Gerasimenko A.N. // *Science and Business: Ways of Development*, **10**(88), 37-40, 2018 (In Russian).

## **Modern Technologies for Building a Wireless Sensor Network**

**D.A. Onyshko<sup>1</sup>, P.Yu. Zhmaylov<sup>1</sup>, D.D. Fugarov<sup>2\*</sup>, O.A. Purchina<sup>2</sup>**

<sup>1</sup>*M.I. Platov South-Russian State Polytechnic University (NPI), Novochoerkassk, Russia*

<sup>2</sup>*Don State Technical University, Rostov-on-Don, Russia*

\*[ddf\\_1@mail.ru](mailto:ddf_1@mail.ru)

The report presents one of the promising options for building wireless sensor networks based on modern MeshLogic technology [1 – 3]. In the process of expert analysis, certain features associated with the process of organizing a network based on this technology were identified and described. Wireless sensor network is a new class of wireless systems, which is a distributed, self-organizing and is the fault-tolerant network of individual sensors with autonomous power sources. A network sensor is an electronic device that may contain a processor, memory, DAC and ADC, radio transceiver, power source, and various sensors. The nodes of such a network are capable of relaying messages along the circuit, providing a significant system coverage area with low transmitter power and, consequently, significant energy saving. MeshLogic technology is a set of hardware and software tools that allow one to implement a set of network protocols for packet data exchange between network elements. This technology is the basis for the organization of wireless sensor networks for various fields of application, with certain features that are reflected at the application level of the embedded software of the network elements, as well as in the configuration of the network stack. The MeshLogic platform uses network devices with equal rights and the same functionality, differences between them are possible only at the application level. Moreover, the MeshLogic system is a peer-to-peer multi-cell network, i.e. packet delivery in the system is carried out from any network node to any other, while all nodes are able to perform the function of a packet relay in the exchange process. Such a network organization provides increased resistance to failure of individual network elements, its independent adaptation to environmental conditions. To organize a sensor network from nodes and a gateway, low-power transceivers of the IEEE 802.15.4 standard of the 2.4 GHz frequency range are used. The distance between the nearest nodes depends on the propagation conditions of the signals and, as a rule, is limited to several tens of meters. Wireless sensor network elements with a certain period perform the measurement of signals from external sensors and their preliminary processing. Then the measurement results are sent over the air to the server. To perform the packet relay function, an automatic search for packet delivery

routes is performed. This search is carried out during the initial deployment of the network, as well as in the event of failure at least one network element. Automatic network reconfiguration provides a high degree of communication reliability compared to wired and traditional wireless data transmission systems. Application of MeshLogic technology provides the following advantages of the sensor network: (i) network configuration flexibility; (ii) insignificant labor costs for the design and deployment of the network; (iii) ease of expansion of the system; (iv) high network stability during failures and even failure of sensor nodes; (v) high energy efficiency. The system gateway stores in its non-volatile memory all the information received from the sensor elements. The archive also records the time of receipt of data and various service information. Thus, the gateway acts as a center for collecting data from distributed sensors on the network. To create an effective wireless sensor network, it is necessary to take into account the features of the application at all its levels. The problem of providing a stable and reliable network is relevant and requires further study.

#### **References**

- [1] Sedov A.V., Onyshko D.A., Lipkin M.S. // *Basic Investigations*, **12**(6), 1134-1138, 2015 (In Russian).
- [2] Onyshko D.A., Fugarov D.D., Nesterchuk V.V., Skakunova T.P. // *Prospective of Science*, **8**(107), 35-38, 2018 (In Russian).
- [3] Onyshko D.A., Fugarov D.D., Skakunova T.P., Gerasimenko A.N. // *Science and Business: Ways of Development*, **10**(88), 37-40, 2018 (In Russian).

## **Controlling the Optoelectrical Properties of Two-dimensional Nanostructures Prepared by Laser Ablation in Liquid**

**Pankaj Koinkar\*, Siddhant Dhongade, Akihiro Furube**

*Department of Optical Science, Tokushima University,  
2-1 Minamijosanjima Cho, Tokushima 7708506, Japan*

[\\*koinkar@tokushima-u.ac.jp](mailto:koinkar@tokushima-u.ac.jp)

Human life becomes easier and convenient because of the recent development and progresses in modern technology, although our life is highly dependent on these technological devices. Technology has advanced with years and it has changed the way of living, traveling, and communication. Such technological changes can be effectively used to contribute and addressed critical issues related to our daily life. Researchers are engaged in performing various experiments and come up with good data and results which benefit society. In this regard, research on two dimensional (2D) nanomaterials attract many researchers due to their excellent physical and chemical properties as compared to bulk counterpart. The 2D nanomaterials are capable to hold the future fabrication of next-generation electronic and optoelectronic devices. The 2D materials can be prepared using many physical and chemical techniques. Among physical methods, laser ablation in a liquid environment is an alternative, simple, and easy method to generate nanomaterials. In the present study, the nanosecond laser ablation is used to produce 2D nanostructures in a liquid environment. The structural and surface morphological studies of prepared 2D nanostructures were studied by various characterization methods. The scanning electron microscopy (SEM),

transmission electron microscopy (TEM) and Raman spectroscopy have been used to reveal surface and structural morphology. It is observed that the laser ablation time is an important factor in determining the size of the nanostructures. The Raman spectra of laser-ablated confirm the formation of nanostructures of different size. It is confirmed that the size of the nanomaterials can be controlled by optimizing various process parameters used for laser ablation method. Furthermore, the influence of laser ablation time on field emission properties has been studied. The field emission current densities and the turn-on fields nanostructures are found to be increased for the laser-ablated nanostructures. The improvement in the field emission characteristics is attributed to the reduction in size and shape of nanostructures. These 2D nanostructures generated by the laser ablation method may be capable of optoelectronic application.

## Highly Stable Pt/C Catalysts with Different Mass Fraction of Platinum

K. O. Paperzh\*, A. A. Alekseenko, A. Y. Nikulin

*Southern Federal University, Rostov-on-Don, Russia*

\*[kpaperzh@yandex.ru](mailto:kpaperzh@yandex.ru)

Platinum-carbon materials are used as a catalytic base for the proton-exchange membrane fuel cells (PEMFC). To select catalysts with optimal functional characteristics, it is necessary to understand how electrochemical parameters (active surface area (ESA), activity in the oxygen reduction reaction (ORR), and stability during stress testing) depend on the crystallite size and the mass fraction of platinum Pt/C materials [1, 2]. The liquid-phase synthesis method described in detail in [2] yielded Pt/C materials with a close platinum crystallite size of about 1.1 nm (with NPs size of about 2 nm (Fig. 1)), but with a different mass fraction of metal from 9 to 40%. The influence of platinum mass fraction on the stability of catalysts during long cycling in the potential range of 0.6 – 1.0 V was determined. For comparison, we took commercial Pt/C catalysts HiSPEC 3000 and HiSPEC 4000. It was shown that with an increase in the mass fraction of platinum, a decrease in ESA is observed (from 131 to 88 m<sup>2</sup>/g (Pt)), this is due to the possible agglomeration of NPs caused by the large amount of Pt per unit surface area of the carbon carrier and, consequently, the narrowing of the distance between particles [2]. In this case, with the growth of ESA, the mass activity of the catalysts also increases.

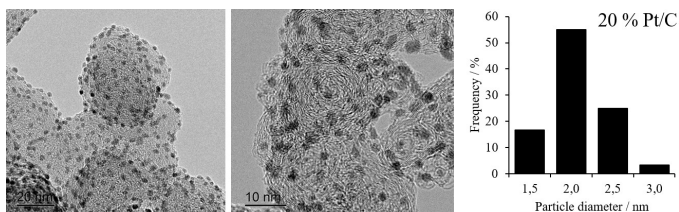


Fig. 1. TEM images and particles size distributions of 20% Pt/C



Pt/C materials containing more than 20% of the mass fraction of platinum are characterized by high relative stability (more than 85%). But the strongest decrease (almost 2 times) in specific activity in ORR after stress testing is observed with a decrease in the mass fraction of Pt. The functional parameters of the materials obtained are superior to those for commercial Pt/C analogues, which makes them promising for use in PEMFC.

#### **Acknowledgement**

This research was financially supported by the Ministry of Science and Higher Education of the Russian Federation (State assignment in the field of scientific activity No. 0852-2020-0019).

#### **References**

- [1] Yano H., Watanabe M., Iiyama A., Uchida H. // *Nano Energy*, **29**, 323 – 333, 2016.
- [2] Alekseenko A.A., Ashihina E.A., Shpanko S.P., Safronko O.I., Guterman V.E. // *Applied Catalysis B: Environmental*, **226**, 608 – 615, 2018.

## **Effect of Lithium Carbonate Modification on the Ferroelectric Phase Transition Diffusion in Lead Ferroniobate Ceramics**

**A.A. Pavelko<sup>1\*</sup>, A.V. Pavlenko<sup>1,2</sup>, A.A. Martynenko<sup>1</sup>, L.A. Reznichenko<sup>1</sup>**

<sup>1</sup>*Research Institute of Physics, Southern Federal University, Rostov-on-Don, Russia*

<sup>2</sup>*Southern Scientific Centre, Russian Academy of Sciences, Rostov-on-Don, Russia*

[\\*aapavelko@sfedu.ru](mailto:*aapavelko@sfedu.ru)

Lead ferroniobate  $\text{PbFe}_{1/2}\text{Nb}_{1/2}\text{O}_3$  (PFN) is one of the most famous representatives of the class of multiferroics, in which the interaction of electrical and magnetic subsystems is observed. Despite the fact that ferroelectric (FE) and magnetic properties combine in PFN only below 140 – 170 K, it remains a very interesting object at the same time both from the applied point of view (use in microwave and sensor technology) and from the position opportunities to study magnetoelectric interaction, often found in the literature as a component of promising multiferroic systems of solid solutions. Despite a rather extensive bibliography, many details of phase transformations in PFN, as well as some features of dielectric responses associated with this, are not fully understood. The purpose of this study was a detailed study of the dielectric properties of PFN in wide temperature (300 – 520 K) and frequency (25 Hz – 2 MHz) ranges, as well as to determine the effect of its modification on lithium carbonate on the degree of smearing of the FE phase transition (PT). For the first time, a method for the qualitative description of PT diffusion was presented in the works of Smolensky, Rolov, Kirillov, and Isupov [1-3]. Later [4], a new empirical relation was proposed that most accurately describes the temperature dependence of the dielectric constant in relaxor ferroelectrics. It was used by us for a quantitative description of the diffusion of FE PT in PFN samples modified with lithium carbonate in the concentration range from 1 to 3 wt.%. The analysis showed that with an increase in the concentration of Li atoms in the system, there is a significant decrease in the dielectric constant at the phase transition point along with a significant increase in its diffusion. Since the observed phenomenon is not accompanied by an unambiguous enhancement of the relaxor properties, it can be concluded that, with an increase in the modifier concentration,

Li atoms prefer to occupy irregular positions in the crystal lattice, which leads to a smearing of phase transitions in the objects.

#### **Acknowledgement**

This work was financially supported by the Ministry of Science and Higher Education of the Russian Federation (State assignment in the field of scientific activity, Southern Federal University, 2020).

#### **References**

- [1] B. N. Rolov // *Sov. Phys.- Solid State*, **6**, 1676-1678, 1965.
- [2] G.A. Smolenskii // *J. Phys. Soc. Jpn.* **28** (Suppl.), 26, 1970.
- [3] V.V. Kirillov, V.A. Isupov // *Ferroelectrics*, **5**, 3, 1973.
- [4] A.A. Bokov, Z.-G. Ye // *Solid State Communications*, **116**, 105-108, 2000.

## **Preparation and Structure of Thin $\text{PbFe}_{0.5}\text{Nb}_{0.5}\text{O}_3$ Films**

**A.V. Pavlenko<sup>1,2</sup>**

<sup>1</sup>*Research Institute of Physics, Southern Federal University, 194, Stachki Ave.,  
Rostov-on-Don, 344090, Russia*

<sup>2</sup>*Federal Research Centre The Southern Scientific Centre of the Russian Academy of Sciences, 41,  
Chekhov Str., Rostov-on-Don, 344006, Russia*

[tolik\\_260686@mail.ru](mailto:tolik_260686@mail.ru)

Currently, Fe-containing multiferroics with a perovskite-type structure are among the most studied objects in physical materials science. It is due to the prospects for using them in microelectronics in various solid-state conditions. The results of  $\text{PbFe}_{0.5}\text{Nb}_{0.5}\text{O}_3$  (PFN) films structure studies are presented. The thin films were prepared by RF cathode sputtering in an oxygen atmosphere. Figure 1 shows the X-ray diffraction results for  $\text{PbFe}_{0.5}\text{Nb}_{0.5}\text{O}_3/\text{Si}$  with a film thickness of 150 nm.

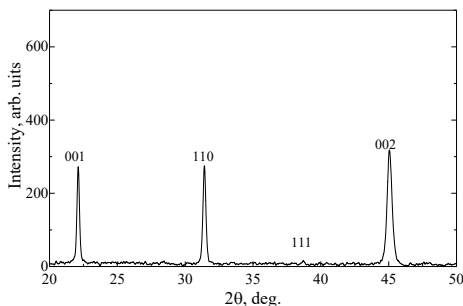


**Fig. 1.** X-ray diffraction pattern for  $\text{PbFe}_{0.5}\text{Nb}_{0.5}\text{O}_3/\text{Si}$  (001) heterostructure

It can be seen that the obtained films are single-phase, polycrystalline with a texture in the direction 001. PFN has unit cell parameters, calculated in the tetragonal approximation, of  $c = 4.023 \pm 0.001 \text{ \AA}$ ;  $a = 4.027 \pm 0.001 \text{ \AA}$  with  $h = 150 \text{ nm}$ . This indicates that deformation of the unit cell is present in the films. Deformation is associated with different unit cells parameters of the film and the substrate. Varying the film thickness in the range 75 – 150 nm practically has not been affected by change in the values of  $c$  and  $a$ .

#### **Acknowledgement**

Research was financially supported by the Ministry of Science and Higher Education of the Russian Federation (State assignment in the field of scientific activity, Southern Federal University, 2020).

## **Piezoelectric and Dielectric Properties of the NaNbO<sub>3</sub>(001)/SrRuO<sub>3</sub>(001)/MgO(001) Heterostructure**

**A.V. Pavlenko<sup>1,2\*</sup>, N.V. Ter-Oganessian<sup>1</sup>**

*<sup>1</sup>Research Institute of Physics, Southern Federal University,  
194, Stachki, Ave., Rostov-on-Don, 344090, Russia*

*<sup>2</sup>Federal Research Center the Southern Scientific Centre of the Russian Academy of Sciences, 41,  
Chekhov Str., Rostov-on-Don, 344006, Russia*

*\*[tolik\\_260686@mail.ru](mailto:tolik_260686@mail.ru)*

Currently, much attention is paid to the development of synthetic routes and electrophysical studies of thin film heterostructures of active dielectrics. This is mainly due to the prospects of their use in modern micro- and nanoelectronics. This work presents the results of a study of piezoelectric and dielectric properties of single-crystal thin NaNbO<sub>3</sub> films grown in an oxygen atmosphere on a SrRuO<sub>3</sub>(001)/MgO(001) substrate. At room temperature, NaNbO<sub>3</sub> films were characterized by average dielectric constant values of  $\epsilon/\epsilon_0 \sim 900 - 1000$ , low loss tangent  $\tan\delta \sim 0.02 - 0.11$ , and high dielectric controllability  $k = [\epsilon/\epsilon_0(0) - \epsilon/\epsilon_0(100 \text{ kV/cm})]/[\epsilon/\epsilon_0(U=0)] = 0.5$ . The measurements of the piezoelectric modulus  $d_{33}$  (Fig. 1), suggest that NaNbO<sub>3</sub> films are characterized by spontaneous polarization with a polarization component directed towards the substrate. When a positive voltage is applied to the upper electrode, polarization switching is observed at  $U \sim 20 \text{ kV/cm}$ , whereas during further increase of voltage  $d_{33}$  increases and reaches its saturation of  $\sim 100 \text{ pC}\cdot\text{N}^{-1}$  at values of  $U \sim 100 \text{ kV/cm}$ . The reasons for the appearance of a ferroelectric state in NaNbO<sub>3</sub> films as well as interpretation of the obtained results are discussed.

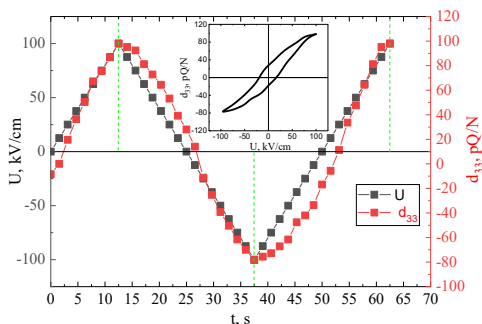


**Fig. 1.**  $d_{33}(U)$  dependence of the Al/NaNbO<sub>3</sub>/SrRuO<sub>3</sub>/MgO heterostructure

### Acknowledgement

The work was financially supported by the Russian Science Foundation, project No. 19-12-00205.

## Influence of Acid Treatment on the Functional Characteristics of PtCu/C Electrocatalysts

A. S. Pavlets<sup>1\*</sup>, A. A. Alekseenko<sup>1</sup>, N. Yu. Tabachkova<sup>2</sup>, V. E. Guterman<sup>1</sup>

<sup>1</sup>*Southern Federal University, Rostov-on-Don, Russia*

<sup>2</sup>*National University of Science and Technology "MISIS", Moscow, Russia*

\*[angelina.pavlez@mail.ru](mailto:angelina.pavlez@mail.ru)

Catalysts based on Pt-Cu nanoparticles show increased activity in oxygen reduction reaction (ORR), high electrochemically active surface area (ESA) and stability during prolonged cycling. However, it is known that during the catalyst work, copper undergoes selective dissolution from nanoparticles. Thus, for such systems, acid treatment is used, which allows one to pre-dissolve copper and its oxides from the surface of the catalyst [1]. We obtained several PtCu/C materials with a gradient structure and carried out their acid treatment as an additional step in the synthesis [2]. The composition of the catalysts is from PtCu<sub>0.34</sub> to PtCu<sub>0.39</sub>. The materials showed a high ESA from 46 to 52 m<sup>2</sup>/g (Pt), activity in ORR from 222 and to 332 A/g (Pt), and increased stability in prolonged stress testing (at least 85%). Transmission electron microscopy (TEM) is presented for one of the materials before and after acid treatment (Fig. 1). Acid treatment not only makes it possible to prevent the dissolution of copper when working in the MEA, but also to increase the specific characteristics due to the reorganization of nanoparticles.

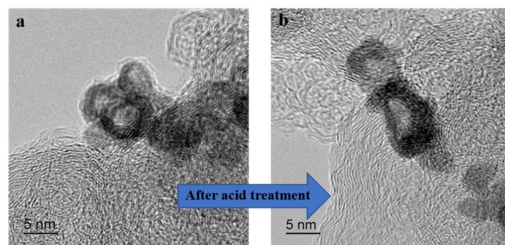


**Fig. 1.** TEM of one of the PtCu/C catalysts before (a) and after (b) acid treatment

### **Acknowledgement**

This research was financially supported by the Ministry of Science and Higher Education of the Russian Federation (State assignment in the field of scientific activity No. 0852-2020-0019).

### **References**

[1] Mani P., Srivastava R., Strasser P. // *J. Power Sources*, **196**, 666 – 673, 2011.

[2] Alekseenko A. A., Guterman V. E., Belenov S. V., Menshikov V. S., etc. // *Int. J. Hydrogen Energy*, **43**, 3676 – 3687, 2018.

## **Analysis of Process Preparation of Process Polymer Mixtures**

**D.V. Petrenko<sup>1</sup>, D. D. Fugarov<sup>1\*</sup>, O. A. Purchina<sup>1</sup>, D.A. Onyshko<sup>2</sup>**

<sup>1</sup> *Don State Technical University, Rostov-on-Don, Russia*

<sup>2</sup> *South-Russian State Polytechnic University (NPI) named after M.I.Platov, Novocheerkassk, Russia*

\*[ddf\\_1@mail.ru](mailto:ddf_1@mail.ru)

Mixing processes are widely used in the production of polymers, this is due to the fact that the polymer in its pure form is not used for the manufacture of products because it does not have characteristic properties [1]. The whole thing is that the polymer receives its characteristic properties only when various pigments, fillers, dyes and other components are added to it, namely for this mixing process is used [2]. The mixtures consist of several components, if any component in a percentage ratio exceeds the rest, then it is called a dispersed medium, and the remaining components are the dispersible phases [3]. One of the tasks is to evaluate the quality of the obtained mixture [4]. The quality assessment is carried out as follows. Several samples are taken from the mixture, but not less than ten. The main condition is the volume of samples, which should be at least 1000 times larger than the volume of the smallest particle. The main problem is that the number of particles will be different in each sample. Existing automated lines that mix polymers with different ingredients consist of various automation techniques that continuously produce blends in accordance with software-defined preparation recipes [5].

## References

- [1] Poluyan A.Y., Fugarov D.D., Purchina O.A., Nesterchuk V.V., Smirnova O.V., Petrenkova S.B. // *Journal of Physics: Conference Series "International Conference Information Technologies in Business and Industry 2018 - Microprocessor Systems and Telecommunications"*. 022013, 2018.
- [2] Fugarov D.D., Gerasimenko Y.Y., Nesterchuk V.V., Gerasimenko A.N., Onyshko D.A. // *Journal of Physics: Conference Series*. 012055, 2018.
- [3] Fugarov D.D. In: *2019 International Conference on "Physics and Mechanics of New Materials and Their Applications"*, PHENMA 2019, Hanoi, Vietnam, November 7 – 10, 2019, Hanoi University of Science and Technology: Hanoi. 119-120, 2019.
- [4] Solomentsev K.Y., Fugarov D.D., Purchina O.A., Poluyan A.Y., Nesterchuk V.V., Petrenkova S.B. // *Journal of Physics: Conference Series*. **1015**, 032179, 2018.
- [5] Y.O. Chernyshev, O.A. Purchina, A.Y. Poluyan, D.D. Fugarov, A.V. Basova, O.V. Smirnova // *Journal of Theoretical and Applied Information Technology*. **80**(1), 13-20, 2015.

## Numerical Study on Screening of Surface Waves Using a Rectangular Open Trench

A.N. Petrov\*, A.A. Belov, M.V. Grigoryev

*Research Institute for Mechanics, National Research Lobachevsky State University of Nizhny Novgorod, 23, Gagarin Avenue, Building 6, Nizhny Novgorod 603950, Russia*

\*[andrey.petrov@mech.unn.ru](mailto:andrey.petrov@mech.unn.ru)

In this work, the efficiency of the rectangular open trench in the scattering of the surface waves in the soil is studied. The influence of the trench depth on the screening effect produced by it is investigated. The soil is modeled as a fully saturated poroelastic half-space subjected to a vertical step load producing the surface waves. To analyze the problem, the three-dimensional boundary element model in the Laplace domain is used, a parametric study is carried out considering different trench depth values. The dynamic response of surface displacements in the time domain is obtained using the convolution quadrature method. The screening efficiency of the open trench is investigated by means of the index  $A_{rf}$ , which is defined as the ratio of the displacement amplitude in the case of the trench presence with respect to the displacement amplitude and in the case of its absence. Based on the numerical tests the contour diagrams of the amplitude reduction ratio  $A_{rf}$  are drawn. It is shown that the screening efficiency of the open trench is significantly governed by its depth. A more complete understanding of the resulting effects requires extensive research with various types of dynamic loads and geometries.

### **Acknowledgement**

The work was carried out with the financial support of the Ministry of Science and Higher Education of the Russian Federation (task 0729-2020-0054).

# The Investigation of the Influence of Rapid Thermal Annealing Temperature on the Formation of Cobalt Oxide Films

V.V. Petrov<sup>1</sup>, V.V. Polyakov<sup>1</sup>, Yu.N. Varzarev<sup>1</sup>, V.V. Bespoludin<sup>1\*</sup>, E.M. Bayan<sup>2</sup>

<sup>1</sup>*Institute of Nanotechnology, Electronics and Electronic Equipment Engineering, Southern Federal University, Taganrog, Russia*

<sup>2</sup>*Chemical Department, Southern Federal University, Rostov-on-Don, Russia*

\*[bespoludin@sfedu.ru](mailto:bespoludin@sfedu.ru)

Currently, metal oxides are one of the most promising materials for use as a sensitive layer in gas sensors due to a number of advantages such as: high gas sensitivity, selectivity, low cost, etc. One of such promising metal oxide materials for use in gas sensors is cobalt oxide, which has such advantages as: sensitivity to a large number of industrial gases, high selectivity, durability, i. e. ability to withstand a large number of gas injection cycles. There are two main types of cobalt oxides,  $\text{Co}_3\text{O}_4$  and  $\text{CoO}$ . Both cobalt oxides are *p*-type semiconductors [1]. The aim of this work is to determine the optimal regimes of rapid thermal annealing (RTA) by halogen lamps for the formation of cobalt oxide films. Metal cobalt films were deposited on a pre-cleaned sital substrate by vacuum-thermal spraying. The thickness of these films was  $0.5 \mu\text{m}$ . After that, the obtained cobalt films for the formation of oxides were annealed by rapid thermal annealing (RTA) using halogen lamps in air at temperatures of  $400^\circ\text{C}$ ,  $500^\circ\text{C}$ ,  $600^\circ\text{C}$  and  $700^\circ\text{C}$ . After rapid thermal annealing, the films were investigated by X-ray phase analysis. It was found that the formation of cobalt oxides does not occur at RTA temperatures of  $400^\circ\text{C}$  and  $500^\circ\text{C}$ , and peaks of metallic cobalt (111) ( $2\theta = 44.560^\circ$ ) are observed in the diffraction patterns, see Fig. 1(c) and (d). An annealing temperature of  $600^\circ\text{C}$  allows the formation of cobalt oxide. So, at RTA temperatures of  $600^\circ\text{C}$  and  $700^\circ\text{C}$ , cobalt oxide  $\text{Co}_3\text{O}_4$  is formed. It can be seen from the characteristic peaks of this oxide at angles  $2\theta$  equal to  $31.42^\circ$ ,  $37.04^\circ$ ,  $41.32^\circ$ ,  $45.02^\circ$ ,  $59.56^\circ$ ,  $65.5^\circ$ ,  $69.04^\circ$ .

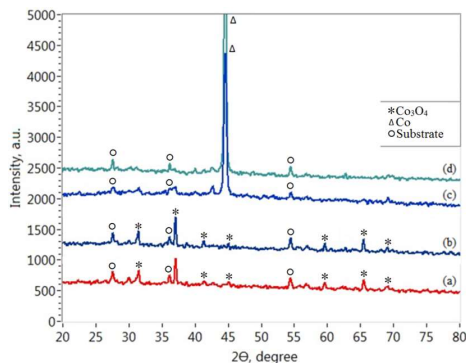


**Fig. 1.** Influence of temperature (RTA) on the formation of cobalt oxide films at annealing temperature of Co: (a)  $700^\circ\text{C}$ ; (b)  $600^\circ\text{C}$ ; (c)  $500^\circ\text{C}$ ; (d)  $400^\circ\text{C}$

Figure 1 shows that all diffractograms contain peaks of polycrystalline alumina, which is the main substrate material. The studies showed that RTA at temperatures above 600 °C allows one to form the phase of cobalt oxide (Co<sub>3</sub>O<sub>4</sub>) from metal cobalt, and a temperature below 500 °C is insufficient for the formation of cobalt oxide.

#### **References**

[1] Vishal Balouria, Arvind Kumar, S. Samanta, S. Bhattacharya, A. Singh et al. // *AIP Conf. Proc.*, **1451**, 289-291, 2012.

## **Turbulent Blood Flow in a Cylindrical Vessel with an Irregular Walls Profile**

**T.A. Petrukhina\*, N.M. Polyakova**

*Southern Federal University, Rostov-on-Don, Russia*

\*[tatjana.petrukhina2013@yandex.ru](mailto:tatjana.petrukhina2013@yandex.ru)

The problem of stationary turbulent rotationally symmetric flow of a liquid in an infinite cylindrical vessel with irregular walls is considered. The asymptotic model of the process based on the Navier-Stokes equations for a viscous incompressible liquid is constructed. The kinematic viscosity of a liquid depends on the axial and radial coordinates. It is also assumed that on the side surface of the cylinder, the viscosity is zero. The non-slip condition of liquid on non-linear sections of boundary is replaced by Navier boundary conditions, namely the tangent velocity at the boundary is proportional to the tangent stress. On straight sections of the boundary, the usual non-slip condition is maintained. At high values of the average axial velocity, wall vortices are formed in the neighborhood of the irregular walls. For quasi-stationary problem, when the pressure gradient depends on time, a change in the pressure gradient causes a rearrangement of the vortex structures. The model does not contain the nonlinear and inertial terms. It allows us to obtain an analytical solution describing the liquid flow. The finite element method is used for numerical investigation of impurity transport in a given quasi-stationary liquid flow. The main attention in the calculations is focused on the case of the boundaries with small periodic roughness, when the average boundary is straight and the non-slip condition is valid on the averaged boundary (but not on the roughness). For a blood vessel, both the case of the passive impurity transport (blood clots) and the case of an impurity interacting with the vessel walls (parietal blood clots) are considered. Various mechanisms of impurity interaction with walls are proposed and investigated.

#### **Acknowledgement**

Research was financially supported by Southern Federal University, grant No. VnGr-07/2020-04-IM (Ministry of Science and Higher Education of the Russian Federation).



## Waste Water Treatment in Reservoir Pressure Support Systems

A.E. Pianov, D. D. Fugarov\*, O. A. Purchina, N.V. Rasteryaev

\*[ddf\\_1@mail.ru](mailto:ddf_1@mail.ru)

Specialists working in the field of water treatment at power plants deal mainly with fresh water, relatively clean, with a low content of petroleum products and mechanical impurities [1]. In oil and gas production, water is supplied to water treatment facilities much more complex from the viewpoint of both composition and purification technologies [2]. These are highly mineralized waters of oil-bearing horizons, often with a large amount of sand or proppant particles, and the so-called "commodity" water, characterized, in addition to mineralization, by a high content of mechanical impurities (mainly ferromagnetic particles) and petroleum products [3]. Corrosion damage to which metal of pipes and equipment is subjected in this case causes not only corrosive aggressiveness of the liquid itself, but also abrasive wear caused by mechanical impurities [4]. In general, the following measures are needed to protect the environment from reservoir water pollution: (i) ensuring the deep treatment of field wastewater; (ii) wide use of anticorrosive coatings and chemical reagents for corrosion protection of oil-producing equipment; (iii) full use of waste water produced in the fields in the reservoir pressure maintenance system; (iv) monitoring of surface water condition and quality of waste water used in formation pressure maintenance system [5].

### References

- [1] Poluyan A.Y., Fugarov D.D., Purchina O.A., Nesterchuk V.V., Smirnova O.V., Petrenkova S.B. // *Journal of Physics: Conference Series "International Conference Information Technologies in Business and Industry 2018 - Microprocessor Systems and Telecommunications"*. 022013, 2018.
- [2] Fugarov D.D., Gerasimenko Y.Y., Nesterchuk V.V., Gerasimenko A.N., Onyshko D.A. // *Journal of Physics: Conference Series*. 012055, 2018.
- [3] Fugarov D.D. In: *2019 International Conference on "Physics and Mechanics of New Materials and Their Applications"*, PHENMA 2019, Hanoi, Vietnam, November 7 – 10, 2019, Hanoi University of Science and Technology: Hanoi. 119-120, 2019.
- [4] Solomentsev K.Y., Fugarov D.D., Purchina O.A., Poluyan A.Y., Nesterchuk V.V., Petrenkova S.B. // *Journal of Physics: Conference Series*. **1015**, 032179, 2018.
- [5] Y.O. Chernyshev, O.A. Purchina, A.Y. Poluyan, D.D. Fugarov, A.V. Basova, O.V. Smirnova // *Journal of Theoretical and Applied Information Technology*. **80**(1), 13-20, 2015.

# Random Vortex Method for Modelling Flow of Viscous Incompressible Fluid in Bounded Regions

A. S. Piskunov\*, Yu. E. Drobotov\*\*

*Southern Federal University, Rostov-on-Don, Russia*

\*[andrey91y@yandex.ru](mailto:andrey91y@yandex.ru), \*\*[yu.e.drobotov@yandex.ru](mailto:yu.e.drobotov@yandex.ru)

The problem on viscous incompressible flow is considered for a bounded region. The Navier–Stokes equations with vorticity are studied, and the Lagrangian specification of the flow field is used to apply the random vortex method [1 – 4], which accelerates computations in comparison with analytical and grid ones. Thus, the movement of a vortex particle in a channel in the Cartesian coordinates is expressed as

$$\begin{aligned}x_i(t + \Delta t) &= x_i(t) + v_{x,i} \Delta t + r_i \cos \theta, \\y_i(t + \Delta t) &= y_i(t) + v_{y,i} \Delta t \sin \theta,\end{aligned} \quad i = 1, \dots, N_k + M, \quad k = 1, \dots, K,$$

where  $\theta$  is a random number from the set of uniformly distributed over the interval  $(0; 2\pi)$ ,  $N_k$  is the amount of the liquid particles in the channel for the  $k$ -th iteration,  $\Delta t$  is the time step for the iteration,  $K$  is the number of iterations and  $M$  is the number of liquid particles at the boundary of the channel. An important feature of the research is calculating a Green's function for the Navier–Stokes equations. The one modifies key parameters of the random vortex algorithm significantly, if the boundary conditions in the problem are considered within a nontrivial geometry.

## **Acknowledgement**

Research was financially supported by Southern Federal University, grant No. VnGr-07/2020-04-IM (Ministry of Science and Higher Education of the Russian Federation).

## **References**

- [1] Kostecki S. W. // *Studia Geotechnica et Mechanica*. **XXXVI**(4), 57–63, 2014.
- [2] Kostecki S. W. // *Archives Civil Mech. Eng.*, **8**(3), 73–89, 2008.
- [3] Lewis R. I. // *J. Mech. Eng. Sci.* **23**, 1–12, 1981.
- [4] Sumbatyan M. A., Piskunov A. S. In: *Proceedings of XIX International Conference “Modern Problems of Continuum Mechanics”*, Southern Federal University, Rostov-on-Don, **2**, 228–232, 2018.

## **Applying Artificial Intelligence Techniques to Redistribute Connections between Outputs**

**O. A. Purchina<sup>1</sup>, D. D. Fugarov<sup>1\*</sup>, S.R. Cherenok<sup>1</sup>, D.A. Onyshko<sup>2</sup>**

<sup>1</sup>*Don State Technical University, Rostov-on-Don, Russia*

<sup>2</sup>*M.I. Platov South-Russian State Polytechnic University (NPI), Novocherkassk, Russia*

[\\*ddf\\_1@mail.ru](mailto:ddf_1@mail.ru)

Redistribution of connections between outputs is possible if the outputs are functionally equivalent [1]. The purpose of the redistribution is to reduce the density of the routing areas, reduce the length of the connections, reduce the number of intersections, increase the degree of integration, etc. [2]. Advantages of the ant colony method include guaranteed convergence to the optimal solution and a higher rate of finding the optimal solution than traditional methods. Shortcomings consist in that the result of the method depends quite strongly on the initial search parameters, which are selected experimentally, as well as the absence of a detailed study of the search space [3]. Paper [4] describes a method of solving the problem of distribution of connections between outputs, based on modeling of collective alternative adaptation. Experimental studies have shown that the use of the algorithm gives a significant decrease in the initial density of the channel, the total length of horizontal fragments and the total number of irreducible intersections of connections with each other [2].

### **References**

- [1] Poluyan A.Y., Fugarov D.D., Purchina O.A., Nesterchuk V.V., Smirnova O.V., Petrenkova S.B. // *Journal of Physics: Conference Series*, **1015**, 022013, 2018.
- [2] Fugarov D.D., Gerasimenko Y.Y., Nesterchuk V.V., Gerasimenko A.N., Onyshko D.A. // *Journal of Physics: Conference Series*, **1015**, 012055, 2018.
- [3] Solomentsev K.Y., Fugarov D.D., Purchina O.A., Poluyan A.Y., Nesterchuk V.V., Petrenkova S.B. // *Journal of Physics: Conference Series*, **1015**, 032179, 2018.
- [4] Chernyshev Y.O., Purchina O.A., Poluyan A.Y., Fugarov D.D., Basova A.V., Smirnova O.V. // *Journal of Theoretical and Applied Information Technology*, **80**(1), 13-20, 2015.

## **Algorithm for Redistribution of Connections between Outputs**

**O. A. Purchina<sup>1</sup>, D. D. Fugarov<sup>1\*</sup>, A.V. Fedorov<sup>1</sup>, D.A. Onyshko<sup>2</sup>**

<sup>1</sup>*Don State Technical University, Rostov-on-Don, Russia*

<sup>2</sup>*M.I. Platov South-Russian State Polytechnic University (NPI), Novocherkassk, Russia*

[\\*ddf\\_1@mail.ru](mailto:ddf_1@mail.ru)

Redistribution of connections between outputs is possible if the outputs are functionally equivalent [1]. As an estimate of the length of the chain, a rectangle semiperimeter describing the contacts

connected by the chain is used, instead of using the total conductor length criterion, relying on topology-independent trace modeling (TP-free), a target function is used to more accurately estimate the cluster of conductors [2]. The switching network is broken down into an ordered set of areas, each of which is part of the next-in-order area [3]. Recently, methods based on the application of artificial intelligence methods have been increasingly used to solve various "complex" problems, which include problems of distribution (or attachment) of circuits behind outputs [4]. Especially there is a rapid growth of interest in the development of algorithms inspired by natural systems [3].

#### **References**

- [1] Chernyshev Y.O., Purchina O.A., Poluyan A.Y., Fugarov D.D., Basova A.V., Smirnova O.V. // *Journal of Theoretical and Applied Information Technology*, **80**(1), 13-20, 2015.
- [2] Poluyan A.Y., Fugarov D.D., Purchina O.A., Nesterchuk V.V., Smirnova O.V., Petrenkova S.B. // *Journal of Physics: Conference Series*, **1015**, 022013, 2018.
- [3] Fugarov D.D., Gerasimenko Y.Y., Nesterchuk V.V., Gerasimenko A.N., Onyshko D.A. // *Journal of Physics: Conference Series*, **1015**, 012055, 2018.
- [4] Solomentsev K.Y., Fugarov D.D., Purchina O.A., Poluyan A.Y., Nesterchuk V.V., Petrenkova S.B. // *Journal of Physics: Conference Series*, **1015**, 032179, 2018.

## **Search Procedure Based on Modelling Collective Alternative Adaptation**

**O. A. Purchina<sup>1</sup>, D. D. Fugarov<sup>1\*</sup>, S. O. Lagoyda<sup>1</sup>, D. A. Onyshko<sup>2</sup>**

<sup>1</sup>*Don State Technical University, Rostov-on-Don, Russia*

<sup>2</sup>*M.I. Platov South-Russian State Polytechnic University (NPI), Novocherkassk, Russia*

\*[ddf\\_1@mail.ru](mailto:ddf_1@mail.ru)

Adaptation is the ability of a living organism or technical system to change its state and behavior (parameters, structure, algorithm and functioning) depending on the change in environmental conditions by accumulating and using information on it [1]. The process of search adaptation has the following many-stage character, at each stage of which the adapting effect on the object is determined, increasing its efficiency and optimizing quality criteria. Initial connection to outputs is given [2]. On each iteration under the action of adaptive action group, re-switching of units is performed, which does not change logical function of circuit [3]. As a model of the learning system, Cetlin M.L. proposed a probabilistic learning machine called an adaptation machine. The state of the adaptation machine corresponds to some alternative of adaptive effect on the object [2]. In the process of adaptation based on the responses of the external environment, the machine changes to the state corresponding to the best alternative of adaptive action on the object [4].

#### **References**

- [1] Solomentsev K.Y., Fugarov D.D., Purchina O.A., Poluyan A.Y., Nesterchuk V.V., Petrenkova S.B. // *Journal of Physics: Conference Series*, **1015**, 032179, 2018.
- [2] Fugarov D.D., Gerasimenko Y.Y., Nesterchuk V.V., Gerasimenko A.N., Onyshko D.A. // *Journal of Physics: Conference Series*, **1015**, 012055, 2018.
- [3] Poluyan A.Y., Fugarov D.D., Purchina O.A., Nesterchuk V.V., Smirnova O.V., Petrenkova S.B. // *Journal of Physics: Conference Series*, **1015**, 022013, 2018.

[4] Chernyshev Y.O., Purchina O.A., Poluyan A.Y., Fugarov D.D., Basova A.V., Smirnova O.V. // *Journal of Theoretical and Applied Information Technology*, **80**(1), 13-20, 2015.

## **Application of Hybrid Immune Algorithms to Solve Fuzzy Optimization Problems**

**O. A. Purchina<sup>1</sup>, A.Y. Poluyan<sup>1</sup>, D. D. Fugarov<sup>1\*</sup>, D.A. Onyshko<sup>2</sup>**

<sup>1</sup>*Don State Technical University, Rostov-on-Don, Russia*

<sup>2</sup>*M.I. Platov South-Russian State Polytechnic University (NPI), Novocherkassk, Russia*

[\\*ddf\\_1@mail.ru](mailto:ddf_1@mail.ru)

The main purpose of the study is to develop effective methods and algorithms based on the principles of hybrid operation of the immune system and evolutionary search to determine a global optimal solution for optimization problems [1]. It is proposed to use the integration of modified evolutionary algorithms and immune algorithms to solve the problem [2]. There is no precise method for effectively solving fuzzy optimization problems in polynomial time. However, evolutionary bionic methods proved to be suitable for solving these problems by determining close to optimal solutions in acceptable time [3]. The hybrid algorithm is able to provide multiple solutions that represent a trade-off between multiple goals. Very little research has focused on optimizing more than one goal, and even lesser studies had a clearly considered variety of solutions that is crucial to the good performance of any evolutionary calculation method [3, 4].

### **References**

- [1] Poluyan A.Y., Fugarov D.D., Purchina O.A., Nesterchuk V.V., Smirnova O.V., Petrenkova S.B. // *Journal of Physics: Conference Series*, **1015**, 022013, 2018.
- [2] Solomentsev K.Y., Fugarov D.D., Purchina O.A., Poluyan A.Y., Nesterchuk V.V., Petrenkova S.B. // *Journal of Physics: Conference Series*, **1015**, 032179, 2018.
- [3] Fugarov D.D., Gerasimenko Y.Y., Nesterchuk V.V., Gerasimenko A.N., Onyshko D.A. // *Journal of Physics: Conference Series*, **1015**, 012055, 2018.
- [4] Chernyshev Y.O., Purchina O.A., Poluyan A.Y., Fugarov D.D., Basova A.V., Smirnova O.V. // *Journal of Theoretical and Applied Information Technology*, **80**(1), 13-20, 2015.

# Chemical Ordering, Magnetic and Ferroelectric Phase Transitions in Multiferroic $\text{BiFeO}_3 - A\text{Fe}_{1/2}\text{Sb}_{1/2}\text{O}_3$ ( $A = \text{Pb, Sr}$ ) Solid Solution Ceramics Fabricated by a High-pressure Synthesis

S.I. Raevskaya<sup>1</sup>, N.M. Olekhovich<sup>2</sup>, A.V. Pushkarev<sup>2</sup>, Y.V. Radyush<sup>2</sup>, S.P. Kubrin<sup>1</sup>, V.V. Titov<sup>1</sup>, E.A. Artseva<sup>1</sup>, I.P. Raevski<sup>1\*</sup>, S.I. Shevtsova<sup>1,3</sup>, C-C. Chou<sup>4</sup>, M.A. Malitskaya<sup>1</sup>

<sup>1</sup>Research Institute of Physics and Faculty of Physics, Southern Federal University, 344090, Rostov-on-Don, Russia

<sup>2</sup>Scientific-Practical Materials Research Centre of NAS of Belarus, 220072, Minsk, Belarus

<sup>3</sup>Institute of Earth Sciences, Southern Federal University, 344090, Rostov-on-Don, Russia

<sup>4</sup>National Taiwan University of Science and Technology, Taipei, 106, Taiwan

\*[igorraevsky@gmail.com](mailto:igorraevsky@gmail.com)

Ceramic samples of  $(1-x)\text{BiFeO}_3 - x\text{PbFe}_{1/2}\text{Sb}_{1/2}\text{O}_3$  and  $(1-x)\text{BiFeO}_3 - x\text{SrFe}_{1/2}\text{Sb}_{1/2}\text{O}_3$  solid solutions with a perovskite structure were obtained using high-pressure synthesis at 6 GPa. Room temperature Mössbauer spectra of the compositions with  $0.6 \leq x \leq 1$  show the quadrupole-split lines. For compositions with  $0.8 \leq x \leq 1$  a singlet component, being a fingerprint of the Fe and Sb ordering [30], was present as well, its intensity being increased as  $x$  grows. Dielectric studies, corresponding to the ferroelectric phase transition, strongly deviates downward from a straight line, connecting the  $T_m$  values of the end components of the solid solution. Such type of  $T_m(x)$  dependence is typical for binary solid solutions having as one of the components highly chemically  $B$ -site ordered double perovskite [1, 2]. Magnetic phase transition temperatures  $T_N$  of  $(1-x)\text{BiFeO}_3 - x\text{PbFe}_{1/2}\text{Sb}_{1/2}\text{O}_3$  compositions with  $0.6 \leq x \leq 1$  are substantially lower than those of  $(1-x)\text{BiFeO}_3 - x\text{PbFe}_{1/2}\text{Nb}_{1/2}\text{O}_3$  ones with the same  $x$  values. This difference seems to be due to the chemical ordering of  $\text{Fe}^{3+}$  and  $\text{Sb}^{5+}$  ions as the ordering lowers the number of the Fe-O-Fe bonds which determine the  $T_N$  value [3]. As both X-ray diffraction and Mössbauer studies have shown that long-range chemical ordering of these ions is observed only for compositions with  $x \geq 0.9$ , the ordering is believed to realize at the nanoscale (short-range or local ordering). These data show the possibility of tailoring the  $T_N$  values of multiferroic solid solutions by changing the chemical ordering degree of  $B$ -site ions. The  $T_N$  values of  $(1-x)\text{BiFeO}_3 - x\text{SrFe}_{1/2}\text{Sb}_{1/2}\text{O}_3$  compositions are lower than those of  $(1-x)\text{BiFeO}_3 - x\text{PbFe}_{1/2}\text{Sb}_{1/2}\text{O}_3$  ones with the same  $x$  values. This difference is presumably due to the possibility of additional magnetic superexchange between  $\text{Fe}^{3+}$  ions via the empty  $6p$  states of  $\text{Bi}^{3+}$  and  $\text{Pb}^{2+}$  ions in the latter solid solution [4, 5].

## Acknowledgements

This study was funded by the Russian Foundation for Basic Research (Grants 18-52-00029, and 20-52-00045) and Belarusian Republican Foundation for Fundamental Researches (Grants T18R-048 and T20R-169).

## References

- [1] K. Uchino, S. Nomura // *Jpn. J. Appl. Phys.* **18**, 1493, 1979.
- [2] X. Yang, C. Wang, F. Zhuo, et al // *Mater. Design.* **183**, 108168, 2019.
- [3] M. A. Gille // *J. Phys. Chem. Sol.* **13**, 33, 1960.

[4] R. De Sousa, M. Allen, M. Cazayous // *Phys. Rev. Lett.* **110**, 267202, 2013.

[5] I. P. Raevski, S. P. Kubrin, S. I. Raevskaya et al // *Phys. Rev. B*, **80**, 024108, 2009.

## Effect of Driving Torque on Interfacial Creep Generation for Shrink-fitted Bimetallic Work Roll Considering Elastic Deformation of Shaft

Rahimah Abdul Rafar\*, Nao-Aki Noda, Xuchen Zheng, Hiroyuki Tsurumaru, Yudai Taruya, Yoshikazu Sano

*Department of Mechanical Engineering, Kyushu Institute of Technology, Kitakyushu, Japan*

\*[eimah7178@gmail.com](mailto:eimah7178@gmail.com)

Various metallic rolls are used in the rolling line of the steelworks, for example, rolling roll, pickling roll, plating roll, sink roll and steel sheet transporting roll. Since those rolls are usually operated consecutively, wear and roughness always appear on the roll surface. After the abrasion, most of the conventional solid type rolls must be replaced totally since the shaft and body are integrated. However, if the body and the shaft are formed into a jointed structure for example shrink-fitted structure, only the worn body portions are required to be replaced. Regarding a shrink-fitted construction type, the interfacial creep sometimes appears between the shaft and the shrink-fitted sleeve. This interfacial creep can be regarded as the relative displacement between the sleeve and the shaft, which often causes the roll damage. In the previous study, the FEM simulation is performed to clarify the effect of driving torque on the interfacial creep by considering the driving motor torque. In this paper, the FEM analysis of the effect of driving torque on the interfacial creep is performed by changing the shaft from a rigid body to an elastic body.

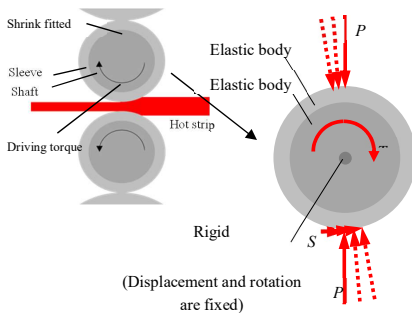


**Fig.1.** Modelling of FEM2D model

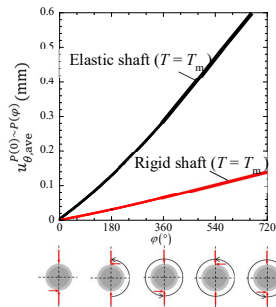


**Fig. 2.** Comparison of history of mean displacements for rigid shaft ( $T = T_m$ ) and elastic shaft ( $T = T_m$ )

Fig. 1 shows the numerical simulation model used in this study. Fig 2 shows the relationship between the load shift angle  $\phi$  and the average interface displacement  $u_{\theta,ave}^{P(0) \sim P(\phi)}$ . From Fig. 2, it is

found that the relative displacement in the interfacial creep is accelerated by the presence of the motor torque significantly. The effects of motor drive torque on the displacement and average displacement along the interface were also discussed by varying the motor torque.

## Microaccelerometer Based on Self-organizing Semiconductor Heterostructures

A. Sh. Rakhmatulin\*, V. D. Popov

*Southern Federal University, Department of Construction and Technology of Electronic Devices,  
347922, Taganrog, Russia*

[\\*rahmatulin@sfnedu.ru](mailto:*rahmatulin@sfnedu.ru)

The use of accelerometers is increasing every year, both in consumer electronics from toys to smartphones, and in the industrial field, for example, space satellites, rockets and military equipment in general, due to the relatively small price, small size and low power consumption. In this paper, we consider the development (see Fig. 1) and simulation of a tunnel-type micromechanical accelerometer.

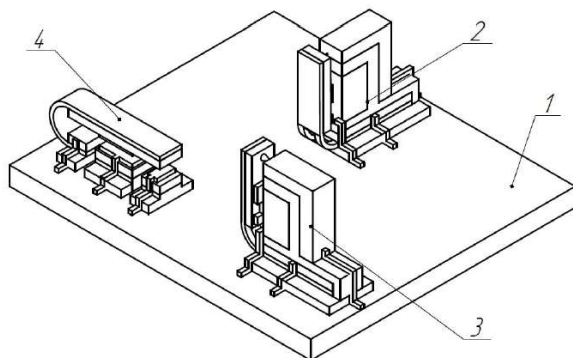


**Fig. 1.** Structure of three-axis accelerometer: (1) silicon substrate; (2) sensor, measuring  $X$ -deviation; (3) sensor that measures the deviation along  $Y$ -axis; (4) sensor, measuring deviation in  $Z$ -axis

A feature of the proposed sensor is a design that includes a nanoscale displacement transducer based on the tunnel effect, as well as a technological manufacturing route, including a self-assembly operation based on controlled self-organization of mechanically strained Ga/As and In/As semiconductor heterostructures. Distinctive features of the proposed design are: (i) the possibility of its integral production by group processing methods using standard technological operations; (ii) the possibility of precision formation of a tunneling contact with a gap of the order of a few nanometers; (iii) the possibility of incorporating into the structure of a functionally and



technologically integrated calibration system and accelerometer signal processing circuitry, recording linear acceleration on all planes, high precision design. The integrated circuit provides a signal pick-up, its amplification and processing, followed by transmission in analog or digital form. Based on the results of modeling the developed structure, a high sensitivity of the structure was determined, which can predetermine its use. A conclusion was drawn about the possible construction of this structure on an industrial scale. It was obtained that when applying acceleration on one axis, then offsets on the other axes almost never happen. This fact suggests that the structure of the accelerometer is noise immunity. For example, highly sensitive microelectromechanical accelerometers can be used in some special areas, in particular for monitoring seismic activity, as well as for registering microvibrations in high-precision industries.

### **Nitrate Graphite Co-intercalated with Carboxylic Acids: Structural Reorganization and Carbon Nanoparticles Obtaining**

**E.V. Raksha<sup>1\*</sup>, A.A. Davydova<sup>1</sup>, Yu.V. Berestneva<sup>2\*\*</sup>, O.N. Oskolkova<sup>1</sup>, P.V. Sukhov<sup>1</sup>,  
V.A. Glazunova<sup>3</sup>, G.K. Volkova<sup>3</sup>, V.V. Gnatovskaya<sup>1</sup>, O.M. Padun<sup>1</sup>,  
M.V. Savoskin<sup>1</sup>, I.A. Verbenko<sup>4</sup>, Yu.I. Yurasov<sup>4,5</sup>**

<sup>1</sup>*L.M. Litvinenko Institute of Physical Organic and Coal Chemistry, Donetsk, 283114, Ukraine*

<sup>2</sup>*Federal Scientific Centre of Agroecology, Complex Melioration and Protective Afforestation of the Russian Academy of Sciences, 97, Universitetskij prospekt, Volgograd, 400062, Russia*

<sup>3</sup>*Donetsk Institute for Physics and Engineering named after A.A. Galkin, Donetsk, Ukraine*

<sup>4</sup>*Research Institute of Physics, Southern Federal University, Rostov-on-Don, Russia*

<sup>5</sup>*Southern Scientific Centre RAS, Rostov-on-Don, Russia*

\*[elenaraksha411@gmail.com](mailto:elenaraksha411@gmail.com); \*\*[berestnevayuv@mail.ru](mailto:berestnevayuv@mail.ru)

Synthesis of graphite nitrate co-intercalation compounds (GNCCs) with a variety range of organic compounds makes it possible to control the stability/lability of the GNCCs that is promising for the further production of carbon nanoparticles based on them. Structural characteristics of the obtained GNCCs with carboxylic acids were determined from X-ray patterns of GNCCs samples. Noticeable structural reorganization of the GNCC with acetic acid was observed by XRPD method (Fig. 1). Additional information on the behavior of GNCCs with carboxylic acids and esters in a solvent medium used for their liquid-phase exfoliation, and possible competition of organic cointercalants during the GNCCs formation was obtained by NMR <sup>1</sup>H spectroscopy. We have demonstrated the possibility of graphene-like particles as well as nanoscrolls obtaining by liquid phase exfoliation of the GNCCs assisted with sonication (Fig. 2). Planar sizes of the as-prepared few-layer graphenes reached several tens of μm according to TEM data (Fig. 2). The length and diameter of nanocrolls formed in the system varies over a wide range.

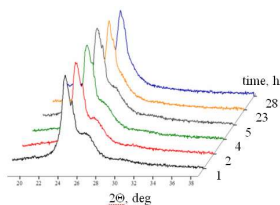


**Fig. 1.** X-ray patterns of the GNCC with acetic acid at different intervals after synthesis

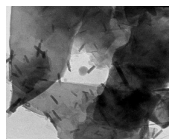
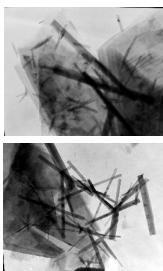


**Fig. 2.** Representative TEM images of carbon nanoparticles, obtained by sonication of the GNCC with acetic acid in ethanol

### **Acknowledgement**

The work was supported by the Ministry of Education and Science of the Russian Federation: projects №№ 3.6371.2017/8.9, 3.6439.2017/8.9 (the basic part of the state task).

## **Problems of Hydrothermal Synthesis of Sodium Bismuth Titanate**

**E. A. Reshetnikova\*, I. V. Lisnevskaya, A. I. Terekhin**

*Faculty of Chemistry, Southern Federal University,  
7, Zorge Str., Rostov-on-Don, 344090, Russia*

\*[brightc@yandex.ru](mailto:brightc@yandex.ru)

We have studied phase formation processes during sodium bismuth titanate,  $\text{Na}_{0.5}\text{Bi}_{0.5}\text{TiO}_3$  (NBT), synthesis under hydrothermal conditions at a temperature of 230 °C for 24 and 48 h using stoichiometric mixtures of titanium oxide and bismuth hydroxide and NaOH solutions in the concentration range 5–30 M [1]. The results demonstrate that, at sodium hydroxide concentrations in the range  $\leq 10$  M, there is almost no reaction between the starting reagents. In the concentration range 10–15 M, two-phase products are formed, containing a perovskite-like phase and the  $\text{Bi}_{12}\text{Ti}_{20}$  bismuth titanate. Single-phase samples with the perovskite structure are formed at NaOH concentrations from 18 to 20 M, but their composition differs considerably from the stoichiometric one ( $\text{Na}_{0.61-0.69}\text{Bi}_{0.39-0.31}\text{Ti}_{2.89-2.81}\delta_{0.11-0.19}$ , where  $\delta$  stands for an oxygen vacancy). In the NaOH concentration range 22–30 M, first partial and then complete  $\text{Bi}^{3+}$  dissolution occurs. Increasing the synthesis time helps to stabilize the perovskite phase. The single-phase NBT ceramics have resistivity of  $1.3 \times 10^9 \Omega\cdot\text{cm}$ , dielectric permittivity  $\epsilon/\epsilon_0 = 360$ , dielectric loss tangent  $\tan \delta = 0.15$ , longitudinal electromechanical coupling coefficient  $K_p = 0.068$ , piezoelectric charge coefficients  $d_{31} = 6.7 \text{ pC/N}$  and  $d_{33} = 9 \text{ pC/N}$ , and piezoelectric voltage coefficients  $g_{31} = 2.07 \text{ mV}\cdot\text{m/N}$  and  $g_{33} = 2.84 \text{ mV}\cdot\text{m/N}$ . The relatively low piezoelectric performance of the ceramics is obviously due to the imperfect structure of the synthesized phases.

### **Reference**

[1] E. A. Reshetnikova, I. V. Lisnevskaya, A. I. Terekhin // *Inorganic Materials*, 56(1), 83–90, 2020.

## Use of Mathematical Methods in Hydrochemical Researches of Natural Waters

A.N. Reshetnyak<sup>1\*</sup>, O.S. Reshetnyak<sup>1,2\*\*</sup>

<sup>1</sup>*Southern Federal University, Rostov-on-Don, Russia*

<sup>2</sup>*Hydrochemical Institute of Roshydromet, Rostov-on-Don, Russia*

\*[reshetnyak\\_a\\_n@mail.ru](mailto:reshetnyak_a_n@mail.ru), \*\*[osreshetnyak@sfedu.ru](mailto:osreshetnyak@sfedu.ru)

The formation of the chemical composition of natural waters is influenced by a large number of factors (natural and man-made) of different strength and orientation. For this reason the currently available hydrochemical information characterizing the quality of water may be heterogeneous. In general, the variational series of water quality data are numerous, so is difficult to reveal any regularity of their variation. On the one hand, the series of hydrochemical data have all the properties of statistical aggregates, on the other hand, they have a number of specific features. Mostly hydrochemical data have the properties of non-equidistance (uneven sampling), heterogeneity (due to changes in chemical analysis methods or observation conditions and the formation of the chemical composition of natural waters) and temporal non-stationarity (daily, annual fluctuations as well as longer periodic processes known as the hydrochemical regime of rivers). Typically, samples of hydrochemical data are rarely subject to the law of normal distribution, with the exception of individual chemicals. Therefore, it is necessary to use the methods of nonparametric statistics in the statistical processing of data. One of the stages of data processing should be a check for the normality of distribution according to one of the widely used criteria (Smirnov, Kolmogorov-Smirnov, etc.) and the selection of genetically homogeneous aggregates accounting the processes that determine the chemical composition of natural waters, primarily, accounting hydrological phases. Violation of the normality of the distribution of hydrochemical data introduces a restriction on the use of a number of standard statistical estimates (calculation of arithmetic mean, geometric mean, span, variance, etc.), traditionally used in the analysis of long-term observation data. For the correct statistical analysis of hydrochemical data in case of distribution deviations from the normal law or the unknown distribution law as well as with short samples it is recommended to use the so-called robust, or stable (noise-resistant) approaches. According to Huber, they can be divided into approaches based on the use of L-, R-, and M-estimates. The L-estimates are linear combinations of ordinal statistics (median, truncated average, winsorized average, etc.). R-estimates are determined using rank statistics, M-estimates are determined similarly to the maximum likelihood method using various weighting functions. The use of the maximum likelihood principle originates from the works of D.A. Rodionova in the classification of geological objects. This approach implies the selection of homogeneous groups when there are more than two data sets. Further, multidimensional grouping methods have been developed and the grouping method widely used in recent years is formulated in such a way that the separation of the initial heterogeneous population into homogeneous groups is carried out by dichotomous division. The consistent application of the rule for checking the stability of intergroup boundaries allows us to eliminate erroneous delimitations. When one needs for processing large arrays of heterogeneous data the use of multidimensional statistics can serve as an auxiliary procedure that automates the collection and generalization of primary information, presents it in a compact form, classifies it, and filters out gross errors, and highlights the main factors. The principal

component method helps researchers to cope with these tasks. Using of the principal component method allows one to obtain mathematical models without loss of information content up to the stage of modeling hydrochemical processes.

#### ***Acknowledgement***

The study was conducted as part of the work of the Student Scientific Society “Modern Problems of Environmental Geochemistry” at the Institute of Earth Sciences, SFedU.

## **Eco-friendly Electric Tourism Boat Design for Prone Rivers. Case Study: at Kalimas River, Surabaya, Indonesia**

**R. A. Retno Hastijanti<sup>1\*</sup>, M. Bayu Abisatya<sup>2</sup>**

*<sup>1</sup>Architecture Department, University of 17 Agustus 1945 (UNTAG) Surabaya, Indonesia*

*<sup>2</sup>Design and Construction Department, Surabaya State Polytechnic of Shipping, Indonesia*

*\*[retnohasti@untag-sby.ac.id](mailto:retnohasti@untag-sby.ac.id)*

Surabaya is one of the biggest metropolitan cities in Indonesia, it has scarcest natural beauty, therefore to increase tourism in the city, it must be improved by urban tourism. Currently the city of Surabaya has a river boat tour of the Kalimas river, which has the potential to be developed into one of the main attractions of tourism in the city of Surabaya, currently the ship used for the Kalimas river tourism is conventional power boat, where they use gasoline-powered outboard engines, capable of polluting the river ecosystem. The current battery's and electric outboard motors technology are experiencing rapid technological advances which have the ability to compete. In order to replace conventional outboard engines, and also be more environmentally friendly, there is a necessity in waters that have fragile ecosystems such as the Kalimas river. The design and survey results can be determined that the designed ship is capable of carrying 20 visitors and from that the tour boat will have a length of 12 meters, a width of 3 meters, and a draft of 0.37 meters, The electric motor used is Torqeedo deep blue 25 RLX with maximum output power 17 kWh, and for an operational duration of 4 hours is equipped with battery module capacity of 31 kWh. To determine the stability of the ship, a stability analysis was carried out using IMO Intact Stability A.749 (18) and good running results were obtained, as well as calculating the estimated production costs of electrically powered tourist boats to be efficient.

## Turing Instability in the Gierer-Meinhardt System

S.V. Revina<sup>1,2\*</sup>, A.S. Ryabov<sup>2\*\*</sup>

<sup>1</sup>*Southern Mathematical Institute of the Vladikavkaz Scientific Center of the Russian Academy of Sciences, Vladikavkaz, Russia*

<sup>2</sup>*I. I. Vorovich Institute for Mathematics, Mechanics and Computer Sciences, Southern Federal University, Rostov-on-Don, Russia*

\*[svrevina@sfedu.ru](mailto:svrevina@sfedu.ru), \*\*[calling-windows@yandex.ru](mailto:calling-windows@yandex.ru)

At the present time, a significant attention is given to the analysis of nonlinear parabolic systems, called reaction-diffusion systems. These partial differential equations have found a wide range of practical applications in theoretical biology, chemistry, physiology. In this paper, we consider the classical Gierer-Meinhardt system, which is an activator - substrate system and, in particular, describes the process of regeneration of parts of the hydra body. It is assumed that the system is considered in an arbitrary bounded domain, on the boundary of which the Neumann boundary conditions are satisfied. As the parameters change, spatially inhomogeneous structures with complex behavior resulting from bifurcations born in such systems. Of particular importance are spatially inhomogeneous solutions of the reaction-diffusion equations arising from spatially homogeneous solutions in the result of diffusion instability. The mechanism of diffusion instability was proposed by A. Turing in 1952 to describe the process of morphogenesis. Later, the term "Turing instability" was used for diffusion instability in reaction-diffusion systems. The equilibrium position of a system of partial differential equations is called Turing unstable, if it is stable for the system in the diffusionless approximation, but loses stability in the presence of diffusion. The region in the parameter space of the system in which the Turing instability occurs is called the Turing instability region. Despite the large number of publications on Turing instability in reaction-diffusion systems, many problems remain unexplored. As a rule, only the region of necessary Turing instability conditions is analytically investigated, while numerical methods are used to construct the region of sufficient conditions. In the present study, the approach of work [1] is used to analytically describe the domain of sufficient Turing instability conditions. An analytical description is given of the region of necessary and sufficient Turing instability conditions in the Gierer – Meinhardt system, and a range of critical wave numbers is found under which this instability arises, depending on the ratio of the diffusion coefficients of the activator and substrate. Using the Lyapunov-Schmidt method, spatially inhomogeneous stationary structures are found that are formed at a critical value of the diffusion parameter.

### **Acknowledgement**

Research was financially supported by Southern Federal University, grant No. VnGr-07/2020-04-IM (Ministry of Science and Higher Education of the Russian Federation).

### **Reference**

[1] Revina S. V., Lysenko S. A. In: *Proceedings of Eight China-Russian Conference, Southern Federal University, I. I. Vorovich Institute of Mathematics, Mechanics and Computer Science*, 44–48, 2019.

## The Use of Plasma Chemical Methods for Producing Carbon Nanostructures Based on SiC

A.A. Rezvan\*, V.S. Klimin, I.N. Kots, O.A. Ageev

*Institute of Nanotechnologies, Electronics, and Electronic Equipment Engineering,  
Southern Federal University, Taganrog, Russia*

\*[arezvan@sfedu.ru](mailto:arezvan@sfedu.ru)

Si is still main semiconductor material for modern electronics, however, in a number of areas it is starting to lose ground. Speaking about the power electronics area, the most promising materials here are GaN and silicon carbide SiC [1]. Recently, with discovery of layer etching techniques, interest in SiC has again increased, which allows formation of functional elements corresponding to given parameters on its surface with high accuracy. This work is aimed at demonstrating the relevance of applying layer-by-layer etching technique for the formation of emission carbon nanoscale structures on surface of SiC based on plasma chemical etching. The work was carried out on carbon surface of plates of intrinsic SiC. After that, samples were placed in vacuum chamber of focusing ion beam module and oriented so that stream of accelerated ions fell on the substrate in the normal direction. The working vacuum during exposure of the beams was maintained at  $(1 - 2) \times 10^{-4}$  Pa. At this stage, an array of pointed cathodes was formed on surface of SiC. The carbon nanosize layer was formed by etching atomic layer in a fluoride plasma. SF<sub>6</sub> was used as a fluorine containing gas, which made it possible to etch surface layer of SiC. At the same time, their crystal lattice removed only Si and formed a thin carbon layer on surface of samples. The study of surface topology at each iteration was carried out using scanning electron microscopy. These structures have the same electrical parameters of carbon nanotubes, however, technology obtained allows one to form emission structures at lower temperatures and shorter preparation times, meeting the specified parameters. At the end of a series of experimental studies, it was found that the presented technology for producing graphene films on the surface of SiC wafers by etching on the atomic layer allows one to obtain a carbon structure in accordance with the specified parameters at lower temperatures than during the thermal destruction of SiC substrates.

### **Acknowledgements**

This work was supported by Grant of the President of the Russian Federation No. MK-3512.2019.8. The results were obtained using the equipment of the Research and Education Center and Center for Collective Use "Nanotechnologies" of Southern Federal University.

### **Reference**

[1] Rezvan A.A., Klimin V.S. *Abstracts & Schedule of the 2017 International Conference on "Physics and Mechanics of New Materials and Their Applications" (14-16 October, 2017, Jabalpur, India)*, PDPM Press: Jabalpur, 198, 2017.

## Carbon Based Nanoelectronics Device Sensitive to Gas Parameters

A.A. Rezvan\*, V.S. Klimin, J.V. Morozova

*Institute of Nanotechnologies, Electronics, and Electronic Equipment Engineering,  
Southern Federal University, Taganrog, Russia*

\*[arezvan@sfedu.ru](mailto:arezvan@sfedu.ru)

Currently, carbon has become a widely available material for various devices that can find their application in our daily lives. Already there are a number of developments on formation on its basis of solar cells, rechargeable batteries, touch displays, various coatings and so on. This fact is explained by a wide range of various properties and parameters of carbon [1 – 3]. Moreover, in addition to physical and electrical, there is particular interest to chemical parameters of carbon, consisting in using carbon in sensor devices. So relevant is the use of carbon nanoscale structures to obtain devices that are sensitive to changes in environmental characteristics, in particular, a pressure sensor. Si-plates were used to form the sensor. Surfaces of plates underwent standard cleaning and degreasing operations, as well as grinding and polishing. Then, Ni based contacts were formed on several plates by magnetron sputtering. A carbon nanoscale layer was deposited on the obtained layer using the method of plasma chemical vapor deposition. For formation of structures, a mixture of gases from acetylene and argon was introduced into the working chamber. The resulting plates were connected using the anode welding method. The end of research work was formation of upper contacts and electrodes.

According to the obtained data, volt-ampere characteristics were constructed from experimental studies, the dependences on which completely satisfy the Paschen law. The sensitivity of the experimental layout is  $2.4 \times 10^{-8}$  A/Pa.

### **Acknowledgements**

This work was supported by Grant of the President of the Russian Federation No. MK-3512.2019.8. The results were obtained using the equipment of the Research and Education Center and Center for Collective Use "Nanotechnologies" of Southern Federal University.

### **References**

- [1] Rezvan A.A., Klimin V.S. *Abstracts & Schedule of the 2017 International Conference on "Physics and Mechanics of New Materials and Their Applications" (14-16 October, 2017, Jabalpur, India)*, PDPM Press: Jabalpur, 197, 2017.
- [2] Rezvan A.A., Klimin V.S. *Abstracts & Schedule of the 2017 International Conference on "Physics and Mechanics of New Materials and Their Applications" (14-16 October, 2017, Jabalpur, India)*, PDPM Press: Jabalpur, 198, 2017.
- [3] Rezvan A.A., Klimin V.S. *Abstracts & Schedule of the 2017 International Conference on "Physics and Mechanics of New Materials and Their Applications" (14-16 October, 2017, Jabalpur, India)*, PDPM Press: Jabalpur, 199, 2017.

## **Effects of Water pH and Immersion Time on Water Absorption Behavior and Mechanical Properties of Carbon Fiber Reinforced Bio Plastic Composites**

**Ri-ichi Murakami<sup>1\*</sup>, Wahyu Solafide<sup>2\*\*</sup>**

*<sup>1</sup>Department of Materials Science and Engineering, National Taiwan University of Science and Technology, 43 Sec. 4 Keelung Rd, Taipei 106, Taiwan*

*<sup>2</sup>Institute Teknologi Sumatera, Terusan Ryacudu, Way Hui, Jati Agung, Lampung Selatan 35365, Indonesia*

\*[anewmoon816@gmail.com](mailto:anewmoon816@gmail.com); \*\*[wahyu.sipahutar@mt.itera.ac.id](mailto:wahyu.sipahutar@mt.itera.ac.id)

The objective of this research is to study the effects of water pH and immersion time on water absorption and mechanical properties of carbon fiber reinforced bio plastic composites. The composite samples were exposed into three different water conditions such as distilled and salt water. The composites were immersed for 1, 3, 5, 10, 15, 20, 25, 30, 35 and 40 days, respectively. The entire preparation and test follow the ASTM standards. After immersing for 40 days, the highest moisture absorption was found for the composites immersed in distilled water. Also, it is found that SEM images have shown many voids on the tensile fracture surface of the composite immersed in distilled water. Therefore, the high amount moisture absorption results in the presence of voids in a composite. For the composite immersed in normal water, the mechanical properties (Young's modulus and tensile strength) decreased with increasing the immersion time. Moreover, the effect of the moisture absorption on the mechanical properties and the fracture surface was discussed by the thermal behavior that the glass transition temperature,  $T_g$ , decreased with increasing the immersion time. The glass transition temperature of the composite linearly decreased when the quantity of moisture absorption increased.

## **Cost and Quality Analysis of Using Steel Fibers in a Strong Pavement Using Laboratory Experimental Method**

**Risma Marleno\*, Fajar Romadhon, Gede Sarya, Hari Susanto**

*Department of Civil Engineering, University of 17 Agustus 1945 Surabaya Indonesia*

\*[marleno\\_ts@gmail.com](mailto:marleno_ts@gmail.com)

Indonesia as a developing country is still using concrete in its construction. By modifying one or more component on the concrete construction, it will affect the cost-saving and the quality of the construction. The current innovation in concrete technology in a developing country is the mixture of steel fiber in concrete construction. This study aims to find and compare the cost and quality of the use of steel fiber (dramix) and iron wire mesh in the rigid pavement. The method used in this study is a laboratory experiment. The study results that steel fiber costs less and is more economic than reinforcing steel in the rigid pavement. 1 m<sup>3</sup> concrete with reinforcing iron wire mesh, m8



costs Rp. 2,138,343.26. However, concrete is a mixture of 10% steel fiber (dramix) costs Rp. 1,798,089.00, that is there is a cost savings of Rp. 340,254.26 per 1 m<sup>3</sup>. The mixing of steel fiber in concrete through 28 days has greater compressive strength than the ordinary concrete mix with compressive strength value of  $f_c' = 29.07$  MPa. However, concretes with the mixture of steel fiber (dramix) has more compressive strength that varies in value: for 10%,  $f_c' = 29.34$  MPa; for 15%,  $f_c' = 29.38$  MPa; for 20%,  $f_c' = 29.41$  MPa, and for 30%,  $f_c' = 29.58$  MPa. In the flexural strength test, the concrete with iron wire mesh m8 results in flexural strength of  $f_c' = 4.978$  MPa. However, a concrete with the mixture of steel fiber (dramix) has more flexural strength that varies in value; for 10%,  $f_c' = 5.173$  MPa; for 15%,  $f_c' = 5.316$  MPa; for 20%,  $f_c' = 5.458$  MPa, and for 30%:  $f_c' = 5.707$  MPa.

## **The Effect of Temperature during the Growth of CNTs on the Structure of Ni/TiN/Si**

**N.N. Rudyk\*, O.I. Il'in, A.V. Guryanov, M.V. Il'ina, A.A. Fedotov**

*Southern Federal University, Institute of Nanotechnologies, Electronics and Electronic Equipment Engineering, Taganrog, 347922, Russia*

[\\*rudyk0918@gmail.com](mailto:*rudyk0918@gmail.com)

The rapid development of the market for portable devices generates a request for the creation of compact sources of electrical energy. One of the promising areas for the creation of miniature energy sources is the development of piezoelectric nanogenerators. Carbon nanotubes (CNTs) with a piezo- and flexoelectric effect [1] are potentially the basis for the creation of such converters. To increase the efficiency of current generation, vertically aligned CNT arrays are used. Moreover, the generation efficiency is determined by the geometric dimensions of the CNTs. The PECVD method allows the formation of CNT arrays in a wide range of geometric parameters. The height, diameter, density and material of the contact layer can significantly affect the CNTs structural characteristics and their properties [2]. Thus, the determination of laws of influence of technological modes of the formation of CNT arrays on their geometric parameters by the PECVD is an actual task. In this work, we studied the effect of the CNT arrays growth temperature by PECVD on their geometric parameters such as diameter and height. Experimental studies were carried out on the Ni/TiN/Si structure. The catalytic layer (Ni, 15 nm) and the contact layer (TiN, 100 nm) were formed by magnetron sputtering on Auto500 (BOC Edwards, UK). TiN was chosen as the contact layer, because it has a low contact resistance with nanotubes, is chemically stable, and also allows the formation of CNT arrays by tip-mechanism under wide range technological modes. CNTs were formed in the temperature range 615 – 690 °C with a step of 15 °C. It was found that a whole temperature range of 615 – 690 °C is applicable for the formation and growth of CNTs on the TiN contact layer. With increasing temperature, the average diameter of nanotubes increases from 47 to 78 nm, which may be due to an increase in the diameter of Ni catalytic centers due to the coalescence of small particles into larger ones and increasing surface diffusion [3]. The minimum deviation in diameter was  $\pm 15$  nm and was observed at 660 °C. It was established that the CNT height decreased with increasing process temperature. This may be due to the fact that with increasing temperature,

the desorption rate of carbon-containing gas increases. Taking into account the increase in the CNTs diameter with increasing temperature, it can be assumed that for CCs with a larger diameter, the formation of a larger number of CNT layers is occurring. As a result, the resulting growth rate decreases. This result can be used to develop and create nanogenerators and flexoelectric converters based on aligned carbon nanotubes.

#### **Acknowledgement**

This work was financially supported by the RFBR (project No. 20-37-70034).

#### **Reference**

- [1] Il'ina M.V., Il'in O.I., Guryanov A.V., Osotova O.I., Ageev O.A. // *Fullerenes Nanotub. Carbon Nanostructures* **28**, 78–82, 2020.
- [2] Adam J. Clancy, Mustafa K. Bayazit, Stephen A. Hodge, Neal T. Skipper, Christopher A. Howard and Milo S. P. Shaffer // *Chem. Rev.* **118** 7363–7408, 2018.
- [3] Il'in O.I., Rudyk N.N., Fedotov A.A., Il'ina M.V., Cherednichenko D.I., Ageev O.A. // *Nanomaterials*. **10**, 554, 2020.

## **Molecular Composition of the White Spot Lesion Detected on the Human Molar**

**E.V. Sadyrin<sup>1\*</sup>, M.V. Swain<sup>1,2</sup>, A.L. Nikolaev<sup>1</sup>, A.S. Vasiliev<sup>1</sup>, D.V. Yogina<sup>3</sup>,  
N.V. Lyanguzov<sup>4</sup>, S.Yu. Maksyukov<sup>3</sup>, S.M. Aizikovich<sup>1</sup>**

<sup>1</sup>*Don State Technical University, Rostov-on-Don, Russia*

<sup>2</sup>*University of Sydney, Sydney, Australia*

<sup>3</sup>*Rostov State Medical University, Rostov-on-Don, Russia*

<sup>4</sup>*Southern Federal University, Rostov-on-Don, Russia*

\*[ghostwoode@gmail.com](mailto:ghostwoode@gmail.com)

Researches of early clinically visible stage of carious disease – natural proximal white spot lesion (WSL) from a microstructural point of view, in addition to conventional bitewing X-ray techniques used in medical practice, provides a better understanding of the changes in the carious enamel. Raman spectroscopy enables researchers to study accurately the molecular composition of carious lesions [1]. A number of solutions for the non-invasive *in vivo* detection of early caries various methods were proposed [2, 3]. The present work addresses the problem *in vitro* tracing the changes in molecular composition that emerge in human molar at the stage of WSL by means of Raman spectroscopy. The spectra were collected using a He-Ne laser (wavelength of the laser excitation was 633 nm) in the device (inVia Reflex, Renishaw, UK) with an Edge filter. We used the backscattering scheme with a Leica optical microscope. The resolution of the spectra did not exceed 0.5 cm<sup>-1</sup>. The laser beam diameter on the sample surface was equal to 1–2 μm (the preparation included cutting using a precision saw followed by grinding and polishing procedures). The Raman spectra measured were corrected using the Bose–Einstein temperature factor. During the research we kept the sample wet with Hanks' balanced salt solution with thymol. The research resulted in detection of some repeatable features connected to changes in the molecular composition in the carious areas (the most intense PO<sub>4</sub><sup>3-</sup> band shift, change in its full width at half maximum and a new band appearance, detected and described for the WSL).

### **Acknowledgements**

This work was supported by the grant of the Government of the Russian Federation (grant No. 14.Z50.31.0046). E.V. Sadyrin was supported by the scholarship of the President of the Russian Federation No. SP-3672.2018.1. The tooth was extracted in the Dental Department of Rostov State Medical University Clinic for orthodontic reasons, local independent ethics committee of Rostov State Medical University approved the study. Experiments were conducted in Nanocenter of Research and Education Center "Materials" (<http://nano.donstu.ru>) of Don State Technical University and Faculty of Physics, Southern Federal University.

### **References**

- [1] Wang Y., Spencer P., Walker M. P. // *Journal of Biomedical Materials Research Part A*, **81**(2), 279-286, 2007.
- [2] Akkus A., Yang S., Akkus O., Lang L. // *Journal of Operative and Esthetic Dentistry*, **1**(1), 1-5, 2016.
- [3] Yakubu E., Li B., Duan Y., Yang S. // *Biomedical Optics Express*, **9**(12), 6009-6016, 2018.

## **Analysis of Resistance Factor and Application Strategy of Work Safety and Health Applications Construction Project Workers in Tulungagung Regency**

**Sajiyo<sup>1\*</sup>, Faiz Muhammad Azhari<sup>2</sup>, Haris Muhamadun<sup>2</sup>, Priyoto<sup>3</sup>**

<sup>1</sup>*Department of Industrial Engineering, University of 17 Agustus 1945 Surabaya Indonesia*

<sup>2</sup>*Department of Civil Engineering, University of 17 Agustus 1945 Surabaya Indonesia*

<sup>3</sup>*Department of Architecture, University of 17 Agustus 1945 Surabaya Indonesia*

\*[sajiyo@untag-sby.ac.id](mailto:sajiyo@untag-sby.ac.id)

In the implementation of physical development, Occupational Safety and Health (OSH) issue is generally still ignored in Indonesia, especially in public work construction with the construction of simple buildings. This is evidenced by the high number of work accidents in construction. Workers in the construction service sector consist of 7-8% of total workers in all sectors and contribute 6.45% of GDP in Indonesia. The construction service sector is one of the sectors with the highest risk of work accidents. Therefore, the authors conducted an analysis of health and safety application in construction project workers in Tulungagung Regency. To find out the barriers to the implementation of Occupational Safety and Health and how the strategic efforts made improve the application of OSH to construction project workers in Tulungagung Regency. In this study, quantitative methods are used, and data analysis is performed by multiple linear regression analysis and SWOT analysis, but before multiple regression testing is performed first, the validity and reliability tests are performed using the SPSS statistical program. Regression analysis is intended to be able to find out what factors can significantly hinder the application of OSH to Construction Project Workers in Tulungagung Regency, while SWOT analysis is carried out to find out what factors are strengths, weaknesses, opportunities, and threats in the implementation of OSH. Thus, company management can implement relevant and effective strategies so that the application of Occupational Safety and Health to construction project workers in Tulungagung Regency can increase, which in turn reduces work accident rates and improves performance.

## Monomethylamine Isolation Process

F.D. Savriddinov<sup>1</sup>, D. D. Fugarov<sup>1\*</sup>, O. A. Purchina<sup>1</sup>, D.A. Onyshko<sup>2</sup>

<sup>1</sup>Don State Technical University, Rostov-on-Don, Russia

<sup>2</sup>South-Russian State Polytechnic University (NPI) named after M.I. Platov,  
Novocherkassk, Russia

\*[ddf\\_1@mail.ru](mailto:ddf_1@mail.ru)

Monomethylamine, an organic substance derived from ammonia, is a colorless gas. Widely used in the production of insecticides, monomethylhydrazine, which is a component of fuel for rockets, is also used in the manufacture of drugs and explosive substances are obtained from it. However, the most important is the use of monomethylamine in the synthesis of vulcanization accelerators, fungicides, corrosion inhibitors, bactericidal preparations, additives to lubricating oils, this direction is decisive in the development of the production of this substance, therefore, the issues associated with the improvement of technological schemes for the isolation of monomethylamine today are extremely relevant [1]. On an industrial scale, methylamine is obtained from mixtures obtained by methanol vapor phase catalytic amination at high temperatures and pressure. The methanol-ammonia ratio regulates the total composition of methylamine mixtures. Isolation of monomethylamine is carried out by rectification. Moreover, methylamine can be prepared by reaction of ammonia and methyl chloride. In the process of production of monomethylamine, control of process parameters is necessary practically without human participation, this will allow timely warning about the presence of unacceptable deviations in process parameters, which will quickly eliminate the emergency situation [1].

### References

- [1] Fugarov D.D. In: *2019 International Conference on "Physics and Mechanics of New Materials and Their Applications"*, PHENMA 2019, Hanoi, Vietnam, November 7 – 10, 2019, Hanoi University of Science and Technology: Hanoi. 119-120, 2019.
- [2] Poluyan A.Y., Fugarov D.D., Purchina O.A., Nesterchuk V.V., Smirnova O.V., Petrenkova S.B. // *Journal of Physics: Conference Series "International Conference Information Technologies in Business and Industry 2018 - Microprocessor Systems and Telecommunications"*. 022013, 2018.
- [3] Solomentsev K.Y., Fugarov D.D., Purchina O.A., Poluyan A.Y., Nesterchuk V.V., Petrenkova S.B. // *Journal of Physics: Conference Series*. **1015**, 032179, 2018.
- [4] Fugarov D.D., Gerasimenko Y.Y., Nesterchuk V.V., Gerasimenko A.N., Onyshko D.A. // *Journal of Physics: Conference Series*. 012055, 2018.

## **Topological Optimization of the Support of the Control Panel of a Numerically Controlled Machine**

**I.V. Semenchatenko\*, A.A. Matrosov**

*Don State Technical University, 1, Gagarin Sq., Rostov-on-Don, 344010, Russia*

[\\*ivan5570c@gmail.com](mailto:ivan5570c@gmail.com)

A modern design approach involves the efficient use of materials in the design. Reducing weight, changing the shape of the construction as a whole or its individual elements allows to achieve improvement in a number of indicators. These indicators include: time for design development and manufacturing, construction costs, transportation and operating costs, etc. Such tasks are structural optimization problems, i. e. generating an optimal design of load-bearing mechanical constructions. At the same time, the parameters optimized are not numerical. A variety of optimization problems are topological optimization problems, which allow us to obtain the optimal shape of the good for given loads and boundary conditions, under given operating conditions. The use of such an optimization can significantly reduce the time devoted to design, therefore, to increase the life cycle of the good, to more widely use the capabilities of both traditional manufacturing methods and additive technologies. One of the effective optimization criteria may be, for example, minimizing the total weight of construction. In this case, of course, volume forces and external loads are taken into account. Using the Autodesk Fusion 360 software package, topological optimization of the support of the machine control panel with numerical control was performed. In series with a step of 10%, a series of calculations was carried out with a different degree of filling of the volume of the support, namely from 10% to 90% of the filling while maintaining the nature and magnitude of external loads and the conditions of fastening (steel 45, the support is rigidly fixed with bolts passing through the corresponding holes). The option with 10% coverage is not further considered, since there are no contact zones between the created structures. For the remaining options, a stress state calculation was performed. In the result of these calculations, it was found that only starting with the option with 50% coverage, the support can withstand a given external load. Thus, topological optimization acts as the basis for the preliminary design of a lightweight part. At the same time, there are no algorithms for choosing one or another option. To study the stress distribution, and, consequently, the design operability, it is necessary to perform a separate analysis.

## Effect of Heating Rate on Mechanical Properties of Polymer Matrix of Carbon/PEKK Composites in Thermoforming Process

Seong-Jae Park<sup>1</sup>, Yu Tianyu<sup>1</sup>, Kyo-Moon Lee<sup>1</sup>, Soo-Jeong Park<sup>2</sup>, Yun-Hae Kim<sup>1,2†</sup>

<sup>1</sup>*Department of Marine Equipment Engineering, Graduate School, Korea Maritime and Ocean University, 727 Taejong-ro, Yeongdo-gu, Busan, 49112, Republic of Korea*

<sup>2</sup>*Department of Ocean Advanced Materials Convergence Engineering, Korea Maritime and Ocean University, 727 Taejong-ro, Yeongdo-gu, Busan, 49112, Republic of Korea*

†[yunheak@kmou.ac.kr](mailto:yunheak@kmou.ac.kr)

Interests in thermoplastic composites are growing because of the properties such as high production rates, recycling possibilities, weldabilities, and a low level of moisture uptake. However, the high viscosity and temperature in processing thermoplastic polymer make it challenging to be used. Accordingly, studies have been conducted to optimize and stabilize the autoclave process. Moreover, other methods such as vacuum-assisted oven consolidation and thermoforming are considered a breakthrough to reduce the production costs and processing time. Thermoforming is a manufacturing process where a blank is heated to a processing temperature and moved to a mold for compression and cooling. In previous studies, the cooling rate is regarded as related to mechanical and thermal properties. Although the processing temperature in the heating process of thermoforming affects interactions between resin matrix and fiber reinforcement, influences have not been investigated. Therefore, in this study, the effect of the heating rate on the mechanical properties of the matrix was evaluated and analyzed.

### **Acknowledgment**

This work was supported by the Technology Innovation Program (No. 20007444), funded by the Ministry of Trade, Industry & Energy (MOTIE, Korea).

## Mathematical Simulation Testing of Some Building Materials

I.A. Serebryanaya, A.A. Matrosov\*, D.A. Nizhnik, N.A. Poryadina

*Don State Technical University, 1, Gagarin Sq., Rostov-on-Don, 344010, Russia*

\*[amatrosov@donstu.ru](mailto:amatrosov@donstu.ru)

The paper analyzes the ratio of friction forces and shear stresses arising at the upper and lower boundaries of a brick during standard compression tests [1 – 3]. A brick is modeled by a body in the shape of a rectangular parallelepiped. It is accepted that the material is transversely isotropic. A uniformly distributed load, corresponding to the compressive strength of the specimen, acts on the upper surface of the body from the side of the press metal plate. The lower surface of the body rests on a fixed metal press plate. The lateral borders of the body are free from external influences. The numerical experiment was performed in the ANSYS 19.2 finite element analysis software package

on a model broken by an eight-node three-dimensional finite element. According to the results of a numerical study, it was found that the distribution of the stress field in the samples leveled by grinding, as well as using a cement-sand mortar, is characterized by the compression effect due to friction. The calculation of the stress state before the detachment of the side surfaces is made according to the criterion of Mohr strength. The largest equivalent stresses are directed horizontally, therefore, fracture cracks should have a vertical orientation. Further loading leads to a redistribution of stresses in the remaining part of the body. The action of maximum tangential stresses causes further destruction of the body with a sharp drop in its bearing capacity. Thus, according to the results of the calculations it was found that the friction forces arising from standard tests significantly affect the deformation conditions of the samples and lead to a distortion of the test results. To reduce this effect, it is necessary to adjust the standard test method.

### **References**

- [1] Lukinova N.A., Matrosov A.A., Nizhnik D.A., Serebryanaya I.A., Terekhina Y.V. // *MATEC Web of Conferences*, **132**, 03002, 2017.
- [2] Lukinova N.A., Matrosov A.A., Nizhnik D.A., Serebryanay I.A., Terekhina Yu.V. *Abstracts & Schedule of the 2017 International Conference on "Physics and Mechanics of New Materials and Their Applications"* (14-16 October, 2017, Jabalpur, India), PDPMPress: Jabalpur, 134-135, 2017.
- [3] Poryadina N.A., Serebryanaya I.A. *Materials of the All-Russian Scientific Conference "Intelligent Technologies and Problems of Mathematical Modeling"*. Rostov-on-Don: DSTU Press, 42-43, 2018 (In Russian).

## **Simplified Analytical Expressions for Indentation Stiffness of Coated Solids and its Application for Experimental Analysis**

**Sergei M. Aizikovich\*, Andrey S. Vasiliev, Boris I. Mitrin, Evgeniy V. Sadyrin**

Research and Education Center "Materials", Don State Technical University,  
1 Gagarin sq., Rostov-on-Don 344000, Russia

[\\*saizikovich@gmail.com](mailto:*saizikovich@gmail.com)

Nanoindentation is widely used to determine the mechanical characteristics of coatings. However, analysis of the experimental results is usually made with the help of classical theoretical results for the homogeneous non-coated materials. Such an approach can lead to significant error in evaluation of Young's modulus of thin coatings especially in the case of sufficient difference of the elastic moduli of the coating and substrate. Approximated analytical solutions for the contact problems for coated elastic solids are presented in a form convenient for the analysis of the experimental results. Special attention is paid to the construction of simplified explicit expressions for the indentation stiffness and indentation force. Detailed analysis of the accuracy of the obtained results is made. Good agreement of the theoretical and experimental results is observed for the samples with various coating thicknesses. Application of the results for evaluation of the Young's modulus of thin coatings is discussed.

### **Acknowledgement**

This work was supported by the Government of the Russian Federation (grant No. 14.Z50.31.0046).

## Structure, Mechanical and Electrophysical Characteristics of Li-ion Conducting Ceramics $\text{Li}_{1.3}\text{Al}_{0.3}\text{Ti}_{1.7}(\text{PO}_4)_3$

O.B. Shcherbina\*, G.B. Kunshina, V.V. Efremov

*I.V. Tananaev Institute of Chemistry - Subdivision of the Federal Research Centre "Kola Science Centre of the Russian Academy of Sciences", Apatity, Russia*

\*[o.shcherbina@ksc.ru](mailto:o.shcherbina@ksc.ru)

Solid electrolytes with Li-ion conductivity and crystal structure NASICON are perspective for development of solid-state batteries with high energy density and improved safety compared to existing lithium-ion systems [1]. It is important that these materials have suitable mechanical characteristics along with high ion and low electron conductivity, electrochemical stability in contact with metal lithium. The aim of this work is determination of mechanical and electrochemical characteristics of oxide solid electrolytes  $\text{Li}_{1.3}\text{Al}_{0.3}\text{Ti}_{1.7}(\text{PO}_4)_3$  and  $\text{Li}_{1.3}\text{Al}_{0.3}\text{Ti}_{1.7}(\text{PO}_4)_3$  doped with  $\text{B}_2\text{O}_3$ . Single phase powder solid electrolyte  $\text{Li}_{1.3}\text{Al}_{0.3}\text{Ti}_{1.7}(\text{PO}_4)_3$  (LATP) was synthesized by crystallization from liquid peroxide precursor at temperature of 700 – 800 °C [2]. Calculated amount of shredded powder  $\text{B}_2\text{O}_3$  was added to solid electrolyte LATP, mixed, pressed into tablets and sintered in programmable muffle furnace MIMP-3P at 1000 °C for 2h. Sintered LATP and LATP( $\text{B}_2\text{O}_3$ ) ceramic density was measured by hydrostatic weighting. Ceramic microstructure was studied using scanning electron microscope SEM LEO 420 and image processing program Scan Master. Elastic and mechanic characteristics of ceramics were studied by probe method by a probe microscope "NANOSKAN" [3]. Microhardness ( $H$ , GPa) was detected by comparative sclerometry and Young's modulus ( $E$ , GPa) with help of stress–strain curve slope. A mode I stress intensity factor  $K_{\text{IC}}$  ( $\text{MPa}\cdot\text{m}^{1/2}$ ) was evaluated due to model Anstis et al [4]. The criterion is a crack resistance of a material. It was shown that doping of LATP with  $\text{B}_2\text{O}_3$  in the amount up to 3 wt% leads to a decrease in porosity, increase in ceramic grains adhesion and improvement of material mechanical characteristics: for LATP  $\sim E = 70.2 \pm 1.2$  GPa;  $H = 4.1 \pm 0.7$  GPa;  $K_{\text{IC}} = 0.93 \pm 0.6$   $\text{MPa}\cdot\text{m}^{1/2}$ ; for LATP( $\text{B}_2\text{O}_3$ )  $\sim E = 86.5 \pm 2.1$  GPa;  $H = 5.8 \pm 0.8$  GPa;  $K_{\text{IC}} = 1.0 \pm 0.3$   $\text{MPa}\cdot\text{m}^{1/2}$ . Ion conductivity ( $\sigma$ , S/cm) of LATP and LATP( $\text{B}_2\text{O}_3$ ) was studied by spectroscopy of electrochemical impedance in the frequency range 10 –  $2 \times 10^6$  Hz in a cell with blocking graphite electrodes by an impedance meter Elins Z-2000. Hodographs of electrochemical impedance show a substantial increase in grain boundaries resistance for LATP( $\text{B}_2\text{O}_3$ ) samples containing dopant ( $\text{B}_2\text{O}_3$ ) in amount 1 – 3 wt%. This leads to an increase in general ion conductivity of the ceramics to values  $2.5 \times 10^{-4}$  S/cm at room temperature. Dependence was determined for hardness characteristics and microhardness on content of  $\text{B}_2\text{O}_3$  boron oxide in LATP ceramics.

### References

- [1] J. Wolfenstine, J.L. Allen, J. Sakamoto, D.J. Siegel, H. Choe // *Ionics*, **24**, 1271-1276, 2018. <https://doi.org/10.1007/s11581-017-2314-4>
- [2] G.B. Kunshina, V.V. Efremov, E.P. Lokshin // *Russ. J. Electrochem.*, **49**, 725-731, 2013. <https://doi.org/10.1134/S1023193513070082>
- [3] I. I. Maslenikov, V. N. Reshetov, A. S. Useinov // *Instrum. Exp. Tech.*, **58**, 711 – 717, 2015. <https://doi.org/10.1134/S0020441215040223>



[4] G.R. Anstis, P. Chantikul, B.R. Lawn, D.B. Marshall // *J. Am. Ceram. Soc.*, **64**, 533-538, 1981. <https://doi.org/10.1111/j.1151-2916.1981.tb10320.x>

## Mixed Yttrium Tantalo-Niobates

O. B. Shcherbina\*, S. M. Masloboeva, M. N. Palatnikov

*I.V. Tananaev Institute of Chemistry - Subdivision of the Federal Research Centre «Kola Science Centre of the Russian Academy of Sciences», Apatity, Russia*

\*[o.shcherbina@ksc.ru](mailto:o.shcherbina@ksc.ru)

Yttrium tantalo-niobates are a new class of effective X-ray fluorescent materials used as radiopaque substances in medical diagnostics [1]. These luminescent materials show high absorption of X-rays and radiate in the blue and near ultraviolet optical spectrum. These materials are aimed at a decrease in X-ray radiation in order to obtain a clear image in medical diagnostics. Existence in the  $\text{YNb}_x\text{Ta}_{1-x}\text{O}_4$  matrix of both niobium and tantalum increases energy exchange between luminescent centers. At certain ratios of  $\text{NbO}^+$  and  $\text{TaO}^+$  complexes this situation can lead to stimulation of radiative ability of the material [2]. This report studies obtaining processes of mixed tantalo-niobates of yttrium  $\text{YNb}_x\text{Ta}_{1-x}\text{O}_4$  ( $x = 0 - 1$ ) by sol-gel. Mixed tantalum and niobium hydroxides were precipitated by ammonia from a mixture of high purity fluorine Ta and Nb containing solutions. Volumes of solutions provided gave composition of  $\text{YNb}_x\text{Ta}_{1-x}\text{O}_4$ . The precipitate was thrice pulp washed by deionized water for removing of  $\text{F}^-$  ions at solid to liquid phase ratio  $S:V_L=1:3$  and dried at  $100^\circ\text{C}$ . After that a  $\text{Y}(\text{NO}_3)_3$  solution was added to a precipitate in the given volume. 25% solution of  $\text{NH}_4\text{OH}$  was added to the pulp until  $\text{pH} \sim 8 - 9$ . The residue was filtered, washed with deionized water and dried at  $90^\circ\text{C}$ , then sintered at  $\sim 1000^\circ\text{C}$ ,  $\sim 1200^\circ\text{C}$ ,  $\sim 1400^\circ\text{C}$  for 3h with obtaining the powder of  $\text{YNb}_x\text{Ta}_{1-x}\text{O}_4$ . Steps of obtaining  $\text{YNb}_x\text{Ta}_{1-x}\text{O}_4$  ( $x = 0 - 1$ ) revealed by using TGA were confirmed by XRD (diffractometer Shimadzu XRD-6000 with a counter speed 1 deg/min ( $\text{CuK}\alpha$  radiation)). Databases ICDD (PDF 4, relies 2020) were used for phase identification. It has been established that after annealing at  $\sim 400^\circ\text{C}$  and  $500^\circ\text{C}$ , the material stays XRD amorphous; at  $\sim 500 - 600^\circ\text{C}$ , a phase  $\text{Y}_2\text{O}_3$  starts to appear on the background of amorphous area. In the area  $\sim 600 - 640^\circ\text{C}$ , samples contain  $\text{Y}_2\text{O}_3$  (ICDD 071-0049) and  $\text{Nb}_2\text{O}_5(\text{Ta}_2\text{O}_5)$  starts to appear. At temperature of  $\sim 800^\circ\text{C}$ , a crystallization of  $\text{YNbO}_4$  (ICDD 023-1486) starts. A phase composition of a precipitate  $\text{YNb}_x\text{Ta}_{1-x}\text{O}_4$  ( $x = 0.9$ ) annealed at  $\sim 1000 - 1400^\circ\text{C}$  is shown in Table 1. At annealing temperature of  $1000^\circ\text{C}$  the mixture contains single oxides  $\text{Y}_2\text{O}_3$ ,  $\text{Nb}_2\text{O}_5$  and  $\beta$ -fergusonite (ICDD 023-1486), see Table 1. At increase in the annealing temperature to  $1200^\circ\text{C}$ , the main phases are  $\text{YNbO}_4$  and  $\text{YTaO}_4$  probably, with partial substitution of tantalum by niobium in the structure and traces of  $\text{Nb}_2\text{O}_5$  and  $\text{Ta}_2\text{O}_5$ . Only at temperature of  $1400^\circ\text{C}$ , formation of solid solution  $\text{YNb}_x\text{Ta}_{1-x}\text{O}_4$  is observed. Note that XRD analysis reveals morphotropic area of co-existence monoclinic and tetragonal phases (see Table 1). Average particle sizes of synthesized powders (Table 1) were calculated due to specific surface area (BET, FlowSorb II 2300; TriStar 3020 V1. 03). Samples prepared at different thermal treatment modes have shown changes in morphology and particle sizes with an increase in the temperature. At an increase in the annealing

temperature, shape of particles becomes almost spherical and they tend to form clusters. Particle size increases (Table 1).

**Table 1.** Phase composition and average particle size ( $\alpha$ ) of  $\text{YNb}_x\text{Ta}_{1-x}\text{O}_4$  ( $x=0.9$ ) powders.

$T_{\text{annealing}}, ^\circ\text{C}$	Phase composition* of solid solutions $\text{YNb}_x\text{Ta}_{1-x}\text{O}_4$ due to JCPDS	$\alpha, \mu\text{m}$
1000	$\text{Y}_2\text{O}_3$ (071-0049), $\text{Nb}_2\text{O}_5$ (027-1003) – orthorhombic $\text{YNbO}_4$ (023-1486) – monoclinic $\beta$ -fergusonite, $\text{Nb}_2\text{O}_5$ (015-0166) – monoclinic	0.37
1200	$\text{YNbO}_4$ (023-1486), $\text{YTaO}_4$ (024-1425) – monoclinic – $M^1$ -fergusonite, $\text{YTaO}_4$ (050-0846) – tetragonal, $\text{Ta}_2\text{O}_5$ (025-0922)	0.52
1400	$\text{YNbO}_4$ (072-2077) – monoclinic, $\text{YTaO}_4$ (050-0846) – tetragonal	0.94

\*Phases are presented in the order of their quantity from larger to lesser

Luminescence spectra of yttrium tantalate-niobates was registered at 300 K by a spectrofluorimeter Shimadzu RF-5301 PC. For all synthesized yttrium tantalate-niobates, the excitation wavelength was  $\lambda_{\text{ex}} = 250$  nm. Research revealed that the highest luminescence intensity in the area of 300 – 600 nm with a maximum at  $\lambda_{\text{max}} \sim 400$  nm is shown by luminophores  $\text{YNb}_{0.7}\text{Ta}_{0.3}\text{O}_4$  with a monoclinic unit cell distortion. Thus, despite traditional solid phase synthesis [2], sol-gel allows drastically uniform initial mixtures, notably decrease temperature and longitude of synthesis and obtain single phase compositionally uniform fine-dispersive powders of yttrium tantalate-niobates.

#### References

- [1] Zuev M., Larionov L.P. // *Open Journal "Investigated in Russia"*, **11**, 933 – 949, 2008. <http://zhurnal.ape.relarn.ru/articles/2008/087.pdf>.  
[2] Voloshyna O., Boiaryntseva I., Spassky D., Sidletskiy O. // *Solid State Phenomena*, **230**, 172 – 177, 2015.

## Solubility Features of Rare Earth Elements in BST-ceramics. Part I: Large-sized Ln

L.A. Shilkina\*, S.V. Khasbulatov, L.A. Reznichenko

<sup>1</sup>Research Institute of Physics, Southern Federal University, Rostov-on-Don, 344090, Russia

\*[lid-shilkina@yandex.ru](mailto:lid-shilkina@yandex.ru)

It is known that the dielectric and piezoelectric properties of ferroelectric solid solutions (SSs), in particular  $(\text{Ba}, \text{Sr})\text{TiO}_3$ , can be corrected by introducing modifiers into their composition. In this paper, we present the results of a study of the structure and properties of SS  $\text{Ba}_{1-x}\text{Sr}_x\text{TiO}_3$  modified with large-sized rare earth elements, whose ionic radius is in the range 1.04 – 0.94 Å (La-Gd). For modification, we selected SSs from different regions of the phase diagram of the  $\text{BaTiO}_3 - \text{SrTiO}_3$  system:  $\text{Ba}_{0.8}\text{Sr}_{0.2}\text{TiO}_3$  from the tetragonal (T) region,  $\text{Ba}_{0.5}\text{Sr}_{0.5}\text{TiO}_3$  from the pseudocubic (Psc) region, and  $\text{Ba}_{0.2}\text{Sr}_{0.8}\text{TiO}_3$  from the cubic (C) region [1]. The modification was carried out in accordance with the formulae:  $\text{Ba}_{0.76}\text{Ln}_{0.04}\text{Sr}_{0.2}\text{TiO}_3$ ,  $\text{Ba}_{0.475}\text{Ln}_{0.025}\text{Sr}_{0.5}\text{TiO}_3$ ,  $\text{Ba}_{0.19}\text{Ln}_{0.01}\text{Sr}_{0.80}\text{TiO}_3$ . Samples are made by solid-phase synthesis followed by sintering using conventional ceramic

technology. Despite the fact that the difference between the ionic radii of Ba and Ln is 33 – 47% in the La-Gd series, which suggests limited solubility and the formation of impurity phases, XRD analysis showed a pure perovskite phase in all samples. In Fig. 1, the dependences of the unit cell volume,  $V$ , of the SSs on the ionic radii Ln for coordination number 12 are shown. It can be seen that the value of the  $V$  cell of doped SSs is much smaller than the  $V$  cell of the initial SSs, which indicates the embedding of all modifiers in the structure of the latter. It was established, that in SS with  $x = 0.2$ , T-symmetry changed to C-symmetry, the phase state of the SS with  $x = 0.50$  shifted to the initial stage of spinodal decomposition or to the metastable region of the phase diagram of the system (Ba, Sr)TiO<sub>3</sub>, and in SS with  $x = 0.80$ , the real (defective) structure changed, which resulted in an increase in the wavelength of the defect density from ~ 130 Å to 180 – 200 Å.

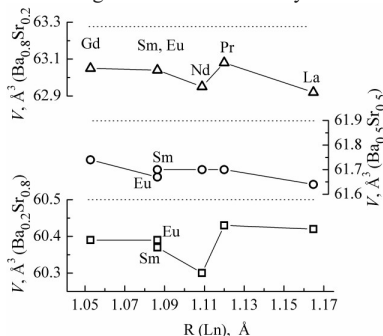


**Fig. 1.** Dependences of the  $V$  unit cell of doped SSs  $\text{Ba}_{1-x}\text{Sr}_x\text{TiO}_3$  with  $x = 0.2, 0.5, 0.8$  on the ionic radius Ln. Dotted lines show the unit cell volume of unmodified

#### Acknowledgement

Research was financially supported by the Ministry of Science and Higher Education of the Russian Federation (State assignment in the field of scientific activity, Southern Federal University, 2020)

#### Reference

[1] S.V. Khasbulatov, L.A. Shilkina, H.A. Sadykov, A.A. Pavelko, A.T. Kozakov, S.P. Kubrin, I. N. Andryushina, L.A. Reznichenko // *Bull. Russ. Acad. Sci. Phys.* **80**(11), 1364-1366, 2016.

## Solubility Features of Rare Earth Elements in BST-ceramics. Part II: Small-sized Ln

L.A. Shilkina\*, S.V. Khasbulatov, L.A. Reznichenko

<sup>1</sup>Research Institute of Physics, Southern Federal University, Rostov- on-Don, 344090, Russia

\*[lid-shilkina@yandex.ru](mailto:lid-shilkina@yandex.ru)

In accordance with the conditions of isomorphism, small-sized lanthanides cannot replace Ba in SSs  $\text{Ba}_{1-x}\text{Sr}_x\text{TiO}_3$ , since the difference between the ionic radii of Ba and Ln from Tb to Yb is 55 –

70%. In this case, only microisomorphism is possible, which also significantly affects the properties of ferroceramics. The present work is devoted to the study of the solubility of Tb – Yb lanthanides and its effect on the structure of BST ceramics. The X-ray phase analysis showed the presence of  $\text{Ln}_2\text{Ti}_2\text{O}_7$  compounds with a pyrochlore structure in almost all SSs. All doped SSs retained the symmetry of the initial SS: tetragonal at  $x = 0.2$ , pseudocubic at  $x = 0.5$ , and cubic at  $x = 0.8$ . The relative intensities of the strong pyrochlore peak and the difference between the ionic radii of the  $A$ -cation,  $\bar{R}$ , (Ba and Sr taking into account molar concentrations) and Ln are given in Table 1. Figure 1 shows the dependences of the unit cell volume,  $V$ , of all SSs and  $c/a$  of SS with  $x = 0.2$  on the ionic radius Ln for coordination number 12. Fig.1 shows that  $V$  of doped SSs in the Ho – Yb series are less than  $V$  of initial SSs, but the difference does not exceed the measurement error  $\Delta V = 0.05 \text{ \AA}^3$ . The minimum amount of  $\text{Tb}_2\text{Ti}_2\text{O}_7$  in SSs with  $x = 0.2, 0.5$  and its absence in SS with  $x = 0.8$  indicates the partial solubility of Tb in all SSs. The remaining lanthanoides exhibit microisomorphism.

**Table 1.** Relative intensity,  $I_{rel}$ , of X-ray peak 222 of  $\text{Ln}_2\text{Ti}_2\text{O}_7$  pyrochlore in X-ray diffraction patterns of SSs and  $\Delta \bar{R}$ , %.

Chemical composition $A$ -cation	Tb		Dy		Ho		Er		Tm		Yb	
	$I_{rel}$	$\Delta \bar{R}$	$I_{rel}$	$\Delta \bar{R}$	$I_{rel}$	$\Delta \bar{R}$	$I_{rel}$	$\Delta \bar{R}$	$I_{rel}$	$\Delta \bar{R}$	$I_{rel}$	$\Delta \bar{R}$
$\text{Ba}_{0.76}\text{Ln}_{0.04}\text{Sr}_{0.2}$	5	51	10	53	13	56	12	58	13	58	14	66
$\text{Ba}_{0.475}\text{Ln}_{0.025}\text{Sr}_{0.5}$	3	45	8	47	9	50	10	52	8	52	9	59
$\text{Ba}_{0.19}\text{Ln}_{0.01}\text{Sr}_{0.80}$	–	39	–	40	–	44	2	45	2	45	2	53

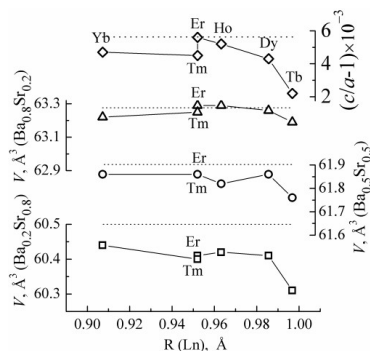


**Fig. 1.** Dependences of the  $V$  unit cell of SSs  $\text{Ba}_{1-x}\text{Sr}_x\text{TiO}_3$  with  $x = 0.2, 0.5, 0.8$  and, the degree of tetragonality for SS with  $x = 0.2$  on the ionic radius Ln; dotted lines show the value of these values in unmodified TR

### Acknowledgement

Research was financially supported by the Ministry of Science and Higher Education of the Russian Federation (State assignment in the field of scientific activity, Southern Federal University, 2020).

# Experimental Confirmation of Spinodal Decomposition in the $\text{Ba}_{1-x}\text{Sr}_x\text{TiO}_3$

L.A. Shilkina\*, S.V. Khasbulatov, L.A. Reznichenko, S.I. Dudkina

Research Institute of Physics, Southern Federal University, Rostov-on-Don, 344090, Russia

\*[lid-shilkina@yandex.ru](mailto:lid-shilkina@yandex.ru)

In [1], on the basis of X-ray diffraction studies, we constructed a phase diagram of the  $(1-x)\text{BaTiO}_3 - x\text{SrTiO}_3$  system at room temperature, which includes two morphotropic phase transitions. The first, well-known, transition from the tetragonal (T) phase to the pseudocubic (Psc) phase occurs in the range  $0.2 < x < 0.3$ , and the second transition from the Psc phase to the cubic (C) phase occurs in the range  $0.7 < x < 0.8$ . Fuks D et al. [2] calculated the theoretical phase diagram, according to which the solid solutions (SSs) of the  $\text{Ba}_x\text{Sr}_{1-x}\text{TiO}_3$  system at room temperature in the range  $0.20 < x < 0.80$  are in the state of spinodal decomposition. The presented work gives experimental confirmation of the theoretical phase diagram. The Psc phase, that we discovered is located precisely in the region of spinodal decomposition of SSs according to [2]. The X-ray diffraction pattern of SSs in this region is characterized by single broadened peaks, and near  $x = 0.5$ , the fine structure of the peaks demonstrates their doubleness. Figure 1(a) shows the diffraction peaks 200 and 111 of SS with  $x = 0.5$ , on which seen a small but distinct splitting into two peaks, the corresponding unit cell parameters are:  $a_1 = 3.956 \text{ \AA}$ ,  $a_2 = 3.951 \text{ \AA}$ . Figure 1(b) shows the dependences of the coherent scattering regions,  $D(x)$  and microstrains  $\Delta d/d(x)$  in the interval  $0 \leq x \leq 0.4$ . It is seen that after separation of the second phase from the matrix in the range:  $0.25 \leq x < 0.275$ ,  $D$  decreases from 110 to 30 nm, and  $\Delta d/d(x)$  has not a sharp maximum before decay and a sharp drop after it, as is typical for a phase transition along type of nucleation and growth. For example, in the  $\text{PbZr}_{1-x}\text{Ti}_x\text{O}_3$  system, upon the nucleation of rhombohedral phase clusters inside the T-phase ( $x = 0.70 - 0.75$  Ti) before the separation of the new phase clusters,  $\Delta d/d$  increased from  $0.6 \times 10^{-3}$  to  $30 \times 10^{-3}$ , and after their separation decreased to  $0.2 \times 10^{-3}$  [3]. Thus, our experiment confirms the correctness of the theoretical phase diagram.

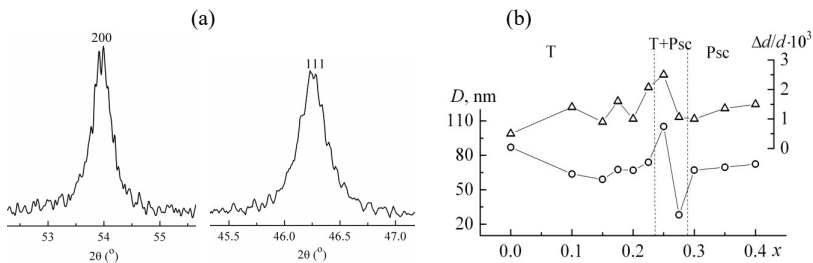


Fig. 1

## Acknowledgement

Research was financially supported by the Ministry of Science and Higher Education of the Russian Federation (State assignment in the field of scientific activity, Southern Federal University, 2020).

## References

- [1] S.V. Khasbulatov, L.A. Shilkina, H. A. Sadykov et al. // *Bull. Russ. Acad. Sci. Phys.* **80**(11), 1364-1366, 2016.
- [2] Fuks D., Dorfman S., Piskunov S., Kotomin E.A. // *Phys. Rev. B.* **71**, 014111-9, 2005.
- [3] L.A. Shilkina, P.G. Grin', L.A. Reznichenko et al. // *Phys. Sol. State.* **58**(3), 551-556, 2016.

## Analysis of Material Properties Using Machine Learning

O.V. Shilyaeva<sup>2</sup>, A.V. Cherpakov<sup>1,2\*</sup>, R.I. Shakhanov<sup>2</sup>, C.-Y. Jenny Lee<sup>3</sup>, Y.-M. Liu<sup>3</sup>

<sup>1</sup>*Southern Federal University, Rostov-on-Don, Russia*

<sup>2</sup>*Don State Technical University, Rostov-on-Don, Russia*

<sup>3</sup>*Department of Electric Communication Engineering, National Kaohsiung University of Science and Technology, Kaohsiung, Taiwan (R.O.C.)*

\*[alex837@yandex.ru](mailto:alex837@yandex.ru)

At the moment, there is a high growth rate of machine learning, which deals with various tasks of a wide range. There are not many studies that help solve the problem of assessing the properties of materials that can be used in the construction and design of various objects. The objects of research in this report are the properties of various materials and the analysis of their properties depending on the applied impact. The aim of the study is to determine the properties of such materials for their further use in industrial projects in the modeling and production of various types of elements and structures. Material properties can be assessed based on non-destructive testing methods. One of these methods is the indentation of some rigid indenter into the surface of the material. By obtaining plastic deformations on the surface of the material (holes), assessing their sizes, depth, and other characteristics, the material properties are determined, such as: modulus of elasticity, ultimate strength, dynamic viscosity, Brinell hardness. It is required to build a recurrent neural network with the LSTM architecture that performs regression analysis and approximates the output information depending on input data. The properties obtained in the result of the operation of the neural network are the main ones in determining the bearing capacities of steel structures and their general strength, which are important for modeling and subsequent manufacturing of structures. It is also possible to talk about new results of the application of machine learning in this area and the subsequent more comprehensive development of the implementation of machine learning, when solving problems of this type. As a result, an information system is being implemented that allows one to analyze the properties of various materials under various conditions, such as using different set-ups and other factors that affect the results of experiments. The information system collects, stores, and analyzes the properties of materials received at the input of the neural network, based on qualitative experimental pre-introduced reference values. To achieve the set task, modern technologies for constructing and training a recurrent neural network with the LSTM architecture were applied, as well as web programming technologies were used and actual tools for implementing the software product were used.

### **Acknowledgement**

Research was financially supported by Southern Federal University, grant No. VnGr-07/2020-04-IM (Ministry of Science and Higher Education of the Russian Federation).

## **Assessment of Crack Resistance of Bridge Reinforced Concrete Piles**

**E.A. Shlyakhova<sup>1</sup>, I.A. Serebryanaya<sup>1\*</sup>, I.O. Egorochkina<sup>1</sup>, A.V. Cherpakov<sup>1,2</sup>**

<sup>1</sup>*Don State Technical University, 1, Gagarin Sq., Rostov-on-Don, 344010, Russia*

<sup>2</sup>*Southern Federal University, Rostov-on-Don, Russia*

\*[silveririna@mail.ru](mailto:silveririna@mail.ru)

Providing standardized quality indicators for reinforced concrete piles for bridge construction is an essential requirement in their manufacture. A mandatory controlled parameter, along with indicators such as strength, density, frost resistance and water resistance, is crack resistance. It is known that crack resistance and its quantitative characteristics are the main indicators of the quality of the material used in structural calculations based on the laws of fracture mechanics of solids. Determination of crack resistance of bridge piles is a rather time-consuming process. This process requires the availability of a specially equipped testing ground for the release of large production areas, special handling equipment, a large number of additional devices, etc. One of the non-destructive diagnostic methods is the vibration method, based on the analysis of the parameters of the natural vibrations of the structures under investigation. The analysis of works [1 – 5] shows that the vibration diagnostics allows one to set the number, type, localization, parameters of the defects of the object. Moreover, it allows one to evaluate the strength and deformation properties of building structures. It is proposed to apply the method of vibration diagnostics with the subsequent simulation of the kinetics of the development of structural deformation in the ANSYS software package for continuous monitoring of the crack resistance of piles. In this case, the results of continuous laboratory control of the values of actual strength and density of concrete for each filling of factory-made piles are used as input parameters.

### **References**

- [1] A.V. Cherpakov, E.A. Shlyakhova I.O. Egorochkina Y.A. Kokareva // *Materials Science Forum.* **931**, 373-378, 2018.
- [2] A.V. Cherpakov, A.N. Soloviev, V.V. Gricenko, O.U. Goncharov // *Defence Science Journal.* **66**(1), 44-50, 2016.
- [3] Cherpakov A., Egorochkina I., Shlyakhova E., Kharitonov A., Zarovy A., Dobrohodskaya S. // *MATEC Web of Conferences*, **106**, 04009, 2017.
- [4] Poryadina N.A., Serebryanay I.A., Matrosov A.A., Nizhnik D.A. In: *Construction and Architecture. Faculty of Industrial and Civil Engineering.* Rostov-on-Don. 124-127, 2017 (In Russian).
- [5] Matrosov A.A., Serebryanay I.A., Lukinova N.A., Nizhnik D.A., Terekhina Yu.V. In: Abstracts & Schedule of the 2018 International Conference on “Physics and Mechanics of New Materials and Their Applications” (9-11 August, 2018, Busan, South Korea), Korea Maritime and Ocean University Press: Busan, 238, 2018.

## Optical and EXAFS Studies of $\text{NaNbO}_3$ – $\text{NaTaO}_3$ Solid Solution Crystals

V.A. Shuvaeva<sup>1</sup>, I.P. Raevski<sup>1\*</sup>, A.M. Glazer<sup>2</sup>, S.I. Raevskaya<sup>1</sup>, G.A. Simachkova<sup>1</sup>,  
V.V. Titov<sup>1</sup>, M.A. Malitskaya<sup>1</sup>

<sup>1</sup>Research Institute of Physics and Faculty of Physics, Southern Federal University,  
Rostov-on-Don, 344090, Russia

<sup>2</sup>Department of Physics, Oxford University, Parks Road, Oxford, OX1 3PU, UK

\*[igorraevsky@gmail.com](mailto:igorraevsky@gmail.com)

$\text{NaNbO}_3$ -based solid solutions are prospective environmentally-friendly materials for piezoelectric, pyroelectric, electrostrictive and energy storage applications [1 – 4]. In the present work flux-grown  $(1-x)\text{NaNbO}_3-x\text{NaTaO}_3$  (NNT- $x$ ) solid solution crystals are studied in order to take a further insight into the nature of phase transition diffusion in  $\text{NaNbO}_3$ -based solid solutions. Both ceramic and single-crystal NNT- $x$  compositions with  $x > 0.5$  are known to exhibit a diffuse dielectric permittivity  $\epsilon$  maxima [1]. Temperature-dependent optical studies of NNT crystals were carried out by the rotating polarizer method, using the Metripol ([www.metripol.com](http://www.metripol.com)) microscope system [5] and a precise heating stage (Linkam HFS91). False-colour images showing values of  $|\sin\delta| = |\Delta n \cdot L \cdot 2\pi/\lambda|$  ( $\Delta n$  is the birefringence,  $L$  is the crystal thickness,  $\lambda = 600$  nm is the light wavelength) and the orientation of the optical indicatrix at every point of the crystals were obtained in the temperature range from 20 to 600 °C. Birefringence values were extracted from the  $|\sin\delta|$  data. Optical studies have shown that the value of  $|\sin\delta|$  of pure  $\text{NaNbO}_3$  exhibits an abrupt jump at 370 °C, corresponding to the well-known first-order antiferroelectric phase transition. No such jumps are observed at higher temperatures. High-temperature phase transitions which occur at 480, 520, 575 °C and according to the X-ray diffraction studies are due to the rotation of oxygen octahedra, manifest themselves only through a change in the period of  $|\sin\delta|$ . Two types of optical extinction, namely symmetrical and parallel ones have been observed in two domains of the crystal below the phase transition and only parallel extinction at higher temperatures. This is in a total agreement with the earlier optical studies of  $\text{NaNbO}_3$  crystals. NNT-0.6 crystal displays sharp jumps of birefringence  $\Delta n$  at 580 °C and at 480 °C, which can be attributed to the rotational phase transitions. Below  $\approx -100$  °C the  $\Delta n(T)$  dependence changes a slope indicating a diffuse phase transition. This result agrees well with the data of dielectric measurements, which show that NNT-0.6 crystal has a diffused maximum of dielectric permittivity  $\epsilon$ . Its temperature  $T_m \approx -100$  °C is close to the temperature of the kink in the  $\Delta n(T)$  dependence and is practically independent on frequency in the 1 – 100 kHz range. Nb K-edge extended X-ray absorption fine structure (EXAFS) spectra of the pure NN and NNG-0.6 crystals were measured in the transmission mode at the Synchrotron Radiation Source (SRS, Daresbury). Comparison of Fourier Transforms (FTs) of Nb K-EXAFS spectra of NN and NNT-0.6 shows that a partial substitution of Ta for Nb leads to a decrease in the displacements of Nb atoms from the centers of oxygen octahedra.

### Acknowledgement

This study is supported by Russian Science Foundation (project 19-12-00205).

### References

- [1] I.P. Raevski, L.A. Reznitchenko, M.A. Malitskaya, et al // *Ferroelectrics*. **299**, 95, 2004.
- [2] Z. Liu, T. Lu, J. Ye, et al // *Adv. Mater.* **3**, 1800111, 2018.



- [3] S. I. Raevskaya, M. A. Malitskaya, C-C. Chou, et al // *Phys. Status Solidi A*. **216**, 1800972, 2019.  
[4] M. Zhou, R. Liang Z. Zhou, X. Dong // *J. Amer. Ceram. Soc.* **103**, 193, 2020.  
[5] A.M. Glazer, J.G. Lewis, W. Kaminsky // *Proc. R. Soc. London. Ser. A*. **452**, 2751, 1996.

## **Influence of Organic Coatings Formation Conditions on Their Morphology and Protective Properties**

**E.N. Sidorenko\*, S.P. Shpanko, M.A. Bunin**

*Southern Federal University, Rostov-on-Don, 344006, Russia*

[\\*si-do-re@mail.ru](mailto:si-do-re@mail.ru)

The protective properties and morphological features of organic coatings received on the surface of low-alloy steel by adsorption method from an inhibited solution of sulfuric acid were studied. The inhibitor was a substituted benzimidazole derivative (surface-active substance, SAS). The SAS was doped by thiocyanate ions, introduced in the form of KNCS. The dependences of organic coatings properties and characteristics on the KNCS ( $C_{KNCS}$ ) concentration and on the film formation time  $t$  were studied. The growth regularities of the protection degree of these coatings with a decrease in  $C_{KNCS}$  and an increase in  $t$  were established earlier [1]. The protective effect of the organic compound significantly increased when thiocyanate anions were introduced into the inhibited acid solution. However, this effect is somewhat reduced with a further increase in  $C_{KNCS}$ . Such an effect of sulfur containing compounds is associated with their dual influence at the state of the interphase boundary. The recharging of the steel surface and the blocking of adsorption-active centers are the consequences of this effect. The analysis of various samples surface topography images was performed. The purpose of that analysis was to find out the relationship between the protection degree of the composite SAS, the concentration of  $C_{KNCS}$ , and the features of the surface micro-relief. To get these data the scanning electron and atomic force microscopes were applied. From the AFM, 2D and 3D surface images of the inhibited samples were obtained: the scan relief height distribution histograms, the arithmetic and geometric roughness values, the surface structural peculiarities distribution in sections of the scans surface. All that data allowed us to find the correlation between the protective effect of the inhibitor,  $C_{KNCS}$  and  $t$ . The analysis of the inhibited samples surface morphology indicates the resulting coatings heterogeneity. The steel surface is covered completely with conical globules. Difficulties in the formation of large globules and a decrease in the film roughness are due to the  $C_{KNCS}$  increase. With an increase in the film formation time, the larger sized globules grow, and the surface roughness increases. Coalescence of globules and formation of large globular aggregates occurred with an additional increase in  $t$  and  $C_{KNCS}$ . Thus, the protective properties of organic coatings are determined by the concentration of thiocyanate anions in the composite inhibitor and the morphology of the precipitates formed. Large aggregates of coalescent globules with clear border outlines provide a high protection degree of the steel surface from corrosion and are formed at a long adsorption time and optimal concentration of thiocyanate anions.

### **Reference**

[1] Shpanko S.P., Sidorenko E.N., et al In: *Proceedings of the 2018 International Conference on Physics and Mechanics of New Materials and Their Applications*, Ivan A. Parinov, Shun-Hsyung Chang, Yun-Hae Kim (Eds.). Nova Science Publishers, New York, 13-19, 2019.

## **Microwave Energy Absorption and Radiation Spectra of Lead Ferrowolframate Ceramics**

**E.N. Sidorenko\*, V.G. Smotrakov, M.A. Marakhovskiy**

*Southern Federal University, Rostov-on-Don, 344006, Russia*

\*[si-do-re@mail.ru](mailto:si-do-re@mail.ru)

The absorption and radiation spectra of a ceramic ferromagnet–lead ferrowolframate  $\text{PbFe}_{2/3}\text{W}_{1/3}\text{O}_3$  (PFW) have been studied in the radio frequency range of 3.2 – 12 GHz. It is known that ferroelectric and magnetic subsystems coexist in this compound. Such materials are promising for creating devices, the magnetic properties of which can be controlled by an electric field and (or) change their electrical properties by a magnetic field. Ceramic samples of ferroelectric relaxor PFW were obtained by spark plasma sintering at a temperature of 700 C. The samples were shaped like a disk with a diameter of 10 mm and a height of 1 mm. Their domain structure was studied using an electron microscope. The work used the same microwave technique as before [1]. To measure spectra in the frequency range of 3.2 – 12 GHz, three replaceable generators with panoramic VSWR and attenuation meters were used. The test sample was located on the surface of the microstrip line (MSL) as in dielectric resonator antennas. The electromagnetic field radiation spectra and the electromagnetic field direction diagrams at the vicinity of the disk were obtained using receiving antennas in the form of a pin-type or loop-type vibrator. The absorption spectra of PFW are strongly rugged and have several sharp large (30 – 40 dB) maximum of the resonant type. The type of spectra, the number of maxima in the spectrum and their values depend on external factors such as: temperature, uniaxial mechanical pressure, displacement of the sample relative to the central conductor of the MSL, the angle of rotation of the sample around its own axis. We have studied the spectra of integral radiation of electric field strength and magnetic field induction at different heights from the sample surface. The maximum height at which the detected antenna signal could still be measured using a digital voltmeter without an additional amplifier is 60 mm. The angular distribution of the intensity of the electric field of the PFW resonator at various distances from its side surface is studied at the frequency of the maximum radiation of the electromagnetic field. The impact of a constant magnetic field with induction  $B = 0.375$  T did not change the absorption spectra of PFW, in contrast to the changing spectra of composite compositions based on manganite [2]. The obtained data confirm the presence of polar nanoregions (clusters) in PFW ceramics at a considerable distance from the temperature of the diffuse phase transition. Absorption spectra with a large number of resonance-type maxima indicate the existence of various ensembles of oscillators with their own resonant frequencies in the PFW domain structure. These oscillators can be domain walls of mechanical twins in clusters of ceramics, making elastic vibrations in the electromagnetic field.

## References

- [1] Sidorenko E.N., Chan Thi Beat Ngoc, Prikhodko G.I., Natkhin I.I., Shloma A.V., Kharchenko D.G. // *Journal of Advanced Dielectrics*. 10(01-02), 2060020, 2020.
- [2] Sidorenko E.N., Privalov E.E., Demchenko A.A., Kabirov Yu.V., Chebanova E., Nathan I.I. *Radiation and Scattering of Electromagnetic Waves*. RSEMW. 464 – 467, 2019.

## Photoluminescence of Nominally Pure Lithium Niobate Crystals Grown by Different Technologies

N.V. Sidorov<sup>1</sup>, N.A. Teplyakova<sup>1</sup>, M.V. Smirnov<sup>1\*</sup>, M.N. Palatnikov<sup>1</sup>, V.B. Pikylev<sup>2</sup>

<sup>1</sup>Tananaev Institute of Chemistry – Subdivision of the Federal Research Centre “Kola Science Centre of the Russian Academy of Sciences”, Apatity, Russia

<sup>2</sup>Petrozavodsk State University, Petrozavodsk, Russia

\*[max-17000@yandex.ru](mailto:max-17000@yandex.ru)

Photorefractive LiNbO<sub>3</sub> crystal has a variety of intrinsic defects in its structure. They form many localized energy levels in the band gap, location of which depends on the Li/Nb ratio [1]. Excited electrons relaxing to a ground state through energy levels in the band gap lead to both the energy transfer to the lattice phonons and the appearance of radiation with a certain wavelength. The latter determines the luminescent characteristics of optical materials based on a LiNbO<sub>3</sub> crystal. It is of interest to find out the influence of the defective structure on the luminescent properties of nominally pure LiNbO<sub>3</sub> crystals depending on the Li/Nb ratio. The results of photoluminescence in a nominally pure congruent crystal (LiNbO<sub>3cong</sub>), as well as in crystals obtained by two technologies: from a melt with 58.6 mol. % Li<sub>2</sub>O (LiNbO<sub>3stoich</sub>) and HTTSSG (High temperature technology top speed solution growth) from congruent melt with the addition of flux 6 wt. % K<sub>2</sub>O (LiNbO<sub>3stoich</sub>:K<sub>2</sub>O) are observed. Photoluminescence spectra were recorded with a SL100M spectrograph (Solar TII) with a CCD detector (FLICCDML0673710). He-Cd laser was used as excitation source. There are a wide halo at the range from 380.0 to 650.0 nm and sharp increase of luminescence intensity (> 700.0 nm) in the photoluminescence spectra of LiNbO<sub>3stoich</sub>, LiNbO<sub>3stoich</sub>:K<sub>2</sub>O and LiNbO<sub>3cong</sub> crystals obtained from the sample volume. The halo at 527.0 nm (LiNbO<sub>3stoich</sub>), 613.0 nm (LiNbO<sub>3cong</sub>) and 612.0 nm LiNbO<sub>3stoich</sub>:K<sub>2</sub>O is complex and consists of five individual bands. Luminescence centers in form of Nb<sub>Li</sub> defects in LiNbO<sub>3</sub> crystals correspond to the luminescence bands at 510.0 – 520.0 nm [2]. The intensity of luminescence bands with maxima at 510.0 – 527.0 nm increases in the series of LiNbO<sub>3stoich</sub>, LiNbO<sub>3stoich</sub>:K<sub>2</sub>O, and LiNbO<sub>3cong</sub> crystals. It indicates a sequential increase in the number of Nb<sub>Li</sub> defects. Moreover, the shift of some emission bands in LiNbO<sub>3cong</sub> crystal to long-wavelength range in comparison with LiNbO<sub>3stoich</sub> was observed. It may be caused by changing the absorption edge values equal to 3.48 and 3.72 eV for LiNbO<sub>3stoich</sub> and LiNbO<sub>3cong</sub> crystals, respectively [3]. It is known that hydrogen is located at three positions in the LiNbO<sub>3</sub> structure [3]. Consequently, the defects in form of Me-OH also leads to additional effects connected with the energy transfer and the appearance of new emission centers. The photoluminescence intensity in LiNbO<sub>3</sub> crystals close to the stoichiometric composition was lower than in a congruent crystal. An increase in the Li/Nb ratio leads to the shift

of photoluminescence bands to the short-wavelength region of the spectrum and the change of fundamental absorption edge of the crystals. In addition to point defects in the cationic sublattice, complex defects due to the presence of OH groups in the structure can also contribute to photoluminescence.

### References

- [1] N.V. Sidorov, T.R. Volk, B.N. Mavrin, V.T. Kalinnikov. Lithium niobate: defects, photorefraction, vibrational spectrum, polaritons. Moscow: Nauka, 2003 (In Russian)
- [2] M.H.J. Emond, M. Wiegel, G. Blasse, R. Feigelson // *Mat. Res. Bull.* **28**(10), 1025-1028, 1993.
- [3] N.V. Sidorov, M.N. Palatnikov, N.A. Teplyakova, A.V. Syuy, E.O. Kile, D.S. Shtarev // *Inorg. Mater.* **54**(6), 581–584, 2018.

## Structural Particularities of LiNbO<sub>3</sub>:B (0.55, 0.69, 0.83 mol. % B<sub>2</sub>O<sub>3</sub>) with R (Li/Nb) Close to Stoichiometric

N.V. Sidorov, N.A. Teplyakova, R.A. Titov\*, M.N. Palatnikov, I.V. Biryukova

*Tananaev Institute of Chemistry – Subdivision of the Federal Research Centre “Kola Science Centre of the Russian Academy of Sciences”, Apatity, Russia*

[\\*r.titov@kcs.ru](mailto:r.titov@kcs.ru)

There are two methods for growing crystals close to the stoichiometric composition: growing from a Li<sub>2</sub>O – Nb<sub>2</sub>O<sub>5</sub> melt with 58.60 mol. % Li<sub>2</sub>O and from a congruent melt with ~ 6 wt. % alkaline solvent (flux) K<sub>2</sub>O (HTTSSG method - High temperature top speed solution growth). The first method is used rarely due to the high heterogeneity of the composition and refractive index of the grown crystal along the growth axis. The HTTSSG method is much more complicated although it allows us to obtain stoichiometric single crystals of a high degree of compositional uniformity. In this work, we have studied nominally pure LiNbO<sub>3</sub> crystals with different Li/Nb ratios grown from a congruent melt with a flux of B<sub>2</sub>O<sub>3</sub>. A LiNbO<sub>3</sub>:B crystal (0.55 – 0.83 mol. % B<sub>2</sub>O<sub>3</sub>) was obtained using direct solid-phase alloying [1]. The boron does not enter the lithium niobate crystal structure, since the LiNbO<sub>3</sub> phase does not have a solubility region of boron in the solid state. But boron compounds can be used as a flux. At the same time, LiNbO<sub>3</sub>:B crystals are close to a stoichiometric crystal by the number of the structural defects, but differ from it by a significantly smaller photorefractive effect. A calculation based on the Curie temperature of LiNbO<sub>3</sub> crystals has shown that an increase in the boron concentration in the charge leads to an increase in the Li/Nb ratio and Li content in the grown crystals. Moreover, the LiNbO<sub>3</sub>:B crystals are characterized by decrease in the number of Nb<sub>Li</sub> defects. For LiNbO<sub>3</sub>:B (0.55 mol. % B<sub>2</sub>O<sub>3</sub>),  $T_c = 1145$  K, Li/Nb = 0.942, [Li] = 48.56 mol. % [2], [Nb<sub>Li</sub>] = 0.976 mol. %. For LiNbO<sub>3</sub>:B (0.83 mol. % B<sub>2</sub>O<sub>3</sub>),  $T_c = 1189$  K, Li/Nb = 0.970, [Li] = 49.76 mol. % [2], [Nb<sub>Li</sub>] = 0.503 mol. %. The linewidths in the Raman spectra of LiNbO<sub>3</sub>:B crystals, corresponding to vibrations of intra-octahedra cations (150 – 300 cm<sup>-1</sup>), are less than the corresponding linewidths of the spectrum of the LiNbO<sub>3</sub> crystal and coincide with the linewidths in the spectrum of a stoichiometric crystal [3]. The Raman spectra data indicate ordering of structural units of the cation sublattice along the polar axis. The widths of the components of the

absorption band of the IR spectra of  $\text{LiNbO}_{3\text{stoich}}$  and  $\text{LiNbO}_3\text{:B}$  crystals (0.55 and 0.83 mol. %  $\text{B}_2\text{O}_3$ ) are narrower than that in a congruent crystal, which reveals a higher ordering of the proton sublattice in a  $\text{LiNbO}_{3\text{stoich}}$  and  $\text{LiNbO}_3\text{:B}$  (0.55 and 0.83 mol. %  $\text{B}_2\text{O}_3$ ) crystals than in a congruent crystal. It was shown that structuring the congruent melt by nonmetallic element boron can adjust the number of point defects ( $\text{Nb}_{\text{Li}}$ ) and the Li/Nb ratio. Note that both the increase in the lithium content and trace amounts of boron ( $10 \times 10^{-4}$  wt. %) increase ordering of the structural units of the cation sublattice along the polar axis in a nominally pure  $\text{LiNbO}_3\text{:B}$  crystal. It brings the structure of  $\text{LiNbO}_3\text{:B}$  crystals closer to stoichiometric composition. Thus a nominally pure  $\text{LiNbO}_3\text{:B}$  demonstrates a high optical damage resistance. Moreover, boron compounds reduce the content of multiply charged transition metal impurities in the crystal, which significantly affect photorefractive effect.

### References

- [1] M. N. Palatnikov, N. V. Sidorov, In: *Oxide Electronics and Functional Properties of Transition Metal Oxides*, A. Pergament (Ed.). New York: Nova Science Publishers, 31 – 168, 2014.  
 [2] H. M. O'Bryan, P. K. Gallagher, C. D. Brandle // *J. Amer. Ceram. Soc.*, **68**(9), 493 – 496, 1985.  
 [3] Sidorov N. V., Teplyakova N. A., Titov R. A., Palatnikov M. N. // *Tech. Phys.*, **63**(12), 1758 – 1766, 2018.

## Piezoelectric Characteristics of Ternary Solid Solutions $(1 - x - y)\text{BiFeO}_3 - x\text{PbFe}_{0.5}\text{Nb}_{0.5}\text{O}_3 - y\text{PbTiO}_3$

**E.I. Sitalo, N.A. Boldyrev\***

*Research Institute of Physics, Southern Federal University,  
 Rostov-on-Don, 344090, Russia*

[\\*nboldyrev@sfsedu.ru](mailto:nboldyrev@sfsedu.ru)

Unalloyed samples of solid solutions of the ternary system  $(1 - x - y)\text{BiFeO}_3 - x\text{PbFe}_{0.5}\text{Nb}_{0.5}\text{O}_3 - y\text{PbTiO}_3$  ( $y = 0.05, 0.175 \leq x \leq 0.325$ ) were prepared by the solid-phase reactions technique with following sintering using conventional ceramic technology. X-ray diffraction analysis revealed the rhombohedral structure in all solid solutions (Fig. 1a). Studying the dielectric characteristics of ceramics revealed that samples with  $x > 0.225$  demonstrate relaxor-like behavior. It was manifested in presence of the maxima on the  $\epsilon'/\epsilon_0(T)$  dependencies shifting to the higher temperature region with increasing  $f$ . Fig. 1b shows the concentration dependence of the piezoelectric module  $d_{33}$  of the ceramics. The value of  $d_{33}$  initially reaches the minimum at  $x = 0.25$  (the first relaxor in this section) and then increases with increasing PFN concentration. The highest piezoelectric constant of 50 pC/N for  $x = 0.325$  ceramic is much larger than  $d_{33} = 15$  pC/N achieved in BF-PT ceramics fabricated by conventional solid-phase reactions method [1] and reasonably close to the value of 87 pC/N found in BF-PT ceramics prepared by much more complicated technique [2]. This result confirms the efficiency of PFN for modification of BF-PT solid solution system.

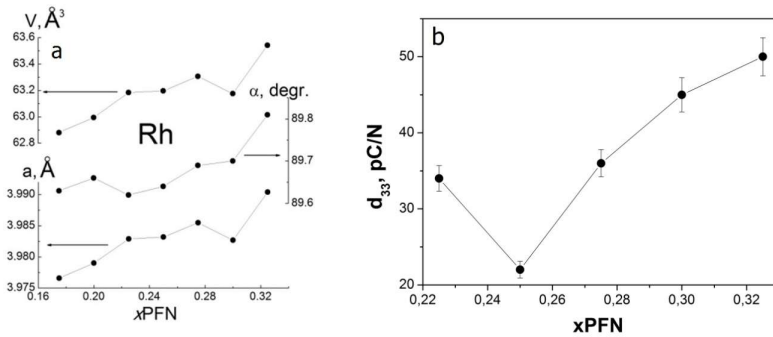


Fig. 1. Concentration dependencies of the unit cell parameters  $V$ ,  $\alpha$  and  $a$  (a) and  $d_{33}$  (b) at room temperature

### Acknowledgements

The work was supported by the Ministry of Science and Higher Education of the Russian Federation (State assignment in the field of scientific activity, Southern Federal University, 2020) with equipment of the CCU "EETPS", RIF SFedU.

### References

- [1] T.P. Comyn, T. Stevenson, A.J. Bell // *J. Phys. IV Fr.* **128**, 13–17, 2005.
- [2] H. Amorín, C. Correas, C. M. Fernández-Posada, O. Peña, A. Castro, M. Algueró // *J. Appl. Phys.* **115**, 104104, 2014.

## Microstructure, Ferroelectric and Piezoelectric Properties of Textured Bismuth-containing Ceramics

E.I. Sitalo\*, V.G. Smotrakov

Research Institute of Physics Southern Federal University, Rostov-on-Don, 344090, Russia

\*[sitalo@sfedu.ru](mailto:sitalo@sfedu.ru)

Bismuth titanate with a layered perovskite-like structure ( $\text{Bi}_4\text{Ti}_3\text{O}_{12}$ , BLSF) was of great interest for use in piezoelectric sensors at high temperature due to its high Curie temperature ( $T_C = 675^\circ\text{C}$ ) and strong ferroelectric polarization [1]. The aim of the study is to investigate the processes of crystalline texture formation in polycrystalline BLSF and to establish the dependence of the electrophysical properties of ceramics on the degree of texturing. Ceramics were textured using the hot stamping method developed at the Research Institute of Physics [2]. The mechanism of the method is that the workpiece is subjected to uniaxial pressure and free radial deformation occurs due to the plastic flow of the material until the workpiece fills the free volume of the mold, which is created by placing the workpiece in the mold with a gap. The study of the microstructure of ceramics showed that an increase in the firing temperature in the range of  $950 - 1050^\circ\text{C}$  causes a sharp decrease in porosity and increases the density to  $7.95 \text{ g/cm}^3$ , which is 98% of theoretical. An

X-ray analysis was performed and microstructural studies were carried out, which revealed the formation of an axial texture in ceramics. The features of the switching processes of textured ceramics are revealed. The characteristics of the polarization switching of ceramics in the directions parallel and perpendicular ( $\perp$ ) of the pressure axis during hot processing were obtained from the dielectric hysteresis  $P(E)$  loops, i.e. axis axial texture. The  $\perp$ -cut ceramics are characterized by a more complete polarization switching, which is associated with the additional orientation of the (001) crystallographic planes in the textured material, as well as the presence of a threshold switching field. In the temperature range from  $-196$  to  $+600$  °C, the anisotropy of the electrophysical properties of ceramics was studied due to the presence of a crystalline texture in it. The dielectric constant, electrical conductivity, piezoelectric and elastic coefficients were measured for sections of ceramics of different orientations relative to the axis of the texture. The anisotropy of the dielectric constant and electrical conductivity manifests itself weakly at room temperature and increases sharply when approaching the Curie temperature. In the temperature range  $+20 - 400$  °C the high thermal stability of the piezoelectric module  $d_{33}$ , measured by the quasistatic method, was established.

#### **Acknowledgements**

The work was supported by the Ministry of Science and Higher Education of the Russian Federation (State assignment in the field of scientific activity, Southern Federal University, 2020) with equipment of the CCU "EETPS", RIF SFedU.

#### **References**

- [1] Xudong Li, Lingli Zhu et al. // *J. Appl. Phys.* **127**, 044102 (2020).
- [2] E.G. Fesenko, V.P. Zavyalov et al. A method of manufacturing a high-density piezoelectric ceramic // *USSR author's certificate* No. 1286576, MKI CO4B 35/64.

## **Determination of the Physical Constants of a Piezomagnetolectric Layered Composite**

**A.N. Soloviev<sup>1,2\*</sup>, Do Thanh Binh<sup>2</sup>, V.A. Chebanenko<sup>3\*\*</sup>, A.V. Derkun<sup>2</sup>**

*<sup>1</sup>Don State Technical University, Rostov-on-Don, Russia*

*<sup>2</sup>I. I. Vorovich Mathematics, Mechanics and Computer Science Institute, Southern Federal University, Rostov-on-Don, Russia*

*<sup>3</sup>Federal Research Center "Southern Scientific Center of the Russian Academy of Sciences", Rostov-on-Don, Russia*

\*[solovievarc@gmail.com](mailto:solovievarc@gmail.com); \*\*[valera.chebanenko@yandex.ru](mailto:valera.chebanenko@yandex.ru)

A layered composite consisting of alternating piezoelectric and piezomagnetic layers is considered. Such layered stack can be used as a piezoactive layer in a bimorph structure, in which these layers are glued to the middle passive layer i.e., a substrate. The presented piezoelectric element can be used as a piezoelectric generator (PEG) for energy harvesting device which works in an external alternating magnetic field. An alternating magnetic field is associated with some electromagnetic device or may be artificial due to the rotation of some mechanism on which the permanent magnets

are located. To calculate the characteristics of the PEG, such as resonant frequencies, output potential, etc., it is necessary to know the effective physical constants of a multilayer package. Methods for determining these effective properties are developed in this study. A finite element model of the representative volume of the composite is constructed and a number of static boundary value problems are solved, which have analytical solutions for a homogeneous medium. Several ways of determining effective constants are considered. Namely, the well-known volume fractions method, the method of averaging the characteristics of internal fields over the volume and the method proposed in the work, in which additional data for solving the inverse coefficient problem are "measured" at the boundary of the body. Numerical calculations were carried out in plane and three-dimensional formulations, in which various ratios of layer thicknesses and their number were considered. The obtained results of calculating the effective physical constants of the composite showed good agreement between the proposed method and the procedure for averaging over the area.

#### ***Acknowledgement***

This work was supported by the Government of the Russian Federation, contract No. 075-15-2019-1928.

## **Applied Theory of Bending Vibrations of a Bimorph with Two Active Composite Piezomagnetolectric Layers**

**A.N. Soloviev<sup>1,2\*</sup>, Do Thanh Binh<sup>2</sup>, V.A. Chebanenko<sup>3\*\*</sup>, E.V. Kirillova<sup>4</sup>**

*<sup>1</sup>Don State Technical University, Rostov-on-Don, Russia*

*<sup>2</sup>I. I. Vorovich Mathematics, Mechanics and Computer Science Institute,  
Southern Federal University, Rostov-on-Don, Russia*

*<sup>3</sup>Federal Research Center "Southern Scientific Center of the Russian Academy of Sciences",  
Rostov-on-Don, Russia*

*<sup>4</sup>RheinMain University of Applied Sciences, Wiesbaden, Germany*

*\*[solovievarc@gmail.com](mailto:solovievarc@gmail.com); \*\*[valera.chebanenko@yandex.ru](mailto:valera.chebanenko@yandex.ru)*

The theory is based on the plane problem of steady bending vibrations of a plate. The plate consists of three layers. The outer two layers are two identical piezoactive layers made of composite piezomagnetolectric material. Between them there is a substrate i.e., a purely elastic layer. It is assumed that the considered composite material is a package consisting of alternating piezoelectric and piezomagnetic layers. Therefore, to simplify the problem, when describing piezoactive bimorph layers, the effective physical constants of a multilayer package will be used. The presented problem is solved within the framework of the linear theory of piezomagnetoelastocity. An applied theory is built on the basis of hypotheses about the distribution of mechanical, electric and magnetic fields using the variational principle. Within the framework of the constructed theory, the problem of finding the natural frequencies of the plate is solved, and the values of the mechanical, electrical and magnetic field characteristics are calculated. The constructed applied theory of bimorph bending can be used to calculate a piezoelectric generator (PEG) for energy harvesting from an external alternating magnetic field. An alternating magnetic field is associated with some



electromagnetic device or may be artificial due to the rotation of some mechanism on which the permanent magnets are located.

#### ***Acknowledgement***

This work was supported by the Government of the Russian Federation, contract No. 075-15-2019-1928 and by the Russian Foundation for Basic Research grant No. 19-08-00365\_A.

## **Study of the Efficiency of Using Porous Piezoceramics in a Stack-type Piezoelectric Generator**

**A.N. Soloviev<sup>1,2\*</sup>, Do Thanh Binh<sup>2</sup>, V.A. Chebanenko<sup>3\*\*</sup>, P.A. Oganesyanyan<sup>2</sup>**

*<sup>1</sup>Don State Technical University, Rostov-on-Don, Russia*

*<sup>2</sup>Vorovich Mathematics, Mechanics and Computer Science Institute, Southern Federal University, Rostov-on-Don, Russia*

*<sup>3</sup>Federal Research Center "Southern Scientific Center of the Russian Academy of Sciences", Rostov-on-Don, Russia*

[\\*solovievarc@gmail.com](mailto:solovievarc@gmail.com); [\\*\\*valera.chebanenko@yandex.ru](mailto:valera.chebanenko@yandex.ru)

It is known that piezoelectric materials are widely used as actuators, sensors and generators in mechanical engineering and aerospace for monitoring the health of structures, shape control, active suppression of parasitic vibrations, noise suppression, etc. In the field of energy harvesting by using piezoelectric materials, free mechanical energy present in structures is converted into electrical energy, and its subsequent transformation into suitable for powering low-power devices. In this work, within the framework of the previously developed mathematical model, we study the efficiency of a stack piezoelectric generator based on composite piezoelectric materials. The device is a multilayer transducer consisting of several layers of porous piezoelectric ceramics, connected in parallel into a single electric circuit. By modeling composite piezoelectric layers, previously calculated effective material constants were used. The analysis of the considered devices is carried out depending on the percentage of porosity of the piezoelectric ceramics and geometric dimensions. It is shown that with an increase in the percentage of porosity, the output electrical characteristics of the generator improve. As a result, a set of values of the geometric parameters of the device and values of the porosity of the material was obtained, on the basis of which it is possible to manufacture PEG with the maximum possible output power.

#### ***Acknowledgments***

This work was supported by the Government of the Russian Federation, contract No. 075-15-2019-1928 and by the Russian Foundation for Basic Research grant No. 19-08-00365\_A.

## The Simplest Mathematical Models of Wheat Ear Dynamics

A.N. Soloviev\*, A.A. Matrosov, I.A. Panfilov, O.N. Lesnyak, D.A. Nizhnik

*Don State Technical University, 1, Gagarin Sq., Rostov-on-Don, 344010, Russia*

\*[solovievarc@gmail.com](mailto:solovievarc@gmail.com)

The work is devoted to the urgent task of today, namely the development of new highly effective physicommechanical methods for harvesting grain crops and the design of appropriate equipment [1, 2]. Static and dynamic deformation of a stem with an ear of wheat is considered. The purpose of this report is to determine the factors affecting the stem for subsequent isolation of the grain. Two stages of grain ripening are considered: at the early stage, the grain is attached by the stalk to the ear, at the second stage there is no stalk, the connection of grain with the spike is carried out by means of scales. Deformation is considered within elastic limits until the destruction of plant elements. An ear with a stem is an elastic body, one size of which is much larger than the other two, in addition, the geometric and mass characteristics of the stem and ear are significantly different from each other. The grain size is much smaller than the size of the stem and spike. The statement of the problem is carried out in the framework of the linear theory of elasticity and represents the initial-boundary-value problem in the case of non-stationary effects on the plant and boundary-value problems with static exposure and with steady vibrations. The simplest mathematical model is a model consisting of absolutely solid bodies interconnected by elastic bonds. Rods with a given moment of inertia act as such bodies, and spiral springs serve as elastic bonds [3, 4]. A more complex model is the Euler-Bernoulli rod model. If at the same time we assume that the beam consists of two homogeneous parts (stem and spike), then in this case, in a static and harmonic analysis, a solution can be constructed analytically. In the general case, the characteristics of the cross-section and the mechanical properties depend on the longitudinal coordinate of the beam, which leads to boundary value problems with variable coefficients, which can be solved analytically only in some special cases and require numerical solutions. An analysis of the results for different degrees of grain ripening made it possible to assess the applicability limits of the described models and give recommendations on the parameters of the impact of the working body of the combine on the ear.

### References

- [1] Matrosov A.A., Serebryanaya I.A. In: *Materials of the International Scientific and Practical Conference "Construction-2013"*. Rostov-on-Don: RGSU Press, 75-76, 2013 (In Russian).
- [2] Lysenok O.I., Matrosov A.A. In: *Materials of the 7th International Scientific and Practical Conference (Interagromash-2014)*. Rostov-on-Don: DSTU Press, 86-87, 2014 (In Russian).
- [3] Lachuga Yu.F., Matrosov A.A., Panfilov I.A., Pakhomov V.I., Rudoy D.V. In: *Abstracts of the XIV All-Russian School "Mathematical Modeling and Biomechanics at a Modern University"*. Rostov-on-Don: SFedU Press, 91, 2019 (In Russian).
- [4] Lachuga Yu.F., Soloviev A.N., Matrosov A.A., Panfilov I.A., Pakhomov V.I., Rudoy D.V. In: *2019 International Conference on "Physics and Mechanics of New Materials and Their Applications"*, PHENMA 2019, Hanoi, Vietnam, November 7 – 10, 2019, Hanoi University of Science and Technology: Hanoi, 179 – 180, 2019.

## The Use of Porous Piezoelectric Ceramics in a Piezoelectric Composite of 1-3 Connectivity

A.N. Soloviev<sup>1,2\*</sup>, A.V. Nasedkin<sup>2\*\*</sup>, Do Thanh Binh<sup>2</sup>, V.A. Chebanenko<sup>3\*\*\*</sup>,  
P.A. Oganesyan<sup>2</sup>

<sup>1</sup>*Don State Technical University, Rostov-on-Don, Russia*

<sup>2</sup>*Vorovich Mathematics, Mechanics and Computer Science Institute, Southern Federal University, Rostov-on-Don, Russia*

<sup>3</sup>*Federal Research Center "Southern Scientific Center of the Russian Academy of Sciences", Rostov-on-Don, Russia*

\*[solovievarc@gmail.com](mailto:solovievarc@gmail.com); \*\*[nasedkin@math.sfedu.ru](mailto:nasedkin@math.sfedu.ru); \*\*\*[valera.chebanenko@yandex.ru](mailto:valera.chebanenko@yandex.ru)

A piezoelectric composite of 1-3 connectivity is considered, which is a certain passive matrix filled with parallel piezoactive rods. These piezoelectric rods are polarized along their length and undergo tensile-compressive deformation. In this case, the main coefficient that characterizes the efficiency of converting mechanical energy into electrical energy is the piezo module  $d_{33}$ . If solid piezoceramic is used as a piezoactive material, then usually its rigidity is much higher than that of the matrix. It is possible to overcome this difference by using porous piezoelectric ceramics. It is known from the literature that for porous piezoceramics the magnitude of the piezoelectric modulus  $d_{33}$  is practically independent of the percentage of porosity, and in some cases, it becomes larger than for solid piezoceramics. Determination of the physical properties of such a composite is carried out in two stages. At the first stage, the finite element package ACELAN-COMPOS determines the elastic, piezoelectric and electrical properties of porous piezoelectric ceramics, as a composite 3-0, for a discrete set of its percentage of porosity. At the second step, the data of the first stage are used, also in the ACELAN-COMPOS package to determine the physical constants of the composite 1-3 of connectivity. In this case, both the percentage of porosity of the piezoceramic and its volume fraction in the composite vary.

### **Acknowledgement**

This work was supported by the Government of the Russian Federation, contract No. 075-15-2019-1928.

## Finite-element Modeling of Soft Biological Tissues Indentation

A.N. Soloviev<sup>1,2\*</sup>, A.S. Vasiliev<sup>1</sup>, I.A. Panfilov<sup>1</sup>, A.S. Lednov<sup>1</sup>, E.V. Sadyrin<sup>1</sup>

<sup>1</sup>*Don State Technical University, Rostov-on-Don, Russia*

\* [solovievarc@gmail.com](mailto:solovievarc@gmail.com)

One of the most actual problems arising during keratoprosthesis development is modelling of interaction of such an implant with the cornea soft tissues. The mathematical model should contain

the mechanical properties of these soft tissues. One of the ways to determine these properties *in vivo* is to conduct a nanoindentation experiment for cornea thus obtaining "load –displacement" functional relationship. This dependence can serve as additional information for solving the inverse coefficient problem. The paper considers a contact problem for soft biological tissue in the framework of a poroelastic water-saturated medium described by the Bio model, which is the prototype of the cornea of the eye. Within the framework of plane deformation, two types of boundary conditions for pore pressure under a smooth flat punch and their influence on the relationship between the indentation depth and the contact force are investigated. The first type corresponds to the impermeability condition, the second type corresponds to the proportionality of pore pressure to contact stresses. Moreover, various boundary conditions on the surface of the body outside the punch are considered: impermeability of the boundary and zero pore pressure. A set of mechanical boundary conditions under the punch is also considered: smooth contact, rigid adhesion, and contact with friction. The problems are solved numerically using the finite element method for the model material. It is concluded that it is necessary to compare the calculation results with a full-scale experiment for a material with specified properties. Such a comparison will allow one to build an adequate mathematical model for the pore pressure under the punch.

#### **Acknowledgement**

This work was supported by the Government of the Russian Federation (grant No. 14.Z50.31.0046).

## **Effect of Focal Position on Cut Surface Quality in Laser Cutting of 50 mm Thick Stainless Steel**

**M.K. Song<sup>a</sup>, J.E. Kim<sup>b</sup>, J.H. Jung<sup>c</sup>, D.S. Shin<sup>d</sup>, J. Suh<sup>d</sup>, S.J. Lee<sup>d</sup>, J.D. Kim<sup>e\*</sup>**

<sup>a</sup>*Laser Advanced Machining Support Center, Korea Maritime and Ocean University, Busan, Korea*

<sup>b</sup>*Ocean Science and Technology School, Korea Maritime and Ocean University, Busan, Korea*

<sup>c</sup>*Graduate School, Korea Maritime and Ocean University, Busan, Korea*

<sup>d</sup>*Busan Machinery Research Center, Korea Institute of Machinery & Materials, Busan, Korea*

<sup>e</sup>*Division of Marine Engineering, Korea Maritime and Ocean University, Busan, Korea*

\*[jdkim@kmou.ac.kr](mailto:jdkim@kmou.ac.kr)

The technology for dismantling nuclear power structures is complex and difficult, similar to their construction technology. Furthermore, structure dismantling requires a wide variety of technology to prevent radiation leak and is a large-scale process that takes as long as 60 years in some cases. Because workers do not have access to the inside of a nuclear power plant, a remote dismantling system using automated devices such as robot is required for structure dismantling. Cutting technology, which is currently used for structure dismantling in the nuclear power industry, includes abrasive mixed waterjet, diamond wire cutting, and plasma arc cutting. However, because these methods contain complex mechanisms, their application is limited. Hence, recently, high-power laser cutting that facilitates easy automation and long-distance remote control based on fiber transmission have attracted considerable attention in the nuclear power plant demolition industry [1, 2]. In this study, the parameters for underwater laser cutting of 50 mm thick stainless steel, which is typically used in nuclear power structures, are investigated. The focal position of laser beam

significantly affects the cutting quality. In particular, in the cutting of the thick sample, change in the focal position determines the kerf width and the roughness of the cut surface.

#### **References**

- [1] Ana Beatriz Lopez, Eurico Assuncao, Luisa Quintino, Jonathan Blackburn, Ali Khan // *Nuclear Engineering and Technology*. **49**, 865-872, 2017.  
[2] Abdul Fattah Mohd Tahir, Syarifah Nur Aqida // *Optics & Laser Technology*. **92**, 142–149, 2017.

## **Reinforcing Effects of CNT Nanofiller for Enhancing the Interfacial Bonding Strength of Filament Wound FRP Composites**

**Soo-Jeong Park, Yun-Hae Kim<sup>†</sup>**

*<sup>1</sup>Department of Ocean Advanced Materials Convergence Engineering, Korea Maritime and Ocean University, 727 Taejong-ro, Yeongdo-gu, Busan, 49112, Republic of Korea*

*<sup>†</sup>[yunheak@kmou.ac.kr](mailto:yunheak@kmou.ac.kr)*

Nanofillers used in polymer composites have attracted considerable attention in reinforcement or functionalization. The nanofillers are a lightweight material and have advantages in the process, even without a change in scale, because the performance can be dramatically improved with only a small amount. In this respect, in this study, carbon nanotube (CNT) was used to overcome the limitations of failure such as band slip, resin-rich phenomena cross-ply region according to the filament wound structure's winding angle. According to previous studies, CNT has been excellently utilized to improve interfacial bonding strength in general fiber reinforced plastic (FRP) laminates. However, the CNT is limited in use, such as non-uniform dispersibility due to aggregation in industrial production of bulk scale. In other words, reinforcing CNTs throughout the structure may act as a weakness that degrades the structure's performance.

Therefore, in this study, to maximize the interfacial reinforcement effect of CNT, the reinforcement effect of CNT according to the reinforcement of each layer in the filament wound cylinder structure is analyzed under various loads. In other words, the CNT nanofiller was applied to local layers rather than full-scale filament wound FRP composites. Its effects on physical interfacial bonding strength and failure behavior were evaluated. Besides, the roles of CNT nanofiller was investigated by specifying interfacial defects such as interplay voids.

#### **Acknowledgment**

This work was supported by the Technology Innovation Program (No. 20005403), funded by the Ministry of Trade, Industry & Energy (MOTIE, Korea).

## Study of the Influence of the Configuration of a Rotary Mixer on the Quality Indicators of the Mixture

S.A. Stel'makh<sup>1\*</sup>, E.M. Shcherban'<sup>1</sup>, I.A. Parinov<sup>2</sup>, A.V. Cherpakov<sup>1,2</sup>, J.-P. Wang<sup>3</sup>

<sup>1</sup>Don State Technical University, Rostov-on-Don, Russia

<sup>2</sup>Southern Federal University, Rostov-on-Don, Russia

<sup>3</sup>Department of Naval Architecture Engineering, National Kaohsiung University of Science and Technology, Kaohsiung, Taiwan (R.O.C.)

[\\*au-geen@mail.ru](mailto:au-geen@mail.ru)

The research substantiates the relevance of the influence on the mixing process of the geometric parameters of a rotary mixer, the design of the mixing body, its location in the volume of the mixer, the shape of the mixer and its geometry [1]. The aim of the study was the influence of the ratio of the height of the mixture and the diameter of the mixer on the quality of the mixture and power consumption. The height (depth) of the liquid (foam concrete mixture) in the mixer vessel ( $H_{mix}$ ) (for mixers with paddle mixers) is in practice taken equal to the vessel diameter ( $D$ ), that is,  $H_{mix} = D$ . However, in the case of designing a mixer having a different height of the mixture in container, the question arises whether this will affect the homogeneity of the mixture density in the volume of the mixture and the power consumed for mixing. The ratio  $H_{mix}/D$  affects the density of the foam concrete mixture. Fig. 1 shows the dependence of the coefficient of homogeneity of the foam concrete mixture by density  $K_{chm} = \bar{\rho}_{min}/\bar{\rho}_{max}$  on the ratio  $H_{mix}/D$ .

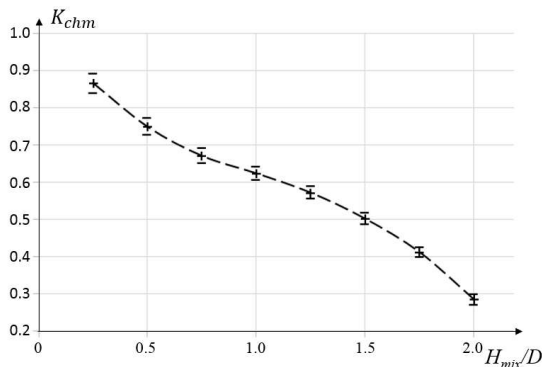


Fig. 1. Dependence of the homogeneity of the foam concrete mixture on the ratio  $H_{mix}/D$

The experiment was carried out on a cylindrical mixer with a conical bottom. The density of the foam concrete mixture in the mixer volume was measured by sampling after preparing the mixture through the discharge valves installed on the mixer body along the entire height with a step of 300 mm. Fig. 1 shows that with an increase in the loading height of the mixture, the homogeneity of the

mixed mixture steadily decreases. This is explained by the fact that the circulation flow rate  $q$  decreases with an increase in the height of the mixture, the nature of the movement of the mixture from the turbulent regime turns into a laminar one, and the turbulent transfer of particles of the mixture between the central zone and the peripheral zone decreases.

#### **Acknowledgement**

Research was financially supported by Southern Federal University, grant No. VnGr-07/2020-04-IM (Ministry of Science and Higher Education of the Russian Federation).

#### **Reference**

[1] Sergey A. Stel'makh, Evgenii M. Shcherban, Anatolii I. Shuiskii, Al'bert Yu. Prokopov, Sergey M. Madatyan, Ivan A. Parinov Alexander V. Cherpakov // *Applied Sciences (MDPI)*. **10**(22), 8055-8075, 2020.

## **Structure Features of BiFeO<sub>3</sub> Thin Film on Magnesium Oxide Substrate**

**D.V. Stryukov<sup>1\*</sup>, A.V. Pavlenko<sup>1,2</sup>**

<sup>1</sup>*Southern Scientific Centre of the Russian Academy of Sciences,  
41, Chekhov Str., Rostov-on-Don, 344006, Russia*

<sup>2</sup>*Research Institute of Physics, Southern Federal University,  
194, Stachki, Ave., Rostov-on-Don, 344090, Russia*

[\\*strdl@mail.ru](mailto:*strdl@mail.ru)

Multiferroics, are materials possessing simultaneously two or more primary ferroic-like properties. Among multiferroics, BiFeO<sub>3</sub> (BFO) is the most widely considered compound because of coexistence of remarkable structural, ferroelectric, magnetic and optical properties in its thin films at room temperature.

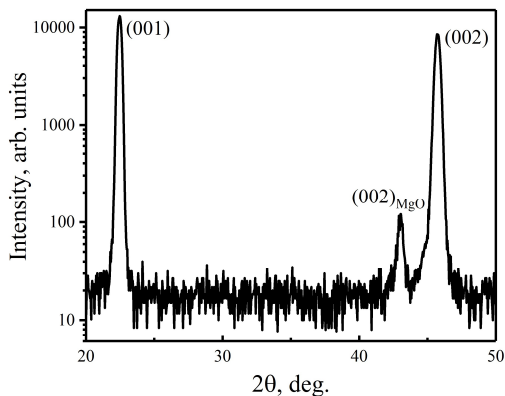


**Fig. 1.** XRD pattern of BFO/MgO(001) heterostructure

It makes BFO a unique candidate for multifunctional device applications. This paper presents the results of the structure investigation of BFO thin films, which were grown on single-crystal MgO(001) substrates by RF-cathode sputtering technique. By X-ray diffraction studies (Fig. 1) of the BFO/MgO heterostructure, it has been revealed that the BFO film was sputtered epitaxially. No impurity phases have been found. It has been established that the unit cell has a rhombohedral structure. The unit cell parameters are  $a = 0.3964 \pm 0.0001$  nm;  $\alpha = 89.8^\circ$ . Preliminary work on the synthesis of  $\text{Sr}_x\text{Ba}_{1-x}\text{Nb}_2\text{O}_6$ /BFO two-layer structures on MgO(001) substrates have been carried out.

#### ***Acknowledgements***

This work was performed in the framework of a state assignment for the Southern Scientific Center of the Russian Academy of Sciences (project No. 01201354247) and a grant of the President of the Russian Federation (project No. MK-678.2020.2).

## **Lamination Design for Composite Material Application of Ship Radar Mast**

**Sung-Won Yoon, Chang-Wook Park\***

Research Institute of Medium & Shipbuilding, 38-6, Noksan Industrial Complex-232 Ro,  
Gangseo-Gu, Busan, Republic of Korea

\*[cwpark@rims.re.kr](mailto:cwpark@rims.re.kr)

International Maritime Organization (IMO) regulations on carbon dioxide and greenhouse gas emissions have come into force, requiring energy saving and eco-friendly material technology. Therefore, there is a need for a lightweight material that can maintain stability and durability in an extreme marine environment and which has excellent mechanical performance. As the IMO's environmental regulations have been strengthened to increase the energy efficiency of ships, the IMO has also begun to consider operational economics such as energy reduction through lightening the hull. Demand for lighter weight technology using composite materials is increasing. Examples would include lightweight large structures using composite materials, composite materials replacing metal design parts, and polymer composite materials applicable to marine environments. When the existing metal material is replaced with a composite material, the cargo transport volume increases due to weight reduction and the operational efficiency is improved, so that a high economic effect can be expected. In this study, analysis is carried out on the application of a ship radar mast. In the composite material, the mechanical properties vary depending on the laminated pattern of the reinforcing material. The properties of the composite materials were calculated using the computer simulation program. The laminate patterns are an important factor in determining the strength and life of the final structure. In this study, the structural safety was analyzed for the laminate patterns. The laminating pattern and order were finally decided considering the results of the finite element analysis (FEA).



## **A Study on Structural Design and Analysis of 18ft CFRP Leisure Boat**

**Sung-Youl Bae<sup>1\*</sup>, Yun-Hae Kim<sup>2</sup>**

*<sup>1</sup>Center of Ceramic Fiber Commercialization, Korea Institute of Ceramic Engineering and Technology, Busan, Korea*

*<sup>2</sup>Department of Ocean Advanced Materials Convergence Engineering, Korea Maritime and Ocean University, Busan, Korea*

[\\*boxer2002@hanmail.net](mailto:*boxer2002@hanmail.net)

The purpose of this study is to develop a lightweight design model for an 18ft leisure boat. The existing leisure boat is manufactured by GFRP material and hand lay-up process. CFRP is applied on the new design to reduce the weight of boat, and automated tape laying machine is applied manufacturing process of the lightweight boat. The newly designed CFRP model is 30% lighter than the existing GFRP model. Moreover, it was confirmed that the newly designed lightweight hull has sufficient structural integrity compared to the existing hull through the structural integrity evaluation by FEA.

## **The Treatment of Restaurant Wastewater Containing Oil and Grease by Using Immersed Membrane Bioreactor: Design Concept, Application and its Maintenance in Indonesia**

**Supardi\*, Elisa Sulistyorini**

*Mechanical Engineering Department, University of 17 Agustus 1945 Surabaya, Indonesia*

[\\*supardis@gmail.com](mailto:*supardis@gmail.com)

Restaurant business has been growing rapidly in Indonesia these days. As the consequence of this growth, a large amount of wastewater containing a great amount of oil and grease from the leftovers of food discharged to the sewage system every day. This will pose some adverse impacts to the environment and human beings if the appropriate treatment is not performed. One of the advanced wastewater treatment plant, membrane bioreactor (MBR), has been claimed to have more advantages over conventional activated sludge (CAS) in terms of high efficiency of contaminant removal and not-so-large space required. Several references about MBR technology have been reviewed and corresponded with the restaurant wastewater issues (primarily oil and grease content), and its condition in Indonesia. Based on this study, a design concept of biotreatment by using isolated microorganisms and physical means by using immersed membrane is given for the lab-scale study. The lab-scale experiment is then needed to explore the feasibility of full-scale application in restaurant and foodservice operation in Indonesia. The implementation of immersed membrane bioreactor (iMBR), however, has a major drawback refers to as membrane fouling. This fouling can reduce the performance and lifespan of membrane, which then lead to an increase in

maintenance and operating costs. This study also provides an overview of membrane fouling and several factors affecting it, as well as its mitigating strategies in iMBR full-scale application.

## **Determination of the Tribological Properties of the Oil Saturated Composite under Dynamic Effects Depending on the Viscosity of the Liquid Phase**

**T.V. Suvorova, O.A. Belyak\***

*Rostov State Transport University, Rostov-on-Don, Russia*

*\*o\_bels@mail.ru*

Recently, oil-filled nanocomposites, which are used for assemblies and parts of tribological applications, have become widespread. The components of the considered composite materials have viscoelastic properties and the properties of a viscous fluid [1]. When designing such new composite materials, the actual and practically unexplored task is to study the influence of dynamic effects arising due to vibration on the antifriction properties of the tribosystem. To study the patterns of changes in the stress-strain state of a tribosystem, a dynamic contact problem is solved taking into account friction in the contact area for a base with a microstructure. For this purpose, the contact problem of steady-state oscillations of a punch with a flat sole on a heterogeneous base is considered, taking into account friction in the contact area. The heterogeneous base is described by the Biot-Fraenkel equations in terms of displacements [2]. Using the integral Fourier transform, the problem is reduced to an integral equation of the first kind with a difference kernel. The integral equation was solved numerically based on the modified collocation method [3]. Depending on the viscous properties of the liquid filler and the degree of saturation of the viscoelastic matrix of the material with it, contact pressures and tangential displacements in the contact region were studied. The results of numerical analysis are consistent with the field experiment for a low-saturated composite with a matrix of the aromatic polyamide phenylene with nanoscale additives and a viscous cylindrical filler oil.

### ***Acknowledgement***

This study was supported by the Russian Science Foundation (project No. 18-08-00260).

### ***References***

- [1] Ivanochkin P.G., Suvorova T.V, Danilchenko S.A., Novikov E. S., Belyak O.A. // *Vestnik RGUPS*. **4**(72), 18-25, 2018 (In Russian)
- [2] Belyak O.A., Suvorova T.V. // *Ecological Bulletin of Research Centers of the Black Sea Economic Cooperation*. **3**(16), 33-39, 2019.
- [2] Kolesnikov V.I., Belyak O.A., Kolesnikov I.V, Suvorova T.V. // *Doklady Akademii Nauk. Physics, Technical Sciences*. **2**(491), 5–9, 2020.

## **A Novel Universal Voltage-mode Inverse Filter for Signal Processing**

**Ta-Chi Jeang, Po Cheng Ke, Hung-Yu Wang\*, Tsair-Fwu Lee, Chien-Liang Chiu**

*Department of Electronic Engineering, National Kaohsiung University of Science and Technology, Kaohsiung, Taiwan, R.O.C.*

[\\*hywang@nkust.edu.tw](mailto:hywang@nkust.edu.tw)

Inverse filters are used in numerous situations, such as communication, speech processing, audio and acoustic systems, and instrumentation [1 – 6]. They are put to use to recover the input signal from the available distorted output signal resulted from the signal progress. The realization of universal inverse filter received much attention due to its convenience of realizing different type inverse filter functions. In this report, a novel universal voltage-mode inverse filter is proposed. It can realize various inverse filter functions by using the same scheme. HSPICE simulations are performed to verify the feasibility of the proposed structure. Its workability is shown by the simulated results.

### **Acknowledgement**

This research was funded by the Ministry of Science and Technology of the Republic of China, grant numbers MOST 108-2622-E-992-012-CC3 and 108-2622-8-992-301-TE2.

### **References**

- [1] O. Kirkeby, P. A. Nelson // *Journal of the Audio Engineering Society*, 47(7-8), 583–595, 1999.
- [2] J. K. Tugnait // *IEEE Transactions on Signal Processing*, 45(3), 658-672, 1997.
- [3] E. M. Hamed, L. A. Said, A. Madian, A. G. Radwan // *Circuits, Systems and Signal Processing*, 39(1), 2-29, 2020.
- [4] D. R. Bhaskar, M. Kumar, P. Kumar // *Analog Integrated Circuits and Signal Processing*, 97, 149–158, 2018.
- [5] H. Y. Wang, C. T. Lee // *Electronics Letters*, 35, 1889-1890, 1999
- [6] H. Y. Wang, S. H. Chang, T. Y. Yang, P. Y. Tsai // *Circuits and Systems*, 2, 14-17, 2011.

## **Intensity of Singular Stress Field Analysis for Scarf Joint**

**R. Takaki\*, N. A. Noda, B. Wang, S. Wang, Y. Sano, Y. Takase**

*Department of Mechanical Engineering, Kyushu Institute of Technology, Kitakyushu, Japan*

[\\*takaki.rei244@mail.kyutech.jp](mailto:takaki.rei244@mail.kyutech.jp)

Semiconductor packaging contains various interfaces composed of different materials combinations, such as connection between semiconductor and substrate, sealing with resin, multilayer structuring of semiconductor chip and wiring, etc. To ensure the reliability, it is indispensable to evaluate the peeling strength properly. The peel strength of dissimilar bonding interface varies greatly depending on material combination, load type, bonding condition, and the like. In previous study, the

debonding strength of the butt joints was expressed by the intensity of singular stress field (ISSF). In this study, the debonding strength evaluation will be investigated for scarf joint under tension by considering ISSF. Then, the debonding condition will be compared with the butt joint. Fig. 1 shows relationship between the critical remote tensile stress  $\sigma_{yc}^{\infty}$  and adhesive thickness  $h$ . Fig. 2 shows the critical singular stress distribution  $\sigma_{\theta c}(r)$  near the interface corner. Fig.2 is obtained by considering ISSF. The critical remote tensile stress  $\sigma_{yc}^{\infty}$  increases with decreasing adhesive thickness as shown in Fig. 1. However, critical singular stress distribution  $\sigma_{\theta c}(r)$  can be expressed by almost one curve independent of adhesive thickness except when the thickness is extremely thick.

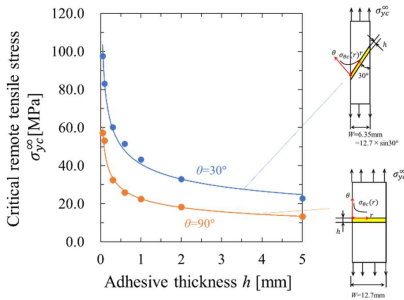


**Fig. 1.** Relationship between the critical remote tensile stress  $\sigma_{yc}^{\infty}$  and adhesive thickness  $h$  for scarf joint and butt joint

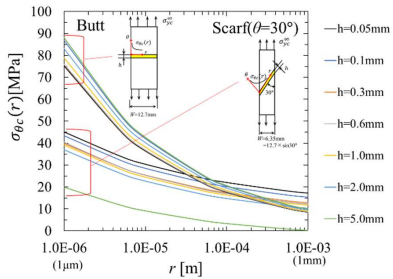


**Fig. 2.** Critical singular stress distribution  $\sigma_{\theta c}(r)$  at near the interface corner for scarf joint and butt joint

## Dielectric Tunability of Multicomponent Relaxor Ceramics

M.V. Talanov

Research Institute of Physics, Southern Federal University, Rostov-on-Don, 344090, Russia

[mvtalanov@sfdedu.ru](mailto:mvtalanov@sfdedu.ru)

Ferroelectric materials demonstrate nonlinear dielectric response under applied electric field ( $E$ ). Dielectric tunability can be defined as  $n(E) = [\epsilon(0) - \epsilon(E)]/\epsilon(0)$ , where  $\epsilon(0)$  and  $\epsilon(E)$  represent the dielectric permittivity at  $E = 0$  kV/cm and at a certain electric field, respectively. The study of dielectric tunability is necessary for the use of materials in filters, phase shifters etc. Moreover, the behavior of dielectric tunability reflects the fundamental features of the ferroelectric/dielectric material response to an applied electric field. Relaxor ferroelectrics differ from other dielectric materials by extremely high values of dielectric constant and dielectric tunability, which at room temperature can reach values of  $> 10,000$  and  $> 75\%$ , respectively. Therefore, the aim of this work was to establish the dielectric tunability of multicomponent relaxor ceramics. The object of the study was the ceramics of the multicomponent system

$(\text{Pb}_{0.95}\text{Ba}_{0.05})(\text{Zn}_{1/3}\text{Nb}_{2/3})_y(\text{Mg}_{1/3}\text{Nb}_{2/3})_m(\text{Ni}_{1/3}\text{Nb}_{2/3})_n\text{Ti}_x\text{O}_3$  with a wide variation in the concentrations of the components. The choice of the object of study is due to a combination of high piezoelectric and dielectric parameters of individual compositions, as well as a variety of polar states (ergodic relaxor, relaxor with diffused transition to the ferroelectric state, normal ferroelectric) in the system. The  $\varepsilon(E)$  dependences were measured at room temperature in the *ac* measuring electric field into range of 0.1 – 100 kHz on a test system including an Agilent 4263B LCR-meter. The measurements were carried out using reversible changes in the *dc* electric field in the range from –20 to +20 kV/cm. The report presents the main results of the study. In particular, the dependences of dielectric parameters on the concentrations of individual components ( $\text{PbTiO}_3$  and  $\text{PbNi}_{1/3}\text{Nb}_{2/3}\text{O}_3$ ) of solid solutions are obtained. The relationship between the dielectric parameters, crystal structure and polar states of the studied objects is established. Moreover, it was shown that the study of the dielectric permittivity in strong electric fields makes it possible to clarify the boundaries between adjacent polar states at the  $x - T$  phase diagram, which are difficult to identify based on the separate results of dielectric spectroscopy or X-ray diffraction. In the course of the study, the compositions, promised for practical applications of solid solutions, with the dielectric permittivity of ~ 16,500 and the dielectric tunability of more than 90%, were identified.

#### **Acknowledgements**

This work has been done on equipment of Collective use center "Electromagnetic, electromechanical and thermal properties of solids", Southern Federal University. This work was financially supported by the State assignment in the field of scientific activity, Southern Federal University, 2020.

## **Dielectric Properties of Bismuth-containing Pyrochlores: A Comparative Analysis**

**M.V. Talanov<sup>1\*</sup>, A.A. Bush<sup>2</sup>, K.E. Kamentsev<sup>2</sup>**

<sup>1</sup>*Research Institute of Physics, Southern Federal University, Rostov-on-Don, 344090, Russia*

<sup>2</sup>*Research Institute of Solid-state Electronics Materials, Russian Technological University (RTU MIREA), Moscow, 119454, Russia*

[\\*mvtalanov@sfedu.ru](mailto:mvtalanov@sfedu.ru)

Bismuth-containing pyrochlores are of great interest due to their dielectric and optical properties as well as photo-catalytic activity. One of the distinctive structural features of bismuth-containing pyrochlores is disordered displacement of  $\text{Bi}^{3+}$  cations with a lone-electron pair. According to a number of researchers, temperature-activated hopping of bismuth atoms between symmetrically equivalent positions is a source of dielectric relaxation in bismuth-containing pyrochlores, for example, in  $\text{Bi}_{1.5}\text{Zn}_{1.0}\text{Nb}_{1.5}\text{O}_7$  (BZN) [1]. However, among all the known bismuth-containing pyrochlores, one compound, namely  $\text{Bi}_2\text{Ti}_2\text{O}_7$  stands out fundamentally due to the absence of any compositional disorder. Earlier, large impurity-free single crystals were grown and their structure and dielectric properties were investigated [2]. In particular, it was shown that, unlike other bismuth-containing pyrochlores, attempts to describe the dielectric relaxation of  $\text{Bi}_2\text{Ti}_2\text{O}_7$  single crystals using the Arrhenius equation lead to physically insignificant values of the fitting parameters.

However, the relaxation behavior is well described by the empirical Vogel-Fulcher relation, which is typical for many dipole and spin glasses, as well as relaxor ferroelectrics. The discovered relaxor-like behavior of the  $\text{Bi}_2\text{Ti}_2\text{O}_7$  single crystal makes it a candidate-material for studying aspects of geometric frustration related with pyrochlore structure in non-magnetic medium. The aim of this study was to compare the dielectric properties of various bismuth-containing pyrochlores, which are characterized by both disordered displacement of  $\text{Bi}^{3+}$  cations and dielectric relaxation. Fitting parameters of the Arrhenius equation were analyzed for various bismuth-containing pyrochlores with and without compositional disorder in the cationic sublattices. The details of the relationship between the bismuth ions displacements, room temperature dielectric constant and dielectric relaxation parameters are discussed in the report.

#### **Acknowledgement**

This work was supported by the Russian Science Foundation, Project 20-72-00086.

#### **References**

- [1] S. Kamba, V. Porokhonsky, A. Pashkin, V. Bovtun, J. Petzelt, J.C. Nino, S. Trolier-McKinstry, M. T. Lanagan, C. A. Randall // *Physical Review B*. **66**, 054106, 2002.
- [2] A. A. Bush, M. V. Talanov, A. I. Stash, S. A. Ivanov, K. E. Kamentsev // *Cryst. Growth Des.* **20**, 824 – 831, 2020.

## **A Neural Network Analysis to The Risk Factors of Type 2 Diabetes**

**Te-Jen Su\*, Feng-Chun Lee, Shih-Ming Wang**

*Department of Electronic Engineering, National Kaohsiung University of Sciences and Technology, Kaohsiung, Taiwan*

\*[sutj@kuas.edu.tw](mailto:sutj@kuas.edu.tw)

International Diabetes Federation (IDF) announced that there are currently 463 million adults worldwide with diabetes, and the diabetic population in Taiwan has been growing. According to data from the National Health Insurance Bureau (MOHW), the prevalence of diabetes among adults in Taiwan has reached 5% and is increasing every year. In 2016, diabetes caused 56 million deaths worldwide. The World Health Organization (WHO) revealed that 1 from 11 adults has diabetes, but 1 from 2 adults is not diagnosed. By 2030, one from ten adults will have diabetes. This shows that diabetes is an important public health problem. It is one of the four major non-communicable diseases that world leaders must act on. About 8% of Taiwanese adults have diabetes, which can cause many complications, such as cardiovascular disease, visual impairment, amputation, kidney disease, etc. Cardiovascular disease is the most common complication of diabetes. It has the highest mortality rate and greatly increases medical expenses. This study used neural networks to create a predictive model that can be used as a diagnostic reference for healthcare professionals.

## **Particle Swarm Optimization Implementation on the Fault Diagnosis of Gearbox**

**Te-Jen Su\*, Tzung-Shiarn Pan, Tsung-Ying Li**

*Department of Electronic Engineering National Kaohsiung University of Sciences and Technology, Kaohsiung, Taiwan*

\*[sufj@kuas.edu.tw](mailto:sufj@kuas.edu.tw)

Condition monitoring and fault diagnosis both are issues which people attach importance to. We research particle swarm optimization based on the parameters and the functions of algorithm to propose modified particle swarm optimization algorithm. We do research on the theory and methods of the gearbox intelligent fault diagnosis based on particle swarm optimization algorithm. We solve the problems of multi points sensor's location and positioning by proposing modified location of the gearbox sensors based on modified particle. According to the outputs of gearbox finite element, we also build the adaptation based on modal assurance criterion. We prove the rationality of this method with the results of the gearbox experimental modal analysis and the frequency response characteristics analysis. We propose intelligence fault diagnosis method based on dynamic acceleration constant and modified speed of particle self-adaptation. We use time-domain and frequency-domain characterizations of gearbox vibration signal as neural network input, while the main fault form of gearbox as output to build neural network fault diagnosis system which is based on PSO. In the process of training and judgement, PSO is used as a rough optimization or off-line learning process which can adjust and optimize the global network parameters. While neural network learning is used as a fine optimization or on-line learning process which can optimize local parameters. We hope that the intelligent diagnosis method can improve the fault diagnosis performance of the gearbox and provide a solution for the efficiency and the accuracy of non-linear complex system fault diagnosis and for the improvement of automated diagnosis.

## **A Scissor Jack Mechanism Shear Mode Piezoelectric Energy Harvester for Wind Mill**

Tejkaran Narolia<sup>1\*</sup>, Vijay K. Gupta<sup>1</sup>, I.A. Parinov<sup>2</sup>

<sup>1</sup>*PDPM IITDM Jabalpur, India,*

<sup>2</sup>*Southern Federal University, Rostov-on-Don, Russia*

\*[tejkaran.narolia@iitdmj.ac.in](mailto:tejkaran.narolia@iitdmj.ac.in)

Day per day consumption of traditional energy sources and their harmful effects on humans and other creatures have increased the attention of the scientists to alternative. Energy harvesting from the wind or water flows caused by piezoelectric material is the best alternative. On other hand, the small-power sensors, actuators and wireless communications devices are run on batteries [1]. The

replacement of batteries in small power consuming wireless sensors, implantable medical devices, and structural health monitoring system become a tough and tedious task [2]. Rezaei-Hosseinabadi et al. [3] developed a topology for lift-based wind turbine piezoelectric harvester without contact vibration mechanism. Xie et al. [4] designed a ring piezoelectric energy harvester having inner and outer concentric ring. The results show that power 5274.8 W has been generated at radius 0.5 m of the harvester. Wang and Liu [5] fabricated a shear mode piezoelectric energy harvester for harnessing the power from pressurized water flow. FEM simulation and experiments results show that the open circuit peak to peak voltage vary from 72 mV to -72 mV. Zhou et al. [6] combined shear mode ( $d_{15}$ ) piezoelectric constitutive equations and single degree of freedom vibration system to harvest the energy from cantilever. Frequency dependent peak to peak voltage and power has been found out. Assembly of energy harvester is shown in Fig.1. For extracting power from wind mill, shaft is coupled to the wind mill. The major components of the harvester are a scotch yoke mechanism, two piezoelectric scissor jacks and two springs with spring constant  $k_s$ . The scotch yoke mechanism, shown in Fig. 2, is used to convert the rotary motion into a translated motion [7]. A sliding pair of slotted rod and cylinder mounted on the rotating wheel confirms the motion only in the normal direction to the shaft axis. When the shaft rotates with an angular velocity,  $\omega$ , the eccentricity,  $Y$ , of cylinder and wheel, displaces the end of the slotted rod from the starting point in time,  $t$ , by an amount  $Z_s = Y \sin \omega t$ . Figure 3(a) shows the piezoelectric-scissor jack mechanism, consisting of four arms of uniform length.

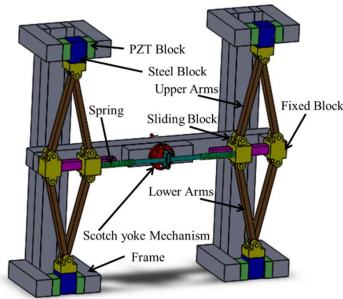


**Fig. 1.** Simple Configuration of Energy Harvester

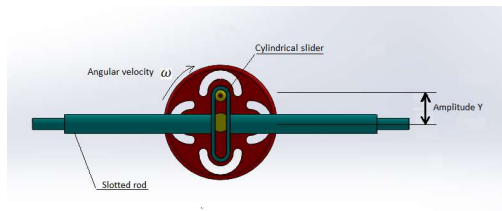


**Fig. 2.** Scotch yoke mechanism



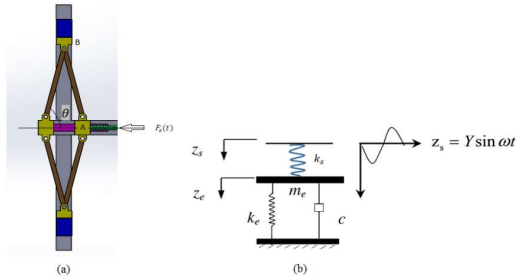


**Fig. 3.** (a) Scissor jack mechanism and (b) equivalent damped mass-spring model

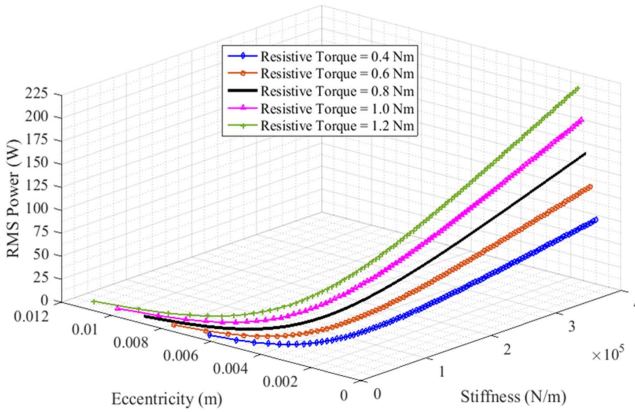


**Fig. 4.** Variation in RMS of electric power with spring stiffness

The lower ends of the upper two arms are hinged at fixed and sliding block for making turning pair and upper ends of arms hinged together to form self-turning pair. The material of arms of scissor jack is steel and the cross-section is square in plausibility with a side of square is  $s$  and the length of the arm is  $l$ . Electrical power was calculated against various physical and geometrical parameters of the harvester. Analytical formulation indicates that the execution of the harvester mainly depends on the stiffness of the spring and eccentricity of the scotch yoke mechanism. It is considered that the wind turbine is situated in areas of repugnant wind with a cut-in speed of 4.75 m/s for a turbine with three blades of 1 m length [8]. Figure 4 shows the influence of the spring stiffness  $k_s$  on the output electric power corresponding to the scissor jack angle, speed of the turbine, thickness and side of the PZT bar as  $80^\circ$ , 50 rad/s, 0.1 m and 20 mm, respectively. The generator resistive torque,  $k_s Y^2$ , is considered in the range between 0.4 to 1.2 N/m. The electric power rises nonlinearly with increase in the stiffness of spring. At the resistive torque of 0.4 N/m, the RMS of the power varies from 2.006 W to 69.51 W, corresponding to stiffness value between

100 kN/m<sup>2</sup> to 400 kN/m<sup>2</sup>. Similarly, at the resistive torque of 1.2 N/m, the RMS of the power varies from 6.0019 W to 208.55 W with the same variation in stiffness of the spring. At constant resistive torque  $k_s Y^2$  a rise in the spring stiffness would lead to a decrease in the magnitude of  $Y$ , and increase in the magnitude of the applied force on the PZT bars. So, an increase in the spring stiffness, decreases the eccentricity to maintain a constant resistive torque and allows one to obtain higher efficiency of the harvester. Adversely increase in the eccentricity  $Y$  at constant spring stiffness  $k_s$  increases the magnitude of the working force  $k_s Y$ , but simultaneously increases the resistive torque, thus reducing the effectiveness of the harvester at low wind speed areas.

#### **Acknowledgement**

Research was partially financially supported by RFBR grant No. 19-08-00365.

#### **References**

- [1] W. Wang, F. Ismail, F. Golnaraghi // *IEEE Trans. Fuzzy Syst.*, **12**(5), 710–723, 2004.
- [2] M. Bhardwaj, T. Garnett, A. P. Chandrakasan // *Commun. 2001. ICC 2001. IEEE Int. Conf.* **3**, 785–790, 2001.
- [3] N. Rezaei-Hosseinabadi, A. Tabesh, R. Dehghani, A. Aghili // *IEEE Trans. Ind. Electron.*, **62**(6), 3576–3583, 2015.
- [4] X. D. Xie, Q. Wang, N. Wu // *Int. J. Eng. Sci.*, **77**, 71–78, 2014.
- [5] D.-A. Wang, N.-Z. Liu // *Sensors Actuators A Phys.*, **167**(2), 449–458, 2011.
- [6] L. Zhou, et al. // *Sensors Actuators, A Phys.*, **179**, 185–192, 2012.
- [7] Scotch Yoke. [https://en.wikipedia.org/wiki/Scotch\\_yoke](https://en.wikipedia.org/wiki/Scotch_yoke).
- [8] D. H. Wood // *Wind Eng.*, **25**(4), 249–255, 2001.

## **Viscous Oil Cooling Unit**

**V.A. Temnenko<sup>1</sup>, D. D. Fugarov<sup>1\*</sup>, O. A. Purchina<sup>1</sup>, D.A. Onyshko<sup>2</sup>**

<sup>1</sup>*Don State Technical University, Rostov-on-Don, Russia*

<sup>2</sup>*South-Russian State Polytechnic University (NPI) named after M.I. Platov, Novocherkassk, Russia*

\*[ddf\\_1@mail.ru](mailto:ddf_1@mail.ru)

Today the current problem is the increase of automation level of one of the stages of petrochemical production of polymer threads, namely automation of technological process of cooling the viscous oil products [1]. The general principle of operation of the cooling unit is as follows: the fan sucks air into the installation chamber from the room and/or outside, depending on the time of year where it is mixed, filtered, cooled, moistened with sharp steam and heated to a given temperature [2]. The air is cooled by cold water, which is supplied to the coil through a closed circulation system from the cold-water preparation unit. Cooling air is heated to the specified temperature using electric heaters [3]. The automated control system of the cooling plant has the following requirements: it is necessary to provide alarm of the main emergency parameters, continuous monitoring of process parameters, to display process parameters on mnemonic circuits, to keep a set of process parameters within the specified limits, control of various mechanisms and devices of the process service,

recording the various transient states of the process [4]. To meet these requirements, it is necessary to automate the process using the modern software logic controller [5].

### References

- [1] Fugarov D.D., Gerasimenko Y.Y., Nesterchuk V.V., Gerasimenko A.N., Onyshko D.A. // *Journal of Physics: Conference Series*. 012055, 2018.
- [2] Poluyan A.Y., Fugarov D.D., Purchina O.A., Nesterchuk V.V., Smirnova O.V., Petrenkova S.B. // *Journal of Physics: Conference Series "International Conference Information Technologies in Business and Industry 2018 - Microprocessor Systems and Telecommunications"*. 022013, 2018.
- [3] Fugarov D.D. In: *2019 International Conference on "Physics and Mechanics of New Materials and Their Applications", PHENMA 2019*, Hanoi, Vietnam, November 7 – 10, 2019, Hanoi University of Science and Technology: Hanoi. 119-120, 2019.
- [4] Y.O. Chernyshev, O.A. Purchina, A.Y. Poluyan, D.D. Fugarov, A.V. Basova, O.V. Smirnova // *Journal of Theoretical and Applied Information Technology*. **80**(1), 13-20, 2015.
- [5] Solomentsev K.Y., Fugarov D.D., Purchina O.A., Poluyan A.Y., Nesterchuk V.V., Petrenkova S.B. // *Journal of Physics: Conference Series*. **1015**, 032179, 2018.

## Determination of OH-group Concentration and Point Defects in LiNbO<sub>3</sub>:Zn Crystals

N.A. Teplyakova, N.V. Sidorov, M.N. Palatnikov, L.A. Bobreva\*

*Tananaev Institute of Chemistry - Subdivision of the Federal Research Centre "Kola Science Centre of the Russian Academy of Sciences", Apatity, Russia*

\*[l.bobreva@ksc.ru](mailto:l.bobreva@ksc.ru)

We carried out studies of effect of the crystal composition on the concentration of point defects  $Nb_{Li}$  and  $V_{Li}$  the concentration of OH-groups and the nature of complex defects associated with OH-groups in the LiNbO<sub>3</sub>:Zn (4.54, 4.68, 6.50 mol% of ZnO), (LiNbO<sub>3</sub> <sub>stech</sub>) (LiNbO<sub>3</sub> <sub>congr</sub>) crystals by infrared (IR) absorption spectra in the frequency range of stretching vibrations of hydrogen bonds. Doped zinc crystals at concentrations close to the second threshold value (7.0 mol% ZnO) have a low photorefractive effect and a coercive field. These crystals are promising as nonlinear optical materials for converting laser radiation including on periodically polarized domains. We have grown the crystals by the Czochralski method in air from using the Crystal-2 apparatus at the ICT KSC RAS. IR spectra were measured using a Bruker IFS 66 v/s spectrometer. Many physical properties of a lithium niobate crystal can be improved by changing the state of defectiveness of its structure. The presence of point defects of  $Nb_{Li}$ , which are deep electron traps, significantly affects the photorefractive properties of LiNbO<sub>3</sub> crystals [1]. Moreover, in LiNbO<sub>3</sub> crystals grown in air, there are always hydrogen atoms bound to oxygen atoms by hydrogen bonds. In the structure of the LiNbO<sub>3</sub> <sub>congr</sub> crystal,  $Nb_{Li}$  defects present ~ 1 mol% and  $V_{Li}$  defects present ~ 4 mol % [1]. When a LiNbO<sub>3</sub> <sub>congr</sub> crystal is doped Zn cations,  $Nb_{Li}$  defects will be displaced from the structure and due to the conservation of charge neutrality of the cationic sublattice the number of  $V_{Li}$  defects will change [1]. These structural changes can be traced by infrared spectra. According to the Li-vacancy compensation model [1], the concentration of point defects  $Nb_{Li}^{4+}$  and  $V_{Li}^{-}$  can be calculated using

the formulas proposed in [2]. According to the calculation results, there are no NbLi defects in the structure of the LiNbO<sub>3</sub>:Zn crystal (4.54 mol% ZnO). A further increase in the Zn concentration leads to the appearance of Nb<sub>Li</sub> defects and several absorption bands are already present in the IR spectrum. From the IR spectrum the concentration of OH<sup>-</sup>-groups can be calculated according to the Clavier method [3]. The calculation showed the minimum content of hydrogen atoms in LiNbO<sub>3</sub>:Zn crystals at an alloying element concentration near the second concentration threshold (7.0 mol% ZnO). Moreover, in heavily doped LiNbO<sub>3</sub>:Zn crystals, there are more free protons (contributing to the conductivity) than in lightly doped and nominally pure crystals, which can lead to higher electrical conductivity thermal fixation rate of holograms and a decrease in the photorefraction effect.

### References

- [1] Sidorov N.V., Wolf, T.R., Mavrin, B.N., V.T. Kalinnikov. Lithium Niobate: Defects, Photorefraction, Vibrational Spectrum, Polaritons. Moscow: Nauka, 2003, 255 p.  
[2] Salloum M.Y., Grunsky O.S., Manshina A.A., Tveryanovich A.S., Tveryanovich Y.S. // Russian Chemical Bulletin, **58**(11), 2228-2232, 2009.  
[3] Klauer S. // *Physical Review B*, **45**, 2786-2799, 1992.

## Experimental and Computational Studies on Stiffness Properties of Nanoclay-Incorporated FRPs with Different Nano-Structures

Tianyu yu<sup>1</sup>, Zixuan Chen<sup>2</sup>, Soo-Jeong Park<sup>3</sup>, Yun-Hae Kim<sup>1,3†</sup>

<sup>1</sup>Department of Marine Equipment Engineering, Graduate School, Korea Maritime and Ocean University, 727 Taejong-ro, Busan, 49112, Republic of Korea

<sup>2</sup>School of Aerospace Engineering and Applied Mechanics, Tongji University, 1239 Siping Road, Shanghai, 200092, PR China

<sup>3</sup> Department of Ocean Advanced Materials Convergence Engineering, Korea Maritime and Ocean University, 727 Taejong-ro, Yeongdo-gu, Busan, 49112, Republic of Korea

†[yunheak@kmou.ac.kr](mailto:yunheak@kmou.ac.kr)

Halloysite nanotubes (HNTs) are innovative natural clay materials with unique multi-walled continuous hollow tubular structures. This study investigated the stiffness properties of different-structured HNTs incorporated basalt fiber reinforced polymers (BFRPs) by combining experimental and computational approaches. The amorphous HNTs (AHNTs) were synthesized by heat treatment under 1000 °C, sustaining four hours. The AHNTs shown in Fig. 1(a) presents the flattened structures obtained by transmission electron microscopy (TEM). The Fourier-transform infrared spectroscopy (FTIR) shown in Fig. 1(b) validates the amorphous structure after heat treatment. Incorporation of HNTs effectively improved the bending strength and interlaminar shear strength (ILSS) of BFRPs. The computational results obtained based on the Eshelby-Mori-Tanaka model demonstrate effectiveness on stiffness enhancement with flattened structure. The tendency of experimental and computational results are identical. Moreover, the stress concentration factor during transverse loading in the representative volume element (RVE) can be reduced by

toughening the matrix, which contributes to the higher through-thickness strength of HNT-incorporated BFRPs.

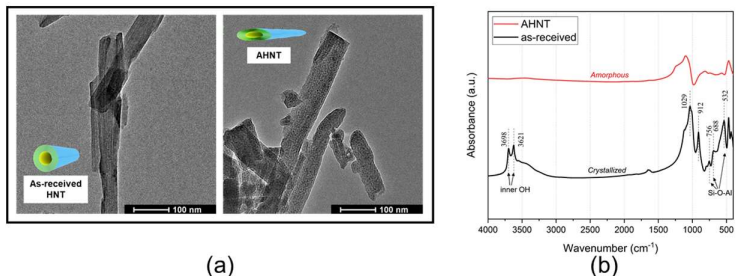


Fig. 1. TEM photographs (a) and FTIR spectra (b) of as-received HNT and AHNT

### Acknowledgment

This work was supported by the Technology Innovation Program (No. 20005403), funded by the Ministry of Trade, Industry & Energy (MOTIE, Korea).

## Meso- and Microstructural Anomalies in Ceramics of Ferroactive Solid Solutions

S.V. Titov\*, L.A. Shilkina, V.V. Titov, A.V. Pavlenko, I.A. Verbenko, L.A. Reznichenko

*Research Institute of Physics, Southern Federal University, Rostov-on-Don, Russia*

\*[svtitov@sfedu.ru](mailto:svtitov@sfedu.ru)

Objects with a combination of fundamentally different macroscopic properties (dielectric, piezoelectric, magnetic, optical, elastic) are of most interest to modern researchers. The reason for this interest is the desire to reduce the cost of scientific and technical products and make them universal. In recent decades, researchers have begun to examine in detail the structure of matter in the solid state, characterizing it as a combination of nano- and microstructural complexes, often possessing scale invariance properties in a certain range of scales. X-ray and multifractal studies of the structure of solid solutions, promising both as an independent basis for ferroelectric materials and as one of the components of new solid solutions, were carried out in the work. The objects of study are  $\text{PbFe}_{0.5}\text{Nb}_{0.5}\text{O}_3$  with the addition of  $\text{MnO}_2$  (PFNM) and  $\text{Li}_2\text{CO}_3$  (PFNL), introduced in excess of stoichiometry in an amount of 1% wt. each, and  $\text{Bi}_{1-x}\text{La}_x\text{MnO}_3$  with  $0.4 \leq x \leq 0.6$ . Using X-ray diffraction analysis, the phase composition, unit cell parameters, and the degree of perfection of the crystal structure were determined. For multifractal parameterization, the following parameters were used [1]: (i) the fractal dimension  $D_0$ ; (ii) the “orderliness” parameter  $\Delta_\infty = D_1 - D_q$  at  $q \gg 1$ ; (iii) the “homogeneity” parameter  $f_\infty = f[\alpha(q)]$  at  $q \gg 1$ . Multifractal scanning was

performed to identify the spatial arrangement of heterogeneities in the ceramic microstructure: images of vast areas (containing 2000 or more grains) of the ceramic surface were examined and areas with parameters significantly different from the region average were revealed. The study revealed a number of factors that critically affect the quality of the ceramics structure. The optimal compositions and temperature conditions for solid solutions are established. A number of meso- and microstructural anomalies were recorded, caused by both technological influences and the interaction of components in solid solutions. The character of the parameter  $f_{\infty}$  distribution in  $\text{Bi}_{1-x}\text{La}_x\text{MnO}_3$  ceramics in the form of alternating bands with high and low values is revealed. Decreasing  $f_{\infty}$  is associated with an increase in microdeformation of the solid solution' crystalline cell. The occurrence of such anomalies is considered as one of the stages of deformation in progress. This stage precedes the transition of stability loss processes to the macro-level and the subsequent destruction of the material. A multilevel approach to structural research allows us to identify how changes in the composition and technological regulations affect the properties of ceramics; it is useful in the development of new highly efficient ferromagnetic materials.

#### **Acknowledgement**

Research was financially supported by the Ministry of Science and Higher Education of the Russian Federation (State assignment in the field of scientific activity, Southern Federal University, 2020).

#### **Reference**

[1] G. V. Vstovskii, A. G. Kolmakov, I. Zh. Bunin, *Introduction to the Multifractal Parameterization of Material Structures*. Center for Regular & Chaotic Dynamics, Izhevsk, 2001 (In Russian).

## **Resistive Switching in Nanocrystalline ZnO Films for Next Generation Memory Development**

**R.V. Tominov\*, V.I. Avilov, A.A. Avakyan, V.A. Smirnov**

*Southern Federal University, Institute of Nanotechnology, Electronics and Electronic Equipment Engineering, 2, Schevchenko Str., Taganrog, 347928, Russia*

[\\*roman.tominov@gmail.com](mailto:roman.tominov@gmail.com)

The development of electronic technology is aimed at creating computer memory that can meet the growing demand for energy efficiency, compactness and speed of computing systems. There are several technologies that can combine the advantages of read-only memory and random-access memory, the most promising of which is the non-volatile resistive memory ReRAM [1]. The ReRAM memory element has a relatively simple structure consisting of an oxide layer located between two conductive contacts. The principle of operation of ReRAM is based on the effect of resistive switching, namely a change in the resistance of an oxide film between high resistance states (HRSs) and low resistance states (LRSs) under the influence of an electric field. The effect of resistive switching is demonstrated by many metal oxides, among which nanocrystalline zinc oxide grown using the pulsed laser deposition method is particularly notable for its speed and energy efficiency. However, for the manufacture of a new generation of computer memory, there are

currently no systematic studies of the effect of resistive switching in nanocrystalline zinc oxide, which is the aim of this work. Nanocrystalline ZnO films were grown by pulsed laser deposition at Al<sub>2</sub>O<sub>3</sub>/TiN structure. Zn was used as a target. Deposition was under the following conditions: wafer temperature 500 °C, substrate – target distance 40 mm, O<sub>2</sub> pressure 1 mTorr, pulse energy 300 mJ, number of pulses 5000, frequency 10 Hz. Electrical measurements were performed using semiconductor characterization system Keithley 4200-SCS (Keithley, USA) with W probes. During the measurement, the TiN bottom contact was grounded, and the tungsten probe was used as the top contact. As a result, 30 current-voltage characteristics (CVCs) were obtained at one point with a voltage scan from –3 V to +3 V. The average CVC and the dependence of HRS and LRS on the number of switching cycles at the point are plotted. Analysis of the results obtained showed, that resistance of the ZnO nanocrystalline film in the HRS was equal to  $0.35 \pm 0.14 \text{ M}\Omega$  and  $56.31 \pm 1.54 \text{ M}\Omega$  in the LRS. HRS/LRS ratio was equal to 160. Resistance dispersion can be due to uneven distribution of the defects in the volume of nanocrystalline ZnO oxide film during resistance switching. The obtained results can be used for technological processes of nanocrystalline ZnO film based on the next generation of computer memory.

#### **Acknowledgement**

This research is supported by the Russian Foundation for Basic Research under grants No. 19-29-03041\_mk.

#### **Reference**

[1] Smirnov V. A., Tominov R. V., Avilov V. I., Alyabieva N. I., Vakulov Z. E., Zamburg E. G., Ageev O. A. // *Semiconductors*. **53**(1), 72 – 77, 2019.

## **Piezoelectric Sensitivity of Modern Lead-Free 1–3-Type Composites Based on Domain-Engineered Single Crystals: Longitudinal and Hydrostatic Responses**

**V. Yu. Topolov\*, A. O. Denisova**

*Department of Physics, Southern Federal University, Rostov-on-Don, 344090, Russia*

[\\*vutopolov@srfedu.ru](mailto:vutopolov@srfedu.ru)

In the last decade, many examples of novel lead-free piezo-active composites were discussed owing their piezoelectric performance, electromechanical coupling, anisotropy factors, and other characteristics that are important for various applications. Among piezoelectric materials to be applied as main components of the modern lead-free composites, one can choose ferroelectric domain-engineered single crystals (SCs) with the perovskite-type structure and piezoelectric coefficients  $d_{ij}$  [1 – 4] that are comparable to those of conventional PZT-type ferroelectric ceramics in the poled state. Hereby we mention alkali niobate-based SCs with the large piezoelectric coefficient  $g_{33}$  [4] related to the longitudinal response. This is important to take into account when creating novel composites, for instance, of the 1–3 type [2, 3, 5] with parallel long SC rods in large matrices. In the present study, we analyse some relationships between the microgeometry and piezoelectric coefficients of the 1–3-type piezo-active composites wherein the ferroelectric domain-engineered alkali niobate-based SCs are main components. Of great interest are the 1–3-type composites with the large effective piezoelectric coefficients  $g_{33}^*$  and  $g_n^* = g_{33}^* + g_{32}^* + g_{31}^*$ .

These parameters are related to the longitudinal ( $g_{33}^*$ ) and hydrostatic ( $g_h^*$ ) responses of the composite sample. Taking into account specifics of the microgeometry of these composites (i.e., a system of long parallel SC rods surrounded by a heterogeneous polymer matrix), the poling direction (along the  $Ox_3$  axis) and the elastic anisotropy of their heterogeneous matrices, we consider examples of the composites for which conditions:

- (i)  $g_{33}^* > 1 \text{ V m/N}$  and  $g_h^* > 1 \text{ V m/N}$ ,
- (ii)  $g_{33}^* > 1 \text{ V m/N}$  and  $0.1 \text{ V m/N} < g_h^* < 1 \text{ V m/N}$ ,
- (iii)  $0.1 \text{ V m/N} < g_{33}^* < 1 \text{ V m/N}$  and  $0.1 \text{ V m/N} < g_h^* < 1 \text{ V m/N}$

hold. We analyse the role of the heterogeneous matrix in forming the high piezoelectric sensitivity of the 1–3-type composite in specific volume-fractions, and cases (i) and (ii) are in the focus of attention. Main representatives to be of interest due to the large  $g_{33}^*$  and  $g_h^*$  values are the SC/porous polymer (1–3–0 connectivity) and SC-1/SC-2/polymer (1–0–3 connectivity) composites. In addition, we consider the novel 1–3–0 composite wherein the porous polymer matrix contains two kinds of air pores [5]. We take into account specifics of elastic properties of the matrix surrounding the SC rods and discuss ways to form a large elastic anisotropy of the matrix and a high piezoelectric sensitivity of the composite. Some ways to increase the  $g_h^*/g_{33}^*$  ratio are highlighted in the context of connectivity patterns and components of the 1–3-type composites. The studied lead-free composites can be applied as elements of piezoelectric sensors, transducers, hydrophones, etc.

#### **Acknowledgement**

Research was financially supported by Southern Federal University, grant No. VnGr-07/2020-04-IM (Ministry of Science and Higher Education of the Russian Federation).

#### **Reference**

- [1] D. Zhou, K. H. Lam, Y. Chen et al. // *Sens. a. Actuat. A.* **182**, 95, 2012.
- [2] V. Yu. Topolov, C. R. Bowen, A. N. Isaeva // *IEEE Trans. Ultrason., Ferroelec., a. Freq. Cont.* **65**, 1278, 2018.
- [3] V. Yu. Topolov, C. R. Bowen, A. N. Isaeva, A. A. Panich // *Phys. Stat. Sol. A.* **215**, 1700548, 2018.
- [4] X. Huo, R. Zhang, L. Zheng et al. // *J. Am. Ceram. Soc.* **98**, 1829, 2015.
- [5] V. Yu. Topolov, A. N. Isaeva, P. Bisegna // *J. Phys. D: Appl. Phys.* **53**, 395303, 2020.

## **Piezoelectric Sensitivity and Anisotropy in 1–3-type Composites Based on Ferroelectric Lead-free Single Crystals**

**V. Yu. Topolov<sup>1\*</sup>, A. N. Isaeva<sup>1</sup>, C. R. Bowen<sup>2</sup>**

<sup>1</sup>*Department of Physics, Southern Federal University, Rostov-on-Don, 344090, Russia*

<sup>2</sup>*Department of Mechanical Engineering, University of Bath, Bath BA2 7AY, UK*

\*[vutopolov@sfedu.ru](mailto:vutopolov@sfedu.ru)

An interest in 1–3-type composites that are based on ferroelectric domain-engineered alkali niobate – alkali tantalate single crystals (SCs) [1, 2] originates from the piezoelectric performance and anisotropy of these composites. The use of a lead-free SC component with large piezoelectric



coefficients  $g_{3j}$  [3] and varying the microgeometric characteristics of the matrix leads to a high piezoelectric sensitivity of the composite. In the present study, we show an influence of the matrix on the piezoelectric coefficient  $g_{33}^*$ , thickness electromechanical coupling factor (ECF)  $k_t^*$  and related anisotropy factors of the 1–3-type composite with two SC components. The studied composite consists of a system of long SC-1 parallelepiped-shaped rods and a 0–3 SC-2 / polymer matrix (Figure). The SC-1 rods with square bases are poled along [001] of the perovskite unit cell, and the spontaneous polarisation of each SC-1 rod is  $\mathbf{P}_3^{(1)} \uparrow \uparrow OX_3$ . Such a composite is characterised by 1–0–3 connectivity [2]. It is assumed that the SC-2 inclusions are regularly distributed in the large polymer matrix, and the shape of each inclusion obeys the equation  $(x_1/a_1)^2 + (x_2/a_2)^2 + (x_3/a_3)^2 = 1$ . Hereby  $\rho_t = a_1/a_3$  is the aspect ratio of the SC-2 inclusion. Among lead-free SC components of interest, we consider the ferroelectric [001]-poled  $(K_{0.562}Na_{0.438})(Nb_{0.768}Ta_{0.232})O_3$  (KNN-T) SC-1 for the rods and piezoelectric  $Li_2B_4O_7$  (LBO) SC-2 for inclusions in the 0–3 matrix. By varying  $\rho_t$  even at a relatively small volume fraction of the SC-2 inclusions  $m_i = 0.1$ , we observe an influence of  $\rho_t$  on the piezoelectric sensitivity, electromechanical coupling and anisotropy factors of the 1–0–3 composite (Table).

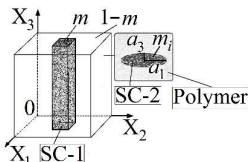


**Table.** Piezoelectric coefficient  $g_{33}^*$  (in mV m/N), thickness ECF  $k_t^*$ , and anisotropy factors  $g_{33}^*/|g_{31}^*|$ ,  $g_{31}^*$  and  $k_t^*/|k_p^*|$  of the 1–0–3 KNN-T SC/LBO SC/polyethylene composite at the volume fraction of LBO  $m_i = 0.1$  in the 0–3 matrix

$\rho_t$	$g_{33}^*$	$k_t^*$	$g_{33}^*/ g_{31}^* $	$k_t^*/ k_p^* $	$g_{33}^*$	$k_t^*$	$g_{33}^*/ g_{31}^* $	$k_t^*/ k_p^* $
	At the volume fraction of SC-1, $m = 0.1$				At the volume fraction of SC-1, $m = 0.2$			
0.01	510	0.749	4.46	9.27	300	0.800	3.83	9.30
0.1	566	0.773	4.47	8.14	315	0.812	3.83	8.71
0.5	599	0.788	4.49	7.70	323	0.819	3.89	8.47
1	604	0.791	4.60	7.70	324	0.820	3.96	8.46
5	608	0.793	5.40	8.12	325	0.821	4.45	8.54
10	609	0.793	6.20	8.46	325	0.821	4.89	8.51

The large  $g_{33}^*$  and  $k_t^*$  values and considerable anisotropy factors  $g_{33}^*/|g_{31}^*|$  and  $k_t^*/|k_p^*|$  suggest that the studied composite can be of interest for piezoelectric sensor, transducer and related applications.

#### Acknowledgement

Research was financially supported by Southern Federal University, grant No. VnGr-07/2020-04-IM (Ministry of Science and Higher Education of the Russian Federation).

#### Reference

- [1] V. Yu. Topolov, C. R. Bowen, A. N. Isaeva, A. A. Panich // *Phys. Stat. Sol. A*. **215**, 1700548, 2018.
- [2] V. Yu. Topolov, C. R. Bowen, A. N. Isaeva // *IEEE Trans. Ultrason., Ferroelec., a. Freq. Contr.* **65**, 1278, 2018.
- [3] X. Huo, L. Zheng, R. Zhang et al. // *CrystEngComm*. **16**, 9828, 2014.

# Strength of Protective Sheet in Multi-Layered Pipe Plug Used for Repair and Maintenance of Underground Piping

H. Tottori\*, N. A. Noda, G. Gao, Y. Sano, A. Kai

Department of Mechanical Engineering, Kyushu Institute of Technology, Kitakyushu, Japan

\*[tottori.hisanori731@mail.kyutech.jp](mailto:tottori.hisanori731@mail.kyutech.jp)

The water and sewer system are becoming obsolete in Japan. It is necessary to find out a suitable water stopping method to reinforce and repair the underground pipe without stopping the water supply system and sewer functions as shown in Fig. 1. We focused on sewer pipe plug in Fig. 2 that can be installed and removed shortly having various diameters and used conveniently. In this study, two types of protective sheets were investigated experimentally. The sheet specimens are prepared with and without slit and seams.

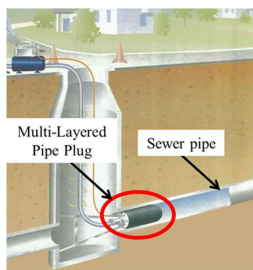


Fig. 1. Image of using Multi-Layered Pipe Plug

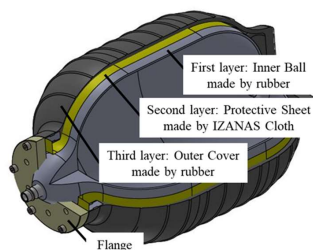


Fig. 2. Image of Multi-Layered Pipe Plug

Table 1. Fracture stress of IZANAS cloth without seams and with seams

Types	Sample No.	Specimen	Number of slits	Test width w [mm]	Fracture Stress $\sigma_B = F/A$ [MPa]	Cross-Sectional area [mm <sup>2</sup> ]	Average Fracture Stress $\sigma_B^{ave}$ [MPa] ( $\sigma_B^{ave}/\sigma_{B0}^{ave}$ )
Type-A without seams	A1-No.1	1 pair of slit in Fig.3	2	25	201	25×1	$\sigma_{B0}^{ave} = 200$ (100%)
	A1-No.2		2	25	195		
	A1-No.3	1 pair of slit in Fig.3	2	12.5	203	12.5×1	
	A1-No.4		2	12.5	201		
Type-B with seams	B0-No.1	with seams in Fig.4	0	50	30	50×1	$\sigma_{B0}^{ave} = 34$ (17%)
	B0-No.2		0	50	38		

Table 1 shows the fracture stress of the IZANAS cloth specimens. Fig. 3 shows the sheet without seams with slits. Fig.4 shows the sheet with seams without slits. The specimen without seams need double slits to eliminate the gripping part fracture. The tensile strength of the IZANAS cloth obtained as  $\sigma_{B0}^{ave} = 200\text{MPa}$  as shown by A1 in Table. 1. The average

fracture stress of the seamed specimens is  $\sigma_B^{ave} = 34\text{MPa}$ , which is 17% of  $\sigma_{B0}^{ave} = 200\text{MPa}$  as shown by B0 in Table. 1.



Fig. 3. Specimen without seam with slits



Fig. 4. Specimen with a seam without slits

## Operation Modes of the Automated Gas Monitoring System in the Pipeline

K. M. Ugrovatov<sup>1</sup>, D. D. Fugarov<sup>1\*</sup>, O. A. Purchina<sup>1</sup>, D.A. Onyshko<sup>2</sup>

<sup>1</sup>Don State Technical University, Rostov-on-Don, Russia

<sup>2</sup>South-Russian State Polytechnic University (NPI) named after M.I.Platov, Novocherkassk, Russia

\*[ddf\\_1@mail.ru](mailto:ddf_1@mail.ru)

Currently, more than 80% of the country's population use gas fuel in everyday life, and most of the apartments are gasified with liquefied gas [1]. Natural gas is used mainly by industry and in thermal power, which accounts for about 50% of gas consumed, including 26% at power plants of the Ministry of Energy, 15% in heating boilers and 14% in industrial boilers [2]. There is not a single branch of the national economy where gas is not used. Today, the state of the gas industry and the economic situation require organizations delivering gas to the end user to strengthen control over both gas supply regimes, the state of the gas distribution network, and the amount of gas transferred [3]. The main parameter that characterizes the state of the gas distribution network is the gas pressure [4]. In this regard, it can be concluded that the issues related to the study of the operation modes of the automated gas control system in the pipeline are relevant [5].

### References

- [1] Poluyan A.Y., Fugarov D.D., Purchina O.A., Nesterchuk V.V., Smirnova O.V., Petrenkova S.B. // *Journal of Physics: Conference Series "International Conference Information Technologies in Business and Industry 2018 - Microprocessor Systems and Telecommunications"*. 022013, 2018.
- [2] Fugarov D.D., Gerasimenko Y.Y., Nesterchuk V.V., Gerasimenko A.N., Onyshko D.A. // *Journal of Physics: Conference Series*. 012055, 2018.
- [3] Y.O. Chernyshev, O.A. Purchina, A.Y. Poluyan, D.D. Fugarov, A.V. Basova, O.V. Smirnova // *Journal of Theoretical and Applied Information Technology*. **80**(1), 13-20, 2015.
- [4] Solomentsev K.Y., Fugarov D.D., Purchina O.A., Poluyan A.Y., Nesterchuk V.V., Petrenkova S.B. // *Journal of Physics: Conference Series*. **1015**, 032179, 2018.
- [5] Fugarov D.D. In: *2019 International Conference on "Physics and Mechanics of New Materials and Their Applications"*, PHENMA 2019, Hanoi, Vietnam, November 7 – 10, 2019, Hanoi University of Science and Technology: Hanoi. 119-120, 2019.

## **Is the Majority Gypsum for Ceiling Choosing on Housing and Buildings in Surabaya, Indonesia?**

**Uniek Praptiningrum W\*, Joko Santoso\*\***

*Department of Architecture, Faculty of Engineering Universitas 17 Agustus 1945 Surabaya, Indonesia*

\*[uniek@untag-sby.ac.id](mailto:uniek@untag-sby.ac.id); \*\*[joko\\_santos@untag-sby.ac.id](mailto:joko_santos@untag-sby.ac.id)

To implement architectural works, such as residential, houses, and buildings; the shape and its facade, including the interior, construction and building materials are elements that need to be considered. In architectural works, structures election, construction and interior building materials are not only considered in terms of strength and durability, but also from the ease of obtaining the materials, as well as adjusting the shape, and installation. In order to be categorized as good architectural works, buildings should have: attractive appearance, wide and comfortable, beautiful views, safe construction, easy to maintain and simple inform, has local wisdom and nature and environmental friendly. This research is focused more specifically toward the trend of the selection/use of structures, construction and building materials for ceiling, especially interior ceiling frames in residential/buildings in Surabaya. From a temporary survey, it was found that 75% from 120 residents of residential and buildings in Surabaya chose to use gypsum for its structure and the construction of the roof frame. While the remaining 25% choose a combination between gypsum, wood, drywall and other materials. The purpose of this study is to find out the enthusiasm/tendency of Surabaya residents and their reasons for determining the interior especially for ceiling, structure and the construction of building materials for the ceiling frame of residential houses/buildings. What are the elements from the architectural viewpoint to become one of the considerations? The methods used are both field survey by distributing questionnaires and direct interviews with respondents. The provisional results obtained are a tendency to prioritize the ease of monitoring and current trends compared to maintaining local wisdom and nature friendly and healthy environment. It can be seen from the increasing number of houses and buildings built using modern building materials. This trend is not only possessed by the middle and upper class as in some real estate areas in Surabaya, but it has also penetrated in to residential housing among the middle and lower classes such as in residential houses in several areas in Surabaya.

## **The Variable Order Riesz Potential on Quasimetric Sphere in the Variable Exponent Hölder Space**

**B. G. Vakulov, Yu. E. Drobotov\***

*Southern Federal University, Rostov-on-Don, Russia*

\*[yu.e.drobotov@yandex.ru](mailto:yu.e.drobotov@yandex.ru)

The Riesz potential type operator of a variable complex order  $\alpha(x)$  is considered as

$$(K^{\alpha(\cdot)} f)(x) := \int_{S^{n-1}} \frac{f(\sigma)}{d^{n-1-\alpha(x)}(x, \sigma)} d\sigma, \quad x \in S^{n-1},$$

where  $d(x, \sigma)$  is a quasimetric on the  $n$ -dimensional unit sphere  $S^{n-1}$  with radius  $r$  and center  $x_c$ , embedded in the real vector space  $\mathbb{R}^n$ , i.e.

$$S^{n-1} := \{ \sigma = (\sigma_1, \dots, \sigma_n) \in \mathbb{R}^n : d(x_c, \sigma) < r \}, \quad x_c \in \mathbb{R}^n.$$

The condition for  $K^{\alpha(\cdot)}$  is a bounded operator from the space  $L^p(S^{n-1})$  to the variable exponent Hölder space

$$H^{\lambda(\cdot)}(S^{n-1}) := \{ f \text{ is continuous on } S^{n-1} : \forall x \in S^{n-1} \quad M_d(f, x, t) \leq C t^{\lambda(x)}, \quad t < 1, \quad 0 < C < \infty, \}$$

defined by the local continuity modulus

$$M_d(f, x, t) := \sup_{y \in S^{n-1}; d(x, y) \leq t} |f(x) - f(y)|,$$

are investigated, which is the basis for constructing the solution of the integral equation

$$(E - K^{\alpha(\cdot)})f = g, \quad E f = f.$$

As the one is of interest within mathematical modelling in mechanics and material sciences [1], the results are to serve to expand the relevant theories. The background of the research is [2], in which the reflection between Hölder spaces by  $K^{\alpha(\cdot)}$  was considered for a quasimetric homogeneous space.

#### **Acknowledgement**

Research was financially supported by Southern Federal University, grant No. VnGr-07/2020-04-IM (Ministry of Science and Higher Education of the Russian Federation).

#### **References**

- [1] Tarasov V. E. *Fractional Dynamics: Applications of Fractional Calculus to Dynamics of Particles, Fields and Media*. Berlin, Germany: Springer, 2010.  
 [2] Vakulov B. G., Samko N. G., Samko S. G. // *University News North-Caucasian Region. Natural Sciences Series. Special Issue*, 40–45, 2009.

## **On Smoothness of the Solution of an Integral Equation with the Spatial Riesz Potential Type Operator**

**B. G. Vakulov, Yu. E. Drobotov\*, G. S. Kostetskaya**

*Southern Federal University, Rostov-on-Don, Russia*

\*[yu.e.drobotov@yandex.ru](mailto:yu.e.drobotov@yandex.ru)

Riesz kernels include the ones of the classical potential theory, such as the Newtonian and logarithmic ones, and Green kernels associated with a region as special and limiting cases, which makes the Riesz potential type operators of interest for applications in mathematical physics,

mechanics and material science. Here, the potential type operator with the bounded and sufficiently smooth differential characteristic  $a(\cdot)$  is considered in the following way:

$$(K_a^\alpha f)(x) = \int_{\mathbb{R}^n} \frac{a(x-t)f(t)}{|x-t|^{n-\alpha}} dt, \quad 0 < \alpha < n.$$

Under certain conditions [1], the inverse operator  $(K_a^\alpha)^{-1}$  can be represented as the convolution

$$(K_a^\alpha)^{-1} f = D_\Omega^\alpha f + \mu_\alpha * f,$$

where  $\mu_\alpha(x)$  is integrable and  $D_\Omega^\alpha$  is the hypersingular integral with the characteristics  $\Omega(\cdot)$

$$(D_\Omega^\alpha f)(x) = \frac{1}{d_{n,l}(\alpha)} \int_{\mathbb{R}^n} \frac{(\Delta_t^l f)(x)}{|t|^{n+\alpha}} \Omega(t) dt, \quad 0 < \alpha < l,$$

$(\Delta_t^l f)(x)$  is a finite difference of the function  $f$  with the center  $x$  of the order  $l$  with the step  $t$ ,  $d_{n,l}(\alpha)$  is the normalizing constant such that  $D_\Omega^\alpha = (-\Delta)^{\alpha/2}$ . The latter provides therefore the solution of the integral equation:

$$(E - K_a^\alpha) f = g, \quad E f = f,$$

in the terms of  $D_\Omega^\alpha$ , and the presented research considers its smoothness in the terms of weighted Hölder spaces. Moreover, the results on applications in various computational problems are demonstrated and new mathematical models, valuable for practical use, are outlined.

#### **Acknowledgement**

Research was financially supported by Southern Federal University, grant No. VnGr-07/2020-04-IM (Ministry of Science and Higher Education of the Russian Federation).

#### **Reference**

[1] Vakulov B. G., Kostetskaya G. S., Drobtov Y. E. In: Nekrasova, I., Karnaukhova, O., Christiansen, B. (Ed.), *Fractal Approaches for Modeling Financial Assets and Predicting Crises*. IGI Global, 249–273, 2018. <http://doi:10.4018/978-1-5225-3767-0.ch013>

## **Effect of Laser Pulses Energy on the Morphology and Electrical Properties of LiNbO<sub>3</sub> Thin Films Grown by Pulsed Laser Deposition**

**Z.E. Vakulov<sup>1\*</sup>, D.A. Khakhulin<sup>2</sup>, A.A. Geldash<sup>2</sup>, V.S. Klimin<sup>2</sup>, O.A. Ageev<sup>2</sup>**

<sup>1</sup>*Federal Research Centre The Southern Scientific Centre of the Russian Academy of Sciences (SSC RAS), Rostov-on-Don, Russia*

<sup>2</sup>*Southern Federal University, Research and Education Centre «Nanotechnology», Taganrog, Russia*

\*[zakhar.vakulov@gmail.com](mailto:zakhar.vakulov@gmail.com)

Advances in wireless technology and MEMS made it possible to use energy converters as an alternative to conventional electrochemical batteries, which are now widely used as a power source

for portable electronic devices. Besides, the battery life frequently is limiting the operational time of the device itself. Replacing or recharging batteries is often ineffective. Therefore, the harvesting and conversion of environmental energy into electric energy is considered today as a prospective alternative to electrochemical batteries and can act as an independent power source for portable devices and wireless sensors. Currently, one of the most promising areas within this field is the conversion of the environment mechanical energy (vibrations) into electrical energy by the piezoelectric effect. For expanding the scope of possible applications of such devices, the use of lead-free piezoelectric materials is of particular interest. One of the potential materials for use in piezoelectric converters is  $\text{LiNbO}_3$ , thanks to high Curie temperature and the absence of lead. One of the urgent tasks in the formation of thin metal oxides films is the study of processes that affect the preservation of the stoichiometric composition. The composition determines the structural and electro-physical properties of the formed films, which will allow the use of  $\text{LiNbO}_3$  films as part of mechanical energy converters. Pulsed laser deposition (PLD) allows the complex oxides films stoichiometric fabrication when a specific threshold value of the laser pulse power is exceeded. However, the physical mechanisms underlying this phenomenon have not yet been detailed clarified. Thus, the purpose of this work is to study the influence regularities of laser pulses energy during the deposition of  $\text{LiNbO}_3$  films by PLD on morphology and electro-physical parameters of the films.  $\text{LiNbO}_3$  films were deposited by the PLD method using a Pioneer 180 module (Neocera Co., USA) of the NANOFAB NTK-9 cluster nanotechnological complex (NT-MDT, Russia). The number of pulses was constant and kept at 50,000 with 10 Hz a pulse repetition rate. The energy of laser pulses varied in the range from 180 mJ to 220 mJ. The films were fabricated at the substrate temperature of 600 °C. The results show that with an increase in laser pulses energy from 180 mJ to 220 mJ, the thickness of  $\text{LiNbO}_3$  films increases from  $132.3 \pm 8.8$  nm (film deposition rate of 1.47 nm/min) to  $153.9 \pm 0.5$  nm (film deposition rate of 1.71 nm/min). Raise in grain size can be associated with coalescence processes caused by the higher kinetic energy of the ablated particles due to increased laser pulses energy from 180 mJ to 200 mJ. Further increase in laser pulses energy above 200 mJ, ablated particles have smaller sizes, which leads to the formation of a fine-grained film. Increase in laser pulses energy from 180 mJ to 220 mJ, the concentration of charge carriers of  $\text{LiNbO}_3$  films decreases from  $8.6 \times 10^{15} \text{ cm}^{-3}$  to  $1.0 \times 10^{13} \text{ cm}^{-3}$ . The charge carriers mobility increases from  $0.43 \text{ cm}^2/\text{V}\cdot\text{s}$  to  $80.4 \text{ cm}^2/\text{V}\cdot\text{s}$ , which may be associated with enhancing stoichiometry during heat and mass transfer within transition space as well as decreasing in the defectiveness of the films, which indicates a transition from the evaporation to ablation mode. The obtained results are promising to the fabrication of innovative energy converters for the Internet of Things devices based on lead-free ferroelectric films.

#### ***Acknowledgement***

The reported study was funded by the Russian Foundation for Basic Research, project No. 19-38-60052.

## Numerical Study of Impurity Transport in Thin Horizontal Layer with a Free Boundary for the Stationary Turbulent Fluid Flow

A. V. Vasilev\*, E. V. Shiryaeva

*Southern Federal University, Rostov-on-Don, Russia*

[\\*avvasiliev1995@gmail.com](mailto:*avvasiliev1995@gmail.com)

The behavior of an impurity in a stationary turbulent flow is numerically studied with the help finite element method. An asymptotic model based on the Navier–Stokes equations is used as a mathematical model of process. It is assumed that the liquid layer has a free surface, is in the gravity field, and the thickness of the layer is much smaller than the horizontal size. Moreover, it is assumed that the turbulent viscosity depends on the coordinates and vanishes at the lower boundary of the layer (reservoir bottom). A special feature of the model is the rejection of the non-slip conditions for viscous liquid to the lower boundary of the layer. This allows us to reject the hypothesis of instantaneous adaptation and set the relief of the lower boundary arbitrarily. The asymptotic model does not contain inertial and nonlinear terms. In this case, the flow of the liquid is described by analytical formulae. The flow velocity has a logarithmic profile along the vertical coordinate and a singularity at the lower boundary of the layer. To prevent the occurrence of a singularity in the vicinity of the lower boundary layer, a fictitious surface is introduced that simulates the roughness of the reservoir bottom. This situation is typical when describing turbulent flows. To study the behavior of an impurity the main attention is focused on the construction of special numerical approximations for equations describing the transport of passive impurity particles by the fluid flow, that settle to the reservoir bottom under the influence of gravity. The sedimentation process is modeled by various theoretical and semi-empirical relationships that take into account particle size and shape, sedimentation rate, drag coefficients, and other factors. Computational experiments are shown that the impurity transport near the lower boundary, at almost any sedimentation rate, is mainly determined by the topography of the reservoir bottom. It is shown that bottom vortex flows are formed in the depressions of the bottom. These vortex flows capture the impurity and block its propagation along the stream. At certain values of the liquid flow parameters in the vicinity of the lower boundary, counter-flows of liquid may occur. In this case, when the impurity reaches the lower boundary of the layer, a significant distortion of the impurity spot occurs. The computational experiment also allowed us to specify the optimal approximation of the convective terms of the impurity transport equation. This made it possible to significantly improve the accuracy of calculations. In particular, a pseudo-conservative scheme has been constructed for the finite element method, which allowed us to satisfy the conservation law of the amount of impurity with high accuracy. The calculations presented are shown good agreement with the experimental data available in the literature.

### ***Acknowledgement***

The results of this research were financially supported by the Southern Federal University, grant No. VnGr-07/2020-04-IM (Ministry of Science and Higher Education of the Russian Federation).



## Development and Application of a Convolutional Neural Network Based on the Generated Data Set in Identification Problems

P.V. Vasiliev\*, A.V. Senichev, A.I. Novikova

*Don State Technical University, Rostov-on-Don, Russia*

\*[lyftzeigen@mail.ru](mailto:lyftzeigen@mail.ru)

Modern production processes place high demands on product quality control, which can be carried out at various stages of both production itself and further operation. This aspect plays a huge role in many industries, science and technology. Timely diagnosis, prediction and identification of defects is a necessary measure that can prevent many negative consequences occurring in the result of failures and breakdowns of both structural elements and systems as a whole. In the result of the rapid growth in the volume of road surfaces and along length, the complexity of conducting complex diagnostics and constant monitoring of road networks increases [1, 2]. Timely detection and elimination of malfunctions can reduce the risk of uncontrolled events that can entail significant expenses aimed at eliminating the consequences. Existing research trends show that deep convolutional neural networks are highly effective for the automatic analysis of large volumes of images. They are also effective in identifying features. Using these features, it is possible to analyze problem areas of the road surface. To solve complex informal problems of segmentation, forecasting and classification, artificial neural networks are widely used. A variety of neural network architectures and techniques make it possible to solve a wide range of problems [3, 4]. In this report, we propose a neural network data processing method that automates the process of knowledge representation and helps to reduce development costs and time. Creating a training set, which is a pair of images, requires real human time, concentration and attention. Therefore, to solve the problem of developing and training a convolutional neural network, we used a software-generated data set, which allowed us to significantly reduce the preparation time and increase its size. The generation of the data set occurs programmatically. The size of the output images and the parameters of the generated defects, in this case, cracks on the surface of the road surface, are set. The main texture of the generated images are real data. Using a special algorithm, based on the specified parameters, cracks are generated and combined with the texture layer. The result is a data set consisting of the constructed images and their corresponding binary masks, which reflect the degree of presence of the defect and its features. We conducted a comparative analysis of the operation of a neural network trained on a generated data set and a data set marked up by a person manually. The proposed approach shows the possibility of its application in a small amount of real data. The possibility of more successful augmentation of data, as compared to classical methods, was also demonstrated. Software crack generation gives a more diverse result of artificially increasing the data set, which helps to improve the quality of the neural network as a whole. Due to its flexibility and the ability to obtain large volumes of images in a short time, without human intervention, the approach has proven itself in the development and debugging of new neural network architectures.

### ***Acknowledgement***

This work was supported by the RFBR in the framework of the project 19-08-00074.

## References

- [1] Shi Yong, Cui Limeng, Qi Zhiquan, Meng Fan, Chen Zhensong // *IEEE Transactions on Intelligent Transportation Systems*. 17, 1-12, 2016.
- [2] Kapela Rafal, Rydzewski Paweł, Michał Wyczalek, Błoch Adam, Śniatała Paweł, Pożarycki Andrzej, Rybarczyk Adam, Turkot Adam. In: *Proc. 22nd Int. Conf. "Mixed Design of Integrated Circuits and Systems"*, June 25-27, 2015, Toruń, Poland, 579-584, 2015.
- [3] C. Szegedy et al. In: *2015 IEEE Conference on Computer Vision and Pattern Recognition (CVPR)*, Boston, MA, 1-9, 2015.
- [4] Eisenbach M., Stricker R., Seichter D., Amende K., Debes K., Sesselmann M., Ebersbach D., Stöckert U., Gross H.-M. In: *Int. Joint Conf. on Neural Networks (IJCNN)*, Anchorage, USA, 2039-2047, 2017.

## Investigation of Stress Localization at the Interface of a Coating and a Substrate Based on the Gradient Model of Thermoelasticity

A.O. Vatulyan<sup>1,2\*</sup>, S.A. Nesterov<sup>1</sup>

<sup>1</sup>*Southern Mathematical Institute - Branch of VSC RAS, Vladikavkaz, Russia*

<sup>2</sup>*Southern Federal University, Rostov-on-Don, Russia*

\*[vatulyan@math.rsu.ru](mailto:vatulyan@math.rsu.ru)

To protect parts from high temperature effects, thin-layer heat-protective coatings made of both homogeneous and functionally graded materials are widely used. Large concentrations of stresses can occur at the interface between dissimilar materials, which greatly affect the strength of the product. However, the stress concentration cannot be determined by solving boundary value problems of classical thermoelasticity. Recently, gradient models taking into account scale effects have been used more and more often to solve problems of mechanics of layered bodies. The work considers the equilibrium of the system "functionally graded coating – substrate", modeled in the form of an inhomogeneous strip. The lower boundary of the coating-substrate system is rigidly pinched and maintained at zero temperature, and the heat flux is localized at the upper boundary free of stresses in the final segment. The Lamé parameters, thermal conductivity coefficient and thermal stress coefficient are piecewise continuous functions in thickness. Based on the Lagrange variational principle, equations of gradient thermoelasticity, boundary and contact conditions for the strip are obtained. The gradient model proposed by Aifantis, in comparison with the classical model of thermoelasticity, has one additional scale parameter. The study begins by finding the temperature distribution. The solution is based on a combination of the Fourier transform and the shooting method. After finding the temperature, the Fourier transform is applied to study the stress-strain state of the coating-substrate system. The problem is reduced to the canonical system of ordinary differential equations in transformants. To solve on the basis of the shooting method, a number of auxiliary Cauchy problems are formed. For each problem, we have a system of differential equations in the presence of a small coefficient at the first derivative. To solve the rigid system of equations, the Gear method is used, implemented in the Maple computing environment. The inverse of the Fourier transform is based on the theory of residues. Computational experiments

were performed for specific materials. It was found that the stress distribution far from the interface and the fixing point corresponds to the solutions of the classical model of thermoelasticity. However, there is a local stress concentration at the band boundary that cannot be predicted in the classical model. The influence of the ratio of elastic modulus, thermal conductivity, thermal expansion, as well as the values of the scale parameter and the relative thickness of the coating on the level of temperature stresses is studied.

#### **Acknowledgement**

The work is supported by the Russian science Foundation (project No. 18-11-00069).

## **On Boundary Integral Equations in the Problem of Wave Propagation in Topographic Waveguides**

**A.O. Vatulyan\*, L.I. Parinova\*\***

*I. I. Vorovich Institute of Mathematics, Mechanics and Computer Science,  
Southern Federal University, 8a, Milchakov Street, Rostov-on-Don, 344090, Russia*

\*[aovatulyan@sfedu.ru](mailto:aovatulyan@sfedu.ru); \*\*[lparinova@sfedu.ru](mailto:lparinova@sfedu.ru)

The study of the features of changes in the velocities of acoustic waves in wedge-shaped elastic topographic waveguides is important for flaw detection. The results obtained in the process of solving problems of wave propagation in elastic media are used to develop and improve compact devices for processing acoustic signals. Plate elastic waveguides are used as delay lines. Wedge-shaped structures drawn out false signals and serve as filters in various acoustic electronic devices. Measurement of the speed of propagation of surface elastic waves allows detecting defects in welding and adhesive structures, as well as monitoring the condition of the cutting tool edge. Previously, studies of the features of the propagation of wedge waves in an isotropic medium were carried out. It was proved that the wave field, which is localized near the edge of the wedge, had not dispersion. It was shown that the problems of wave propagation along the edge of an infinite isotropic wedge-shaped waveguide were reduced to eigenvalue problems and could be solved using finite-element approaches. In the case of an anisotropic medium, the study of the features of the propagation of wave fields was carried out by the authors in a number of works for topographic waveguides of various cross-sections, for a wedge in the case of a small opening angle. This study is based on the use of analogs of the plate models of Kirchhoff and Timoshenko and also the Hamilton-Ostrogradsky variational principle, while finding the stationary value and constructing the dispersion set, the Ritz method was applied [1 – 4]. In this report, a new approach is proposed to study wave processes in a topographic waveguide with an arbitrary cross-section. On the base of the Fourier transform and the analysis of the characteristic polynomial, new non-classical boundary integral equations with smooth kernels are constructed in the framework of the approach [5]. A simplification of the general system for antisymmetric vibrations of a wedge with an arbitrary opening angle is carried out. The main methods of discretization, based on the use of boundary-element approximations and the Galerkin method, are present, which allow us to approximately construct dispersion relations and estimate the values of velocities depending on the parameters of the problem.

### **Acknowledgement**

This study was funded by RFBR, project number 19-31-90079.

### **References**

- [1] A. O. Vatulyan, L. I. Parinova, In: *Advanced Materials – Techniques, Physics, Mechanics and Applications, Springer Proceedings in Physics*, Ivan A. Parinov, Shun-Hsyung Chang, Muaffaq A. Jani, Eds., Heidelberg, New York, Dordrecht, London: Springer Cham, **193**, 309 – 317 (2017).
- [2] A. O. Vatulyan, L. I. Parinova, *University News. North-Caucasus Region. Natural Sciences Series*, **3**, 10, 2018.
- [3] L. I. Parinova. In: *Advanced Materials Proceedings of the International Conference on “Physics and Mechanics of New Materials and Their Applications”, PHENMA 2018, Springer Proceeding in Physics*, Ivan A. Parinov, Shun-Hsyung Chang, Yun-Hae Kim, **224**, 487 – 494, 2019.
- [4] A. O. Vatulyan, L. I. Parinova. In: *Advanced Materials - Proceedings of the International Conference on “Physics and Mechanics of New Materials and Their Applications”, PHENMA 2019, Springer Proceedings in Materials*, Ivan A. Parinov, Shun-Hsyung Chang, Banh Tien Long (Eds.). Springer Nature, Cham, Switzerland, **6**, 383 – 389, 2020.
- [5] A. O. Vatulyan // *Doklady RAN*, **333**(3), 312-314, 1993.

## **Numerical Calculation of Stresses Arising in the Steering Axle of the Combine**

**D.V. Velibekov, A.A. Matrosov\***

*Don State Technical University, 1, Gagarin Sq., Rostov-on-Don, 344010, Russia*

[\\*amatrosov@donstu.ru](mailto:*amatrosov@donstu.ru)

The mechanical basis of the agricultural combine is its chassis. In the running gear, two main parts can be distinguished, namely the drive axle and the steering axle. In the work, using the numerical finite element methods, the steering axle bridge for different loading modes was calculated. The first loading mode corresponds to movement along a stubble with a horizontal non-uniform relief [1, 2]. The second loading mode corresponds to the movement along the field with a transverse slope, comprising an angle  $\alpha$  with the horizon line. The angle  $\alpha$  is taken equal to  $8^\circ$ . The calculations were carried out for the steering axle of the Don-1500 combine. The geometric model of the bridge is built in the three-dimensional modeling system Compass-3D and exported to ANSYS. The stress-strain state of the steering axle was calculated in the ANSYS 19 R2 finite element analysis software package. A linear statement of the problem of the theory of elasticity is adopted. The element Solid 65 is selected as the final element. The step of splitting the finite element mesh is 5 mm. In the result of calculations, it was shown that when the loading regime changes, the nature of the stress distribution does not change qualitatively. However, quantitatively, in the case of movement along an inclined surface, the maximum voltage value increases. Namely, when moving along a stubble with a horizontal uneven relief, the stresses reach a maximum value of 138 MPa. When moving along a stub with a transverse slope, the stresses reach a maximum value of 158 MPa. Moreover, in the first loading mode (the case of movement along the stubble with a horizontal uneven relief), the safety factor for yield strength is 1.81. In the second loading mode (movement along the stubble with a transverse slope), it is 1.52. The minimum allowable values of the safety factor for yield

strength are values in the range of 1.3 – 1.5. Thus, the stresses arising in the steering wheel axle are permissible in terms of the safety factor in both loading modes.

### **References**

- [1] Dyachenko N.V., Matrosov A.A. In: *Materials of the International Scientific and Practical Conference (Interagromash-2009)*. Rostov-on-Don: DSTU Press, 97-99, 2009 (In Russian).
- [2] Ziborov E.N., Matrosov A.A. In: *Materials of the 3rd International Scientific and Practical Conference (Interagromash-2010)*. Rostov-on-Don: DSTU Press, 199-200, 2010 (In Russian).

## **Application of Neural Networks to the Sensors Data Processing Problem**

**N.N. Ventsov\*, L.A. Podkolzina\*\***

*Don State Technical University, 344000, Rostov-on-Don, Russia*

*\*[myvnn@list.ru](mailto:myvnn@list.ru), \*\*[podkolzinalu@gmail.com](mailto:podkolzinalu@gmail.com)*

The identification and construction of adequate mathematical models of elements and the control object of a complex system is an important basis for the high-qualitative functioning of a whole process. In connection with the growth and complication of industrial processes, the problem of monitoring the state of the objects of complex systems is urgent. Although using sensors is becoming increasingly ubiquitous, key challenges remain in improving the accuracy of their operation. The identification of failures and anomalies in telemetric information coming from sensors is an integral part of the work on assessing the state of complex objects in many fields of scientific and industrial activity. Telemetry (data streams about the position of the object, the parameters of the external environment and equipment) is of the greatest interest. It contains important information about the condition of the facility and the environment. This data requires automated data flow analysis tools. New methods of control are needed using modern computing technologies, a method for detecting anomalies in telemetry data, as well as means of response in the event of malfunctions and short-term equipment. Recently, as deep learning has proven effective in many areas, many deep methods have been explored to solve problems in recognizing human activity. The report discusses the proposed architecture of deep learning to use the relationships built into various types of input data. However, many of them do not take into account the modeling of multimodal inputs necessary for constructing a solution when operating a system of several sensors. At the same time, the required accuracy has not yet been achieved by working with data from sensors. The aim of the scientific work is the general problem of detecting malfunctions of the equipment of a control system. The solution to the monitoring system of sensors is based on the determination of assumptions about the credibility of the testimony based on the available data on the probabilities of sensor failure. General issues of monitoring and processing information flows, including approximation and interpolation of experimental data, are considered. In this report, we propose one of the possible approaches to solving the problem of identifying complex objects and control systems. In the work, a fuzzy-probabilistic approach is used in combination with neural network technology for solving the control problem of the studied object. For modeling were used TensorFlow, Keras, PyTorch. A system for monitoring telemetry data from sensors has been developed. The results of solving the problems of processing information flows using a cluster

computer are present. The estimation of the required level of performance of the hardware-software complex is given.

***Acknowledgement***

This work was supported by RFBR grant No. 19-01-00357.

## **A Case Study of Renewable Energy Development in Indonesia**

**Victoria Aurellia Sri Paramita Putri<sup>1</sup>, Erni Puspanantasari Putri<sup>2\*</sup>**

*<sup>1</sup>Department of Industrial Engineering, University of Pembangunan Nasional Veteran (UPN Veteran) East Java, Surabaya, Indonesia*

*<sup>2</sup>Department of Industrial Engineering, University of 17 Agustus 1945 (UNTAG) Surabaya, Indonesia*

[\\*erniputri@untag-sby.ac.id](mailto:erniputri@untag-sby.ac.id)

The energy crisis has now hit many countries, not only from onward countries but developing countries are also experiencing the same thing. Long-standing levels of energy consumption such as petroleum have a negative impact on the environment. The process of developing renewable energy in various countries including Indonesia must be carried out immediately to meet the requirements of the society in the next few years. Renewable energy is an option to meet energy requirements. As a tropical country, Indonesia has a favorable geographical location with a variety of natural conditions that have the potential to produce renewable energy. The use of renewable energy has also become one of the government programs listed in the national energy policy, namely the government has targeted its utilization of up to 23% in 2025. Further, Indonesia is expected to become an industrial country that has added value by reducing the use of fossil energy in 2045. Hence, Indonesia is demanded to be able to develop and use renewable energy efficiently. The trend in the use of energy in the future is to provide more opportunities for local governments to manage the use and supply of energy sources. This study discusses five case studies of the development of new renewable energy in Indonesia which, include the development of (i) Solar Power Plant on Karampuang Island, West Sulawesi; (ii) Wind Power Plant in Sidenreng Rappang (Sidrap), South Sulawesi; (iii) Hydroelectric Power Plant in Cihea Village, Cianjur; (iv) Sea Wave Power Plant in the Larantuka Strait, East Nusa Tenggara and (v) Waste Power Plants in Several Major Cities.

## **Stabilographic Complex Based on Virtual Games Using AR Technology for Training and Rehabilitation of Athletes**

**V.Yu. Vishnevetskiy<sup>1\*</sup>, A.V. Golda<sup>1</sup>, A.A. Sliva<sup>2</sup>**

<sup>1</sup>*Southern Federal University, Taganrog, 347922, Russia*

<sup>2</sup>*OKB RITM, Taganrog, 347900, Russia*

[\\*yuvishnevetsky@mail.ru](mailto:yuvishnevetsky@mail.ru)

Training of high-level athletes, and even more so, world-class ones, at the present stage of sports development is not possible without attracting funds to objectify the knowledge of the coach about the functional state of the athlete and his special technical level. The problem of obtaining and interpreting this information is very relevant both for solving the problems of selecting the most promising mid-level and novice athletes, and for completing teams that are optimal in terms of compatibility and coherence. Multi-channel complex consists of stabilizing platform and is specialized for rehabilitation of motor disorders and improvement of movement coordination in athletes of the highest category on the base of analysis of center of mass position and movement. The developed methods of training, rehabilitation and diagnostics of athletes of various specializations are required to guarantee: (i) comfort of human examination, which is carried out on a special power-coordinate platform and does not require special training and mounting of sensors on the subject; (ii) short examination time (1-1.5 min); (iii) informative nature of the survey; (iv) high sensitivity, which will allow one to assess the reaction to physical and mental effects, to take medications, etc.; (v) multifunctionality (diagnostics of a wide range of diseases and pre-diseases, control and objectification of human movements, rehabilitation of postural function disorders). In conditions of limited use of medicinal means, the presented method will allow one to bring the results of athletes to the world level, using only instrumental methods. The complex uses virtual gaming technologies with a high proportion of the game element. Using AR technologies, it will allow one to implement a more authentic image for real conditions.

### ***Acknowledgement***

This research was supported by Foundation for Assistance to Small Innovative Enterprises (FASIE).

## **Evaluation of Information Characteristics of Underwater Communication Channel of Divers Using Parametric Arrays**

**V.Yu. Vishnevetskiy<sup>1\*</sup>, D.A. Kolesnik<sup>1</sup>, I.B. Starchenko<sup>2</sup>**

<sup>1</sup>*Southern Federal University, Taganrog, 347922, Russia*

<sup>2</sup>*Parametrika LCC, Taganrog, 347902, Russia*

[\\*vuvishnevetsky@mail.ru](mailto:vuvishnevetsky@mail.ru)

The estimation of the amount of information received in the result of measurements and intended for transmission over a communication channel is crucial in the development and operation of systems. The quality of the received information also plays an important role, but the criteria and methods for evaluating the quality of information are not yet fully developed. When calculating the information characteristics of hydroacoustical telemetry systems, the most important parameters are the intensities of acoustic signal and noise at the receiving point and in the receiving path band. The ratio between the bandwidth of the channel and the performance (intensity) of the source determines the ability to achieve the required accuracy when transmitting data over the communication channel. Based on these values, taking into account the conditions of sound propagation, the required values of the parameters of the emitted signal are calculated. Using information theory and Nyquist–Shannon sampling theorem, an expression for calculation of the bandwidth of hydroacoustic communication channel using parametric arrays was obtained. It is shown that the channel capacity depends on the bandwidth of transmitted frequencies, signal power, interference power, and characteristics of the water environment. This allows us to draw a conclusion about the limited capacity of the hydroacoustic communication channel. The restriction is caused primarily by strong sound absorption, which narrows the range of operating frequencies of hydroacoustical telemetry system to a value of about 100 kHz, as well as the constant presence of noise interference in the channel, which has a significant level in the frequency band of the speech signal.

#### ***Acknowledgement***

This research was supported by Foundation for Assistance to Small Innovative Enterprises (FASIE).

### **Correlation Method for Estimating Dynamic Loading of Drives of Active Working Tools**

**I.N. Vislousova\*, V.V. Kotov, O.N. Lesnyak, A.A. Matrosov, A.N. Soloviev**

*Don State Technical University, 1, Gagarin Sq., Rostov-on-Don, 344010, Russia*

[\\*vislousova-irina@mail.ru](mailto:vislousova-irina@mail.ru)

The work studies the dynamics of multi-mass systems with non-linear characteristics. The obtained results are applied to evaluation of dynamic loading of drives of active working tools of agricultural machines, in particular, harvesting machines [1, 2]. For this purpose, the correlation method of research is used. The method is based on the direct transformation of correlation functions of nonlinear members of small oscillation equations. Most probabilistic methods require reducing the



nonlinear characteristics of the system to analytical (smooth, differentiable) functions. The correlation method can be applied directly to essentially nonlinear systems, including systems with nonanalytic nonlinear functions. The method is based on the direct transformation of correlation functions of nonlinear members of small oscillation equations. This study considers oscillations of a single-mass dynamic system with a nonlinear elastic characteristic, which is an arbitrary (non-analytical) function of the generalized coordinate. Resistance forces are reduced to the case of linear friction. As a driving force, a random normal stationary process with known mathematical expectation, dispersion, and spectral density is applied to the input of the system. A restoring force is a nonlinear elastic characteristic of a system. If it is given by an odd function, then at centered input the output process can also be considered centered. To construct an approximate stationary solution, an unknown random function is represented as a series by degrees of normal process with unknown dispersion. The corresponding two-dimensional distribution also accepts normal. The considered method allows one to investigate dynamic processes in drive mechanisms of working elements with oscillatory motion, having essentially nonlinear characteristics (gaps, side plays, overrunning couplings, nonlinear position functions), but also in other systems subject to random input influences [3].

#### **References**

- [1] Vislousova I.N., Kotov V.V., Mikhalev A.I. In: *Collection of Scientific Papers of the Scientific and Methodological Conference (ITNO-2014)*. Rostov-on-Don: DSTU Press, 469, 2014 (In Russian).
- [2] Vislousova I.N., Lesnyak O.N. In: *Materials of the 10th International Scientific and Practical Conference (Interagromash-2017)*. Rostov-on-Don: DSTU Press, 61-65, 2017 (In Russian).
- [3] Kislyakov E.A., Matrosov A.A. In: *Abstracts & Schedule of the 2018 International Conference on "Physics and Mechanics of New Materials and Their Applications"* (9-11 August, 2018, Busan, South Korea), Korea Maritime and Ocean University Press: Busan, 196, 2018.

## **Generation and Diagnostics of Glow Discharges for Biomedical, Agricultural and Gas Conversion Applications**

**Vladislav Gamaleev\*, Masaru Hori**

*Centre for Low Temperature Plasma Science, Nagoya University, Nagoya, Japan*

[\\*vlad@plasma.engg.nagoya-u.ac.jp](mailto:*vlad@plasma.engg.nagoya-u.ac.jp)

Rapid development of atmospheric-pressure plasma sources over the last two decades has led to the use of plasma in a large number of applications where samples are not compatible with low-pressure conditions. Moreover, the development of nonequilibrium plasmas allowed the plasma treatment of biological targets and opened door for the use of plasma technologies in medicine, agriculture, and even farming [1]. On the other hand, growing demands in nitric compounds, which are a crucial part of most fertilizers, led to the requirement for large-scale production of ammonia and nitric oxide, which are commonly used as a precursor for the synthesis of more complex molecules. There are few works reporting on nitrogen fixation using atmospheric-pressure plasma sources with

considerably high efficiency that, together with use of renewable-energy sources (solar- and wind-power plants), can make plasma a “green” technology for nitrogen fixation [2]. According to recent reports, one of the most efficient plasma sources for nitrogen fixation is “gliding glow” reactor [2]. Moreover, there are few works concerning application of glow discharges in medicine and agriculture [1]. In general, glow discharges are one of most studied types of plasma; however, most detailed studies were done in low-pressure conditions. Two main features are required for the possible application of glow discharge in gas conversion, medicine and agriculture: operation at atmospheric pressure and easy scaling. There are many works concerning the generation and diagnostics of glow discharges in various gases at atmospheric pressure using subcentimeter gaps between electrodes, but works are limited on the generation and diagnostics of glow discharges in centimeter-order gaps filled with atmospheric-pressure molecular gases, including air. In this work, we propose method of generation of stable centimeter-scale re-pulsing glow discharge in ambient air, which will improve efficiency of electric power use during plasma treatment. Re-pulsing glow discharges were characterized by current and voltage measurements, and optical emission spectrometry. It was found that, at a certain range of parameters, the discharge could be stabilized even in the presence of external gas flow and parameters of the plasma could be precisely controlled using regulation of power supply and gas flow. The generation of stable and controllable centimeter-scale glow discharge looks promising for use in energy-efficient gas conversion and agriculture. In the presentation, plasma generation process, electrical parameters of the plasma and results of optical diagnostics together with examples of application in gas conversion and agriculture will be demonstrated.

#### ***Acknowledgement***

This work was supported by the JSPS KAKENHI Grant Number 19H05462.

#### ***References***

- [1] V. Gamaleev, N. Iwata, G. Ito, M. Hori, M. Hiramatsu, M. Ito // *Appl. Sci.* **10**, 801, 2020.
- [2] V. Gamaleev, N. Iwata, M. Hiramatsu, M. Ito // *Jpn. J. Appl. Phys.* **59**, SHHF04, 2020.

## **Thermally Expanded Graphite: Sorption Properties and Carbon Nanoparticles Obtaining**

A.A. Voitash<sup>1,2</sup>, E.V. Raksha<sup>1\*</sup>, A.A. Davydova<sup>1</sup>, Yu.V. Berestneva<sup>2\*\*</sup>, A.V. Muratov<sup>1</sup>,  
A.B. Eresko<sup>1</sup>, V.A. Glazunova<sup>3</sup>, M.V. Savoskin<sup>1</sup>, I.A. Verbenko<sup>4</sup>, Yu.I. Yurasov<sup>4,5</sup>

<sup>1</sup>L.M. Litvinenko Institute of Physical Organic and Coal Chemistry, Donetsk, 283114, Ukraine  
<sup>2</sup>Federal Scientific Centre of Agroecology, Complex Melioration and Protective Afforestation of the Russian Academy of Sciences, 97, Universitetskij prospekt, Volgograd, 400062, Russia  
<sup>3</sup>Donetsk Institute for Physics and Engineering named after A.A. Galkin, Donetsk, Ukraine  
<sup>4</sup>Research Institute of Physics, Southern Federal University, Rostov-on-Don, Russia  
<sup>5</sup>Southern Scientific Centre RAS, Rostov-on-Don, Russia

\*[elenaraksha411@gmail.com](mailto:elenaraksha411@gmail.com); \*\*[berestnevayuv@mail.ru](mailto:berestnevayuv@mail.ru)

Ternary graphite nitrate co-intercalation compounds with ethyl formate, ethyl acetate, acetic acid, formic acid, and 1,4-dioxane were prepared and used as a source of thermally expanded graphite (TEG). Obtained cointercalates demonstrated a good thermal expansion ability: the thermal expansion coefficient determined for considered compounds was within 340 – 380 cm<sup>3</sup>·g<sup>-1</sup>. The sorption properties of TEG relative to aromatic hydrocarbons (Fig. 1) as well as a number of new derivatives of condensed 1,2-diazepines were studied.

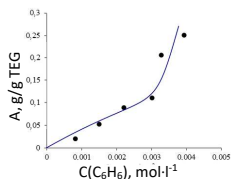


**Fig. 1.** Adsorption isotherm of benzene from aqueous solution with TEG, obtained from graphite nitrate co-intercalated with ethyl formate and acetic acid

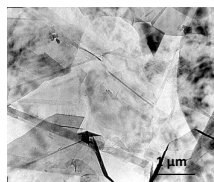


**Fig. 2.** Representative TEM image of carbon nanoparticles, obtained by TEG sonication in ethanol

The sorption capacity investigations were carried out by UV spectroscopy at 20 °C. Carbon nanoparticles (few-layer graphenes and nanoscrolls) were obtained by sonication of thermally expanded graphite in liquid media. The sedimentation stability of the as-prepared few-layer graphene suspensions was shown to increase in a series of alcohols: methanol < ethanol < isopropanol < phenylmethanol < tert-butanol. Planar sizes of the as-prepared few-layer graphenes reached several tens of μm and the thickness was within 1 – 10 atomic layers according to TEM data (Fig. 2).

#### **Acknowledgement**

The reported study was funded by RFBR according to the research project No. 19-33-50154.

## **Cracker Control System Upgrade**

D.A. Volkov<sup>1</sup>, D. D. Fugarov<sup>1\*</sup>, O. A. Purchina<sup>1</sup>, D.A. Onyshko<sup>2</sup>

<sup>1</sup>Don State Technical University, Rostov-on-Don, Russia  
<sup>2</sup>South-Russian State Polytechnic University (NPI) named after M.I. Platov,  
Novocherkassk, Russia

\*[ddf\\_1@mail.ru](mailto:ddf_1@mail.ru)

In modern geopolitical conditions, Russia especially needs new modern large-scale production of deep hydrocarbon processing in order to increase domestic value added and prevent raw material dependence [1]. However, to normalize the situation, systematic work is needed both as from the Government of the Russian Federation to develop new clusters, as from large and medium-sized businesses to create a large number of new large and medium-sized high-tech industries in oil and gas chemistry [2]. Modernization of the existing control system of the thermal cracking unit consists in replacement of obsolete equipment with new, more accurate, advanced and reliable ones, and application of new control algorithms ensuring efficient and safe operation of the equipment [3]. The modernization of the management system is the cheapest, that is not requiring significant capital investments, and a fast-paying action to improve production efficiency, its safety, energy efficiency and, therefore, reduce the cost of production [4, 5].

#### **References**

- [1] Fugarov D.D., Gerasimenko Y.Y., Nesterchuk V.V., Gerasimenko A.N., Onyshko D.A. // *Journal of Physics: Conference Series*. 012055, 2018.
- [2] Poluyan A.Y., Fugarov D.D., Purchina O.A., Nesterchuk V.V., Smirnova O.V., Petrenkova S.B. // *Journal of Physics: Conference Series "International Conference Information Technologies in Business and Industry 2018 - Microprocessor Systems and Telecommunications"*. 022013, 2018.
- [3] Fugarov D.D. In: *2019 International Conference on "Physics and Mechanics of New Materials and Their Applications"*, PHENMA 2019, Hanoi, Vietnam, November 7 – 10, 2019, Hanoi University of Science and Technology: Hanoi. 119-120, 2019.
- [4] Y.O. Chernyshev, O.A. Purchina, A.Y. Poluyan, D.D. Fugarov, A.V. Basova, O.V. Smirnova // *Journal of Theoretical and Applied Information Technology*. **80**(1), 13-20, 2015.
- [5] Solomentsev K.Y., Fugarov D.D., Purchina O.A., Poluyan A.Y., Nesterchuk V.V., Petrenkova S.B. // *Journal of Physics: Conference Series*. **1015**, 032179, 2018.

## **Researching the Phenomenon of Nonlinear Diffraction in Structure of Microwave Integrated Circuits**

P. Yu. Voloshchenko, Yu. P. Voloshchenko\*

\*[yvoloshchenko@yandex.ru](mailto:yvoloshchenko@yandex.ru)

Currently, the differentiation of electromagnetic field sources on primary and secondary is used for obtaining the graphical and analytical operators for mathematical modeling the analog and digital integrated circuits in the gigahertz and terahertz ranges using engineering methods, such as methods of equivalent circuits and non-autonomous block [1, 2]. The obligatory application of the recursion and the energy conservation principles, assumptions and presupposition defined by the design of electronic devices and supply wires are the specific features of this phenomenological formalization of nonlinear and wave electric processes. These graphical and analytical dependencies determine the input of constant or variable electromotive forces without specifying micro- and nanoscale interelectrode space, electrical conductivity and dielectric constant, used substances and materials, manufacturing technology of parts and components of microwave integrated circuits. These data are necessary to analyze correctly the electromagnetic waves diffraction and to verify the results of the energy efficiency estimation for non-autonomous blocks of “open” electronic device systems. At the same time, the information about the origins of self-excitation and oscillation regeneration, signal composition along galvanic and wireless connections in them is not distorted. Therefore, it is important to identify the integration of discrete electronic devices that are influencing each other in a common inhomogeneous electromagnetic field and designed as a combination of one primary source and many secondary sources of voltage and current waves using the method of invariant modeling the nonlinear composition of electrical signals in microwave integrated circuits. The purpose of the report is to present the results obtained in the analytical calculation of the diffraction of electromagnetic waves emitted by electronic devices and in the verification measurement of the external characteristic of a signal secondary source, which corresponds to the amplitude-frequency characteristic of a resistive-negatron nonlinear element. The summation of controlled sources in the microwave range, considered as a voltage and current sources, simultaneously takes into account the interference phenomenon in the waveguide channel between dependent secondary and primary power sources and the signal composition along the “long” supply conductors, which establish uncontrolled feedback connections in the microwave integrated circuit. The research presents a synthesis of topology of lumped and wave equivalent circuits modeling a single pair of electronic devices and the reverse symbolic analysis, which is intended to study the amplification and absorption modes of oscillation energy in the circuit. The synthesized topology allows one to control the intensity of the electromagnetic field inside and outside the micro-systems of the gigahertz and terahertz ranges. Mathematical models of integrated circuit elements were experimentally verified in the antenna chamber. The verification results fully confirmed the correctness of the used graphic and analytical dependencies of the integrated circuit engineering model and the reliability of the symbolic analysis of nonlinear diffraction in the free space surrounding the circuit.

#### **References**

[1] P. Yu. Voloshchenko, Yu. P. Voloshchenko. In: *International Conference on “Physics and Mechanics of New Materials and Their Applications” (PHENMA 2019)*. Hanoi, Publishing House for Science and Technology, 334–335, 2019.

[2] P. Yu. Voloshchenko, Yu. P. Voloshchenko. *Modeling the Electric Charge Transfer in Electrovacuum Devices with Electrostatic Control*. Taganrog, Southern Federal University Press, 2019. <https://elibrary.ru/item.asp?id=41480834> (in Russian).

## **Topology Synthesis of Integrated Circuits of the Giga and Terahertz Range by the Method of Non-autonomous Blocks**

**P. Yu. Voloshchenko, Yu. P. Voloshchenko\***

*Engineering Technological Academy, Southern Federal University, 2, Shevchenko Str., Taganrog, 347900, Russia*

[\\*yvoloshchenko@yandex.ru](mailto:yvoloshchenko@yandex.ru)

The modern theoretical description of analog and digital integrated circuits made of different materials and operating in stationary and switching modes, is based on the superposition principle and electrical circuits in the form of autonomous blocks. Autonomous blocks include linear passive and active elements. At the same time, it is known that only using the amplitude-dependent models allow one to describe correctly the multifactor mechanism for converting the energy of free charges in micro and nanoscale transit-time regions of semiconductor and vacuum electronic devices [1, 2]. Therefore, it is relevant to study various types of nonlinear elements with one, two, three, and larger number of ports that together form a nonreciprocal multiterminal network, which is used in the non-autonomous block method for the synthesis of the microwave integrated circuits topology. The report presents the results of a theoretical and experimental study of a consistent non-autonomous four-terminal with distributed parameters, loaded with a resistive-negatron nonlinear element. Its graphical and analytical dependencies are used to verify the modeling methods of microwave electronic micro- and nanosystems operating in common electromagnetic field. The fact is that the initial and boundary conditions in electronic devices, coupled with power conductors in a single unit, depend on the signal intensity and the duration of signals transmission according to Kirchhoff laws and the Tellegen's theorem. Therefore, the following two items are the features of a non-autonomous block modeling. First, presenting the block as a lumped and wave equivalent circuit simultaneously, that is valid in the electronic wave circuit theory. Equivalent circuits mutually determine the multimode properties of a non-autonomous block, calculated as the algebraic summation of coherent influences and reactions under the diffraction of the electromagnetic field of an electronic device. Second, an analytical solution of energy state equations is obtained, which forms the target optimization functions for microwave integrated circuits under an energy saving considerations. The study of the electronic wave circuit based on the model of a balanced four-port network eliminate the influence of a nonlinear signal composition, interference phenomena in the connections of microwave integrated circuits, while researching the influence of the regeneration of electronic device oscillatory power on the coherent control of boundary conditions in devices. In the practice of verification modeling of microwave integrated circuits containing a negatron-IMPATT diode, the balanced mode is usually provided by a ferrite circulator placed at the terminals of a non-autonomous block. The correctness of modeling techniques for electronic micro- and nanosystems in the microwave range was verified by comparison with the results of an experimental

study. An analysis of the characteristics obtained analytically and experimentally showed the adequacy and consistency of modeling techniques with electrical and physical processes in electronic microwave circuits with active nonlinear elements.

### **References**

[1] P. Yu. Voloshchenko, Yu. P. Voloshchenko. In: *International Conference on "Physics and Mechanics of New Materials and Their Applications" (PHENMA 2019)*. Hanoi, Publishing House for Science and Technology, 335–336, 2019.

[2] P. Yu. Voloshchenko, Yu. P. Voloshchenko. In: *International Conference on "Physics and Mechanics of New Materials and Their Applications" (PHENMA 2018)*. Busan, Korea Maritime and Ocean University, 376-377, 2018. <https://elibrary.ru/item.asp?id=36342999>

## **Monitoring and Evaluation System of Contractor's Performance Achievement in Road Preservation in Long Segment Contract in East Java**

**Wateno Octomo<sup>a\*</sup>, Bambang Andrianto<sup>a</sup>, Herry Widhiarto<sup>b</sup>, Dwi Yuli Rakhmawati<sup>c</sup>**

*<sup>a</sup>Master of Civil Engineering, University of 17 Agustus 1945 Surabaya Indonesia*

*<sup>b</sup>Department of Civil Engineering, University of 17 Agustus 1945 Surabaya Indonesia*

*<sup>c</sup>Department of Industrial Engineering, University of 17 Agustus 1945 Surabaya Indonesia*

[\\*profwateno.wiro@gmail.com](mailto:profwateno.wiro@gmail.com)

Along 2361 km of national road in East Java Province, spread across several locations especially north coast causeway, there are minor and severe damage suffered. The reconstruction was performed by long segment road preservation activities in 100 – 200 km-package, but there were premature damages before the designed period. Monitoring and performance evaluation of contractors are necessary to be done. The objective of this research was to obtain a monitoring and evaluation system of contractors comprehensively and quantitatively by mapping the level of contractor's problem in performing routine maintenance of the road by long segment and to obtain the score of every factor as well as to get contractors performance value. The primary data collection was done to get data on the level of the contractors' performance problem and road preservation performance, while secondary data were the response time of damage repair. The analysis was performed using SEM (Structural Equation Modelling) and descriptive analysis of the results of monitoring and evaluation of the contractor's performance. To know the score of every factor, analysis by SEM from the result of Confirmatory Factor Analysis (CFA) was done using AMOS ver.21. CFA analysis showed that the indicators that have effects were seven out of 10 for workers, seven out of 10 for consultants expert, six out of 11 for PPK performance, seven out of 11 for material use, six out of 10 for heavy equipment, six out of nine for quality test equipment, four out of nine for work method, five out of six for financial condition, six out of 11 for environmental condition, and seven out of 10 for limitation of performance indicator achievement. SEM analysis resulted in influence score of 31% for workers, 14% for consultants experts, 10% for PPK performance, 7% for material use, 0 for heavy equipment and quality test equipment, 5% for work method, 8% for financial condition, 15% for environmental condition, and 10% for limitation of performance indicator achievement. The value of contractor's performance achievement obtained

from the sum of the product of mean and the result of SEM analysis for each variable is 59, which means fall into the category of “poor” (below 60). Performance improvement from monitoring consultants experts, heavy equipment, quality test equipment, environmental condition, and performance indicator fulfillment is required to increase the value of a contractor's performance.

## **Preparation of TiO<sub>2</sub>-WS<sub>2</sub>-Au Composite Using Hydrothermal Synthesis for Photocatalytic Activity under Visible Light**

**Wu Kejun<sup>1\*</sup>, Pankaj Koinkar<sup>1</sup>, Akihiro Furube<sup>1\*\*</sup>**

*1Department of Optical Science, Tokushima University, 2-1 Minamijosanjima-cho, Tokushima, Tokushima, 770-8506, Japan*

\*[c501738003@tokushima-u.ac.jp](mailto:c501738003@tokushima-u.ac.jp); \*\*[furube.akihiro@tokushima-u.ac.jp](mailto:furube.akihiro@tokushima-u.ac.jp)

Titanium oxide is well-known as a photocatalytic material due to its excellent photoactivity, high stability, low cost and eco-friendly nature. The numerous research reports on photocatalytic activities of TiO<sub>2</sub> suggests that the large gap energy (3.2 eV) limits its absorption of solar radiation in the UV range as well as the rapid recombination of photogenerated electron-holes pairs. In this relation, various approaches were attempted to provide visible-light response and electron-hole recombination rate. The doping or decoration of metal nanoparticle is an effective way to increase the photocatalytic activity of TiO<sub>2</sub>. Nanomaterials in the form of nanoparticles or nanosheets show significantly different characteristics than bulk materials. Currently, new nano-functional materials which are atomically thin inorganic layered materials called as two-dimensional (2D) nanomaterials have attracted great attention because of its exceptional electrical and optical properties. Tungsten disulfide (WS<sub>2</sub>) is 2D nanomaterial, which has superior properties such as high conductivity, excellent catalytic activity, and high thermochemical stability. The ultrathin WS<sub>2</sub> displays unusual electrical, optical and chemical properties, and can be used in promising applications such as photocatalysts, photodetectors and field emission devices. In the present study, WS<sub>2</sub> nanosheet and gold nanoparticle were used to extend the visible light absorption region of TiO<sub>2</sub>. Moreover, a ternary composite, consisting of three materials with different energy levels was prepared, in which the electrons excited will form a cycle to reduce the recombination of electrons-holes pairs enhancing the property of photocatalyst and the photocatalytic activity of TiO<sub>2</sub>. First, WS<sub>2</sub> nanosheet was prepared using-ultra-sonication method. Then, WS<sub>2</sub> nanosheets were exfoliated by sonication to transform nanosheet layers into a few layers of hundred nanometers in size. Furthermore, TiO<sub>2</sub> and WS<sub>2</sub> nanosheets and gold nanoparticles were combined via hydrothermal synthesis at high temperature and long time, which could construct them together to complete the electron cycle as well as to achieve less electron recombination and wider visible light absorption region. The morphology, crystal structures and optical properties of TiO<sub>2</sub>-WS<sub>2</sub>-Au composite were characterized by scanning electron microscopy, Raman scattering spectra, and UV-vis absorption spectra.



# Improve the Efficiency of the Patients' Specific Quality Assurance Procedure in Fields' Optimization Techniques of the Pencil Beam Linear Scanning Proton Therapy

Yang-Wei Hsieh<sup>1,2</sup>, Chao-Hong Liu<sup>1</sup>, I-Hsing Tsai<sup>1</sup>, Zih-Xiang Su<sup>1</sup>, Yu-Hao Chiu<sup>1</sup>,  
Pei-Ju Chao<sup>1,2</sup>, Hung-Yu Wang<sup>1,3</sup>, Yu-Jie Huang<sup>2</sup>, Tsair-Fwu Lee<sup>1,3\*</sup>

<sup>1</sup>Medical Physics and Informatics Laboratory of Electronics Engineering, National Kaohsiung University of Applied Sciences, Kaohsiung, 80778, Taiwan, ROC

<sup>2</sup>Department of Radiation Oncology, Kaohsiung Chang Gung Memorial Hospital and Chang Gung University College of Medicine, Kaohsiung, 83342, Taiwan, ROC

<sup>3</sup>PhD program in Biomedical Engineering, Kaohsiung Medical University, Kaohsiung, 80708, Taiwan, ROC

\*[tflee@nkust.edu.tw](mailto:tflee@nkust.edu.tw); [tflee@kuas.edu.tw](mailto:tflee@kuas.edu.tw)

The aim of this study was to improve the efficiency of the single-field optimization (SFO) and multi-field optimization (MFO) of the patient-specific quality assurance (PSQA) process for the pencil beam linear scanning (PBLs) proton therapy. The study collected 389 proton PSQA field parameters. The process of the PSQA program included field monitoring unit calibration, absolute dose and depth dose measurement, and two-dimensional dose gamma index analysis. MATLAB was used to adopt the concept of supervised learning to build database models. From this, we established a PSQA database and proposed important parameters of the evaluation procedure, defined the spread-out Bragg peak (SOBP) depth of both SFO and MFO technologies, evaluated the Gamma index passing rate of the five defined depths, and quantify protons. For analyzing the dose difference at the beam position, we introduced particle swarm optimization (PSO) to execute the operating point searching, calculated the coordinates of dose specification point (DSP), and provided PSQA program optimization suggestions. In the definition of the longitudinal depth of SOBP, SFO technology defined surface (entrance dose) from the shallow surface of the beam from 0 to 4 cm, the interval from the shallow surface to the target area was defined as Proximal, and the interval of SOBP dose greater than 90% was defined as Proximal-SOBP, Middle-SOBP and Distal-SOBP. The distance between the 80% position of the beam end and the 20% position of the end was defined as the distal falloff area. According to the important parameters of the proton therapy quality assurance program proposed by the database, the results of SFO technology for the field monitoring unit calibration, absolute dose measurement, depth dose measurement, and two-dimensional dose gamma index analysis, were  $1.15\% \pm 0.88$ ,  $-0.77\% \pm 1.30$ ,  $0.25\% \pm 1.05$ ,  $99.41\% \pm 0.67$ , respectively; the MFO technical results were  $1.29\% \pm 1.09$ ,  $-1.23\% \pm 1.13$ ,  $0.67\% \pm 0.94$ ,  $99.26\% \pm 0.62$ , respectively. All parameters are within the standard error  $\pm 5\%$  and the Gamma index passing rate  $\geq 85\%$ , respectively. The MFO technical dose curve was not as obvious as the SFO's dose gradient in terms of quantifying the definition of each depth. The Gamma index pass rate at the end of the beam was 42.86% and 70.8% for the SFO and MFO technologies, respectively. Input dose matrix from PTW Verisoft to MATLAB to execute OPS script and combine the above program optimization suggestions will save 23.5% of the operation time. The implementation of OPS in the PSQA program can improve the efficiency of pre-operations in searching and measuring

the working point. For two-dimensional dose measurement result analysis, it is recommended to merge the Surface and Proximal areas of the SFO technology and Group 1 and Group 2 in the MFO technology into a single unit for measurement. Removal of the measurement of SFO and MFO in the distal falloff area, combined with the above steps, can maximize the efficiency of the PSQA program.

## **A Study on the Micro/Nano Texture Design to Improve the Friction Properties of DLC Thin Films**

**Young Woo Kwon<sup>1</sup>, Mun Ki Bae<sup>1</sup>, Ri-ichi Murakami<sup>2</sup>,  
Tae Gyu Kim<sup>3\*</sup>**

*<sup>1</sup>Department of Nano Fusion Technology, Pusan National University, Busan, Korea*

*<sup>2</sup>Chengdu University, Chengdu, China*

*<sup>3</sup>Department of Nanomechatronics Engineering, Pusan National University, Busan, Korea*

*[\\*tgkim@pusan.ac.kr](mailto:*tgkim@pusan.ac.kr)*

In this study, in order to improve the friction characteristics of DLC thin films, a micro/nano-textured dimple surface was fabricated to present a new synergy lubrication system. The texturing technology of the substrate surface is an effective way to improve the friction properties of the sliding surface. A micro/nano size dimple surface texturing technique was applied using a photolithography process, which is an important part of the semiconductor process. DLC thin films were deposited on a cemented carbide (WC) substrate by plasma chemical vapor deposition (PECVD), and micro/nano-sized dimple patterns having different pattern densities were fabricated, respectively. Dimple texturing was performed in 4 steps, Step 1: DLC thin film deposition process by PECVD method on cemented carbide substrate, Step 2: Micro/nano size pattern formation through photolithography process, Step 3: Re-deposition process of DLC thin films on the formed pattern, Step 4: Lift off process was performed in the order of micro/nano size dimple formation. Tribology test was performed to observe the lubricating mechanism of the fabricated micro/nano texturing functional surface, friction coefficient and wear volume were obtained, and the texturing effect was verified. Moreover, the dimple texturing surface was studied by AFM, XPS, Raman, and Nano-indentation analysis to investigate surface morphology, surface structure, chemical composition, and mechanical properties. As a result, it was found that the micro/nano patterned DLC thin film on the cemented carbide substrate was able to maximize the friction performance only by the physical surface modification of the micro/nano texture without special treatment of chemical surface modification, and it was possible to implement a functional surface.

## **Using Supervised Learning algorithms to Predict the Risk of Thyroid Damage for Head and Neck Cancer Patients after Radiation Therapy**

**Yu-Hao Chiu<sup>1</sup>, Jung-Ting Hsieh<sup>1</sup>, Jia-Yu Chen<sup>1</sup>, Chao-Hong Liu<sup>1</sup>, I-Hsing Tsai<sup>1</sup>,  
Pei-Ju Chao<sup>1</sup>, Hung-Yu Wang<sup>1,3</sup>, Shyh-An Yeh<sup>1,2\*</sup>, Tsair-Fwu Lee<sup>1,3\*\*</sup>**

*<sup>1</sup>Medical Physics and Informatics Laboratory of Electronics Engineering, National Kaohsiung University of Applied Sciences, Kaohsiung, 80778, Taiwan, ROC*

*<sup>2</sup>Department of Radiation Oncology, E-Da hospital, Kaohsiung City, 82445, Taiwan, ROC*

*<sup>3</sup>PhD program in Biomedical Engineering, Kaohsiung Medical University, Kaohsiung, 80708, Taiwan, ROC*

\*[sayeh@outlook.com](mailto:sayeh@outlook.com); \*\*[tflee@nkust.edu.tw](mailto:tflee@nkust.edu.tw)

The aim of this report was using supervised machine learning algorithms to predict the thyroid damage and predictive factors of head and neck cancer patients undergoing radiotherapy. This study collected retrospective data of 160 head and neck cancer patients, excluding 20 patients who had hypothyroidism or other thyroid diseases before receiving radiation therapy, and 3 patients with outlier doses. Through 137 patients, the head and neck cancer patient data are predicted and evaluated using supervised learning algorithms. Candidate factors include gender, age, thyroid volume, total dose, average dose, maximum dose, number of treatments, relative volume of organs under X dose ( $X = 10, 20, 30, 40, 50, 60$  Gy). Cancer patient data were predicted and evaluated by using supervised learning algorithms. Three classification algorithms were selected to improve the classification results by enhancing the overall learning method: decision tree, random forest, and support vector machine (SVM). In order to analyze the relationship between the independent input variables and the relevant characteristics of the dependent variables, Binary Logistic Regression, Pearson product Difference correlation coefficient, and Least absolute shrinkage and selection operator (LASSO) were used to enhance model prediction accuracy and interpretability to better optimize the models. Relevant accuracy (ACC), receiver characteristic curve (ROC), and the area under the receiver characteristic curve (AUC) were used as adjusting model parameters and factor weights as the reference basis for the described statistical tests and models. It is shown the importance of ranking predictors through 3 supervised learning algorithms. The five predictors before the ranking are age, thyroid volume, average dose, V50 and V60 dose factors, of which age and volume factor are negatively correlated. It means that the greater the age and volume, the lower the risk of thyroid damage; the average dose, V50 and V60 are positively correlated, indicating that the larger the average dose, V50 and V60, the higher the risk of thyroid damage. The optimization results of the parameters for predicting the probability of thyroid damage by the three algorithms are as follows. The decision tree algorithm is improved from AUC: 0.653, ACC: 70.6% to AUC: 0.635, ACC: 73.5%; random forest algorithm AUC: 0.793, ACC: 79.4% improved to AUC: 0.827, ACC: 82.4%; SVM algorithm AUC: 0.649, ACC: 79.4% improved to AUC: 0.692, ACC: 79.4%. Among them, the probability of predicting thyroid complications with random forest is relatively accurate. So, through the supervised machine learning algorithm, the probability of predicting thyroid complications after radiotherapy for head and neck cancer patients can be improved. The study found 5 predictors (age, volume, average dose, V50 and V60) are important factors affecting hypothyroidism. The algorithm of this study can be used as a reference for predicting radiotherapy complications and auxiliary medical decisions in the future.

# Experimental Verification for Interfacial Creep Generation for Shrink-fitted Bimetallic Work Roll by Using Miniature Rolling Mill

Yudai Taruya\*, Rahimah Abdul Rafar, Nao-Aki Noda, Xuchen Zheng, Hiroyuki Tsurumaru, Yoshikazu Sano

Department of Mechanical Engineering, Kyushu Institute of Technology, Kitakyushu, Japan

\*[q104070y@mail.kyutech.jp](mailto:q104070y@mail.kyutech.jp)

The bimetallic work rolls are widely used in the roughing stands of hot rolling stand mills. The rolls are classified into two types; one is a single-solid type, and the other is a shrink-fitted construction type consisting of a sleeve and a shaft. Regarding a shrink-fitted construction type, the interfacial creep sometimes appears between the shaft and the shrink-fitted sleeve. The numerical simulation for interfacial creep phenomenon was studied recently. This interfacial creep can be regarded as the relative displacement between the sleeve and the shaft, which often causes the roll damage. This paper confirms the interfacial creep generation in experiment. Rolling process experiments were carried out for hollow shrink-fitted discs. Then, the interfacial creep between shrink-fitted roll was confirmed in the experiment. Fig. 1 shows the experimental specimens used in this study.

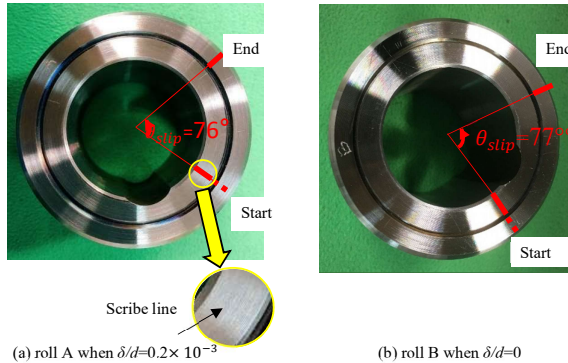


Fig. 1. Angle slipped in the experiment

Table 1 summarizes the slip velocity  $du_{\theta,ave}^{P(0)\sim P(4\pi)} / d\varphi$  and  $u_{\theta,ave}^{P(0)\sim P(2\pi)}$  for the experimental data and numerical simulation. The correspondence was confirmed between the experimental data and the simulation results.

Table 1. Comparison of experimental data and simulation results for

	Shrink-fitting ratio, $\delta/d$	Experiment Data	Simulation Results
$\frac{du_{\theta,ave}^{P(0)\sim P(4\pi)}}{d\varphi} \Big _{\varphi \geq \pi}$		306	

Velocity	0	$0.889 \times 10^{-5}$ mm/deg.	$6.65 \times 10^{-5}$ mm/deg.
	$0.2 \times 10^{-3}$	$0.296 \times 10^{-5}$ mm/deg.	$2.50 \times 10^{-5}$ mm/deg.
Average displacement	0	$0.32 \times 10^{-2}$ mm	$2.7 \times 10^{-2}$ mm
$u_{\theta, ave.}^{P(0) \sim P(2\pi)}$	$0.2 \times 10^{-3}$	$0.17 \times 10^{-2}$ mm	$0.886 \times 10^{-2}$ mm

## Oscillations of Non-axisymmetric Shells: Parameterization and Equations

A.S. Yudin

*I. I. Vorovich Institute of Mathematics, Mechanics and Computer Sciences,  
Southern Federal University, Rostov-on-Don, Russia*

[ayudin@sfedu.ru](mailto:ayudin@sfedu.ru)

Shells closed in the circumferential direction, but without axial symmetry, can be used for modeling a number of technical structures. These include aircraft structures (aircraft fuselages, helicopters), tankers, and ship hulls. Parameterization of such shells can be performed in the class of framed shells with linear surfaces of component sections (module-elements). The module-element is built on two guiding plane contours  $K_0$  and  $K_1$ , defined in local coordinate systems with centers  $O$  and  $O_1$ . Contour equations are converted to a polar coordinate system and are set by analytical curves closed in the circumference (ellipse, special contour, etc.) or piecewise analytic functions. The centers  $O$  and  $O_1$  are connected by a segment that acts as the local axis of the module-element. Contours can have different angles of inclination to this axis. The plane passing through the  $OO_1$  axis intersects the guide contours at points  $M_0$  and  $M_1$ . When this plane rotates, the segment  $M_0M_1$  forms a linear surface stretched over the contours  $K_0$  and  $K_1$ . The shell of a complex structure (CS) is assembled from a chain of module-elements. The axial (main) line of CS can be a multi-link flat polyline with the centers of the frame contours located on it. Guide polygons are required at points where the main line breaks. The CS-surface is constructed in the global Cartesian coordinate system under the assumption that the diametric planes of all the contours are in the same plane. The ability to control the angle of inclination of the guide contour planes allows one to combine them with the configuration of the ends, the junction lines of sections and the external borders of the frames. This simplifies the formulation of boundary conditions and section interface conditions. Equations and metric tensors of the main surfaces of typical module-elements are constructed. The derivation of the main equations is based on the application of the Hamilton – Ostrogradsky principle. Variants of Timoshenko-type and Kirchhoff-type shells are considered. In accordance with the accepted calculation scheme, quasi-one-dimensional systems of ordinary differential equations in matrix form for dimensionless variables are constructed. The construction of the system is associated with a large mass of calculations performed in the integrated package of symbolic transformation technologies. The integrated package also implements a numerical algorithm. To improve the efficiency of the algorithm, when preparing the equations of the boundary value problem, the reference matrices of the coefficients of the resolving system are pre-calculated on a sparse set of axis points along a longitudinal coordinate. Further, the algorithm for solving the boundary value problem, which is reduced to a series of Cauchy problems, uses approximations of the coefficients

of the system through the elements of the reference matrices. The calculation scheme is based on the representation of solutions by trigonometric Fourier series on a circumferential coordinate, the construction of a canonical ODE resolving system connected by circumferential modes for coefficients of series that depend on the longitudinal coordinate, and the solution of boundary value problems for this system using stable numerical methods. The Kantorovich type method is used to remove the circumferential coordinate. In the power scheme, the characteristics of the frames are present in the conditions of interfacing sections. Longitudinal force elements and local mass inhomogeneities are taken into account by the “smearing” method in the attached areas bounded by pairs of coordinate lines. Regular grids of reinforcing edges are taken into account according to the scheme of constructive anisotropy in skewed coordinate systems. Debugging a set of computer programs for a shell is the geometry used in the model hierarchy for simpler shells. Numerical experiments are performed to analyze the stability of calculation, convergence, and accuracy depending on the model type, mode numbers, and the number of grid points.

#### **Acknowledgement**

Research was financially supported by Southern Federal University, grant No. VnGr-07/2020-04-IM (Ministry of Science and Higher Education of the Russian Federation).

## **Vibrations of the Auxetic Shell in the Liquid**

**A.S. Yudin**

*I. I. Vorovich Institute of Mathematics, Mechanics and Computer Sciences,  
Southern Federal University, Rostov-on-Don, Russia*

[ayudin@sfedu.ru](mailto:ayudin@sfedu.ru)

Analysis of vibrations of shell constructions in a liquid is relevant in cases when a high noise level is an undesirable characteristic of the object. The vibration amplitudes of the shell surface in contact with the liquid and the noise levels in the environment are correlated. Therefore, a set of methods is used to reduce vibration and noise levels, which include means of vibration isolation, vibration and noise absorption. Due to the development of new technologies, the analysis of effects from the use of non-traditional materials is also relevant in this area. These include materials with auxetic properties. As shown by mathematical modeling, they give the effect of reducing vibration levels on the example of a thin aircraft-type shell [1]. In this report, the analysis of vibrations in the liquid of a thicker and stronger shell that can withstand a high level of external pressure is performed. In the vibroacoustic calculation of vibrations of shells and a linear medium, the stage of determining the reaction of dynamic pressure on the contact surface is of considerable complexity. To do this, it is necessary to solve the Fredholm-type integro-differential problem on the shell surface using the Helmholtz integral in the correct formulation. Such approaches based on the eigenform method, local impedance modeling method, and iterative methods are developed for shells of revolution [2]. The most convenient and effective method for modeling local impedance is when the type of connection between the amplitude of dynamic pressure and velocity (or displacement) on the shell surface is set *a priori*. To do this, we use the solution of the Helmholtz equation in cylindrical coordinates. The acceptability of this approach was checked by comparison with more accurate

methods on shells of revolution. For vibroacoustic calculations of complex composite structures, calculations of amplitude-frequency characteristics (AFC) are performed on a set of discrete values of the driving frequency parameter. This is quite a long and painstaking work. Examples of such AFC are given in [2]. However, in the case of comparative analysis of the influence of the properties of different materials on the vibrational characteristics, a very convenient model is a reinforced cylindrical shell with a free support of the ends. This model allows representation of the solution in series and construction of the frequency response as a function of the frequency parameter. In addition, this model is also informative for more complex structures, since it is a typical section of composite shells. As the frequency increases, the vibrations are localized to a separate excitable section. This is why the effect of reducing the long structure to a single section works, which determines the main contribution to the acoustic field. Calculations of the effect of acoustic properties of the shell were performed on a cylindrical shell supported by a grid of edges in the circumferential direction, and located in a heavy acoustic environment with a density of water. The frequency of resonances in the medium decreases in relation to the "dry" shell due to the influence of the attached mass of the liquid. However, the positive effect of reducing the vibration levels of the shell with the properties of the auxetic remains.

#### **Acknowledgement**

Research was financially supported by Southern Federal University, grant No. VnGr-07/2020-04-IM (Ministry of Science and Higher Education of the Russian Federation).

#### **References**

- [1] Yudin A. S., Yudin S. A. In: *Proceedings of the 2015 International Conference on Physics and Mechanics of New Materials and Their Applications, devoted to 100-th Anniversary of the Southern Federal University*, Ivan A. Parinov, Shun-Hsyung Chang, Vitaly Yu. Topolov (Eds.). Nova Science Publishers, New York, 447-452, 2016.
- [2] Yudin A.S. In: *Advanced Materials. Physics, Mechanics and Applications*. Springer Proceedings in Physics, Shun-Hsyung Chang, Ivan A. Parinov, Vitaly Yu. Topolov (Eds.). Heidelberg, New York, Dordrecht, London: Springer Cham, **152**, 181-191, 2014.

## **The Dielectric Spectra Study of Polyaniline**

**Y.I. Yurasov<sup>1,2</sup>, A.V. Nazarenko<sup>1\*</sup>, G.K. Timoshenko<sup>2</sup>**

<sup>1</sup>*Southern Scientific Center, Russian Academy of Sciences, Rostov-on-Don, 344006, Russia*

<sup>2</sup>*Research Institute of Physics, Southern Federal University, Rostov-on-Don, 344090, Russia*

[\\*avnazarenko1@gmail.com](mailto:*avnazarenko1@gmail.com)

The study of the relaxor properties of Ferroalloy cermets around the world has been engaged in for more than 50 years. During this time, numerous objects were created that have unique properties and a combination of ferroelectric, piezoelectric and optical properties. Many theories and models have been developed to describe the physical processes occurring in them, including the Arrhenius and Vogel Fulcher laws. The most common model of approximation of the relaxation in magnetoplasma dynamic today is formula Havriliak – Negami [1]. That is why a new model for

describing the complex specific electrical conductivity was obtained on its basis, which has a higher convergence in a wide frequency spectrum  $f = 10^{-3} - 10^8 \text{ Гц}$  [2, 3]:

$$\gamma^* = \gamma_\infty + \sum_{n=1}^{\infty} \frac{\Delta\gamma_n}{(1 + (i\omega\tau_n)^{1-\alpha})^\beta} + \varepsilon''\omega\varepsilon_0 + i\varepsilon'\omega\varepsilon_0 \quad (1)$$

$$\alpha = \frac{kT}{E_a} \ln(Q_\infty), \quad M' = \frac{\varepsilon'}{\varepsilon'^2 + \varepsilon''^2}, \quad M'' = \frac{\varepsilon''}{\varepsilon'^2 + \varepsilon''^2} \quad (2)$$

where  $\gamma^* = \gamma' + i\gamma''$  is the total complex electrical conductivity;  $Q_\infty = \varepsilon'_{\infty}/\varepsilon''_{\infty}$  is the  $Q$ -factor at  $\omega \rightarrow \infty$ ;  $\varepsilon'_{\infty}$  and  $\varepsilon''_{\infty}$  are the real and imaginary parts of the permittivity  $\varepsilon''$  at  $\omega \rightarrow \infty$ , respectively;  $M'$ ,  $M''$  are the real and imaginary parts of module;  $\varepsilon''\omega\varepsilon_0$  is the singular member and  $\varepsilon'\omega\varepsilon_0$ , is the additional member;  $\alpha$  is the parameter of the temperature-frequency distribution of dielectric losses in a nonlinear dielectric,  $\beta = 1 - \alpha$  ( $0 \leq \alpha \leq 1$ ,  $0 \leq \beta \leq 1$ );  $\Delta\gamma_n = \gamma_{Sn} - \gamma_{\infty n}$ ;  $n$  is a number of the relaxation process, and  $\gamma_{Sn} = \gamma_{\infty n-1}$ . The report shows the possibility of using new model (1) to describe the temperature and frequency dependences of a chemical polymer such as polyaniline on the electrical conductivity, which is its distinctive feature from most known polymers, which are insulators under normal conditions. It was found that new model (1) with calculated values of  $\alpha$  from (2), and not empirically selected, has complete convergence with experimental data (see Fig.1).

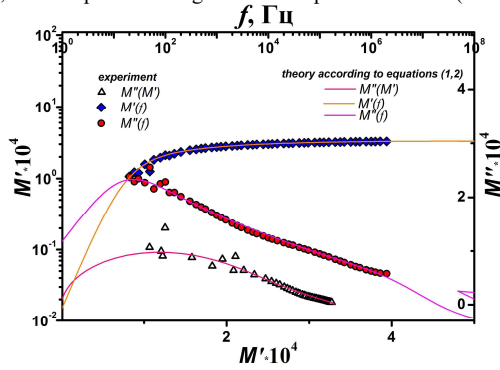


Fig. 1

The results of the study confirm that new model (1), (2) can be used to describe the dielectric spectra of any nonlinear dielectrics, including those with high values of electrical conductivity.

#### Acknowledgements

The work is performed as part of the projects of the SSC RAS State Order (Nos. 01201354240 and 01201354247) and the Ministry of Science and Higher Education of the Russian Federation (State assignment in the field of scientific activity, Southern Federal University, 2020) with the use of equipment of the Centers for Collective Use Nos. 1483136 and 501994.

#### References

- [1] Havriliak S., Negami S. // *Journal of Polymer Science Part C*, **14**(1), 99 – 117, 1966.
- [2] Yurasov Yu.I., Nazarenko A.V. // *Science of the South of Russia*, **15**(1), 31 – 41, 2019.
- [3] Yurasov Yu.I., Nazarenko A.V. // *Journal of Advanced Dielectrics*, **10**(01n02), 2060006, 2020.



## **Study of Fatigue Life Experiments in Bottom Ash /Aluminum Composite Getting T6 Heat Treatment and Artificial Aging**

**Zainun Achmad\*, Dikrie Alief Zaini, M. Kevin Firnanda, Ismail**

*Mechanical Engineering Department, University of 17 Agustus 1945 (UNTAG) Surabaya, Indonesia*

[\\*zainun@untag-sby.ac.id](mailto:*zainun@untag-sby.ac.id)

The process of the manufacture of aluminum composite with reinforcement of coal bottom ash which has gone through an electroless process with an aim to coat the coal bottom by ash powder to stick to the aluminum metal during casting. The strength of aluminum alloy material depends not only on the concentration of the metal alloy, but also how it is treated until the aluminum is ready for use. T6 heat treatment with a dissolving temperature of 510 °C for 1 hour and 2 hours and followed by artificial aging temperatures of 120 °C, 140 °C and 160 °C held for 2 hours. The highest strength values were achieved in the T6 treatment at 510 °C for 1 hour and the temperature of the artificial aging 140 °C for 2 hours. The maximum tensile strength value of 310 MPa, and the yield strength 222.3 MPa were found in the T6 treatment at 510 °C with an artificial aging temperature of 120 °C during 1 hour. Fatigue is a major cause of failure in applications. From the fatigue test, the highest age of fatigue with a load of  $0.87\sigma_{it}$  was in specimens that were manufactured in the T6 treatment at 510 °C with one-hour dissolution time and 120 °C aging temperature for 1 hour and it was equal to 3,466 cycles. The lowest fatigue life in the specimens was attained in the T6 treatment at 510 °C with two-hour dissolution time and at the aging temperature equal to 160 °C for 2 hours; it was 400 cycles. The highest fatigue age with load  $\sigma_y$  was in the specimens manufactured in the T6 treatment at 510 °C with one-hour dissolution time and 140 °C aging temperature for 1 hour and it was equal to 32,566 cycles. The lowest fatigue life in the specimens was attained in the T6 treatment at 510 °C with one-hour dissolution time and at the aging temperature equal to 160 °C for 1 hour; it was 11,333 cycles.

## **Pyroelectric, Bolometric and Flexoelectric Effects Excited in the Volume of Unpolarized Ferroelectric Plates by Periodic Heating of Electrode Surfaces by Modulated Thermal Radiation**

**Yu.N. Zakharov<sup>1</sup>, L.A. Reznichenko<sup>1</sup>, I.A. Parinov<sup>2</sup>, E.I. Sitalo<sup>1\*</sup>, V.A. Chebanenko<sup>3</sup>,  
A.A. Pavelko<sup>1</sup>, L.I. Kiseleva<sup>3</sup>**

<sup>1</sup>*Physics Faculty and Physics Research Institute, Southern Federal University,  
Rostov-on-Don, Russia*

<sup>2</sup>*I. I. Vorovich Mathematics, Mechanics and Computer Science Institute, Southern Federal  
University, Rostov-on-Don, Russia*

<sup>3</sup>*Federal Research Center "Southern Scientific Center of the Russian Academy of Sciences",  
Rostov-on-Don, Russia*

\*[e\\_sitalo@mail.ru](mailto:e_sitalo@mail.ru)

The method of dynamic pyroelectric effect was used in this study to investigate ferroelectric plates with dimensions of  $10 \times 6 \times 0.6 \mu\text{m}^3$  made of hot-pressed ferroelectric ceramics PZT-19 ( $T_C = 300 \text{ }^\circ\text{C}$ ), which did not undergo the process of preliminary polarization, after laser scribing of one surface and grinding with a powder with a particle diameter of up to 10 microns of the opposite surface. The electrodes were deposited by firing silver (Ag). For comparison, a batch of similar plates was made, but did not go through the laser scribing process. It has been established that after firing metal electrodes into opposite surfaces with different depths of mechanical damage, counter-directed stationary deformation gradients and, accordingly, internal electric displacement fields are created in the plate. Such plates retain the values of the pyro- and flexoelectric effects in the ferroelectric phase, as well as the bolometric effect in the paraelectric phase, after repeated heating cycles up to  $350 \text{ }^\circ\text{C}$  and cooling down to  $T_{\text{norm}}$ . In addition, it has been shown that damage to the plate surface prior to electrode firing gives increased values of the response in the paraelectric phase. This indicates that the pyroelectric response at the treated surface consists of the sum of the induced and stationary flexoelectric effect caused by damage. Whereas the plates that did not pass the scribing process will have only an induced flexoelectric effect (due to temperature gradient), which is confirmed by lower pyroelectric response values.

#### ***Acknowledgement***

The work was supported by Russian Foundation for Basic Research, grant No.19-08-00365.

## **Dielectric, Piezoelectric and Magnetodielectric Characteristics of Ceramic Multiferroic Solid Solution Composition $0.5\text{BiFeO}_3 - 0.5\text{PbFe}_{1/2}\text{Nb}_{1/2}\text{O}_3$**

**K.M. Zhidel<sup>1\*</sup>, A.V. Pavlenko<sup>1,2</sup>**

<sup>1</sup>Research Institute of Physics, Southern Federal University,  
194, Stachki Ave., Rostov-on-Don, 344090, Russia

<sup>2</sup>Federal Research Centre The Southern Scientific Centre of the Russian Academy of Sciences, 41,  
Chekhov Str., Rostov-on-Don, 344006, Russia

\*[karinagidele@gmail.com](mailto:karinagidele@gmail.com)

Multiferroics combine both ferroelectric and ferro(antiferro-)magnetic properties in a wide temperature range. Currently, such materials are of great interest for not only theoretical point of view but also practical ones. Physical characteristics (dielectric, magnetodielectric and piezoelectric) of  $0.5\text{BiFeO}_3 - 0.5\text{PbFe}_{1/2}\text{Nb}_{1/2}\text{O}_3$  multiferroic, made in the form of ceramic, are reported. Based on measurements of sample dielectric characteristics, it has been found that at  $T \sim 400$  K the anomalies in the dependences of the real ( $\epsilon'/\epsilon_0$ ) and imaginary ( $\epsilon''/\epsilon_0$ ) parts of the complex dielectric constant are due to the transition of the object from the ferroelectric phase to the paraelectric. At  $T \sim 450$  K, ones are associated with the magnetic transformation occurring at these temperatures in the object. The behavior of  $\epsilon'/\epsilon_0$  and  $\epsilon''/\epsilon_0$  in the high-temperature region is a consequence of the Maxwell-Wagner polarization of the non-Debye type and its corresponding relaxation. It also took place in  $\text{BiFeO}_3$  and  $\text{PbFe}_{1/2}\text{Nb}_{1/2}\text{O}_3$  ceramics. Taking into account the reference data, it has been established that the object under study simultaneously exhibits ferroelectric and magnetic properties at  $T < 450$  K. Attempts have been undertaken to polarize by various technological methods for the studied ceramics. It turned out to be possible to fix only the  $d_{33}$  piezomodule, measured by the quasistatic method, which fell from 24 pC/N to 0 within 240 hours. The investigation of the magnetodielectric effect in high-resistance ceramic samples  $\text{BiFeO}_3$ ,  $\text{PbFe}_{1/2}\text{Nb}_{1/2}\text{O}_3$  and  $0.5\text{BiFeO}_3 - 0.5\text{PbFe}_{1/2}\text{Nb}_{1/2}\text{O}_3$  was performed. It has been discovered that the magnetodielectric effect in them at room temperature in a magnetic induction field of 0.85 T is maximum precisely in  $0.5\text{BiFeO}_3 - 0.5\text{PbFe}_{1/2}\text{Nb}_{1/2}\text{O}_3$  ( $\sim 0.5\%$  at  $B = 0.86$  T). The reasons for the revealed regularities and the nature of the detected phase transformations are discussed.

#### **Acknowledgement**

Research was financially supported by the Ministry of Science and Higher Education of the Russian Federation (State assignment in the field of scientific activity, Southern Federal University, 2020).

## **Investigation of the Parameters of the Convergence of Two Axes of Contacting Circular Parallel Steel Cylinders in Numerical Modeling**

**G.A. Zhuravlev<sup>1</sup>, A. V. Cherpakov<sup>1,2</sup>, Yu. E. Drobotov<sup>1\*</sup>**

<sup>1</sup>*Southern Federal University, Rostov-on-Don, Russia*

<sup>2</sup>*Don State Technical University, Rostov-on-Don, Russia*

The problem of modeling in the ANSYS complex the contacting circular parallel steel cylinders of different radii is considered. The radii of the cylinders were taken as  $R_1 = 10 - 100$  mm. The elastic modulus of the cylinders had the value  $E_1 = E_2 = 2.15 \times 10^{11}$  Pa, Poisson's ratios were taken equal to  $\nu_1 = \nu_2 = 0.3$ . The goal was to study the dependence of the characteristics of the approach of the axes, the contact area, and the stress state of the cylinders, depending on the change in the radius of the first of them. The load on the first cylinder was assumed to be 10000 N/m. Fig. 1a shows the plots of the calculation results showing the values of radii convergence for the upper (1) and lower (2) cylinders, depending on the radius of the upper cylinder  $R_1$ . Analysis shows that these plots have a non-linear logarithmic trend of change. The dependence of the contact area  $l_p$  for two cylinders shown in Fig. 1b also has a nonlinear trend of a certain dependence. A more detailed analysis requires comparing this solution with the analytical one.

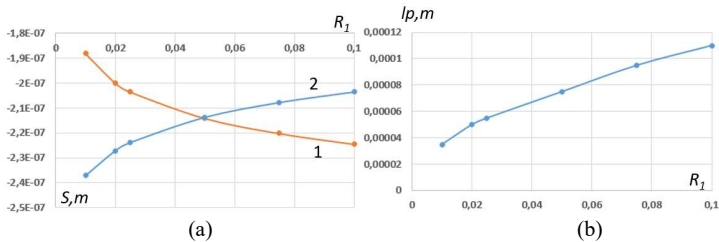


**Fig. 1.** Values of the approach of the radii (a) for the upper (1) and lower (2) cylinders depending on the radius of the upper cylinder  $R_1$ ; (b) dependence of the contact area  $l_p$  for two cylinders

### **Acknowledgement**

Research was financially supported by Southern Federal University, grant No. VnGr-07/2020-04-IM (Ministry of Science and Higher Education of the Russian Federation).

## **Evaluation Criteria for the Influence of the Material Properties of Elastic Cylinders on Their Contact Approach**

**G. A. Zhuravlev\*, Yu. E. Drobotov\*\***

*Southern Federal University, Rostov-on-Don, Russia*

\*[zhur.okp@yandex.ru](mailto:zhur.okp@yandex.ru), \*\*[yu.e.drobotov@yandex.ru](mailto:yu.e.drobotov@yandex.ru)

In theory and practice of contact calculations, there are two entirely opposite views on the influence exerted by the radii of two elastic circular cylinders on their approach. While the methods [1, 2] attribute it to the fully justified classical theory, the method [3] states this influence is absent, as well as the contact deformation of the cylinders depends linearly on loading. The presented analysis proposes that the contact approach  $\delta = \delta_1 + \delta_2$  is independent only on the significantly smaller radius of the cylinders [4, 5], which is reflected in Figs. 1 and 2 by considering steel cylinders with  $\mu = 0.3$  and  $E = 2.15 \times 10^5$  MPa. To prove this effect of the approach, called here “EA”, a theoretical research for various combinations of values of material parameters is carried out, and experimental data are considered in the framework of the developed theoretical models.

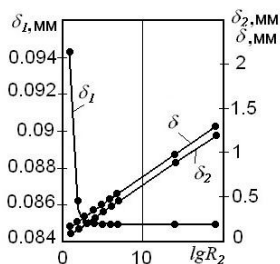


**Fig. 1.** Influence of the radius of greater cylinder  $R_2$  on the components  $\delta_1$  and the approach  $\delta$  of the axes of steel cylinders for  $R_1 = 10$  mm,  $q = 10^4$  N/mm

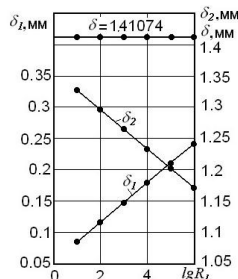


**Fig. 2.** Influence of the radius of smaller cylinder  $R_1$  on the components  $\delta_1$  and the approach  $\delta$  of the axes of steel cylinders for  $R_2 = 10^{20}$  mm,  $q = 10^4$  N/mm

**Acknowledgement**

Research was financially supported by Southern Federal University, grant No. VnGr-07/2020-04-IM (Ministry of Science and Higher Education of the Russian Federation).

**References**

- [1] Koval'skij B. S. *Calculation of Details on Local Compression*. Kharkov, HVKIU, 1967 [In Russian].
- [2] Loo T. T. // *J. Appl. Mech.*, **25**, 122 – 124, 1958.
- [3] Ajrapetov E. L. // *Russian Engineering Research*, **6**, 6–10, 1988.
- [4] Zhuravlev G. A., Karpenko V. A. // *Mechanical Engineering*, **6** (28), 51–55, 2008 [In Russian].
- [5] Zhuravlev G. A. In: *Mixed Problems of Solid Mechanics. Materials of the V Russian Conference with International Participation*, 23 – 25 August, 2005. Saratov, Saratov State University Press, 148–151, (2005) [In Russian].

**Method for Calculating Stress Concentration in Elastoplastic Rod with Two Symmetric Hyperbolic Recesses**

G. A. Zhuravlev\*, Yu. E. Drobotov\*\*

*Southern Federal University, Rostov-on-Don, Russia*

\*[zhur.okp@yandex.ru](mailto:zhur.okp@yandex.ru), \*\*[yu.e.drobotov@yandex.ru](mailto:yu.e.drobotov@yandex.ru)

An approach for approximating the stress-strain state of an elastoplastic rod with two symmetric hyperbolic recesses under transverse bending with compressing and thermal-force loading at the surface layers is considered. Both the concentrator and the area outside it are loaded on the same side of the rod. The approach uses “elastic” solutions with reference to the widely approved kinematic hypothesis of S. P. Timoshenko [1, 2], which say on independence of the distribution law of strains on deforming and strengthening the material:

$$\tilde{\varepsilon}_x(y) = \varepsilon_x(y) \frac{\varepsilon_T}{\varepsilon_l(y_T)},$$

where  $\varepsilon_x(y)$  and  $\tilde{\varepsilon}_x(y)$  are the relative linear deformations at the current point  $y$  for a specific cross-section at  $x = \text{const}$  for an ideal absolutely elastic material and the real one, respectively;  $\varepsilon_T$  is the relative deformation, corresponding to the material yield stress;  $\varepsilon_l(y_T)$  is the criterion value, characterizing transition from elastic deforming to the non-elastic one at the boundary point  $y = y_T$  of the section for ideally elastic material. The Neuber’s solution [3] for the plane problem on stress concentration is used as the “elastic component” of the method. An iterative process is organized then for calculation of residual normal stresses after the elastoplastic deforming, with applying the Ilyushin – Genki theorem and verifying the equilibrium condition. As a result, the stress-strain state of the considered rod is specified with high accuracy and performance. Software implementation and a practical instance of applying the method are discussed.

#### **Acknowledgement**

Research was financially supported by Southern Federal University, grant No. VnGr-07/2020-04-IM (Ministry of Science and Higher Education of the Russian Federation).

#### **References**

- [1] Del' G.D., Chebaevskii B.P., Pronkin A.F. // *Strength Mater.* **3**, 80–83, 1971.
- [2] Troshchenko V.T., Getman A.F. // *Strength Mater.* **4**, 140–144, 1972.
- [3] Neuber H. *Kerbspannungslehre. Theorie der Spannungskonzentration Genaue Berechnung der Festigkeit*. Springer-Verlag Berlin Heidelberg, 2001.

## **Thermostability Ceramics Based on Sodium, Calcium, Strontium Niobates, Depending on the of Synthesis and Sintering Conditions, and Mechanical Processing**

J.Y. Zubarev<sup>1,2\*</sup>, L.A. Reznichenko<sup>2</sup>

<sup>1</sup>*Research and Technology Unit, FKU NPO "STiS" MIA Russia, Rostov-on-Don, 344090, Russia*

<sup>2</sup>*Research Institute of Physics, Southern Federal University,  
Rostov-on-Don, 344090, Russia*

\*[yzubarev@sfedu.ru](mailto:yzubarev@sfedu.ru)

In the last five years, detonation engine researchers, both pulsed and rotational, have achieved significant success. They require extreme accuracy in monitoring and controlling of fuel detonation processes. The processes taking place are accompanied by changes in temperature and pressure. In this work, the phase-electrophysical properties of high-temperature ferro-piezoceramic materials with the participation of layered perovskite-like compounds are considered. These objects have a maximum working temperature reaches 2000 – 3000 K. This is of interest for use in the above devices. The phase diagrams of binary systems of the  $(1-x)\text{NaNbO}_3 - x\text{CaSr}_2\text{Nb}_2\text{O}_7$  ( $0.0 \leq x \leq 1.0$ ;  $\Delta x = 0.05$ , 300 K) type are studied. These include crystallization regions of perovskite-type solid solutions and alternating layered perovskite-like compounds. At the boundary of these phase states, objects with increased reactivity are formed. Due to this, intercalation of gas ions into the structure is possible. The underside mechanism is studied by the example of interaction of ceramics with atmospheric water. In the process of water adsorption, intercalation of hydroxyl groups into the interlayer space occurs. Moreover, under certain conditions, ionic molecules create an active film on the surface of crystalline structures. This process is reversible under the influence of external factors. Significant impact on these properties has thermodynamic background: synthesis conditions and sintering ceramics. Increasing the sintering temperature and the synthesis allows one to obtain optimum characteristics of ceramic objects. Machining, besides changes in the structure and topology, reduces the sintering temperature. The totality of the objects of study can be recommended as components of pulse and rotating detonation engines. However, a variation of the thermodynamic background of these objects can be recommended as devices in microwave technology.

#### ***Acknowledgements***

This work was financially supported by the Russian Federation Ministry of Science and Higher Educations (State assignment in the field of scientific activity, Southern Federal University, 2020). The equipment of the Collective Use Centers “Electromagnetic, Electromechanical and Thermal Properties of Solids” was used at the Research Institute of Physics of the Southern Federal University.

## **Crystal Structure and Dielectric Properties of Layered Perovskite-like Solid Solutions $\text{Bi}_{3-x}\text{Gd}_x\text{TiTaO}_9$ ( $x = 0, 0.1, 0.2, 0.3$ ) with High Curie Temperature**

**S. V. Zubkov**

*Research Institute of Physics, Southern Federal University, 194, Stachki Ave,  
Rostov-on Don, 344090, Russia*

[svzubkov61@mail.ru](mailto:svzubkov61@mail.ru)

The Aurivillius phases  $[\text{Bi}_2\text{O}_2][\text{A}_{n-1}\text{B}_n\text{O}_{3n+1}]$  are well-known ferroelectrics with high Curie temperatures. High-temperature piezoceramics  $\text{Bi}_{3-x}\text{Gd}_x\text{TiTaO}_9$  ( $x = 0, 0.1, 0.2, 0.3$ ) were prepared by a solid-state reaction method [1]. The structural and electrophysical characteristics of  $\text{Bi}_{3-x}\text{Gd}_x\text{TiTaO}_9$  ceramics have been studied. According to the data of powder X-ray diffraction, all the compounds are single-phase with the structures of two-layer Aurivillius phases ( $m = 2$ ) with the orthorhombic crystal lattice (space group  $A21am$ ). The temperature dependence of the relative permittivity  $\epsilon/\epsilon_0(T)$  of the compounds was measured and showed that the Curie temperature of perovskite-like oxides  $\text{Bi}_{3-x}\text{Gd}_x\text{TiTaO}_9$  increases linearly with an increase in the substitution parameter  $x$  to  $T_C = 920$  °C. The activation energies of charge carriers have been found in different temperature ranges.

#### **Reference**

[1] S. V. Zubkov // *Journal of Advanced Dielectrics*, **10**(01n02), 2060002, 2020.

## **Crystal Structure and Dielectric Properties of Layered Perovskite-like Solid Solutions $\text{Bi}_{3-x}\text{Nd}_x\text{TiNbO}_9$ ( $x = 0, 0.2, 0.4, 0.6, 0.8, 1.0$ )**

**S. V. Zubkov**

*Research Institute of Physics, Southern Federal University, 194, Stachki Ave,  
Rostov-on Don, 344090, Russia*

[\\*svzubkov61@mail.ru](mailto:svzubkov61@mail.ru)

The Aurivillius phases  $[\text{Bi}_2\text{O}_2][\text{A}_{n-1}\text{B}_n\text{O}_{3n+1}]$  are well-known ferroelectrics with high Curie temperatures. High-temperature piezoceramics  $\text{Bi}_{3-x}\text{Nd}_x\text{TiNbO}_9$  ( $x = 0, 0.2, 0.4, 0.6, 0.8, 1.0$ ) were prepared by a solid-state reaction method [1]. The structural and electrophysical characteristics of  $\text{Bi}_{3-x}\text{Nd}_x\text{TiNbO}_9$  ceramics have been studied. According to the data of powder X-ray diffraction, all the compounds are single-phase with the structures of two-layer Aurivillius phases ( $m = 2$ ) with the orthorhombic crystal lattice (space group  $A21am$ ). The temperature dependence of the relative permittivity  $\epsilon/\epsilon_0(T)$  of the compounds was measured and showed that the Curie temperature of perovskite-like oxides  $\text{Bi}_{3-x}\text{Nd}_x\text{TiNbO}_9$  decreases linearly with a decrease in the substitution parameter  $x$  to  $T_C = 430$  °C. The activation energies of charge carriers have been found in different temperature ranges as well as dependence of  $T_C$  on  $x$  for  $\text{Bi}_{3-x}\text{Nd}_x\text{TiNbO}_9$  (see Figs.1, 2).



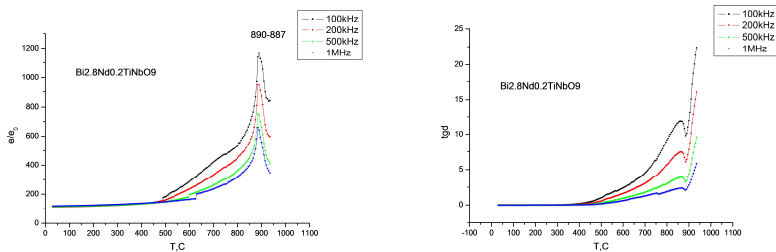


**Fig. 1.** Temperature dependence of the permittivity  $\varepsilon/\varepsilon_0$  and dielectric loss  $\tan\delta$  for  $\text{Bi}_{2.8}\text{Nd}_{0.2}\text{TiNbO}_9$

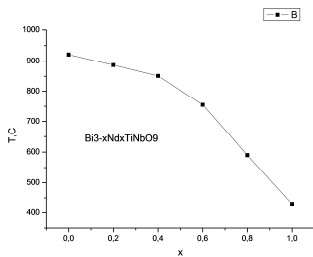


**Fig. 2.** Dependence of Curie temperature on  $x$

**Reference**

[1] S. V. Zubkov // *Journal of Advanced Dielectrics*, **10**(01n02), 2060002, 2020.

**Crystal Structure and Ferroelectrics Properties of Mixed-layer  $\text{Bi}_7\text{Ti}_{4-x}\text{Sn}_x\text{NbO}_{21}$  ( $x = 0.1, 0.2, 0.3, 0.4, 0.5$ ) Ceramics**

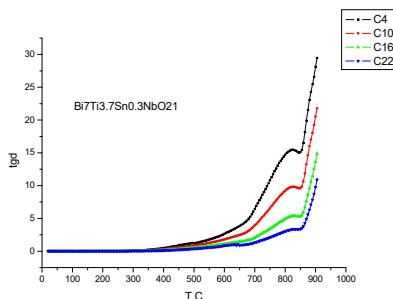
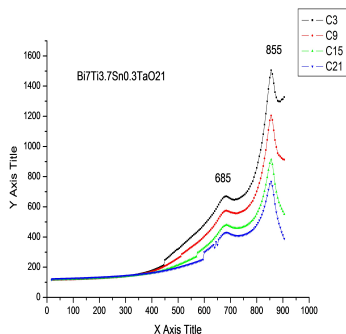
**S. V. Zubkov**

*Research Institute of Physics, Southern Federal University, 194, Stachki Ave, Rostov-on Don, 344090, Russia*

\*[svzubkov61@mail.ru](mailto:svzubkov61@mail.ru)

Layered perovskite-like bismuth oxides with the Aurivillius phase (AP) structure have been known for several decades [1, 2], but interest in them has been growing due to their potential practical applications. APs are promising materials for fabricating high-temperature piezoelectric transducers operating in extreme conditions and are considered as elements of ferroelectric memory devices (FeRAM), as multifunctional materials exhibiting magnetic properties (multiferroics), photoluminescence etc. At the present time, the number of known APs is several hundreds, and this number continues to increase. A number of solid solutions  $\text{Bi}_7\text{Ti}_{4-x}\text{Sn}_x\text{NbO}_{21}$  ( $x = 0.1, 0.2, 0.3, 0.4, 0.5$ ) have been synthesized from oxides by solid-phase reaction. The crystal structure, the electrophysical characteristics and the microstructure of the prepared ceramic samples have been studied. According to X-ray powder diffraction, all the compounds are single-phase with the

structure of mixed-layer Aurivillius phases ( $m = 2.5$ ) with the orthorhombic crystal lattice (space group  $I2cm$ ,  $Z = 2$ ). The activation energies of charge carriers have been found in different temperature ranges.



## References

1. Zubkov S.V., Vlasenko V.G., Shuvaeva V.A., Shevtsova S.I. // *Phys. Solid State*, **58**(1),42, 2016.
2. D.Mercurio, G.Trolliard, THansen, J.P. Mercurio, // *International Journal of Inorganic Materials*, **2**(5), 397-406, 2000.

## Crystal Structure and Ferroelectrics Properties of Mixed-layer Bi<sub>7-x</sub>Y<sub>x</sub>TiNbO<sub>21</sub> ( $x = 0, 0.2, 0.4, 0.6$ ) Ceramics

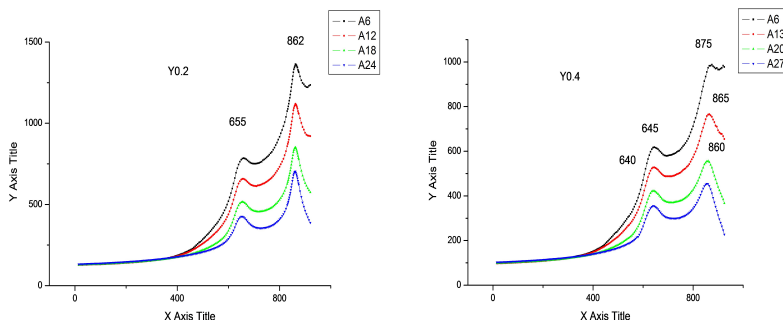
S. V. Zubkov

*Research Institute of Physics, Southern Federal University, 194, Stachki Ave, Rostov-on Don, 344090, Russia*

[svzubkov61@mail.ru](mailto:svzubkov61@mail.ru)

Layered perovskite-like bismuth oxides with the Aurivillius phase (AP) structure have been known for several decades [1, 2], but interest in them has been growing due to their potential practical applications. APs are promising materials for fabricating high-temperature piezoelectric transducers operating in extreme conditions and are considered as elements of ferroelectric memory devices (FeRAM), as multifunctional materials exhibiting magnetic properties (multiferroics), photoluminescence etc. At the present time, the number of known APs is several hundred, and this number continues to increase. A number of solid solutions Bi<sub>7-x</sub>Y<sub>x</sub>TiNbO<sub>21</sub> ( $x = 0, 0.2, 0.4, 0.6$ ) have been synthesized from oxides by solid-phase reaction. The crystal structure, the electrophysical characteristic and the microstructure of the prepared ceramic samples have been

studied. According to X-ray powder diffraction, all the compounds are single-phase with the structure of mixed-layer Aurivillius phases ( $m = 2.5$ ) with the orthorhombic crystal lattice (space group  $I2cm$ ,  $Z = 2$ ). The activation energies of charge carriers have been found in different temperature ranges.



### References

- [1] Zubkov S.V., Vlasenko V.G., Shuvaeva V.A., Shevtsova S.I. // *Phys. Solid State*, **58**(1), 42, 2016.  
 [2] D. Mercurio, G. Trolliard, T. Hansen, J.P. Mercurio // *International Journal of Inorganic Materials*, **2**(5), 397-406, 2000.

## Crystal Structure and Ferroelectrics Properties of Mixed-layer $\text{Bi}_{7-2x}\text{Nd}_{2x}\text{Ti}_4\text{NbO}_{21}$ ( $x = 0.2, 0.4, 0.6, 0.8, 1$ ) Ceramics

S. V. Zubkov

*Research Institute of Physics, Southern Federal University, 194, Stachki Ave, Rostov-on Don, 344090, Russia*

\*[svzubkov61@mail.ru](mailto:svzubkov61@mail.ru)

Layered perovskite-like bismuth oxides with the Aurivillius phase (AP) structure have been known for several decades [1, 2], but interest to them has been growing due to their potential practical applications. APs are promising materials for fabricating high-temperature piezoelectric transducers operating in extreme conditions and are considered as elements of ferroelectric memory devices (FeRAM), as multifunctional materials exhibiting magnetic properties (multiferroics), photoluminescence etc. At the present time, the number of known APs is several hundreds, and this number continues to increase. A number of solid solutions  $\text{Bi}_{7-2x}\text{Nd}_{2x}\text{Ti}_4\text{NbO}_{21}$  ( $x = 0.2, 0.4, 0.6, 0.8, 1$ ) have been synthesized from oxides by solid-phase reaction. The crystal structure, the electrophysical characteristics and the microstructure of the prepared ceramic samples have been

studied. According to X-ray powder diffraction, all the compounds are single-phase with the structure of mixed-layer Aurivillius phases ( $m = 2.5$ ) with the orthorhombic crystal lattice (space group  $I2cm$ ,  $Z = 2$ ). Temperature dependences of the relative permittivity  $\varepsilon(T)$  of the compound have been measured, from which it has been found that the Curie temperature  $T_C$  of perovskite-like oxides  $\text{Bi}_{7-2x}\text{Nd}_x\text{Ti}_4\text{NbO}_{21}$  ( $x = 0.2, 0.4, 0.6, 0.8, 1$ ) decreases linearly as substitution parameter  $x$  decreases. The activation energies of charge carriers have been found in different temperature ranges.

#### **References**

- [1] Zubkov S.V., Vlasenko V.G., Shuvaeva V.A., Shevtsova S.I. // *Phys. Solid State*, **58**(1), 42, 2016.  
[2] D. Mercurio, G. Trolliard, T. Hansen, J.P. Mercurio // *International Journal of Inorganic Materials*, **2**(5), 397-406, 2000.

## **Development of Multi-Layered Sewer Pipe Plug -Ruptured Test and Stress Analysis of Protective Sheet**

**H. Tottori, N.A. Noda, G.Gao, R. Takaki, Y. Sano, A. Kai.**

*Kyushu Institute of Technology*

In recent years, the sewer system in Japan is becoming obsolete. It is, therefore, necessary to reinforce or repair without stopping sewer functions by applying a suitable water stopping method. In this study, a multi-layered sewer pipe plug consisting of the protective sheet and two rubber balls is focused since it can be installed and removed at the construction site in a short time conveniently. This sewer pipe plug has several advantages dealing with various diameters compared to the conventional type. In this study, the rupture test is conducted to improve the water stopping performance. The fractured position of the protective sheet of the sewer pipe plug was investigated experimentally. It was clarified that the maximum stress around the flange portion can be reduced by decreasing the flange inner diameter.

## **Development of Multi-Layered Sewer Pipe Plug-Tensile Strength of Protective Sheet**

**H. Tottori, N.A. Noda, G. Gao, R. Takaki, Y. Sano, A Kai.**

*Kyushu Institute of Technology*

Since Japanese sewer system is becoming obsolete, it is necessary to reinforce and repair the system without stopping sewer functions. In this study, a multi-layered sewer pipe plug consisting of the protective sheet and two rubber balls is focused to be installed and removed conveniently at the construction site. In this paper, a suitable testing method and the strength of the protective sheet are discussed experimentally by changing the specimen geometry providing slit and seams. It is found that the slit specimen is most desirable to obtain the standard tensile strength of UHMWPE cloth named Išanas cloth. It is found that the seamed strength is  $\sigma_B=34\text{MPa}$ , which is about 17% of the standard tensile strength  $\sigma_{B0}=200\text{MPa}$ .

## **Fatigue Strength Improvement of Roller Chain by Press Pitting between Pin and Plate**

**R. Saito, N. A. Noda, Y. Sano, A. Miyagi, T. Okamura.**

*Kyushu Institute of Technology*

To improve the fatigue strength of the roller chain, the fatigue test is conducted by varying the pressfitting ratio between the pin and the holed plate. To model what occurs in a chain under load, a single plate specimen is prepared by press-fitting two pins into two holes at the ends of the plate. The FEM analysis is performed to obtain the stress amplitude and the average stress. The results, in both cases demonstrate that the fatigue strength is improved by the press-fit between the pin and the hole. The fatigue improvement mechanism is discussed based on the stress analysis.

## **How to Estimate Fatigue Strength of Wood Material**

**K. Saito, N. A. Noda.**

*Kyushu Institute of Technology*

When wood materials are used for a mechanical structure, the fatigue strength should be estimated due to repeated loads they receive. This paper reveals that the methods to calculate allowable stresses along with American Society for Testing and Materials (ASTM) and Architectural Institute of Japan (AIJ) can take the strength reduction due to fatigue into account because the ASTM/AIJ allowable stresses against the static strength closely resemble the fatigue limit against the wood static strength.

## **Adhesive Strength Evaluation of Scarf Joint by using Intensity of Singular Stress Field (ISSF)**

**N. A. Noda, R. Takaki, B. Wang, S. Wang, Y. Sano, Y. Takase.**

*Kyushu Institute of Technology*

In previous study, the debonding strength of the butt joints was expressed as a constant value of the critical ISSF (Intensity of Singular Stress Field). In this study, the debonding strength evaluation will be investigated for scarf joint under tension by considering ISSF. This study deals with the scarf joint considering two ISSFs corresponding to two distinct singular stress fields. How to evaluate the scarf joint strength is described in comparison with the lap joint having similar two ISSFs. The debonding strength for scarf joints and lap joints can be expressed by the singular stress  $\sigma_{\theta c}(r)$  almost independent of bondline thickness  $h$ .

## **Fractographic Identification of Fracture Origin in Scarf Joint in Comparison to Butt Joint**

**R. Takaki, N. A. Noda, D. Ishida, Y. Sano, Y. Suzuki.**

*Kyushu Institute of Technology*

In previous study, the ISSF (Intensity of Singular Stress Field) was analyzed at the interface edge. However, the fracture origin controlled by the ISSF was not investigated in detail yet. In this study, the detail experimental observation is performed for the scarf joint specimen to identify the fracture origin. The fracture origin of scarf joint is compared to butt joint. The fractographic observation shows that the fracture originates from microcracks about 10-50 $\mu$ m depth at the interface edge in a similar way the butt joint.

## **Convenient and Accurate Formulas for Stress Intensity Factor Distribution of Semi-Elliptical Surface Crack**

**Y. Takase, N. A. Noda.**

*Kyushu Institute of Technology*

In this paper, the stress intensity factor (SIF) formula  $F_{ISE}$  along the crack front of a semi-elliptical surface crack is studied. The exact SIF solution  $F_{ISE}$  is used by solving the

hypersingular integral equation of the body force method discussed in the previous paper. To obtain the accurate formula, the SIF ratio  $F_{ISE}/F_{IE}$  is focused considering the exact solution  $F_{IE}$  of an elliptical crack. By applying the least squares method to the ratio  $F_{ISE}/F_{IE}$ , accurate and convenient formula is proposed. The proposed formulas may provide the accurate SIF distributions for the aspect ratio  $a/b=1\sim 4$  better than 0.2% accuracy.

## **Effect of Shaft's Rigidity and Motor Torque on Interfacial Slip for Shrink-fitted Bimetallic Work Roll**

**R. A. Rafar, N. A. Noda, H. Tsurumaru, Y. Sano, Y. Takase.**

*Kyushu Institute of Technology*

The bimetallic work rolls are widely used in the roughing stands of hot rolling stand mills. The rolling rolls are classified into two types; one is a single-solid type, and the other is a shrink-fitted construction type consisting of a sleeve and a shaft. Regarding the shrink-fitted type, the interfacial slip occurs and causes damage between the shaft and the shrink-fitted sleeve. In this paper, by varying the shaft material, the FEM simulation is performed to realize the interfacial slip. The effect of the shaft deformation on the interfacial slip is clarified as well as the effects of the shrink-fitting ratio, and motor torque in relation to the slippage zone along the interface.

## **Stress Intensity Factors of Interfacial Crack associated with Different Interface Edge Singularities**

**K. Oda, T. Irie, T. Masuno, N. Tutsumi.**

*Oita University*

The singular stress field near the interface end is determined by the shape of the edge and the combination of materials. In the lap joint and scarf joint, the singular stress field at the interface end can be expressed by superposing the stress fields having the two different singularities,  $\lambda_1$  and  $\lambda_2$ . The stress intensity factor of edge interface crack is controlled by the intensity of the singular stress field near the interface end when the crack length is short. In this study, we investigated a method to separate the stress intensity factor of an edge interface crack into two components related to the singularity indices in a single lap joint. The separated stress intensity factors for interface crack can be obtained by using the stress intensity factor solutions of two different crack lengths.

## **Effect of Hydrogen on Fracture Mechanism in Tensile Test of Carbon Steels**

**N. Tutsumi, K. Oda, K. Miyaji.**

*Oita University*

In order to investigate the effect of hydrogen on fracture mechanism in tensile tests of carbon steels, tensile tests were conducted using hydrogen-charged and uncharged specimens of JIS-SS400 (0.09 mass % C), JIS-S25C (0.27 mass % C) and JIS-S45C (0.46 mass % C). Each specimen was introduced prestrain (0%, 5% and 10%) since the hydrogen content in hydrogen-charged specimens increased as prestrain increased. The tensile strength and yield stress of hydrogen-charged specimens was approximately the same as those of uncharged. However, the reduction of area of hydrogen-charged specimens was smaller than that of uncharged and decreased as hydrogen content increased. On the fracture surface of all the uncharged specimens, many dimples were observed. On the other hand, flat fracture surface was observed on hydrogen-charged specimens of JIS-SS400 and JIS-S25C. However, no flat fracture surface was observed on hydrogen-charged specimens of JIS-S45C. To reveal the reason of the difference, longitudinal cross section near the fracture surface were observed. Many voids were initiated in pearlite structure of hydrogen-charged specimens compared with that of uncharged. And the larger voids were observed in hydrogen-charged specimens of JIS-SS400 since it has more ferrite structure compared with JIS-S25C and JIS-S45C.

## **Proportional Method for Evaluating Intensity of Singular Stress Field for Butt Joint with Adhesive Spew**

**T. Miyazaki, D. Takasuka, K. Naka.**

*University of the Ryukyus*

In this study, a proportional method for evaluating an intensity of singular stress field (ISSF) at an interface corner in a butt joint (BJ) with an adhesive spew is proposed. Square-shaped inclusion models under bi-axial tensile stress and under shear stress are used as reference models. The ISSFs for the BJ are calculated by superposing those for the reference models. The reference and BJ models are analyzed by FEM under the same mesh division and the same material combination, and the stresses applied to the reference models are determined by the FEM stresses at the interface corner. The validity of the present method is examined by applying to the BJ composed of the steel and the epoxy resin. The asymptotic solution obtained by the method is in agreement with the FEM stress distributions. Then, the ISSFs for the BJ are calculated by changing adhesive spew similarly. It is shown that the ISSF normalized by the adhesive thickness is constant independent of the thickness.



## Mechanism of Growth ZnO Nanowires and Applications

C. F. Yang

*National University of Kaohsiung*

The topic of this speech is to investigate “Mechanism of Growth ZnO Nanowires and Applications”, and it has three topics. First, we discussed the mechanism of growth ZnO nanowires under different parameters, including deposition seed layer with different times, different deposition temperatures, and different C<sub>6</sub>H<sub>12</sub>N<sub>4</sub> and Zn(NO<sub>3</sub>)<sub>2</sub>·6H<sub>2</sub>O concentrations. Next, we investigated a new method to grow the In- and Eu-doped ZnO nanowires and discussed the effects of In and Eu concentrations on the growth properties of ZnO nanowires. We would show that as the In and Eu concentrations increased, the needed growth temperatures of ZnO nanowires were reduced. Finally, we used ZnO nanowires and P3HT to fabricate the hetero-junction-based ammonia (NH<sub>3</sub>) gas sensors. The gas sensing properties of pure ZnO nanorods and nanorods-P3HT hetero-junction gas sensors were investigated in detail. The nanowires-P3HT hetero-junction gas sensors showed dramatically enhanced response to ammonia gas, and this device held a great potential for practical applications.

## Photo-Enhanced Field Emission Behavior of CDSSE Microflowers

**A. B. Deore<sup>\*</sup>, M. A. More<sup>\*§</sup>, B. B. MUSMADE<sup>†</sup>, S. D. Nerkar<sup>\*\*</sup>, P. G. CHAVAN<sup>\*\*\*</sup>,  
P. M. KOINKAR<sup>\*\*\*\*§</sup>**

*<sup>\*</sup>Department of Physics, Savitribai Phule Pune University, Pune 411007, India.*

*deoreamol91@gmail.com, §mam@physics.unipune.ac.in*

*<sup>†</sup>D. Y. Patil College of Engineering Akurdi, Pune, Savitribai Phule Pune University, Pune 411044, India.*

*bbmusmade@dypcoeakurdi.ac.in.*

*<sup>\*\*</sup>SVKM's Institute of Technology, Dhule 424001, India.*

*snerkar@gmail.com*

*<sup>\*\*\*</sup>School of Physical Science Kavayitri Bahinabai Chaudhari North Maharashtra University,*

*Jalgaon, 425001, India*

*pgchavan@nmu.ac.in*

*<sup>\*\*\*\*</sup>Department of Optical Science, Tokushima University, 2-1 Minamijosanjima Cho, Tokushima, 7708506, Japan.*

*[koinkar@tokushima-u.ac.jp](mailto:koinkar@tokushima-u.ac.jp)*

In this work, synthesis of well grown cadmium sulphoselenide (CdSSe) microflowers on gold coated silicon substrate using simple and low cost chemical bath deposition technique. The deposited CdSSe film was annealed in a furnace for 30 minutes at 250 oC. Subsequently, annealed CdSSe film further characterized structural, morphological and field emission analysis have been studied. The CdSSe microflowers show photo-sensitive field emission behavior. In photo-sensitive

field emission the emission current rises nearly two to three times of its primary preset value at  $\sim 1 \mu\text{A}$ .

## **Robust Sliding Mode Control of Uncertain Nonlinear Systems**

**B. B. MUSMADE<sup>1†</sup>, Y. P. PATIL<sup>2</sup>, B. M. PATRE<sup>3</sup>**

<sup>1</sup>*D. Y. Patil College of Engineering Akurdi, Pune, Savitribai Phule Pune University, Pune 411044, India.*

*bbmusmade@dypcoekurdi.ac.in.*

<sup>2</sup>*MVP Samaj's K B T College of Engineering, Nashik., Savitribai Phule Pune University Pune, patil.yogesh@kbtcoe.org*

<sup>3</sup>*S. G. G. S. Institute of Engineering and Technology, Nanded, India.. bmpatre.sggs.ac.in*

In this paper, a class of uncertain nonlinear systems is investigated and a sliding mode control design is presented. The method is proposed for uncertain systems with model uncertainties, nonlinear dynamics and external disturbances. Using nominal system and related bounds of uncertainties, a chattering alleviating scheme is also proposed, which can ensure the robust sliding mode control law. The control performance is validated by simulation. The study shows that the proposed controller is effective compared to existing controllers.

## **Investigation of Electrical Properties of PEALD Deposited Ti/Al<sub>2</sub>O<sub>3</sub>/Al/Si MIM Capacitors**

**S. PATIL<sup>1</sup>, V. BARHATE<sup>1</sup>, A. MAHAJAN<sup>1</sup>, H. XU<sup>2</sup>, M. RASADUJJAMAN<sup>2</sup>, J. ZHANG<sup>2</sup>**

<sup>1</sup>*Department of Electronics, School of Physical Sciences, Kavayitri Bahinabai Chaudhari North Maharashtra University, Jalgaon, Maharashtra – 425001, India*

*s.r.patil1992@gmail.com, viral.barhate@gmail.com, ammahajan@nmu.ac.in*

<sup>2</sup>*School of Information Science and Technology, North China University of Technology, Beijing 100144, China*

*haoyu\_xu@outlook.com, rasadphy@duet.ac.bd, zhangj@ncut.edu.cn*

MIM devices fabricated with 10 nm thickness of Al<sub>2</sub>O<sub>3</sub> high-k thin film deposited using plasma-enhanced atomic layer deposition (PEALD) system on Al coated Si Substrate were investigated. The structural, morphological, and electrical properties of Ti/Al<sub>2</sub>O<sub>3</sub>/Al/Si MIM capacitors as-deposited and Post Deposition Annealed (PDA) at different temperatures were studied and compared. Al<sub>2</sub>O<sub>3</sub> thin films were investigated using atomic force microscopy (AFM) and x-ray diffraction (XRD) and Ti/Al<sub>2</sub>O<sub>3</sub>/Al MIM capacitors were characterized by Current-voltage (I-V) and capacitance-voltage (C-V) measurements. The stable phase formation of Ti/Al<sub>2</sub>O<sub>3</sub>/Al MIM

capacitor provides the lowest leakage current density in the range of nA/cm<sup>2</sup> for as-deposited and annealed films was observed.

## **Sol-Gel Deposited Xerogel, Aerogel and Poren Based Porous Low-K Thin Films: A Comparative Investigation**

**S. GUPTA<sup>1</sup>, A. GAIKWAD<sup>1</sup>, A. MAHAJAN<sup>1\*</sup>, L. ONGXIAO<sup>2</sup>, Z. WEI<sup>2</sup>**

<sup>1</sup>*Materials and Devices Laboratory for Nanoelectronics, Department of Electronics, Kavayitri Bahinabai Chaudhari North Maharashtra University, Jalgaon (Maharashtra) 425 001, India, \*ammahajan@nmu.ac.in*

<sup>2</sup>*Department of Applied Physics, China Agricultural University, Beijing, China*

Low dielectric constant (k) films are used as inter layer dielectric in nanoelectronic devices to reduce interconnect delay, crosstalk noise and power consumption. Tailoring capability of porous low-k films attracted more attention. Present work investigates comparative study of xerogel, aerogel and porogen based porous low-k films. Deposition of SiO<sub>2</sub> and incorporation of less polar bonds in film matrix is confirmed using Fourier Transform Infra-Red Spectroscopy. Refractive indices (RI) of xerogel, aerogel and porogen based low-k films observed to be as low as 1.25, 1.19 & 1.14, respectively. Higher porosity percentage of 69.46% is observed for porogen based films while for shranked xerogel films, it is lowered to 45.47%. Porous structure of low-k films has been validated by using FESEM micrograph. The pore diameters of porogen based annealed samples were in the range of 3.53 to 25.50 nm. The dielectric constant obtained from RI for xerogel, aerogel and porogen based films are 2.58, 2.20 and 1.88, respectively.

## **Photochromic Effects in P- and B-Doped Diamond**

**K. N. Boldyrev**

*Institute of spectroscopy, Russian Academy of Sciences, Troitsk, Moscow, 108840, Russia.*

Diamond is an ultrawide-bandgap material (5.47 eV) with many unique properties for the different purposes from power electronics to quantum computing. High electron and hole mobility, and high thermal conductivity, has compelling potential advantages over the most known analogs, such as the narrow-bandgap silicon (Si), in radiation-resistant, high-power, and high-frequency electronics, as well as in deep-UV optoelectronics, quantum information, and extreme-environment applications [1]. As well a diamond is an excellent photoconductor, and this property can be used for UV detectors with ultra-high sensitivity [2]. It is known that p-type semiconducting diamond is synthesized by doping boron impurity. However, it used to be almost impossible to make n-type

diamond. Phosphorus is only an impurity for n-type semiconducting diamond established at this moment. P-donors in a diamond can be used for quantum computing, spin-to-photon conversion, photonic memory, integrated single-photon sources, and all-optical switches because of the read-in/read-out is in the optical region showing extremely high decoherence time up to hours [3]. Earlier studies of the photoconductivity of the phosphorus-doped diamond, which made it possible to register several electronic transitions near 600 meV [4]. These studies gave hope for the presence of photochromic effects in P-doped diamonds, by analogy with such effects in silicon [5]. In addition, based on such effects, it is possible to create a technique for the optical monitoring of the quality and concentration of doping [5,6].

In this work, we report the detail studies of the photochromic effects of the large-sized HPHT-grown high-quality P- and B-doped single-crystal diamonds by the high-resolution photochromic spectroscopy. We found a significant photochromic effect on the electronic transitions of phosphorus. A strong intensity measurement in the absorption spectra is observed under the influence of external optical radiation. In addition, there was a redistribution of intensities in the absorption region of boron and phosphorus, by analogy with the dopant of boron and phosphorus in silicon [5,6]. Based on this effect, a method is proposed for determining the real concentration of boron and phosphorus in a diamond.

A financial support by the Russian Science Foundation under Grant № 19-72-10132 is acknowledged.

- [1] J. Y. Tsao, S. Chowdhury, M. A. Hollis et al., *Adv. Electron. Mater.* 4, 1600501 (2018).
- [2] F. Hochedez, W. Schmutz, Y. Stockman et al., *Adv. Space Res.* 37(2), 303 312 (2006).
- [3] K. Saeedi, S. Simmons, J. Z. Salvail et al., *Science* 342, 830 (2013).
- [4] K. Haenen, K. Meykens, M. Nesladek et al., *Phys. Stat. Sol. a* 181, 11 (2000).
- [5] Test method for low temperature FT-IR analysis of single crystal silicon for III-V impurities SEMI MF 1630-0704 (2004).
- [6] K.N. Boldyrev, N.Yu. Boldyrev, R.V. Kirillin, *Bull. Russ. Acad. Sci. Phys.*, 77(12), 1420 (2013).

## **Infrared Spectra of the $\text{CH}_3\text{NH}_3\text{PbI}_3$ and $\text{CH}_3\text{NH}_3\text{PbBr}_3$ Hybrid Perovskites: Signatures of Phase Transitions and of Organic Cation Dynamics**

**K. N. Boldyrev<sup>1,2</sup>, V.E. Anikeeva<sup>1,2</sup>, O.I. Semenova<sup>3</sup>, M.N. Popova<sup>1</sup>**

<sup>1</sup>*Institute of spectroscopy, Russian Academy of Sciences, Troitsk, Moscow, 108840, Russia.*

<sup>2</sup>*Moscow Institute of Physics and Technology (National Research University), Dolgoprudny, Moscow Region, 141701, Russia*

<sup>3</sup>*A.V. Rzhanov Institute of Semiconductor Physics, Siberian Branch of the Russian Academy of Sciences, Novosibirsk, 630090, Russia*

The organic–inorganic hybrid halide perovskites attract a relentless interest of researchers due to their enormous potential as functional materials, primarily for solar cells, as well as for light emitting diodes, lasers, photodetectors, and thermoelectric devices [1-5]. It should be mentioned that the power conversion efficiency of the solar cells based on hybrid perovskites already exceeds 20%, with the advantage of cost-effective low-temperature synthesis methods [2]. Exceptional functionality of hybrid halide perovskites is due to useful physical properties such as tunable optical bandgap and absorption coefficient [3], long carrier lifetimes, high carrier mobility, and large diffusion lengths [4], low thermal conductivity [5].

Methylammonium lead iodide perovskite  $\text{CH}_3\text{NH}_3\text{PbI}_3$  (MAPbI<sub>3</sub>) is the most studied material among hybrid halide perovskites. Here, we report on the first high-resolution (up to 0.2 cm<sup>-1</sup>) terahertz (far IR) reflection and mid- and near-IR transmission studies of MAPbI<sub>3</sub> large single crystals in a wide range of temperatures (5 – 350 K), carried out with the aim of getting information on low-frequency phonons and multiphonon lattice excitations that could not be obtained by previously used experimental techniques or/and samples [6]. We observed several low-frequency excitations not reported before and made their assignments. Using the literature data on the lattice expansion with temperature and our data on temperature-dependent phonon frequencies we calculated the mode Grüneisen parameters for the strongest low-frequency modes. In addition, we investigated another crystal from this group of organic-inorganic materials - methylammonium lead bromide perovskite  $\text{CH}_3\text{NH}_3\text{PbBr}_3$  (MAPbBr<sub>3</sub>). We have observed all phase transitions by studying low-frequency phonons and multiphonon lattice excitations. By analyzing the temperature behavior of the multi-phonon spectrum, we revealed changes in the dynamics of the  $\text{CH}_3\text{NH}_3^+$  molecular cation, which is important for interpreting physical properties of MAPbI<sub>3</sub> and MAPbBr<sub>3</sub>.

A financial support by the Russian Science Foundation under Grant № 19-72-10132 is acknowledged.

[1] M.A. Green, A. Ho-Baillie; H.J. Snaith, *Nat. Photon* 8, 506 (2014).

[2] S.I. Seok, M. Grätzel, N.-G. Park, *Small* 14, 1704177 (2018).

[3] M.A. Green, Y. Jiang, A.M. Soufiani, A. Ho-Baillie, *J. Phys. Chem. Lett.* 6, 4774 (2015).

[4] T.M. Brenner, D.A. Egger, L. Kronik, G. Hodes, D. Cahen, *Nat. Rev. Mater.* 1, 15007 (2016).

[5] M.A. Haque, S. Kee, D.R. Villalva, W.-L. Ong, D. Baran, *Adv. Sci.* 10, 1903389 (2020).

[6] K.N. Boldyrev, V.E. Anikeeva, O.I. Semenova, M.N. Popova, *J. Phys. Chem. C* 124(42), 23307 (2020).

## **Fabrication and evaluation of Ca-doped SrTiO<sub>3</sub> thermoelectric materials by molten salt method**

**K. I. MURAI, T. NISHIURA, R. NAGATA, T. MORIGA**

*Graduate School of Technology, Industrial Social Science, Tokushima University, 2-1 Minami-josanjima*

*Tokushima, 770-8506, Japan*  
[keimurai@tokushima-u.ac.jp](mailto:keimurai@tokushima-u.ac.jp)

In this study, we focused on the molten salt method and attempted a simple synthesis of  $\text{SrTi}_{0.8}\text{Co}_{0.2}\text{O}_3$ . It was clarified that  $\text{SrTi}_{0.8}\text{Co}_{0.2}\text{O}_3$  can be obtained under relatively mild conditions by using the molten salt. In all samples, the electrical conductivity increased with increasing temperature. Compared with the sample without the molten salt, the electric conductivity of the samples with the molten salt were greatly improved. The sample using the KCl-NaCl mixed salt showed the highest electrical conductivity of 83 S / cm at 973 K. The relative densities of all the samples using the molten salt were above 85%. It is considered that the improvement in the electrical conductivity is partly due to the increase in the relative density.

Keywords: Molten salt method; Ca-doped  $\text{SrTiO}_3$ ; thermoelectric material.

## LOCAL ELECTRONIC AND ATOMIC STRUCTURES OF THE MIXED B-SITE IONS IN $\text{SrFe}_{1-x}\text{Mn}_x\text{O}_{3-\delta}$ STUDIED WITH X-RAY ABSORPTION SPECTROSCOPY

*M. OISHI<sup>1,\*</sup>, T. SAKURAGI<sup>1</sup>, F. FUJISHIRO<sup>2</sup>, T. INA<sup>3</sup>, H. YAMAGISHI<sup>4</sup>, I. WATANABE<sup>4</sup>, T. OHTA<sup>4</sup>*

*<sup>1</sup>Graduate School of Technology, Industrial and Social Science, Tokushima University,  
2-1 Minamijosanjima cho, Tokushima 770-8506, Japan*

*\*oishi.masatsugu@tokushima-u.ac.jp*

*<sup>2</sup>Faculty of Science and Technology, Kochi University, 2-5-1 Akebono-cho, Kochi-shi, Kochi,  
780-8520, Japan*

*<sup>3</sup>Japan Synchrotron Radiation Research Institute, 1-1-1 Kouto, Sayo-cho, Sayo-gun, Hyogo 679-  
5198, Japan*

*<sup>4</sup>SR center, Ritsumeikan University, 1-1-1 Higashinoji Kusatsu Shiga 525-8577, Japan*

Local electronic and atomic structures of the B-site ions in perovskite  $\text{SrFe}_{1-x}\text{Mn}_x\text{O}_{3-\delta}$  were evaluated with X-ray absorption spectroscopy (XAS) at Mn, Fe K and L-edges and O K-edge. The energy of LIII and LII-edge peaks for Mn and Fe ions stayed unchanged against the change in Mn content x. The analysis of Mn K-edge extended X-ray absorption fine structure (EXAFS) revealed that Mn-O polyhedra kept as an octahedron with  $\text{Mn}^{4+}$  irrespective of the x value, agreeing with the results of L-edge spectra. The Fe K-edge EXAFS analysis showed that the Fe-O distance decreased with decrease of the Mn contents, suggesting that the ratio of  $\text{FeO}_5$  polyhedra to  $\text{FeO}_6$  octahedra is increased due to smaller oxygen amount. By analyzing both the K-edge and L-edge spectra, we clarified the local electronic and atomic structural changes, particularly occurred in the B-site mixed perovskite oxides.

Keywords: Oxygen storage materials, B-site mixed perovskite-type oxide, K- and L-edge XAS

## LIQUID EXFOLIATION OF GRAPHENE OXIDE NANORIBBONS USING CHEMICAL ASSISTED LASER ABLATION

S. DHONGADE<sup>†</sup>, P. KOINKAR<sup>†,\*</sup>, A. FURUBE<sup>†,\*</sup>, S. SUGANO<sup>‡</sup>

<sup>†</sup>*Department of Optical Science, Tokushima University, 2-1 Minamijosanjima Cho,  
Tokushima 7708506, Japan  
c501938021@tokushima-u.ac.jp, \*koinkar@tokushima-u.ac.jp, \*furube.akihiro@tokushima-  
u.ac.jp*

<sup>‡</sup>*Tokushima University, 2-1 Minamijosanjima Cho,  
Tokushima 7708506, Japan  
[sugano@tokushima-u.ac.jp](mailto:sugano@tokushima-u.ac.jp)*

The interest toward two dimensional (2D) materials is gradually increasing because of their structure at nanoscale and great importance for electronic and optical applications. In this study, we show the synthesis of graphene oxide micro-ribbons fabricated by chemical assisted-laser ablation method. In order to confirm the formation of graphene oxide (GO), UV-visible spectroscopy (UV-vis) and Raman spectroscopy are used to observe surface morphological feature and structural details. In addition, a possible mechanisms for the growth of GO nanoribbon is discussed. This work indicates a new method to develop GO nanostructures and related nanomaterials.

Keywords: Laser ablation in liquid, Graphene oxide, UV-visible spectrum, Raman spectrum

## AUTHOR INDEX

- Abdulahidov K.G., 57, 163, 197  
Adeel Ahmad Jamil, 31  
Afonin S. M., 32  
Ageev O.A., 106, 228, 284  
Aizikovich S.M., 197, 232  
Akihiro Furube, 205, 302  
Aleksandrova A., 169  
Aleksenko A.A., 182, 206, 210  
Alexander N. Epikhin, 41, 44  
Alexander Gerasimenko, 165  
Alexander Markov, 165  
Alexandra Starnikova, 33  
Alexey M. Kolesnikov, 34  
Andjikovich I. E., 53  
Andreeva T.M., 35  
Andrey S. Vasiliev, 36, 237  
Andris Chate, 111  
Andros N.V., 36  
Andryushin K.P., 37 – 39, 183  
Andryushina I.N., 37 – 39  
Anikeev M.V., 149  
Aridi M. R., 40  
Arkadiy N. Soloviev, 41, 43, 44, 45,  
Artseva E.A., 220  
Avakyan A.A., 276  
Avilov V.I., 46, 276  
Bae M. K., 131  
Balakirev S. V., 75, 95, 106  
Bambang Andrianto, 301  
Banh Tien-Long, 169  
Bardakova R.A., 47  
Bayan E.M., 48, 213  
Bayu Abisatya M., 226  
Bei-fen Siew, 53  
Belenov S.V., 193  
Belov A.A., 212  
Belyak O.A., 49, 50, 264  
Belyankova T. I., 51, 52  
Moguchih E.A., 182  
Morozova J.V., 229  
Morshneva I.V., 36  
Moysa M.O., 183  
Muhyin, 184  
Mukesh Kumar Roy, 124  
Mun Ki Bae, 132, 304  
Muratov A.V., 297  
Nadegda Glushko, 44  
Nagaenko A. V., 141, 183  
Nakagaito A. N., 185  
Nao-Aki Noda, 53, 221, 306  
Nasedkin A.V., 152, 186, 257  
Nassar M.E., 186  
Natalia V. Petrovskaya, 187  
Naumenko D.V., 112, 172  
Nazarenko A.V., 188, 309  
Nedin R.D., 190  
Nemchenko I.V., 191  
Nesterov S.A., 192, 288  
Nevelskaya A.K., 193  
Nguyen Duc-Toan, 169  
Nguyen Phu Thuong Luu, 194  
Nguyen Van Dung, 195  
Nikiforova N.A., 39  
Nikolaev A. L., 170, 197, 232  
Nicholas Kiprotich Cheruiyot, 87  
Nick Yanie, 125  
Nikitenko D.V., 155  
Nikulin A.Y., 206  
Nikulina A.A., 120  
Nizhnik D.A., 236, 256  
Noda N.A., 40, 139, 197, 265, 280  
Novikov E.S., 159  
Novikova A.I., 287  
Oganesyan P.A., 255  
Olekhovich N.M., 220  
Onyshko D.A., 114 – 117, 191, 199, 200, 202,



- Berestneva Yu.V., 223, 297  
 Bespoludin V.V., 213  
 Biao Wang, 53  
 Biryukova I.V., 250  
 Bobreva L.A., 273  
 Bocharova O. V., 53  
 Boev E.V., 174, 175  
 Bogachev I.V., 54 – 56  
 Bogatin A. S., 57  
 Boldyrev N.A., 58, 141, 142, 251  
 Bondar A., 114  
 Boris V. Bondarev, 60, 61  
 Boris I. Mitrin, 237  
 Bowen C.R., 278  
 Boyev N.V., 62  
 Brazhnikov V.A., 63  
 Budi Witjaksana, 64  
 Bunin I. Zh., 65  
 Bunin M.A., 247  
 Buravchuk N. I., 66, 69  
 Bush A.A., 267  
 Chang S.-H., 76 – 78, 101  
 Chang-Wook Park, 73, 262  
 Chao-Hong Liu, 303, 305  
 Chebakov M.I., 73, 74  
 Chebanenko V.A., 45, 76, 253 – 255,  
 257, 312  
 Chen D., 197  
 Cherenok S.R., 217  
 Chernenko N.E., 75, 95, 106  
 Cherpakov A.V., 76 – 78, 92, 100 – 104,  
 244, 245, 260, 314  
 Chia-Chi Yen, 79  
 Chien-Liang Chiu  
 Chih-Chin Chuang, 85  
 Chih Chin Yang, 80, 81, 83  
 Chih-Feng Yen, 179  
 Chin-Feng Lin, 85  
 Chin Ko Yeh, 86, 126  
 Chitsan Lin, 31, 86, 87, 96, 126  
 Choi J. G., 131  
 Chou C.-C., 220  
 Chyi-Da Yang, 179  
 Da-Ying Chou, 79  
 Daniil O. Nepryakhin, 88  
 204, 211, 217 – 219, 234, 272,  
 281, 298  
 Oskolkova O.N., 223  
 Osotova O. I., 123  
 Padun O.M., 223  
 Palatnikov M.N., 98, 239, 249, 250, 273  
 Palchikov A.A., 182  
 Panfilov I.A., 196, 256, 257  
 Pankaj Koinkar, 205, 302  
 Paperj K.O., 182, 206  
 Parinov I.A., 76 – 78, 89, 100 – 104, 180, 260,  
 269, 312  
 Parinova L.I., 289  
 Parshina N.V., 173  
 Pavel Akishin, 111  
 Pavel A. Oganessian, 43, 45  
 Pavel Vasilevsky, 165  
 Pavelko A.A., 207, 312  
 Pavlenko A.V., 136, 188, 207 – 209, 261, 275, 313  
 Pavlets A.C., 210  
 Pei-Ju Chao, 303, 305  
 Petrenko D.V., 211  
 Petrov A.N., 175, 212  
 Petrov V.V., 48, 213  
 Petrukhina T.A., 214  
 Pianov A.E., 215  
 Pilipenko E.A., 122  
 Piskunov A. S., 216  
 Po Cheng Ke, 265  
 Poddubny A.A., 74  
 Podkolzina L.A., 291  
 Polupanov N.V., 46  
 Poluyan A.Yu., 219  
 Polyakov V.V., 213  
 Polyakova N.M., 214  
 Ponomarev A.A., 200  
 Popov V.D., 222  
 Poryadina N.A., 236  
 Priyoto, 233  
 Purchina O. A., 63, 114 – 117, 140, 151, 153, 191,  
 199, 200, 202, 204, 211, 215, 217  
 – 219, 234, 272, 281, 298  
 Pushkarev A.V., 220  
 Putri E. P., 66, 69  
 Radyush Y.V., 220

Danilchenko D.A., 73  
 Davydova A.A., 223, 297  
 Denis Ermakov, 105  
 Denis V. Krasnov, 41  
 Denisova A. O., 277  
 Deog-Hee Doh, 178  
 Derkun A.V., 253  
 Dian-Min Lin, 79  
 Dikrie Alief Zaini, 311  
 Dmitry K. Nadolin, 43  
 Dmitry Telyshev, 165, 166  
 Dneprovski V.G., 89  
 Do Thanh Binh, 253 – 255, 257  
 Dodonov M.V., 171  
 Dong-Ho Yang, 90  
 Drobotov Yu.E., 35, 91 – 93, 216, 282,  
 283, 314 - 316  
 Dudkina S.I., 94, 141, 142, 154, 243  
 Dukhan D.D., 95  
 Duy-Hieu Nguyen, 96  
 Dwi Yuli Rakhmawati, 125, 184, 301  
 Edi Santoso, 97  
 Efremov V.V., 98, 238  
 Egorochkina I.O., 99 – 104, 245  
 Elisa Sulistyorini, 263  
 Elizaveta Smirnova, 165  
 Endija Namsone, 105  
 Eremenko M.M., 75, 95, 106  
 Eresko A.B., 297  
 Erni Puspanantasari Putri, 107 – 110, 292  
 Ershin V. A., 158  
 Eugenia Davydova, 165  
 Evgenia Kirillova, 45  
 Evgeniy V. Sadyrin, 237  
 Evgeny Barkanov, 111  
 Ezhova O.A., 112, 172  
 Fahreza Rukmana Witjaksono, 184  
 Faiz Muhammad Azhari, 233  
 Fajar Romadhon, 230  
 Fedorov A.V., 217  
 Fedotov A.A., 231  
 Feng-Chun Lee, 268  
 Filimonov A.V., 150  
 Fomenko S.I., 113, 121  
 Fugarov D. D., 63, 114 – 117, 140, 151,  
 Raevskaya S.I., 157, 158, 220, 246  
 Raevski I.P., 157, 158, 220, 246  
 Rahimah Abdul Rafar, 221, 306  
 Rakhmatulin A. Sh., 222  
 Raksha E.V., 223, 297  
 Rasteryaev N.V., 63, 140, 151, 153, 215  
 Reshetnikova E. A., 224  
 Reshetnyak O.S., 225  
 Reshetnyak V.N., 225  
 Retno Hastijanti R.A., 226  
 Revina S.V., 227  
 Reznichenko L.A., 37 – 39, 94, 141, 142, 154,  
 183, 207, 240, 241, 243, 275,  
 312  
 Reznitchenko L.A., 317  
 Rezvan A.A., 148, 228, 229  
 Ri-ichi Murakami, 2306 304  
 Risma Marleno, 126, 230  
 Romadhon, 64  
 Rozhkov E. V., 76  
 Rudyk N.N., 231  
 Ryabov A.S., 227  
 Sadyrin E. V., 232, 257  
 Sajjiyo, 233  
 Sano Y., 40, 139, 197, 265, 280  
 Sarychev D. A., 158  
 Saveliev D.A., 202  
 Savoskin M.V., 223, 297  
 Savriddinov F.D., 234  
 Sedov A. V., 53  
 Semenchatenko I.V., 235  
 Senichev A.V., 287  
 Seong-Jae Park, 164, 236  
 Serebryanaya I.A., 99, 236, 245  
 Sergei M. Aizikovich, 36, 237  
 Sergei Selishchev, 165, 166  
 Sergei S. Volkov, 36  
 Shakhanov R.I., 244  
 Sharapov N.A., 46  
 Shcherban' E.M., 260  
 Shcherbina O.B., 98, 238, 239  
 Sheng Min Huang, 179  
 Shevtsova S.I., 220  
 Shih-Ming Wang, 268  
 Shihova E.P., 157

153, 191, 199, 200, 202,  
 204, 211, 215, 217 – 219,  
 234, 272, 281, 298  
 Gao G., 280  
 Gavrishchakin G.D., 134, 135  
 Gayduchik A.V., 199  
 Gede Sarya, 230  
 Geguzina G.A., 118  
 Geldash A.A., 284  
 Glazer A.M., 246  
 Glazunova E.V., 120, 122, 141, 223, 297  
 Glushkov E.V., 121  
 Glushkova N.V., 121  
 Gnatovskaya V.V., 223  
 Golda A.V., 293  
 Golub M.V., 113  
 Gorbenko Ie. Ie., 122  
 Grigoryev M.V., 212  
 Guan-Fan Chen, 79  
 Guryanov A.V., 123, 231  
 Guryanova O. V., 66, 69  
 Guterman V.E., 210  
 Gyanendra Pratap Singh, 124  
 Han M. S., 143  
 Hanie Teki Tjendani, 125, 126  
 Hari Susanto, 230  
 Haris Muhammadun, 233  
 Harjo Seputro, 176  
 Herry Widhiarto, 301  
 Hiroyuki Tsurumaru, 221, 306  
 Hsueh Chen Shen, 86, 126  
 Hudhiyantoro, Budi Santoso, 164  
 Hung Yeh Lin, 80  
 Hung-Yu Wang, 265, 303, 305  
 I-Hsing Tsai, 303, 30  
 I Made Kastawan, 127  
 I Nyoman Sutantra, 127  
 Ichlas Wahid, 97, 128  
 Igumnov L.A., 174  
 Il'in O.I., 123, 231  
 Il'ina M.V., 123, 231  
 Inui Y., 139  
 Ipatov A.A., 128  
 Irina Gulyaeva, 33  
 Isaeva A. N., 129, 278  
 Shilkina L.A., 94, 141, 142, 240, 241, 243, 275  
 Shilova N. V., 162  
 Shilyaeva O.V., 77, 78, 244,  
 Shin D.S., 258  
 Shiryaeva E. V., 286  
 Shlyahova S.A., 157  
 Shlyakhova E.A., 99 – 104, 245  
 Shpak A.N., 113  
 Shpanko S.P., 57, 247  
 Shu-Yuan Lin, 79  
 Shun-Hsyung Chang, 81, 83, 85, 179  
 Shuvaeva V.A., 246  
 Shyh-An Yeh, 305  
 Sidashov A.V., 159  
 Siddhant Dhongade, 205, 304  
 Sidorenko E.N., 57, 247, 248  
 Sidorov N.V., 249, 250, 273  
 Siew B., 139  
 Silcheva A.G., 136  
 Silin M. Yu., 158  
 Sliva A.A., 293  
 Simachkova G.A., 246  
 Sitalo E.I., 58, 251, 252, 312  
 Sizov V.P., 181  
 Smirnov M.V., 249  
 Smirnov V.A., 46, 276  
 Smotrakov V.G., 247, 252  
 Solodovnik M. S., 75, 95, 106  
 Soloviev A.N., 76 – 78, 196, 253 – 257, 294  
 Song M. K., 143, 258  
 Soo-Jeong Park, 90, 132, 133, 164, 236, 259, 274  
 Sri Astutik, 64  
 Starchenko I.B., 144, 156, 294  
 Stel'makh S.A., 260  
 Storozhenko V.Yu., 48  
 Stryukov D.V., 261  
 Suei Chang Wu, 126  
 Suh J., 258  
 Sukhov P.V., 223  
 Sukon Aduldaecha, 107, 108  
 Sung-Won Yoon, 73, 262  
 Sung-Youl Bae, 90, 263  
 Supardi, 263  
 Sutikno, 127  
 Suvorova T.V., 50, 264

Ismail, 311  
 Ivan A. Parinov, 81, 83, 85  
 Ivanov A. E., 44  
 Jang T. H., 131  
 Jenny Chih-Yu Lee, 179  
 Jenny Lee C.-Y., 104, 244  
 Jeong-Hyo Hong, 132  
 Jeong Wan Kim, 132  
 Jeong-Woong Hong, 178  
 Jia-Yu Chen, 305  
 Jin-Cheol Ha, 133  
 Jityaev I.L., 134, 135  
 Joko Santoso, 282  
 Jung J.H., 258  
 Jung-Ting Hsieh, 305  
 Kai A., 280  
 Kaidashev E.M., 137, 138, 163, 197  
 Kalinchuk V. V., 51, 52, 53  
 Kalinin V.A., 137, 138  
 Kamentsev K.E., 267  
 Kara-Murza S.V., 136  
 Karapetyan G.Ya., 137, 138, 163  
 Katsumoto Y., 185  
 Kawano R., 139  
 Kaydashev V. E., 137, 163  
 Kazimirov N.I., 114  
 Kazmenko M.I., 140  
 Kazmina M. A., 197  
 Kevin Firnanda M., 311  
 Khabarova I.A., 65  
 Khabibulla Abdullin, 33  
 Khakhulin D.A., 284  
 Khanazaryan A.D., 113  
 Khasbulatov S.V., 141, 142, 240, 241,  
 243  
 Kim J.D., 143, 144, 258  
 Kim J.E., 143, 258  
 Kim J.S., 144  
 Kim T.G., 131  
 Kirichenko I.A., 144  
 Kirillova E., 254  
 Kirtan K. Sahu, 145  
 Kiseleva L.I., 312  
 Kislitsyn V.O., 137, 138  
 Klimin V.S., 148, 228, 229, 284  
 Svetlichnyi A.M., 134, 135  
 Swain M. V., 232  
 Ta-Chi Jeang, 265  
 Tabachkova N.Yu., 210  
 Tae Gyu Kim, 132, 304  
 Takagi H., 185  
 Takaki R., 197, 265  
 Takase Y., 197, 265  
 Takata K., 40  
 Talanov M.V., 266, 267  
 Tamarkin M.A., 196  
 Tang Z., 157  
 Taran V.M., 171  
 Tatarinov A.M., 121  
 Tekhteleev Yu.V., 136  
 Te-Jen Su, 268, 269  
 Tejkaran Narolia, 269  
 Temnenko V.A., 272  
 Teplyakova N.A., 249, 250, 273  
 Ter-Oganessian N.V., 209  
 Terekhin A. I., 224  
 Terehov V.V., 116  
 Tianyu yu, 132, 274  
 Timoshchenko G.K., 309  
 Tisno Subroto, 125  
 Titov R.A., 250  
 Titov S.V., 275  
 Titov V.V., 157, 158, 220, 246, 275  
 Tiwi Sri Rejeki, 164  
 Tominov R.V., 276  
 Topolov V.Yu., 129, 277, 278  
 Tottori H., 280  
 Triger E.V., 39  
 Trofimenko A.D., 117  
 Troitskaya E.P., 122  
 Tsair-Fwu Lee, 79, 265, 303, 305  
 Tsung-Ying Li, 269  
 Tukodova O. M., 51, 52  
 Tzung-Shiarn Pan, 269  
 Ugrovatov K. M., 281  
 Uniek Praptiningrum, W, 282  
 Vakulov B. G., 92, 282, 283  
 Vakulov Z.E., 284,  
 Varavka V.N., 159  
 Varzarev Yu.N., 213

Klunnikova Yu.V., 149, 150  
 Kolesnik D.A., 294  
 Kolomiitsev A.S., 134, 135  
 Kolosova E.M., 74  
 Kompaniets A.A., 151  
 Kondratyev D.E., 115  
 Korchikova N.V., 136  
 Kornievsky A.S., 152  
 Korolenko S.V., 153  
 Kostetskaya G. S., 283  
 Kotov V.V., 294  
 Kotova A.A., 47  
 Kots I.N., 228  
 Kovalenko M. I., 154  
 Kovalets A.I., 134, 135  
 Kozmin A.A., 163  
 Krasnyakova T.V., 155  
 Kravchuk D.A., 144, 156  
 Kubrin S.P., 157, 158, 220  
 Kudryakov O.V., 159  
 Kunshina G.B., 238  
 Kurakin L.G., 160 – 162  
 Kurdoglyan A.V., 160  
 Kutepov M.E., 137, 138, 163  
 Kyo-Moon Lee, 164, 236  
 Lagoyda S.O., 218  
 Laksono Djoko Nugroho, 164  
 Le Thi Hieu, 87  
 Lednov A.S., 257  
 Lee S.J., 258  
 Lesnyak O. N., 44, 256, 294  
 Levan Ichkitidze, 165, 166  
 Levi G. Yu., 168  
 Lin C.-F., 77, 78  
 Lisnevskaya I.V., 163, 169, 224  
 Litvinchuk S.Yu., 128  
 Liu X., 139  
 Liu Y.-M., 103, 244  
 Luyen The-Thanh, 169  
 Lyanguzov N.V., 197, 232  
 Lyasnikova A. V., 170, 171  
 Lysenko I.A., 161  
 Lysenko I. E., 112, 172  
 Lysenko S.A., 161  
 Mac Thi-Bich, 169  
 Vasiliev A.S., 232, 257  
 Vasilev A. V., 286  
 Vasiliev P. V., 287  
 Vatulyan A. O., 56, 288, 289  
 Velibekov D.V., 290  
 Ventsov N.N., 291  
 Verbenko I.A., 94, 120, 122, 141, 142, 155, 223,  
 275, 297  
 Victor Petrov, 33  
 Victoria Aurellia Sri Paramita Putri, 109, 110, 292  
 Vijay K. Gupta, 145, 269  
 Vishnevetskiy V. Yu, 293, 294  
 Vislousova I.N., 294  
 Vladislav Gamaleev, 295  
 Voitash A.A., 297  
 Volkov D.A., 298  
 Volkova G.K., 223  
 Volkova M.G., 48  
 Voloshchenko P.Yu., 299, 300  
 Voloshchenko Yu.P., 299, 300  
 Vorovich E. I., 51, 52  
 Vovchenko D.V., 117  
 Vu Thi Lan Anh, 195, 196  
 Wang B., 139, 265  
 Wang J.-P., 260  
 Wang S., 265  
 Wateno Oetomo, 64, 126, 301  
 Wahyu Solafide, 230  
 Wei-Chun Lin, 79  
 Wisanukorn Lukkhasorn, 86, 87, 126  
 Wu Kejun, 302  
 Xi Liu, 53  
 Xuchen Zheng, 221, 306  
 Yang C.-C., 76, 104  
 Yang C.-D., 100, 102  
 Yang-Wei Hsieh, 303  
 Yeh M.-Y., 100, 102  
 Yi Tseng Li, 83  
 Yogina D.V., 232  
 Young Woo Kwon, 304  
 Yoshihiro Deguchi, 178  
 Yoshikazu Sano, 53, 221, 306  
 Yu-Hao Chiu, 303, 305  
 Yu Hsuan Hsu, 81  
 Yu-Jie Huang, 303

Maksyukov S.Yu., 232  
 Malitskaya M.A., 157, 158, 220, 246  
 Malyshev I. V., 173  
 Malysheva I. S., 174  
 Malyukov S.P., 150  
 Marakhovskiy M.A., 247  
 Markov I. P., 174, 175  
 Martynenko A.A., 207  
 Masaru Hori, 295  
 Masloboeva S.M., 239  
 Matrosov A.A., 47, 235, 236, 256, 290,  
 294  
 Maula Nafi, 97, 128, 176  
 Melnikova I. P., 170  
 Miakisheva O.A., 121  
 Michael Swain, 44  
 Michael Yu. Zhukov, 88  
 Migal Yu.F., 176  
 Mikhail Belodedov, 166  
 Mikhail Savelev, 165  
 Mikhailova I.B., 168  
 Min-He Zhan, 79  
 Min Yen Yeh, 179  
 Minasyan T.A., 137, 163  
 Miroschnichenko I.P., 180, 181  
 Mitchenko S.A., 155  
 MURAI K. I., 332  
 OISHI M., 333  
 Yu Liang Hsiao, 81, 83  
 Yu Tianyu, 164, 236  
 Yudai Taruya, 221, 306  
 Yudin A. S., 307, 308  
 Yun-Hae Kim, 90, 132, 133, 164, 236, 259, 263,  
 274  
 Yurasov Yu.I., 188, 223, 297, 309  
 Yuto Inui, 53  
 Zabiyaka I.Yu., 159  
 Zainun Achmad, 311  
 Zakharov Yu.N., 312  
 Zau Wen Kuo, 86  
 Zhidel K.M., 136, 313  
 Zhmaylov P.Yu., 204  
 Zhuang J., 157  
 Zhuravlev G.A., 93, 314 - 316  
 Zifeng S., 40  
 Zi-Hao Wang, 79  
 Zih-Xiang Su, 303  
 Zixuan Chen, 274  
 Zong Hsien Wu, 81, 83  
 Zubarev J. Y., 317  
 Zubkov S.V., 318 – 321  
 Zubova T.A., 148  
 Zulfiqar Ali, 31



2020 International Conference on "Physics and Mechanics  
 of New Materials and Their Applications" (PHENMA 2020)  
 Kitakyushu, Japan, March 26 – 29, 2021

## Participating Countries and Organizations

### Australia

- University of Sydney, Sydney

### Belarus

- Scientific-Practical Materials Research Centre of NAS of Belarus, Minsk

### China

- Chengdu University, Chengdu
- College of Engineering, Dali University, Dali, Yunan

- Electronic Materials Research Laboratory, Key Laboratory of the Ministry of Education, International Center for Dielectric Research, School of Electronic and Information Engineering, Xi'an Jiaotong University, Xi'an, Shaanxi
- School of Aerospace Engineering and Applied Mechanics, Tongji University, Shanghai

### **Egypt**

- Faculty of Electronic Engineering, Menoufia University, Menouf

### **Germany**

- RheinMain University of Applied Sciences, Wiesbaden

### **India**

- Natural Science Discipline, PDPM, Indian Institute of Information Technology, Design and Manufacturing Jabalpur, Madhya Pradesh

### **Indonesia**

- Department of Architecture, Faculty of Engineering Universitas 17 Agustus 1945 Surabaya
- Department of Industrial Engineering, University of Pembangunan Nasional Veteran (UPN Veteran) East Java, Surabaya
- Department of Industrial Engineering, University of 17 Agustus 1945 (UNTAG) Surabaya
- Departement of Mechanical Engineering, Faculty of Industrial Technology, Institut Teknologi Sepuluh Nopember Surabaya
- Design and Construction Department, Surabaya State Polytechnic of Shipping, Surabaya
- Department of Mechanical Engineering, University of 17 Agustus 1945 Surabaya
- Institute Teknologi Sumatera, Lampung Selatan

### **Japan**

- Centre for Low Temperature Plasma Science, Nagoya University, Nagoya
- Department of Mechanical Engineering, Kyushu Institute of Technology, Kitakyushu
- Department of Optical Science, Tokushima University, Tokushima
- Graduate School of Advanced Technology and Science, Tokushima University, Tokushima
- Graduate School of Technology, Industrial and Social Sciences, Tokushima University, Tokushima

### **Kazakhstan**

- Al Farabi Kazakh National University, National Nanotechnology Laboratory of Open Type, Almaty

### **Latvia**

- Institute of Materials and Structures, Riga Technical University, Riga

## **Republic of Korea**

- Busan Machinery Research Center, Korea Institute of Machinery & Materials, Busan
- Center of Ceramic Fiber Commercialization, Korea Institute of Ceramic Engineering and Technology, Busan
- Daewoo Shipbuilding & Marine Engineering Co., Ltd., Busan
- Department of Marine Equipment Engineering, Graduate School, Korea Maritime and Ocean University, Busan
- Department of Ocean Advanced Materials Convergence Engineering, Korea Maritime and Ocean University, Busan
- Department of Nano Fusion Technology, Pusan National University, Busan
- Department of Nanomechanics Engineering, Pusan National University, Busan
- Division of Mechanical Engineering, Korea Maritime and Ocean University, Busan
- Division of Marine Engineering, Korea Maritime and Ocean University, Busan
- Division of Refrigeration & Air-conditioning Engineering, Korea Maritime and Ocean University, Busan
- Electro-Medical Device Research Center, Korea Electrotechnology Research Institute, Ansan
- Graduate School, Korea Maritime and Ocean University, Busan
- Korea Marine Equipment Research Institute, Busan
- Laser Advanced Machining Support Center, Korea Maritime and Ocean University, Busan
- Ocean Science and Technology School, Korea Maritime and Ocean University, Busan
- Research Institute of Medium & Shipbuilding, Busan
- R&D Center, Control Factory, Busan

## **Russia**

- Bauman Moscow State Technical University, Moscow
- Chemistry Department, Southern Federal University, Rostov-on-Don, Russia
- Department of Construction and Technology of Electronic Devices, Southern Federal University, Taganrog
- Department of Theoretical and Applied Mechanics, Don State Technical University, Rostov-on-Don
- Department of Mechanics of Composite Materials and Structures, Perm National Research Polytechnic University, Perm
- Department of Nanotechnologies and Microsystems, Southern Federal University, Taganrog
- Don State Technical University, Rostov-on-Don
- Engineering Technological Academy, Southern Federal University, Taganrog
- Faculty of Physics, Southern Federal University, Rostov-on-Don
- Federal Scientific Centre of Agroecology, Complex Melioration and Protective Afforestation of the Russian Academy of Sciences, Volgograd
- Yu. A. Gagarin State Technical University, Saratov



- Hydrochemical Institute of Roshydromet, Rostov-on-Don
- Institute of Biomedical Systems of National Research University of Electronic Technology “MIET”, Moscow
- Institute for Bionic Technologies and Engineering of I.M. Sechenov First Moscow State Medical University, Moscow
- Institute of Comprehensive Exploitation of Mineral Resources of the Russian Academy of Sciences (IPKON RAS), Moscow
- Institute of Earth Sciences, Southern Federal University, Rostov-on-Don
- Institute of High Technology and Piezo Technic, Southern Federal University, Rostov-on-Don
- Institute for Mathematics, Mechanics and Informatics, Kuban State University, Krasnodar
- Institute of Nanotechnologies, Electronics, and Equipment Engineering, Southern Federal University, Taganrog
- Laboratory of Nanomaterials, Southern Federal University, Rostov-on-Don
- LLC STC “RUS”, Saint-Petersburg
- Moscow Aviation Institute, Moscow
- Moscow Institute of Physics and Technology, Dolgoprudny
- National Research University of Electronic Technology (Moscow Institute of Electronic Technology MIET), Moscow
- National University of Science and Technology «MISIS», Moscow
- OKB RITM, Taganrog
- OOO "Parametrica", Taganrog
- Peter the Great St. Petersburg Polytechnic University, St. Petersburg
- Petrozavodsk State University, Petrozavodsk
- M.I. Platov South-Russian State Polytechnic University (NPI), Novocherkassk
- Research and Education Center "Materials", Don State Technical University, Rostov-on-Don
- Research and Education Centre “Microsystem Technics and Multisensor Monitoring Systems”, Southern Federal University, Taganrog
- Research and Education Mathematical Center “Mathematics for Future Technologies”, Nizhny Novgorod
- Research Institute for Mechanics, National Research Lobachevsky State University of Nizhny Novgorod, Nizhny Novgorod
- Research Institute of Physics, Southern Federal University, Rostov-on-Don
- Research Institute of Solid-State Electronics Materials, Russian Technological University (RTU MIREA), Moscow
- Research and Technology Unit, FKU NPO "STiS" MIA Russia, Rostov-on-Don
- RITVERC JSC, St. Petersburg
- Rostov State Medical University, Rostov-on-Don
- Rostov State Transport University, Rostov-on-Don
- Smart Materials Research Institute, Southern Federal University, Rostov-on-Don
- Southern Mathematical Institute of the Vladikavkaz Scientific Center of the Russian Academy of Sciences, Vladikavkaz
- Southern Scientific Centre RAS, Rostov-on-Don
- St. Petersburg Academic University RAS, St. Petersburg

- I.V. Tananaev Institute of Chemistry – Subdivision of the Federal Research Centre «Kola Science Centre of the Russian Academy of Sciences», Apatity
- Water Problems Institute of the Russian Academy of Sciences, Moscow

### **Taiwan**

- Chang Gung University College of Medicine, Kaohsiung
- College of Maritime, National Kaohsiung University of Science and Technology, Kaohsiung
- Department of Business Management, National Sun Yat-Sen University, Kaohsiung
- Department of Electrical Engineering, National Kaohsiung University of Science and Technology, Kaohsiung
- Department of Electronic Engineering National Kaohsiung University of Sciences and Technology, Kaohsiung
- Department of Marine Environmental Engineering, National Kaohsiung University of Science and Technology, Kaohsiung
- Department of Materials Science and Engineering, National Taiwan University of Science and Technology, Taipei
- Department of Microelectronics Engineering, National Kaohsiung University of Science and Technology, Kaohsiung
- Department of Naval Architecture Engineering, National Kaohsiung University of Science and Technology, Kaohsiung
- Department of Nutrition, Institute of Biomedical Nutrition, Hung-Kuang University, Taichung
- Department of Orthopedic, Kaohsiung Municipal Min-Sheng Hospital, Kaohsiung
- Department of Radiation Oncology, E-Da Hospital, Kaohsiung
- Department of Radiation Oncology, Kaohsiung Chang Gung Memorial Hospital, Kaohsiung
- Medical Physics and Informatics Laboratory of Electronics Engineering, National Kaohsiung University of Applied Sciences, Kaohsiung
- National Taiwan University of Science and Technology, Taipei
- PhD program in Biomedical Engineering, Kaohsiung Medical University, Kaohsiung
- Tygood Cosmos Vital Force Technology Corporation

### **Thailand**

- Faculty of Business Administration and Accountancy, Khon Kaen University (KKU), Khon Kaen

### **UK**

- Department of Mechanical Engineering, University of Bath, Bath
- Department of Physics, Oxford University, Parks Road, Oxford

### **Ukraine**

- A.A. Galkin Physics and Technology Institute, Donetsk
- A.A.Galkin Institute for Physics and Engineering, Donetsk
- Institute of Physical Organic and Coal Chemistry, Donetsk
- L.M. Litvinenko Institute of Physical Organic and Coal Chemistry, Donetsk
- Lugansk National Agrarian University, Lugansk
- Lugansk Taras Shevchenko State University, Lugansk

### **Vietnam**

- Department of Automotive Engineering, Ho Chi Minh City University of Technology (HUTECH), Ho Chi Minh City
- Faculty of Environmental, Hanoi University of Mining and Geology, Hanoi
- Faculty of Mechanical Engineering, Haiphong University, Haiphong City
- Faculty of Mechanical Engineering, Hung yen University of Technology and Education, Hung yen
- School of Mechanical Engineering, Hanoi University of Science and Technology, Hanoi City



2020 International Conference on "Physics and Mechanics of New Materials and Their Applications" (PHENMA 2020)  
Kitakyushu, Japan, March 26 – 29, 2021

## SCHEDULE OF INTERNATIONAL CONFERENCE ON "PHYSICS AND MECHANICS OF NEW MATERIALS AND THEIR APPLICATIONS" (PHENMA 2020), March 26–29, 2021

### On/Offline Presentaion

- Presentation Instrument: Zoom
- Presentation Room No.: Meeting Room 1, Meeting Room 2, Meeting Room 3, Meeting Room 4

Date	March 26 (On/Offline Schedule)	
15:00~18:00 (UTC+9)	<b>Registration</b>	
	- On/Offline Registration Check	
Date	March 27 (Online Schedule-Meeting Room 1)	
	<b>Opening Ceremony</b> Chairperson: N.A. Noda	
15:00~15:20 (UTC+9)	<ol style="list-style-type: none"> <li>1. <b>Opening</b> - Prof. N.A. Noda, Organizer of PHENMA2020</li> <li>2. <b>Welcome Address</b> - Yun-Hae Kim (Korea Maritime and Ocean University, Korea)</li> <li>3. <b>Congrats Address</b> - I.A. Parinov (Southern Federal University, Russia) - S.-H Chang (National Kaohsiung University of Science and Technology, Taiwan)</li> </ol>	
	<b>Plenary Speech</b>	
15:20~15:45 (UTC+9)	<b>Ri-ichi Murakami</b> (Chengdu University, China) anewmoon816@gmail.com	Effects of Water pH and Immersion Time on Water Absorption Behavior and Mechanical Properties of Carbon Fiber Reinforced Bio Plastic Composites
15:45~16:00 (UTC+9)	<b>Break</b>	
	<b>Keynote Speech</b> Chairperson: Genji Hotta	
16:00~16:25 (UTC+9)	<b>A.V. Lyasnikova</b> (Don State Technical University, Russia) lyasnikovaav@mail.ru	Improving the Functional Characteristics of Biocompatible Coatings of Bone Implants due to Modification of the Initial Powders
16:25~16:50 (UTC+9)	<b>Cheng-Fu Yang</b> (National University of Kaohsiung, Taiwan) cfyang@nuk.edu.tw	Mechanism of Growth ZnO Nanowires and Application
16:50~17:00 (UTC+9)	<b>Break</b>	
	<b>General Presentation</b> <b>Session A-1</b> Chairperson: Pankaj Koinkar	
17:00~17:15	<b>Pankaj Koinkar</b>	Controlling the Optoelectrical Properties of Two-

(UTC+9) <b>Invited Speech</b>	(Tokushima University, Japan) koinkar@tokushima-u.ac.jp	Dimensional Nanostructures Prepared by Laser Ablation in Liquid
<b>17:15~17:25</b> (UTC+9)	<b>Chih Chin Yang</b> (National Kaohsiung University of Science and Technology, Taiwan) chchyang@nkust.edu.tw	Respiration Sensing Devices Based on Indium Nitride <i>p-n</i> Heterostructure on Silicon Porous Substrate
<b>17:25~17:35</b> (UTC+9)	<b>I.V. Bogachev</b> (Southern Federal University, Russia) bogachev89@yandex.ru	On the Identification of the Characteristics of Functional-Gradient Plates in the Framework of the Kirchhoff and Timoshenko Models
<b>17:35~17:45</b> (UTC+9)	<b>Jeong-Wan Kim</b> (Pusan National University, Korea) tgkim@pusan.ac.kr	MgF <sub>2</sub> Nanoparticle Coating to Improve the Efficiency of Light Hazzard in DSLR Cameras
<b>17:45~17:55</b> (UTC+9)	<b>Biao Wang</b> (Kyushu Institute of Technology, Japan) gongliwangbiao@163.com	Nut Height Effect on Anti-Loosening Performance of Pitch Difference Bolt Nut Connections
<b>17:55~18:05</b> (UTC+9)	<b>Break</b>	
	<b>General Presentation Session A-2</b> Chairperson: <a href="#">Soo-Jeong Park</a>	
<b>18:05~18:20</b> (UTC+9) <b>Invited Speech</b>	<b>Soo-Jeong Park</b> (Korea Maritime and Ocean University, Korea) blue9069@naver.com	Reinforcing Effects of CNT Nanofiller for Enhancing the Interfacial Bonding Strength of Filament Wound FRP Composites
<b>18:20~18:30</b> (UTC+9)	<b>Noriko Tutsumi</b> (Oita University, Japan) tsutsumi-noriko@oita-u.ac.jp	Effect of Hydrogen on Fracture Mechanism in Tensile Test of Carbon Steels
<b>18:30~18:40</b> (UTC+9)	<b>N.V. Andros</b> (Southern Federal University, Russia) andross@mail.ru	Occurrence of 3D Periodic Convective Flows in a Vertical Layer with Moving Boundaries
<b>18:40~18:50</b> (UTC+9)	<b>Ta-Chi Jeang</b> (National Kaohsiung University of Science and Technology, Taiwan) hywang@nkust.edu.tw	A Novel Universal Voltage-Mode Inverse Filter for Signal Processing
<b>18:50~19:00</b> (UTC+9)	<b>Kinjirou Saito</b> (Kyushu Institute of Technology, Japan) saito.h2c.kinjiro@jp.nipponsteel.com	Special Sliding Door with Storable Handrail to Support Senior and Handicapped Persons to Walk by Themselves

<b>Date</b>	<b>March 27 (Online Schedule-Meeting Room 2)</b>	
	<b>General Presentation Session B-1</b> Chairperson: <a href="#">Sung-Youl Bae</a>	
<b>17:00~17:15</b> (UTC+9) <b>Invited Speech</b>	<b>Sung-Youl Bae</b> (Korea Institute of Ceramic Engineering and Technology, Korea) bsy@kicet.re.kr	A Study on Structural Design and Analysis of 18ft CFRP Leisure Board
<b>17:15~17:25</b> (UTC+9)	<b>Erni Pusanantarsi Putri</b> (University of 17 Agustus 1945)	A Case Study: Application of Business Process Re-Engineering in the Company

17:25~17:35 (UTC+9)	<b>Yu-Hao Chiu</b> (National Kaohsiung University of Applied Sciences, Taiwan) sayeh@outlook.com	Using Supervised Learning Algorithms to Predict the Risk of Thyroid Damage for Head and Neck Cancer Patients after Radiation Therapy
17:35~17:45 (UTC+9)	<b>Young-Woo Kwon</b> (Pusan National University, Korea) tgkim@pusan.ac.kr	A Study on the Micro/Nano Texture Design to Improve the Friction Properties of DLC Thin Films
17:45~17:55 (UTC+9)	<b>V.A. Chebanenko</b> (Federal Research Center "Southern Scientific Center of the Russian Academy of Sciences", Russia) valera.chebanenko@yandex.ru	Applied Theory of Bending Vibrations of a Bimorph with Two Active Composite Piezomagnetolectric Layers
17:55~18:05 (UTC+9)	<b>Break</b>	
	<b>General Presentation Session B-2</b> Chairperson: Ji-Eon Kim	
18:05~18:20 (UTC+9) <b>Invited Speech</b>	<b>Ji-Eon Kim</b> (Korea Maritime and Ocean University, Korea) wldjs010@naver.com	A Study on the Removal of Paint and Oxide Layer on the Steel Surface by Laser Beam Scanning Method
18:20~18:30 (UTC+9)	<b>Duy-Hieu Nguyen</b> (National Kaohsiung University of Applied Sciences, Taiwan) ctlin@nkust.edu.tw	Investigating the Effectiveness of Shore-Line Power Using AERMOD Model under the Aspect of Ship Emission
18:30~18:40 (UTC+9)	<b>Hisanori Tottori</b> (Kyushu Institute of Technology, Japan) tottori.hisanori731@mail.kyutech.jp	Development of Multi-Layered Sewer Pipe Plug - Ruptured Test and Stress Analysis of Protective Sheet
18:40~18:50 (UTC+9)	<b>Jeong-Hyo Hong</b> (Korea Maritime and Ocean University, Korea) sea0628@naver.com	Experimental Study on Mechanical Properties of Sandwich Composites with Integrating Auxetic-Core Structure Using FDM 3D Printer
18:50~19:00 (UTC+9)	<b>A.N. Isaeva</b> (Southern Federal University, Russia) isaeva.ashura@yandex.ru	Piezoelectric Sensitivity and Anisotropy in 1-3 Type Composites Based on Ferroelectric Lead-Free Single Crystals

<b>Date</b>	<b>March 27 (Online Schedule-Meeting Room 3)</b>	
	<b>General Presentation Session C-1</b> Chairperson: Chitsan Lin	
17:00~17:15 <b>(Invited Speech)</b>	<b>Chitsan Lin</b> (National Kaohsiung University of Applied Sciences, Taiwan) ctlin@nkust.edu.tw	Using a Novel Graphene-Ceramic Composite material in the Adsorption of Aromatic Volatile Organic Compounds
17:15~17:25	<b>Kazuhiro Oda</b> (Oita University, Japan) oda-kazuhiro@oita-u.ac.jp	Stress Intensity Factors of Interfacial Crack Associated with Different Interface Edge Singularities
17:25~17:35	<b>Sung-Won Yoon</b> (Research Institute of Medium & Shipbuilding, Korea) swyoon@rims.re.kr	Lamination Design for Composite Material Application of Ship Radar Mast

<b>17:35~17:45</b> (UTC+9)	<b>A.N. Isaeva</b> (Southern Federal University, Russia) isaeva.ashura@yandex.ru	Figures of Merit of Novel Piezo-Active Lead-Free Composites
<b>17:45~17:55</b> (UTC+9)	<b>Yudai Taruya</b> (Kyushu Institute of Technology, Japan) q104070y@mail.kyutech.jp	Experimental Verification for Interfacial Creep Generation for Shrink-fitted Bimetallic Work Roll by Using Miniature Rolling Mill
<b>17:55~18:05</b> (UTC+9)	<b>Break</b>	
	<b>General Presentation</b> <b>Session C-2</b> Chairperson: <a href="#">Tac-Hwan Jang</a>	
<b>18:05~18:20</b> (UTC+9) <b>Invited Speech</b>	<b>Tac-Hwan Jang</b> (Pusan National University, Korea) taehwan110@hanmail.net	Multi-Layer Thin Film Deposition for High-Performance X-Ray Field Emission Characteristics
<b>18:20~18:30</b> (UTC+9)	<b>Te-Jen Su</b> (National Kaohsiung University of Sciences and Technology, Taiwan) sutj@kuas.edu.tw	A Neural Network Analysis to The Risk Factors of Type 2 Diabetes
<b>18:30~18:40</b> (UTC+9)	<b>Tatsujiro Miyazaki</b> (University of the Ryukyus, Japan) t-miya@tec.u-ryukyuu.ac.jp	Proportional Method for Evaluating Intensity of Singular Stress Field for Butt Joint with Adhesive Spew
<b>18:40~18:50</b> (UTC+9)	<b>Rahimah Abdul Rafar</b> (Kyushu Institute of Technology, Japan) eimah7178@gmail.com	Effect of Shaft's Rigidity and Motor Torque on Interfacial Slip for Shrink-fitted Bimetallic Work Roll
<b>18:50~19:00</b> (UTC+9)	<b>M.K. Song</b> (Korea Maritime and Ocean University, Korea) mooburi@hanmail.net	Effect of Focal Position on Cut Surface Quality in Laser Cutting of 50 mm Thick Stainless Steel

<b>Date</b>	<b>March 27 (Online Schedule-Meeting Room 4)</b>	
	<b>General Presentation</b> <b>Session D-1</b> Chairperson: <a href="#">Chang-Wook Park</a>	
<b>17:00~17:15</b> (UTC+9) <b>Invited Speech</b>	<b>Chang-Wook Park</b> (Research Institute of Medium & Shipbuilding, Korea) cwpark@rims.re.kr	Mechanical Properties of Large-Scale Composite Structures according to Process Condition
<b>17:15~17:25</b> (UTC+9)	<b>Rahimah Abdul Rafar</b> (Kyushu Institute of Technology, Japan) eimah7178@gmail.com	Effect of Driving Torque on Interfacial Creep Generation for Shrink-fitted Bimetallic Work Roll Considering Elastic Deformation of Shaft
<b>17:25~17:35</b> (UTC+9)	<b>Yang-Wei Hsieh</b> (National Kaohsiung University of Applied Sciences, Taiwan) tflee@nkust.edu.tw	Improve the Efficiency of the Patients' Specific Quality Assurance Procedure in Fields' Optimization Techniques of the Pencil Beam Linear Scanning Proton Therapy
<b>17:35~17:45</b> (UTC+9)	<b>Yu. E. Drobotov</b> (Southern Federal University, Russia) yu.e.drobotov@yandex.ru	Evaluation Criteria for the Influence of the Material Properties of Elastic Cylinders on Their Contact Approach

<b>17:45~17:55</b> (UTC+9)	<b>B.B. Musmade</b> (Savitribain Phule Pune University, India) bbmusmade@dypcoeakurdi.ac.in	Robust Sliding Mode Control of Uncertain Nonlinear Systems
<b>17:55~18:05</b> (UTC+9)	<b>Break</b>	
	<b>General Presentation</b> <b>Session D-2</b> Chairperson: Genji Hotta	
<b>18:05~18:20</b> (UTC+9) <b>Invited Speech</b>	<b>Yasushi Takase</b> (Kyushu Institute of Technology, Japan) takase.yasushi415@mail.kyutech.jp	Convenient and Accurate Formulas for Stress Intensity Factor Distribution of Semi-Elliptical Surface Crack
<b>18:20~18:30</b> (UTC+9)	<b>Seong-Jae Park</b> (Korea Maritime and Ocean University, Korea) kay9601@naver.com	Effect of Heating Rate on Mechanical Properties of Polymer Matrix of Carbon/PEKK Composites in Thermoforming Process
<b>18:30~18:40</b> (UTC+9)	<b>Yu. E. Drobotov</b> (Southern Federal University, Russia) yu.e.drobotov@yandex.ru	Method for Calculating Stress Concentration in Elastoplastic Rod with Two Symmetric Hyperbolic Recesses
<b>18:40~18:50</b> (UTC+9)	<b>Hsueh Chen Shen</b> (National Kaohsiung University of Sciences and Technology, Taiwan) ctlin@nckust.edu.tw	A Study on Nitrogen oxides from Coal and Waste Tires in Different Proportion of Mixed Burning
<b>18:50~19:00</b> (UTC+9)	<b>K.N. Boldyrev</b> (Institute of Spectroscopy, Russian Academy of Sciences, Russia) Kn.boldyrev@gmail.com	Infrared Spectra of the $\text{CH}_3\text{NH}_3\text{PbI}_3$ and $\text{CH}_3\text{NH}_3\text{PbBr}_3$ Hybrid Perovskites: Signatures of Phase Transitions and of Organic Cation Dynamics

<b>Date</b>	<b>March 28 (Online Schedule-Meeting Room 1)</b>	
	<b>Keynote Speech</b> Chairperson: Pankaj Koinkar	
<b>15:00~15:25</b> (UTC+9)	<b>N.A. Noda</b> (Kyushu Institute of Technology, Japan) noda.naoaki844@mail.kyutech.jp	Adhesive Strength Evaluation of Scarf Joint by using Intensity of Singular Stress Field (ISSF)
<b>15:25~15:50</b> (UTC+9)	<b>M.A. More</b> (S.P. Pune University, India) mam@physics.unipune.ac.in	Dimensional Materials: Field Emission Characteristics
<b>15:50~16:00</b> (UTC+9)	<b>Break</b>	
	<b>General Presentation</b> <b>Session A-3</b> Chairperson: Yu.E. Drobotov	
<b>16:00~16:15</b> (UTC+9) <b>Invited Speech</b>	<b>Yu. E. Drobotov</b> (Southern Federal University, Russia) yu.e.drobotov@yandex.ru	The Variable Order Riesz Potential on Quasimetric Sphere in the Variable Exponent Höder Space
<b>16:15~16:25</b> (UTC+9)	<b>Dong-Hun Yang</b> (Korea Maritime and Ocean University, Korea) dhyang1@hanwha.com	A Study on Lightweight Design of Ultra High-Pressure Composite Pressure Vessel for Hydrogen Gas



16:25~16:35 (UTC+9)	<b>Wu Kejun</b> (Tokushima University, Japan) c501738003@tokushima-u.ac.jp	Preparation of TiO <sub>2</sub> -WS <sub>2</sub> -Au Composite Using Hydrothermal Synthesis for Photocatalytic Activity under Visible Light
16:35~16:45 (UTC+9)	<b>Min Yen Yeh</b> (National Kaohsiung University of Applied Sciences, Taiwan) minyen@nkust.edu.tw	Preparation of Zinc Silicate Doped with Manganese Phosphor by Hydrothermal Method
16:45~16:55 (UTC+9)	<b>Rei Takaki</b> (Kyushu Institute of Technology, Japan) takaki.rei244@mail.kyutech.jp	Fractographic Identification of Fracture Origin in Scarf Joint in Comparison to Butt Joint
16:55~17:05 (UTC+9)	<b>Min-Gyu Jeon</b> (Korea Maritime and Ocean University, Korea) Jeon85@kmou.ac.kr	Temperature Measurement of Turbulent Flame using CT-TDLAS (Computed Tomography-Tunable Diode Laser Absorption Spectroscopy)
17:05~17:15 (UTC+9)	<b>Kei-Ichiro Murai</b> (Tokushima University, Japan) keimurai@tokushima-u.ac.jp	Fabrication and Evaluation of Ca-Doped SrTiO <sub>3</sub> Thermoelectric Materials by Molten Salt Method
17:15~17:25 (UTC+9)	<b>Erni Puspantasari Putri</b> (University of 17 Agustus 1945)	Case Study of the Keys to Success of Supply Chain Management in Company
17:25~17:35 (UTC+9)	<b>Tianyu Yu</b> (Korea Maritime and Ocean University, Korea) yutianyukmou@gmail.com	Experimental and Computational Studies on Stiffness Properties of Nanoclay-Incorporated FRPs with Different Nano-Structures
17:35~17:50 (UTC+9)	<b>Break</b>	
	<b>Closing Ceremony</b> Closing address: N.A. Noda, Organizer of PHENMA2020	
17:50~18:10 (UTC+9)	<ol style="list-style-type: none"> <li>1. Summary of PHENMA 2020</li> <li>2. Closing Remarks</li> </ol>	

Date	March 28 (Online Schedule-Meeting Room 2)	
	<b>General Presentation</b> <b>Session B-3</b> Chairperson: Antonio Norio Nakagaito	
16:00~16:15 (UTC+9) <b>Invited Speech</b>	<b>Antonio Norio Nakagaito</b> (Tokushima University, Japan) nakagaito@tokushima-u.ac.jp	Fabrication of Strong Macrofibers from Plant Fiber Bundles
16:15~16:25 (UTC+9)	<b>R. Kawano</b> (Kyushu Institute of Technology, Japan) kawano.ryo621@mail.kyutech.jp	Effect of Pitch Difference and Root Radius on Anti-Loosening Performance of Bolt Nut Connections
16:25~16:35 (UTC+9)	<b>J.S. Kim</b> (Korea Maritime Equipment Research Institute, Korea) jskim@komeri.re.kr	Comparison of Weldability of Laser and Laser-Arc Hybrid Welding for Ship Manufacturing Using Environmentally Friendly Aluminum Alloys
16:35~16:45 (UTC+9)	<b>Adeel Ahmad Jamil</b> (National Kaohsiung University of Science and Technology, Taiwan) ctlin@nkust.edu.tw	A Bag of Expressions-Based Method for the Recognition of Vehicle Make and Model
16:45~16:55 (UTC+9)	<b>Sumit Patil</b> (Kavayitri Bahinabai Chaudhari North Maharashtra University,	Investigation of Electrical Properties of Peald Deposited Ti/Al <sub>2</sub> O <sub>3</sub> /Al/Si MIM Capacitors

	India) ammahajan@nmu.ac.in	
<b>16:55~17:05</b> (UTC+9)	<b>Chih Chin Yang</b> (National Kaohsiung University of Science and Technology, Taiwan) C107187156@nkust.edu.tw	Capacitance Type p-InN/n-Si Heterostructure Sensing Devices on Silicon Unpolished Substrate
<b>17:05~17:15</b> (UTC+9)	<b>Edi Santoso</b> (University of 17 Agustus 1945)	Effect of Voltage and Current to MIG Welding with 1 mm Filler Diameter to the Mechanical Properties of Welded Joints of Commercial Steel
<b>17:15~17:25</b> (UTC+9)	<b>Maula Nafi</b> (University of 17 Agustus 1945)	Microstructure and Tensile Stress Analysis on T6 Heat Treated Aluminum-Bottom Ash Coal Composite made by Squeeze Casting

<b>Date</b>	<b>March 28 (Online Schedule-Meeting Room 3)</b>	
	<b>General Presentation</b> <b>Session C-3</b> Chairperson: Jin-Cheol Ha	
<b>16:00~16:15</b> (UTC+9) <b>Invited Speech</b>	<b>Jin-Cheol Ha</b> (Dali University, China) chnhjc@naver.com	Corrosion Mechanism and Degradation Behaviour of Basalt Fiber Reinforced Composites in Sulfuric Acid Solution
<b>16:15~16:25</b> (UTC+9)	<b>Ryoichi Saito</b> (Kyushu Institute of Technology, Japan) Ryoichi.Saito@sengcia.com	Fatigue Strength Improvement of Roller Chain by Press Pitting Between Pin and Plate
<b>16:25~16:35</b> (UTC+9)	<b>I.V. Bogachev</b> (Southern Federal University, Russia) bogachev89@yandex.ru	Modeling of Biological Tissues Taking into Account the Residual Stress
<b>16:35~16:45</b> (UTC+9)	<b>Chin Ko Yeh</b> (National Kaohsiung University of Science and Technology, Taiwan) ctlin@nkust.edu.tw	Using Activated Quantum Reagent to Transform the Quality of Poultry and Animal Manure and its Recycling
<b>16:45~16:55</b> (UTC+9)	<b>Swati Gupta</b> (Kavayitri Bahinabai Chaudhari North Maharashtra University, India) ammahajan@nmu.ac.in	Sol-Gel Deposited Xerogel, Aerogel and Porogen based Porous Low-K Thin Films: A Comparative Investigation
<b>16:55~17:05</b> (UTC+9)	<b>M.R. Aridi</b> (Kyushu Institute of Technology, Japan) radz7cr@gmail.com	Effect of the Residual Stress to the Fatigue Failure of the Bimetallic Roll in 4-High Rolling Mill
<b>17:05~17:15</b> (UTC+9)	<b>Siddhant Dhongade</b> (Tokushima University, Japan) c501848001@tokushima-u.ac.jp	Liquid Exfoliation of Graphene Oxide Nanoribbons using Chemical Assisted Laser Ablation
<b>17:15~17:25</b> (UTC+9)	<b>Ichlas Wahid</b> (University of 17 Agustus 1945)	Mechanical Properties and Microstructure Analysis of Heated Aluminum-2042 with Variation of Aging Temperature and Aging Time

<b>Date</b>	<b>March 28 (Online Schedule-Meeting Room 4)</b>	
	<b>General Presentation</b> <b>Session D-3</b> Chairperson: K.N. Boldyrev	

<b>16:00~16:15</b> (UTC+9) <b>Invited Speech</b>	<b>K.N. Boldyrev</b> (Institute of Spectroscopy, Russian Academy of Sciences, Russia) Kn.boldyrev@gmail.com	Photochromic Effects in P- and B-doped Diamond
<b>16:15~16:25</b> (UTC+9)	<b>V. Yu. Topolov</b> (Southern Federal University, Russia) vutopolov@sfsedu.ru	Piezoelectric Sensitivity of Modern Lead-Free 1-3-Type Composites Based on Domain-Engineered Single Crystals: Longitudinal and Hydrostatic Responses
<b>16:25~16:35</b> (UTC+9)	<b>Kyo-Moon Lee</b> (Korea Maritime and Ocean University, Korea) world1994@nate.com	Quantifying of the Internal Defects Content in CF-PEKK through Water Absorption Behavior
<b>16:35~16:45</b> (UTC+9)	<b>Te-Jen Su</b> (National Kaohsiung University of Sciences and Technology, Taiwan) sutj@kuas.edu.tw	Particle Swarm Optimization Implementation on the Fault Diagnosis of Gearbox
<b>16:45~16:55</b> (UTC+9)	<b>Hisanori Tottori</b> (Kyushu Institute of Technology, Japan) tottori.hisanori731@mail.kyutech.jp	Development of Multi-Layered Sewer Piper Pulug-Tensile Strength of Protective Sheet
<b>16:55~17:05</b> (UTC+9)	<b>Masatsugu Oishi</b> (Tokushima University, Japan) oishi.masatsugu@tokushima-u.ac.jp	Local Electronic and Atomic Structures of the Mixed B-Site Ions in SrFe <sub>1-x</sub> Mn <sub>x</sub> O <sub>3-δ</sub> Studied with X-ray Absorption Spectroscopy
<b>17:05~17:15</b> (UTC+9)	<b>Hanie Teki Tjendani</b> (University of 17 Agustus 1945)	A System Dynamics Approach to Risk Mitigation in Performance-Based Contract Projects
<b>17:15~17:25</b> (UTC+9)	<b>R.A. Retno Hastijanti</b> (University of 17 Agustus 1945)	Eco-Friendly Electric Tourism Boat Design for Prone Rivers

<b>Date</b>	<b>March 29 (On/Offline Schedule)</b>
<b>15:00~18:00</b> (UTC+9)	<b>Offline Presentation/Technical Tour through Online</b>

## Offline Conference Venue

### ○ Local Secretariat of the Conference

**Address:** Dr. Yasushi Takase, Kyushu Institute of Technology, 1-1, Sensui-cho, Tobata, Kitakyushu-city, Fukuoka 804-8550, Japan

**Fax:** Dr. Yasushi Takase, +81-93-871-8591,

Dept. of Mechanical Engineering, Kyushu Institute of Technology

**Phone:** Nao-Aki Noda, +81-93-871-3124

**E-mail:** takase.yasushi415@mail.kyutech.jp

### ○ General Secretariat of the Conference

**E-mail:** parinov\_ia@mail.ru

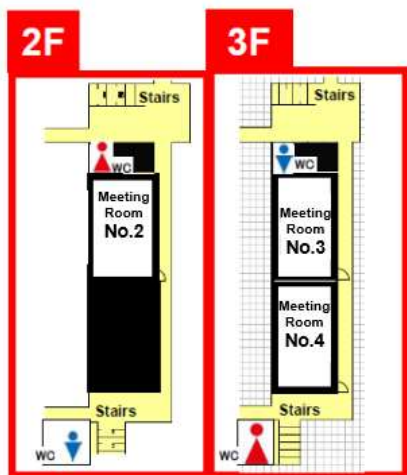
**Web-site:** <http://phenma2020.sfedu.ru/>

**Facebook:** <https://www.facebook.com/PHENMA2020/>

### ○ Locate Map



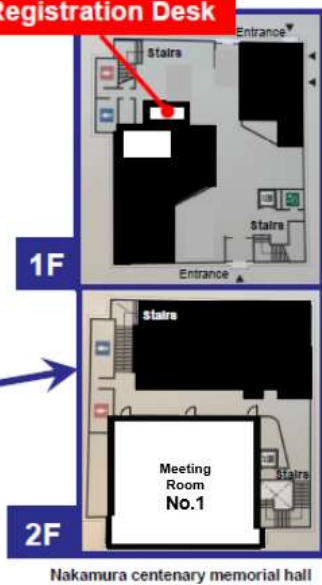
## Floor Map



Education & Research 1



Registration Desk



*Scientific publication*

**2020 International Conference  
on “Physics and Mechanics of New Materials  
and Their Applications” (PHENMA 2020)**

(Kitakyushu, Japan, March 26–29, 2021)

Abstracts and Schedule

Signed to the press on 29.03.2021.

Offset paper. Format 60×84 1/16. Circulation 300 copies.

Usl. pech. list. 20,69. Uch. ed. list. 18,6. Order No. 7995.

Printed in the department of printing, corporate and souvenir products

Publishing and printing complex of the KIBI MEDIA CENTER  
of the Southern Federal University.

344090, Rostov-on-200/1 Stachki Ave., Don, tel. (863) 243-41-66.

